CR 73143

Final Report On

FEASIBILITY STUDY FOR A MULTIPLE SATELLITE SYSTEM

Contract NAS 2-3925

Prepared For

NASA
AMES RESEARCH CENTER
Moffett Field, California

Report SGC 1089R-3
VOLUME II - APPENDICES

SPACE-GENERAL CORPORATION
El Monte, California

FACILITY FORM 602

N67-38549	
(ACCESSION NUMBER)	(THRU)
413	0
(PAGES)	(CODE)
CR# 73143	30
(NASA CR OR TMX OR AD NUMBER)	(CATEGORY)

Final Report On

FEASIBILITY STUDY FOR A MULTIPLE SATELLITE SYSTEM

Contract NAS 2-3925

Prepared For

NASA

AMES RESEARCH CENTER

Moffett Field, California

Approved by:

M. Eimer
Vice President, Engineering

C. A. Lysdale
Program Manager

Report SGC 1089R-3

VOLUME II - APPENDICES

SPACE-GENERAL CORPORATION
El Monte, California

FOREWORD

This final report documents all technical work completed by the Space-General Corporation on the "Feasibility Study for a Multiple Satellite System". It is submitted in partial fulfillment of the requirements of Contract NAS 2-3925. The document consists of two volumes: VOLUME I - SUMMARY, and VOLUME II - APPENDICIES.

The following personnel were responsible for major study tasks, and were primary contributors to the preparation of this final report:

R. L. Phen
Dr. L. Pode
W. F. Storer
E. A. Zeiner
L. B. Wilker

Appendices

Appendix		Page
I	The Major Mission Options	I-1
II	Scientific Implications on Spacecraft Requirements	II-1
III	Preliminary Evaluation of Option 3 Separation Distances and Accuracies	III-1
IV	Selection of Common Orbit Parameters	IV-1
V	Coverage of the Subsolar Line	V-1
VI	Booster Vehicle Considerations	VI-1
VII	Launch Window Considerations	VII-1
VIII	Reference Orbit	XIII-1
IX	Deployment Sensitivities	IX-1
X	Deployment Velocity and Accuracy Requirements	X-1
XI	Aspect Sensing	XI-1
XII	Spin Axis Drift	XII-1
XIII	STADAN Interface	XIII-1
XIV	Communications Link and Tracking Performance Analysis	XIV-1
XV	Satellite Tracking	XV-1
XVI	Communications Coverage	XVI-1
XVII	Magnetic Tape Recorders	XVII-1
XVIII	Multiple Satellite Magnetic Design	XVIII-1
XIX	Reliability Criteria and Analyses	XIX-1
XX	Electromagnetic Interference Control	XX-1
XXI	Environmental Criteria	XXI-1
XXII	System Evaluation for Design	XXII-1
XXIII	Balance Requirements	XXIII-1
XXIV	Thermodynamic Design	XXIV-1
XXV	Power Profile	XXV-1
XXVI	Boom Shadow Considerations and the Effect on Power System Design	XXVI-1

Appendix I

THE MAJOR MISSION OPTIONS

1.0 INTRODUCTION

This Appendix has been developed in support of the coordinated ARC/SGC decision on selection of a scientific mission mode for primary study emphasis*. The preliminary material includes, for each of the primary mission options:

a. A functional sequence
b. A definition of pertinent subsystems and interfaces
c. Relative weight estimates
d. Relative development production cost estimates
e. Relative reliability estimates

2.0 GENERAL COMMENTS

Since the Multiple Satellite Study effort cannot encompass an in-depth investigation of all practical approaches to the scientific mission, a timely decision as to which major mission option is to be emphasized is required. The notes presented herein are intended to facilitate this decision. The options considered are:

Option 1 - No spin axis reorientation, orbit plane near the ecliptic

Option 2 - No spin axis reorientation, orbit plane inclined to the ecliptic

Option 3 - Spin axis reorientation by pallet attitude control system prior to deployment of satellites

Option 4 - Spin axis reorientation by separate satellite systems after deployment from pallet; satellites provide a post-separation orbit and attitude adjustment capability

In the case of the latter two options, to obtain maximum coverage of the subsolar point, the nominal orbit would be chosen to lie close to the ecliptic plane; and the direction of the satellites' spin axes would be brought close to normal to the ecliptic plane, thus keeping the sun line in view at all times. In the case of the first option, the satellites' spin axes will lie in the orbital plane. The requirements for maximum coverage of the subsolar point then conflict

---

*In this Appendix small separation distances only are considered; reference is made to Appendix IV for the implication of large separation distances.

with the requirements for keeping the sun line within the plasma probe's view field throughout the operational lifetime. Option 2 has the orbit plane inclined to the ecliptic providing decreased subsolar coverage than the other options, but does provide that the spin axis is normal to the ecliptic plane. The present notes are directed mainly at a comparison or system implementation. The trade-offs involved in the orbit selection for Option 2 will be considered separately.

In the absence of detailed trade-off studies of the alternative implementations for each option, the implementation concepts projected at this time do not necessarily represent optimum selections. However, the projected concepts are believed to be reasonably representative of main differences between the major mission options. In making these projections, alternatives whose technical feasibility is open to some doubt have been avoided.

Where some desirable but not absolutely essential feature could not be readily provided with one of the mission options, the implementation concept was generally not contrived to provide the feature. For example, in the case of Option 4, in order to implement the spin axis reorientation maneuver, the satellites must carry much of the equipment (such as the pneumatic system and solar sensors) that would be required to provide an orbit adjustment capability. Hence in this case the provision of orbit adjustment capability adds comparatively little to system cost and complexity. Thus the system defined as Option 4 is capable of applying velocity increments after satellite separation to keep the distances between satellites within the bounds desired for the experiments. Since the other options do not lend themselves readily to the provision of such a capability, for present purposes this capability has been considered only for Option 4.

The implementation concepts for each of the options are defined in relatively broad terms, but in sufficient detail to obtain first-cut assessments of relative differences on weight, cost, etc. Undoubtedly, detailed designs would incorporate back-up modes of operation or redundancies to assure the attainment of the desired high reliability level. For present purposes only the primary modes have been considered.

3.0 LAYOUT AND DEPLOYMENT

For this preliminary evaluation, it was assumed that the mission options would not directly lead to a departure from the basic layout of the satellites on the pallet and/or the general technique of deployment considered for the example system in the SGC proposal. This calls for the satellites to be mounted on the pallet in the configuration depicted in Figure 1. The fore and aft satellites are tied together in pairs with the pairs mounted side-by-side on the pallet. They are deployed by first separating satellite pairs from the pallet with spin-off differential velocity increments, and subsequently separating each of the satellites from its partner with axial velocity increments generated by spring action between partners.

In the case of Options 1, 2, and 4, the spin axis of the pallet, which initially is in the orbital plane, would not be reoriented prior to deployment of the satellites. The spin-off deployment would then be timed so that the velocity increments are in the out-of-plane direction while the subsequent axial separations produced are in the in-plane direction. In the case of Option 3, the spin axis of the pallet is reoriented to a direction nearly normal to the orbit. The spin-off is then timed to achieve a velocity increment in the in-plane direction nearly normal to the velocity vector while the subsequent axial separation produces out-of-plane velocity increments.

In the case of Option 4 it may be possible to deploy all four satellites from the pallet simultaneously with spin-off velocity increments, and to subsequently adjust the satellites' orbits using their self-contained velocity increment capabilities. However, it is not apparent at present that a significant advantage could be gained in this way. It seems preferable that the nominal deployment from the pallet be such as to attain the desired differences in the satellites' orbits without counting on subsequent adjustments, since this minimizes the burden on the satellites' systems and enhances the probability of mission success.

It will be noted that for Options 1, 2 and 4, in-plane velocity increments can be applied at two different points; whereas for Option 3 the in-plane velocity increment is applied at only one point.

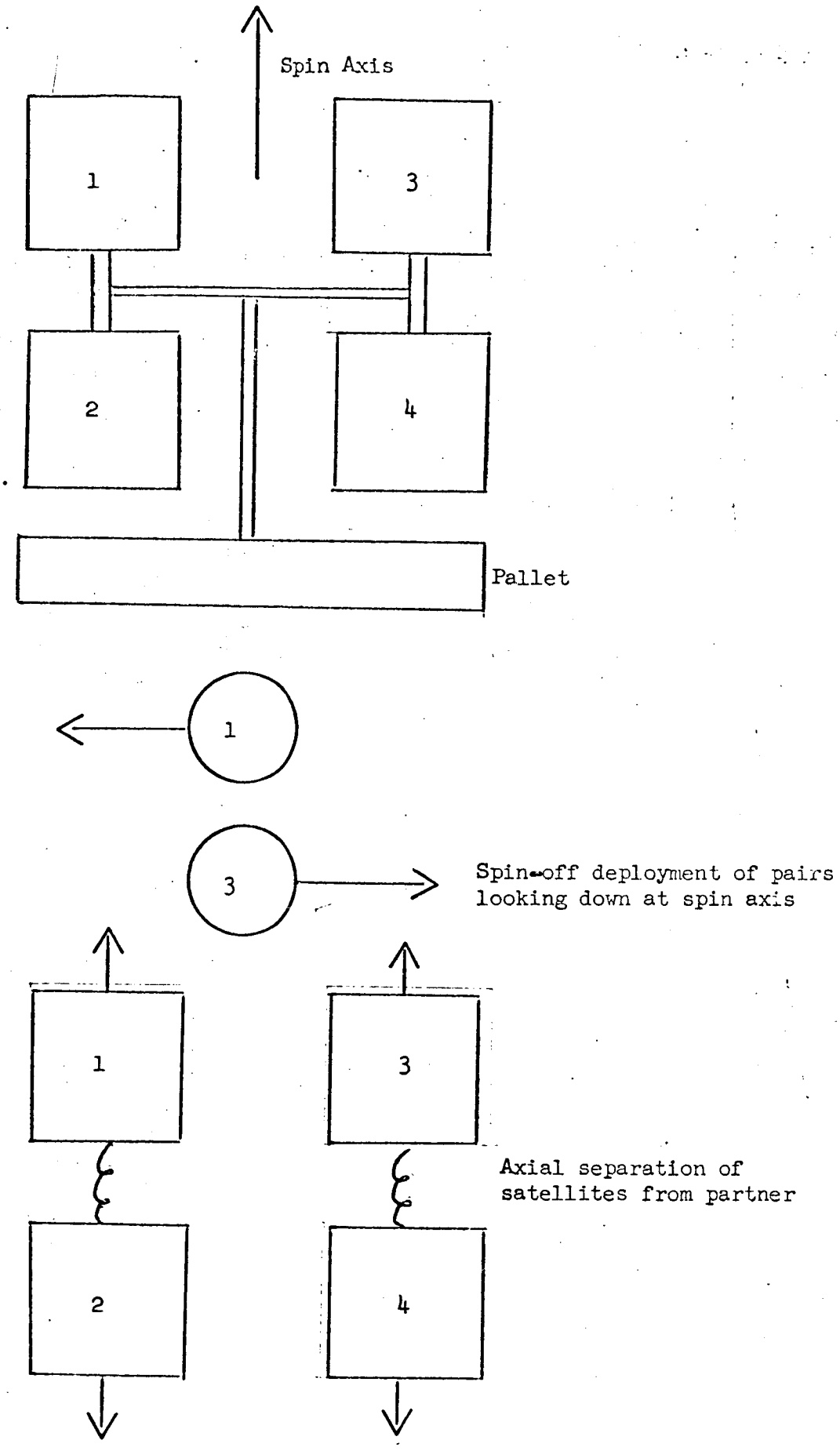

Figure 1. Mounting and Deployment Concept - All Mission Options

4.0 IMPLEMENTATION CONCEPTS

The critical events of the operational sequence for Options 1 and 2 are listed in Table 1. Figure 2 shows the main feature of the pallet/satellite functional interface, highlighting the implementation of sequencing functions.

Table 2 lists the operational sequence and Figure 3 shows the pallet/satellite configuration for Option 3.

The operational sequence for Option 4 is listed in Table 3. Figure 2 is applicable to Option 4 as well as Options 1 and 2, since for these options the pallet/satellite functional interface is the same.

The major difference is the provision of the satellite attitude and orbit adjustment capability for Option 4, which is sketched in Figure 4.

Table 1

OPERATIONAL SEQUENCE, OPTIONS 1 & 2
NO-SPIN AXIS REORIENTATION

1. Inject into orbit with spin axis of vehicle aligned with velocity vector. (A)

2. Separate pallet carrying the four satellites from booster. (A)

3. Deploy pallet's yo-yo despin mechanism. (B)

4. Deploy satellites' antennas and instrument booms. (B)

5. Uncage satellites' precession dampers. (C)

6. Separate satellite pairs from pallet with out-of-plane differential spin-off velocity increments. (D)

7. Separate first pair of satellites (from each other) with in-plane differential axial velocity increment generated by spring action. (C)

8. Separate second pair of satellites with in-plane differential axial velocity increment generated by spring action. (C)

(A) Action initiated by booster.

(B) Action initiated by pallet timer.

(C) Action initiated by ground command through satellites' receivers.

(D) Action armed by ground command through satellites' command receivers and triggered by satellites' sun sensor.

Figure 2.

SKETCH OF SEQUENCING CONFIGURATION FOR OPTIONS 1, 2 & 4
NO REORIENTATION OF PALLET BEFORE SATELLITE DEPLOYMENT

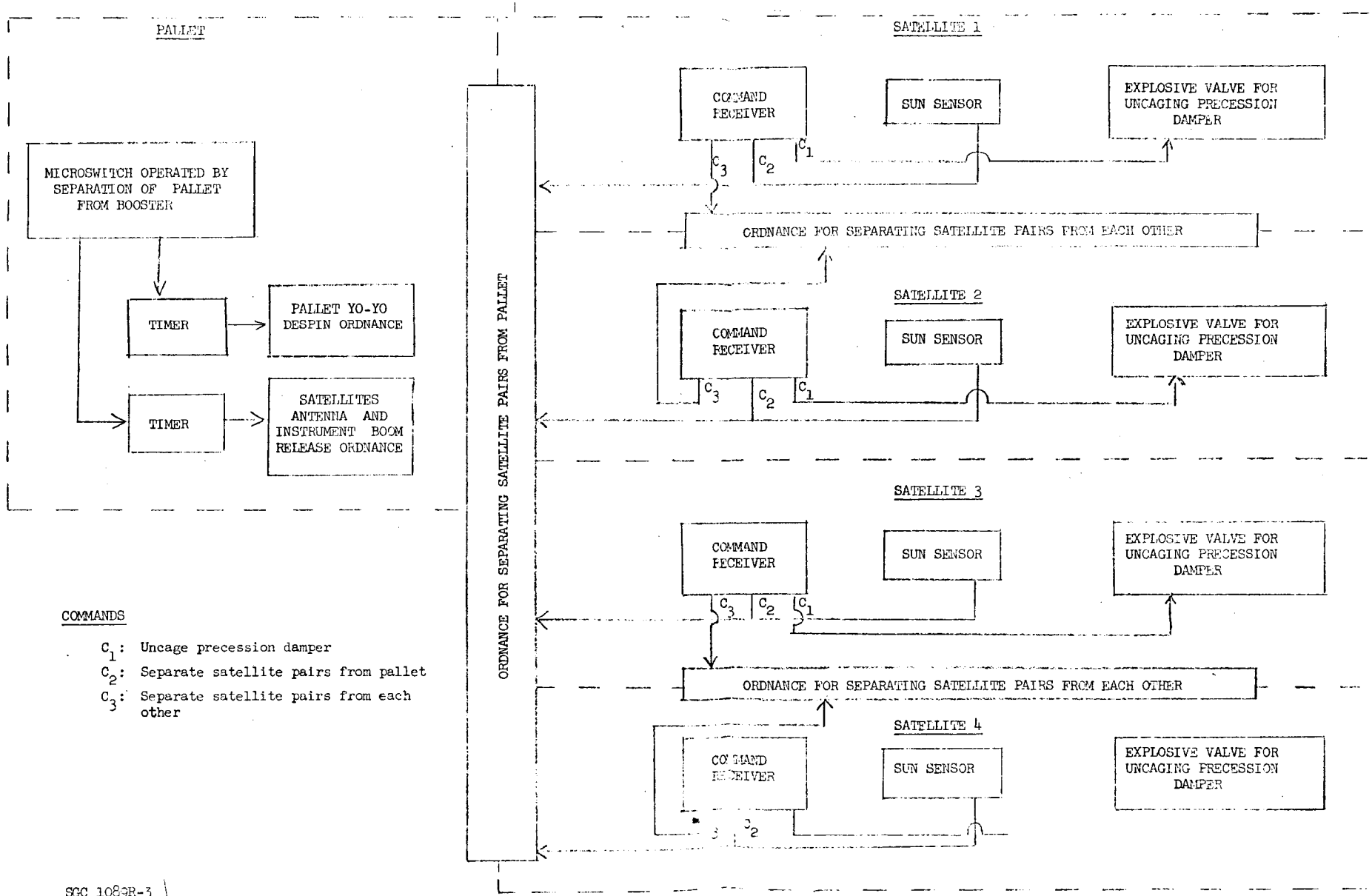

COMMANDS

C_1: Uncage precession damper

C_2: Separate satellite pairs from pallet

C_3: Separate satellite pairs from each other

Table 2

OPERATION SEQUENCE, OPTION 3
PALLET REORIENTATION

1. Inject into orbit with spin axes of vehicle aligned with velocity vector. (A)
2. Separate pallet carrying the four satellites from booster. (A)
3. Deploy pallet's yo-yo despin mechanism. (B)
4. Deploy satellites' antennas and instrument booms and pallet antenna. (B)
5. Uncage satellites' precession dampers. (C)
6. Telemeter and interpret aspect data. (C*)
7. Operate pallet ACS to precess spin axis normal to sun line. (D1)
8. Telemeter and interpret aspect data. (C)
9. Operate pallet ACS to precess spin axis about sun line. (D2/D3)
10. Telemeter and interpret aspect data. (C)
11. Repeat steps 7 to 10 as required to obtain desired spin axis orientation.
12. Separate satellite pairs from pallet with in-plane normal differential spin-off velocity increments. (D4)
13. Separate first pair of satellites with out-of-plane differential axial velocity increments generated by spring action. (C)
14. Separate second pair of satellites with out-of-plane differential axial velocity increments generated by spring action. (C)

(A) Action initiated by booster.

(B) Action initiated by pallet timer.

(C) Action initiated by ground command through satellites' command receivers.

(D) Action initiated through pallet command receiver.

1. Mode 1 - pallet ACS operates to precess spin axis normal to sun line using solar eyes S_1 and S_2.
2. Mode 2 - pallet ACS operates to precess spin axis about sun line in + direction using solar eye S_3.
3. Mode 3 - pallet ACS operates to precess spin axis about sun line in - direction using solar eye S_4.
4. Mode 4 - separation of satellite pairs is armed. Execution is triggered by solar sensor S_5.

* Uses satellites' down link transmission. Aspect inferred from satellites' fan beam antennas and/or auxiliary aspect sensor.

Figure 3

SKETCH OF SEQUENCING CONFIGURATION FOR OPTION 3
PALLET REORIENTED PRIOR TO SATELLITE DEPLOYMENT

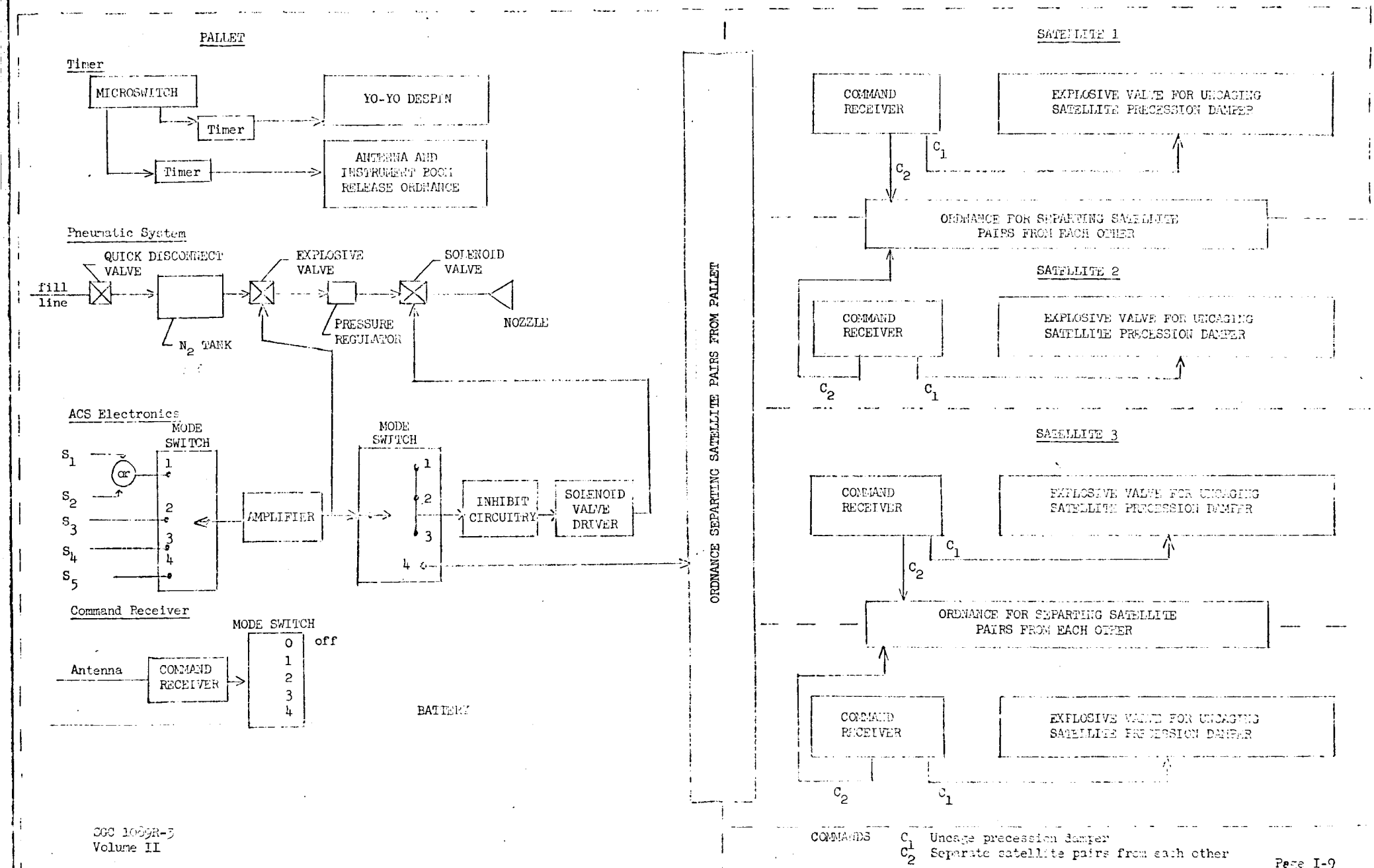

COMMANDS C_1 Uncage precession damper
C_2 Separate satellite pairs from each other

Table 3

OPERATION SEQUENCE, OPTION 4
SEPARATE SATELLITE SPIN AXIS REORIENTATION

1. Inject into orbit with spin axis of vehicle aligned with velocity vector. (A)

2. Separate pallet carrying the four satellites from booster. (A)

3. Deploy pallet's yo-yo despin mechanism. (B)

4. Deploy satellites' antennas and instrument booms. (B)

5. Uncage satellites' precession dampers. (C12)

6. Separate satellite pairs from pallet with cut-of-plane differential spin-off velocity increments. (C10)

7. Separate first pair of satellites with in-plane differential axial velocity increment generated by spring action. (C11)

8. Separate second pair of satellites with in-plane differential axial velocity increment generated by spring action. (C11)

9. Precess spin axis of Satellite 1 to nominal sunline. (C1)

10. Precess spin axis of Satellite 1 about sunline to center satellites' beam transmission pattern on earth. (C2&3)

11. Track Satellite 1, establish ephemeris and adjust orbit. (C4 to 9)

12. Repeat steps 9 to 11 for Satellites 2, 3 and 4.

(A) Action initiated by booster.

(B) Action initiated by pallet timer.

(Cn) Action initiated by ground command through satellites' receivers; executed by mode number n; see sketch of separate Satellite ACS and Orbit Adjustment System.

General Layout

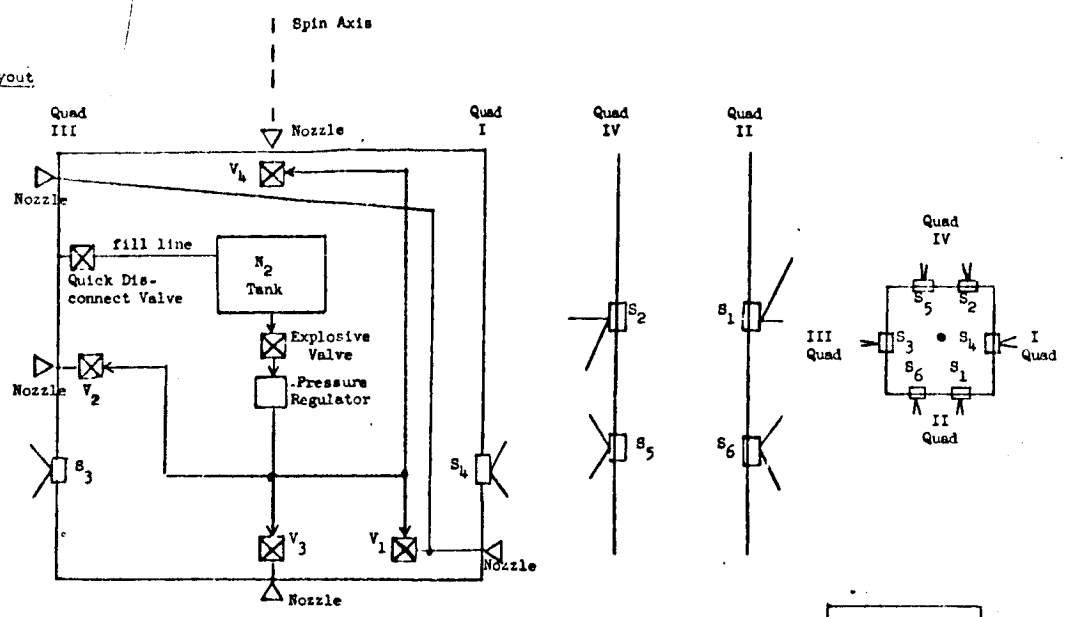

Switching Arrangement

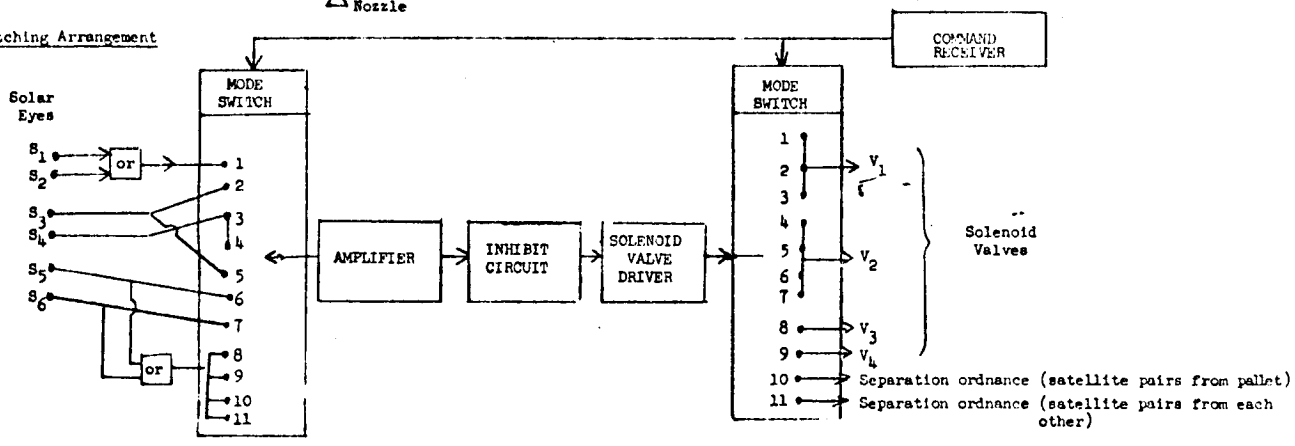

Logic Table

MODE NUMBER	FUNCTION	TRIGGER SOLENOID VALVE	ON SIGNAL FROM SOLAR EYE
1	Precess spin axis to become ⊥ sun line	V_1	S_1 or S_2
2	Precess spin axis about sun line +	V_1	S_3
3	Precess spin axis about sun line -	V_1	S_4
4	Increase velocity in direction of sun line	V_2	S_4
5	Increase velocity in direction opposite to sun line	V_2	S_3
6	Increase velocity in in-plane direction ⊥ to sun line +	V_2	S_5
7	Increase velocity in in-plane direction ⊥ to sun line -	V_2	S_6
8	Increase velocity in out-of-plane direction ⊥ to sun line +	V_3	S_5 or S_6
9	Increase velocity in out-of-plane direction ⊥ to sun line -	V_4	S_5 or S_6
10	Fire ordnance for separation from pallet	ord 1	S_5 or S_6
11	Fire ordnance for separation of pallets from each other	ord 2	-
12	Uncage precession damper	-	-

SKETCH OF OPTION 4 ACS AND ORBIT ADJUSTMENT SYSTEM

5.0 COST, WEIGHT AND RELIABILITY COMPARISONS

Differences among the three basic multiple satellite mission options were investigated and rough order of magnitude costs, weights and reliability differences calculated. Tables 4 - 7 describe the cost and weight differences for the attitude control, communications, power and thermal control subsystems. Table 8 summarizes the cost, weight and reliability differences for the three options. Negative numbers represent weights and costs which are less for the system being compared against. Positive values represent higher weights and costs.

From a weight standpoint Options 1 and 3 are about the same. The additional solar cell panel weights required by Modell are only slightly heavier than the pallet equipment of Option 3. Option 2 is lighter by about 15 lb since no additional solar cells are required compared to Option 3. Mode 4 weighs about 25 lb more than Options 1 and 3 due primarily to the attitude control and orbit adjustment equipment required for each satellite.

Options 1 and 2 are about $400,000 less expensive to develop than Option 3. Production costs of Options 1 and 3 are comparable. The additional solar cells of Mode 1 offset the cost of the pallet equipment of Option 3. Option 2 is about $40,000 cheaper to produce due to the fewer solar cells than Option 1 and lack of an attitude control system. Option 4 is the most expensive, being about $60,000 more expensive to develop than Option 3 and $35,000 more expensive per production system. These costs are due primarily to the attitude control and orbit adjustment subsystem costs.

The reliability difference estimates given in Table 8 represent no consideration of redundancy or marginal failures. Considerations were given only to the differences in equipment and their probability of failure.

Table 4

ATTITUDE CONTROL DIFFERENCES

Factor	Options 1&2 No Reorientation	Option 3 Pallet Reorientation	Option 4 Separate Satellites
Differences	No attitude reorientation before or after separation. See Mode 1&2 block diagram for component description.	Pallet reorients satellite spin axis normal to ecliptic plane before satellite separation. See Option 3 block diagram for component description.	Using individual attitude control systems, the satellites are reoriented after separation. Fan beam antenna assumed as aspect sensor.
Weight Differences		Pallet ACS Weights: ACS Electronics 2.0 Solar Sensor 2.0 Pneumatic System Tank 3.5 Valves 1.5 Lines, Nozzle, Etc. 1.0 10.0 Lbs	Satellite ACS Weights: ACS Electronics 2.0 Solar Sensor, Increment per Satellite 0.5 Pneumatic System Tank 3.5 Valves ACS 1.5 Orbit Adj. 2.5 Lines, Nozzles, Etc. 1.0 11.0/Satellite System ACS Weights: 44.0 Lbs
System Weight Difference With Respect to Option 3	-10 Lbs		+34 Lbs
		Production $ 25,000 R and D $400,000 Total $425,000	Production $ 20,000/Satellite 80,000/System R and D $500,000 Total $530,000
System Cost Difference With Respect to	~ $ 25,000 (Prod. Cost) ~ $400,000 (Develop. Cost)		~ + $ 55,000 (Production Cost) ~ + $100,000 (Development Cost)

Table 5

COMMUNICATION SYSTEM DIFFERENCES

Factor	Option 1&2 No Reorientation	Option 3 Pallet Reorientation	Option 4 Separate Satellites
Differences	Feasibility of using high gain fan beam antennas for this option requires further investigation, but otherwise there is no major satellite communications difference.	Pallet requires command receiver antenna and associated electronics satellite system - same as other options.	Satellite communication system - same as other options.
Weight Differences		Pallet Equipment: Antenna 1 Lb Command Receiver 2-1/2 Electronics, Etc. 1-1/2 5 Lbs	
System Weight Difference With Respect to Option 3	- 5 Lbs		- 5 Lbs
Cost Differences		Equipment Costs: Antenna $ 150 Command Receiver $10,000 Command Decoder $10,000 Harness, Etc. $ 1,000 $21,000 Engineering: Antenna Pattern Test $ 5,000 Command Decoder $10,000 Harness $ 2,000 $17,000	
System Cost Difference With Respect to Option 3	~ - $20,000 (Prod. Cost) ~ - $15,000 (Develop. Cost)		~ - $20,000 (Prod. Cost) ~ - $15,000 (Develop. Cost)

Table 6

POWER SYSTEM DIFFERENCES

Factor	Option 1 No Reorientation	Option 2 No Reorientation	Option 3 Pallet Reorientation	Option 4 Separate Satellite
Differences	Requires 2 ft^2 projected solar cell area on each end of the satellite as well as solar cell around the circumference	Solar cells same as proposal. No battery required for the pallet.	Solar cells are the same as described in the proposal. A silver-zinc battery is required for the pallet.	Solar cells and satellite battery same as proposal.
Weight Differences	4 ft^2 solar cells/satellite @ 1.38#/ft^2 = 5.5#/satellite additional weight over Mode 4.	Same as Mode 4	150 watt-hours silver-zinc pallet battery @ 50 watt hours/lb = 3 lb additional weight over Mode 4.	--
System Weight Difference with Respect to Option 3	+19 lb	-3 lb	--	-3 lb
Cost Differences	Hardware: Additional solar cells over other options = 16 ft^2/system @ \$2/cm^2 (includes final acceptance testing) = \$34,500 Design and Analysis: 3 man-months more than other options = \$12,400 additional cost		Hardware: Pallet battery = \$200	

Table 6

POWER SYSTEM DIFFERENCES

Factor	Option 1 No Reorientation	Option 2 No Reorientation	Option 3 Pallet Reorientation	Option 4 Separate Satellite
	Test: Test planning same for all options. System tests require 1 week/satellite for Option 1 and 2 days/satellite for other options. Assuming test engr. and 1 technician additional cost for Option 1 = $2,600			
	Total difference = $49,500/system	Total difference = 0	Total difference = $200/system	Total difference = 0
System Cost Difference with Respect to Mode 3	$15,000 (Development Cost) + $35,000 (Production Cost)	$-200 (Production Cost)	--	$-200 (Production Cost)

Table 7

THERMAL CONTROL DIFFERENCES

Factor	Option 1 No Reorientation	Option 2 No Reorientation	Option 3 Pallet Reorientation	Option 4 Separate Satellites
Differences	Solar cells on satellite ends make analysis & system design more complicated than the other options.	Satellite thermal control similar to that for Option 3.	1) Pallet requires thermal control as well a satellites. 2) Satellites have no solar cells on ends making passive thermal control easier than Option 1.	Satellite thermal control similar to that for Option 3.
Weight Differences	Weight differences due to thermal control differences cannot be determined at this time, but due to Option 1 being more difficult and relying on less surface area for passive control thicker skins and larger conductive paths may be required than on other systems.	Surface control only -- no weight penalty.	Surface control only -- no weight penalty.	Surface control only -- no weight penalty.
System Weight Difference with Respect to Option 3.	SAME	SAME	SAME	SAME

Table 7

THERMAL CONTROL DIFFERENCES

Factor	Option 1 No Reorientation	Option 2 No Reorientation	Option 3 Pallet Reorientation	Option 4 Separate Satellites
	There is no discernable difference between the hardware and test costs for all options. The analytical costs for this option may be about 500 manhours and 5 computer hours more than the satellite analyses for the other options. Cost difference = $10,000 with respect to Options 2 and 4		A pallet thermal control analysis may cost about 800 manhours and 7 computer hours or about $20,000 with respect to options 1, 2 and 4	
System Cost Difference with Respect to Option 3	-$10,000 (Development Cost)	-$20,000 (Development Cost)	--	-$20,000 (Development Cost)

Table 8

SUMMARY OF WEIGHT, COST AND RELIABILITY DIFFERENCES

Factor	Option 1 No Reorientation	Option 2 No Reorientation	Option 3 Pallet Reorientation	Option 4 Separate Satellites
System Weight Difference with Respect to Option 3	~+ 5 lb	-15 lb	--	~ +25 lb
System Cost Difference with Respect to Option 3	~ -$5,000 (production cost) ~ -$400,000 (development cost)	-$40,000 (production) -$415,000 (development cost)	--	~ +$35,000 (production) ~ +$60,000 (development)
System Reliability Difference with Respect to Option 3	0.5% more reliable	0.5% more reliable	--	4.5% less reliable

Appendix II

SCIENTIFIC IMPLICATIONS ON SPACECRAFT REQUIREMENTS

1.0 INTRODUCTION

A brief discussion of Space-General's understanding of the scientific goals of the Multiple Satellite Mission and the implication of these goals on the spacecraft requirements is presented. In the following paragraphs, the goals are briefly stated; candidate instruments and experiments which have been suggested to achieve these science goals are discussed; implications of the natural phenomena and instrument limitations on spacecraft requirements are investigated; comparisons are made of the scientific capability of the three alternative mission options; and a tentative recommendation of spacecraft and instrument requirements are defined.

2.0 SCIENTIFIC GOALS

The scientific goal of the Multiple Satellite Program is the detailed examination of the interaction of the solar wind and interplanetary magnetic field with the geomagnetic field. Of special interest is the investigation of the plasma discontinuities resulting from the nonuniformity in the emission of the solar wind and variation in the interplanetary magnetic field, such as are associated with solar flares and sun-spot activity. The two basic goals then are to understand (a) the structure of the plasma discontinuities and (b) their interaction with the geomagnetic field. To accomplish these goals the objectives of the multiple satellite experiments are twofold:

(1) to measure the propagation direction and speed of solar wind disturbance fronts in the transition region of the magnetosheath and beyond the magnetosphere;

(2) to derive data permitting temporal and spacial variations in the solar wind to be separately identified.

3.0 EXPERIMENTS AND INSTRUMENTS

Multiple satellites are required to achieve the two scientific objectives. Since three satellites always constitute a plane and a noncoplanar array is required to detect randomly directed disturbance waves, a minimum of four satellites are required. The separation distance requirement of the satellites must be determined

from (a) the need to measure the disturbance propagation with reasonable accuracy and (b) the need to establish spacial gradients so that temporal and spacial variations can be separated. The separation distance requirements to satisfy the first requirement are a function of the disturbance propagation velocity and the instrument response time. The separation distance to satisfy the second requirement is a function of the spacial variation of the plasma and magnetic field and the instrument response time which causes data "smearing" due to the satellite's motion through the media. These may pose conflicting requirements on the separation distance. In this section the natural phenomena and potential instrument characteristics pertinent to the specification of spacecraft requirements are presented.

The relative propagation velocity in the medium is expected to range from 100 to 1000 km/sec. The lower end of this range is expected to occur most frequently and hence is of most immediate interest. The relative propagation velocity is superimposed vectorially on the velocity of the solar wind. Since directions are random, this superposition may add or subtract from the magnitude of the solar wind which is in the range of 300 to 700 km/sec.

The instrument response times are currently understood to be as follows. The Ames plasma probe, as used on Pioneer, has a total response time of about 60 seconds. This includes complete sampling at various energy levels and in the azimuthal and polar planes. This response time could probably be reduced to 25 seconds by reducing the number of energy levels. As will be shown in the following section, this overall response time is orders of magnitude too large for use in determining the disturbance propagation velocity. Two instruments which were included in "Final Proposal for a Multi-Instrument Investigation of Interplanetary Plasma for the 1971 Voyager Mission Technical Section" by Ames Research Center merit consideration. These are the velocity detector and the ion flux detector. They have response times capable of producing one measurement every 0.1 second. The velocity detector determines the peak E/Q value of the primary peak in the ion E/Q spectrum. The ion flux detector measures the total current density carried by the positive particles in the solar wind. Other data on the instruments, including weights, power requirements and bits/sample are given in Table 1. The implication on the spacecraft requirement of the natural phenomena and the instruments, specifically their response times, weights and data rates are presented in the following section.

Table 1

INSTRUMENT CHARACTERISTICS

Instrument	Weight (Lb)	Power Reqmt (Watts)	View Field	Bits/Sample	Minimum Sample Time (Sec)
1. Ames Magnetometer*				30	≈0.1(?)
A-IMP	4.7	.710 avg. 2.7 peak			
Pioneer C & D	6.5	3.0 avg. 6.9 peak			
2. Ames Plasma Probe	6.3	3.0 avg. 3.5 max.	$160^\circ \times 40^\circ$	***azimuth scan-179bps polar scan-136bps max. flux scan-17bps	25
3. Peak Ion Velocity Detector	3.0**	1.8 avg. 2.1 peak	$120^\circ \times 10^\circ$	16	0.1
4. Ion Flux Detector	2.5	0.5 avg. & peak	$30^\circ \times 30^\circ$	8	0.1

* Weight and power data obtained from Dr. Miatech, 10-25-66.

** Weight estimate by R. Silva, 10-24-66.

***Az & polar scans are alternated on Pioneer max. flux scan used only at low data rates.

4.0 IMPLICATIONS OF THE SCIENCE AND INSTRUMENTS ON THE SPACECRAFT REQUIREMENTS

4.1 SATELLITE SEPARATION DISTANCES

4.1.1 DISTURBANCE PROPAGATION VELOCITY EFFECTS

The total propagation velocity will presumably be determined from knowledge of the distances between pairs of satellites and measurements of the differences in the times of front passage. The relative propagation velocity vector would then be derived by subtracting the solar wind velocity vector (which can be obtained directly from the Ames plasma probe).

If the direction of the total propagation velocity was known to be confined to a limited range, consideration might be given to the possibility of arranging the satellite separation distances to best accommodate the prevailing direction; e.g., using greater separation distances in line with the anticipated direction. Beyond the transition region, the propagation velocity can be expected to lie close to the sun line; however, present knowledge and theory indicates no such restriction on the direction of propagation in the transition region. This region is of great interest for the multiple satellite experiments. Accordingly, it is assumed that the system should be designed to achieve at least a minimum degree of accuracy in measuring the propagation velocity for any direction of propagation. It appears that velocity measurements having errors much greater than 100 km/sec. would be of relatively little value, since the propagation velocity can be of that order. Hopefully, the errors can be kept to this order or substantially smaller.

To simplify the assessment of the timing accuracy necessary to achieve the desired accuracy in velocity measurement, the case will be considered where the propagation velocity, V, is in line with the separation distance, D, between a pair of satellites which are taken to be stationary. The time between passage is then given by:

$$T = \frac{D}{V} \tag{1}$$

If ΔT is the error in measuring T, the measured velocity V_M is given by:

$$V_M = V + \Delta V = \frac{D}{T + \Delta T}$$

where ΔV is the error in the velocity measurement. The above expression assumes no error in the knowledge of D, which is a reasonable assumption, since errors in D are of the order of meters while the timing and velocity errors are orders of magnitude

larger. Solving for ΔV and noting that $V = \frac{D}{T}$ yields:

$$\Delta V = \frac{D}{T + \Delta T} - \frac{D}{T} = V \left(\frac{1}{1 + \frac{V\Delta T}{D}} - 1 \right)$$

Clearly, if ΔT is nearly equal to or greater than T, while it may be possible to establish a lower bound for the velocity magnitude, no meaningful quantitive evaluation would be possible. When $\Delta T << T$, differentiation of Equation (1) yields:

$$\Delta V = \frac{-D}{T^2} \Delta T$$

or

$$\Delta V = \frac{-V^2}{D} \Delta T \qquad (2)$$

The velocity error is then proportional to the timing error and increases with the square of the velocity and decreases in inverse proportion to the satellite separation distances.

The velocity error incurred in consequence of timing errors from .01 to 1.0 second for a separation distance from 50 to 5000 km and a range of velocities in the region of interest are listed in Table 2. These results indicate the maximum allowable values of ΔT, as a function of separation distance, would be as follows:

Separation Distance	Maximum Allowable Timing Error
50 km	.01 sec.
500 km	.1 sec.
5000 km	1.0 sec.

The timing errors listed are shared between satellite pairs. Therefore, if each satellite had the timing error shown, the separation distance should be increased by a factor of $\sqrt{2}$ times the separation distance listed.

When the direction of propagation is not in line with the separation distance, the transit time would be decreased and hence the "apparent" velocity of propagation would be increased. However, with the use of four noncoplanar satellites the accuracy of the velocity measurement would be affected mainly by the available separation distances in the direction of propagation and would not be degraded if one or two pairs of satellites are perpendicular to the velocity vector; i.e., in line with the front.

Increasing the separation distances may present some technical problems. Large separation distances in the direction of the orbit could be attained with small separation velocities by changing orbital periods and waiting for the difference in phase to build up, but the large separation distances normal to the orbit, either in-plane or out-of-plane, can only be attained by applying large velocity increments. Separation distances of 50 km can be attained with velocity increments in the order of 1 m/sec; 500 km separation distances would require velocity increments in the order of 10 m/sec; while 5000 km separation distances would require velocity increments in the order of 100 m/sec. Velocity increments in the order of 1 m/sec. can be readily generated by springs. Increments in the order of 100 m/sec. could not practicably be attained with springs and may require the use of small solid rockets. Along with increases in magnitude of the required velocity increments, greater accuracy in the direction of the increments would be necessary to avoid excessive changes in orbital period and perigee attitude. Also, with increased velocity increments complications may arise from second order effects that would otherwise be negligible. If it were necessary to initially separate the satellites over distances as great or greater than 5000 km, the concept of deployment from a single booster would be open to some question, since this is approaching the regime where it would be possible to achieve reasonably accurate intersatellite separation distances with separate launches.

From the above discussion it is obvious that the timing error should be made as small as possible. The timing errors which can be achieved by the satellite are a function of the instrument response time and the satellite spin rate. The Ames plasma probe has an overall response time capability of about 25 seconds, which is orders of magnitude too large for reasonable separation distances. Obviously, a drastic reduction in the data to be collected and/or a drastic increase in the speed of data collection is required. The question then arises as to whether these problems could be mitigated by using separate instruments (a) to detect passage of the front and (b) to measure the details of the condition prior and subsequent to the front passage. In addition to magnetometer readings, which would detect several but not all types of discontinuities, some particle measurements would be necessary. Instruments 3 and 4 (Table 1) or modifications of them, could provide the required plasma data. These instruments are capable of sampling every 0.1 second, but they do so only in a direction defined by the spacecraft spin rate and their view field. For instance, if one set of instruments is used, the sampling of a given direction will be a direct function of the spin rate and therefore the spin rate determines the timing error.

Table 2

EFFECT OF TIMING ERRORS ON MEASUREMENT OF PROPAGATION VELOCITIES

D = 5000 km

V km/sec	T sec	ΔT = +10 sec ΔV km/sec	-10 sec ΔV km/sec	ΔT = +1 sec ΔV km/sec	-1 sec ΔV km/sec	ΔT = +.1 sec ΔV km/sec	-.1 sec ΔV km/sec	ΔT = +.01 sec ΔV km/sec	-.01 sec ΔV km/sec
200	25.0	-57	+133	-8	+8	-1	+1	-.1	+.1
400	12.5	-178	+1600	-30	+35	-3	+3	-.3	+.3
600	8.3	--	--	-62	+85	-7	+7	-.7	+.7
800	6.25	--	--	-110	+152	-13	+13	-1	+1
1000	5.0	--	--	-167	+250	-20	+20	-2	+2

D = 500 km

V km/sec	T sec	ΔT = +10 sec ΔV km/sec	-10 sec ΔV km/sec	ΔT = +1 sec ΔV km/sec	-1 sec ΔV km/sec	ΔT = +.1 sec ΔV km/sec	-.1 sec ΔV km/sec	ΔT = +.01 sec ΔV km/sec	-.01 sec ΔV km/sec
200	2.5	--	--	-57	+133	-8	+8	-1	+1
400	1.25	--	--	-178	+1600	-30	+35	-3	+3
600	.83	--	--	--	--	-62	+85	-7	+7
800	.625	--	--	--	--	-110	+152	-13	+13
1000	.50	--	--	--	--	-167	+250	-20	+20

D = 50 km

V km/sec	T sec	ΔT = 10 sec ΔV km/sec	-10 sec ΔV km/sec	ΔT = +1 sec ΔV km/sec	-1 sec ΔV km/sec	ΔT = .1 sec ΔV km/sec	-.1 sec ΔV km/sec	ΔT = .01 sec ΔV km/sec	-.01 sec ΔV km/sec
200	.25	--	--	--	--	-57	+133	-8	+8
400	.125	--	--	--	--	-178	+1600	-30	+35
600	.083	--	--	--	--	--	--	-62	+85
800	.0625	--	--	--	--	--	--	-110	+152
1000	.0500	--	--	--	--	--	--	-167	+250

D = Distance between satellites

V = Velocity of propagation

T = Transit time between satellites

ΔT = Error in measuring Transit Time

ΔV = Error in measuring propagation velocity

-- = Indicates that no meaningful measurement of propagation velocity is made.

The timing error for various numbers of instruments and spin rates is as follows:

Timing Error

No. of Instr. \ Spin Rate (rps)	1	2
1	1	0.5
2	0.5	0.25
3	0.33	0.167

The timing error is also a function of the instrument viewing angle. In the extreme case, the speed of detection could be made independent of spin rate by using enough sensors with sufficient view fields to cover a solid angle. In this case the speed of detection would be limited mainly by the sensor's response which is in the order of 0.1 second. The above table of timing errors assumes that the view field is less than 360°.

From the above table, it can be seen that three instruments and a spin rate of 2 rps could still require separation distances of the order of 1000 km. Spin rates in excess of about 1-1/2 rps would result in satellite spin-up requirements, since the TAID third stage booster spin rate is 140 rpm, which provides for a satellite spin rate of about 90 rpm with the booms extended. Also, multiple instruments will result in excessive instrument weights and powers, if the weights and powers given in Table 1 are correct.

As a compromise, two sets of instruments (3 and 4 in Table 1) and a spin rate of 1-1/2 rps might be selected with a corresponding separation distance of about 2500 km. This would allow measurement of the net velocity to an accuracy which would provide an indication of the disturbance velocity. The separation distance defined is based on assuming a step function for the disturbance. If the disturbance is not a step function, different separation distances are indicated. For example, if the disturbance has high frequency oscillations superimposed on it or has spectral components which are dispersed in time, they will never be discovered with the specified separation distances and timing errors. If the disturbances has a slow rise time, rather than being step-like, larger separation distances would be required.

4.1.2 SPACIAL SEPARATION CONSIDERATIONS

The expected variation of the plasma parameters, particularly in the transition region, should also be considered in the selection of the satellite separation distances. Figures 1-4 are reproductions from Reference (1) by Spreiter,

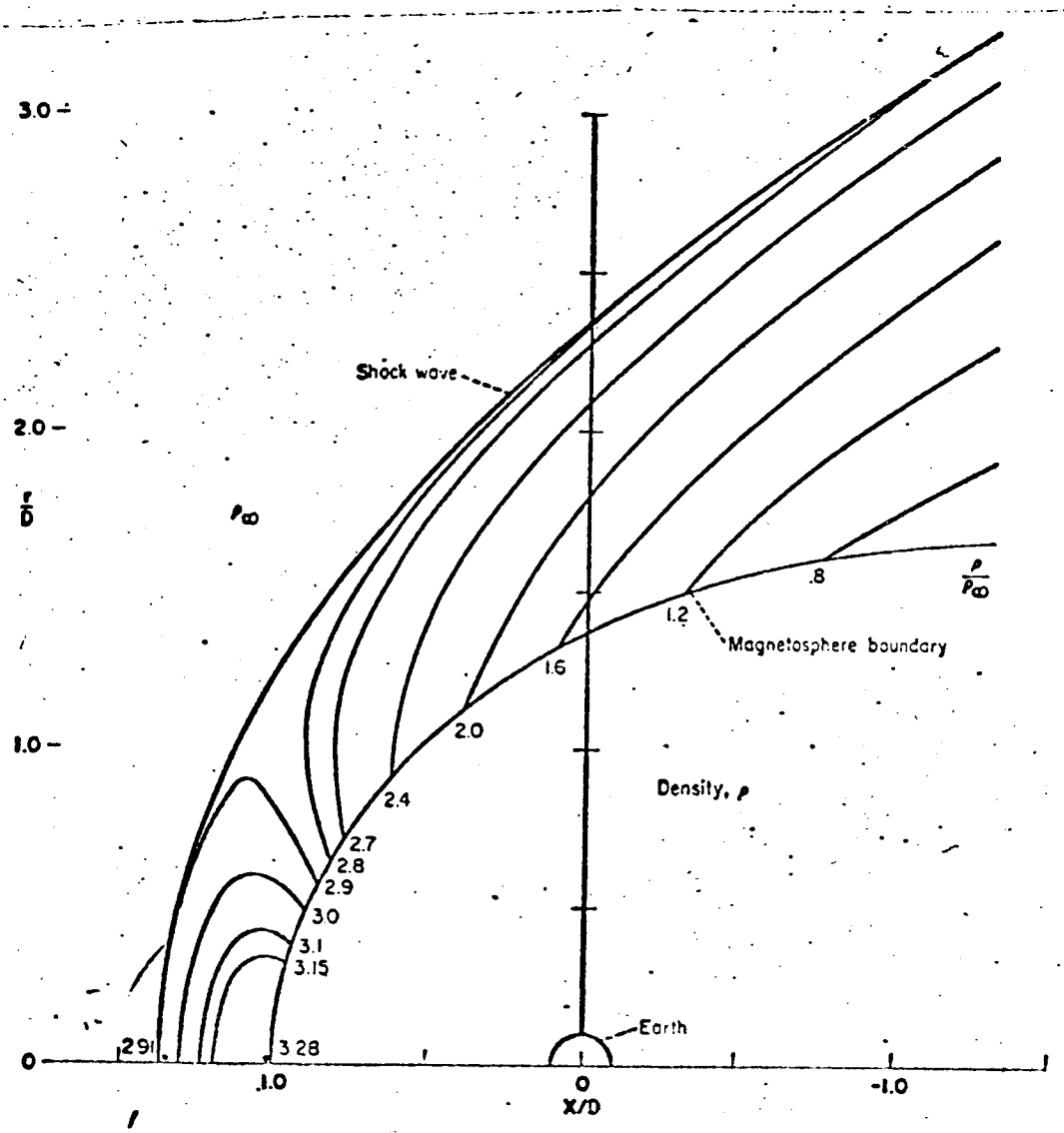

FIG. 6. DENSITY CONTOURS FOR SUPERSONIC FLOW PAST THE MAGNETOSPHERE; $M_\infty = 8, \gamma = 2$.

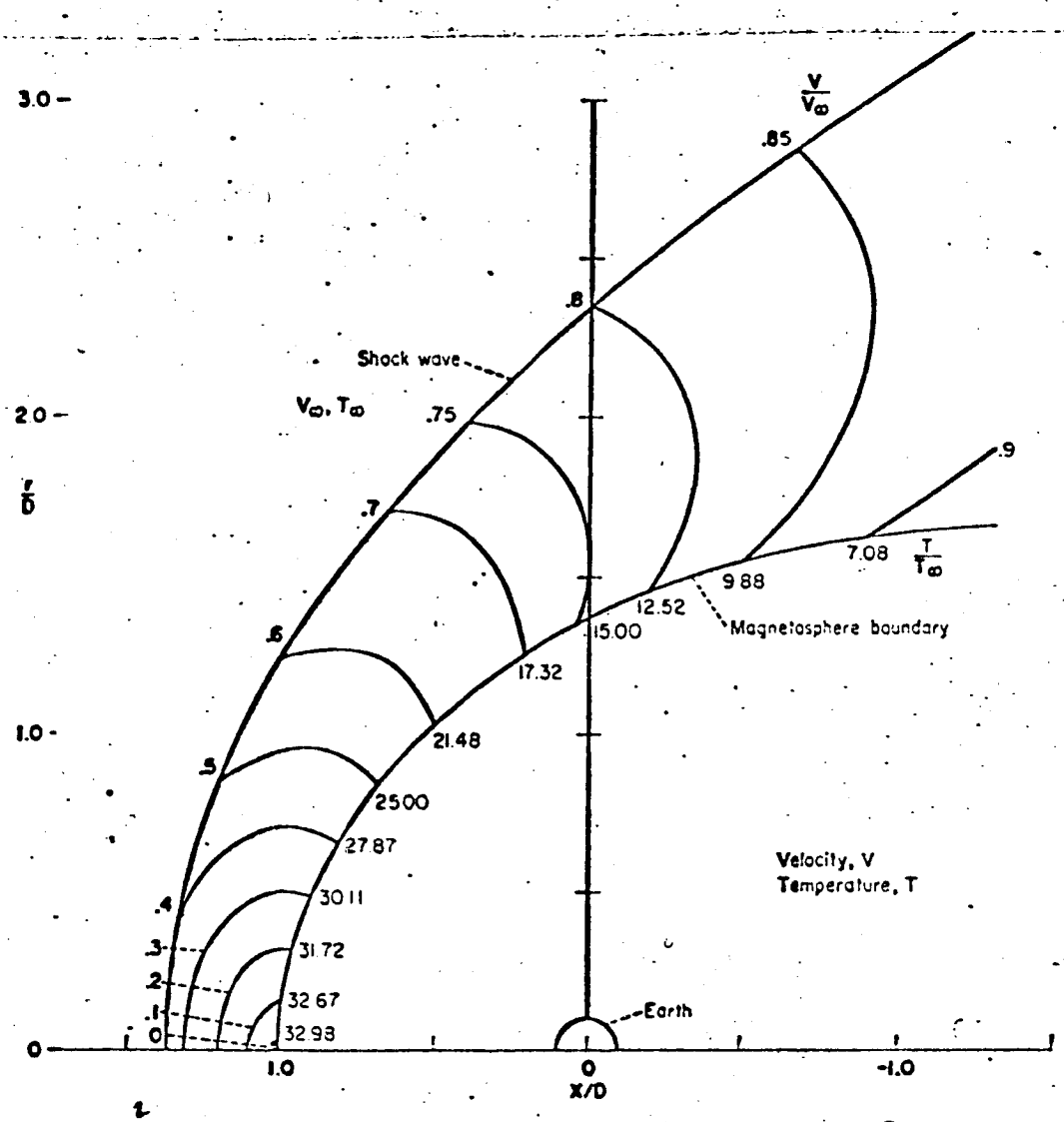

FIG. 7. VELOCITY AND TEMPERATURE CONTOURS FOR SUPERSONIC FLOW PAST THE MAGNETOSPHERE; $M_\infty = 8, \gamma = 2$.

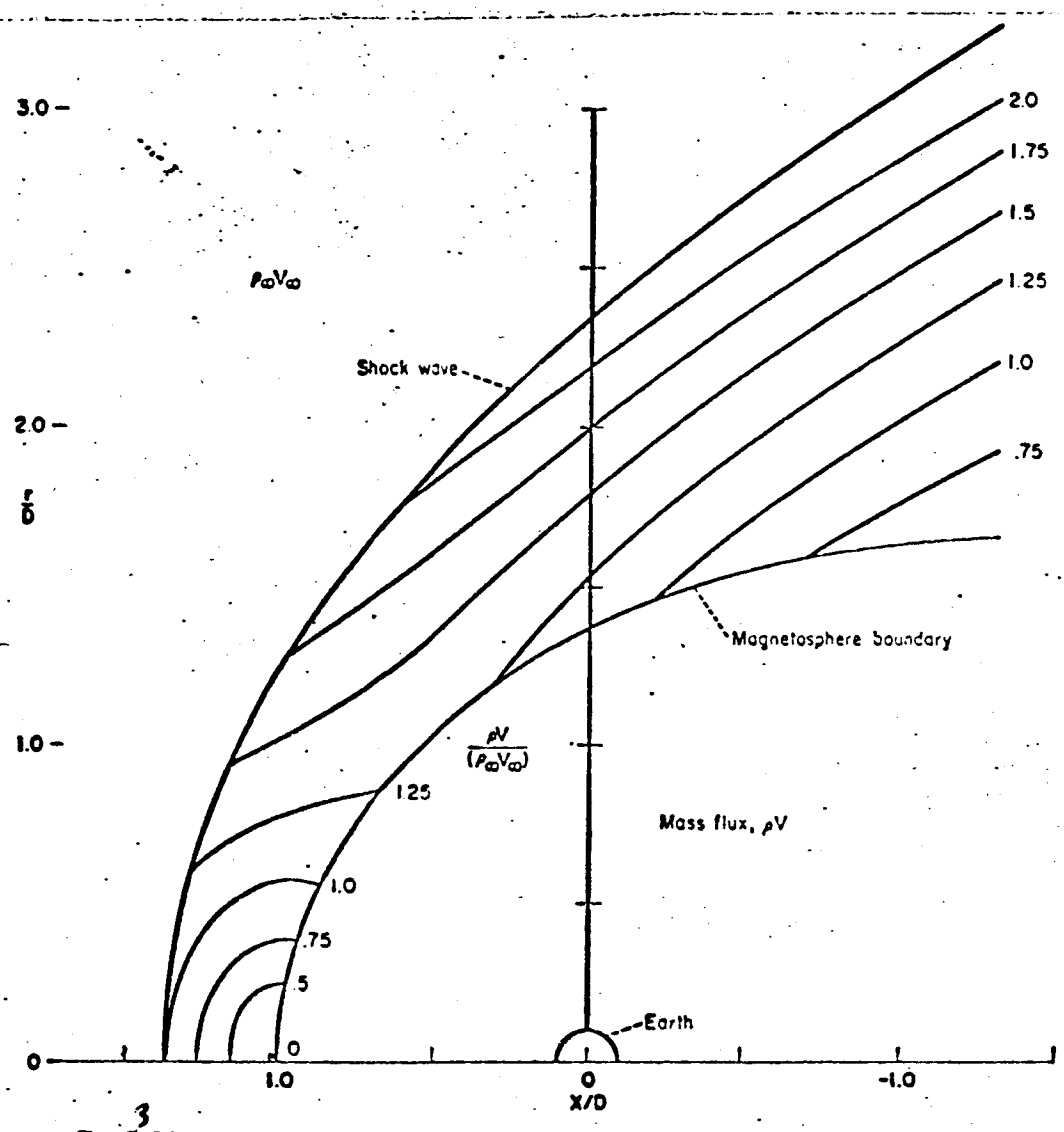

FIG. 8. MASS FLUX CONTOURS FOR SUPERSONIC FLOW PAST THE MAGNETOSPHERE; $M_\infty = 8, \gamma = 2$

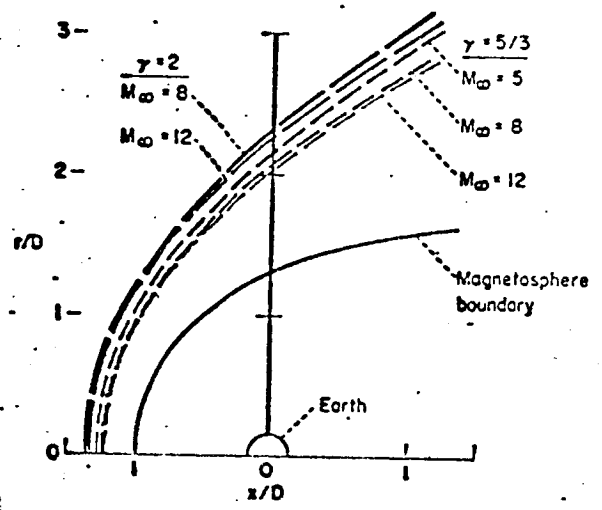

FIG. 13. POSITION OF BOW SHOCK WAVE FOR VARIOUS M_∞ AND γ.

Summers and Alksne. These are theoretical representations of the parametric changes within the transition region. Although these are purely theoretically derived and may be subject to error when the region is viewed empirically, they can provide a means for establishing desired spacing of the satellite. If the magnetosphere boundary is assumed to occur, on the average, at 10 R_e, then the transition region thickness may be assumed to be 2.5 to 4.0 R_e at the earth-sun line. In order to get reasonable resolution within this region, without being so close together that no spacial effects are measured, the satellites should be spaced about 2000 km apart along the earth-sun line. This is about 10% of the transition region thickness, and thus about 10% of the total variation in the transition region along the earth-sun line will be detected by two satellites thus separated. Note that this estimate does not consider the possible effect of "fine structure" plasma turbulence in the transition region; no specific data on the existence or characteristics of phenomena were readily available. The satellite separation distance normal to the earth-sun line, both in the ecliptic plane and normal to it, should be larger than along the earth-sun line in order to detect a comparable change in plasma parameters. A separation of about 3000 km would be more appropriate in this case. These values are comparable to that required by the timing consideration.

The satellites' velocities may also enter significantly into the problems associated with obtaining spacial derivatives. Here what would be desired would be simultaneous measurements of the physical variables. The satellites are, of course, not stationary, but are moving with substantial velocities. With apogee at 20 earth radii, the satellites' velocities with respect to an earth fixed frame would be about 10 km/sec. at perigee; 2.5 km/sec. near 10 earth radii; and about .5 km/sec. near 20 earth radii (apogee). With respect to an inertially fixed frame, the 30 km/sec. velocity of the earth in its rotation about the sun must be added.

Presumably, each of the satellites' systems will be operating asynchronously with respect to the others so that the measurement of a physical variable by one satellite can be separated in time from the measurement of the same variable by another satellite by an interval as large as 1/2 the period of the commutation cycle (this assumes one set of instruments). If the instrument measurement 1/2 period is of the order of 30 seconds, the distance between the points of measurement would be in the order of 75 km greater than the distance if simultaneous measurements were made, when the satellites are at a radius in the region of 10 earth radii (at 10 earth radii they would have velocities of about 2.5 km/sec.). If two sets of instruments and a spin

rate of 2 rps were used, this error would be reduced by a factor of 4 to less than 20 km, which is less than 1% of the desired separation distance as stated above. In inertial coordinates this shift would be 225 km, which is about 10% of the desired separation distance. Interpolation of measurements to obtain estimates of simultaneous readings is feasible only for the lower frequency components of the temporal variations in the field.

Even if the satellite measurements were synchronous to the extent that the measurements of different components are separated in time, the spacial derivatives will be separated in space.

Clearly, to have fine resolution in the definition of the spacial variation of the derivatives will require that data be obtained as rapidly as possible. If the spacial derivatives of many physical variables is desired, this would call for high data rates.

4.2 SPIN RATE

Based upon previous discussions, it becomes clear that the higher the spin rate the lower will be the timing error and the smaller the satellite separation distance. Based upon a no spin-up requirement, 1-1/2 rps is the maximum allowable spin rate. If spin-up is not considered detrimental, acceleration load limits will allow higher spin rates.

4.3 DATA RATE, POWER AND INSTRUMENT WEIGHT

Assuming 1 Ames magnetometer, 1 Ames plasma probe, 2 peak ion velocity detectors and 2 ion flux detectors and a spin rate of 2 rps, currently available information suggests that the data rate would be:

Ames magnetometer	300 bit/sec.
Ames plasma probe	300
Peak ion velocity detector	320
Ion flux detector	160
Total	1,080

Adding syncwords, engineering and attitude data could increase this to about 1500 b/sec. This is not an unreasonable increase over the original 1100 b/sec. specified and may be considered a maximum for all cases of interest.

The suggested instrument complement does present weight and power problems, however, If the values in Table 1 are used (assuming the A-IMP magnetometer), the instrument weight and power requirements are 22.0 pounds and 8.3 watts average, respectively. These values, particularly the weight, must be reduced to make this combination of instruments acceptable.

5.0 ORBIT CONSIDERATIONS

In Figure 5, three orbit orientations are shown superimposed on the mass flux contours of the transition region. The magnetosphere boundary is assumed to be at 10 earth radii. It is obvious that orbit (a), which is normal to the ecliptic, will never sample data in the vicinity of the stagnation point. This fact tends to eliminate this orbit from further consideration. This orbit represents mission Option 2 of the four mission options given in the proposal. Therefore, mission Option 2 appears to be less desirable from a scientific point of view than the other options. The choice between orbits (b) and (c), which are both inclined about 6° to the ecliptic, but tilted differently with respect to the earth-sun line, is not clear. There seems to be little change in the plasma parameters at 6° from the ecliptic so that it is not absolutely necessary for the satellites to pass through the stagnation region of the transition region (orbit (c)). Either orbit (b) or (c) may be selected, depending upon how close to the earth-sun line scientific information is desired.

Looking at the orbits in relationship to the transition region, it appears that excessive time is being spent outside the transition region if the magnetosphere boundary is at or below 10 R_e. Reduction of apogee altitude to 16 earth radii would still allow data to be taken outside the transition region, but would reduce the orbit period and hence the data storage time. Also, a modest payload increase of 10 pounds would be possible. Considering launch errors which can result in apogee variations of approximately 2 R_e, an apogee goal might be 18 R_e if the 12 R_e magnetosphere boundary is considered an appropriate upper limit. This would provide for the possibility of only a short period outside the transition region, however. If this boundary tends to move to greater than 12 R_e for a significant fraction of the time, the original 20 R_e apogee continues to be an excellent choice.

6.0 SCIENTIFIC IMPLICATIONS ON THE MISSION OPTIONS

A primary scientific difference in the mission options is in their instrument view field capability. Except for mission Option 2, which has the satellites launched into a plane substantially inclined to the eciptic, all of the mission options have orbit planes near the ecliptic. Mission 2's orbit was shown to be inferior to the other options' orbit in the previous section. The satellites of mission 1 spin with their spin axis near the ecliptic plane, while the satellites of mission 3 and 4 spin with their axes normal to the ecliptic.

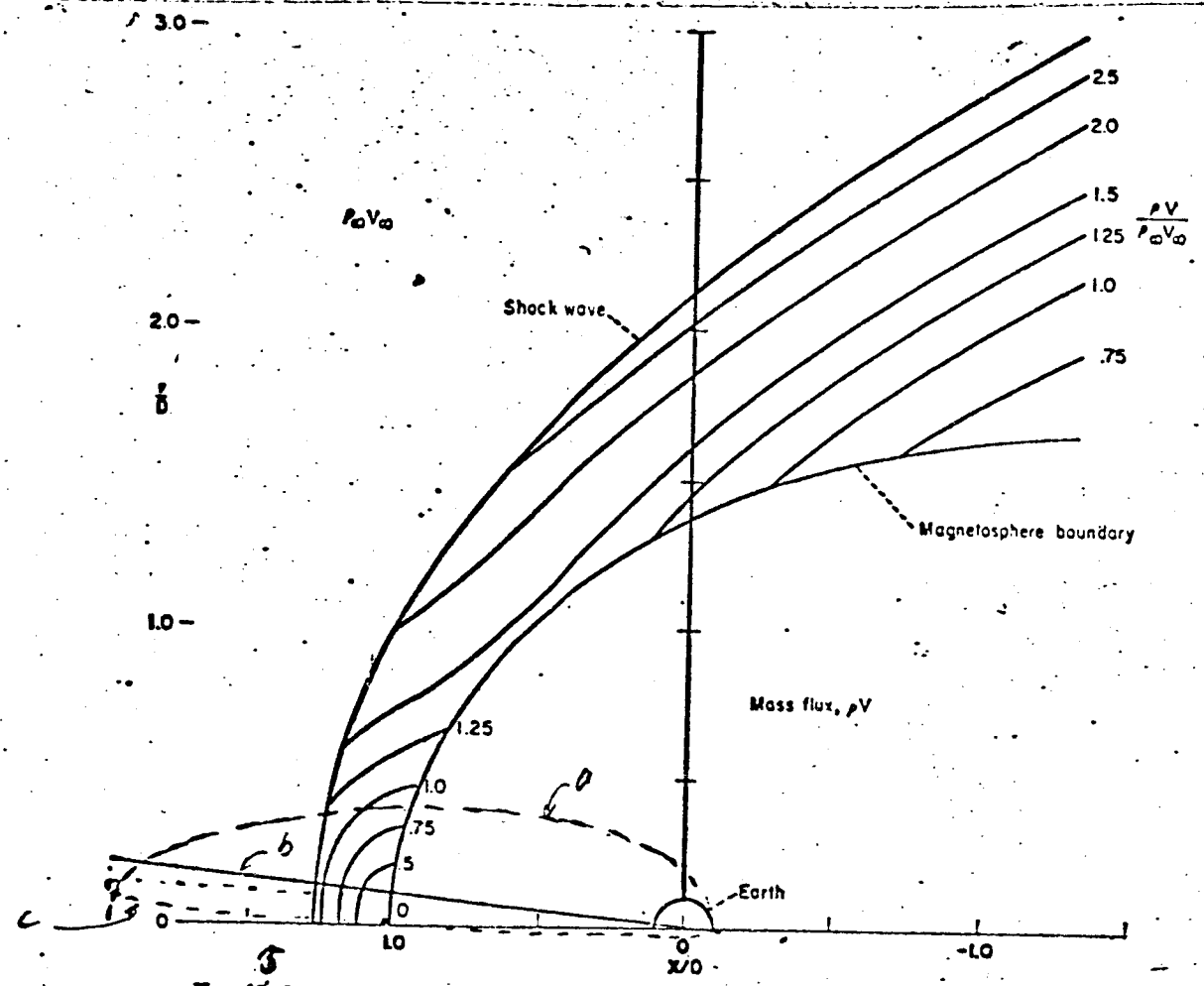

FIG. 12. MASS FLUX CONTOURS FOR SUPERSONIC FLOW PAST THE MAGNETOSPHERE; $M_\infty = 8$, $\gamma = \frac{5}{3}$.

There is no substantial difference in the viewing capability of mission Options 3 and 4. Mission Option 3 uses a pallet to achieve the spin axis perpendicular to the ecliptic, while for Option 4 the satellites separately adjust their spin axis. The orientation of the spin axis makes little difference in the magnetometer measurements and therefore the orientation of the spin axis affects only the plasma measurements.

The view fields of the plasma instruments as currently defined is as follows:

Ames plasma probe	$160^\circ \times 40^\circ$
Peak ion velocity detector	$120^\circ \times 10^\circ$*
Ion flux detector	$30^\circ \times 30^\circ$*

Outside the transition region the preferred viewing direction is sun-oriented. Within the transition region in the subsolar area, the direction of the disturbances is thought to be random and therefore no preferred direction can be established, but the sun should be within the view field.

Based on the instrument view angles and the hypothesized preferred viewing directions, the following conclusions can be drawn. Both mission Option 1 and mission Options 3 and 4 will be seriously hampered by the above view field of the ion flux detector. Mission 1, especially, will be affected, since the sun will remain in this view field little more than one month. With the above view field, the mission Option 1 would be considerably inferior to mission Options 3 and 4. Mission Options 3 and 4 can always maintain the sun within this view field, but would not be able to detect flux disturbance having directions greater than about $\pm 15^\circ$ from the ecliptic plane. This would be limiting, but not nearly so limiting as the effect of the 30° view field on mission Option 1. It is therefore highly desirable to increase the view fields of the peak ion velocity detector and ion flux detector to 160°.

If the ion flux detector view field could be increased to about 160°, then mission Option 1 would not be so seriously limited. With this view field it has been shown that the sun can always be kept within this view field by inclining the orbit plane of mission Option 1 approximately 10° to the ecliptic. However, there will be periods when the sun is viewed at the edge of the instrument's view field which means that some variation of the plasma away from the earth-sun line are not detected. Options 3 and 4 do not have this limitation, since the sun is always approximately centered in the view field.

* Discussions with R. Silva of ARC indicate that these view fields could be increased to 160°.

Based upon view field considerations only, it appears that Option 1 is inferior to Options 3 and 4. If the ratings of the options is based on a scale of 10, where 4 points are assigned if full solid angle coverage is obtained and 6 points if ± 30° from the sun is always swept out by the instrument view field during the 6-month life, then the ratings would be:

Option 1 $\frac{320}{360}(4) + \frac{5}{6}(6) = 8.5$

Options 3 and 4 $\frac{320}{360}(4) + 6 = 9.5.$

View fields of 160° were assumed for all plasma instruments in the above calculation. Both options have 5.8 steradians or 320° solid angle coverage. Options 3 and 4 always have the sun within ± 30°, but for about one month out of six, Option 1 does not meet this criteria.

Therefore, based upon view field and the above ratings, mission Option 1 is about 10% less desirable than Options 3 and 4.

There is one other scientific consideration affecting the relative merits of the three options. The satellites of Option 4 have the capability to vary the separation distance, which could be very useful considering the lack of knowledge of the phenomena to be measured. The satellites of Option 4 are heavier; however, due to the added orbit-keeping capability, this added weight could limit the scientific instrument-carrying capability. The value of the orbit keeping capability or the detriment of the added weight are not easily evaluated at this time, however,

In summary, the scientific capability of the various mission options results in the following ranking:

Scientific Ranking	Mission Option
1	4
2	3
3	1
4	2

The final ranking of the options must also be based upon program cost, reliability, and spacecraft weight.

7.0 SUMMARY OF INSTRUMENT RECOMMENDATIONS AND SPACECRAFT REQUIREMENTS

7.0 RECOMMENDED INSTRUMENTS

The following number and type of instruments or their equivalent are

recommended:

(a) one Ames magnetometer (A-IMP)

(b) one Ames plasma probe*

(c) two peak ion velocity detectors

(d) two ion flux detectors.

The weights of the instruments or their equivalent should be reduced to no more than 15 pounds with a power requirement of about 7 watts, if possible. The polar view angles on all plasma devices should be at least 160°. Response times of all instruments should be as rapid as possible. All instruments measuring the disturbance propagation should have response times of 0.1 second or less.

7.2 SPACECRAFT AND ORBIT REQUIREMENTS

The spacecraft spin rate should be at least 1.5 rps. The maximum data rate capability should be on the order of 1500 bits/sec. The orbit should be aligned as close to the ecliptic as possible. It should intersect the ecliptic at about 10 earth radii. Apogee altitudes of 16 earth radii should be considered to reduce data storage and increase payload.

The satellites should be separated by about 2000 km initially, and capability to vary this distance would be desirable. This separation distance was reviewed by NASA Ames scientists with the subsequent recommendation that a separation distance of 500 to 1000 km be specified based on the development of an integrated instrument complement.

* It has been shown that the response time of the Ames plasma probe is too long for use in measuring disturbance velocities, but it is required to measure the detailed plasma spectrum. The function of this probe may possibly be divided among the four satellites to reduce the data rate requirement and weight for each satellite.

REFERENCES:

1. Spreiter, J. R., Summers, A. L., Alksne, A. Y., "Hydromagnetic Flow Around the Magnetosphere", Planetary and Space Science, Vol. 14, No. 3, pp. 223-253.

Appendix III

PRELIMINARY EVALUATION OF OPTION 3 SEPARATION DISTANCES AND ACCURACIES

1.0 INTRODUCTION

The discussion presented in Appendix X indicates that the attainment of large intersatellite separation distances without excessive growth of the separation along the orbit will require a systems implementation of considerably increased capability. It appears that the required modifications for the alternative mission options then offer little advantage over Option 4, without offering the flexibility of Option 4 in achieving the large separation distances. Since it is clearly desirable that unnecessary complication of the Multiple Satellite system be voided, some time has been taken to define the performance that could be obtained short of recourse to a system with the full capabilities of Option 4.

Option 3 separation distance capabilities are examined in this Appendix assuming separation distance requirements of 500 to 1000 km minimum with a maximum growth not to exceed 15,000 km after six months. This preliminary analysis shows Option 3 to be capable of achieving the required separation distance.

2.0 DEFINITION OF MODIFICATION TO OPTION 3

For this purpose Options 1 and 2 have not been considered since at best they cannot yield the conditions most desired for the experiments. Hence, the main alternative to Option 4 is taken to be Option 3 with the addition of one-shot axial propulsion to the satellites to obtain large out-of-plane separation distances, but without the use of pulsed lateral thrusting to increase in-plane normal separation distances or to correct errors incurred in the tangential velocity increment which leads to growth in separation distances along the orbit.

The operational sequence assumed for this modification of Option 3 is as follows:

1. The pallet carrying the four satellites is injected into orbit by the TAID booster spinning at a rate of about 140 rpm with its spin axis close to the direction of the velocity vector at perigee.

2. Using an ACS system similar to that employed by Pioneer 6, the spin axis of the pallet is reoriented to become aligned with the direction of the normal to the orbit. This is accomplished by (a) precessing the spin axis so that the angle between the spin axis and the sunline becomes equal to the angle between the normal to the orbit and the sunline, and (b) then rotating about the sunline to align the spin axis to normal to the orbit. The first step is referenced to an ACS sun sensor; the second to an auxiliary aspect sensor.

3. After the orientation of the pallet's spin axis is confirmed, Satellite Pairs 1-2 and 3-4 are separated from the pallet by spin-off. This separation is armed by ground command and triggered by a signal from a sun sensor which is positioned so that in the nominal case the velocity increments imparted to the satellite pairs are normal to the orbit. Correction for off-nominal conditions that become known prior to separation is made by adjusting the time when the command for the spin-off separation is given.

4. After separation from the pallet the satellites are separated from their partners by axial springs with small out-of-plane velocity increments.

5. An upward-out-of-plane velocity increment is imparted to Satellite 1 and a downward out-of-plane velocity increment is applied to Satellite 2 by firing small solid rockets in the direction of the satellites' spin axes. These rockets are fired on ground command at about 20 hours from perigee to achieve large out-of-plane separation distances on the sections of the orbit from 6 to 18 R_e. Similarly out-of-plane velocity increments are applied to Satellites 3 and 4. The time of the out-of-plane separations is adjusted to take account of known off-nominal conditions.

3.0 NOMINAL PERFORMANCE

Consideration of the TAID spin-up capability and the probable inertia of the Multiple Satellite Payload indicates that the pallet's spin rate will be about 140 rpm. Consideration of the available envelope indicates that the lateral distance from the centers of mass of the satellite pairs to the pallet's spin axis will be about 1/2 meter. A spin-off separation at 140 rpm from a 1/2 meter arm will impart a velocity increment of about 7.3 meters/sec to each of the satellite pairs. Since the two pairs are spun-off in opposite directions the differential velocity increment would be about 14.7 meters/sec.

In Appendix X a nominal time for application of the in-plane normal velocity increment at 18 hours after perigee was considered to be desirable for a one part deployment in that it provides large in-plane normal separation distances in the region of 10 R_e on both sides of the orbit and is close to optimum with respect to minimization of the accuracy requirements associated with the attainment of an in-plane normal separation distance of specified magnitude.

An in-plane normal differential velocity increment of 14.7 meters/sec applied at 18 hours after perigee would produce in-plane normal separation distances of about 500 km at 10 R_e on both legs of the orbit. In addition to falling far short of the desired separation distance of 1,500 km the pattern of separation distance at larger distances from the earth obtained with this time of application of the in-plane normal velocity increment would be undesirable. It is noted in Figure A that the in-plane normal separation distances for this time of application falls off sharply above 15 R_e. The transition region may extend to 16 R_e along the subsolar line and to even greater distances at angles to the sunline. Hence it is apparent that relatively poor coverage would be obtained with respect to the measurement of the velocities of propagation beyond the transition region.

Larger in-plane normal separation distances in the 15 to 20 R_e region, as well as in the 10 to 15 R_e region on the descending leg of the orbit, could be obtained by an earlier application of the velocity increment, at the expense of smaller in-normal separation distances in the 10 to 15 R_e region on the ascending leg of the orbit and increased sensitivity to errors in the direction of the velocity increment (see Table 1). Since one of the main drawbacks of Option 3 is the

CLEARPRINT PAPER CO. NO. 539X MILLIMETERS 200 BY 250 DIVISIONS PRINTED IN U.S.A. ON CLEARPRINT TECHNICAL PAPER NO. 1015

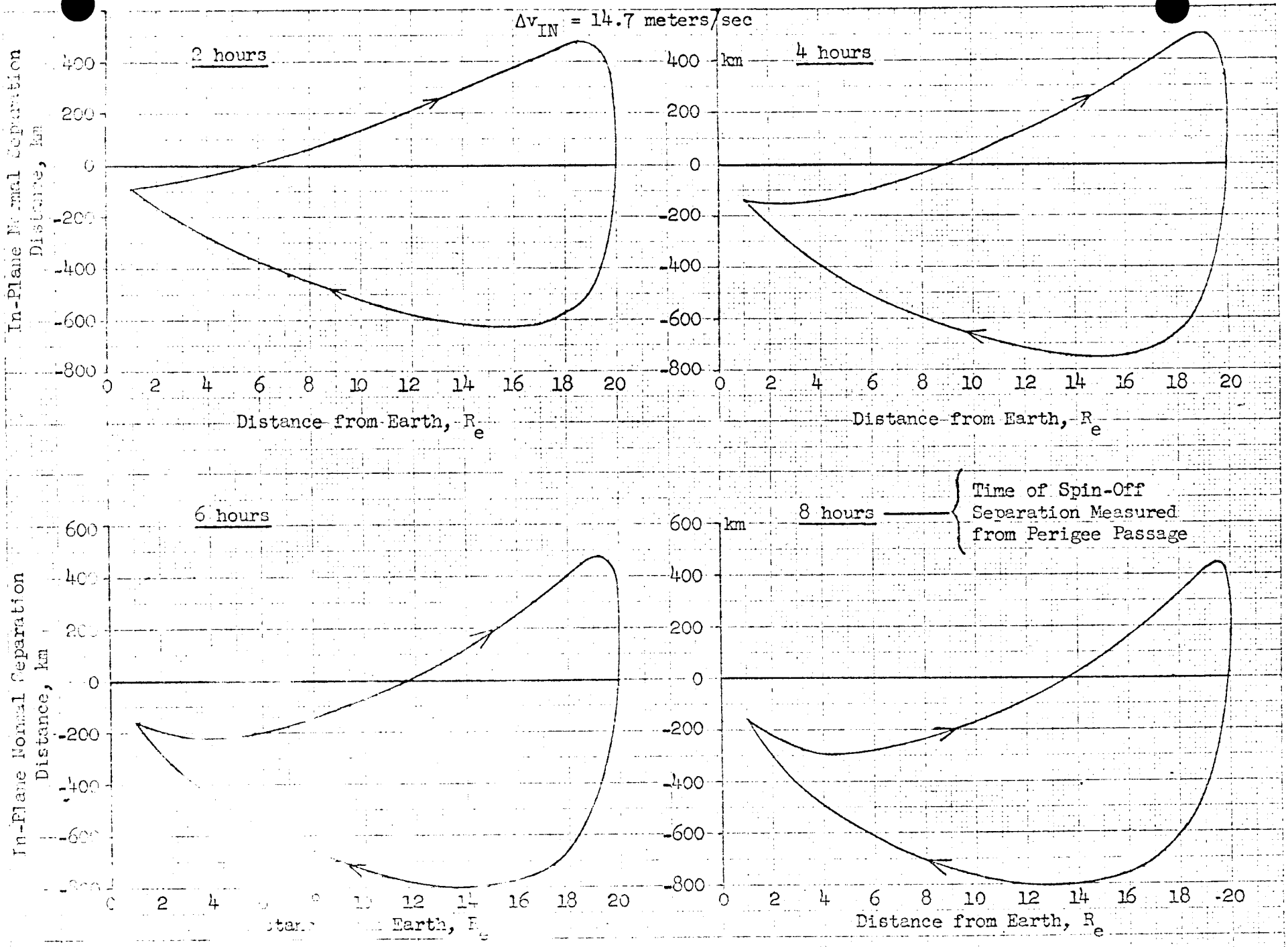

FIGURE A. VARIATION OF IN-PLANE NORMAL SEPARATION DISTANCE WITH DISTANCE FROM CENTER OF EARTH OBTAINED FOR VARIOUS TIMES OF APPLICATION OF THE SPIN-OFF VELOCITY INCREMENT

CLEARPRINT PAPER CO. NO. C39X MILLIMETERS, 200 BY 250 DIVISIONS. PRINTED IN U.S.A. BY CLEARPRINT TECHNICAL PAPER NO. 1015

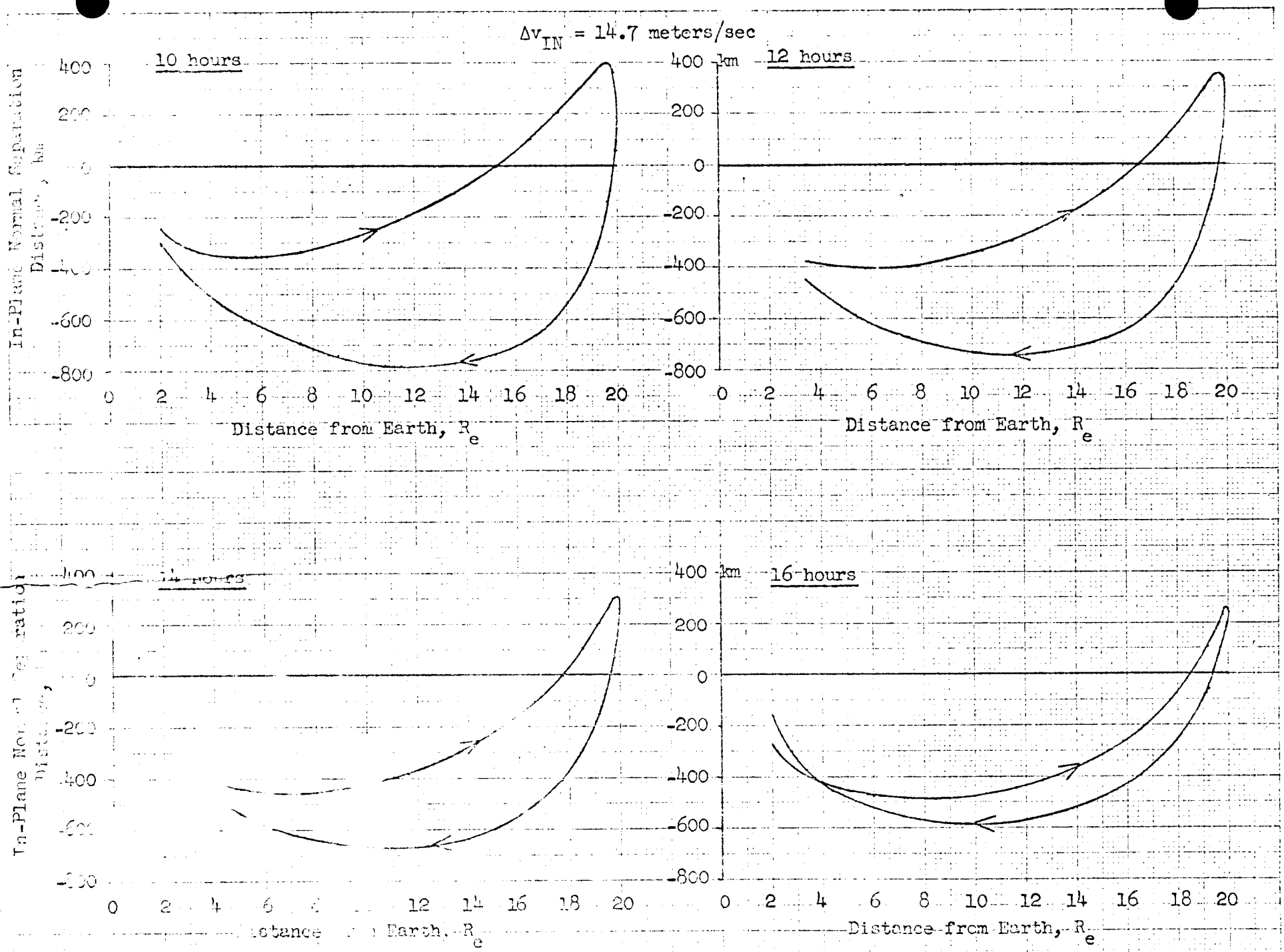

FIGURE A (Continued)

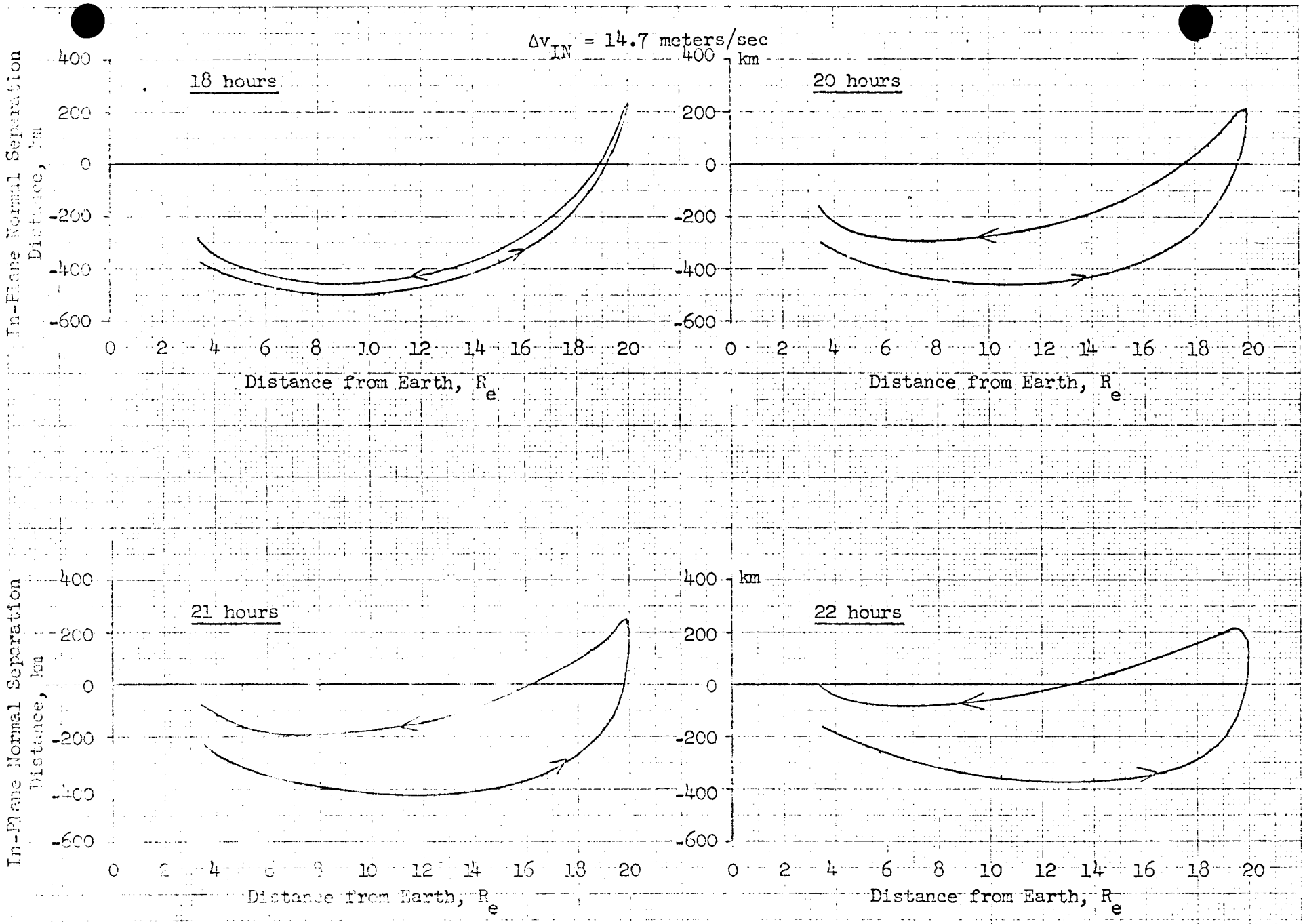

FIGURE A (Continued)

CLEARPRINT PAPER CO. NO. C39X MILLIMETERS 200 BY 250 DIVISIONS PRINTED IN U.S.A. ON CLEARPRINT TECHNICAL PAPER NO. 1015

Δv_{IN} = 14.7 meters/sec

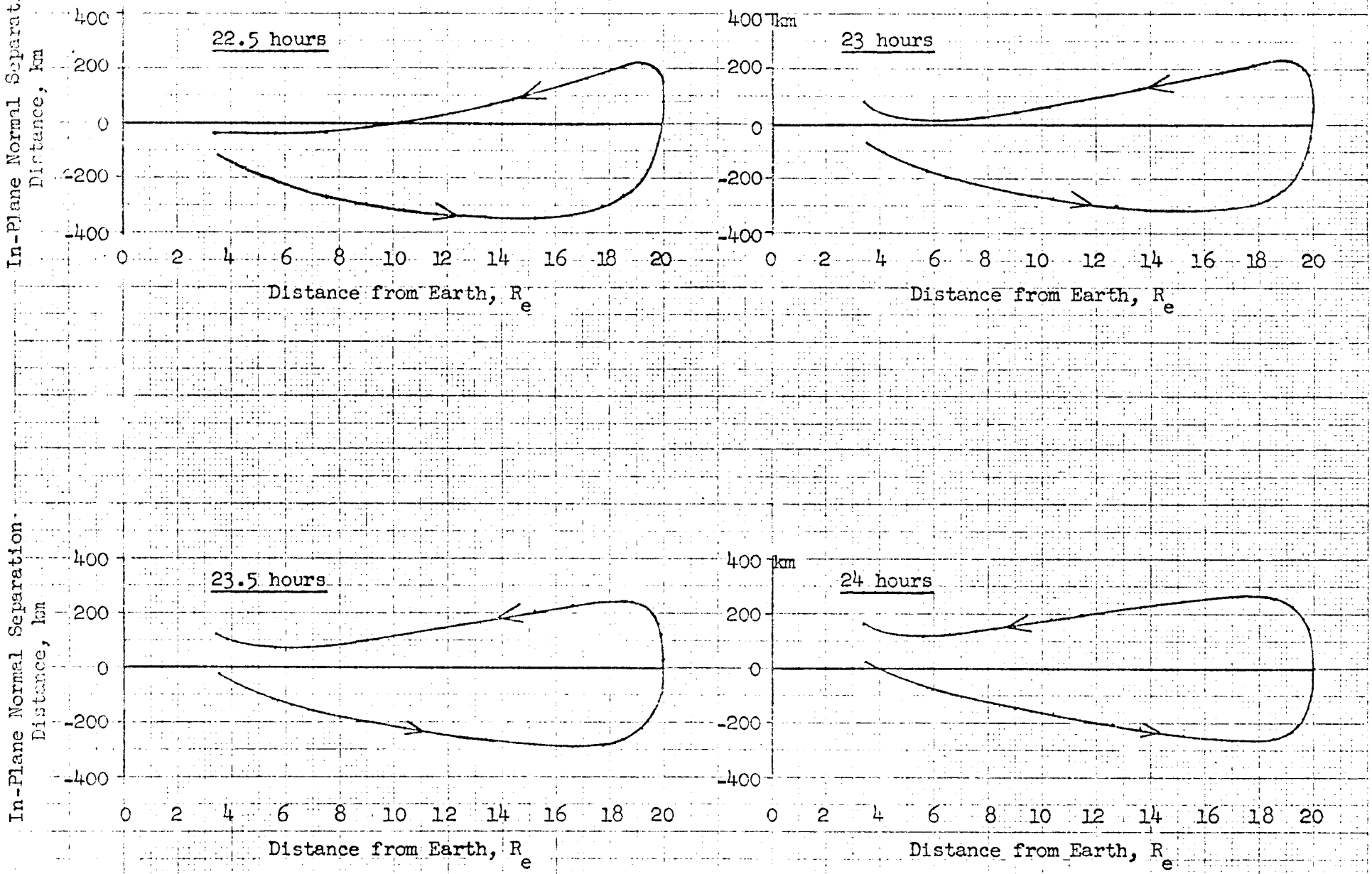

FIGURE A (Continued)

an orbit-fixed reference frame as depicted in Figure A. In this frame the x-coordinate is along the line of apsides positive toward apogee, the z-coordinate is in the direction of the normal to the orbit, positive in the sense of the orbital rotation, the y coordinate is in-plane, normal to x, to form a right-handed set.

Although some interest may be attached to the relationship of the inter-satellite separation distances to the ecliptic plane, it is noted that: the non-coplanarity of the separation distances is independent of the reference frame; the separation distances expressed in the orbital frame can be converted to an ecliptic reference frame through an orthogonal transformation; when the inclination to the ecliptic is very small, the distances given in the orbital frame are closely related to those given in an ecliptic frame.

The use of the orbital reference frame for consideration of the separation distances permits the effects of the components of deployment velocity increments on the component of the separation distances to be more simply stated and visualized. For example, it is clear that in the orbital frame, an in-plane deployment velocity increment will affect only the in-plane components of the separation distances.

It is assumed that the deployment velocity increments will be small relative to the orbital velocity, so that linear approximations are adequate. This permits separate consideration to be given to the effects of the three components of the velocity increments, and the total effect of a given velocity increment vector to be obtained by the superposition of the component effects.

It is convenient to resolve the velocity increment as follows:

Δv_T : in-plane component parallel to the orbital velocity

Δv_{IN}: in-plane component perpendicular to the orbital velocity (positive inward)

Δv_{ON}: out-of-plane component perpendicular to the orbital velocity, i.e., component along the normal to the orbit, positive in the + z direction

These definitions are illustrated in Figure A.

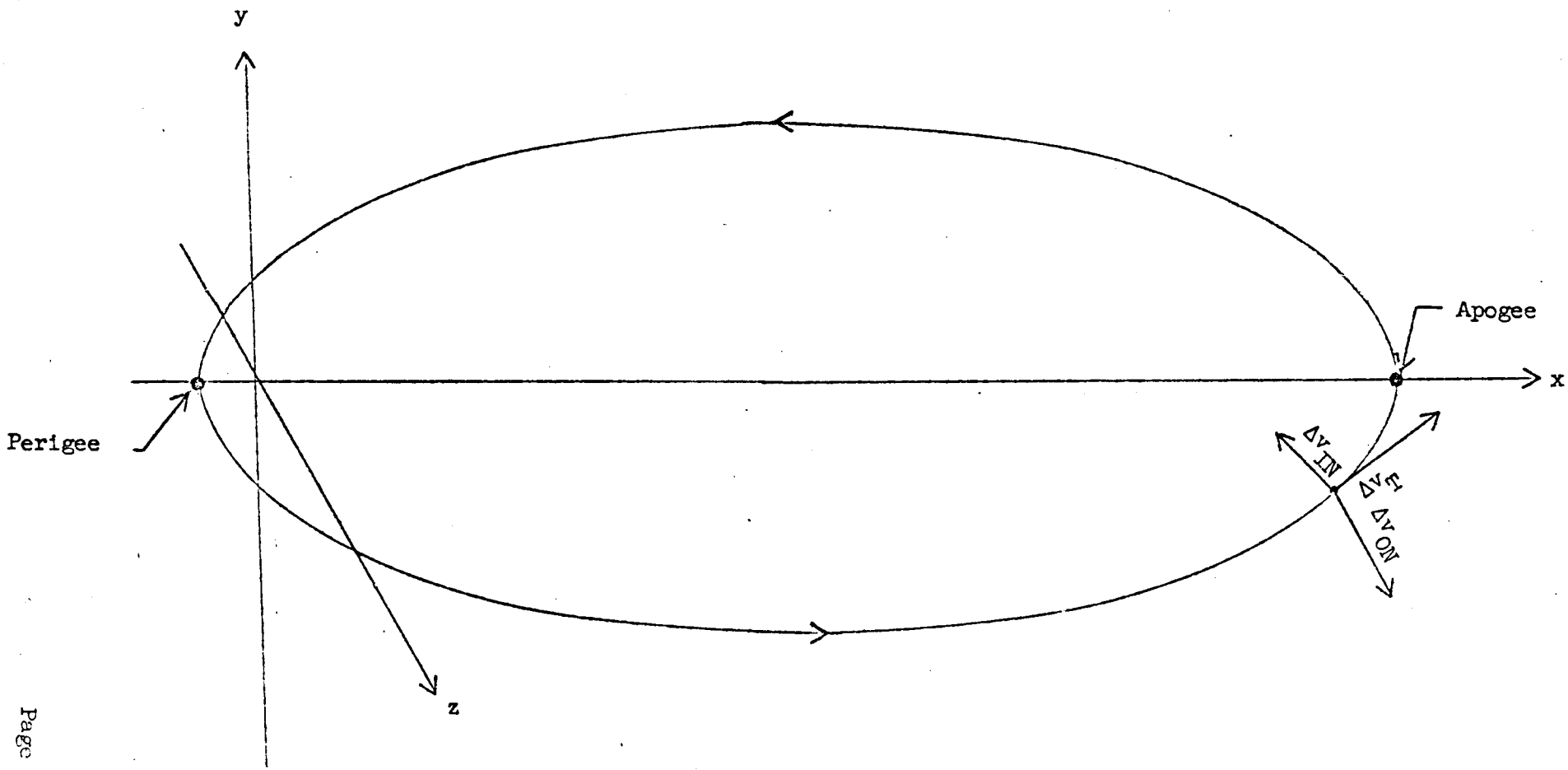

FIGURE A. DEFINITION OF SEPARATION DISTANCE AND DEPLOYMENT VELOCITY INCREMENT COMPONENTS

To provide a basis for the evaluation of deployment techniques, computations have been made to obtain the sensitivities of the component of the intersatellite separation distances to the velocity increment components. For this purpose a reference (280 km x 20 R_e) orbit has been usdd and the effects, based upon Keplerian theory, of a single velocity increment at one point in the orbit in producing separation distances relative to the unperturbed reference orbit have been determined. (The effects of a set of velocity increments applied at different points in the orbit can be built up by the superposition of the effects of single velocity increments.)

The orbital perturbation effects of the velocity increments are divided into 3 categories:

1. In-plane lead time effects
2. In-plane geometric effects
3. Out-of-plane geometric effects

2.0 LEAD TIME EFFECTS

Lead time effects involve no changes in the geometry of the orbit. The satellites are simply displaced within the unperturbed orbit because they pass a given point at a different time. As depicted in Figure B the direction of the intersatellite separation distance rotates as the direction of the velocity vector rotates while the orbit is traversed. If the perturbed satellite is advanced in time it is separated from the unperturbed satellite in the -y direction at perigee; in the +x direction at the semi-minor axis on the ascending leg; in the +y direction at apogee; and in the -x direction at the semi-minor axis on the descending leg. For other points the separation distance is at an angle to the reference axes.

Also because of the variation in the magnitude of the velocity, the magnitude of the separation distance varies as the orbit is traversed. Thus for a given lead time, the separation distance at passing near perigee is about 20 times greater than the separation distance in passing apogee. At the semi-minor axis, i.e., at about 10 R_e, the separation distance is about 5 times greater than at apogee.

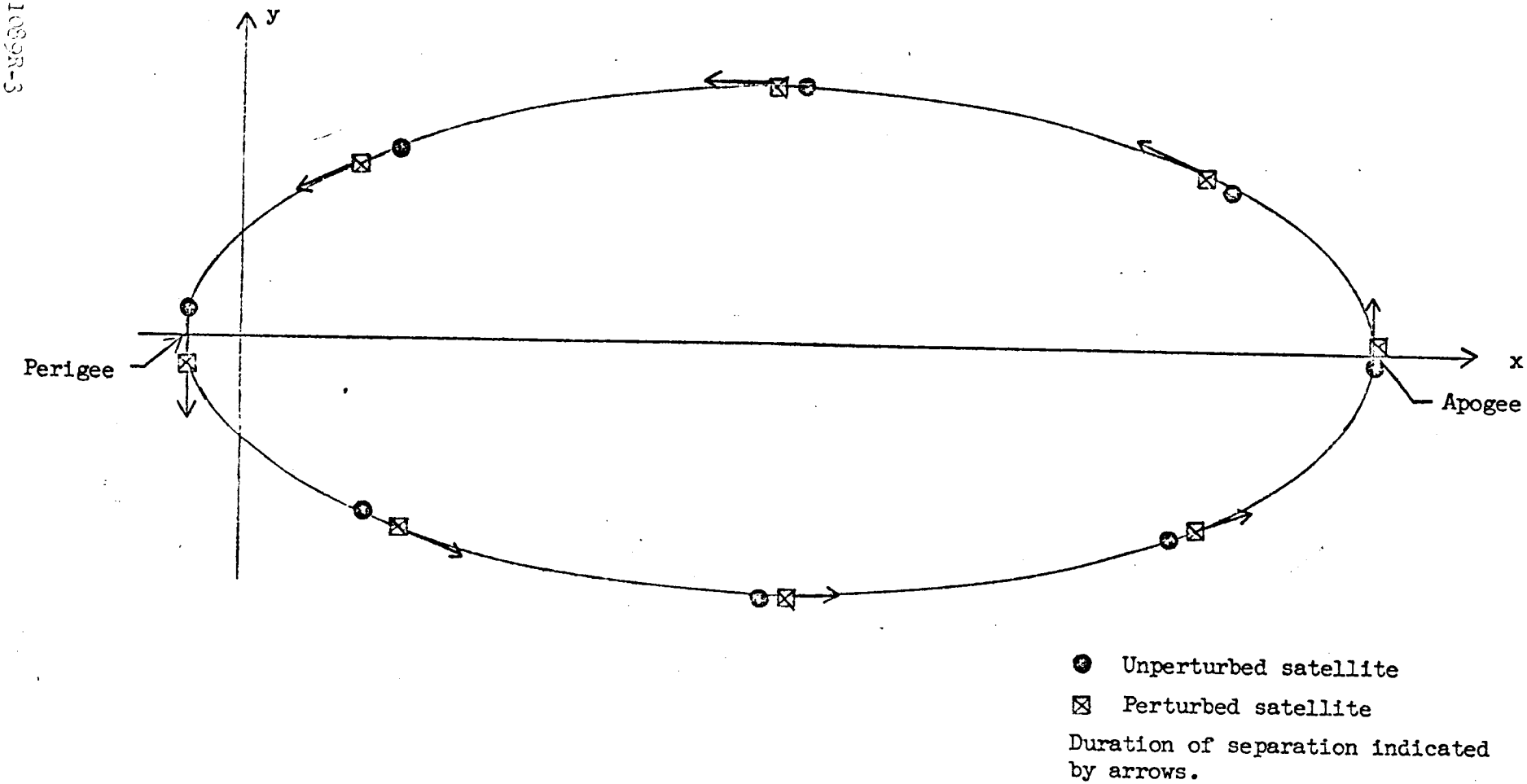

FIGURE B. EFFECT OF TIMING DIFFERENCE ON SATELLITE SEPARATION

The lead time of the perturbed satellite can be conveniently expressed in terms of a percent of the orbital period. For lead times sufficiently small to remain within the linear realm, the separation distances can be taken to be proportional to the lead time. Figures C, D and E show, respectively, the variations in the magnitude of separation distance, the variation in the x component and the variation in the y component of the separation distance, as the satellites traverse the orbit for the case where the perturbed satellite leads by .1% of the orbit period (2.9 minutes). These results are also listed in Table 1. It is seen from Figure C that if the separation in the vicinity of 10 R_e is to be restricted to a maximum value of 15,000 km (after 6 months in orbit) then the maximum allowable lead time between satellites would be about .04 percent of an orbital period.

The lead time between satellites will arise mainly from differences in period. Within the accuracy of linear approximations, neither the in-plane normal or the out-of-plane component of the velocity increment affects the orbital period. However, the tangential component of the velocity increment can have a strong effect on orbital period, particularly when applied near perigee. This is exhibited in Figure F and Table 1 which present the effects of a 1 meter/sec tangential velocity increment applied at different times in the orbit.

After a difference in period has been established the lead time will grow by the difference in period each time the orbit is traversed. Thus in a 6-month period the lead time will grow to about 90 times the difference in orbital period. In the case of an increment applied near perigee, to maintain the restriction on the growth of separation distances to a maximum of 15,000 km in the vicinity of 10 R_e, the tangential component would have to be kept below .1 km/sec.

In addition to the growth in lead time caused by the difference in orbital period, the velocity increment has an immediate effect on lead time, i.e., the orbit is perturbed in such a manner that the effective time of the last perigee passage is changed. Figure G shows the immediate effect of a 1 meter/sec tangential velocity component on the lead time.

Although the in-plane normal velocity increment does not affect the period, it does change the effective time of last perigee passage. This effect is shown in Figure H.

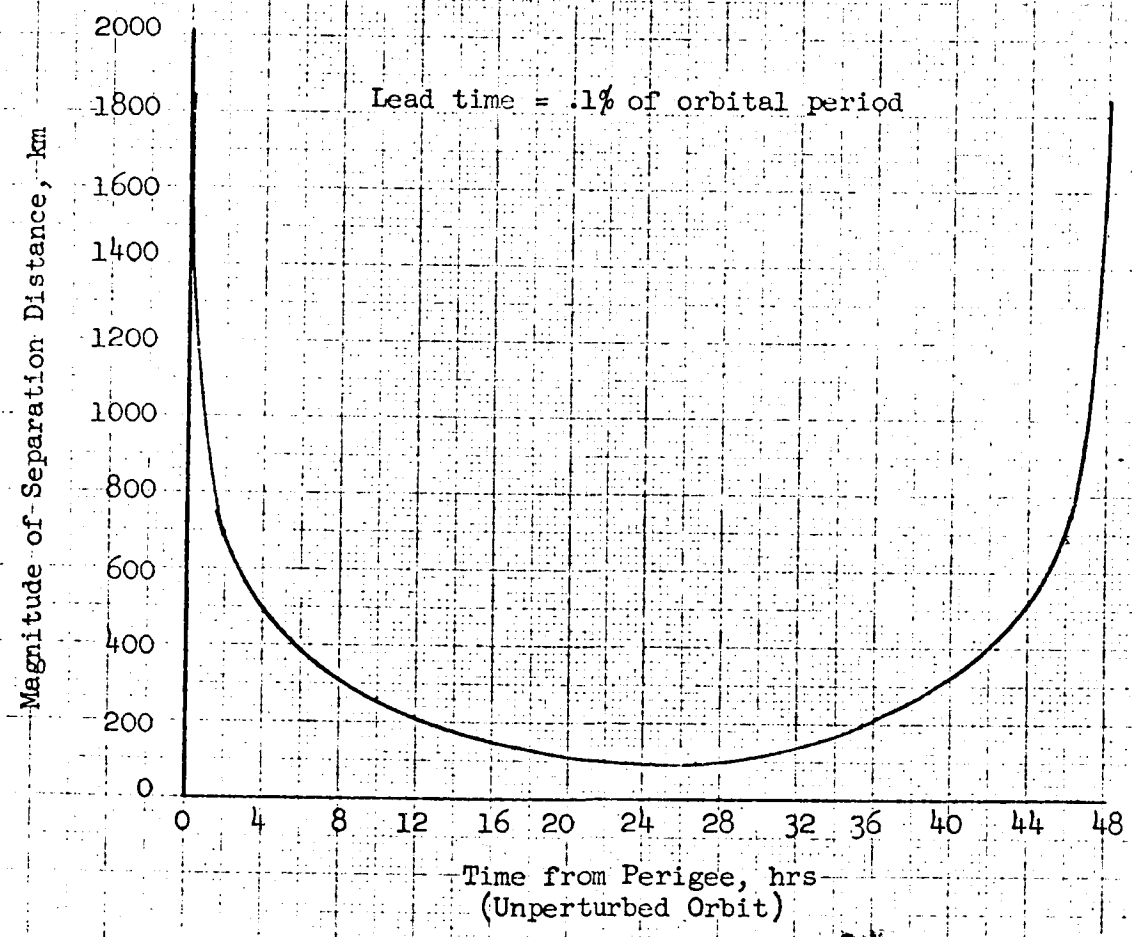

FIGURE C. EFFECT OF LEAD TIME ON SEPARATION DISTANCE

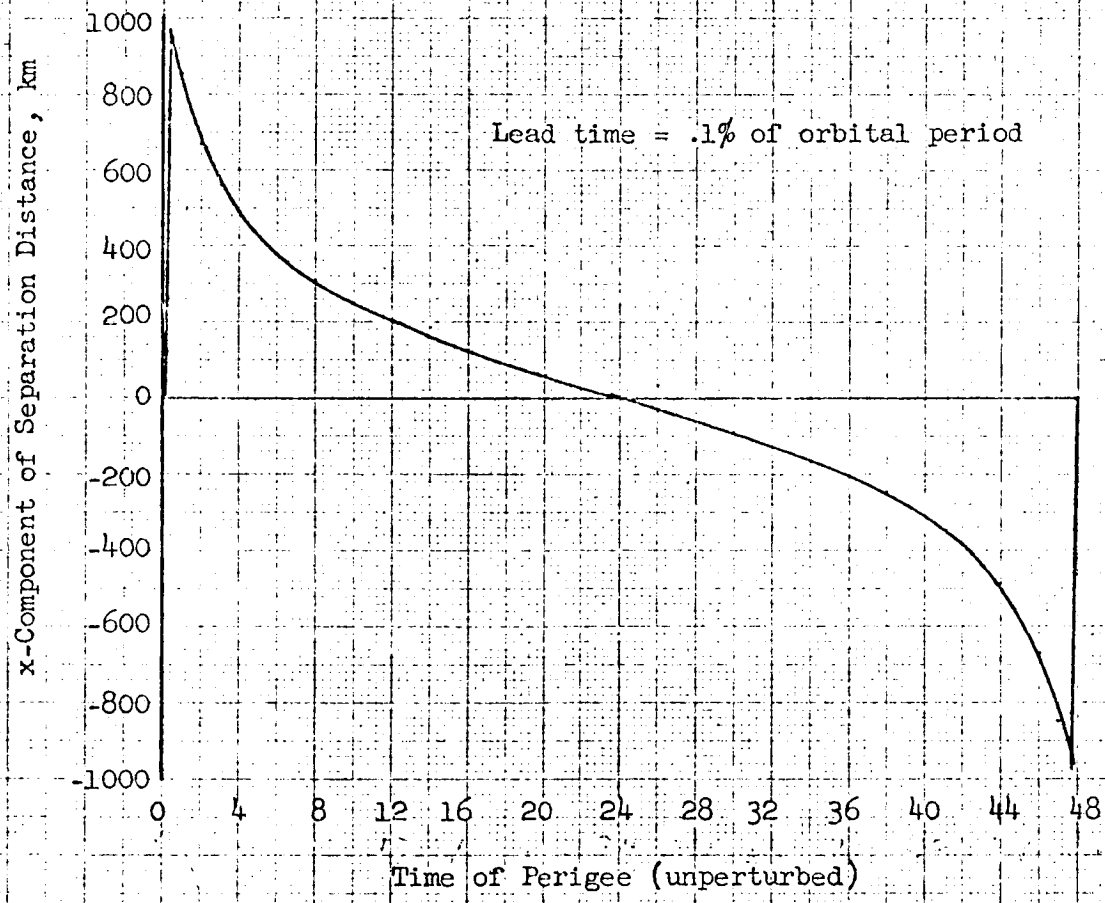

FIGURE D. EFFECT OF LEAD TIME ON x-COMPONENT OF SEPARATION DISTANCE

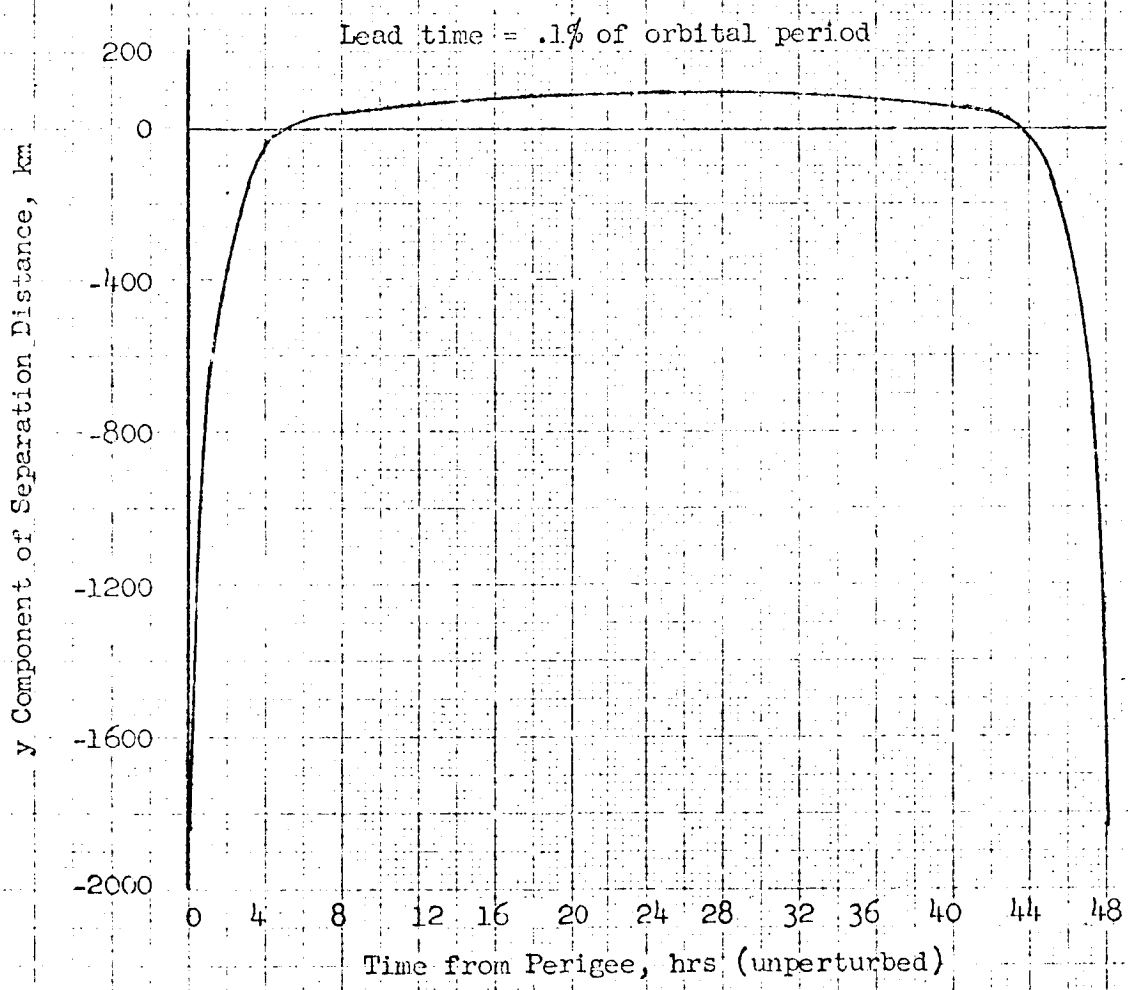

FIGURE E. EFFECT OF LEAD TIME ON y-COMPONENT OF SEPARATION DISTANCE

TABLE 1. IN-PLANE LEAD TIME SENSITIVITIES

Reference Orbit		Effect of .1% of Orbit Period Lead Time on Separation Distance			% Change in Orbital period due to Δv_T = 1 meter/sec	Immediate Effect on Lead Time Change in Time of Last Perigee Passage in 10^{-4} % of Period Due to	
Time From Perigee, hrs	Distance From Earth, R_e	x-Component km	y-Component km	Magnitude km		Δv_T = 1 meter/sec	Δv_{IN} = 1 meter/sec
0	1.044	0	-1843.6	1843.6	.5447		
.5	2.147	966.5	-792.4	1249.8			
1.0	3.492	851.4	-409.1	944.5	.2785	-2.28	2.21
1.5	4.666	747.0	-255.0	789.3			
2.0	5.707	669.0	-171.5	690.7	.2036	-4.11	7.45
2.5	6.646	608.6	-118.5	620.1			
3.0	7.506	559.9	-81.7	565.8	.1668	-6.64	13.50
3.5	8.300	519.2	-54.4	522.0			
4.0	9.039	484.4	-33.4	485.5	.1432	-9.72	20.07
4.5	9.730	454.0	-16.6	454.3			
5.0	10.379	427.1	-2.9	427.1	.1260	-13.19	27.14
6.0	11.568	380.9	18.3	381.4	.1125	-16.98	34.69
7.0	12.632	342.2	33.9	343.9	.1015	-20.97	42.73
8.0	13.590	307.6	45.8	312.1	.0922	-25.09	51.30
9.0	14.455	279.1	55.2	284.5	.0841	-29.22	60.45
10.0	15.238	252.4	62.8	260.1	.0769	-33.24	70.23
11.0	15.946	228.1	69.0	237.7	.0751	-37.00	80.72
12.0	16.584	205.6	74.2	218.6	.0647	-40.32	92.00
13.0	17.159	184.5	78.5	200.6	.0594	-42.95	104.15
14.0	17.673	164.8	82.1	184.1	.0546	-44.59	117.26
15.0	18.131	146.0	85.2	169.0	.0501	-44.84	131.43
16.0	18.535	128.0	87.8	155.2	.0461	-43.20	146.68
17.0	18.886	110.7	89.9	142.6	.0423	-39.03	163.01
18.0	19.187	93.9	91.7	131.2	.0390	-31.53	180.29
19.0	19.440	77.6	93.1	121.2	.0360	-19.75	198.20
20.0	19.645	61.6	94.3	112.6	.0334	-2.66	216.09
21.0	19.804	46.0	95.1	105.7	.0313	+20.67	232.98
22.0	19.916	30.5	95.8	100.5	.0297	+50.85	247.39
23.0	19.983	15.1	96.1	97.3	.0286	+87.72	257.68
24.0	20.000	0.1	96.2	96.2	.0282	130.20	262.34

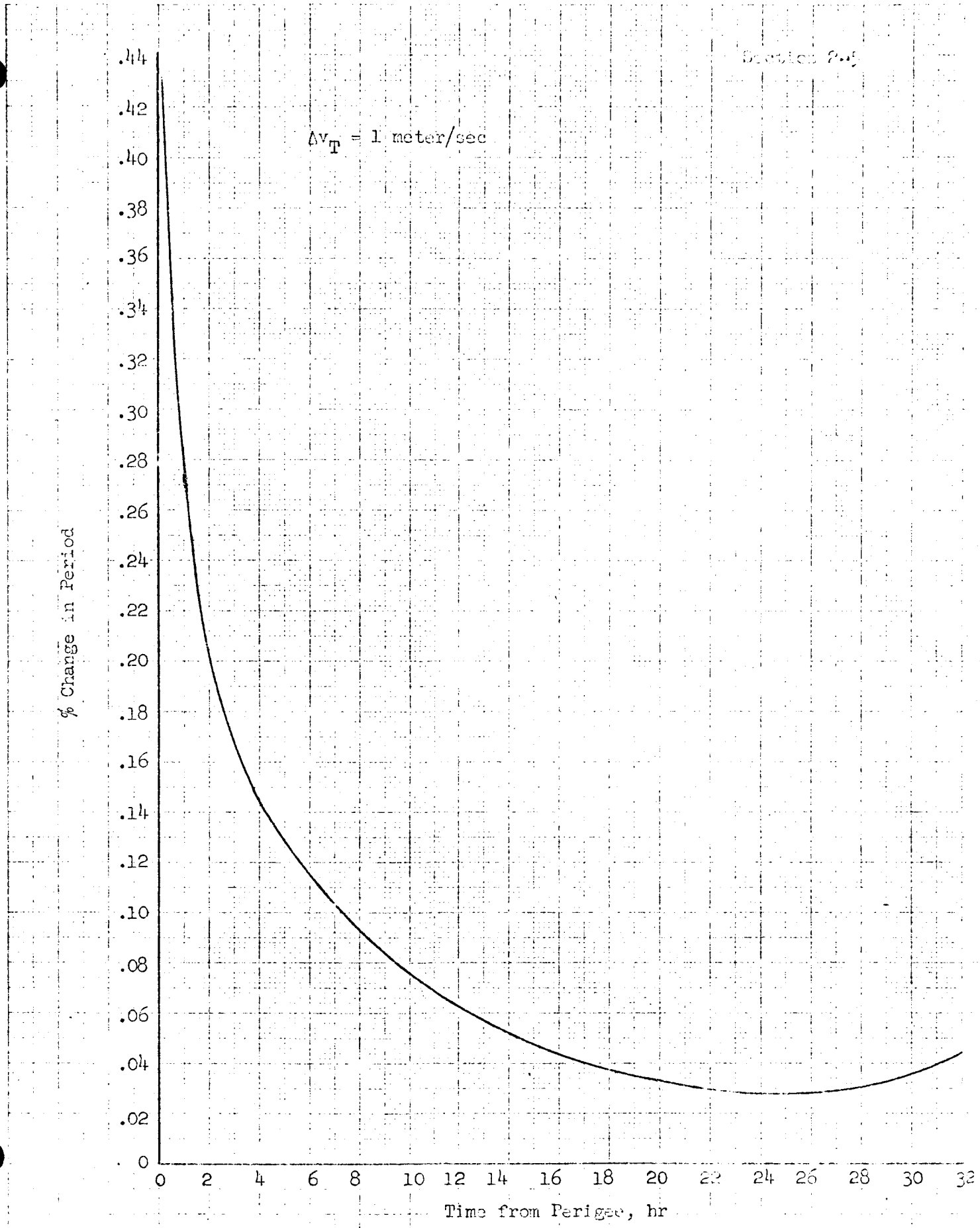

FIGURE F. EFFECT OF TANGENTIAL VELOCITY INCREMENT ON PERIOD

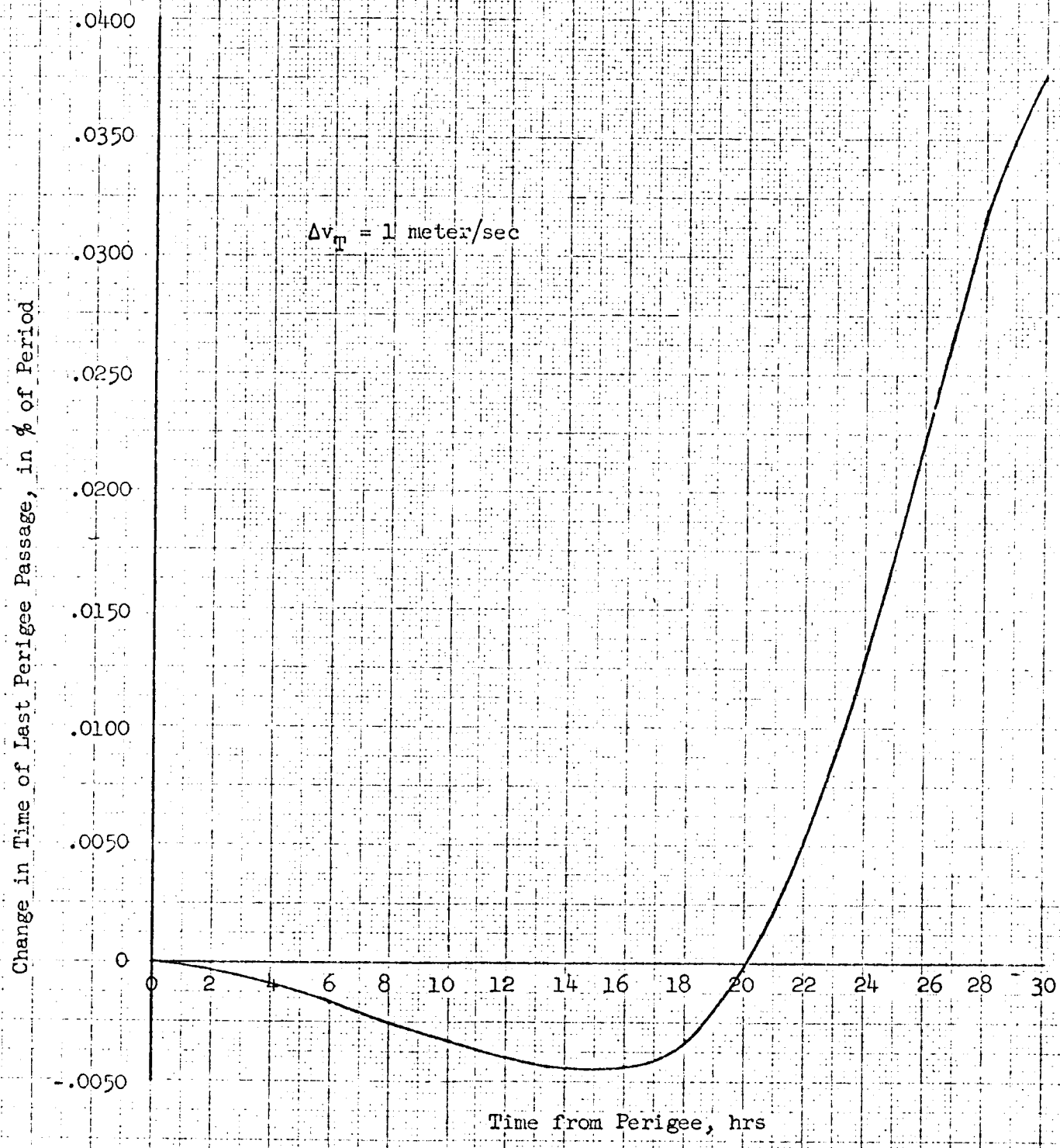

FIGURE G. IMMEDIATE EFFECT OF TANGENTIAL VELOCITY INCREMENT ON LEAD TIME

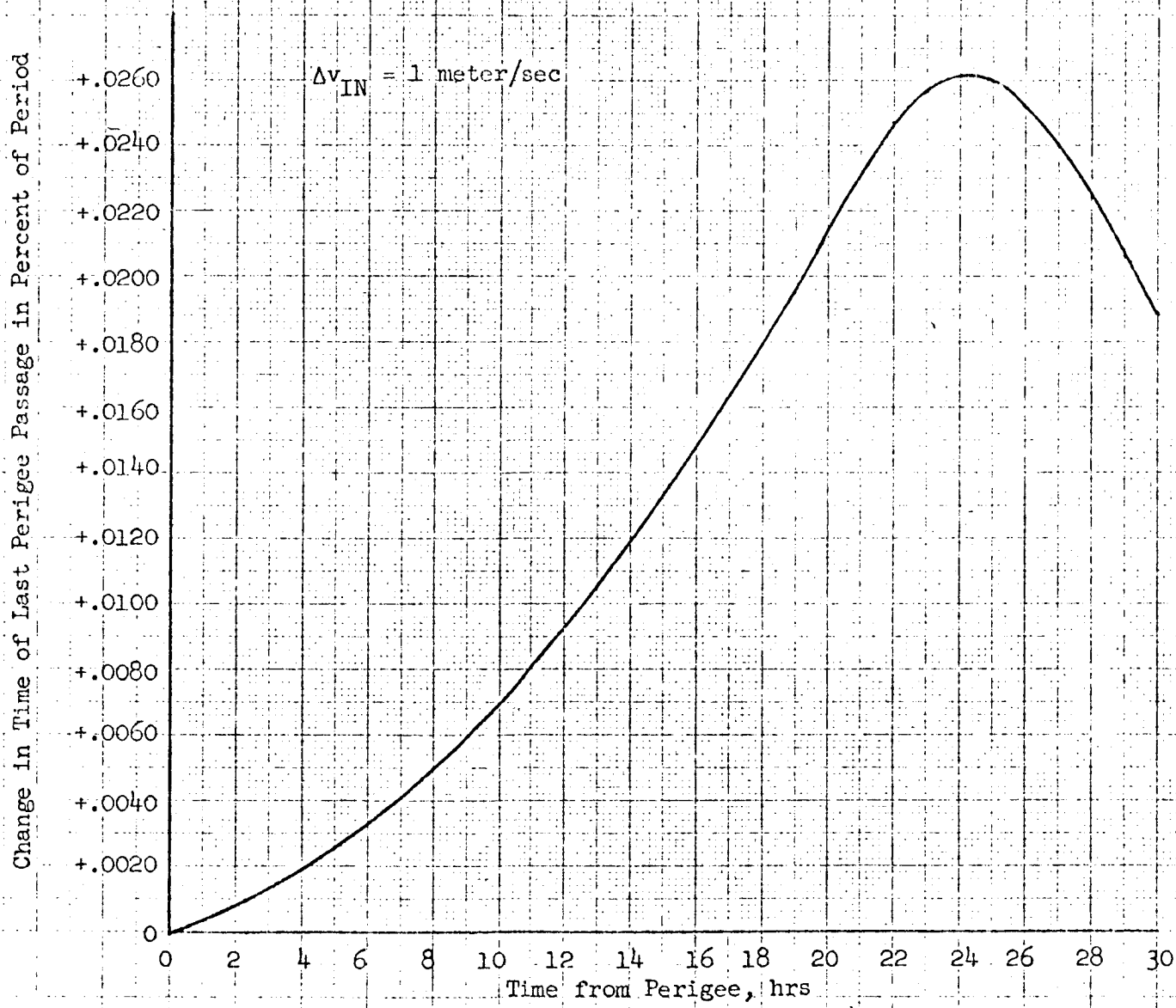

FIGURE H. IMMEDIATE EFFECT OF IN-PLANE NORMAL VELOCITY INCREMENT ON LEAD TIME

PRINTED IN U.S.A. ON CLEARPRINT TECHNICAL PAPER NO. 1015
CLEARPRINT PAPER CO. NO. C 98. MILLIMETERS 200 BY 250 DIVISIONS

3.0 IN-PLANE GEOMETRIC EFFECTS

As noted above, changes in lead time do not produce separations in a consistent direction; the direction of the separation distance rotates with the orbital velocity vector. In order to obtain (a) an x-component of the separation in the vicinity of perigee and apogee, or (b) a y-component in the vicinity of the semi-minor axis, in-plane geometric perturbations are required. As depicted in Figure I, separations in the x direction can be produced by changes in apogee radius and perigee altitude; and separations in the y-direction can be produced by changes in the direction of the line of apsides and/or in the size of the minor axis.

Changes in perigee altitude would generally not be expected to be large enough to be of direct significance in connection with separation distances. However, it is important to take account of changes in perigee altitude in order to protect against an excessive reduction. Also, there is a close connection between changes in perigee altitude, apogee radius and orbital period. Specifically

$$\frac{\Delta\tau}{\tau} = \frac{3}{2}\,\frac{\Delta r_a}{(r_a + r_p)} + \frac{3}{2}\,\frac{\Delta h_p}{(r_a + r_p)}$$

where τ is the nominal orbital period, r_a and r_p are the nominal apogee and perigee radius and h_p is perigee altitude. A 50 km change in apogee radius or in perigee altitude would correspond to a change in period of about .056 percent. This is in excess of the maximum allowable period differences.

Clearly to obtain large changes in apogee radius without large changes in period will require accompanying changes in perigee altitude opposite to the changes in apogee radius. Unless the initial perigee altitude were extraordinarily large, large decreases in perigee altitude must be precluded so that only the case of large decreases in apogee altitude accompanied by large increases in perigee altitude could be considered. Even this choice is restricted by the limitations on the allowable differences in perigee altitude imposed by the necessity of avoiding excessive differences in orbital decay (see Section 2-3, Figure E). For deployment schemes wherein velocity increments of equal magnitude but opposite direction are applied to pairs of satellites (such as, symmetrical spin-off from the pallet or spring-separation of one satellite from another), it would not be possible to increase the perigee altitude of one satellite without decreasing the perigee altitude of its partner.

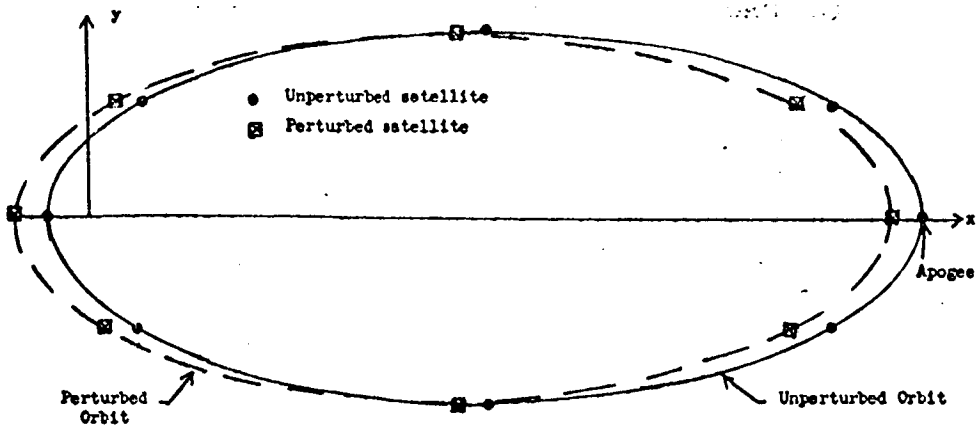

Decrease in Apogee Radius; Increase in Perigee Attitude

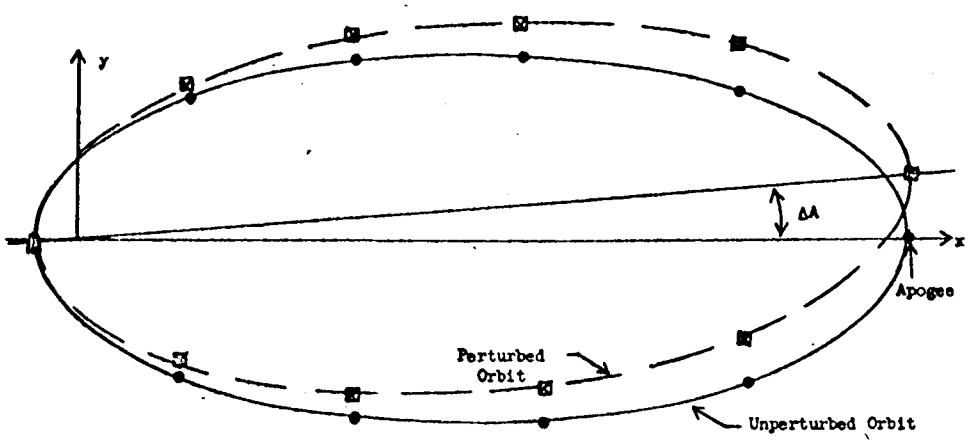

Rotation of Line of Apsides

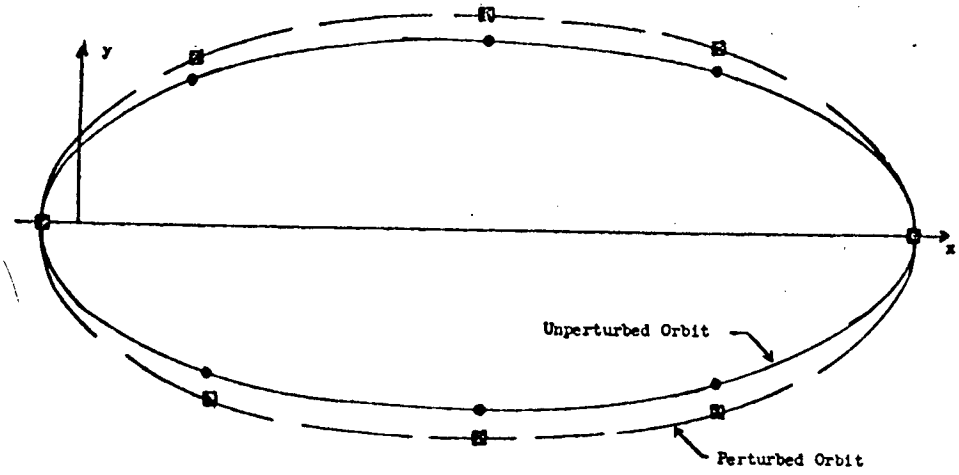

Increase in Semi-Minor Axis

FIGURE I. IN-PLANE GEOMETRIC ORBITAL PERTURBATIONS

If it is necessary to forego the attainment of a large x-component of separation distance in the vicinity of apogee, then near apogee the satellite array will be very nearly planar; all satellites would lie close to a common y-z plane. The possibility of accepting a planar array near apogee rests upon having an apogee radius large enough so that at distances beyond the transition region the direction of velocity vector departs substantially from the direction of the velocity vector at apogee. A non-coplanar array at points beyond the transition region can then be obtained by combinations of separation distances produced by lead time, rotation of the line of apsides, and changes in semi-minor axis (along with out-of-plane separation distances). This is illustrated in Figure J. Such an arrangement will permit 3 dimensional measurement of spacial gradients and disturbance front propagation velocities in the space beyond the transition region. (However, it must be recognized that complete directional information regarding disturbance fronts that happen to be encountered while the satellites are in the vicinity of apogee would not be obtained.)

Because of the high eccentricity of the orbit, except for a small section of the orbit in the vicinity of the semi-latus rectum, the y-components of the separation distances resulting from a rotation of the line of apsides are generally greater than the x-components. For the section of the orbit of most interest, i.e., above 10 R_e, the y-component increases with distance from the center of the earth and is greatest at apogee as indicated in Figure K and Table 2. At a given distance from the earth the sense of the y-component of the separation distance is the same on the descending leg of the orbit as on the ascending leg.

This contrasts with the effect of a change in the length of the semi-minor axis which produces separation distances in the y-direction. that are proportional to the y-coordinate of the point in the unperturbed orbit and thus reaches a maximum at the semi-minor axis and vanishes at apogee and perigee as indicated in Figure L. At a given distance from the earth the y-component of the separation distance on the descending leg is of equal magnitude but opposite direction to that which applies for the ascending leg.

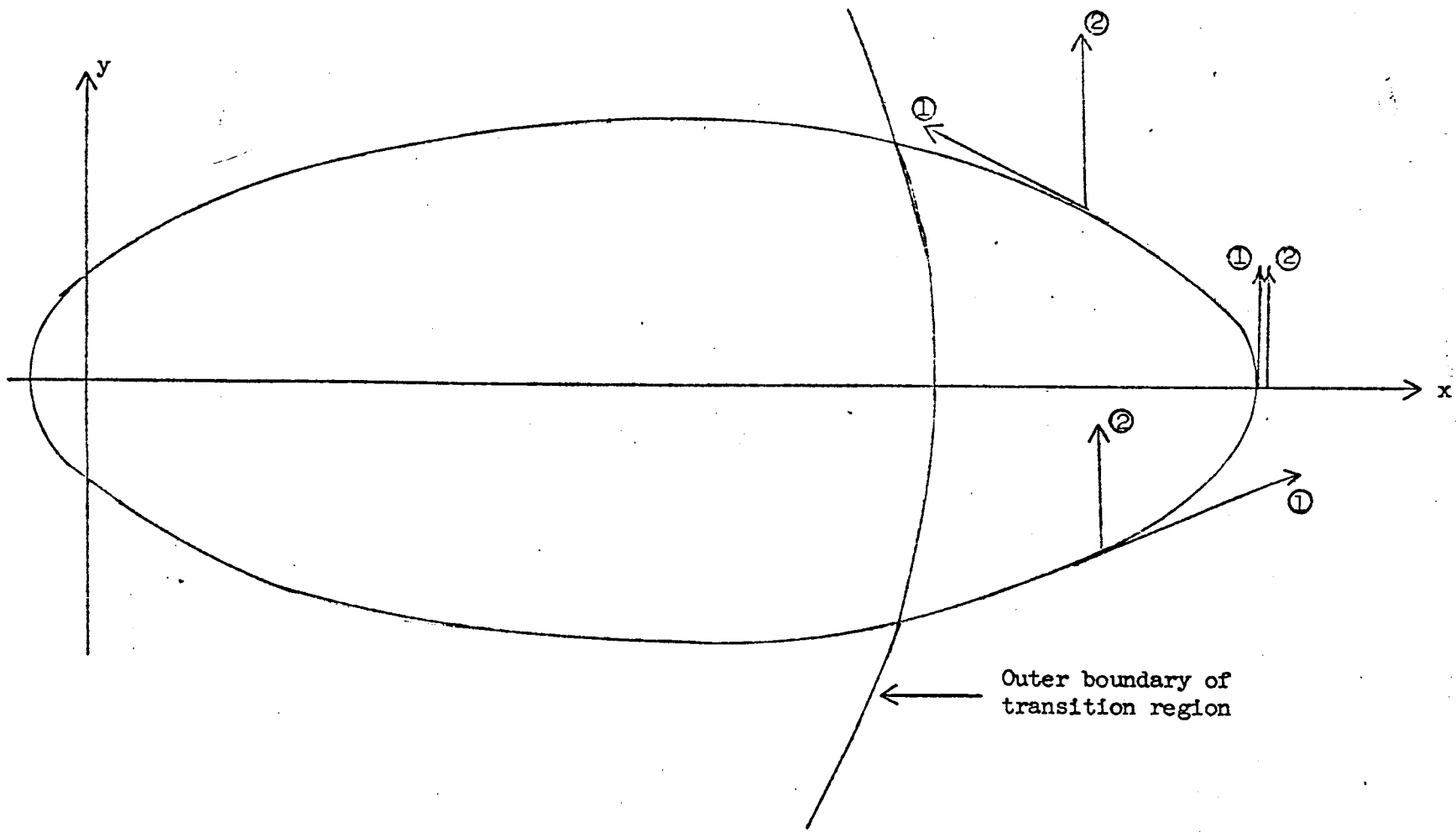

① Direction of separation distance produced by lead time

② Direction of separation distance produced by rotation of line of apsides

FIGURE J. ACHIEVEMENT OF NON-COPLANAR ARRAY BEYOND TRANSITION REGION USING LEAD TIME AND ROTATION OF LINE OF APSIDE EFFECTS

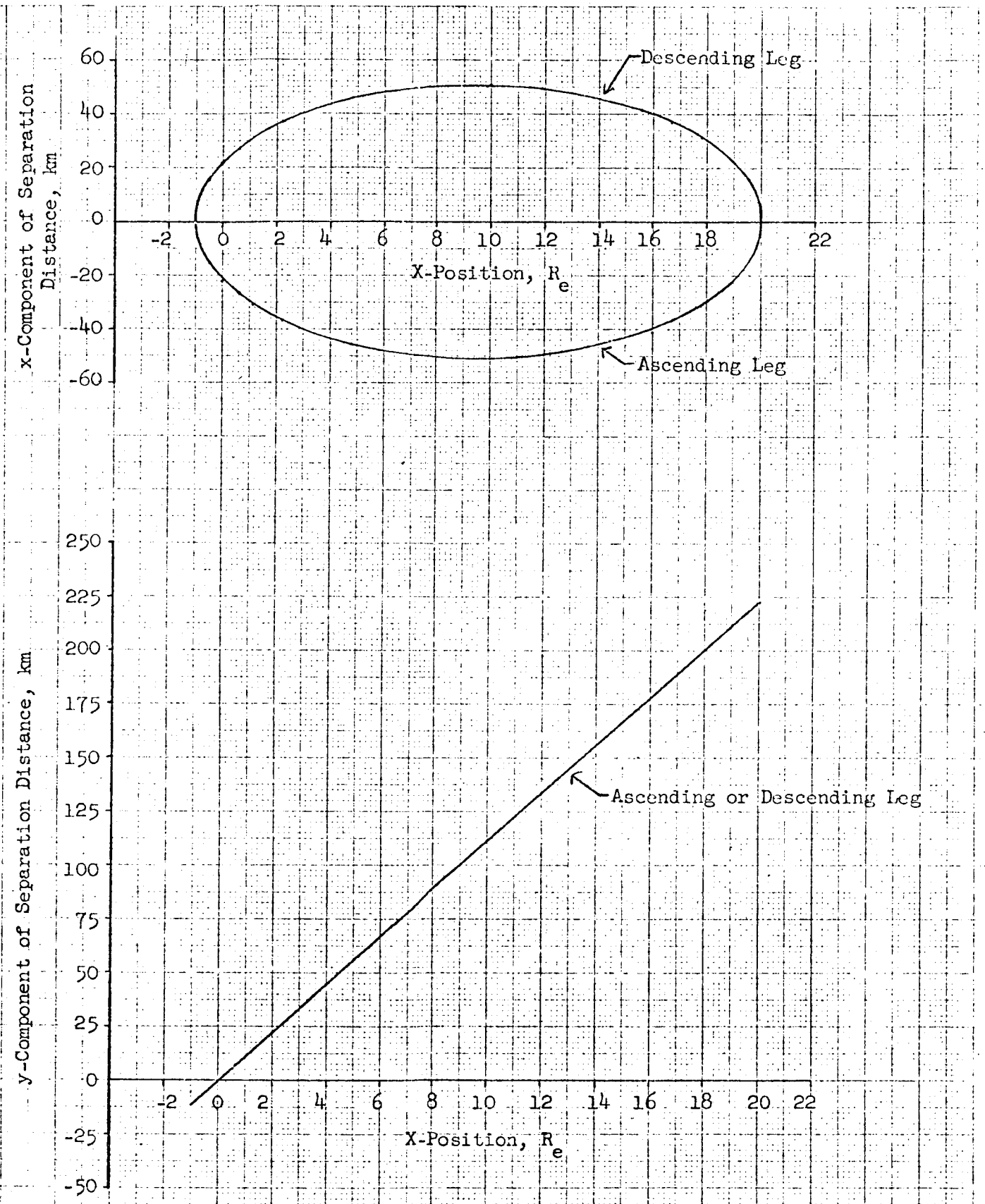

FIGURE K. EFFECT OF .1 deg APSIDAL ROTATION ON IN-PLANE SEPARATION DISTANCE COMPONENTS

Table 2

IN-PLANE GEOMETRIC PERTURBATIONS

Distance From Center of Earth R_e	Effect of a 0.1 deg Apsidal Rotation		Effect of a 100 km Increase in Semi-Minor Axis	Time of Application in Reference Orbit		Tangential Velocity Increment Δv_T = 1 meter/sec				In-Plane Normal Velocity Increment Δv_{IN} = 1 meter/sec		
	x-Component km	y-Component km	y-Component* km	Time From Perigee (Hours)	Distance From The Center Of The Earth (R_e)	Change in Apogee Radius (km)	Change in Perigee Altitude (km)	Change in Semi-Minor Axis (km)	Rotation of The Line of Apsides (10^{-3} deg)	Change in Perigee Altitude** (km)	Change in Semi-Minor Axis (km)	Rotation of The Line of Apsides (10^{-3} deg)
1.044	0	-11.6	0	0	1.044	489.67	0.00	55.9	-0.01	0.02	0.0	11.33
1.5	-15.6	-6.0	-30.6	2	5.709	180.14	3.02	27.2	21.89	6.29	14.5	22.47
2.0	-22.2	0.2	-43.8	4	9.046	124.18	4.65	24.4	22.60	10.24	23.6	23.96
2.5	-27.1	6.4	-53.3	6	11.581	95.18	6.09	24.2	22.63	13.12	30.2	22.92
3.0	-30.9	12.5	-60.8	8	13.610	75.42	7.52	25.1	22.41	15.28	35.2	20.52
4.0	-36.9	24.9	-72.6	10	15.267	60.12	9.12	26.8	22.02	16.82	38.7	17.29
5.0	-41.3	37.2	-81.3	12	16.624	47.36	10.87	29.2	21.33	17.38	40.0	13.51
6.0	-44.7	49.6	-87.9	14	17.725	36.17	12.94	32.4	20.34	18.10	41.7	9.18
7.0	-47.2	61.9	-92.8	16	18.599	26.07	15.38	36.6	18.80	17.57	40.5	4.47
8.0	-49.0	74.3	-96.4	18	19.267	16.86	18.22	41.8	16.47	15.94	36.7	-0.53
9.0	-50.2	86.6	-98.7	20	19.741	8.79	21.28	47.6	12.87	12.75	29.4	-5.45
10.0	-50.7	98.9	-99.8	22	20.030	2.70	24.00	52.8	7.54	7.62	17.6	-9.42
11.0	-50.7	111.3	-99.9	24	20.140	0.03	25.30	55.4	0.81	0.86	2.0	-11.28
12.0	-50.2	123.6	-98.8	26	20.070	1.72	24.47	53.8	-6.14	-6.12	-14.1	-10.11
13.0	-49.0	136.0	-96.5	28	19.824	7.15	21.98	48.9	-11.85	-11.70	-26.9	-6.50
14.0	-47.3	148.3	-93.0	30	19.394	14.87	18.92	43.1	-15.80	-15.33	-35.3	-1.75
15.0	-44.8	160.7	-88.1	32	18.772	23.85	16.01	37.8	-18.43	-17.29	-39.8	3.28
16.0	-41.5	173.0	-81.6	34	17.947	33.74	13.47	33.3	-20.13	-18.04	-41.5	8.12
17.0	-37.1	185.4	-73.0	36	16.901	44.64	11.32	29.9	-21.22	-17.91	-41.2	12.55
18.0	-31.2	197.7	-61.4	38	15.608	56.97	9.48	27.3	-21.92	-17.10	-39.4	16.50
19.0	-22.7	210.1	-44.7	40	14.025	71.56	7.87	25.4	-22.38	-15.69	-36.1	19.88
20.0	0	222.4	0	42	12.091	90.02	6.40	24.3	-22.61	-13.67	-31.5	22.47
				44	9.691	116.12	4.98	24.2	-22.67	-10.97	-25.3	23.96
				46	6.586	162.17	3.43	26.1	-22.25	-7.31	-16.8	23.25
				48	2.046	339.59	0.10	39.0	-17.14	-1.73	-4.0	15.41

* Reverse sign for descending node.

** Change in apogee radius = change in perigee altitude

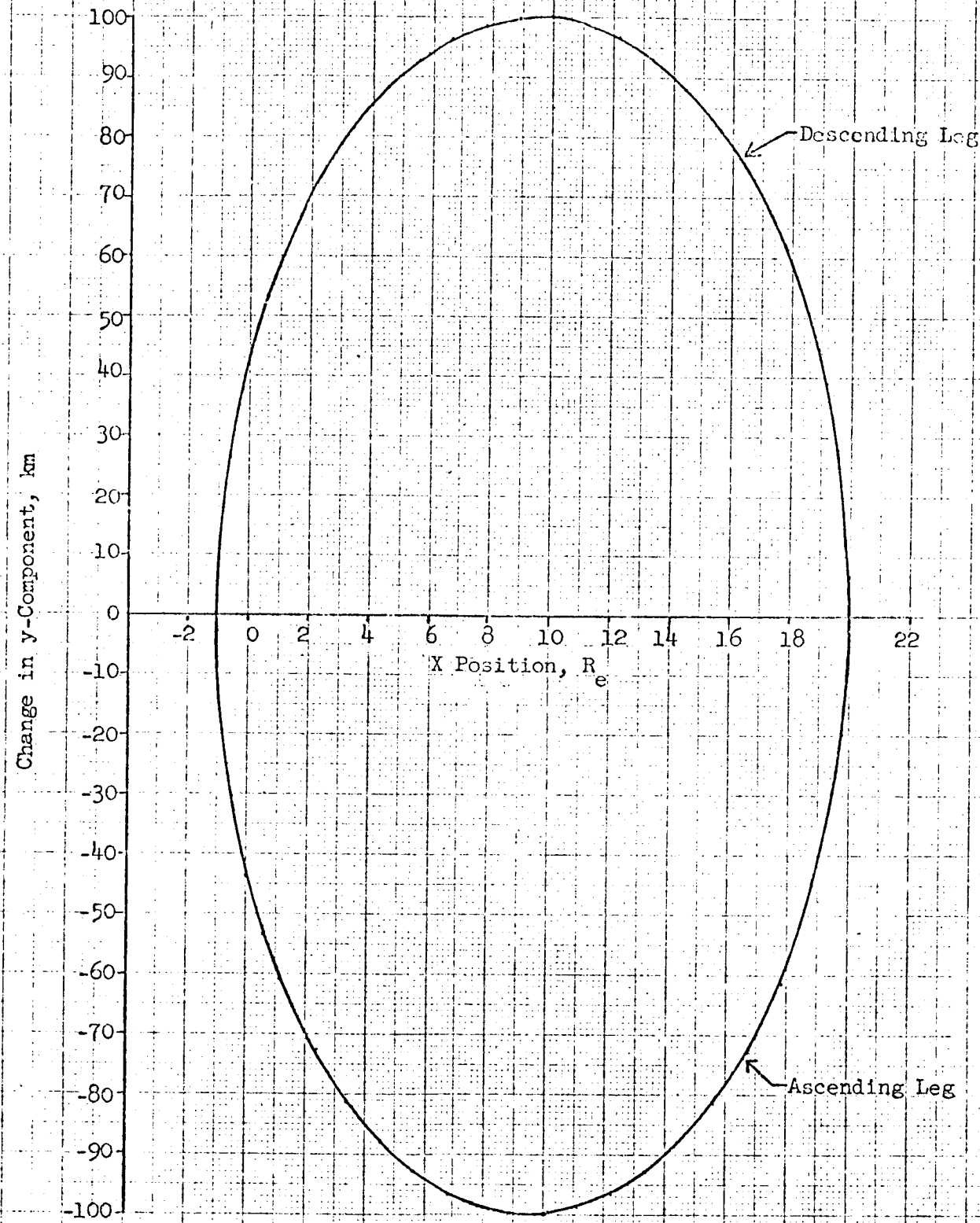

FIGURE L. EFFECT OF 100 km INCREASE OF SEMI-MINOR AXIS ON SEPARATION DISTANCE

There is, of course, a close relationship between the change in the dimension of the semi-minor axis, Δb, and the changes in apogee and perigee. Specifically

$$\Delta b = \frac{1}{2}\left(\frac{1+e}{1-e}\right)^{\frac{1}{2}} \Delta h_p + \frac{1}{2}\left(\frac{1-e}{1+e}\right)^{\frac{1}{2}} \Delta r_a = (2.188)\,\Delta h_p + (.11423)\,\Delta r_a$$

where e is the eccentricity of the orbits and the numerical values apply for the eccentricity of the reference orbit: $e = .9008$. For an in-plane normal velocity increment there is no change in orbital period. Hence in this case it follows automatically that

$$\Delta r_a = -h_p \text{ and}$$

$$\Delta b = \frac{1}{\left(1 - e^2\right)^{\frac{1}{2}}} \Delta h_p = (2.3027)\,\Delta h_p$$

The effects of tangential and in-plane normal velocity components on apogee radius, perigee altitude, the semi-minor axis and the rotation of the line of apsides are presented in Figures M to S and Table 2.

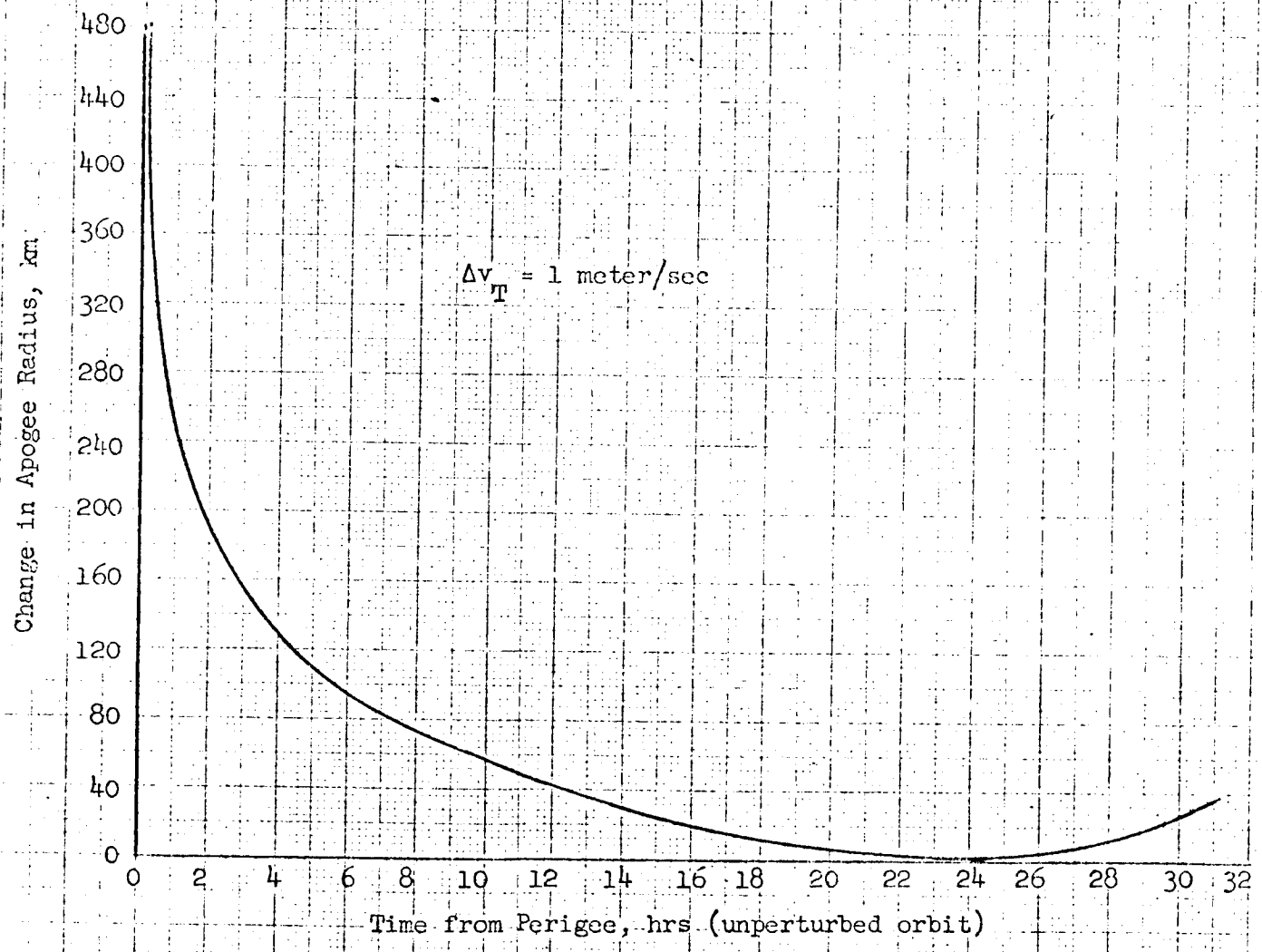

FIGURE M. EFFECT OF TANGENTIAL VELOCITY INCREMENT ON APOGEE RADIUS

PRINTED IN U.S.A. ON CLEARPRINT TECHNICAL PAPER NO. 1015
CLEARPRINT PAPER CO. NO C38X MILLIMETERS 20 HT 250 DIVISIONS

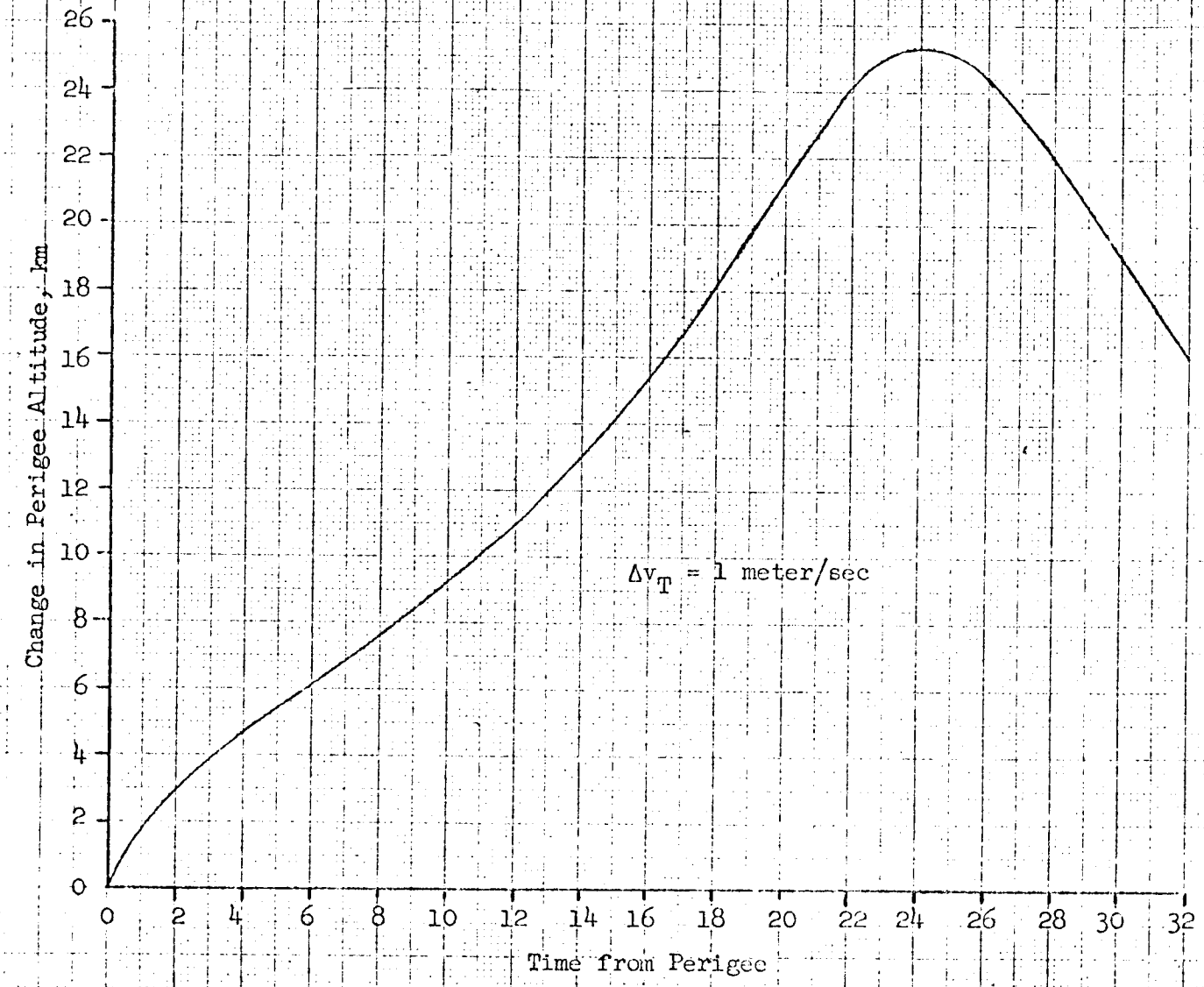

FIGURE N. EFFECT OF TANGENTIAL VELOCITY INCREMENT ON PERIGEE ALTITUDE

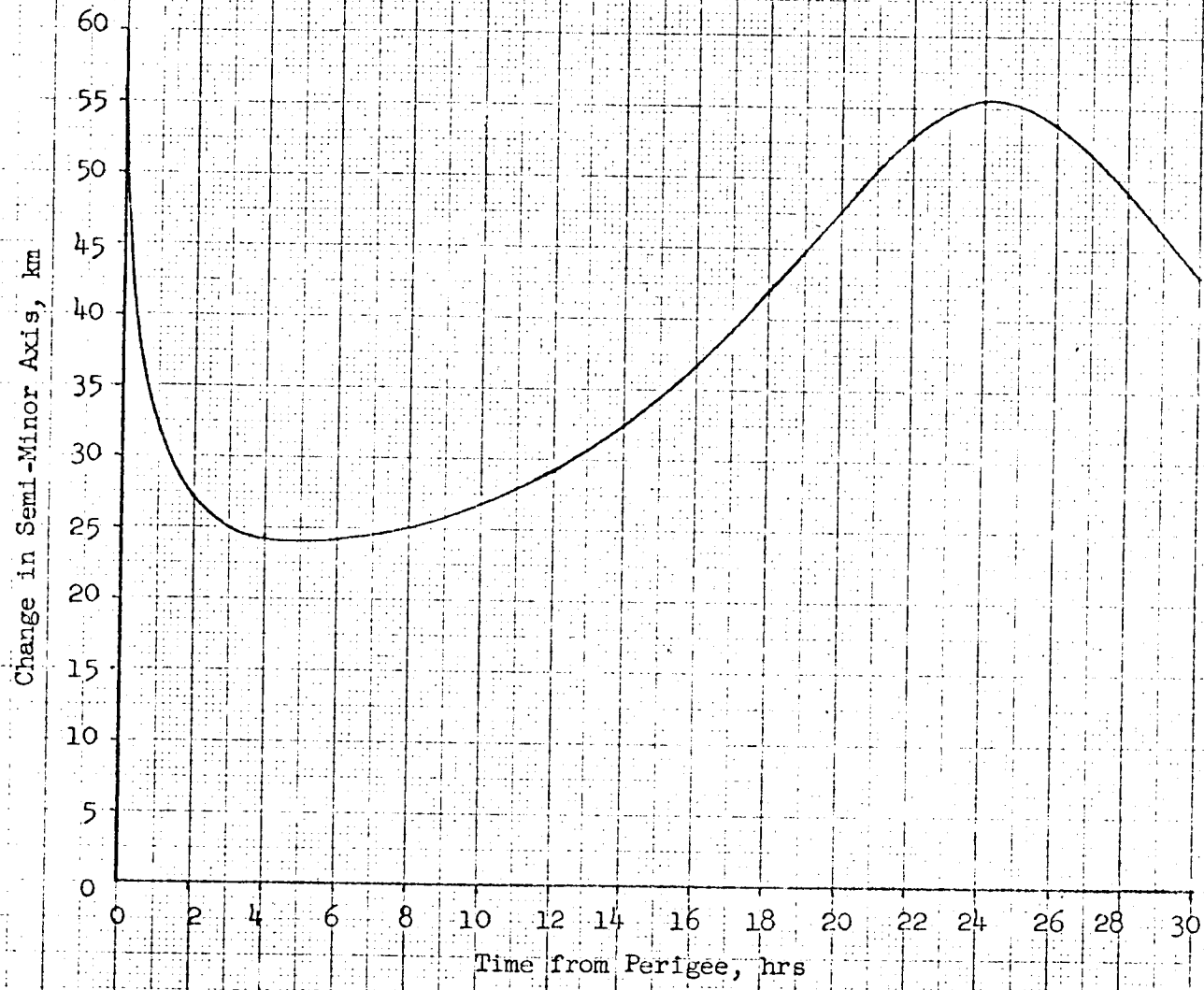

FIGURE O. EFFECT OF TANGENTIAL VELOCITY INCREMENT ON SEMI-MINOR AXIS

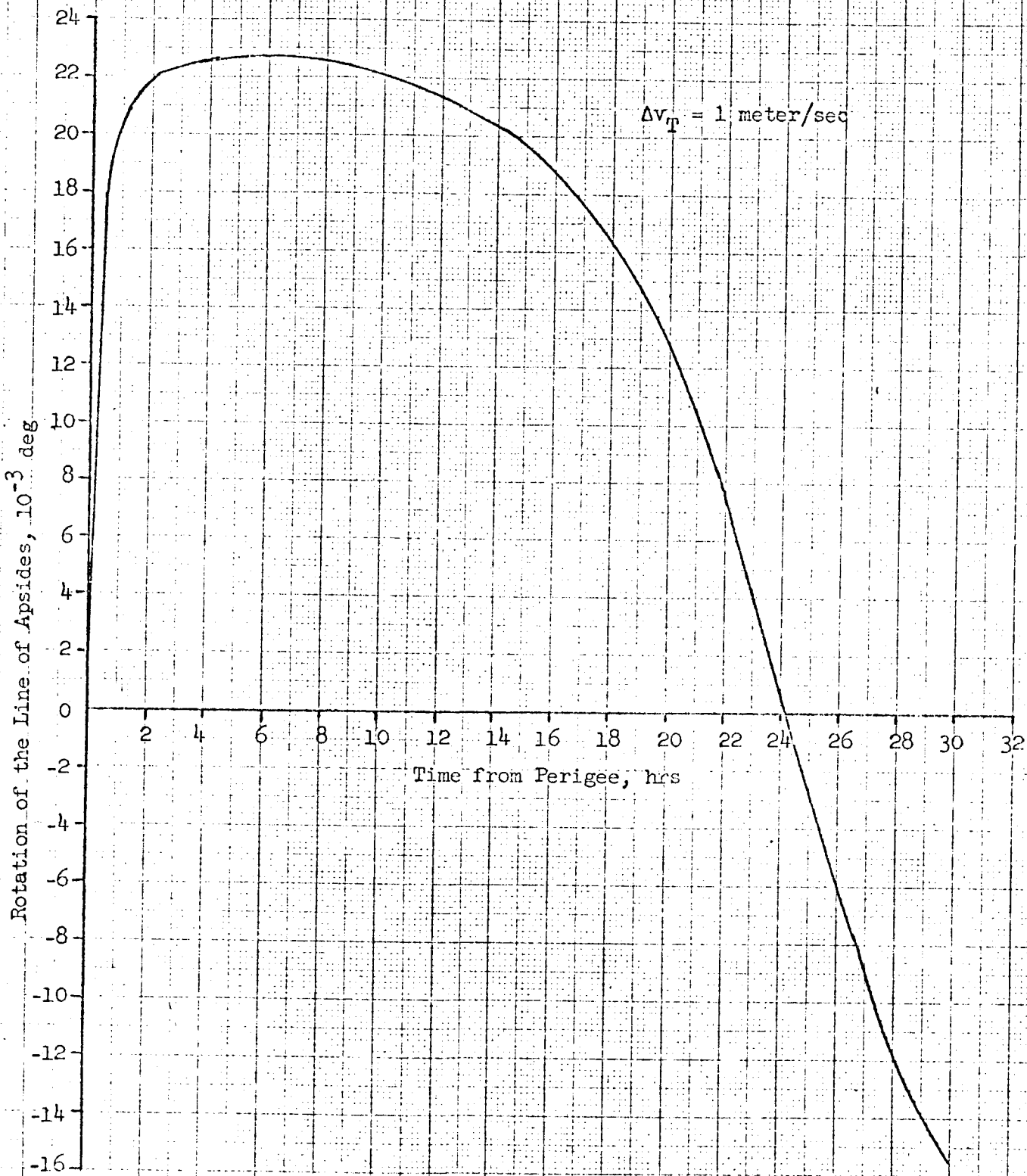

FIGURE P. EFFECT OF TANGENTIAL VELOCITY INCREMENT ON DIRECTION OF LINE OF APSIDES

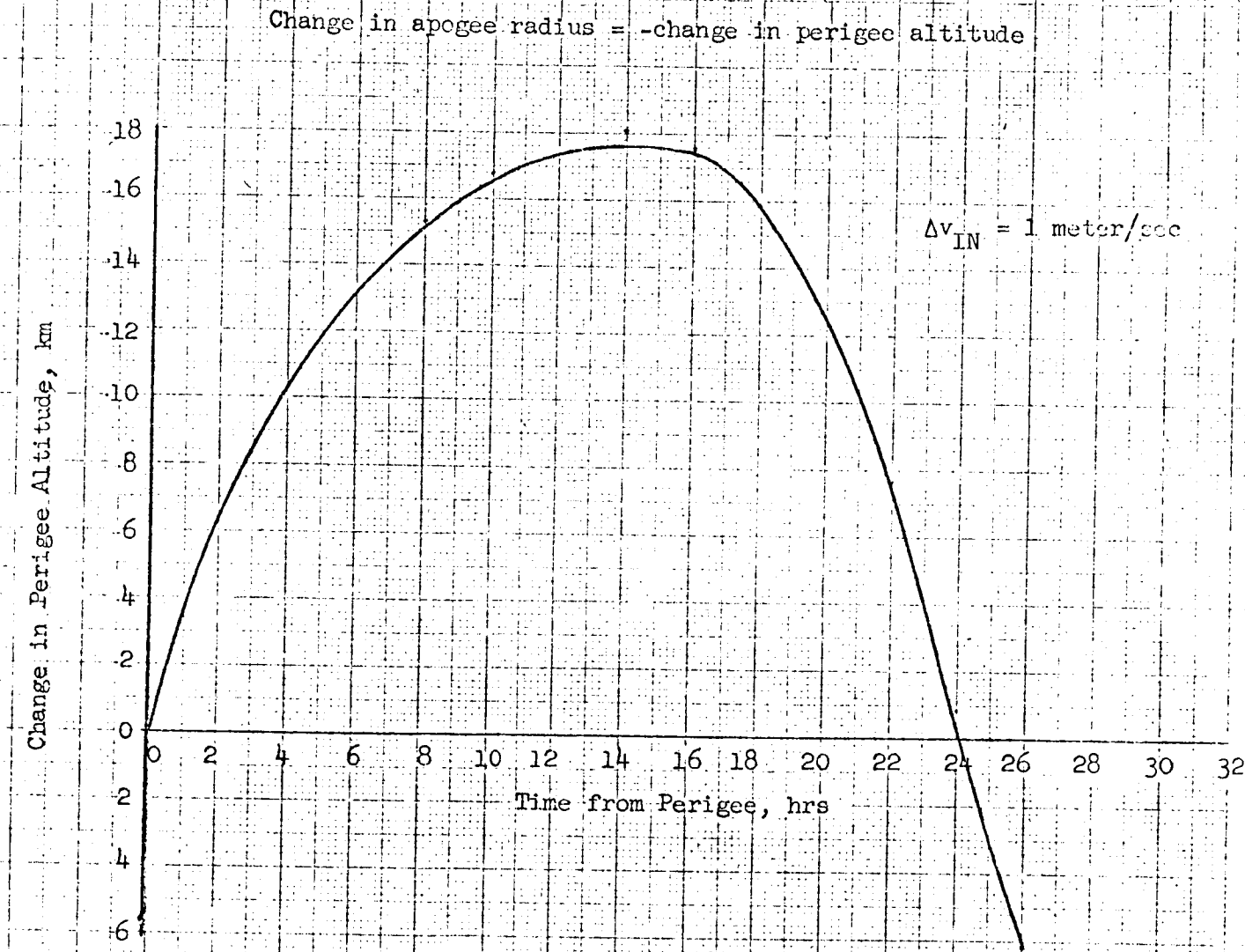

FIGURE Q. EFFECT OF IN-PLANE-NORMAL VELOCITY INCREMENT ON APOGEE RADIUS AND PERIGEE ALTITUDE

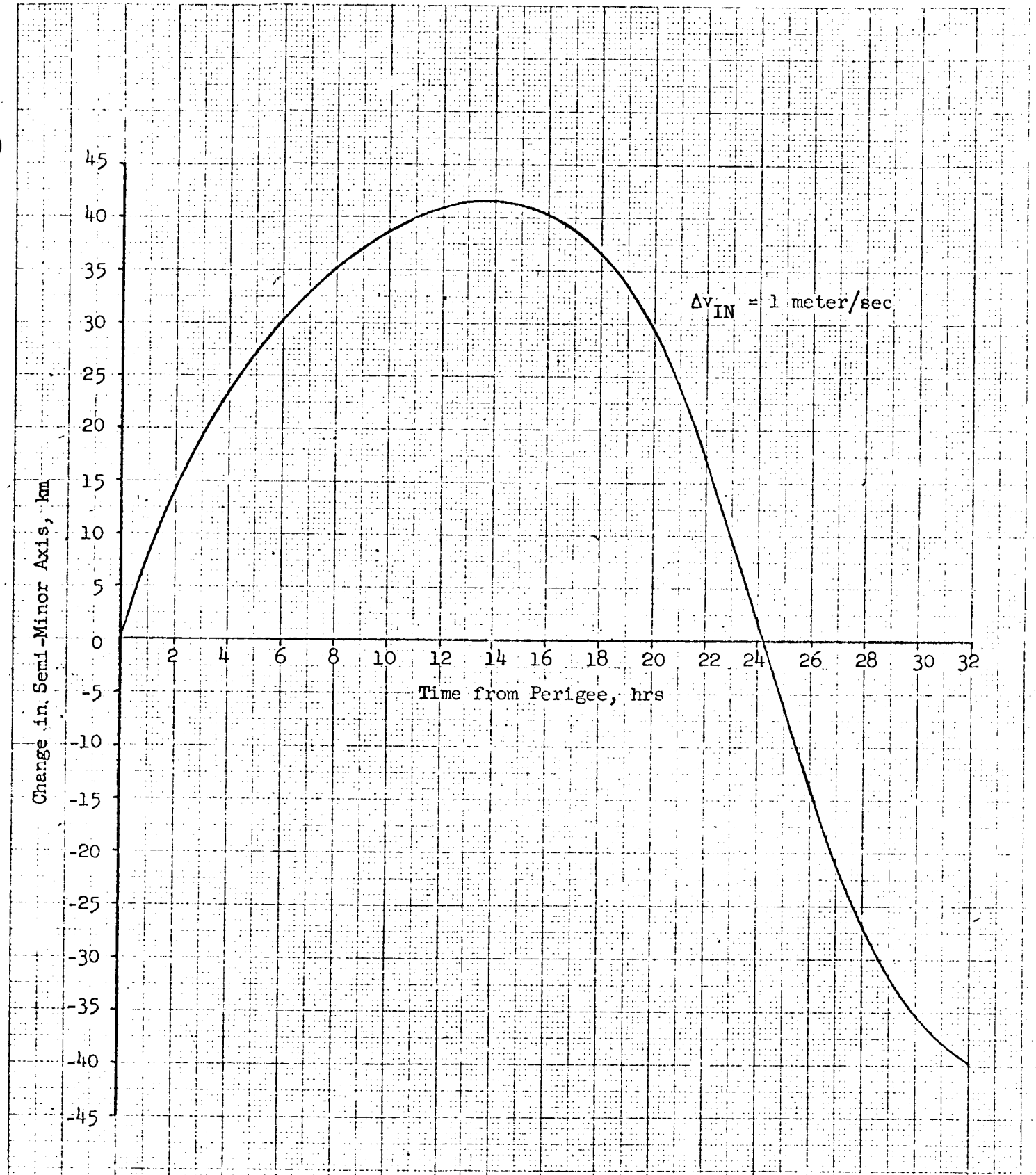

FIGURE R. EFFECT OF IN-PLANE NORMAL VELOCITY INCREMENT ON SEMI-MINOR AXIS

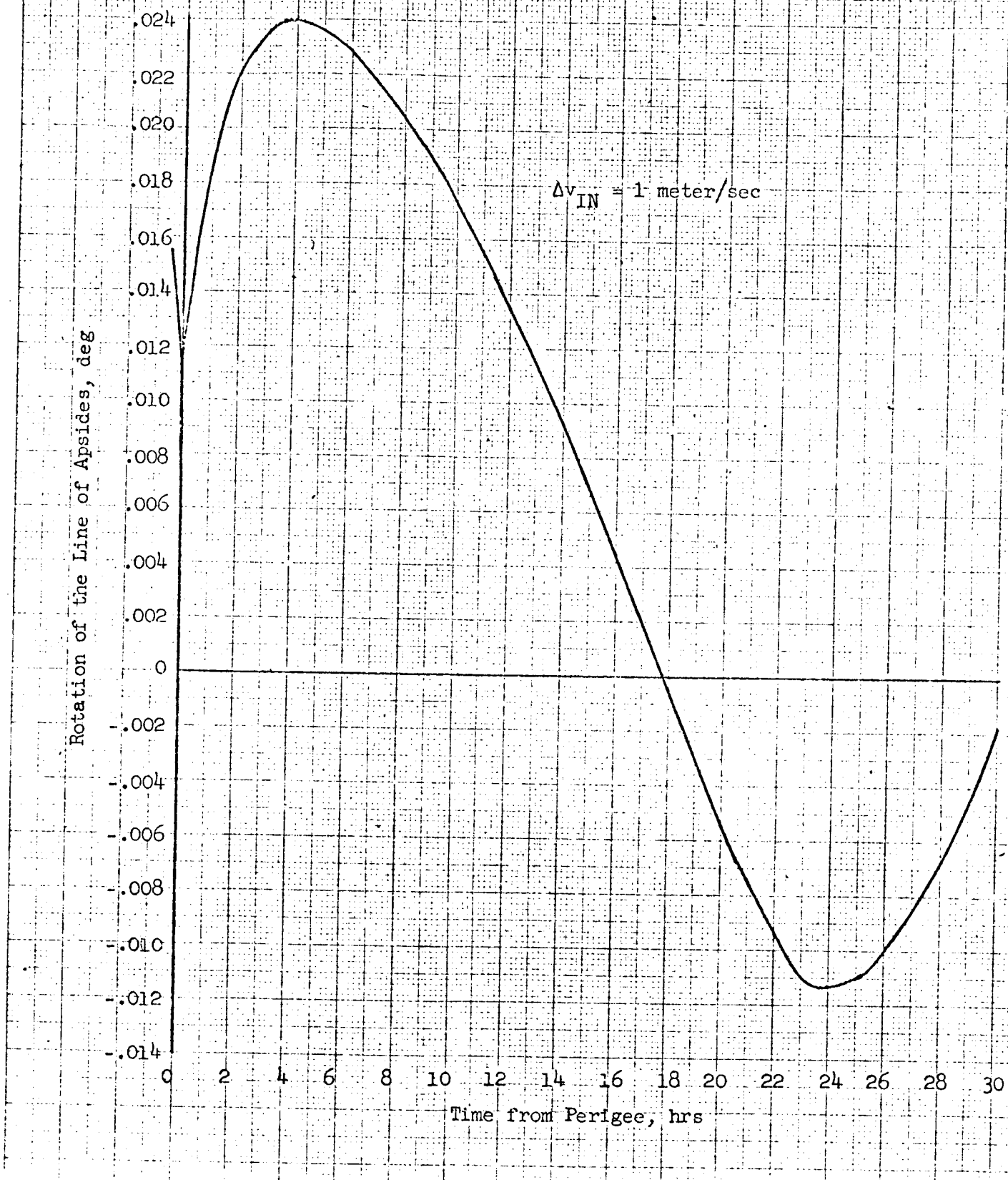

FIGURE S. EFFECT OF IN-PLANE NORMAL VELOCITY INCREMENT ON THE DIRECTION OF LINE OF APSIDES

PRINTED IN U.S.A. ON CLEARPRINT TECHNICAL PAPER NO. 1015
CLEARPRINT PAPER CO. NO. C39X MILLIMETERS 200 BY 270 DIVISIONS

It should be noted that the effects of a velocity increment always combine in such a way that the point of application of the velocity increment remains on the perturbed orbit. For example: an inward normal in-plane velocity increment applied at the semi-minor axis on the ascending leg causes

a. A positive rotation of the line of apsides,

b. An increase in perigee altitude,

c. A decrease in apogee altitude, and

d. An increase in the semi-minor axis.

On the ascending leg at the semi-minor axis, the positive y-component of the separation distance produced by the rotation of the apsides is cancelled by the negative y-component produced by the increase in the semi-minor axis; the positive x-component produced by the rotation of the line-of-apsides is cancelled by the negative x-component produced by the perigee altitude increase and apogee radius decrease. Hence, the point of application of the velocity increment, the semi-minor axis on the ascending leg, remains fixed. At the semi-minor axis on the descending leg the y and the x-components produced by the separate effects are additive; e.g.: the rotation of the line-of-apsides and the increase in the semi-minor axis produce equal positive y-components.

From these considerations it is apparent that a single in-plane normal velocity increment applied at the semi-minor axis on the ascending leg produces a y-component of separation on the descending leg but not on the ascending leg. In the absence of a y-component on the ascending leg, for the section of the orbit in the vicinity of the semi-minor axis, a non-coplanar array could not be obtained so that the time spent passing this section on the ascending leg would not serve the objectives of the experiments. (This situation could be remedied by imparting an outward (negative) in-plane normal velocity increment to a second satellite at the semi-minor axis on the descending leg producing an opposite y-component on the ascending leg along with an increase in perigee altitude.)

4.0 OUT-OF-PLANE EFFECTS

An out-of-plane velocity increment produces a rotation of the orbital plane. To first order apart from the resulting inclination of the perturbed orbit relative to the unperturbed orbit, there are no other changes in the orbit, either in geometry or lead time. The perturbed orbit is rotated about the position vector at the time of application of the velocity increment. Hence, the true anomaly at this time is the true anomaly of the line common to the perturbed and unperturbed orbits.

The relationship between the perturbed and unperturbed orbital planes is precisely analogous to the relationship between the common orbital plane and the ecliptic plane. The z-component of the separation distance, which is produced by and only by the out-of-plane velocity component, depends upon the inclination between the planes and the true anomaly of the common line in the same way as distance from the ecliptic depends upon the corresponding variables (see Figure T). Thus, with appropriate reduction in scaling, Figure B of Appendix V is appropriate to present considerations. Figure U herein was obtained in this way.

The effectiveness of an out-of-plane velocity increment in producing an inclination between the perturbed and unperturbed planes increases as the satellite approaches apogee and its orbital velocity decreases. This is indicated by Figure V which shows the sensitivity of the inclination angle perturbation to out-of-plane velocity increments applied at various times in the orbit. The effectiveness with respect to production of separation distance depends upon the position in the orbit to which reference is made. Figure W shows the effects of out-of-plane velocity increments applied at various times in the orbit on out-of-plane separation distances at apogee. Figure X shows the effects on the separation distances at the semi-minor axis. The sensitivities displayed in Figures V, W, and X are also tabulated in Table 3.

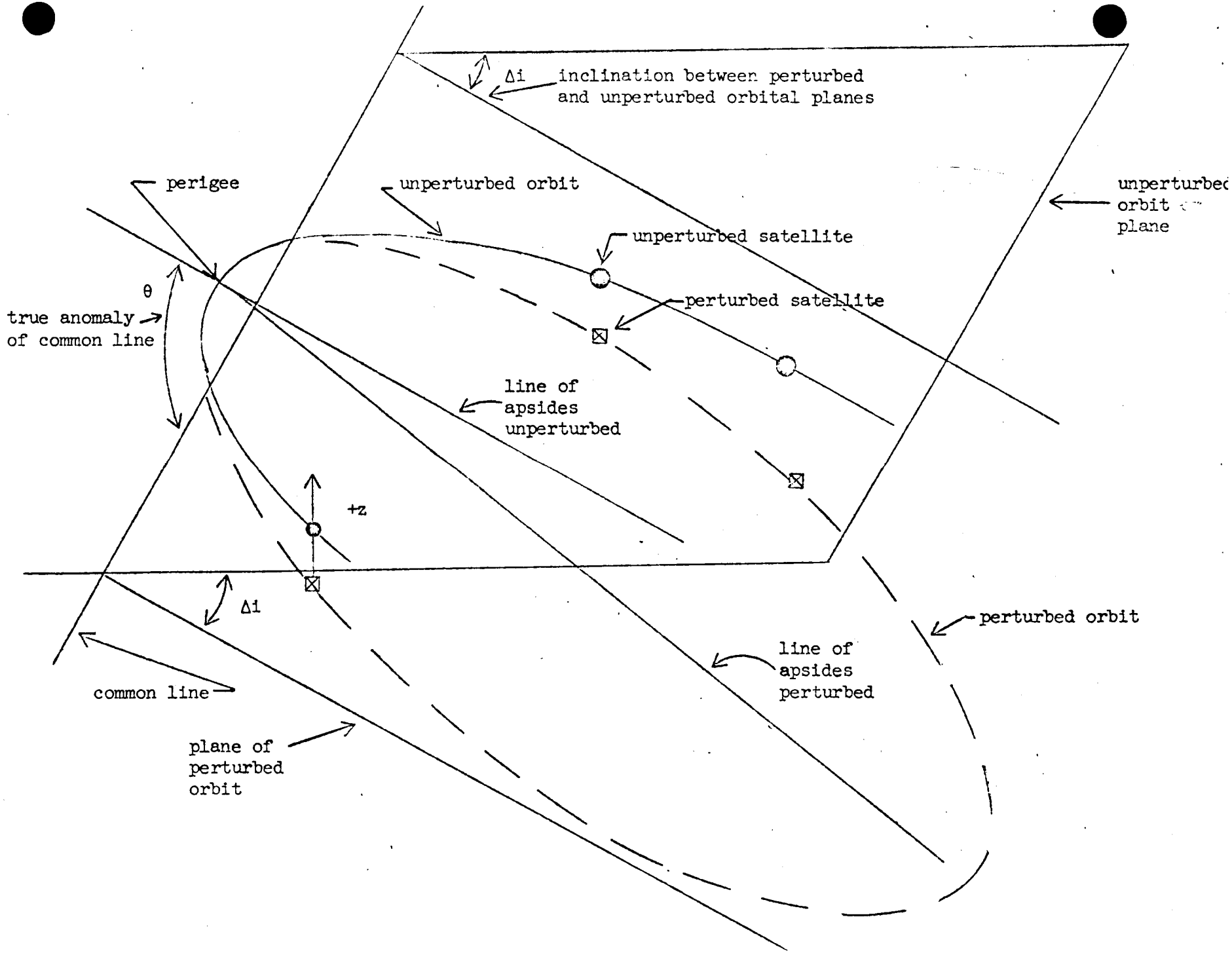

FIGURE T. RELATIONSHIP BETWEEN UNPERTURBED ORBIT AND ORBIT PERTURBED BY OUT-OF-PLANE VELOCITY INCREMENT

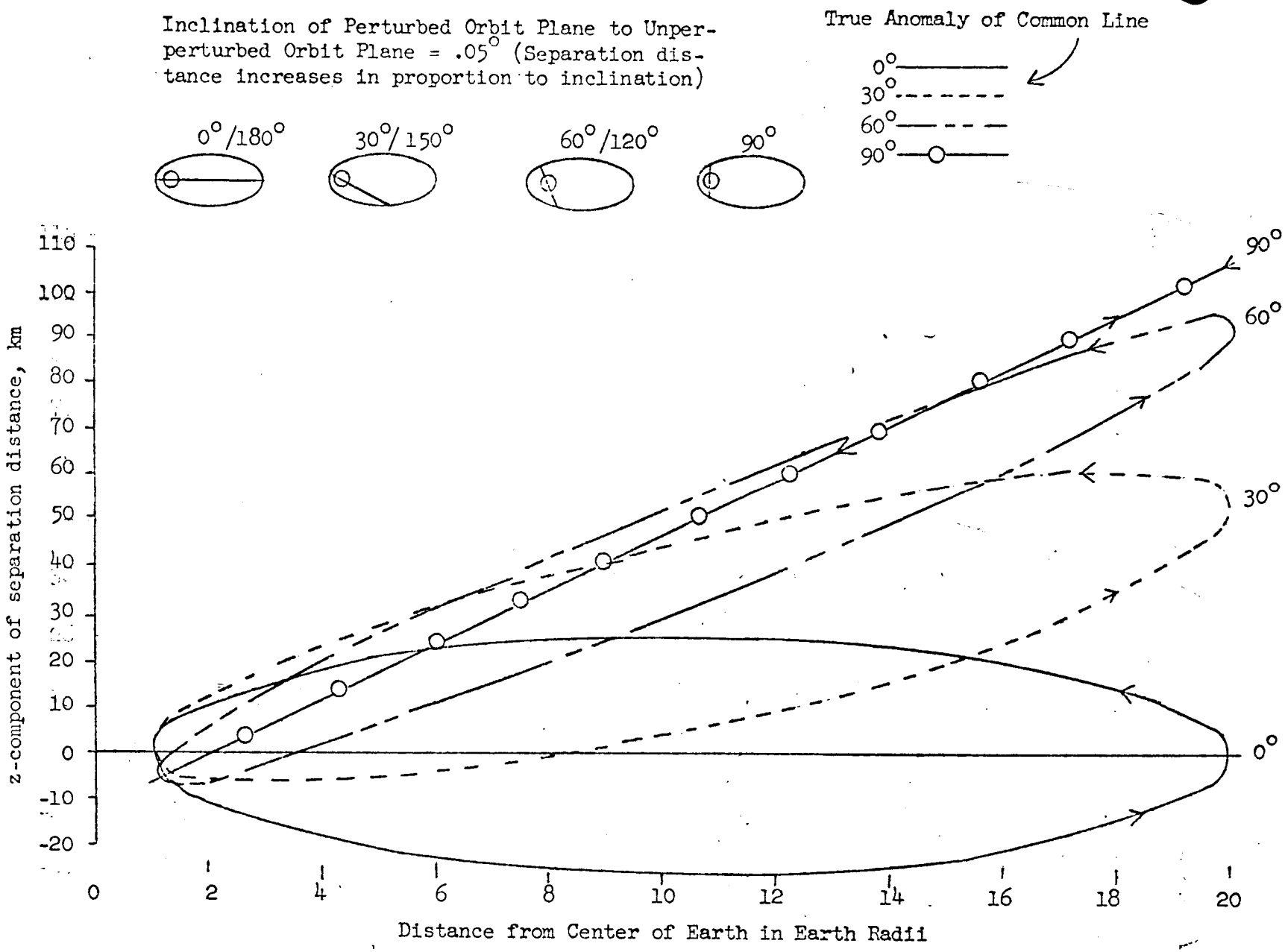

FIGURE U. RELATIONSHIP BETWEEN z-COMPONENT OF SEPARATION DISTANCE, THE INCLINATION BETWEEN PERTURBED AND UNPERTURBED ORBITAL PLANES AND TRUE ANOMALY OF COMMON LINE

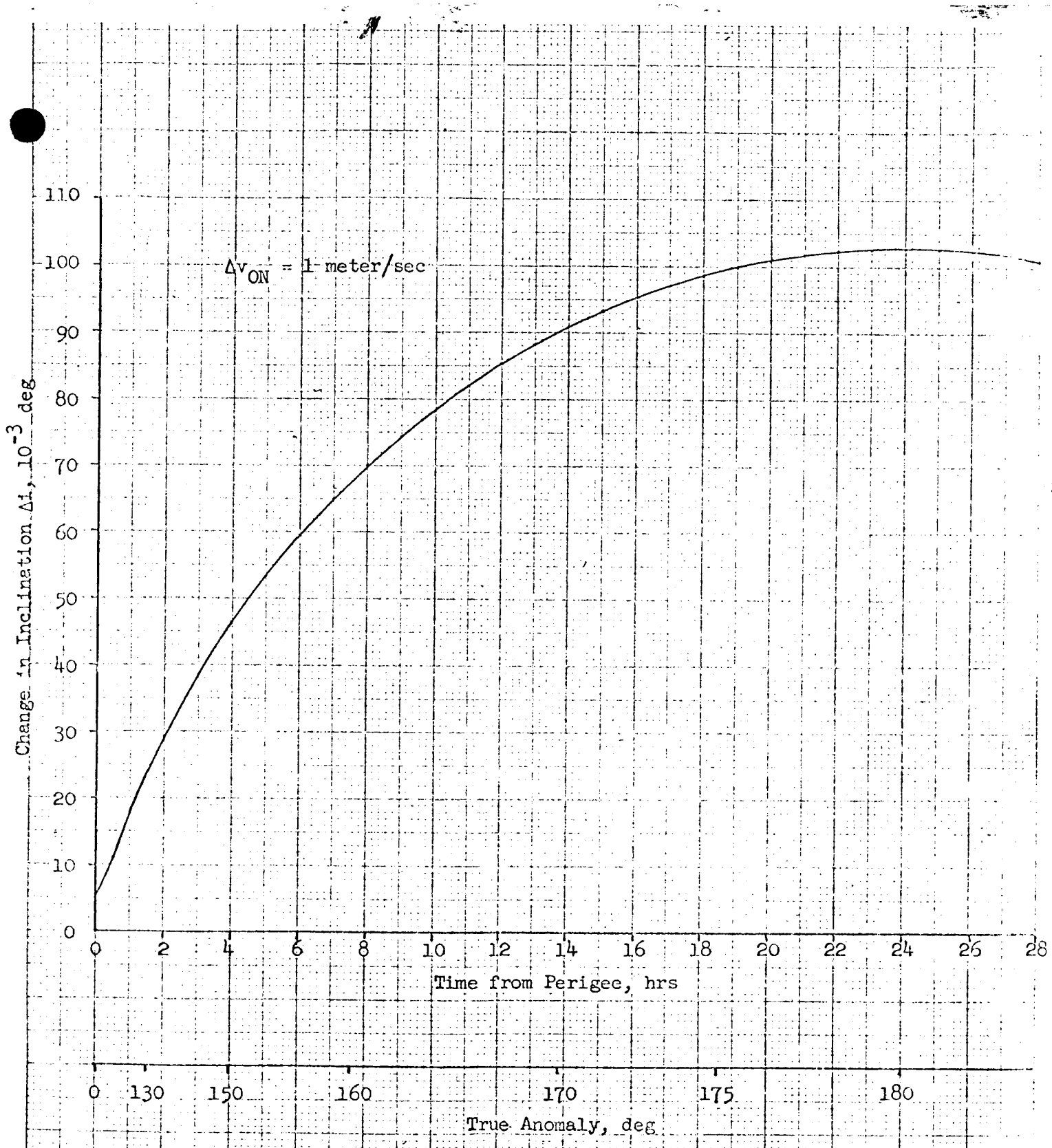

FIGURE V. EFFECT OF OUT-OF-PLANE VELOCITY INCREMENT ON ORBITAL INCLINATION

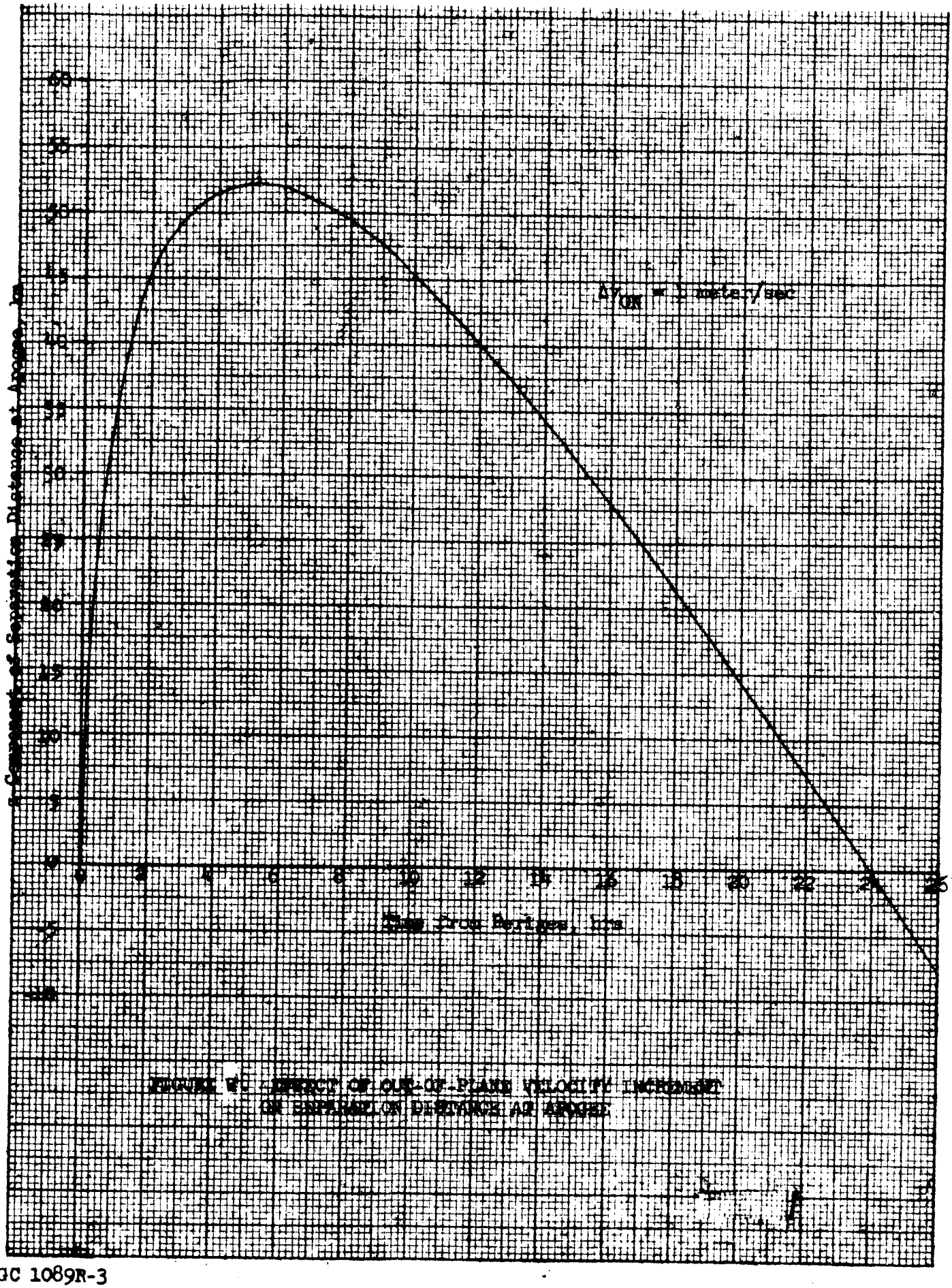

FIGURE [illegible]. EFFECT OF OUT-OF-PLANE VELOCITY INCREMENT ON SEPARATION DISTANCE AT APOGEE

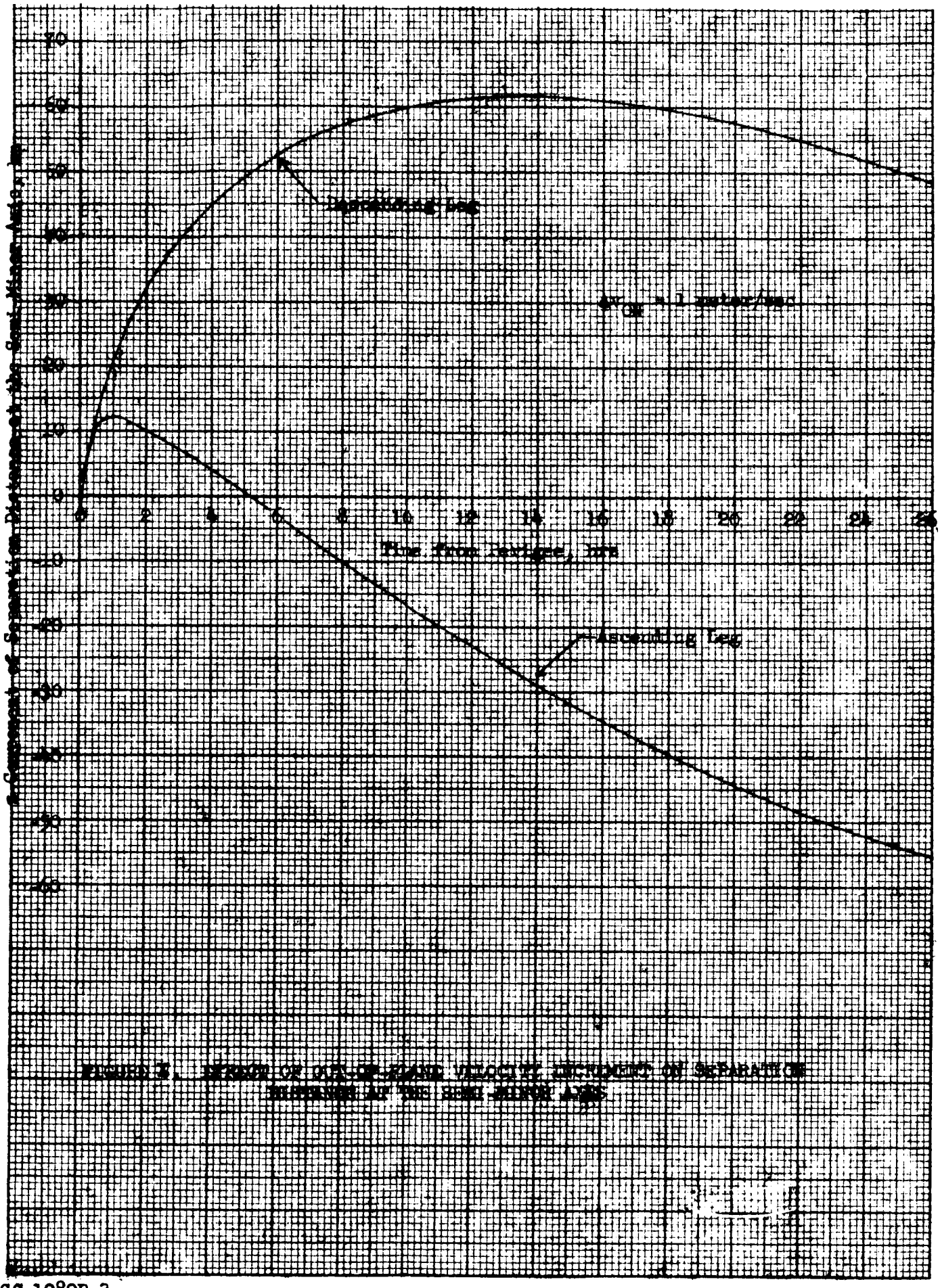

FIGURE X. EFFECT OF OUT-OF-PLANE VELOCITY INCREMENT ON SEPARATION DISTANCE AT THE SEMI-MINOR AXIS

TABLE 3. OUT-OF-PLANE DEPLOYMENT SENSITIVITIES

Reference Orbit		Perturbation due to Δv_{ON} = 1 meter/sec			
			Separation Distance in z-Direction		
				At Semi-Minor Axes	
Time From Perigee hrs	True Anomaly deg	Inclination of Perturbed Orbit, Δi 10^{-3} deg	At Apogee km	Ascending Leg km	Descending Leg km
0	0	5.37	0	2.73	-2.73
0.5	94.80	11.04	24.46	11.12	12.06
1.0	118.63	17.95	35.04	12.24	20.98
1.5	129.63	23.99	41.08	11.69	27.24
2.0	136.39	29.34	45.00	10.54	32.12
3	144.74	38.59	49.54	7.46	39.49
4	150.04	46.47	51.61	4.00	44.91
5	153.88	53.36	52.25	0.42	49.10
6	156.88	59.47	51.94	-3.17	52.40
7	159.34	64.94	50.95	-6.73	55.02
8	161.44	69.86	49.45	-10.22	57.09
9	163.28	74.31	47.55	-13.63	58.70
10	164.91	78.34	45.34	-16.94	59.92
11	166.40	81.97	42.87	-20.17	60.80
12	167.76	85.26	40.19	-23.29	61.38
13	169.03	88.21	37.33	-26.31	61.69
14	170.22	90.86	34.32	-29.23	61.76
15	171.35	93.21	31.19	-32.04	61.60
16	172.42	95.28	27.96	-34.74	61.24
17	173.45	97.09	24.63	-37.34	60.68
18	174.44	98.64	21.24	-39.82	59.95
19	175.41	99.94	17.78	-42.19	59.04
20	176.36	100.99	14.27	-44.45	57.97
21	177.28	101.81	10.73	-46.59	56.75
22	178.20	102.39	7.16	-48.61	55.39
23	179.11	102.73	3.57	-50.50	53.88
24	180.01	102.85	-0.03	-52.27	52.24
25	180.91	102.73	-3.63	-53.91	50.47
26	181.82	102.38	-7.22	-55.41	48.57
27	182.73	101.80	-10.79	-56.78	46.55
28	183.66	100.98	-14.33	-57.99	44.41
29	184.60	99.18	-17.84	-59.06	42.15
30	185.57	98.62	-21.30	-59.96	39.78

Appendix X

DEPLOYMENT VELOCITY AND ACCURACY REQUIREMENTS

1.0 INTRODUCTION

Based upon the deployment sensitivities discussed in Appendix IX, this appendix reviews the general considerations relating to the deployment of the satellites. Minimum velocity increment and accuracy requirements associated with the attainment of large separation distances are derived and consideration is given to the adaptation of the various deployment options projected in Appendix I to the attainment of large separation distance. It appears that obtaining separation distances in the order 2,500 km, while avoiding an unwanted growth in separation distance greater than 7,500 km in 6 months would be difficult for Options 1 to 3, while option 4 could achieve these separation distances. By relaxing the separation requirements from those specified in Appendix II to 500 to 1000 km and a total growth of 15,000 km after 6 months option 3 becomes feasible (see Appendix III).

2.0 GENERAL DEPLOYMENT CONSIDERATIONS

To satisfy the scientific objectives of the mission, it is required that the four satellite array be non-coplanar, particularly in the region of interest, i.e., from about 10 to 18 R_e. This demands that all three components: x, y and z * be represented among the intersatellite separation distances when the satellites traverse this region. The x and y components are obtained from the in-plane components of the deployment velocity increments, while the z component is obtained from the out-of-plane component of the velocity increment.

The in-plane components of the velocity increment affect the in-plane separation distances through:

a. Changes in lead time

b. Rotation of the line of apsides

c. Changes in semi-minor axis, and

d. Changes in apogee radius.

The separation distances produced by changes in lead time are not consistently in the x or y direction but are directed along the orbit following the direction of the orbital velocity vector. These distances also vary in magnitude in proportional to the variation of the magnitude of the velocity vector. They are the only separation distances that are expected to exhibit a marked tendency to grow with time in orbit. This growth stems from differences in orbit period, which causes a steady increase in the lead time. Initial differences in orbital period will arise from the tangential component of the velocity increment. Subsequently differences in period can grow as a result of differences in ballistic coefficient and/or perigee altitude and other secondary effects.

An excessive growth in separation distances due to increasing differences in lead time appears to be undesirable since: (a) in the absence of growth in the other components of the separation distances, the growth due to lead time does not produce a uniform non-coplanar array, i.e., in two directions the separation distances will remain small; the growth would occur in one direction only; (b) when the separation distance in one direction exceeds the scale of spacial variations interpretation of the experimental data may be clouded; in particular, in the presence

* See Figure A, Appendix IX for definition of x, y, z reference axis.

disturbance front curvature, the measurement of propagation velocities which requires data from all four satellites could be adversely affected.

A growth of separation distances to 15,000 km in 6 months was originally advocated in the RFP. Assuming this to be the planned growth, it would appear that growth due to uncontrolled factors should be kept substantially smaller. Accordingly for present purposes allowable growth due to deployment errors has been taken to be 7,500 km in 6-months. Referencing the separation distance to the section of the orbit near 10 R_e, this corresponds to an initial difference in orbital period of .02%.

The requirement for avoiding excessive growth in orbital distances imposes an accuracy requirement on the tangential component of the velocity increment (which is the only component that has a first order affect on the orbital period), Also, as indicated in Figure E of Appendix IV, in order to avoid an excessive growth in period differences, the perigee altitude of the lowest satellite must exceed a value that depends upon the differences in perigee altitude which may be generated by the deployment.

3.0 IN-PLANE SEPARATION REQUIREMENTS

Differences in lead time do not produce separation distances in (a) the y-direction in the vicinity of the semi-minor axis, or (b) in the x-direction in the vicinity of apogee. As discussed in Appendix IX it may be possible to dispense with separation in the x-direction at apogee, but separation in the y-direction near the semi-minor axis is essential.

Separation in the y-direction arises from the effects of apsidal rotation and change in the length of the semi-minor axis. These effects can be obtained from a tangential and/or in-plane normal velocity increment. Figure A shows the effect on the y-component of the separation distance at the semi-minor axis of 1 meter/sec tangential velocity increments applied at various times in the orbit; Figure B shows the effect of in-plane normal velocity increments.

If only small initial separation distances are desired, it is possible to obtain the y-component of the separation distance at the semi-minor axis from the tangential velocity increment alone. This is indicated by the results presented in Figure C which shows the magnitudes of the tangential velocity components required to produce a .04% change in period and the corresponding separations that are obtained in the y-direction at the semi-minor axis. It is seen that a tangential velocity increment of about 1.4 meter/sec applied near apogee will produce, along with the period change, a y-component in the order of 80 km at the semi-minor axis on both the ascending and descending legs of the orbit. (Since in this case, the y-components are produced mainly by an increase in the semi-minor axis, the signs of the component on the ascending and descending legs are opposite.) The corresponding change in perigee altitude would be about 36 km.

Inasmuch as the nominal value of the tangential velocity increment are not to be increased beyond the values corresponding to a .04% change in period, larger values for the y-component of the separation distance at the semi-minor axis must be obtained from the in-plane normal velocity increment; and since the sensitivity to the two in-plane velocity components are of about the same order of magnitude, it is apparent that to obtain a y-component of separation distance very much larger than 80 km will generally require that the normal velocity increment

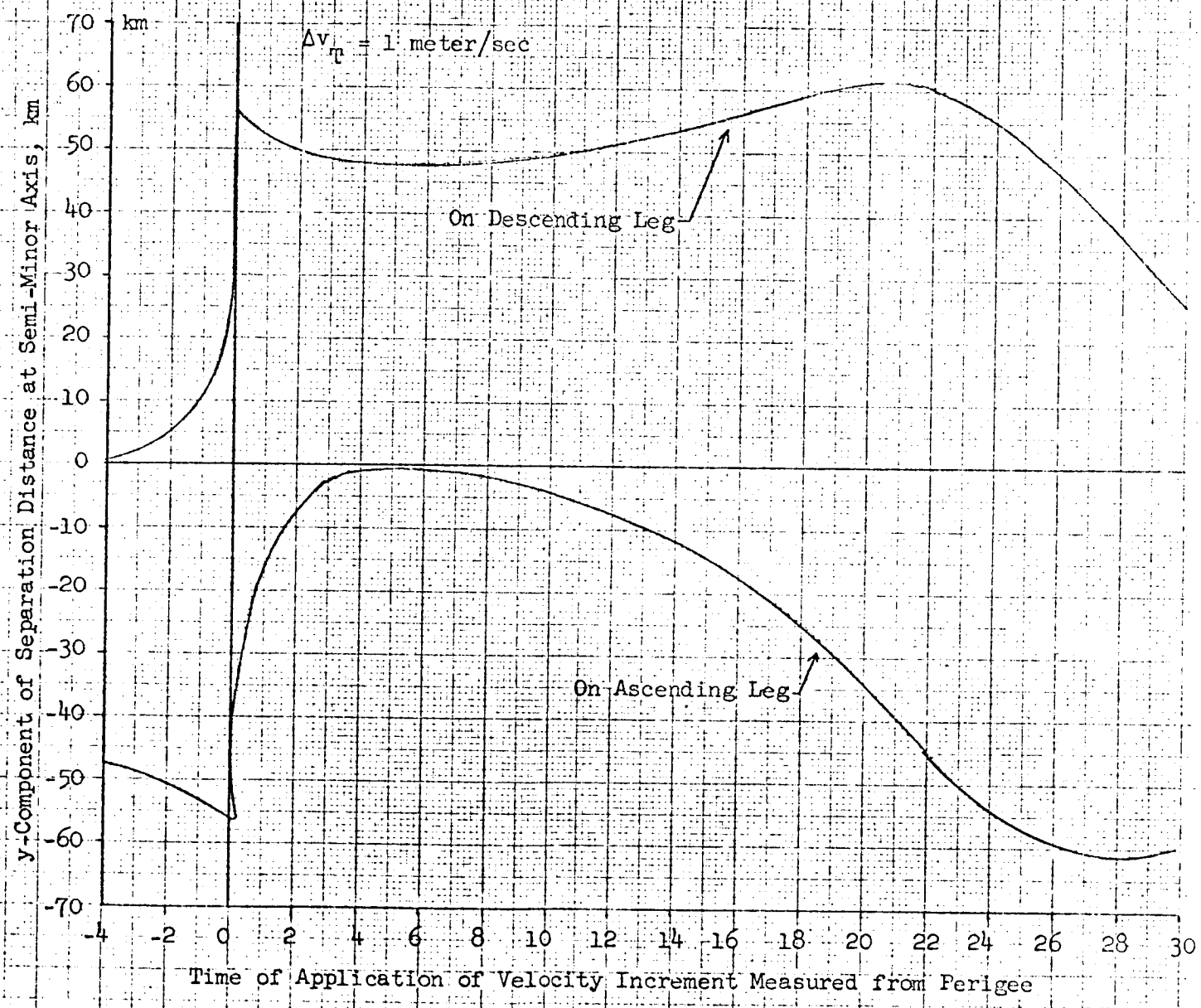

FIGURE A. EFFECT OF TANGENTIAL VELOCITY INCREMENT ON SEPARATION AT THE MINOR AXIS

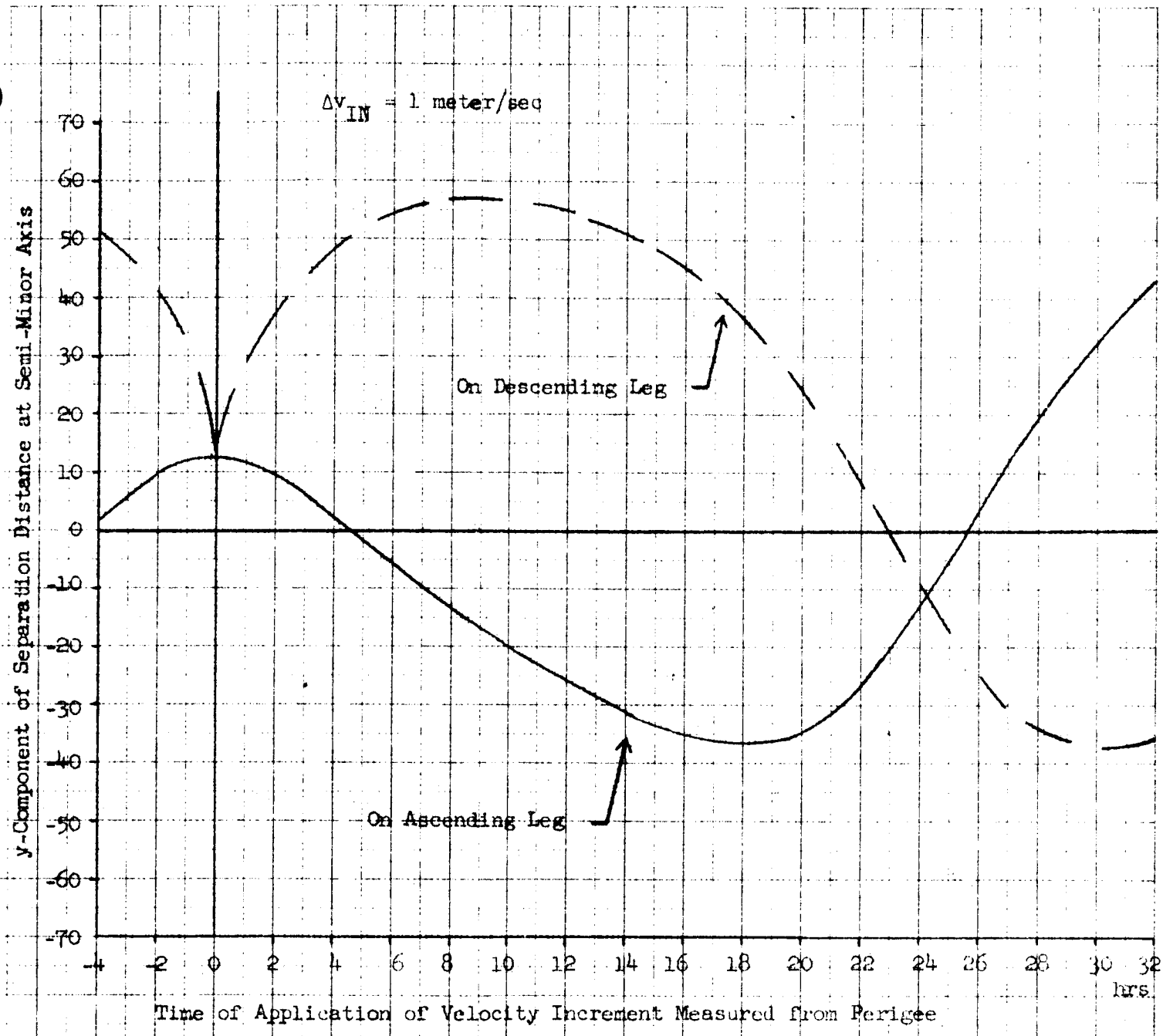

FIGURE B. EFFECT OF IN-PLANE NORMAL VELOCITY INCREMENT ON SEPARATION AT THE MINOR AXIS

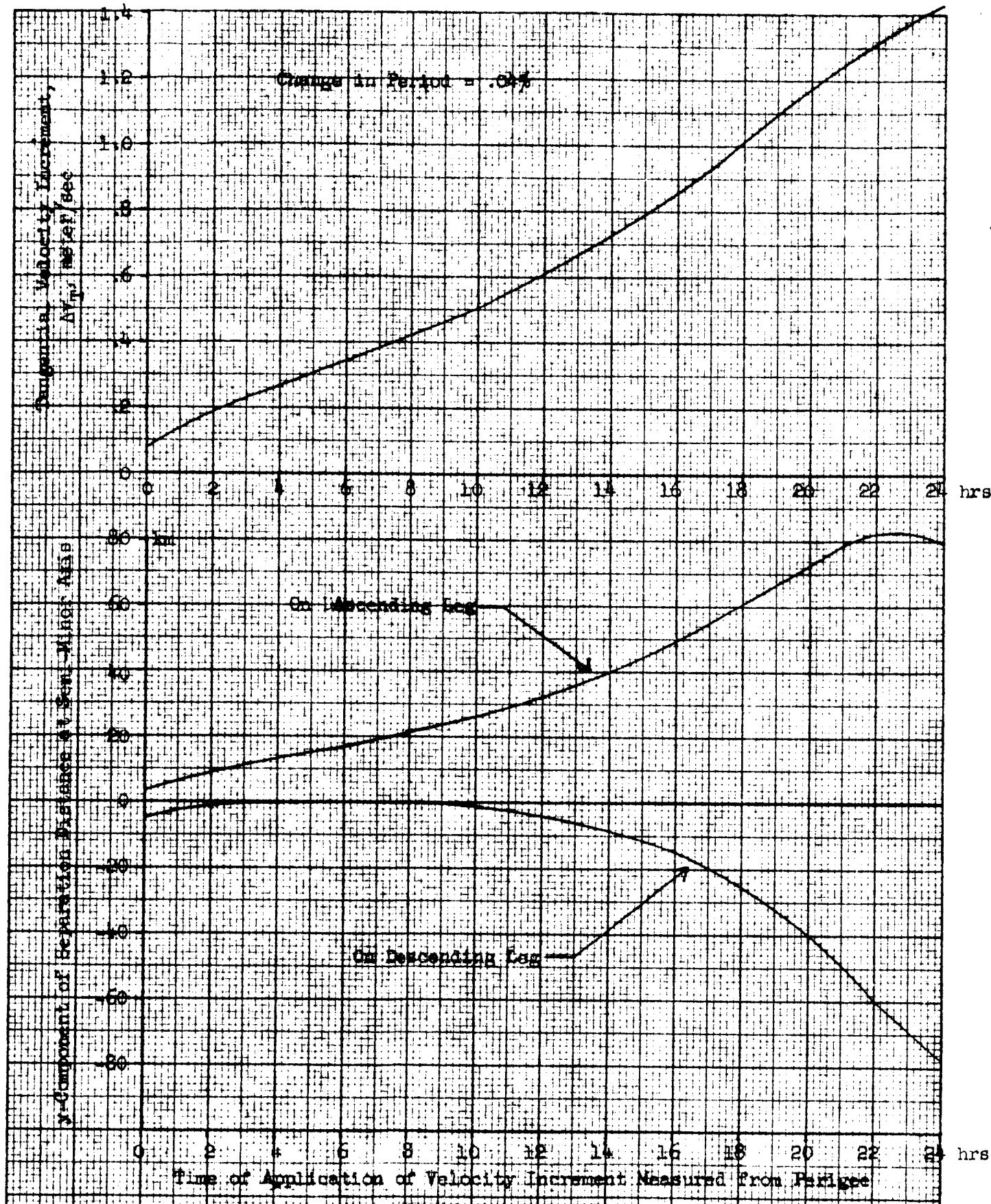

FIGURE C. TANGENTIAL VELOCITY INCREMENT REQUIRED FOR .04% CHANGE IN PERIOD AND CORRESPONDING EFFECTS ON y-COMPONENT OF SEPARATION DISTANCE

K+E 10 X 10 TO ½ INCH 46 1323
7 X 10 INCHES
KEUFFEL & ESSER CO.

be much larger than the tangential component. The velocity increment vector will then be directed very nearly along the normal to the orbit and errors incurred in the direction of applying the increment will have a strong effect on the tangential velocity increment. For the purpose of evaluating the accuracy requirements it will be assumed that the y-component is to be obtained entirely from the in-plane normal velocity increment. (When the in-plane normal velocity increment is much larger than the tangential velocity increment, the presence of a non-zero tangential velocity component chosen to obtain the desired growth in separation distance will increase the accuracy required to prevent an excessive growth in separation distance.)

As seen in Figure B, except for a section of the orbit near apogee, an in-plane normal velocity increment applied on the ascending leg of the orbit produces a y-component at the minor axis that is of greater magnitude on the descending than on the ascending leg. Figure D shows the in-plane normal velocity increments required to make the larger of the two y-components of the separation distance on the minor axis equal to 1,000 km. Also shown in Figure D are the corresponding values of: (a) the smaller of the two y-components of the separation distance on the minor axis, (b) the attitude error that would cause a .02% change in period, and (c) the change in perigee altitude.

These results can be extrapolated for other separation distances by scaling the velocity increment, the smaller y-component and the change in perigee altitude in direct proportion, and the altitude error corresponding to a .02% period change in inverse proportion to the larger y-component.

The results presented in Figure D apply to a one-part deployment, i.e., the in-plane normal velocity increment is applied at only one point in the orbit. This increment could be applied either (a) to one satellite only, or (b) differentially between a pair of satellites. The main difference between these alternatives is that in the former case the sign of the increment could be chosen to increase perigee altitude; in the latter case, of necessity, perigee altitude would increase for one satellite and decrease for the other, but the magnitude of the change for each would be half as great.

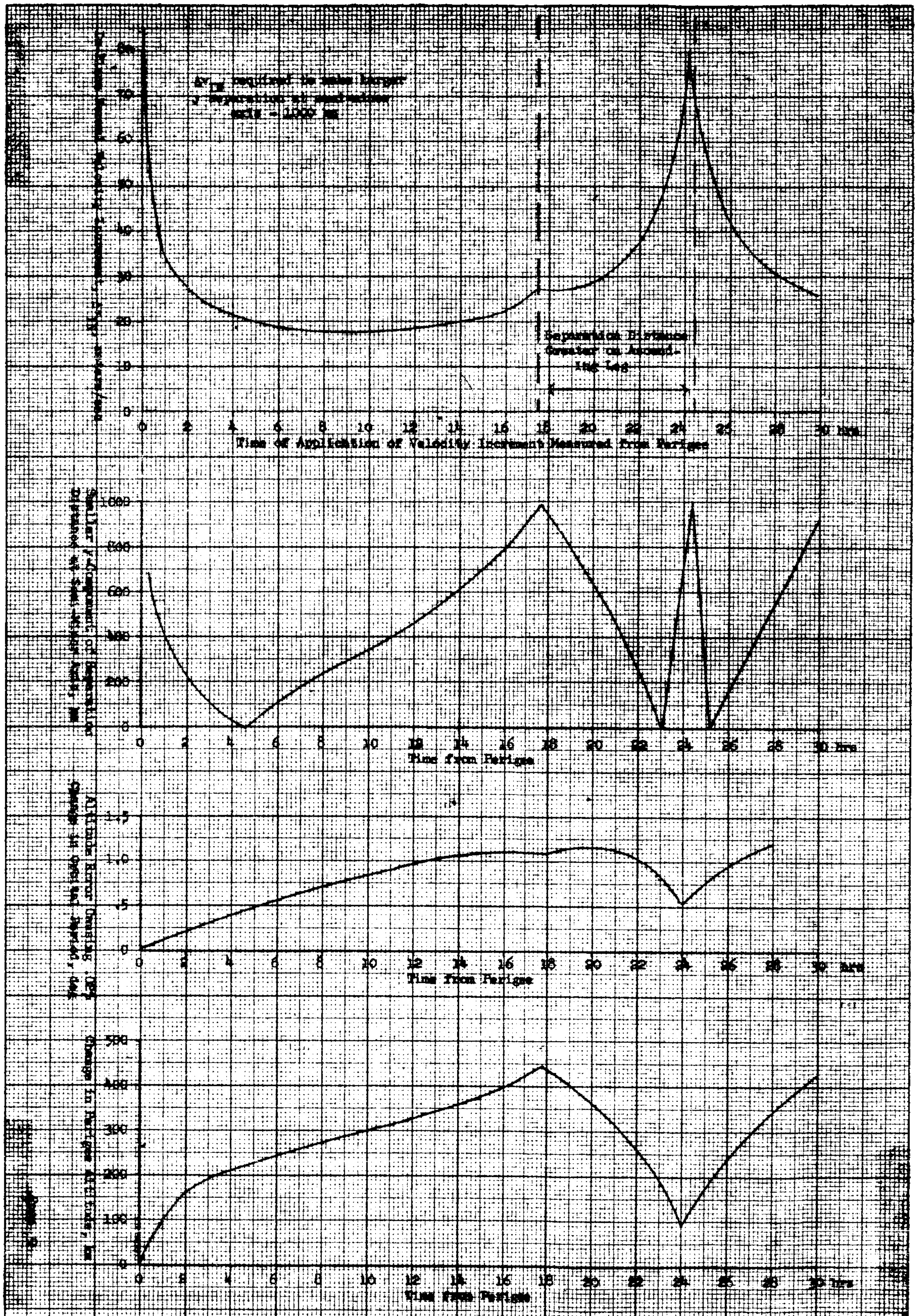

FIGURE D. IN-PLANE NORMAL VELOCITY INCREMENT REQUIRED TO OBTAIN 1000 km y-COMPONENT AT SEMI-MINOR AXIS

Since only one opportunity is available, for a one-part deployment it is important that a sizeable y-component of separation distance be obtained on both legs of the orbit, It is noted in Figure D that a time of application of the velocity increment near 18 hours from perigee does yield nearly equal y-components along with a near-maximum allowable attitude error. Furthermore the magnitude of the velocity increment required for deployment at this time while not minimum is still comparatively small. The main disadvantage of a deployment at this time is the large change in perigee altitude which would require that a larger initial perigee altitude be obtained prior to deployment.

Considerations relating to the application of in-plane normal velocity increments at two or more points in the orbit are rather complex. Depending on the particular circumstances involved in the deployment implementation, advantages could be gained in the way of (a) obtaining large y-components of separation distance at the semi-minor axis on both legs of the orbit and/or better distribution of separation distances normal to the orbit at distances from the earth greater than 10 R_e, with lessor restrictions on the time of application of the velocity increment; (b) restricting perigee altitude changes to increases, and (c) obtaining compensation for some types of altitude errors. However, it seems clear that no advantage would be gained witn regard to magnitude of the velocity increments required and it is unlikely that any large advantage with respect to accuracy requirements would be realized. This is particularly apparent for the case where the velocity increments are always applied differentially between pairs of satellites.

4.0 OUT-OF-PLANE SEPARATION REQUIREMENTS

Velocity and accuracy requirements associated with the attainment of the out-of-plane, i.e., z-component of the distance, depend not only on the magnitude but also on the pattern desired for the out-of-plane separation distance. Both velocity and accuracy requirements are more stringent if a substantial out-of-plane separation distance at apogee is deemed necessary. As apogee is approached and the orbital velocity decreases, the sensitivity of the change in orbital inclination to the out-of-plane velocity increment increases; but full advantage of this increased sensitivity cannot be realized with respect to attaining out-of-plane distances at apogee because the distance of apogee from the axis about which the perturbed plane is inclined is reduced, and finally vanishes as apogee is approached. Hence, to attain substantial out-of-plane separation at apogee with a reasonably sized velocity increment requires that the point of application be well removed from apogee. Removal of the point of application of the velocity increment prevents maximum advantage to be taken of the low sensitivity of the orbital period to tangential velocity that applies near apogee, and thus leads to more stringent accuracy requirements.

These comments are illustrated by the results given in Figure E which show the magnitudes of the out-of-plane velocity increments required to obtain a 1000 km out-of-plane separation distance at apogee and the corresponding attitude errors that would produce a .02% change in orbital period. Also shown in Figure E are the velocity and accuracy requirements for a 1000 km out-of-plane separation distance at the semi-minor axes (i.e., at about 10 R_e). It is seen that from an accuracy viewpoint, the optimum point for the application of the velocity increment for attaining the out-of-plane separation distance at apogee is about 14 hours from perigee; the 1000 km separation distance at the semi-minor axis can be obtained with much smaller velocity increments and much larger allowable directional errors by applying the velocity increment close to apogee, specifically at about 23 hours after perigee passage, but a deployment at this time would yield very little out-of-plane separation at apogee.

Although it may be admissible to accept a near planar satellite array in the vicinity of apogee, the scientific objectives of the mission require that a

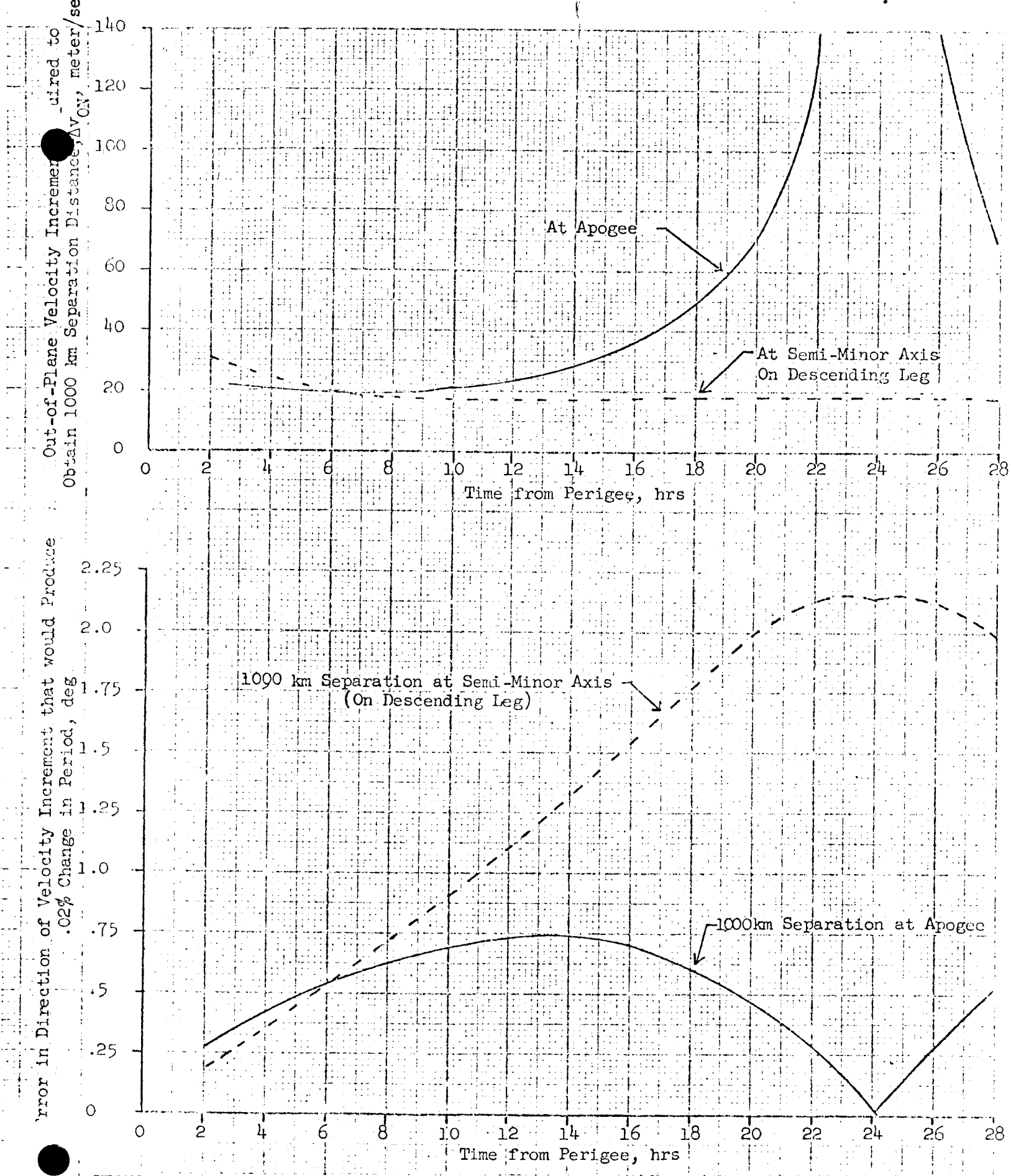

FIGURE E. OUT-OF-PLANE VELOCITY INCREMENT REQUIRED FOR 1000 km SEPARATION DISTANCES AND CORRESPONDING ANGULAR ERROR THAT WOULD CHANGE PERIOD BY .02%

non-coplanar array be obtained at points well beyond the transition region. To satisfy this requirement it is concluded that a substantial out-of-plane separation distance in the vicinity of 18 R_e will be desired. If an out-of-plane velocity increment of about 20 meters/sec is applied at apogee to achieve a 1000 km out-of-plane separation at the semi-minor axis, the out-of-plane separation at 18 R_e would be about 600 km.

Perhaps a better compromise would be obtained by application of the velocity increment somewhat prior to apogee. At about 20 hours from perigee a 20 meter/sec velocity increment produces the out-of-plane separation distances indicated in Figure F. It is seen that separation distances of fairly large magnitude are then obtained in the region of most interest, i.e., from 10 to 14 R_e on both legs of the orbit. At 18 R_e on the leg opposite to that on which the velocity increment is applied at 880 km out-of-plane separation distance is obtained. For such a deployment an error in the direction of the velocity increment of about 2 deg would produce a change of .02% in period.

It is noted that a deployment near 14 hours from perigee, designed to achieve a specified out-of-plane distance at apogee with minimum accuracy requirement, would produce large separation distances in the 10 to 14 R_e region on the opposite leg, but the separation distances in this region on the same leg of the orbit on which the increment is applied would be very small. This problem could be averted through the use of a two-part deployment wherein one velocity increment is applied about 14 hours prior to perigee, and a second velocity increment is applied 14 hours after perigee, with the sense of the increments chosen so that the separation distances produced at apogee are additive. The net result of such a deployment would be to rotate the final perturbed orbit about the semi-latus rectum. Although a rotation about the semi-latus rectum could be achieved by a single velocity increment applied at the crossing of the semi-latus rectum (i.e., about 1/2 hour from perigee), the two-part deployment requires a smaller total velocity increment and is much more tolerant of attitude errors. For a 1000 km out-of-plane separation at about 10 R_e, the velocity increment for a two-part minimum accuracy deployment would be about twice that required to obtain a 1000 km separation at apogee with a single velocity increment, or approximately 60 meter/sec. To the

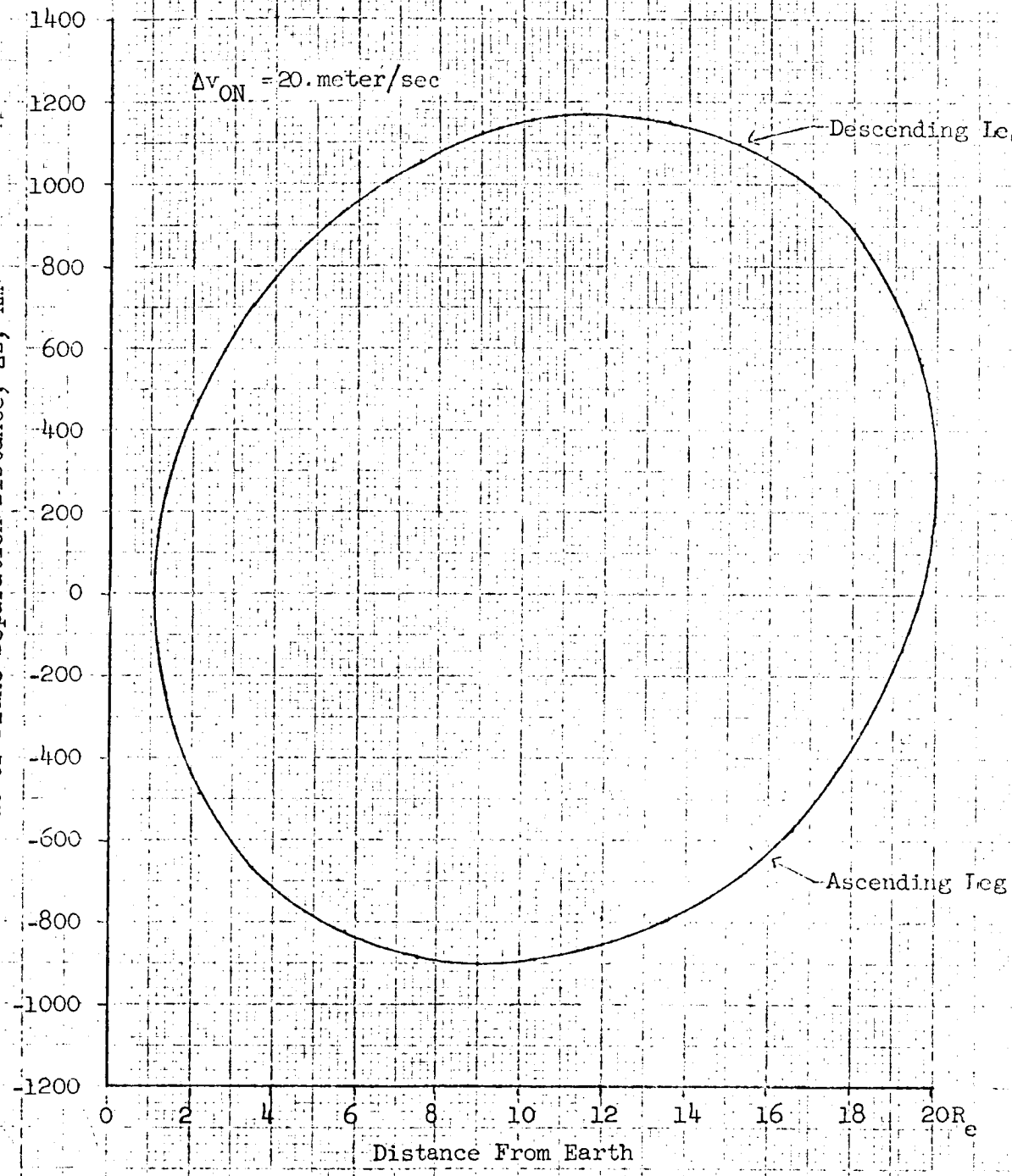

FIGURE F. SEPARATION DISTANCES PRODUCED BY A 1 mps OUT-OF-PLANE VELOCITY INCREMENT APPLIED 20 HOURS AFTER PERIGEE PASSAGE

extent that the attitude errors for the two increments were consistent, the allowable error would be reduced by a factor of two, e.g., the error corresponding to a period change of .02% would be about .4 deg. If the errors were statistically independent a reduction factor of $\sqrt{2}$ would apply yielding an error of about .5 deg for a .02% period change. (In general there may be some possibility for implementing two-part deployments so as to achieve compensation of attitude errors. However, it can be shown that this possibility is not applicable to the type of two-part deployment considered here.)

For the present it will be assumed that out-of-plane deployment using a single velocity increment applied at about 20 hours after perigee is acceptable. The velocity requirement for out-of-plane separation distances in the order of 1000 km will then be about 20 meter/sec with a 2 deg attitude error corresponding to a .02% change in orbital period. Comparison with in-plane requirements, see Table 1, indicates that the out-of-plane requirements are then somewhat less demanding both with respect to velocity and accuracy requirements.

It should also be noted that depending upon the deployment scheme used, the time at which the velocity increments must be applied may be restricted so that the optimum choice with respect to either velocity increment or accuracy requirements is not available. This situation leads to even more stringent requirements.

Table 1

DEPLOYMENT VELOCITY AND ACCURACY REQUIREMENTS

Separation Distance	500 km	1000 km	2500 km
In-Plane Requirements(1)			
Velocity Increment, m/sec	13.	26.	65.
Attitude Error, deg(3)	2.2	1.1	.44
Out-Of-Plane Requirements(2)			
Velocity Increment, m/sec	9.	18.	45.
Attitude Error, deg(3)	4.0	2.0	.8

(1) Assumes in-plane velocity increment applied near 18 hrs from perigee to achieve large y-components of separation distance at the minor axis on both legs of the orbit with near minimum accuracy requirements.

(2) Assumes out-of-plane velocity increment applied at 20 hours after perigee to give distribution of separation distances shown in Figure F.

(3) Attitude error corresponding to .02% change in period is shown. This period change corresponds to the 1/2 the desired rate of separation distance growth along the orbital path.

5.0 ADAPTATION OF THE MISSION OPTIONS

The results presented above indicate that if the initial separation distances normal to the orbital path (which do not "grow" for Keplerian orbits) were to be increased by order of magnitude from the originally contemplated value of 50 km, the deployment schemes projected for the mission options in Appendix I would require modification. Options 1 to 3 make no provision for readjustment of the orbital periods based upon observation of the effects of the deployment velocity increments. Hence, for these options as originally conceived, the required accuracy in establishing the orbital periods would have to be achieved on an open loop basis during the one-shot deployment sequence. For an initial in-plane separation distance of 2,500 km the accuracy of the direction of the deployment velocity increment would have to be better than .5 deg. The attainment of this order of accuracy on an open-loop basis is considered to be impracticable. Because of the weight limitations imposed on the satellites' design, formidable difficulties and considerable technical risk are to be expected in attempting to achieve, on an open loop basis, the minimum accuracy of about 2 deg that would be required for maximum acceptable period uncertainty and an initial in-plane separation distance of 500 km.

In addition to the accuracy problem, it is apparent none of the deployment schemes as previously conceived can provide the magnitudes of the velocity increments required for attaining 500 km initial separation distances in both out-of-plane and in-plane directions. The deployment velocity increments for these schemes were generated by a combination of spin-off and spring separation of the satellites. Assuming a maximum pallet spin rate of 2 rps and a maximum lateral separation of the centers of mass of the satellite pairs of about 1 meter, it is estimated that a differential velocity increment of about 12 meters/sec could be achieved by a spin-off separation. This could provide the velocity increment required for 500 km separation distance either in-plane or out-of-plane but not both. The remaining velocity increment requirement could not feasibly be provided by spring separation. For velocity increments of this magnitude some type of reaction propulsion system would be required. The problems associated with provision of velocity increments of the required magnitude are of course amplified when initial separation distances in the order of 2500 km are considered.

In view of these apparent deficiencies it is pertinent to review each of the Options in some detail to determine to what extent deployment concepts could be modified to accommodate larger intersatellite separation distances.

Option 1 and 2

With regard to deployment there is no essential difference between these Options. In either case the pallet carrying the four satellites is injected into orbit, spinning in the direction inherited from the last booster stage. Nominally this direction would be in line with the velocity vector at perigee. The satellites are deployed from the pallet with no reorientation of the pallet's spin axis and the spin axis of the satellites are not reoriented after separation from the pallet.

Since spin-off velocity increments are necessarily perpendicular to the spin axis, with the inherited direction of the spin axis, spin-off velocity increment can be applied without introducing a tangential velocity component either (a) near apogee (or perigee) to obtain in-plane normal velocity increments, and/or (b) at any point in the orbit to obtain out-of-plane velocity increments.

Spin-off could be used to achieve both out-of-plane and in-plane normal velocity increments by means of an implementation wherein two satellites are first separated from the pallet with out-of-plane velocity increments, while the other two are later separated near apogee with in-plane normal velocity increments. A variation on this scheme is to separate two pairs of satellites with out-of-plane velocity increments and later separate each pair from its partner at apogee with in-plane normal velocity increments. Either implementation faces serious problems in achieving adequate clearance for the first spin-off, and in designing to obtain stable spin dynamic characteristics for the complete pallet, the partially deployed elements and the fully separated satellites.

Even assuming that these problems could be overcome and a 12 meter/sec differential velocity increment can be obtained from a spin-off at 2 rps, the y-component of the separation distance at the semi-minor axis that could be achieved by the in-plane deployment at apogee would be only about 150 km. An increase in spin rate of the magnitude that would be required to obtain a y-component of separation distances at the semi-minor axis in the order of 1000 km would present prohibitive technological problems.

Hence, for Options 1 or 2, for large separation distances spin-off appears to be useful only for generating the out-of-plane velocity increment. Assuming an out-of-plane deployment near 20 hours from perigee to minimize accuracy requirements, an out-of-plane separation distance of about 670 km can be obtained at the semi-minor axis.

To provide the additional velocity increments that are required to complete the deployment, the satellites can be equipped with reaction propulsion system that are operated after the satellites have been separated. Two types of systems can be considered: (a) a system wherein a steady thrust is applied along the spin axis, and (b) a system wherein a pulsed thrust is applied perpendicular to the spin axis, with the pulsing timed to achieve a velocity increment in a fixed direction perpendicular to the spin axis. The first type which is obviously far simpler, can be used for in-plane velocity increments only; the latter could be used for either in-plane or out-of-plane velocity increments.

Velocity increments in the direction of the spin axis would have to be applied near the semi-minor axis. By applying an inward normal velocity increment to one satellite at the semi-minor axis on the ascending leg and an outward in-plane normal to another satellite at the semi-minor axis on the descending leg, y-components at the minor axis on both legs of the orbit can be obtained. To obtain 1,000 km y-components, velocity increments of about 20 meters per second would be required. Assuming a satellite mass of 2 slugs, the impulse required would be about 120 lb-sec. A cold gas system providing this impulse would weigh about 4 pounds. A small solid rocket system would weigh about 2 lbs.

If a 2 deg error were made in applying the velocity increment an unwanted difference in period of about .1% would be incurred. With no subsequent period correction this would cause a growth in separation distance along the orbit near 10 R_e of 37,500 km in 6 months; the unwanted growth would be about 375 km per orbit. In 3 orbits the growth in separation distance would exceed the initial lateral separation.

The unwanted growth in separation distance could be avoided by tracking the satellites after deployment to determine their orbital period and using fore and aft cold gas jets fired on ground command near perigee to correct the orbital

period. Great accuracy in the direction of the velocity increments applied to correct the orbital periods would not be necessary. Errors in the magnitude of these velocity increments should not be serious and could be corrected by a cut-and-try process.

If a laterally firing pulsed thrust system is required in order to achieve greater out-of-plane separation distances than can be practically obtained through spin-off the complexity of the satellite systems for Options 1 or 2 would rival that for Option 4, while still not providing the conditions most desired for the scientific experiments, i.e., an orbit with a low inclination to the ecliptic combined with the satellite spin axis oriented perpendicular to the ecliptic plane.

Option 3

For Option 3 the spin axis of the pallet is reoriented, prior to the deployment of the satellites. Ideally after reorientation the pallet's spin axis would be aligned normal to the ecliptic plane. However, the orbital plane will be inclined to the ecliptic by at least 5 deg and possibly up to about 10 deg. Since an inclination of the pallet's spin axis to the orbital plane would seriously aggravate the deployment problems, for present purposes, it will be assumed that the spin axis of the pallet is nominally aligned to the normal to the orbital plane rather than to the normal to the ecliptic plane.

For this Option spin-off cannot be used to obtain an out-of-plane increment, since the spin-off velocity increments will always be in or close to the orbital plane. By appropriate selection of the time in the spin cycle for separation from the pallet, a spin-off in-plane normal velocity increment can be obtained at any point in the orbit. Based upon the results given in Table 1, a 12 m/sec in-plane normal velocity increment applied by spin-off at about 18 hours after perigee, would yield y-separations at the minor axis crossings of about 460 km. For such a deployment, an error of about 2.4 deg would cause a .02% error in period.

If larger separation distances are sought by increasing the spin-rate, accuracy problems are aggravated because of the increased deployment

velocity, and because of the increased difficulties of obtaining precise control of the direction of the velocity increment. At 4 rps an uncertainty of .002 seconds in the timing of the deployment would cause a directional error of 3 deg and a period change of .05%. Also it is noted that no advantage is gained with respect to impulse requirements if the thrust used for spin-up is not applied on a large moment arm, i.e., through nozzles extended on booms.

To obtain large out-of-plane separation distances the satellites would have to be equipped with axially thrusting reaction propulsion systems. Assuming that the spin axes are normal to the orbital plane, the out-of-plane velocity increment could be applied at any time without generating a tangential component to minimize accuracy requirement. The data given in Table 1 for velocity and accuracy requirements are then applicable.

As opposed to the in-plane deployment where the accuracy in the time in the spin cycle at which the satellites are separated from the pallet is most critical, for the out-of-plane velocity increments the direction of the satellites' spin axes is most critical. Even if precise information regarding the direction of the spin axis is available, there is no simple compensation technique for handling the case where the spin axis is found to depart from the normal to the orbit. Changing the time of application of the out-of-plane velocity increment so as to put the known tilt of the spin axis in the direction normal to the orbit would involve some change in sensitivities. Note that it is necessary to live with both the errors in initial pallet spin axis orientation and the errors due to any shifts in the direction of the satellites' spin axes incurred during spin-off from the pallet, if a subsequent correction of orbital period is not made. The Option 3 implementation errors are analyzed in detail in Appendix III and the resultant array growth modified from that shown in Table 1.

If it is considered necessary to correct the satellites orbital period, the satellites would have to be equipped with laterally thrusting reaction propulsion systems. Such a system would also be required if an increase in the y-component of the separation distance at the minor axis to the order of 2,500 km is desired. Thus if the modifications required to accommodate separation distances as large as 2,500 km are to be made, Option 3 would not be significantly simpler than Option 4. For somewhat relaxed separation distance requirements as specified by Ames scientists, Option 3 has been found to be technically feasible as shown in Appendix III.

The main factors involved in adapting Options 1 to 3 to the attachment of large separation distances are summarized in Table 2.

Option 4

With an increase in stored gas, the deployment implementation concept previously projected for Option 4 (see Appendix I) would in principle be applicable to the attainment of large separation distances. However, for large separation distances it would probably be preferable to revise the deployment implement so that the large velocity increments are always obtained by means of axial thrusts. This is possible in the case of Option 4 because the satellites' spin axes are reoriented after separation from the pallet. Thus the spin axes are initially close to the orbital plane and are later brought close to the normal to the plane. The deployment would then proceed as follows:

1. Two pairs of satellites are separated by spin-off from the pallet with out-of-plane velocity increments.

2. The satellites are separated from their partners using axial springs.

3. In-plane separation is obtained by axial reaction propulsion fired on ground command at the crossing of the minor axis.

4. The orbital periods are determined by ground tracking and any excessive differences are corrected by firing the fore or aft cold gas jets.

5. The satellites' spin axes are reoriented to become aligned to the normal to the orbit.

6. If larger out-of-plane separation distances than were obtained from the spin-off are desired, out-of-plane velocity increment are applied by the firing axial reaction propulsion system.

To save weight, [illegible] small solid rockets could be used for the axial reaction propulsion. In this case separation distances in the order of 2,500 km could be obtained with an addition of about 5 lbs per satellite.

Table 2

ADAPTATION OF OPTIONS 1 TO 3 TO ATTAINMENT OF LARGE SEPARATION DISTANCES

Deployment Implementation	Allowable In-Plane ⊥ Separation Distance, km	Attainable Out-Of-Plane Separation Distance, km	Unwanted Growth in Separation Distance // to Orbit: Per Orbit km	Unwanted Growth in Separation Distance // to Orbit: In 6 Months km	Remarks
OPTION 1 OR 2					
1. Spin-Off/Axial Springs					
2 rps	50	670	120	11,250	Out-of-plane velocity increment applied at 20 hours from perigee; tangential velocity error arises mainly from error in direction of the spin axis which is assumed to be 2 deg.
4 rps	50	1,340	250	22,500	
2. Spin-Off/One-Shot Axial Propulsion					
2 rps	to 2,500	670	940	85,000	Assumes 2 deg error in direction of axial thrust.
4 rps	to 2,500	1,340	950	86,000	
3. Spin-Off/Controlled Axial Propulsion					
2 rps	to 2,500	670	---	---	Axial propulsion system used to obtain in-plane separation distance and to correct orbital periods.
4 rps	to 2,500	1,370	---	---	
4. Spin-Off/Controlled Axial Propulsion/Pulsed Lateral Thrust	to 2,500	to 2,500	---	---	
OPTION 3					
1. Spin-Off/Axial Springs					
2 rps	460	50	100	9,400	Assumes 3 deg error in direction of spin-off velocity increment.
4 rps	940	50	280	25,000	Assumes 4 deg error in direction of spin-off velocity increment.
2. Spin-Off/One-Shot Axial Propulsion					
2 rps	460	to 2,500	230	21,000	Assumes 2 deg error in spin axis orientation plus spin-off error as in (1).
4 rps	940	to 2,500	340	31,000	
3. Spin-Off/One-Shot Axial Propulsion/Pulsed Lateral Thrust	to 2,500	to 2,500	---	---	Pulsed lateral reaction thrust used to increase in-plane separation distance and to trim orbital period to control growth of separation distance parallel to orbit.

22A

Appendix XI

ASPECT SENSING

1.0 INTRODUCTION

The Multiple Satellite system requires the use of aspect sensors for the following functions:

- To provide attitude reference for the pallet's ACS in effecting the reorientation maneuver.
- To trigger the spin-off of the satellite pairs from the pallet
- To provide on-board roll position reference for scientific instruments on the satellites
- To provide data defining the direction of the satellites' spin axes in support of the interpretation of the scientific data.

There is little question that sun sensors will be used for the first step of the pallet's reorientation maneuver, i.e., to bring the pallet's spin axis perpendicular to the sunline and also to reference the rotation of the pallet's spin axis about the sunline during the second step of the reorientation maneuver. Likewise sun sensors will undoubtedly be used to trigger the spin-off separation of the satellite pairs from the pallet and to provide on board roll position reference for the scientific instruments.

The main question involved with regard to aspect sensing is what additional sensor(s) is to be provided to perform the functions for which sun sensors alone are not adequate; specifically:

- To provide the reference required for accurate termination of the second step of the pallet's reorientation maneuver, and
- To provide a complete definition of the direction of the satellites' spin axes.

The former function is the more demanding. As described in Appendix III the accuracy of terminating the pallet's reorientation maneuver affects the accuracy of the deployment of the satellites. For this purpose an accuracy of attitude determination of at least 1 deg, and hopefully better is desired; a two deg accuracy is considered sufficient for monitoring the direction of the satellites' spin axes. Since the direction of the satellites spin axes will be quite stable,

changing only very small fraction of a degree during an orbit, considerable time can be taken for the collection and reduction of aspect data. Less time is available for operation with the pallet since repeated measurements will be needed to trim out the reorientation of the spin axes with precision and an excessively long period of operation of the pallet prior to deployment of the satellites must be avoided.

In spite of the differences in requirements, in order to avoid the need for separate pallet aspect sensors, it is to be hoped that the sensors used to monitor the direction of the satellites' spin axes can also serve the pallet's functions. For the performance of these functions consideration has been given to the following aspect sensors:

a. Directional (fan beam) down-link antenna,

b. Magnetometer, and

c. IR Horizon Crossing Indicator.

On the basis of the discussion of these aspect sensors presented herein, the IR sensor appears to be the most suitable for the Multiple Satellite application.

2.0 FAN BEAM ANTENNA

The use of a narrow fan beam antenna is a potentially attractive technique of aspect sensing in that if the beam pattern is desirable for satisfying communications requirements, aspect sensing is obtained without the cost of additional equipment or increase in system complexity. Also quick response, i.e., practically real time, data can be obtained. This approach was applied by Pioneer VI which achieved an accuracy of about 1 deg in orienting the spacecraft spin axis using a 5 deg fan beam antenna.

However the communications problems for the Multiple Satellite system are quite different from that of Pioneer VI. One of the most significant differences is that the Multiple Satellite communications system is required to operate at relatively small distances from earth as well as larger distances. The requirements for the tape recorder dumping at small distances, i.e., $\leq 6 R_e$ are as critical as the requirements for real time transmission at apogee. At the small distances an excessively narrow fan beam would hurt rather than improve communications coverage by the STADAN stations.

Also for the Multiple Satellite design a difficult if not impossible mechanical problem would be encountered if fixed antennas of the length required for a narrow fan beam are to be mounted on the satellites packaged within the shroud limitations. Study of the Multiple Satellite communications and design problems indicates that fixed fan beam antennas providing a beam width of about 25 deg. could be conveniently mounted within the available envelope and that this beam width would be compatible with the down link transmission requirements. A beam of this width does not permit an accuracy of 1 deg to be obtained in attitude determination and the long travel to the edge of the beam and back to the center which would be required if the Pioneer VI technique were to be followed would impose a burden on the ACS gas supply.

Some use of a 25 deg fan beam antenna in connection with aspect sensing can be made. For example the 25 deg fan beam can be used for a first cut in the reorientation of the pallet's spin axis, i.e., the rotation about the sunline is terminated when sufficient gain is obtained from the fan beam to permit real time down link data transmission. Because of the relatively wide beam there is little danger of overshooting the mark in executing this first cut on pallet's reorientation maneuver. Subsequently the reorientation maneuver is completed using more precise attitude data. Also, after the satellites have been deployed some

deductions can be made regarding the orientation of the satellites' spin axes by noting the times at which the edge of the fan beams cross the STADAN stations. However, it is expected that such interpretations of fan beam data would not be the primary method of monitoring satellites' orientation but would be called for in the event of a suspected system malfunction.

Since a very narrow beam, e.g. in the order of 5 deg would not serve a useful communications purpose, the equipment required for addition of such a beam to be used solely for the purpose of obtaining aspect sensing requirements. An additional antenna switch would be needed. This would entail a reduction in the gain of the wider beam transmission of about 1 dB. The additional switch and the use of deployable antennas would reduce reliability. The application of the narrow beam to aspect sensing both for the pallet and for the satellites would still be very awkward since the STADAN stations will not be the orbital plane and for the Multiple Satellite ranges the angle between the station/spacecraft line-of-sight and the orbital plane will hot be negligible.

3.0 MAGNETOMETER

The use of magnetometers as aspect sensors involves (a) the measurement of the direction of the ambient magnetic field relative to body axes, and (b) the interpretation of these measurements to define the orientation of the spacecraft using exsisting knowledge of the magnetic field relative to an earth fixed frame and information on the position of the spacecraft. In principle from measurements obtained at two or more different spacecraft positions sufficiently separated so that the directions of the ambient fields differ by a substantial angle, the attitude of the spacecraft can be completely determined. The accuracy of the attitude determination depends not only upon the instrument errors, i.e., the accuracy of the measurements but also upon the uncertainties regarding the knowledge of the direction of the field.

Only the main field component, i.e., that generated by the earth has sufficient stability to serve as a basis for an attitude reference. The magnitude of this field decreases approximately with the third power of distance from the earth. Beyond 3 to 4 R_e the use of magnetometer data for attitude determination is totally impractical because the magnitude of the main field no longer predominates over variations due to unaccountable external disturbances. Thus the collection of magnetometer aspect data is restricted to a relatively narrow region close to the earth.

Even within this region the range over which useful data can be collected is restricted by the wide variation of the magnitude of the field. The magnetometer must be designed for some maximum field beyond which it will saturate. Significant contributions to the measurement errors are proportional to the field strength at saturation. Optimum conditions for the magnetometer measurement are obtained when the ambient field strength is close to the saturation value. If the saturation field is made so large that saturation never occurs, i.e., the magnetometer is designed for optimum operation near the lowest (perigee) altitude, then its percentage accuracy will be poor at higher altitudes where the ambient field is reduced. Also at very low altitudes knowledge of the direction of the ambient field is less accurate due to the increased strength of local anomalies and computations are more complicated since retention of higher order harmonics is required.

If the magnetometer is designed to saturate at smaller field strength corresponding to optimum operation at a higher altitude then it will saturate at lower altitudes and some data will be lost. However, since more time is spent at higher altitudes and the visibility of the ground stations is better, it seems adviseable to design for optimum operation at as high an altitude as feasible. This will be limited by the magnitude of the external disturbances. A likely choice for the design altitude appears to be at about 1 R_e, corresponding to a distance from the center of the earth of about 2 R_e and a field strength in the order of 10,000 γ.

Even at this altitude visibility from the STADAN stations will not be very good. Since assurance of real time transmission coverage in the region of interest is doubtful, it will be necessary to rely on the recording and playback to obtain coverage of the passage through perigee from about 3 R_e on the inward to 3 R_e on the outward leg.

The relatively poor coverage and the complicated computations required to extract information on the orientation of the pallet's spin axis would make the application of magnetometer data for control of the pallet's reorientation maneuver difficult. Assume that, with the aid of the satellites' 25 deg. fan beam antennas, a first-cut at the reorientation maneuver is made during the first outward leg after injection into orbit. It is then necessary to wait for a perigee passage to obtain attitude data. This is accomplished by commanding record at about 3 R_e going toward perigee altitude and playing back after passing about 3 R_e outward from perigee. The magnetometer data is then processed through a computer to derive aspect data. Since the first cut was based on the wide fan beam and was conservative, it is likely that the spin axis will be found to be in the order of 10 to 15 deg out. A maneuver must then command on an open-loop basis to correct this this deviation. Inasmuch as it is not adviseable to rely on the accuracy of the open-loop maneuver, another perigee passage is required to get a new reading on attitude. If it is found that the attitude is still somewhat off another open-loop correction is needed and possibly still another perigee passage to confirm the open-loop maneuver would be desired.

This sort of cut-and-try method is expensive in that it may cost three and possibly more orbits before the reorientation maneuver can be completed. Since each orbit takes about two days, a period of 6 or more days of the prime portion of the orbital lifetime would be lost insofar as the collection of data

Table 1

VARIATION OF SENSITIVITY TO DIRECTIONAL ERRORS WITH TIME OF APPLICATION OF IN-PLANE NORMAL VELOCITY INCREMENT

Time of In-Plane Normal Deployment, Hours from Perigee	% Change in Orbit Period per Degree Error in Direction of Velocity Increment Δv_{IN} = 14.7 meters/sec
2	.052
4	.037
6	.029
8	.024
10	.020
12	.017
14	.014
16	.012
18	.0100
20	.0086
21	.0080
22	.0076
22.5	.0075
23	.0073
23.5	.0073
24	.0072

limitations on the magnitude of the in-plane normal separation distances imposed by the limited magnitude of the spin-off velocity increment that can be feasibly obtained and since with the relatively small velocity increment the absolute effect of directional errors would be reduced, it appears that an earlier application of the velocity increment would be more appropriate.

Application of the in-plane normal velocity increment at about 10 hours from perigee passage provides a reasonable compromise. A near maximum in-plane normal separation in the region of 10 R_e of about 800 km is obtained along with separation distances of about 550 and 400 km at 18 and 19.5 R_e. Relative to application of the velocity increment at 18 hours after perigee, the sensitivity to the error in the direction of the velocity increment is increased by a factor of about 2.

The difference in time of application of the in-plane normal velocity increment has little effect on the changes in perigee altitude. In either case, the perigee altitude of Satellite Pair 1-2 is increased by about 120 km while the perigee altitude of Satellite Pair 3-4 is decreased by a like amount.

With out-of-plane velocity increments of 15 meter/sec, separation distances of about 1,500 km between Satellites 1 and 2, and Satellites 3 and 4 are obtained at all of the important sections of orbit. The solid rockets required to obtain this velocity increment will weigh about 1.5 lbs.

In addition to the in-plane normal and out-of-plane separation, a tangential separation, i.e., separation along the orbit, is required to obtain a non-coplanar array. It is noted that for the deployment considered here a tangential separation between Satellite Pairs 1-2 and 3-4 would not be sufficient. To obtain a non-coplanar array, tangential separation distances between Satellites 1 and 2 or 3 and 4 is necessary (see Figure B). This could be obtained by deliberately aligning the spin axes slightly off the normal. For present purposes it will be assumed that this would not be done since it is expected that the inadvertant errors in the direction of spin axes are likely to yield greater tangential separation distances than are required or desired. Since the tangential separation distances

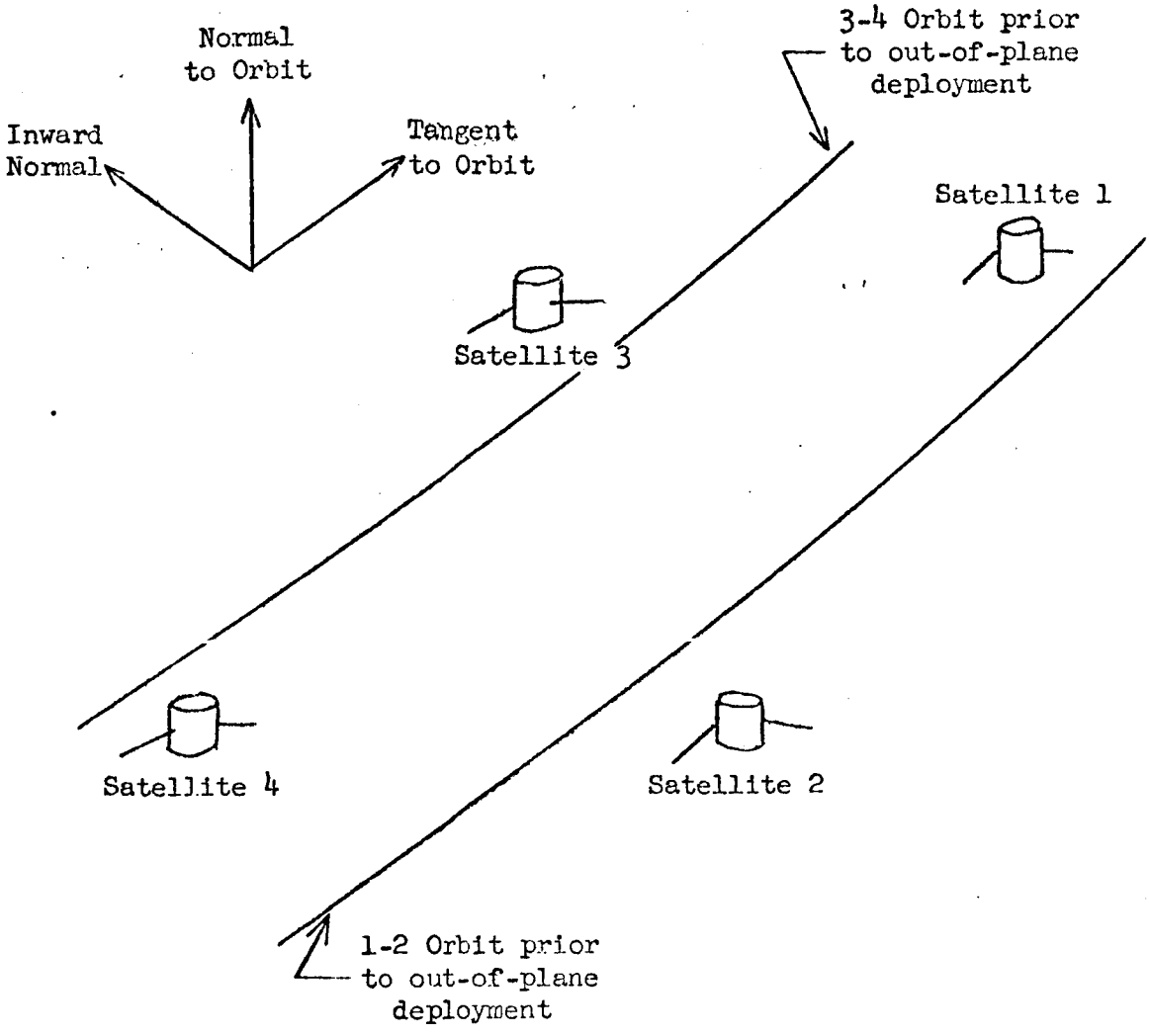

FIGURE B. SATELLITE ARRAY

between Satellites 1 and 2 or between Satellites 3 and 4 can arise only from orbital period differences, this component of the separation distance will: (a) grow with time, and (b) vary in magnitude as the orbit is traversed; the tangential separation distance at 10 R_e will be five times greater than at 20 R_e; and twenty times greater at perigee than at apogee.

4.0 ERROR ANALYSIS

Inasmuch as the implementation under consideration makes no provision for readjustment of the satellites' orbital periods after deployment, the effects of differences in period, incurred during or subsequent to deployment, on the growth of tangential separation distances must be accepted. The period differences incurred during deployment can be attributed to:

a. Errors in the direction of the spin-off velocity increment.

b. Errors in the direction of the out-of-plane velocity increment.

The period differences that develop subsequent to deployment will arise mainly from differences in orbital decay rates resulting from differences in perigee altitudes.

4.1 ERRORS IN DIRECTION OF SPIN-OFF VELOCITY

Table 2 lists the contributions to the errors in the direction of the spin-off velocity increment that lead to a tangential velocity increment and thus to differences in the orbital period. The spin-off velocity increment is nominally in the direction perpendicular to both the pallet's spin axis and the position vector of the satellite pair's center of mass, i.e., the vector normal to the spin axis, passing through the spin axis and the center of mass of the satellite pair. Departures of the pallet's spin axis from its nominal orientation will not contribute to the tangential velocity component: a tilt of the spin axis in the direction of the tangent to the orbit has no effect on the direction of the spin-off velocity increment; a tilt in the direction of the in-plane normal to the orbit causes the direction of the spin-off velocity to shift only in the out-of-plane direction.

Errors incurred in the separation process can be attributed to (a) uncertainties in the forces that may act on the satellite pairs as they are released from the pallet, (b) uncertainties in the time at which the satellite pairs are released, and (c) uncertainties in the location of the center of mass of the satellite pair. These errors, particularly those in the first two categories, are dependent upon the details of the design of the separation system. The development of a design that not only assures a clean separation but also permits the direction of the velocity increment to be predicted with confidence and accuracy can be expected to present one of the major implementation problems for the Multiple Satellite system.

In dealing with this problem ground-based tests can be of only limited value. While it may be possible to perform tests in a vacuum chamber to remove aerodynamic effects, it would not be possible to remove gravitational effects and the simulation of free-space attitude dynamics of the pallet and the satellite pairs would be most difficult. The design of tests to measure the dispersion of the direction of the spin-off velocity increment to an accuracy better than a few degrees is not a simple matter and would undoubtedly add significantly to development costs. Thus it appears likely that chief reliance will have to be placed on theoretical analyses.

Table 2

ESTIMATES OF SPIN-OFF VELOCITY INCREMENT DIRECTIONAL ERRORS

Error Sources	Magnitude of Source Error	Contribution to Directional Error, deg	Contribution to Tangential Velocity, meters/sec	Contribution to Period Difference, % of Period
1. Uncertainty in Reaction Forces at Separation	.05 lb-sec	.2	.05	.004
2. Sun Sensor Error	.1 deg	.1	.03	.002
3. Uncertainty in Action Time	.14 ms	1.2	.31	.024
4. Residual Error in Adjusting for Off-Nominal Conditions	.1 deg	[illegible]	.03	.002
RSS		1.25	.32	.025

The estimates of the disturbance forces that is developed here must be taken with some reservations since in the absence of past flight experience with a similar spin-off separation system and short of in-depth analyses of a specific design it is difficult to obtain an estimate that can be accepted without question.

A design parameter that strongly affects the separation forces is the orientation of the separation planes. The assumed mounting of the satellite pairs on the pallet (see Figure C) is such that it would be impracticable to have the separation planes between the satellite pairs and the pallet perpendicular to the spin axis. As shown in Figure C the separation planes might be perpendicular to the position vector to the centers of mass of the satellite pairs or perpendicular to the nominal direction of the velocity increment.

To minimize the possibility of hanging up it is desirable that the separating sides separation interface remain parallel as the satellite pair moves away from the pallet. It is also desirable that the relative motion of the sides of the interface be very nearly perpendicular to the separation plane through a sufficient distance to assure clearance of any depressions that may be present at the separation interface. If the initial relative motion is perpendicular, shearing action across the interface is avoided. Hopefully, these kinematic features can be obtained without the use of auxiliary reaction forces across the separation plane, such as might be generated by separation springs used to eject the satellite pairs. The presence of such ejection forces could add to the uncertainty of the velocity increment imparted to the satellite pair.

These considerations favor the selection of the separation plane perpendicular to the satellite-pair center-of-mass position vector. With this orientation of the separation plane it is only necessary to free the satellite pairs so that forces can no longer be transmitted to them across the separation planes. Nominally the interaction forces vanish so that the pallet and satellite pairs retain the velocities of their centers of mass and also their angular velocities. Hence the separating sides of the interface remain parallel. Initially, as a result of the differences in centripetal acceleration of the two sides, the pallet side and the satellite pair side separate in the direction perpendicular to the separation plane. For the conditions presently considered the relative acceleration

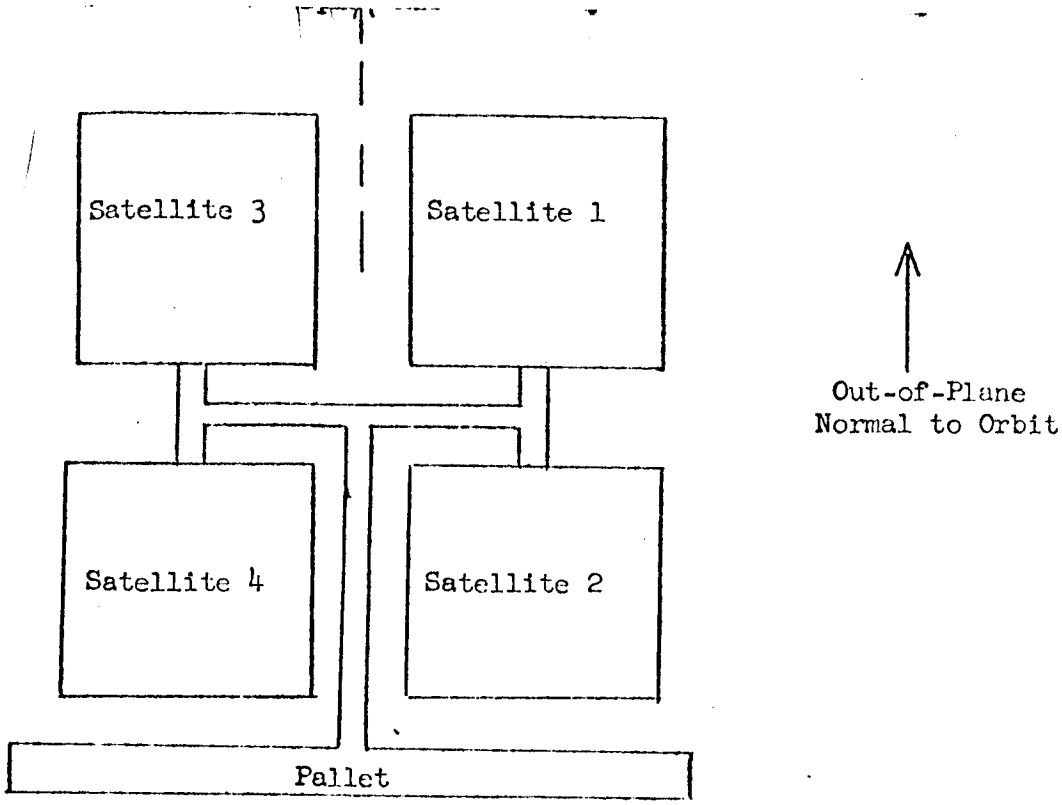

a. Side View of Mounting of Satellites on Pallet

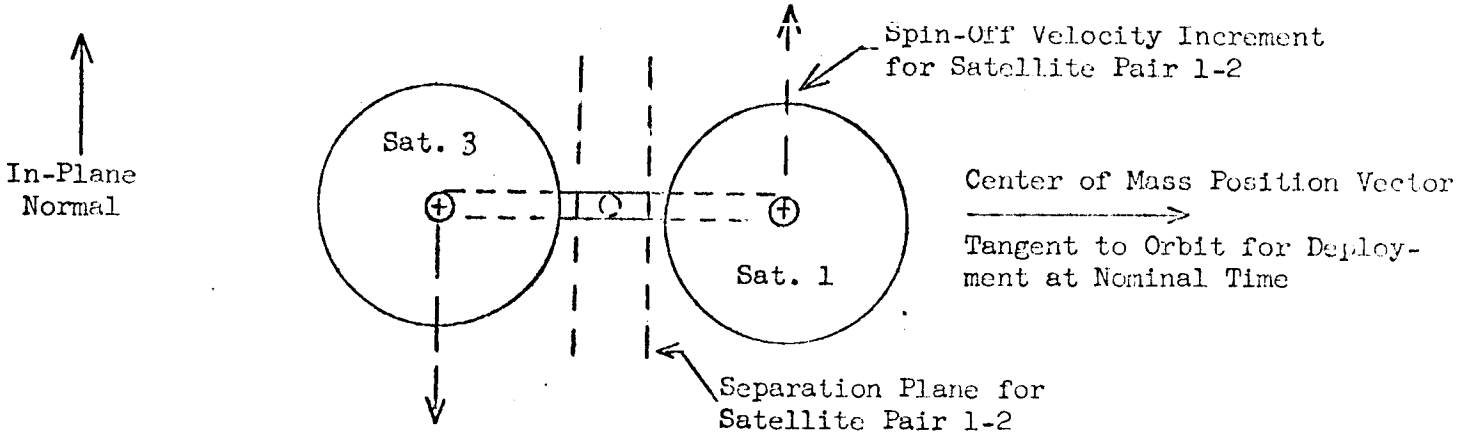

b. View from above of Spin-Off with Separation Planes Perpendicular to Center of Mass Position Vector

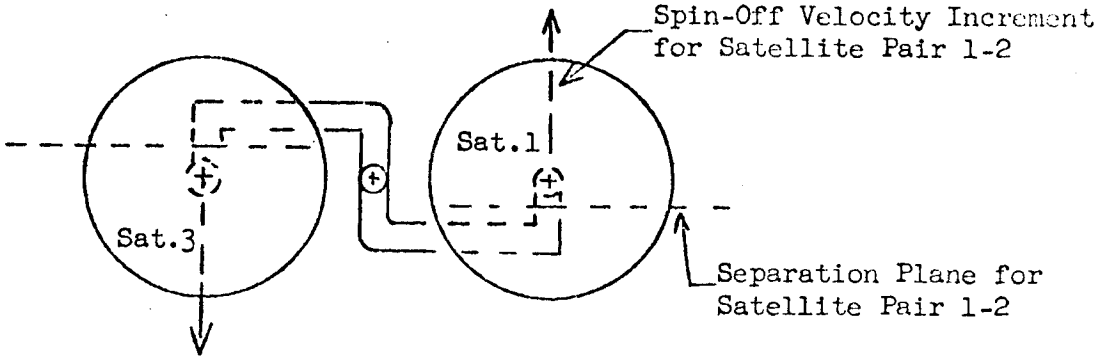

c. View from above of Spin-Off with Separation Plane Perpendicular to the Direction of the Velocity Increment

FIGURE C. ALTERNATIVE SPIN-OFF SCHEMES

would be about 10g. As the sides separate relative motion parallel to the separation plane builds up as shown in Figures D and E. When the sides are 1/4-inch apart the displacement parallel to the separation plane is only about .03 inch. Thereafter the displacement parallel to the separation plane increases more rapidly.

With the separation plane perpendicular to the direction of spin-off velocity increment, in the absence of auxiliary ejection forces, the initial relative acceleration of the two sides of the separation plane would be parallel to the plane. Also for the configuration shown in Figure C-c without auxiliary ejection forces, a clean separation could not be obtained because the distance between the sides of the separation plane would not tend to increase naturally. The application of ejection forces would torque the pallet and this disturbance of the pallet's motion could cause a clearance problem.

It can be shown that if no auxiliary ejection forces are applied, compared to any other orientation, the selection of the separation plane perpendicular to the position vector to the satellite pair center of mass provides the slowest build-up of distance parallel to the separation plane relative to the rate of separation perpendicular to the separation plane. For the assumed mounting of the satellite pairs, this selection also provides the simplest structural configuration.

With the separation plane perpendicular to the center of mass position vector, reaction forces may be inadvertantly transmitted across the separation interface as a result of stress relief and dynamic reactions associated with the separation ordnance. Along with these forces a reaction moment may be applied about the satellite pair's center-of-mass. The forces perpendicular to the separation plane would affect the velocity increment in the direction of the center of mass position vector which is nominally parallel to the tangent to the orbit. To the extent that this velocity increment is predictable, the timing of the separation could be adjusted to avoid a tangential component of the velocity increment; an error will be incurred to the extent that the reaction forces are not predictable. The moment is not of concern in connection with the in-plane velocity increment, but is of concern in connection with the preservation of the direction of spin established by the pallet so as to permit the subsequent out-of-plane velocity increment to be accurately applied.

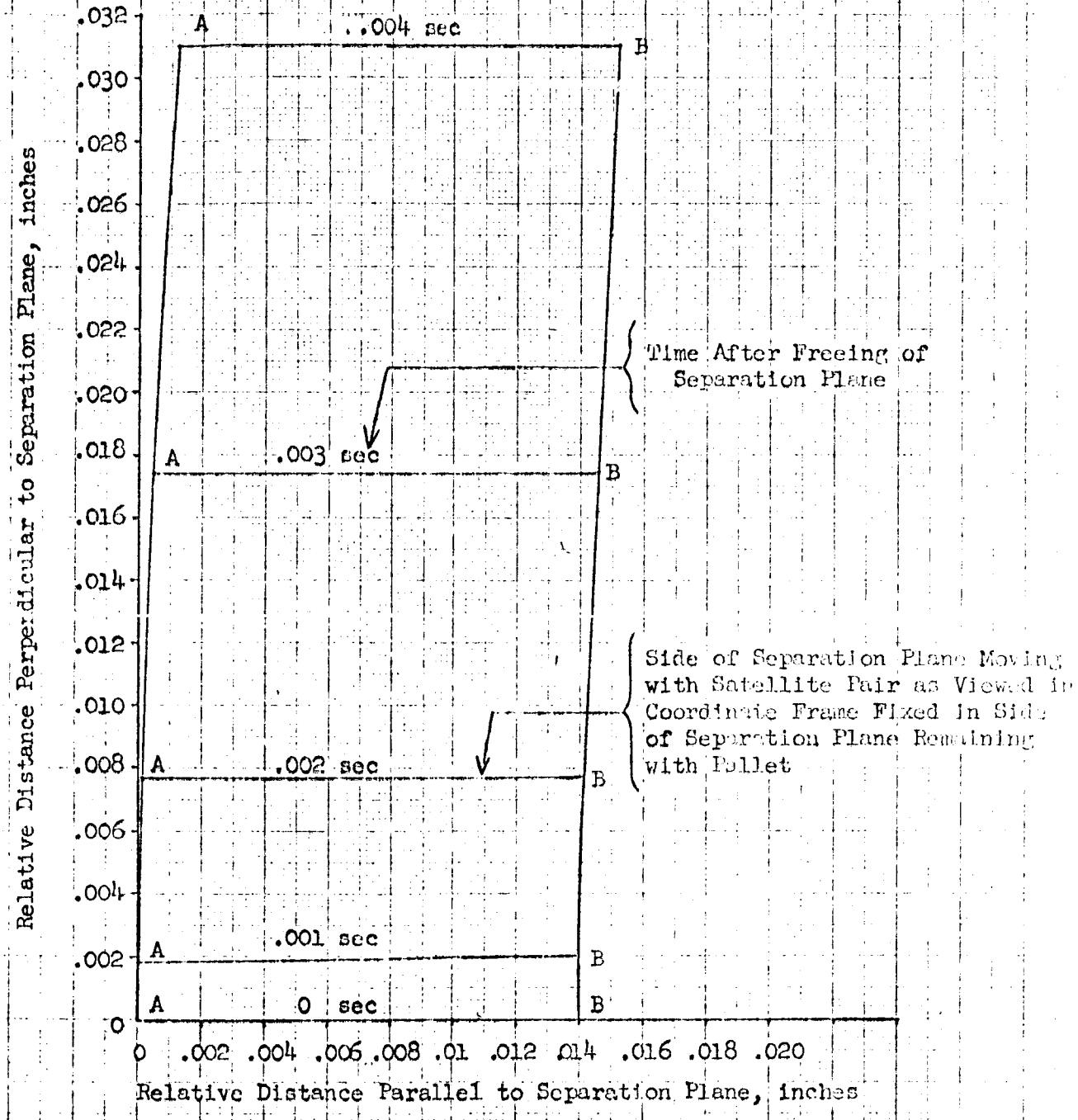

FIGURE D. NOMINAL HISTORY OF RELATIVE POSITIONS OF SIDES SEPARATION PLANE TO .004

(Separation Plane Perpendicular to Position Vector to Center of Mass of Satellite Pairs)

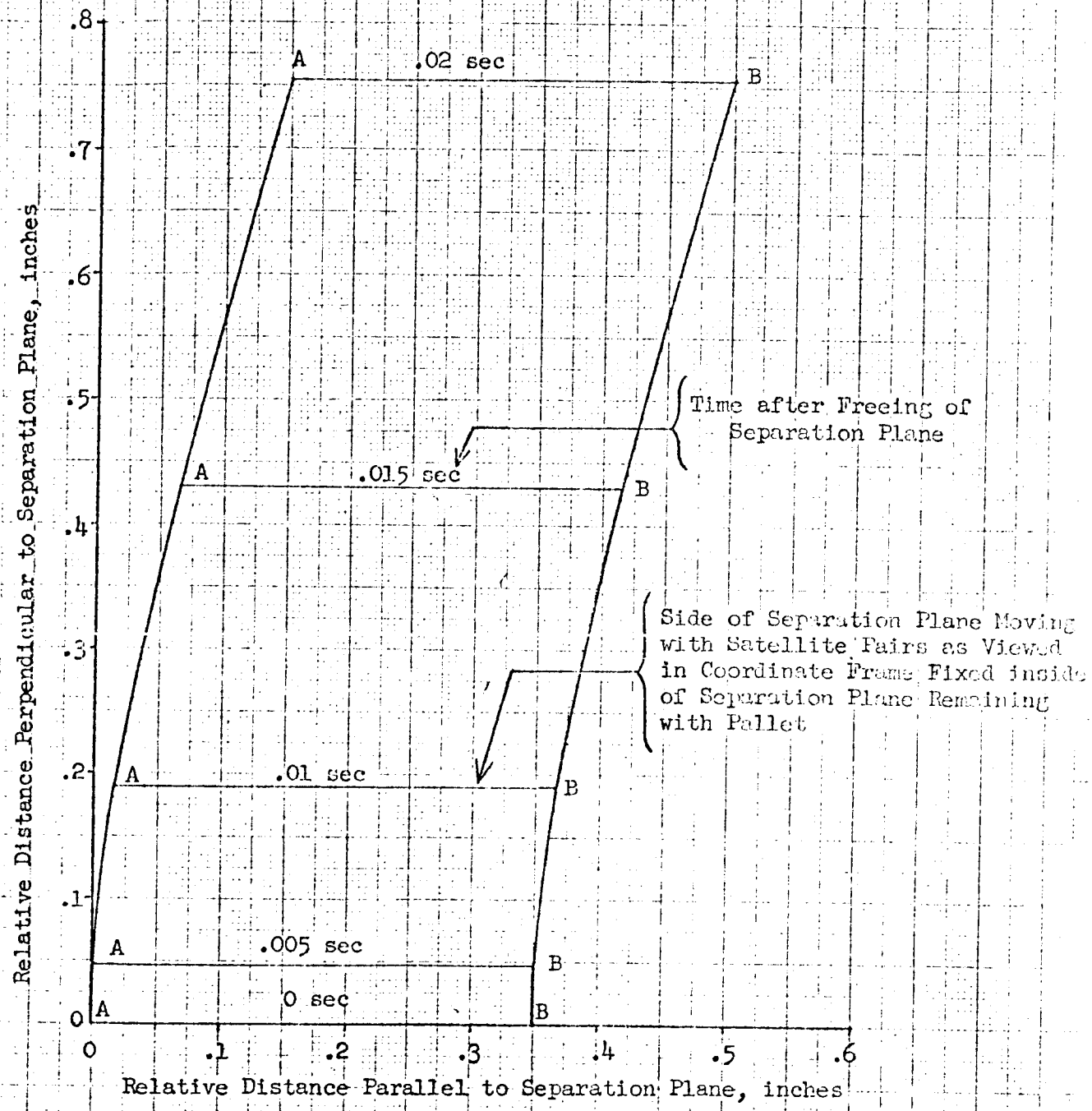

FIGURE E. NOMINAL HISTORY OF RELATIVE POSITIONS OF SIDES OF SEPARATION PLANE TO .02 SEC AFTER SEPARATION

To minimize reaction moments, as well as for reliability considerations, the separation interface will in all likehood be secured by a single fastener. This fastener must support the load due to the centrifugal forces applied by the satellite pair, which is estimated to be in the order of 1,000 pounds. The presence of this tensile load argues against the use of pin-puller separation mechanisms. The probable choice appears to be a frangible bolt.

If the explosives that are typically used to operate such devices were loaded in a small rocket to apply maximum impulse to the satellite pair an impulse in the order of perhaps 5 lb-sec might be delivered. It seems reasonable to assume that the separation mechanism will not be an efficient device for applying impulse to the satellite pair. On this basis the impulse actually delivered whether through stress relief, impact of moving parts or direct application of gas pressures, will be a small fraction of the maximum impulse that could be delivered by the explosive. For present purposes the impulse delivered to the satellite pair will be taken to be 1 lb-sec.

Applied to a satellite pair mass of about 4 slugs this impulse would generate a velocity increment of .25 ft/sec or about .1 meter/sec. Since the nature of the separation interface is such that negative reaction forces could not be transmitted the uncertainty in the velocity increment would be at most .05 meter/sec. With the magnitude of the velocity increment of about 14.7 meter/sec this corresponds to an angular error of .0034 radians or about .2 deg.

Assuming the use of conventional circuitry, the sun sensor signal will be amplified and used to throw a relay that will fire the ordnance to separate the satellite pairs. Review of vendor literature indicates that the sun sensor error could be kept to about .1 deg. Relay and ordnance delay times are typically in the order of .005 second so that the action time between the rise of the sun sensor signal and the release of the satellite pairs would be about 10 milliseconds. Uncertainties in the relay and ordnance delays are generally about .001 sec. Combining the delay uncertainties statistically gives a 1.4 millisecond uncertainty in the action time.

If it were necessary for the successful performance of the mission to reduce the action time and its uncertainty, there is little doubt that this can be done. For example, the ordnance delay time and uncertainty could be substantially reduced with the use of capacitive firing circuits. However, since such improvements would entail some penalty in increased weight and complexity, reduced reliability or increased development requirements, for the present, it is assumed that a standard system is to be used.

The uncertainty in action time translates directly to an error in the direction of the velocity increment. With the pallet spinning at 840 deg/sec the 1.4 millisecond action time uncertainty leads to a 1.2 deg error.

During the mean action time of 10 milliseconds the pallet will rotate about 8.4 deg. Compensation for this rotation would be made by mounting the sun sensor so that it leads the position of the pallet desired at separation by this angle. According to present information the pallet's spin rate will not be known in advance to better than 10%. Hence, if a post-injection correction were not made, a residual error in compensating for the lead time of about .84 deg would be incurred.

However, post-injection correction can and presumably would be made by obtaining accurate data on the pallet's spin rate and changing the time at which the spin-off separation is commanded so that the tangent to the orbit rotates through an angle that adjusts for the off-nominal lead angle and keeps the spin-off velocity increment in the in-plane normal direction.

The need for such a correction technique would be essential in any event to compensate for other off-nominal conditions. The largest of these is expected to be the variation in the direction of the sunline relative to the orbit resulting from the launch window. Assuming a direct-ascent boost trajectory, it will be impractical to change injection conditions relative to the earth. The orbit would rotate with the earth at about .25 deg/minute. A daily $\pm$ 40 minute launch window will then entail a $\pm$ 10 deg range in the relative sunline direction.

This range in relative sunline direction could be accommodated while maintaining an in-plane normal direction for the spin-off velocity increment without changing the orbital position at separation, by providing an adjustable delay between the sun sensor signal and the ignition of the separation. However, it appears preferable to accept a change in orbital position at separation than to provide the additional equipment that would be needed to provide a command-controlled adjustable delay time.

As indicated in Figure F, for a separation nominally at 10 hours from perigee, a $\pm$ 10 deg rotation of the tangent to the orbit is obtained approximately by a $\pm$ 3 hour change in the time of separation. The results presented in Figure A and Table 1 indicate that separation at 7 or 13 hours from perigee will not cause a very great difference in the magnitudes of the separation distances in the sections of the orbit of most interest. However, the sensitivity of the period to errors in the direction of the velocity increment could be increased or decreased by about 20%.

In addition to corrections for the launch window and an off-nominal spin rate, the time of separation would be selected to take account of any booster guidance errors that may influence the direction of the sunline relative to the orbit. Precise orbital data will be available from tracking the pallet. Only the launch window correction is expected to be large enough to cause a very substantial change in the time of separation. Little difficulty is anticipated in selecting the time of separation so that the direction of the spin-off velocity increment is aligned to the perpendicular to the orbit to within .1 deg.

A circumferential shift in the location of the center of mass position vector from its nominal position corresponds to a rotation about the spin axis and will give rise to a tangential velocity component. This error depends upon the effort that is made in locating the precise position of the centers of mass when mounting the satellite pairs on the pallet and in designing to maintain the precision of the center of mass location in flight. With moderate care it is felt that a tolerance of .2 cm could be kept. On an arm of .5 meters this would cause an error of .23 deg.

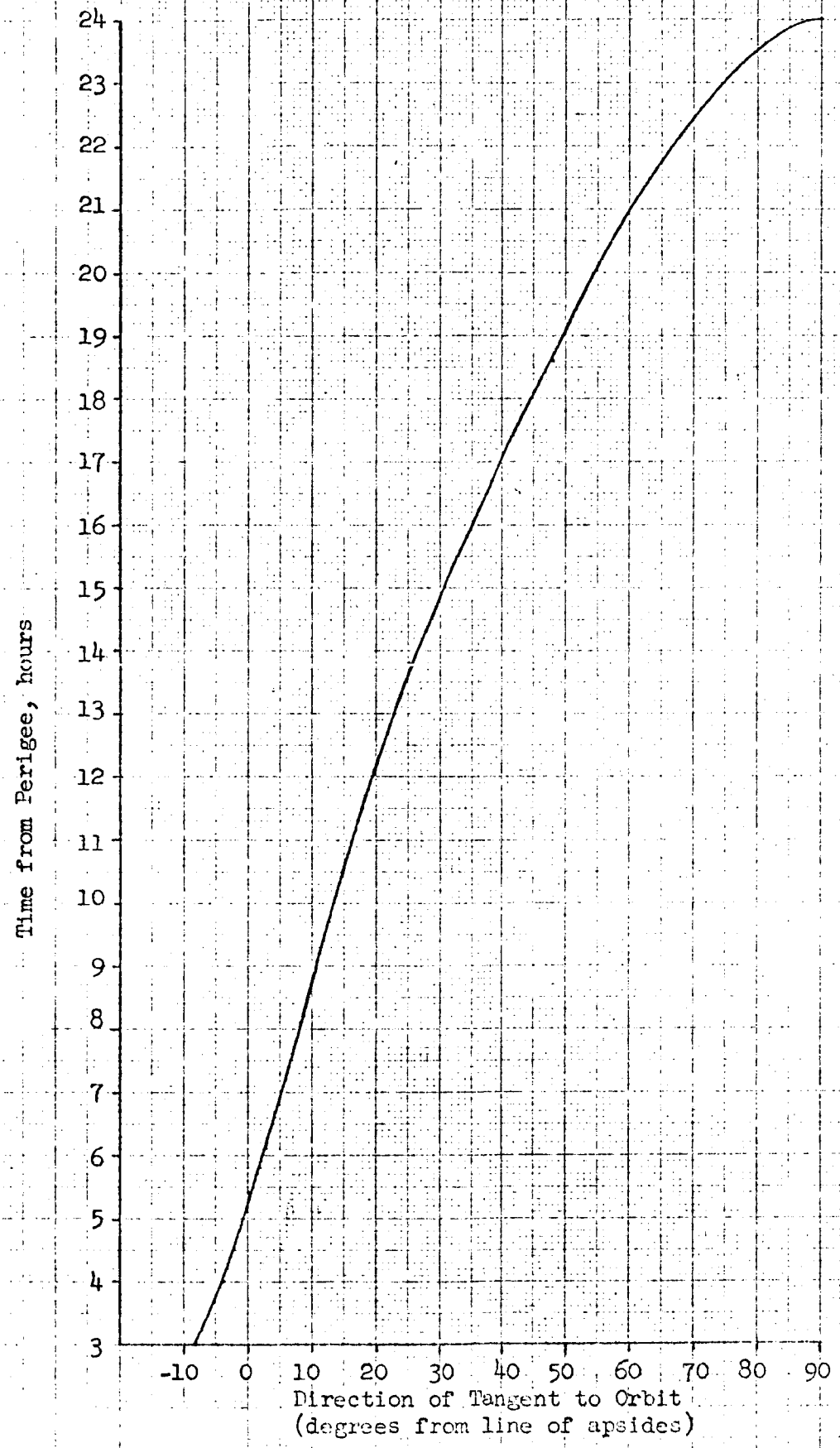

FIGURE F. RELATIONSHIP BETWEEN DIRECTION OF TANGENT TO ORBIT AND TIME FROM PERIGEE

It should be recognized that the accurate positioning of the satellite pairs centers of mass is only one of many requirements that must be met with regard to control of inertial characteristics. This includes: static and dynamic balance of the complete pallet assembly, static and dynamic balance of the satellite pairs and of the separated satellites. The inertial parameters must be accurately controlled both in undeployed and deployed condition, i.e., with booms extended, under boost thrust and spin loading conditions, and both prior and subsequent to the expenditure of propellants such as the ACS cold gas and the solid rockets. Clearly it would not be desirable to impose any unnecessary additional burdens with respect to control of inertial parameters.

4.2 ERRORS IN THE DIRECTION OF THE OUT-OF-PLANE VELOCITY INCREMENT

As listed in Table 3, the factors that may affect the direction of the out-of-plane velocity increment include:

a. Factors that lead to a departure of the pallet's spin axes from the normal to the orbital plane.

b. Factors that cause a shift in the direction of the satellites' spin axes relative to the direction of the pallet's spin axis.

c. Factors that cause a shift in the direction of the out-of-plane velocity increment relative to the direction of the satellite's spin axis.

In the first category, in addition to errors in execution, errors would potentially be incurred as a result of the variations in the direction of the normal to the orbital plane that are inherent in the launch window to be allowed. However, the assumed implementation provides for an almost complete correction for these variations. This is accomplished by:

a. Appropriate adjustment of the precession of the pallet's spin axis about the sunline in completing the reorientation of pallet's spin axis, and

b. Commanding ignition of the rockets that provide the out-of-plane velocity increments to fire at the time when the projection of the sunline in the orbital plane is parallel to the in-plane normal to the orbit.

Within limitations imposed by execution errors, the adjustment of the precession of the pallet's spin axis about the sunline restricts the remaining tilt of the spin axis relative to the normal to the orbital plane to be toward (or away from) the sunline. This selection of the time of application avoids the generation of a tangential component of the velocity increment in consequence of the remaining tilt of the pallet's spin axes.

Assuming that no conflict arises with respect to solar or lunar perturbations, the selection of the nominal time of application of the out-of-plane velocity increment at 20 hours after perigee passage would yield desirable conditions with respect to the initial direction of the sunline relative to the orbit. The initial angle between the sunline and the line of apsides would be about 35 deg

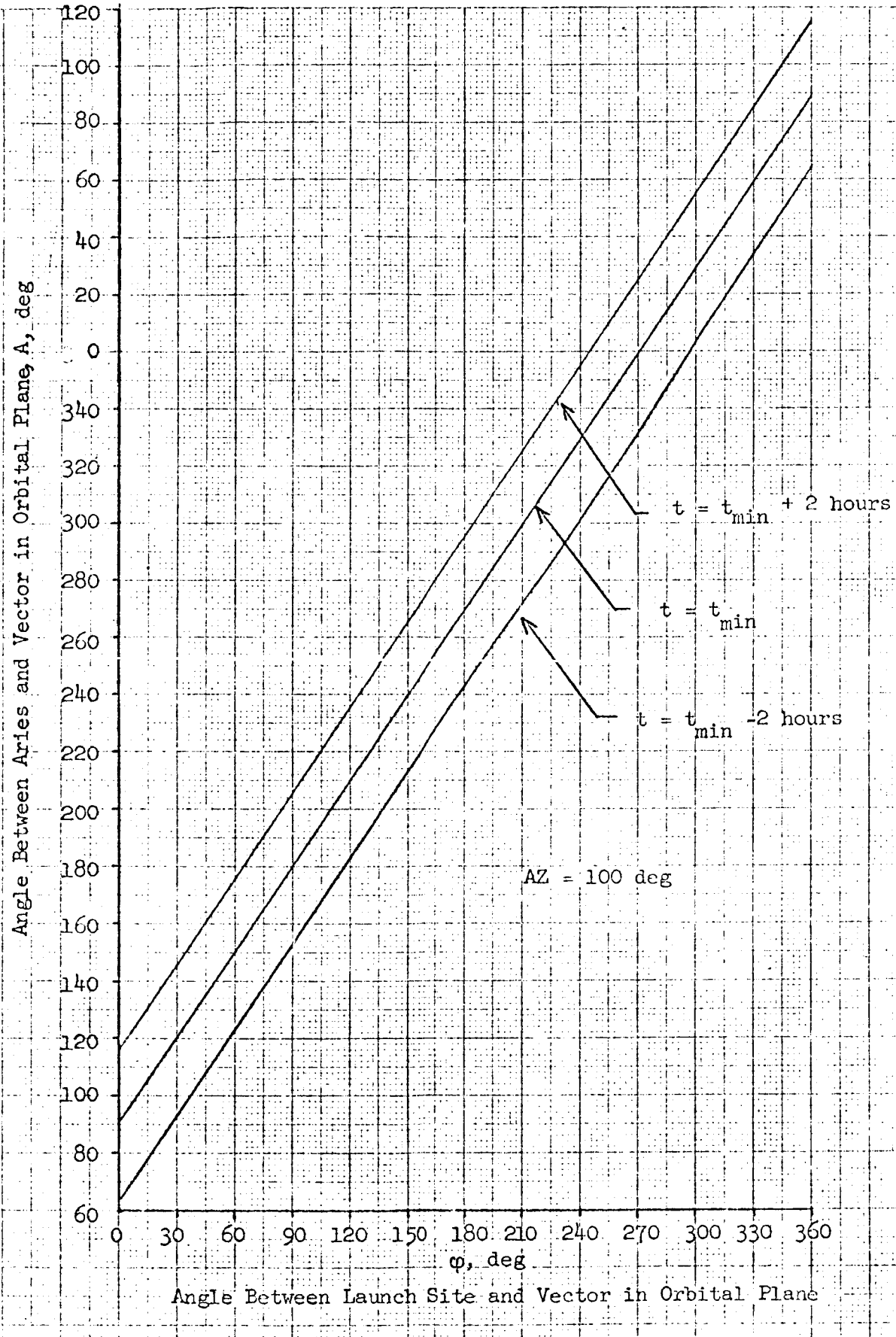

FIGURE L. VARIATION OF A WITH φ AND LAUNCH TIME, AZ = 100 DEG

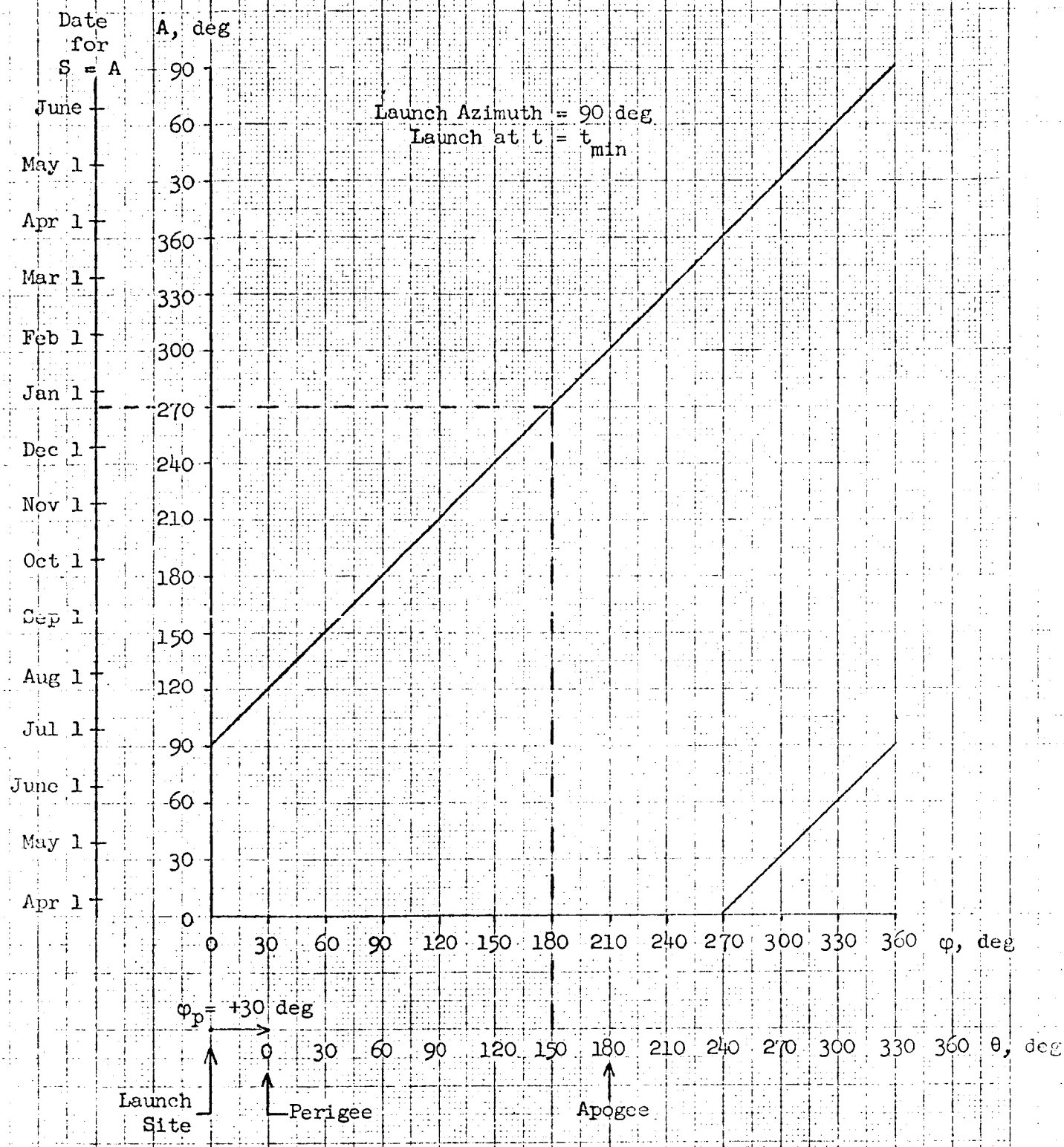

FIGURE M. INTERPRETATION OF RELATIONSHIP BETWEEN A AND φ

would be about 270 deg as indicated by the dashed line. On that date the sunline would be over the vector in the orbital plane at 180 deg from the launch site. If the origin of the φ scale is shifted by φ_p, the shifted scale can be interpreted as true anomaly. In the illustration shown in Figure M, φ_p, was taken to be 30 deg. In this case on December 21 the sunline would be aligned with the position vector on the orbit of the point having a true anomaly of about 150 deg.

The value of (A-S) for any position in the orbit at any date can be readily read off the plot. For example, it is apparent that on December 21, for the apogee radius, the angle (A-S) = s_a would be about 30 deg. About 30 days later, i.e., approximately January 21, the sunline would pass through the apogee radius, i.e., s_a would go to zero.

The relationship between A and φ can also be used to determine the value of φ_p required to obtain a desired initial value of s_a when the launch date is specified. For example, consider the case where the launch is to be on September 21 and a value of s_a of 45 deg is desired to provide a lead time of 45 days before the passage of the sunline over the apogee radius. From Figure M the sunline would start over the point in the orbit for which φ = 90 deg. The value of φ corresponding to apogee must then be 135 deg. Since $\theta = \varphi - \varphi_p$, and for apogee θ = 180 deg, φ_p must be -45 deg. To obtain an initial value of φ_p of -45 deg by using a coast period in a parking orbit would require a coast angle greater than 200 deg. If the launch date were in winter or early spring, the desired lead time could be obtained with relatively short coast periods.

The effects of the launch variables on the angle, D, are shown in Figures N to S. As in the case of Figures J to L, the φ scale can be converted to true anomaly by a shift of origin through the angle φ_p as indicated in Figure T. The angle, D, varies sinusoidally with φ. The point at which D becomes equal to zero identifies the line common to the orbit and ecliptic planes. For the case illustrated, i.e., a launch at $t = t_{min}$ with AZ = 90 deg the value of φ_c is seen to be 90 deg, and with φ_p = 30 deg, the value of θ_c is 60 deg, confirming the results previously obtained.

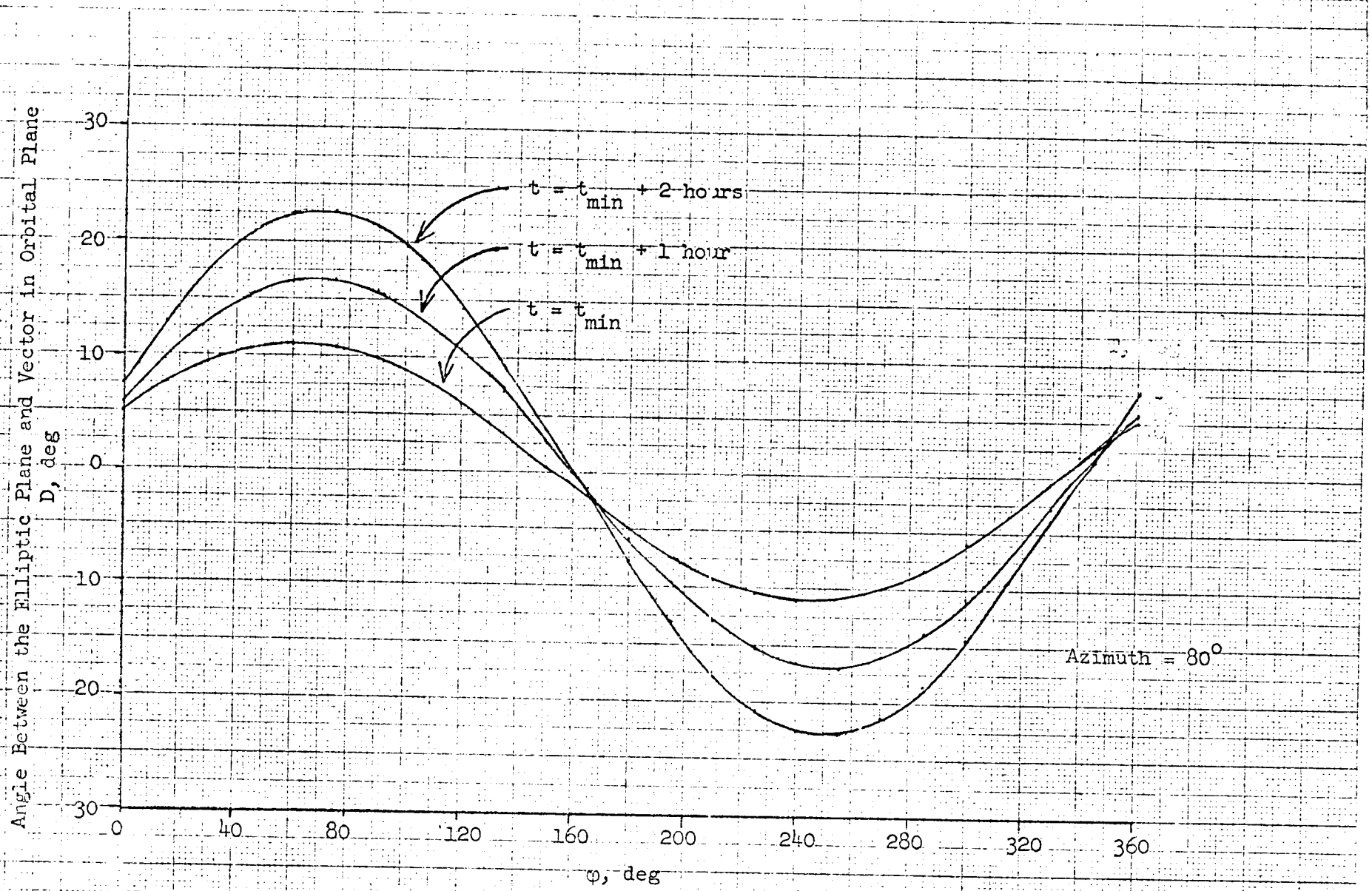

Angle Between Launch Site and Vector in Orbital Plane

FIGURE N. VARIATION OF D WITH φ AND LAUNCH DELAY, AZ = 80 DEG

CLEARPRINT PAPER CO. NO. C39X MILLIMETERS 200 BY 250 DIVISIONS PRINTED IN U.S.A. ON CLEARPRINT TECHNICAL PAPER NO. 1015

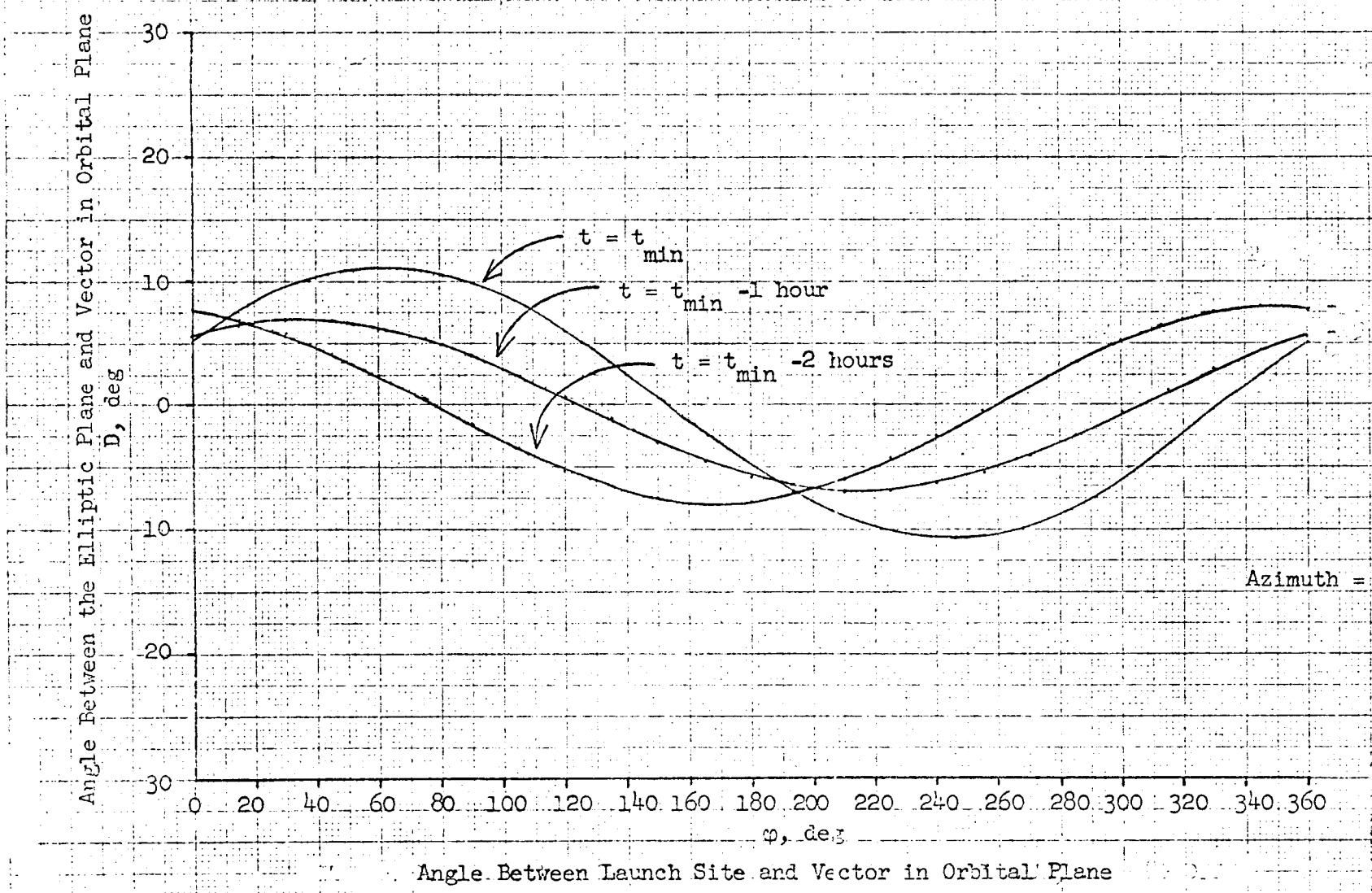

FIGURE O. VARIATION OF D WITH φ AND LAUNCH TIME ADVANCE, AZ = 80 DEG

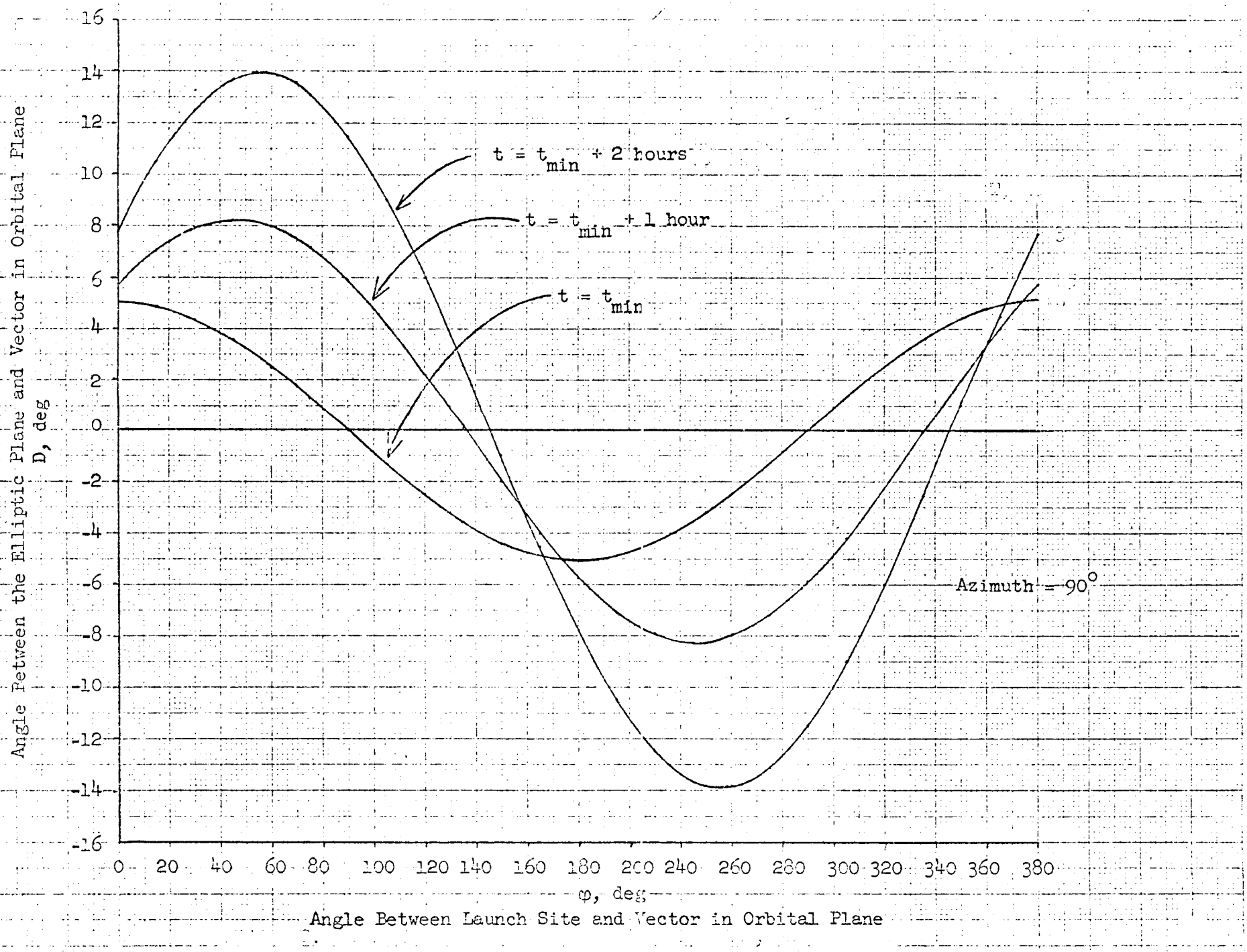

FIGURE P. VARIATION OF D WITH φ AND LAUNCH DELAY, AZ = 90 DEG

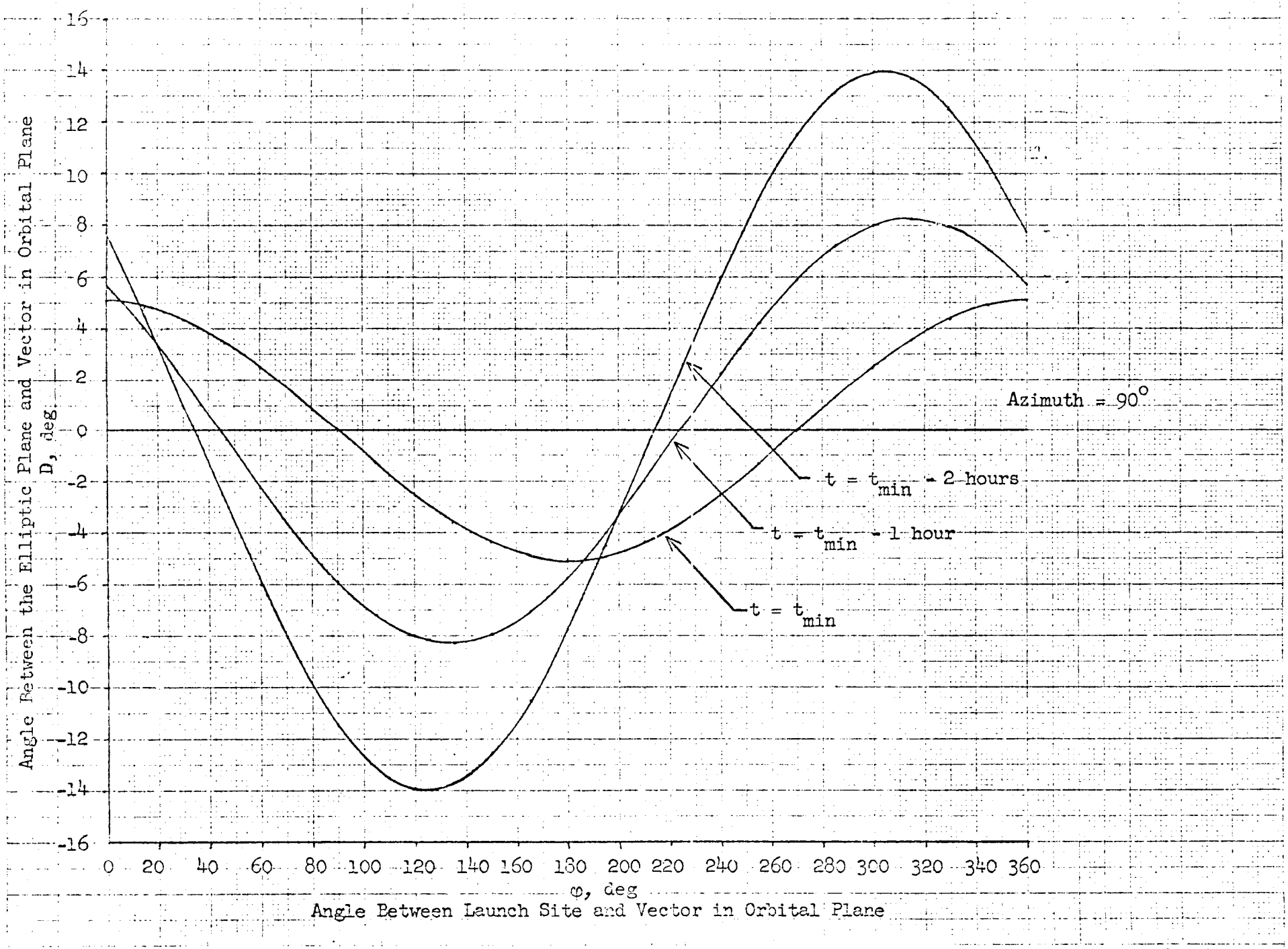

FIGURE Q. VARIATION OF D WITH φ AND LAUNCH TIME ADVANCE, AZ = 90 DEG

CLEARPRINT PAPER CO. NO. C39X MILLIMETERS 200 BY 250 DIV. 10 CM
PRINTED IN U.S.A. ON CLEARPRINT TECHNICAL PAPER NO. 1015

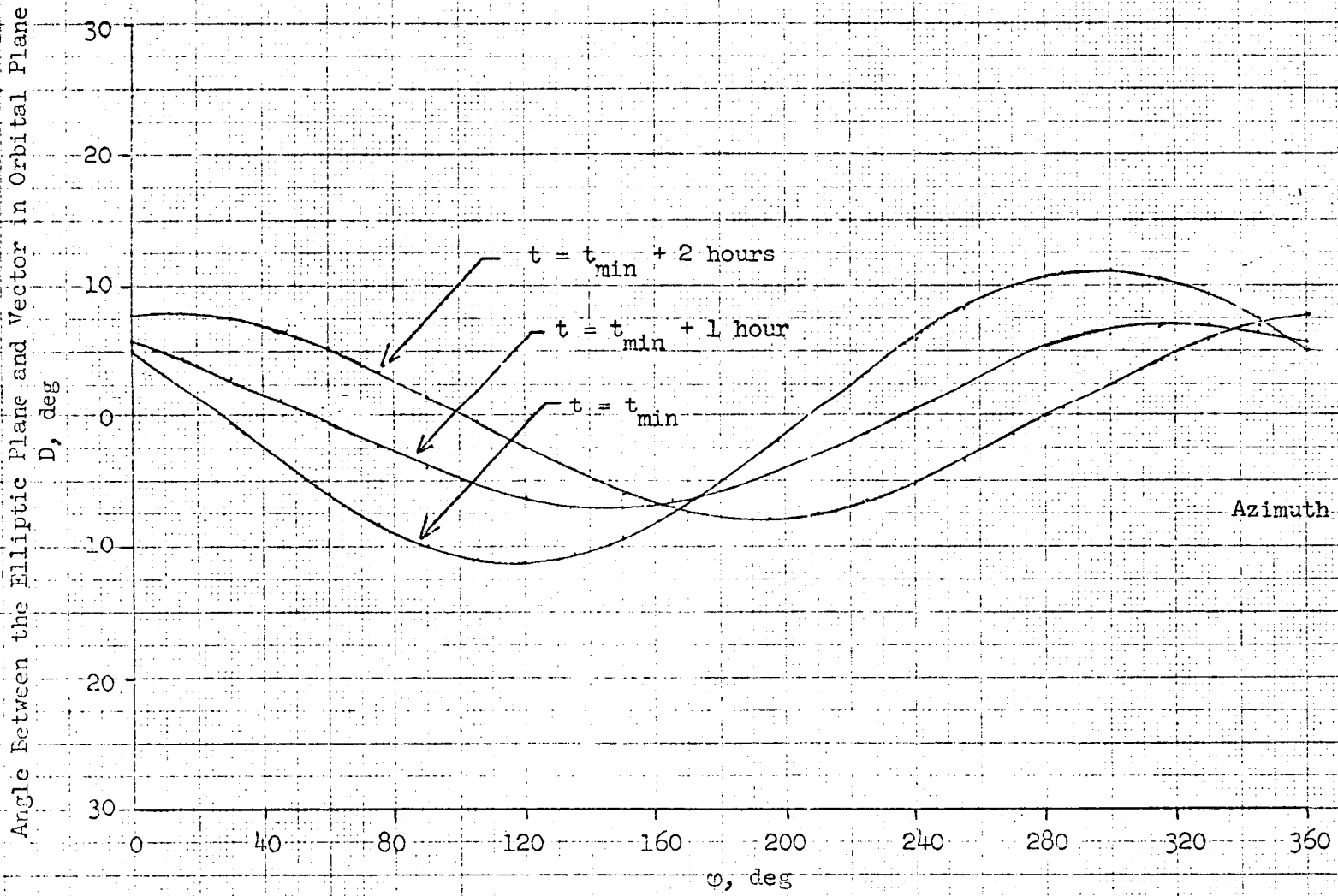

Angle Between Launch Site and Vector in Orbital Plane

FIGURE R. VARIATION OF D WITH φ AND LAUNCH DELAY, AZ = 100 DEG

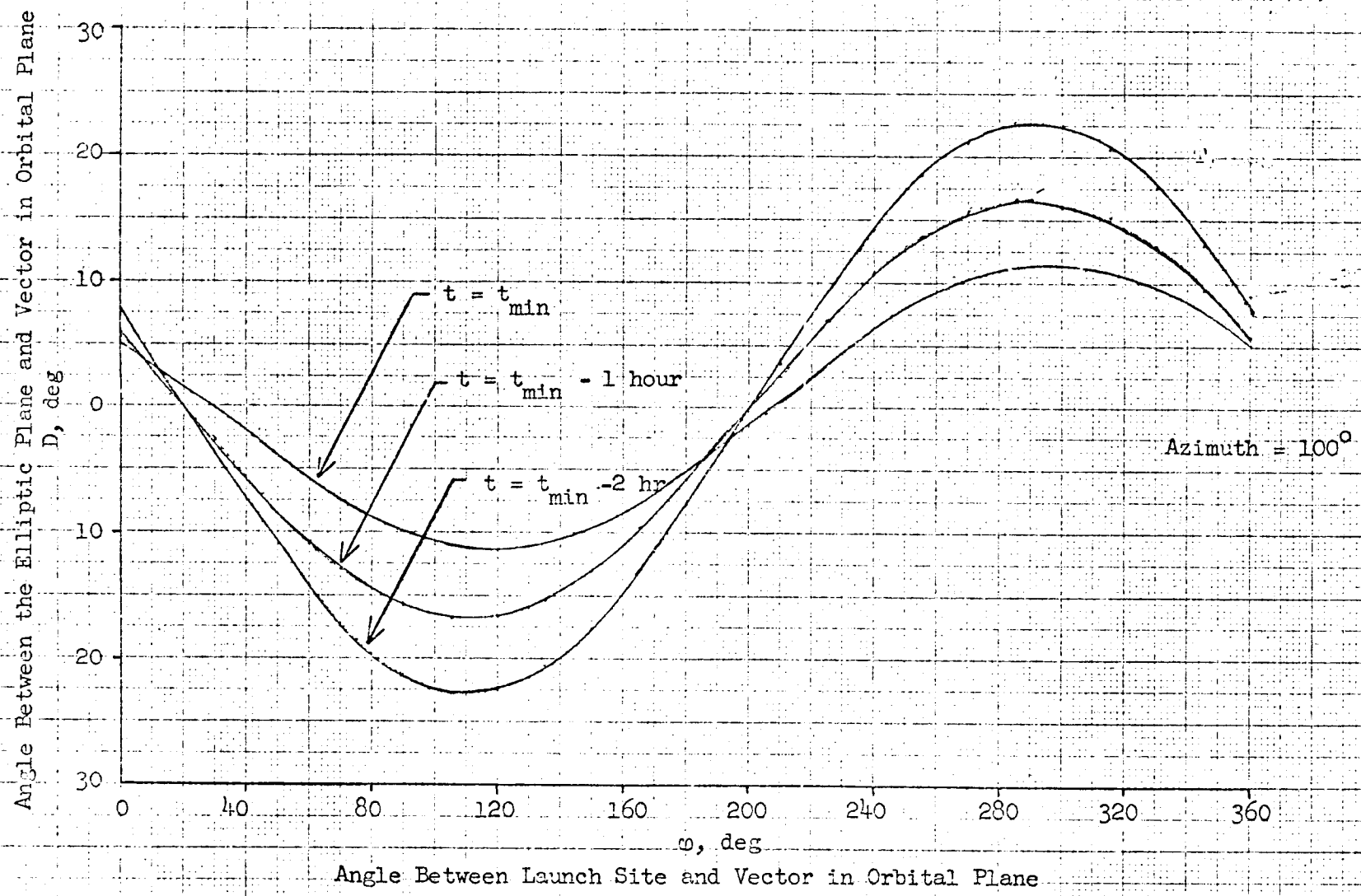

FIGURE S. VARIATION OF D WITH φ AND LAUNCH TIME ADVANCE, AZ = 100 DEG

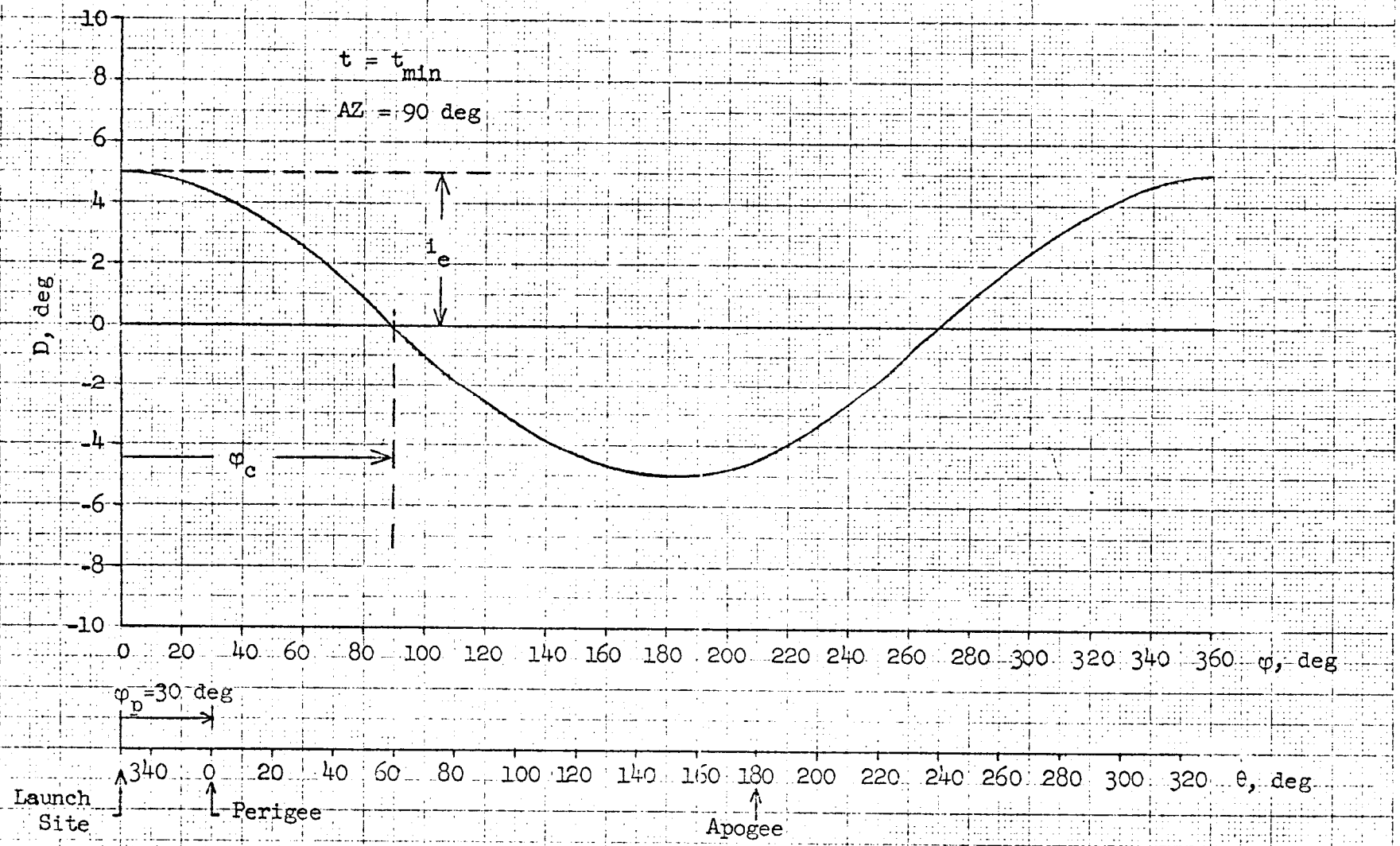

FIGURE T. INTERPRETATION OF RELATIONSHIP BETWEEN D AND φ

The maximum value of D is equal to i_e, the inclination between the orbital plane and the ecliptic plane.

The total angle, S_x, between a vector in the orbital plane and the sunline can be obtained from the relationship:

$$\cos S_x = \cos D \cos (A-S)$$

Except for orbital perturbation effects D and A remain constant and S_x varies mainly in consequence of the 1 deg/day rate of change of S. For any vector the minimum magnitude of S_x is equal to D and occurs when the value of (A-S) becomes equal to zero or 180 deg. The maximum value of S_x is 90 deg and occurs when (A-S) becomes equal to 90 or 270 deg. The former conditions are separated from the latter conditions by quarter year intervals.

The effects of orbital perturbations due to the earth's oblateness on the relative orientation of the sunline can be assessed in the manner previously discussed. Thus the effect of the nodal regression is equivalent to a launch time delay and is estimated to correspond to about 50 minutes delay after 6 months in orbit. The apsidal precession is equivalent to a shift in the origin of the φ variable, or to an increment in φ_p. It is estimated that the effect of the apsidal precession will correspond to an increment in φ_p of about 20 deg after 6 months in orbit.

Appendix VI

BOOSTER VEHICLE CONSIDERATIONS

1.0 INTRODUCTION

The booster vehicle is of considerable importance since:

a. The maximum allowable weight for the satellites and pallet will be limited by the capabilities of the booster vehicle.

b. The booster vehicle costs will be a substantial part of the total mission costs.

c. The total mission reliability will be strongly affected by the booster vehicle reliability.

d. The attainment of an orbit close to the chosen nominal initial orbit depends upon the performance of the launch vehicle guidance system.

e. Launch window restrictions are governed by the limitations on the booster flight trajectory.

f. Initial conditions relating to the orientation and attitude stabilization of the pallet carrying the satellites are inherited from the last stage of the booster vehicle.

Although consideration of these factors in complete detail was beyond the scope of the present study, they have been examined sufficiently to assure the availability of an acceptable booster vehicle. Further study will be required for the selection of the optimum vehicle and the generation of a mission plan defining the operational application of the vehicle in detail.

The purpose of this Appendix is to present the data that has been collected regarding the booster vehicle, in support of the present study.

2.0 PAYLOAD CAPABILITY

2.1 CANDIDATE BOOSTER VEHICLES

2.1.1 THOR DELTA SERIES

In accordance with the ground rules for the present study consideration of the booster vehicle has been confined mainly to the Thor Delta series. This vehicle has undergone and is continuing to undergo evolutionary development. Of the existing versions the best choice would be the DSV-3E* vehicle. This is a three stage vehicle comprised of:

First Stage:	Thrust Augmented Thor (TAT) DSV-3E-1 with TX-33-52 solid motor augmentation
Second Stage:	Improved Delta, DSV-3E-3
Third Stage:	FW-4

The payload capability obtained with this vehicle is shown in Figure 1.

The future version that will most probably be available to the Multiple Satellite Program for launches in the early 1970's is the DSV-3K vehicle which is comprised of:

First Stage:	Thorad (Long Tank Thor) DSV-2L with TX-354 solid motor augmentation
Second Stage:	Improved Delta, DSV-3E-3
Third Stage:	FW-4

This vehicle differs from the present version primarily in the substitution of the Thorad for the TAT first stage. Its payload capability is shown in Figures 2 and 3.

---

*Vehicle and stage designation numbers used here are in accordance with those used in NASA "Certified Launch Vehicle Data".

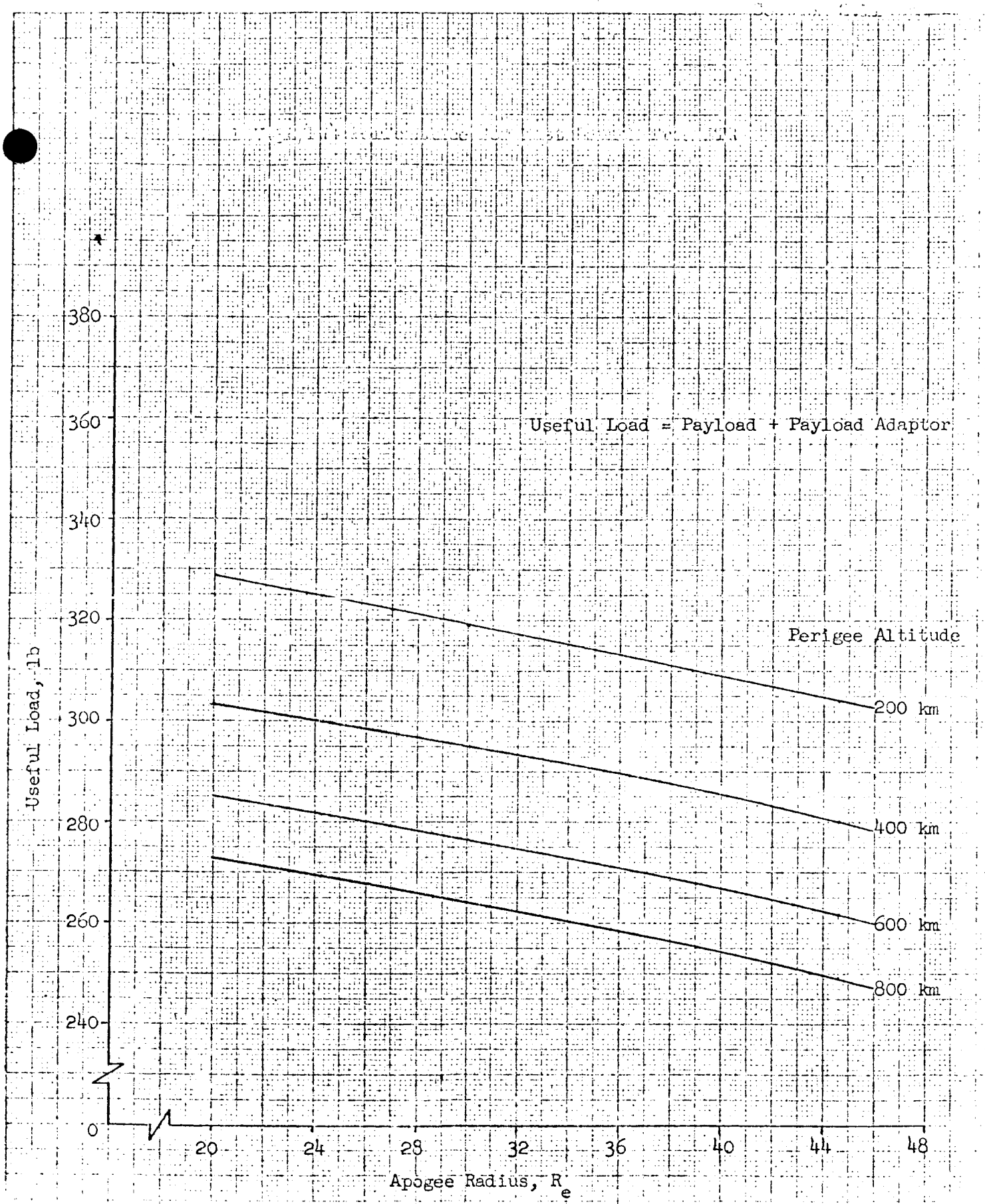

FIGURE 1. DSV-3E/FW4 PERFORMANCE FOR EAST LAUNCH FROM ETR
(Based Upon Computations Made By DAC)

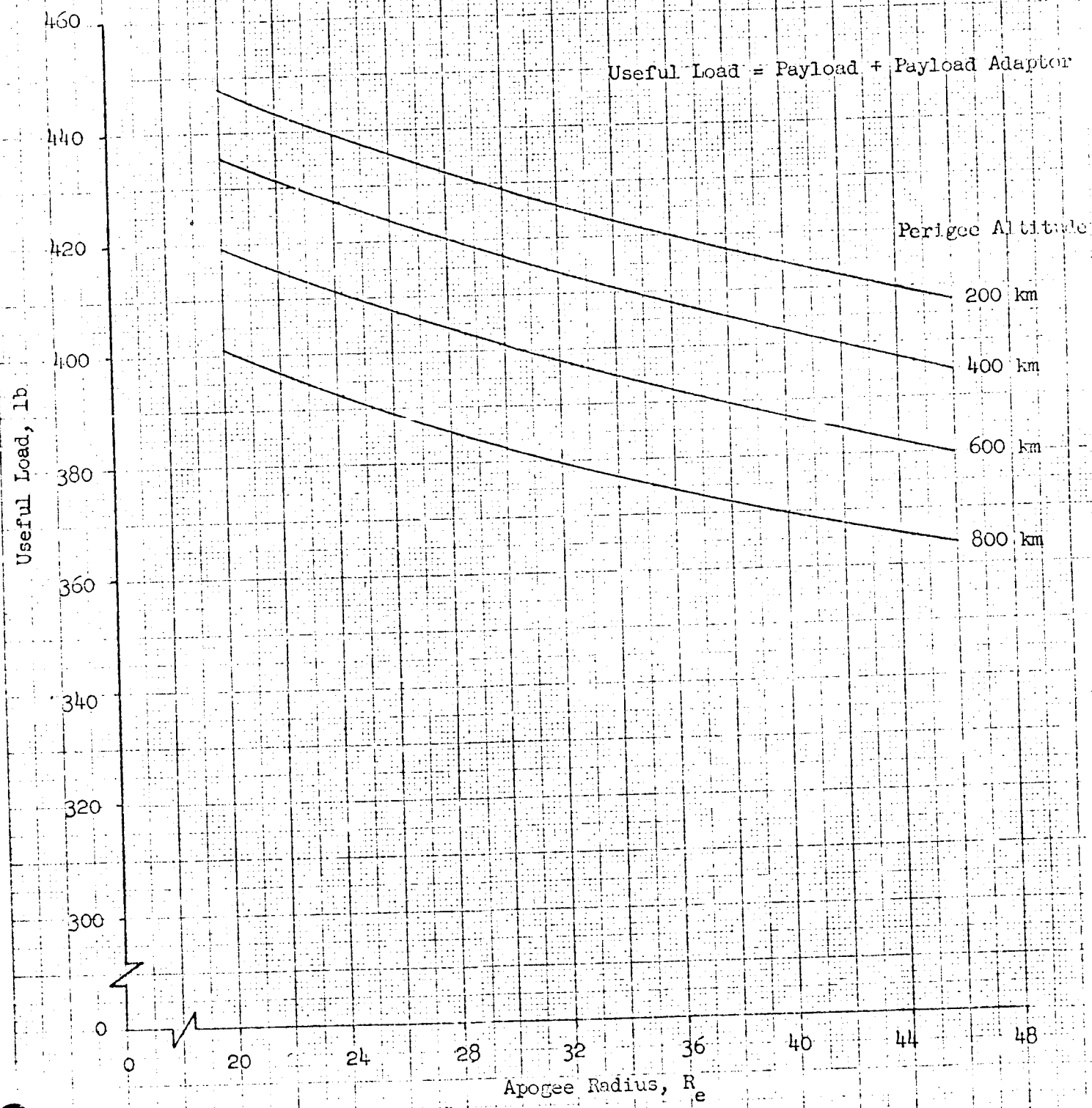

FIGURE 2. DSV-3K PERFORMANCE FOR EAST LAUNCH FROM ETR
(Based Upon Computations Made By DAC)

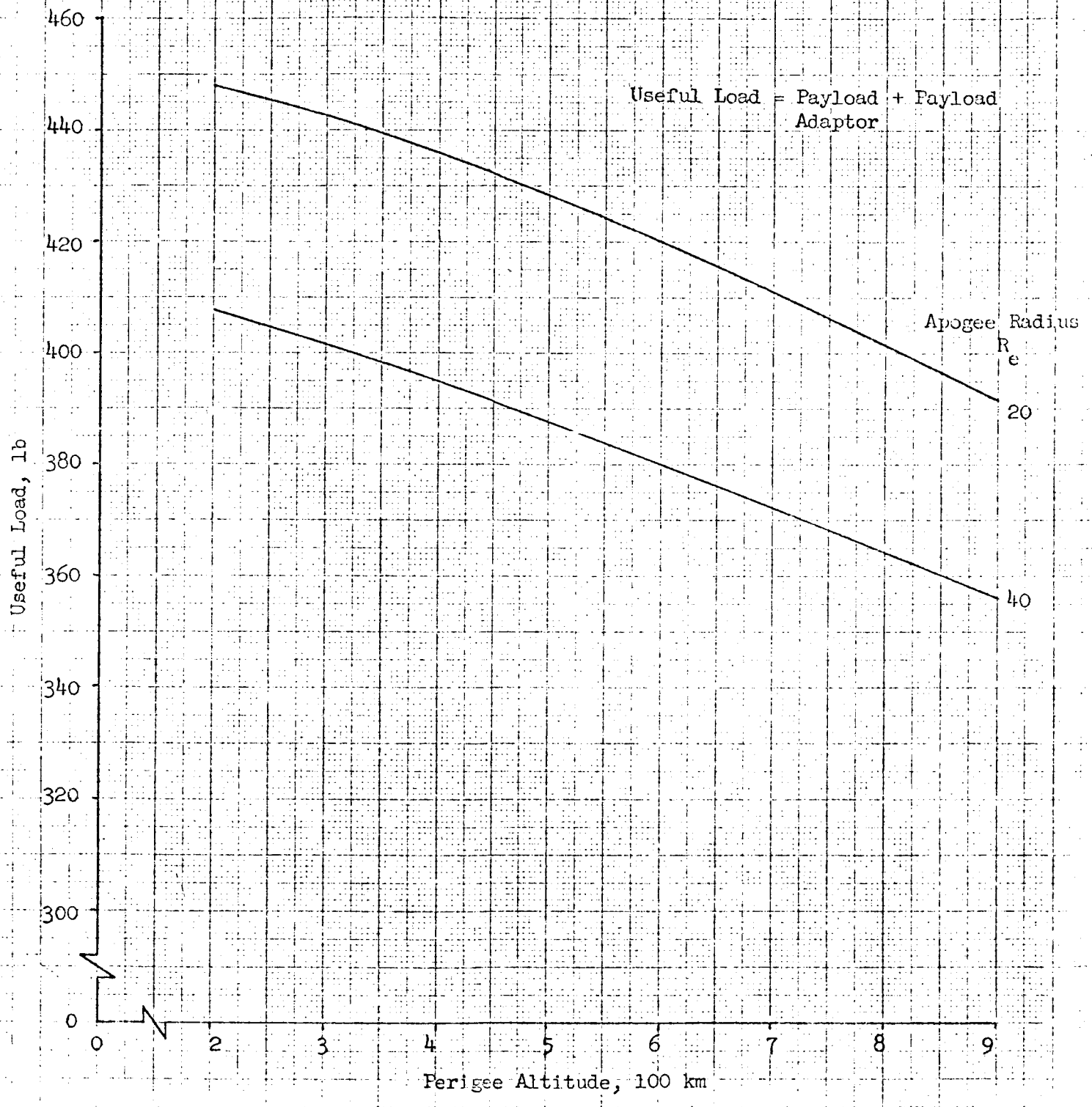

FIGURE 3. DSV-3K PERFORMANCE FOR EAST LAUNCH FROM ETR
(Based Upon Computations Made by DAC)

Additional modifications that are currently in development or under study include: the use of larger solids for the first stage augmentation; the use of higher energy propellants for the second stage; and the substitution of the TE-364 for the FW-4 third stage. While the realization of these developments could benefit the Multiple Satellite application, it is felt that the Multiple Satellite design should be predicated mainly on the developments that are quite certain to proceed. Since some 53 Thorad stages are already on order and the first use of the Thorad with the Delta vehicle is scheduled for 1968, there appears to be little doubt that the present TAT will be phased out and the Thorad will be the standard first stage for the Delta vehicle by the time the multiple satellites are launched. (Similarly the X-258 third stage is currently being superseded by the FW-4.)

Because of the large difference in size, it does not appear likely that the development of the TE-364 third stage would make the FW-4 third stage obsolete. The vehicle will probably be available with alternative third stages. In this case a possible alternative to the DSV-3K will be the DSV-3L vehicle, which differs from the DSV-3K only in the substitution of the TE-364 third stage for the FW-4. The first use of the TE-364 stage with the Delta vehicle is scheduled for this year. Information regarding plans for the future use of this stage is not at hand.

As shown in Figure 4, the DSV-3L would provide a substantial increase in payload capability. However, some problems may be encountered with the Multiple Satellite application. The present design spin rate for the third stage is about 100 rpm which is too low for the currently contemplated Multiple Satellite deployment scheme. If the spin rate cannot be increased to about 140 rpm, the spin rate of the pallet would have to be increased after separation. Also because of the relatively large third stage weight, the use of a parking orbit would not be feasible, and the possibilities for extending the coast period between second stage burnout and third stage ignition, to provide a wider launch window than can be obtained through an optimum direct ascent trajectory, may be minimal.

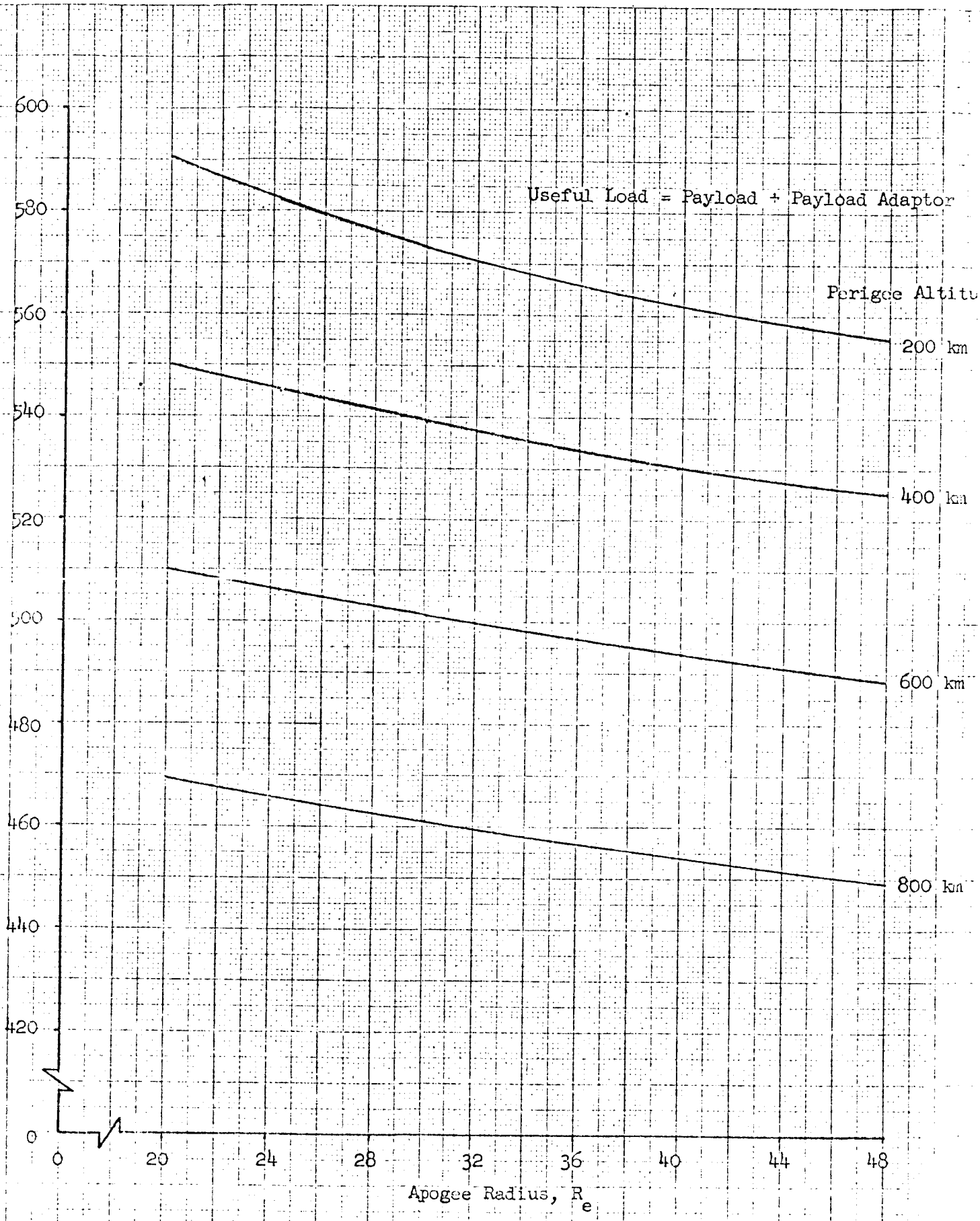

FIGURE 4. DSV-3L PERFORMANCE FOR FAST LAUNCH FROM ETR
(Based Upon Computations Made by DAC)

Since the payload capability of the DSV-3K vehicle appears to be adequate, the availability of this version is assured, and its application to the Multiple Satellite mission is most direct, the present study has been aimed primarily towards assuring the compatibility of the Multiple Satellite design with this version of the booster vehicle.

2.1.2 BURNER II

Boeing has studied the application of its Burner II upper stage to the Multiple Satellite mission. Examination of their results indicates that the use of the Burner II as a third stage above the Thorad/Improved Delta would not improve payload capability in comparison to the use of the FW-4 third stage. Used above the Atlas (SLV-3A) the Burner II could provide a payload capability increase of in order of 230 pounds relative to the DSV-3K. Since a cut-off capability is provided, a reduced dispersion of apogee altitude would be obtained relative to the dispersion that results from the uncertainty in injection velocity when the FW-4, which is not cut-off, is used. However, consideration of the problems arising from variations in apogee altitude indicates that the dispersions obtained without third stage cut-off, though not desirable, will be acceptable. The three axis control capability of Burner II may offer the possibility of achieving the reorientation of the pallet's spin axis without the need for a pallet attitude control system. This approach would involve a radically different design than currently contemplated for use with the spin-stabilized third stage. Inasmuch as no payload advantage is gained with its use above the Thor/Delta, no significant effort was made in the present study to ascertain the compatibility of the Multiple Satellite system design with this stage.

2.1.3 FIVE STAGE SCOUT

Reference to Ling-Tempco-Vought Report No. 23-242, dated 28 September 1965 indicates that the 5-stage Scout could launch a 95-pound payload into a 20 R_e x 100 nmi earth orbit, launching due east from Wallops Island. The current individual satellite design weight is about 85 pounds. The lightest weight obtained for any design previously considered was 65 pounds. Hence, it appears that at most the 5-stage Scout could launch one satellite per launch. The effectiveness of even a 1 satellite per launch scheme is very doubtful since the weight of the satellite would have to be increased to provide an attitude control system for spin axis reorientation, and since the Scout guidance is not nearly accurate enough to match orbital periods so as to avoid excessive growth of separation distances, the satellite would require a substantial orbital period adjustment capability.

2.2 OPERATIONAL FACTORS

The payload capability presented in Figures 1 to 4 have been referenced to the case of a due east launch with an optimum direct ascent booster trajectory. Several operational factors will contribute to variations in payload capability. Range safety and launch window considerations may lead to some departure from optimum trajectories. However, the effects of these factors on payload capability should be relatively minor.

Among the more important factors is the choice of perigee altitude at injection. As a consequence of the deployment velocity increments applied to the satellites after injection of the pallet into orbit, the perigee altitudes of the satellites will suffer changes of about $\pm$ 120 km. In addition, with a lead time of 35 days, the solar perturbation will cause a drop in perigee altitude of about 260 km during the first month after injection into orbit. With a difference in perigee altitude between satellites of about 240 km, it is estimated that the perigee altitude of the lowest satellite must not be lower than about 370 km in order to keep the difference in orbit decay from causing an excessive growth in intersatellite separation distance. In order that the lowest perigee altitude not fall below 370 km, the perigee altitude of the pallet must be about 750 km.

A substantial gain in allowable weight can be obtained if, instead of having the booster vehicle inject the pallet into a 750 km perigee altitude orbit, the booster injects the pallet into a relatively low perigee orbit of about 280 km and a velocity increment is applied to the pallet at first apogee passage to raise perigee altitude. This approach is feasible since the spin axis of the pallet will initially be oriented in a direction reasonably close to the velocity vector at apogee. Hence the required velocity increment can be obtained by means of a small solid rocket firing in the direction of the spin axis. Estimates of the increase in payload capability that could be obtained in this way are presented in Table 1.

It is noted that the increased payload capability would be of most importance if it were necessary to use the DSV-3E version of the booster vehicle. In this case recourse to the use of a pallet velocity increment to increase perigee altitude economically may be mandatory. In the case of the DSV-3K version and particularly with DSV-3L version, the payload capability obtained with direct injection into a 750 perigee altitude orbit appears to be adequate. Hence, for the current design the complication of the pallet design that would be required if the pallet were to provide for the increase in perigee altitude has been avoided.

It should be noted that the estimated requirement for an initial perigee altitude of 750 km is quite conservative in that the drop in perigee altitude due to the solar perturbation has been treated as though it were continually present. This drop will, in fact, not appear immediately and furthermore will not persist, i.e., after about 45 days the perturbation will reverse direction and perigee altitude will subsequently rise. The growth of separation distance resulting from differences in orbital decay that has been allowed, approximately 3,000 km in 6 months in the section of the orbit of most interest, is conservative and could be increased somewhat if necessary. Also some leeway is available in the selection of the lead time, i.e., the number of days from injection to the passage of the sunline over apogee. The lead time affects the phase of the solar perturbation of perigee altitude. The drop in perigee altitude can be reduced by reducing lead time. In fact with sufficient reduction in lead time a benefit instead of a loss could be gained from the solar perturbation.

It is possible, if not probable, that these possibilities for reduction of perigee altitude at injection would lead to an effective increase of payload capability in the order of 20 pounds.

Table 1

DATA ON BOOSTER VEHICLE PAYLOAD CAPABILITY AND COSTS

Vehicle Designation(1)	DSV-3E	DSV-3K	DSV-3L
1st Stage	TAT	Thorad	Thorad
2nd Stage	Improved Delta	Improved Delta	Improved Delta
3rd Stage	FW-4	FW-4	TE-364
Payload Capability			
For East Launch from ETR			
Into 20 R_e x 280 km orbit	318	444	574 lbs
Into 20 R_e x 280 km orbit - Less weight required for ΔV to raise pallet's h_p to 750 km	314(2)	438(2)	566(2) lbs
Into 20 R_e x 750 km orbit	275	405	480 lbs
Cost Per Launch	$3.66 million	$4.06(3) million	$4.15(3) million

(1) In accordance with designations used in NASA "Certified Launch Vehicle Data"

(2) Based upon use of a solid rocket with I_{sp} = 250 sec and mass fraction .5

(3) Includes amortization costs at current rates

3.0 COST AND RELIABILITY

Current estimates of costs for the Thor Delta series vehicles are given in Table 1. To achieve the reliability desired for the Multiple Satellite mission, a booster vehicle reliability of .97 is desired. Although the design reliability for the Thor Delta is .85, current experience based upon 38 missions indicates a reliability of .92. The reliability of the first stage has been 100%; the reliability of the second stage has been .97; the reliability of the third stage has been .95.

The replacement of the X-258 by the FW-4 should improve third stage reliability. The change in the first stage from the TAT to the Thorad involves little in the way of system modification. Hence it is felt that past 1st stage experience is indicative, and that during the years prior to the Multiple Satellite launch there is a good change that the reliability of the vehicle will grow to attain the goal of .97.

4.0 GUIDANCE ACCURACY

Since the errors in injection conditions are trajectory dependent, precise error estimates cannot be made until the details of the nominal boost flight trajectories are established. The values given in Table 2, which were applicable to the Pioneer A mission, are considered to be typical for high energy missions similar to the Multiple Satellite mission, where no yaw maneuver is made and the coast period between second stage burnout and third stage ignition is not prolonged. However, ~~since~~ the third stage is a major error contributor; ~~and~~ because of the heavier payload, the third stage velocity increment for the Multiple Satellite will be smaller, and smaller errors than those listed in Table 2 are to be expected for the Multiple Satellite mission. Also, the errors listed in Table 2 refer to the DSV-3E vehicle using the X-258 third stage. It is believed that the FW-4 third stage will prove to be more accurate both in the direction and magnitude of the velocity increment. Scout experience using the FW-4 indicates a 3σ velocity magnitude error of close to 1%.

Table 2

DELTA GUIDANCE ACCURACY FOR PIONEER A MISSION

Booster Vehicle: DSV-3E (X-258)

Third Stage Burnout Parameter	Nominal Value	One Sigma Error
Time from Liftoff, sec	968	-
Inertial Velocity Magnitude, fps	36190	64
Flight Path Angle, deg	2.26	0.36
Azimuth, deg	115.3	0.36
Altitude, nmi	172.3	11.0
Latitude, deg	14.2N	0.07
Longitude, deg	31.9W	0.11
Pitch/Yaw Attitude Error	-	1.23

The replacement of the TAT by the Thorad is expected to have no major effect on guidance accuracy. The use of the TE-364 third stage might degrade accuracy to some extent as a result of a proportionally larger third stage velocity increment. Prolonged coast periods would also tend to increase directional errors.

The most significant guidance error is the error in velocity magnitude. This error results mainly from the absence of a third stage cutoff capability. For a 400 pound payload the velocity increment applied by the FW-4 third stage will be about 2,400 meter/sec. Assuming a 1% error (3σ), the error in velocity magnitude would be about 24 meter/sec. This would cause a dispersion in apogee radius of about 11,700 km or about 1.8 earth radii, 3σ. Since a reduction in apogee radius is much less desirable than an increase in apogee radius, it will probably be desirable to bias the dispersion in favor of larger apogee radius. This might be done by increasing the nominal second stage velocity increment and decreasing the propellant pad of the second stage.

Apart from the error in velocity magnitude, none of the other guidance errors is large enough to pose any serious problems for the Multiple Satellite mission.

5.0 LAUNCH WINDOW RESTRICTIONS

The role of the booster vehicle in connection with launch window considerations has been discussed in Appendix VII. The most critical factors are the central angle φ_p between the launch site and the perigee radius of the orbit into which the pallet is injected, and particularly the extent to which this angle can be varied. For an optimum direct ascent boost flight trajectory the value of this parameter will be fixed. It is estimated that an annual launch window of about $\pm$ 20 days can be obtained with fixed φ_p.

Widening of the launch window requires variation of φ_p. At some cost in payload capability increased values of φ_p could be obtained by extending the coast period between second stage burnout and third stage ignition. It appears likely that the width of launch window could be doubled in this way with relatively small loss in payload.

To obtain a very wide launch window, i.e., in the order of 1/2 year or more, would require injection into a parking orbit with a first burn of the second stage and restart of the second stage for ejection from the parking orbit. Currently the 3-stage Thor/Delta vehicles are not equipped with a second stage restart capability. However, a restart capability exists and has been flown on the two stage vehicle, and presumably can be adapted to the 3-stage configuration. The duration of the coast period in parking orbit is limited to about 3000 seconds by the second stage ACS cold gas presently supplied. If the cold gas supply were increased, the coast period would be restricted by the 4,000 second limitation of the present second stage autopilot programmer.

For more detailed definition of launch window restrictions, further studies of the boost flight trajectory and vehicle constraints is required. This includes:

- Generation of the nominal boost flight trajectory with some precision to fix the value of φ_p for the optimum direct ascent case. This in turn would fix the optimum launch data more precisely.
- Study of the trade-off between φ_p range and payload capability to determine to what extent widening of the launch window is feasible without restart of the second stage.
- Investigation of the restart capability that is likely to be available and the effects of extended periods in parking orbit on payload capability and guidance accuracy.
- Review of the operational problems involved in meeting an assigned time-of-day launch time; making minor day-to-day adjustments in flight plan; and making major changes in the flight plan involving reprogramming of the autopilot.

6.0 INITIAL ATTITUDE STABILIZATION CONDITIONS

The initial conditions relating to the pallet's attitude stabilization and control that are inherited from the booster's third stage are:

a. Spin rate,

b. Direction of the spin axis, and

c. Amplitude of coning motion.

The initial spin rate of the pallet is important in that it determines the velocity increment obtained by the in-plane spin-off separation of the satellites from the pallet. Also the satellites' spin rate at completion of deployment scales down from the pallet's initial spin rate. Based upon an early estimate of the payload moment-of-inertia, it appeared that an initial spin rate of about 140 rpm would be attainable with the existing complement of 3rd stage spin-up rockets. Calculations relating to the deployment velocity increment and the satellites' spin rate have been based upon this nominal initial spin rate. However, the payload moment of inertia for the current design (about 32 slug-ft^2) turned out to be substantially larger than earlier estimates. Also the arm at which the satellites are deployed is smaller than had been anticipated. Since special 2nd stage spin-up rockets will be required, in any event, it may be desirable to spin-up to the maximum allowable rate, which is 200 rpm. This would compensate for the reduced deployment arm and restore the estimate of the spin-off velocity increment.

Since the spin-up of the third stage is open-loop with respect to rate, a substantial dispersion in spin rate, about 10% 3σ, is expected. To avoid the error in the direction of the spin-off velocity increment that would otherwise be made as a result of spin-rate uncertainty, a precise measurement of spin rate will be obtained from the satellites' aspect sensors prior to the spin-off separation, and the time of commanding separation will be adjusted so that the direction of the velocity increment remains perpendicular to the orbital velocity vector.

It is assumed that the nominal direction of the spin axis at separation from the third stage will be in or close to the direction of the velocity vector at perigee. As indicated in Table 2 an attitude error of about 1.23 deg 1σ or about 5 deg 3σ is expected at 3rd stage burnout. As a result of tip-off disturbances the departure of the direction of the pallet's spin axis from nominal after separation may be somewhat greater. However, there are no stringent requirements on the accuracy of the initial direction of the pallet's spin axis. The main consideration is that the pallet's ACS requires the initial direction of the spin axis to be at least 10 deg from the sunline. The direction of the sunline will be at least 45 degrees from the direction of the perigee velocity vector.

Hence an initial error in the direction of the spin axis of nearly 35 degrees could be tolerated. An error of this magnitude is extremely improbable.

The initial amplitude of coning motion is of concern only to the extent that coning motion might interfere with the separation of the payload from the 3rd stage. In this respect the Multiple Satellite payload is not essentially different from any other payload served by the booster vehicle. Hence no difficulty in separation is anticipated. After separation, the pallet's precession dampers will cause the initial coning to decay long before operation of the pallet's ACS is to be initiated.

Appendix VII

LAUNCH WINDOW CONSIDERATIONS

1.0 INTRODUCTION

In the selection of launch conditions, the factors affecting the coverage of the subsolar line are of prime concern. As discussed in Appendix V, these factors are:

a. The inclination of the orbital plane with respect to the ecliptic plane.

b. The orientation of the sunline relative to the orbit.

c. The true anomaly of the common line.

Attention must be given not only to the attainment of desirable initial values for these parameters, but also to the maintenance of desirable conditions during the operational lifetime, particularly the first portion of the operational lifetime, in the face of orbital perturbation effects.

The major orbital perturbation effects that can influence the factors affecting subsolar coverage are those due to the earth's oblateness and solar and lunar gravitation. The latter perturbations can also have a strong influence on perigee altitude. Hence, it would be desirable that initial conditions with respect to these perturbations be such that a favorable perturbation; e.g., increasing trend in perigee altitude is obtained, or that at least an unfavorable trend; e.g., a marked decrease in perigee altitude, is avoided.

The purpose of this Appendix is to review the effects of launch conditions on the aforementioned factors; to determine the nature of any conflicts that may be involved in achieving favorable values for all parameters and/or obstacles imposed by the booster vehicle constraints; to make a preliminary assessment of the potential effects of the orbital perturbations; and to obtain a preliminary estimate of launch window limitations.

2.0 REVIEW OF FACTORS AFFECTING SUBSOLAR LINE COVERAGE

As described in Appendix V, the minimum initial inclination to the ecliptic plane is obtained by a due east launch, AZ = 90 degrees, at that time of day, $t = t_{min}$, when the launch site is closest to the ecliptic plane. Under these conditions for a launch from ETR, an initial inclination to ecliptic plane of slightly greater than 5 degrees is obtained. After consideration of other factors, orbital perturbation effects, etc., the selection of nominal values for t and AZ might be reconsidered. However, it appears unlikely that there would be any very substantial change from the conditions: $t = t_{min}$; AZ = 90 degrees.

The annual variation of the time of day corresponding to $t = t_{min}$ is shown in Figure A. Figure B shows the effects of small departures from t_{min} and AZ = 90 degrees on inclination to the ecliptic. Figure C shows the launch azimuths which for given values of $(t - t_{min})$ yield the smallest inclination to the ecliptic and the corresponding values of the inclination to the ecliptic.

A launch azimuth of 90 degrees is desirable not only for obtaining minimum inclination to the ecliptic at $t = t_{min}$, but also for obtaining maximum payload capability. An estimate of the variation in payload capability with launch azimuth is presented in Figure D. Also shown in Figure D is the change in apogee radius that would be incurred, if as appears more likely, a shift in azimuth is accommodated not by changing payload weight, but by accepting the change in apogee radius.

Since the conditions of most interest for the Multiple Satellite experiments are obtained when apogee is in the general direction of the sunline, it is desirable that this condition be encountered early in the operational lifetime when the probability of successful collection of data is greatest. A lead time of about 35 days before the sunline passes over apogee is considered to be a suitable choice. Allowing a few orbits for completion of the deployment of the satellites from the pallet, the first two months of data collection will then cover a range of about ± 30 deg. in the sunline position relative to apogee. As described in Appendix III, this choice for the initial orientation of the sunline relative to the orbit is consistent with the projected technique for handling the out-of-plane deployment for Option 3. (The main emphasis of present considerations will relate to this option.)

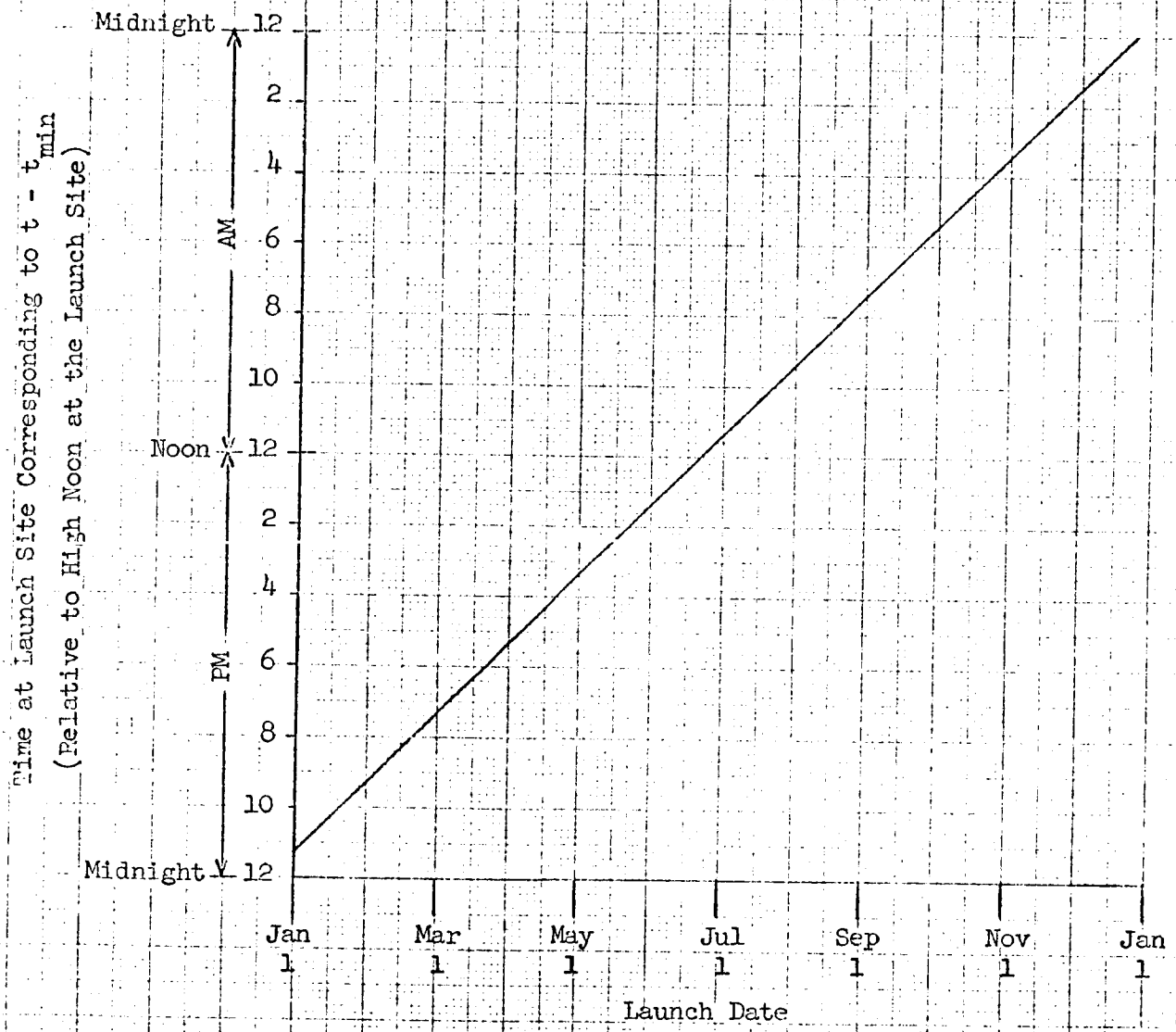

FIGURE A - TIME OF DAY CORRESPONDING TO $t - t_{min}$

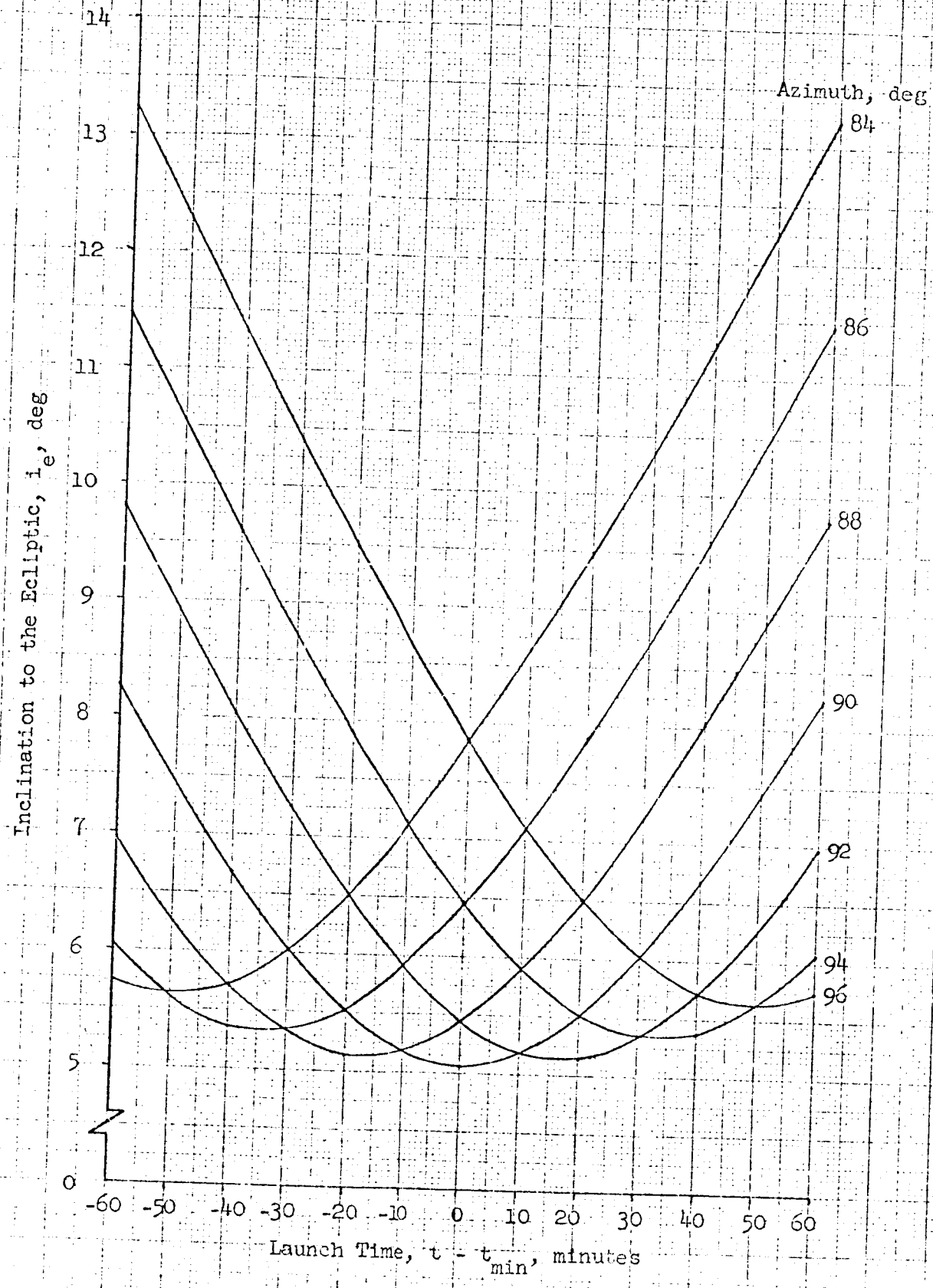

FIGURE B. EFFECT OF LAUNCH TIME AND AZIMUTH ON INCLINATION TO ECLIPTIC

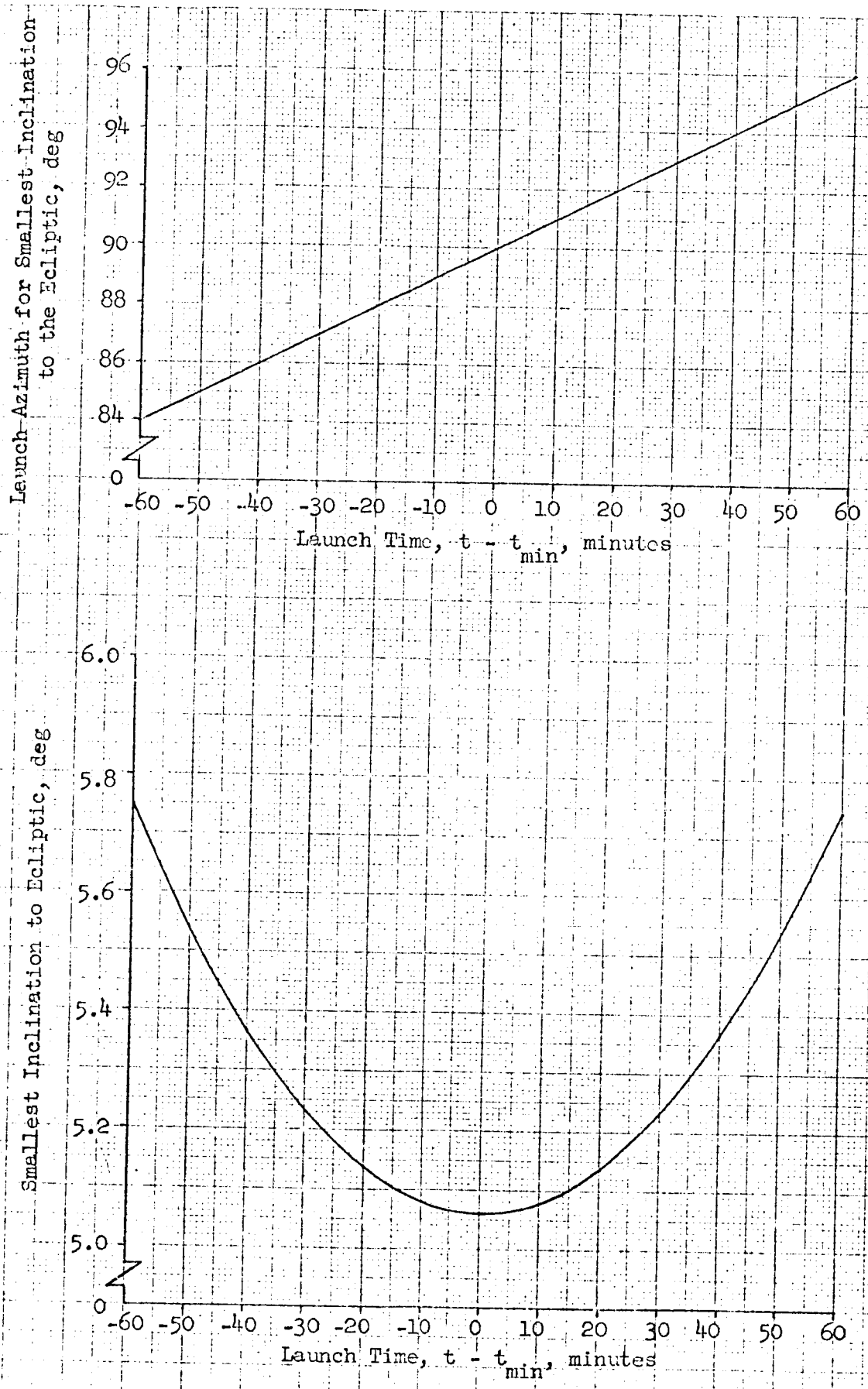

FIGURE C. VARIATION OF LAUNCH AZIMUTH FOR SMALLEST INCLINATION TO ECLIPTIC WITH LAUNCH TIME

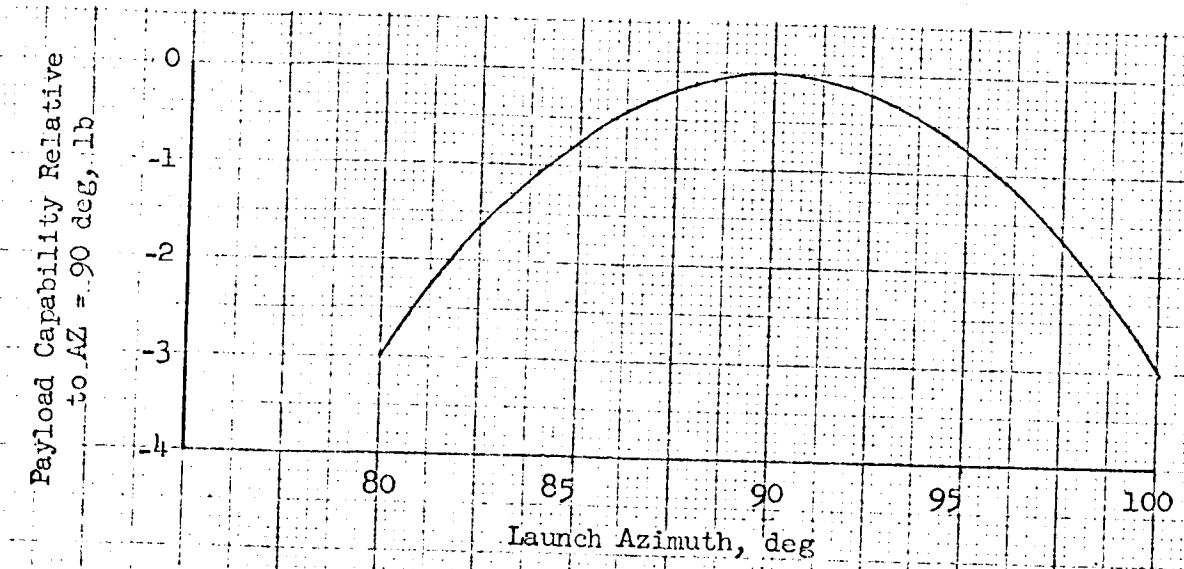

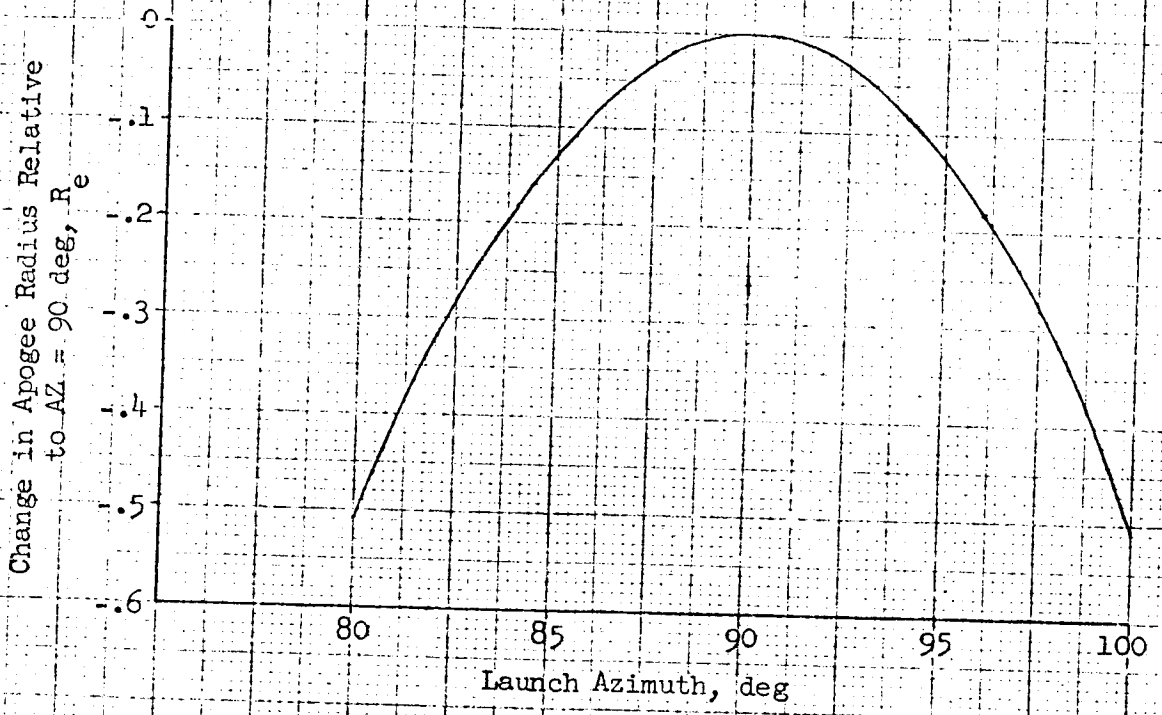

FIGURE D. EFFECT OF LAUNCH AZIMUTH ON PAYLOAD AND APOGEE RADIUS

The values of ϕ_p, the angle between the launch site and perigee required to obtain the desired lead time, can be determined using the results presented in Appendix V. Specifically, from the data given in Figures J to M of Appendix V, it can be shown that the angle s_a is given approximately by:

$$s_a = -S + \phi_p + .22\ (t - t_{min}) + 270 \qquad (1)$$

where all angles are expressed in degrees and $(t - t_{min})$ is given in minutes. For the range of launch conditions of present interest, the launch azimuth has no significant effect on s_a. The value of s_a in degrees is equal to the lead time in days. The value of S in degrees is approximately equal to the number of days from the vernal equinox.

The value of ϕ_p required to obtain a value of $s_a = 35$ degrees for a launch at $t = t_{min}$ is defined by Equation (1) as a function of the launch date. This relationship is shown in Figure E. For a direct ascent booster trajectory, optimized with respect to payload capability, the value of ϕ_p will be fixed. Current estimates indicate that this value of ϕ_p will be about 30 degrees. With such a boost trajectory, the desired lead time, along with minimum inclination to the ecliptic, could be obtained on only one day of the year. As indicated in Figure E, this date would be about December 15.

With a fixed value of ϕ_p, a widening of the annual launch window can be obtained by:

a. Departing from the launch conditions: $t = t_{min}$; AZ = 90 degrees, at the cost of an increase in initial inclination to the ecliptic, and/or

b. Accepting a range of values of the lead time.

Figure F shows the effect of departing from the nominal launch time and date on lead time. Restricting the range of lead time to 25-45 days and the range of $(t - t_{min})$ to $\pm$ 45 minutes, and assuming that a scheduled launch time of day can be closely met, it is found that a launch window of about $\pm$ 20 days could be obtained with a fixed ϕ_p. A launch window of about $\pm$ 10 days can be obtained from the $\pm$ 45 minute range of $(t - t_{min})$ while holding a fixed lead time.

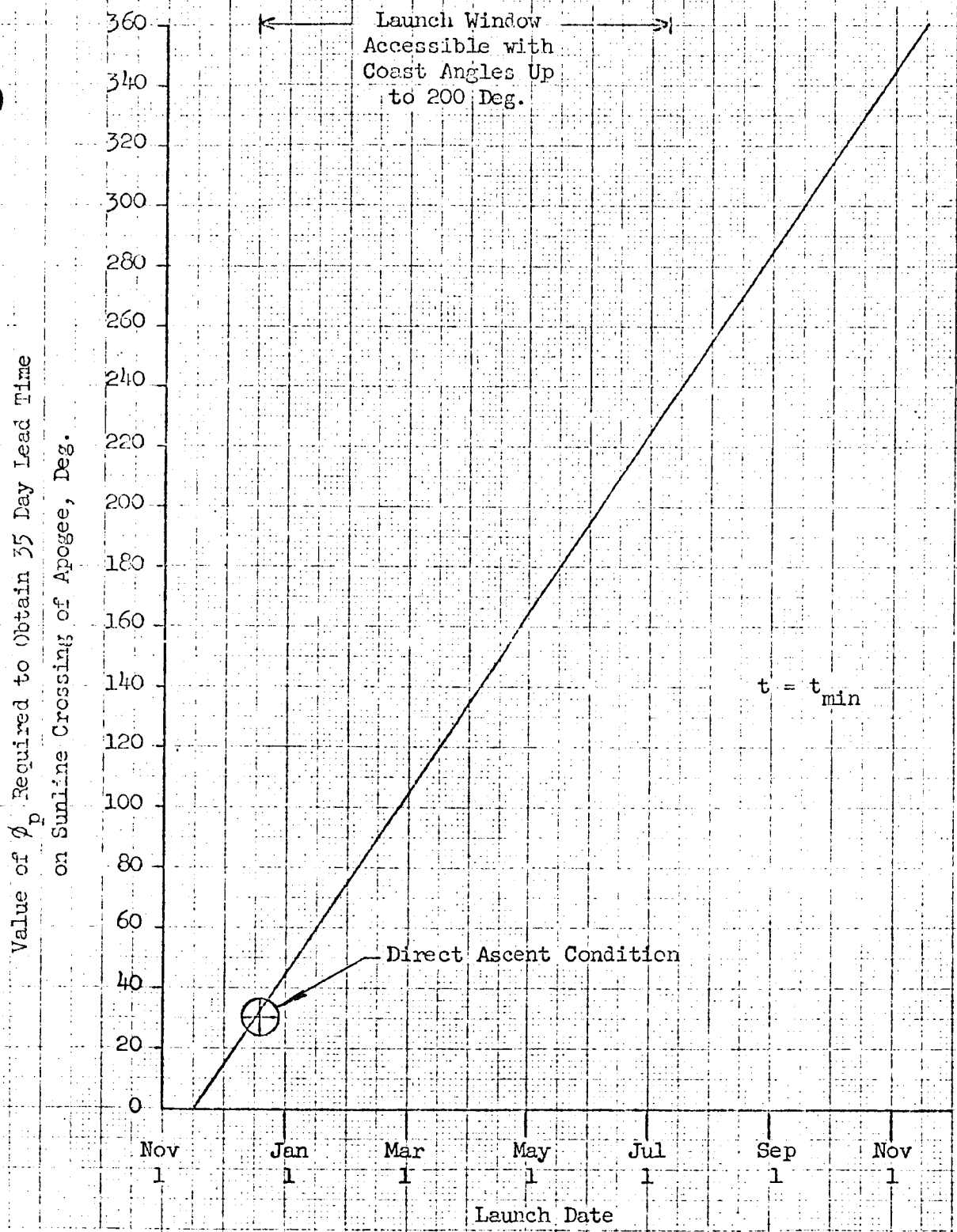

FIGURE E - VARIATION OF REQUIRED VALUE OF ϕ_p WITH LAUNCH DATE

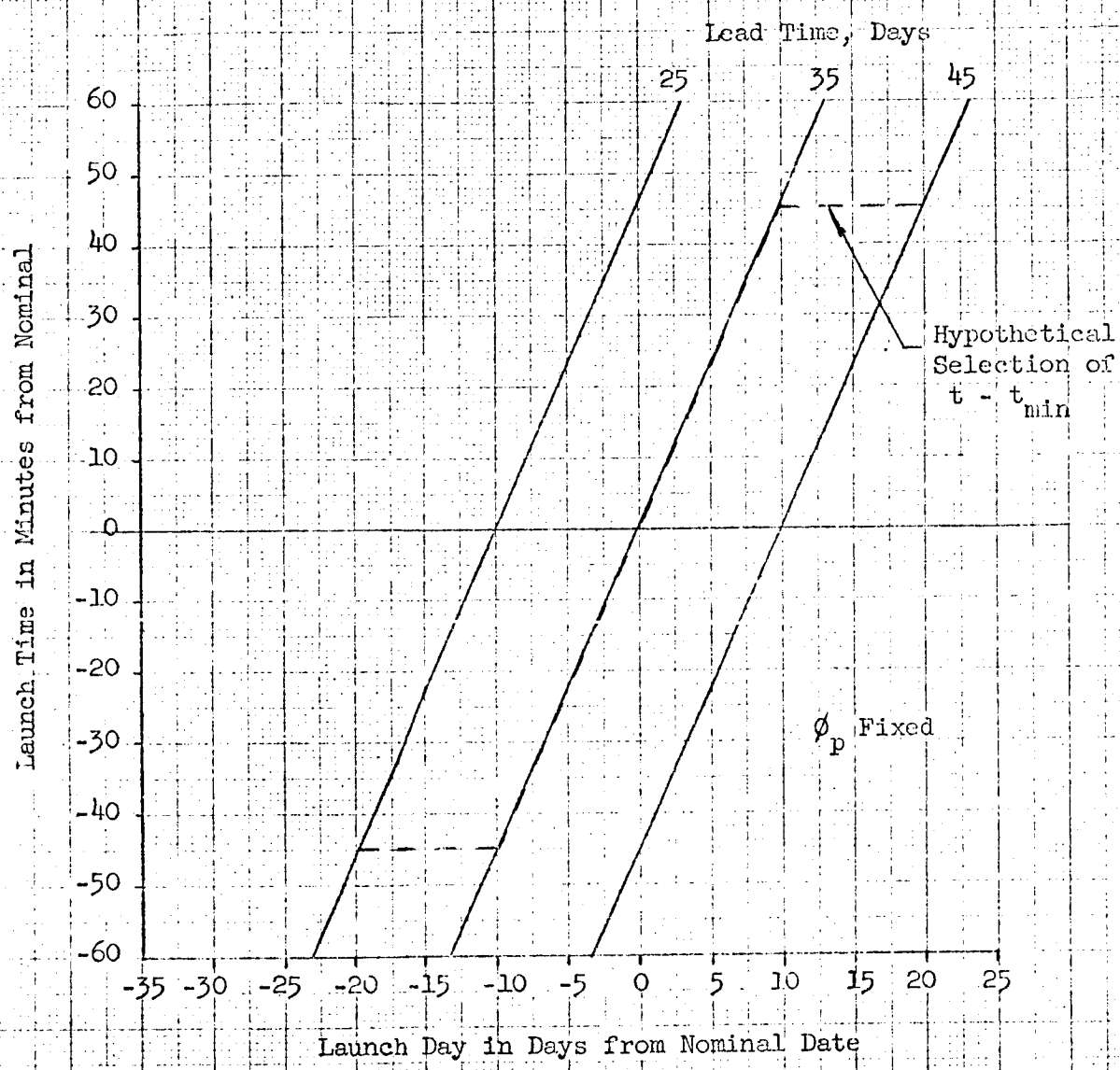

FIGURE F - EFFECT OF LAUNCH TIME AND DATE ON LEAD TIME

Further widening of the launch window requires variation of ϕ_p. The value of ϕ_p cannot be feasibly reduced to any great extent. An increase in ϕ_p can be obtained either (a) by increasing the coast period between second stage burnout and ignition of the third stage, or (b) by injecting into a parking orbit with a first burn of the second stage and ejecting from the parking orbit with a second burn of the second stage. The former alternative involves a payload penalty that increases with increased coast time. The latter alternative requires restart of the second stage. A restart capability is available and has been used with the two-stage TAID booster vehicle configuration. Presumably, the restart capability can be adapted for the three-stage configuration, although some minor additional development may be needed. At best, some reduction in reliability would be involved.

In any case, it must be recognized that to effect a change in the flight program so as to obtain a change in ϕ_p is not a simple matter. It is necessary to reset the flight programmer. This could require a down time of several days. To keep prelaunch operational problems to a practicable level, the flight programs involved must be restricted to a reasonably small number and each program must be retained for a reasonably large number of days. It is felt that the time on stand with a fixed flight program should not be reduced below about 20 days.

It should be noted that in principle a fixed flight program would fix the nominal launch azimuth as well as the nominal ϕ_p. However, it is understood that the BTL radio guidance system has the capability of departing from the nominal launch azimuth to a limited degree. This is done by taking into account the fixed flight program for the open-loop guidance portion of the second and third stage flight to achieve an ultimate orbit in the desired plane. To a degree, depending upon the departure from the nominal azimuth, the trajectory obtained would be slightly dog-legged.

An assessment of the possibilities for increasing ϕ_p without recourse to restarting the second stage awaits evaluation of the loss in payload capability. It is noted that if ϕ_p could be increased to 60 degrees with an acceptable payload reduction, the launch window could be extended an additional 40 days. More specifically, with two flight programs (one providing a ϕ_p of 30 degrees, and the other

a ϕ_p of 60 degrees, allowing a $\pm$ 45 minute range in $(t - t_{min})$ and a $\pm$ 10 day range in lead time) a window from about 25 November to 13 February could be obtained.

The duration of the coast period is limited to about 3000 seconds by the cold gas available for the second stage ACS. With a parking orbit period of about 90 minutes, this would permit a coast angle of about 200 degrees. If the nitrogen supply were increased, the 4,000 second capacity of the Delta programmer would become main constraint. The coast angle would then be limited to about 266 degrees. Reference to Figure E indicates that with a 200 degree coast angle available, nominal launch dates could be chosen between December 15 to July 7. With a 266 coast angle available, the choice of nominal launch dates could be extended to about September 12.

It is noted that each of the types of boost flight trajectories; viz:

a. Optimum direct ascent

b. Extended coast period with no restart of the second stage

c. Injection out of parking orbit with restart of the stage

has drawbacks. In the first case, the annual launch window is severely restricted. A schedule delay could involve nearly a year's postponement of the launch date. In the second case, the launch window is widened to a degree, but only at some cost in payload or in apogee radius. The third case incurs the risks involved in the restart of the second stage. Fortunately, the opportunities for application of the three types of trajectories occur in calendar sequence. Hence, it may not be necessary to make a hard choice between the alternatives. Instead, the optimum direct ascent trajectory being the most desirable can be given first priority. If the launch window associated with this trajectory is missed, and it is considered preferable that a less desirable trajectory be used rather than suffer a year's postponement, the extended coast period without restart trajectory could be used. If the launch window associated with this second priority booster trajectory is missed, the use of a parking orbit with restart of the second stage can be resorted to as a last recourse. Since the status of the restart capability could improve in

the time prior to that currently anticipated for the Multiple Satellite launch, it is felt that a final decision as to whether such recourse will or will not be taken should be deferred.

Figure G shows the effect of small variations of t from t_{min} and AZ from 90° on ϕ_c. For sufficiently small variations, φ_c can be represented by a linear approximation. Using such an approximation, true anomaly of the line common to the orbital and ecliptic planes, $\theta_c = \phi_e - \phi_p$, is given by:

$$\theta_c = -\phi_p + (t - t_{min}) - 10\,(AZ - 90) + 90 \qquad (2)$$

The variation of initial value of θ_c with launch date for launches with $t = t_{min}$, AZ = 90 degrees and ϕ_p equal to the value required for a lead time of 35 days is shown in Figure H.

As discussed in Appendix V, the value of θ_c affects the orbital distribution of distances from the ecliptic plane. To obtain best coverage of the sub-solar point, it is desired that the section of the orbit from 10 to 16 R_e lie close to the ecliptic plane. To be taken into account in the case of Option 3, is the fact that the array of intersatellite separation distances obtained on the descending leg of the orbit will be more compatible with the desired experiment conditions than on the ascending leg. It is therefore advantageous to favor the descending leg; i.e., to select the value of θ_c insofar as possible to keep the descending leg close to the ecliptic plane. This condition is best obtained with values of θ_c roughly in the range from 0 to +30 degrees or equivalently 180 to 210 degrees. On this basis the yearly intervals during which the nominal initial values of θ_c are in the most favored range are indicated in Figure H. It is seen that the center of one interval occurs near February 1 and the other near August 1. The width of the intervals of favored values of θ_c is in the order of one month.

(If the satellite array were symmetrical with respect to obtaining desirable properties on both legs of the orbit, the advantageous θ_c range could extend from -30 to +30 degrees or from 150 to 210 degrees, thus widening each of the favored interval by about a month.)

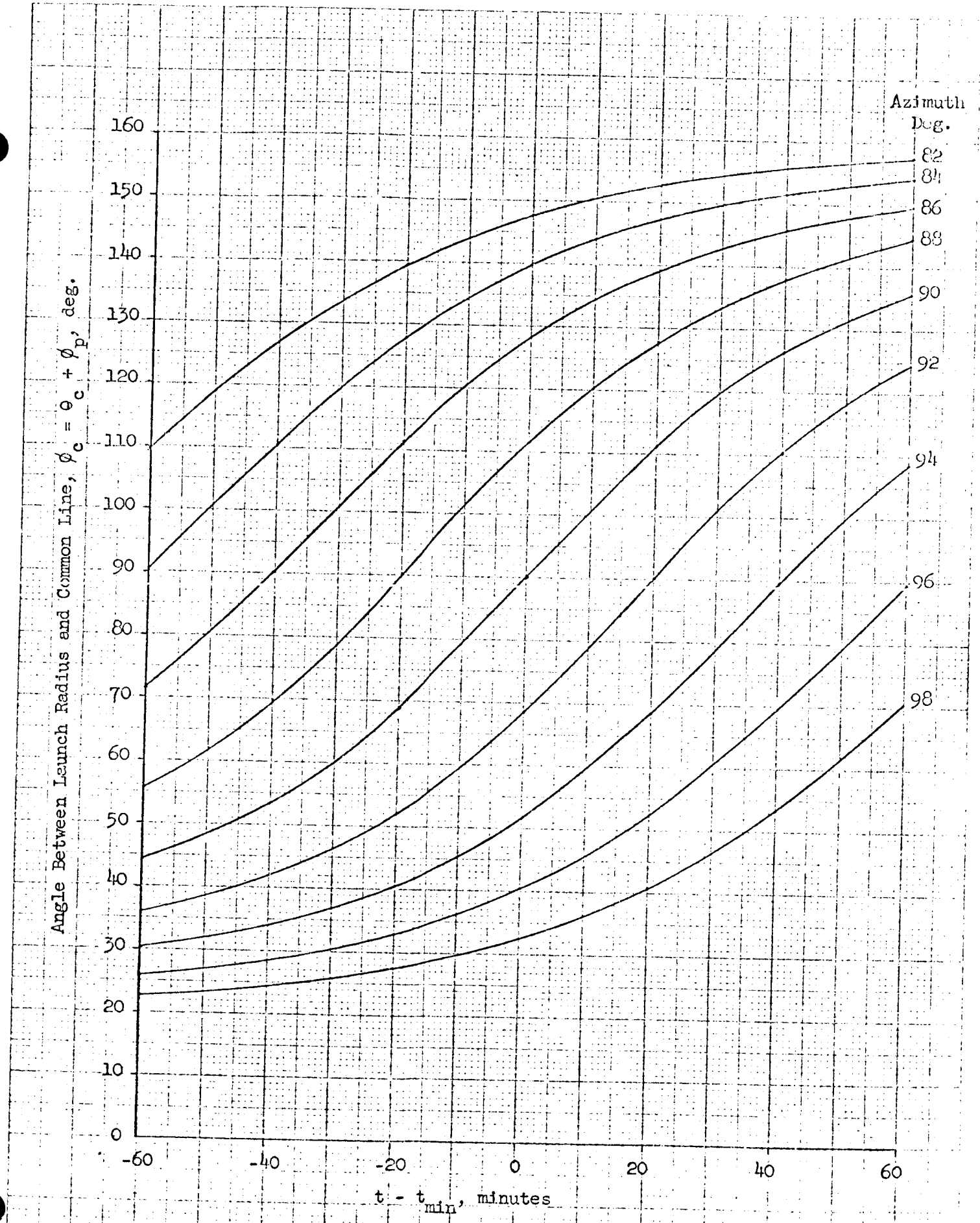

FIGURE G - EFFECT OF LAUNCH TIME AND AZIMUTH ON THE ANGLE BETWEEN THE LAUNCH RADIUS AND THE COMMON LINE

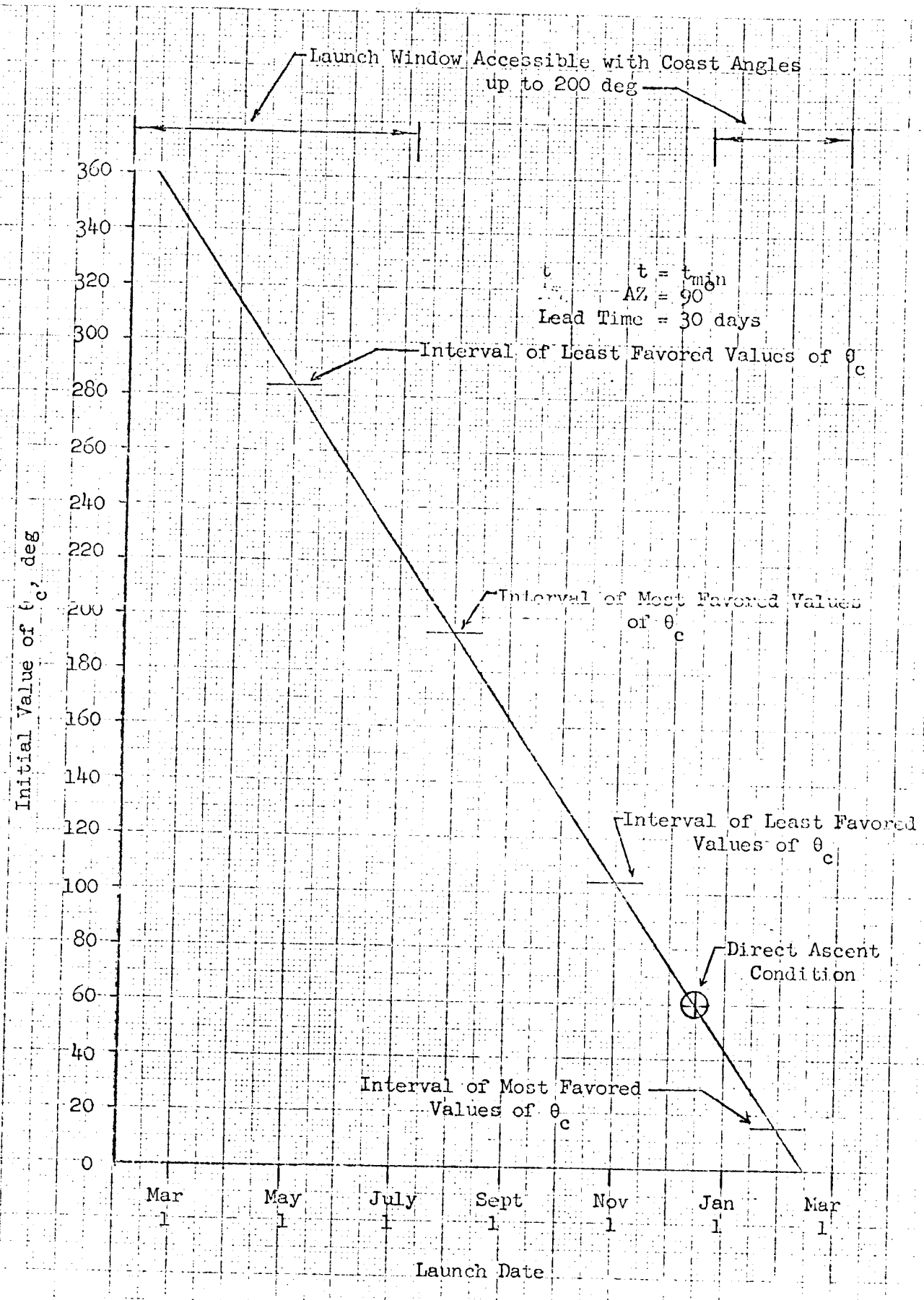

FIGURE H. VARIATION OF NOMINAL INITIAL VALUE OF θ_c WITH LAUNCH DATE

The largest distances from the ecliptic on the descending leg of the orbit are obtained when the value of θ_c is in the range from 90 to 120 degrees. Hence, for the Option 3 deployment, this range of values of θ_c is least favored. The intervals of least favored values of θ_c are centered on dates of about May 1 and November 1 and also extend for about a month. If a launch cannot be made in the most favored interval, as would be hoped for, at least it should be possible to avoid a launch during the least favored intervals.

On a given date with a fixed value of ϕ_p, the values of t and AZ cannot be chosen to obtain optimum conditions with respect to inclination and lead time and also θ_c. However since the "nominal" values of t and AZ have been chosen to minimize inclination, the effects of small variations in t and AZ on inclination are of second order. (Also, the effect of AZ on payload or apogee radius is of second order.) Hence, within limits, the values of t might be chosen to minimize the deviation from the nominal lead time and the value of AZ might be selected to optimize θ_c.

The minimization of the deviation from the nominal lead time is relatively straightforward. Subject to a constraint imposed on $|(t - t_{min})| \leq 45$ minutes, the choice of t is then as indicated by the dashed line on Figure F. The choice of AZ to optimize θ_c depends upon the nominal value of θ_c, which is equal to $(90 - \phi_p)$. If the nominal value is above the favored range; i.e., θ_c = 0 to 15 degrees, or θ_c = 180 to 195 degrees, a decrease in AZ would be desirable; if the nominal value of θ_c is below the favored range, an increase in θ_c is desirable.

On the other hand, although the effects of small deviations from the nominal values of t and AZ an inclination are of second order, as mentioned above and shown in Figure C, the increase in inclination could be minimized by choosing AZ in accordance with the deviation of t from nominal. If the nominal value of θ_c is above the favored region, positive values of $(t - t_{min})$ are fortuitous in that an increase in azimuth will then both reduce θ_c and, to a point, also reduce i_e. For negative values of $(t - t_{min})$, the effect of AZ on θ_c and i_e would be conflicting. Such conflicts are minimal when a nominal value of θ_c within or close to the favored range can be obtained. In other cases, the resolution of such conflicts requires detailed study of the particular circumstances of the launch window.

Figure I illustrates the conditions obtained when $\phi_p = 30$ degrees and the value of t is selected to minimize the deviation from the nominal lead time while the value of AZ is selected to minimize the inclination to the ecliptic in accordance with the value of t. It is seen that in this case the value of θ_c remains nearly constant throughout the 40-day launch window interval. Its value of to about 60 degrees is larger than would be desired.

Figure J shows the conditions obtained with $\phi_p = 30$ deg when an alternative selection of launch time and azimuth is made. In this case the launch parameters were chosen: (a) to keep θ_c equal to about 40 degrees; (b) to avoid inclinations greater than 6 degrees and minimize inclination insofar as possible; (c) to favor the shorter lead time within the range 25 to 45 days. The latter condition is introduced to minimize the adverse effects of the solar perturbation on perigee altitude, which as will be discussed shortly grows more severe with increased lead time.

The results presented in Figure J indicate that the reduced value of θ_c can be obtained with relatively small increases in inclination. At the same time the likelihood of a large lead time is reduced while the 40-day width of the launch window is retained. The lower values of θ_c should more than offset the slightly larger inclinations to the ecliptic insofar as having the section of the orbit of most interest close to the ecliptic plane is concerned.

As described in Appendix V, as a result of the orbital perturbations arising from the earth's oblateness are expected to reduce θ_c by about 35 degrees during the first 3 months in orbit. In this case, the initial values of θ_c obtained with the selection of t and AZ shown in Figure J would result in very desirable values of θ_c during the most important part of the orbital lifetime. However, before this conclusion can be substantiated, the effects of the solar and lunar perturbations must be taken into account.

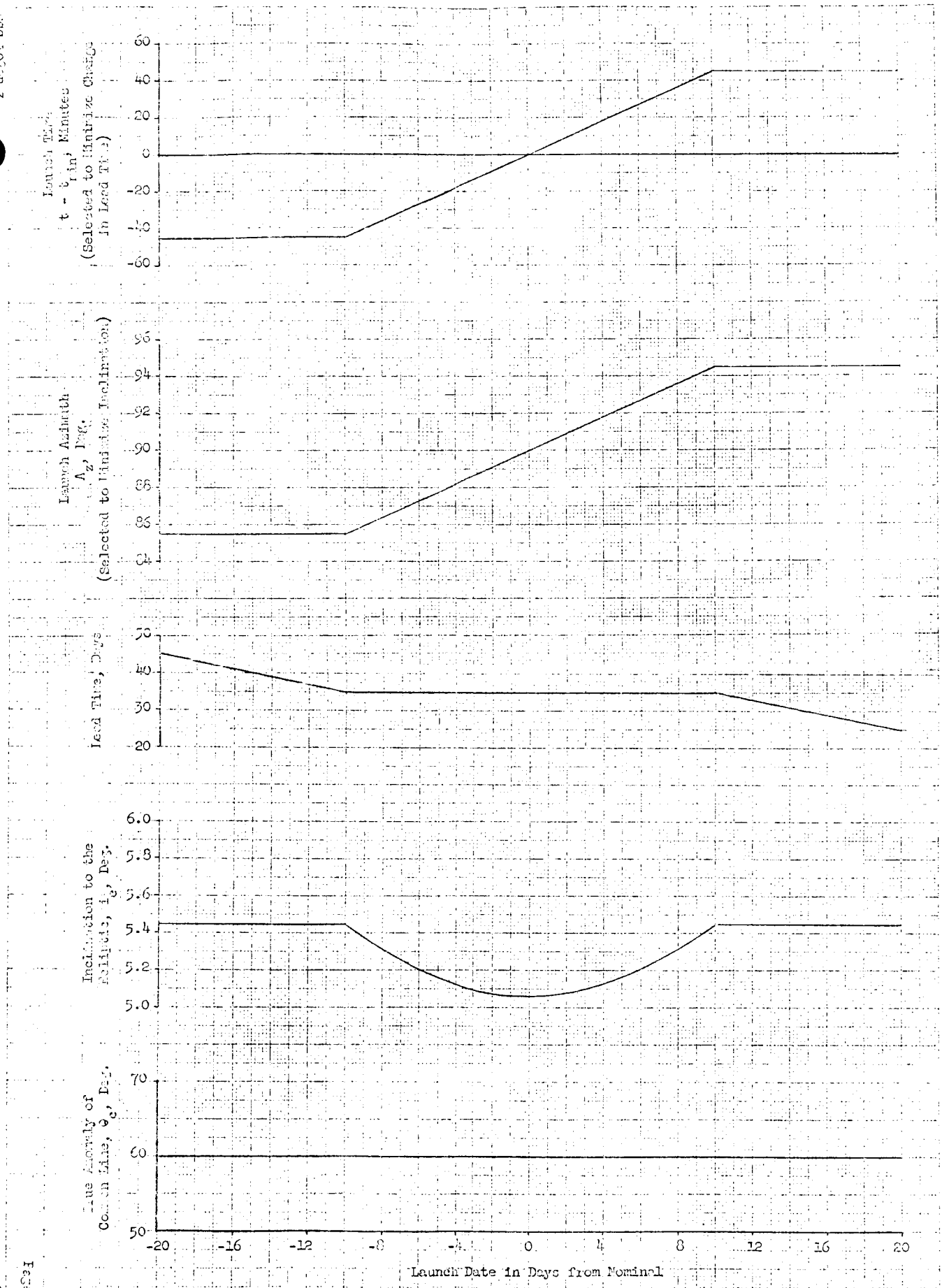

FIGURE I - VARIATION OF LAUNCH CONDITIONS WITH LAUNCH DATE. ϕ_p = 30 DEG.
t CHOSEN TO MINIMIZE DEVIATION FROM NOMINAL LEAD TIME.
Λ_z CHOSEN TO MINIMIZE INCLINATION TO THE ECLIPTIC.

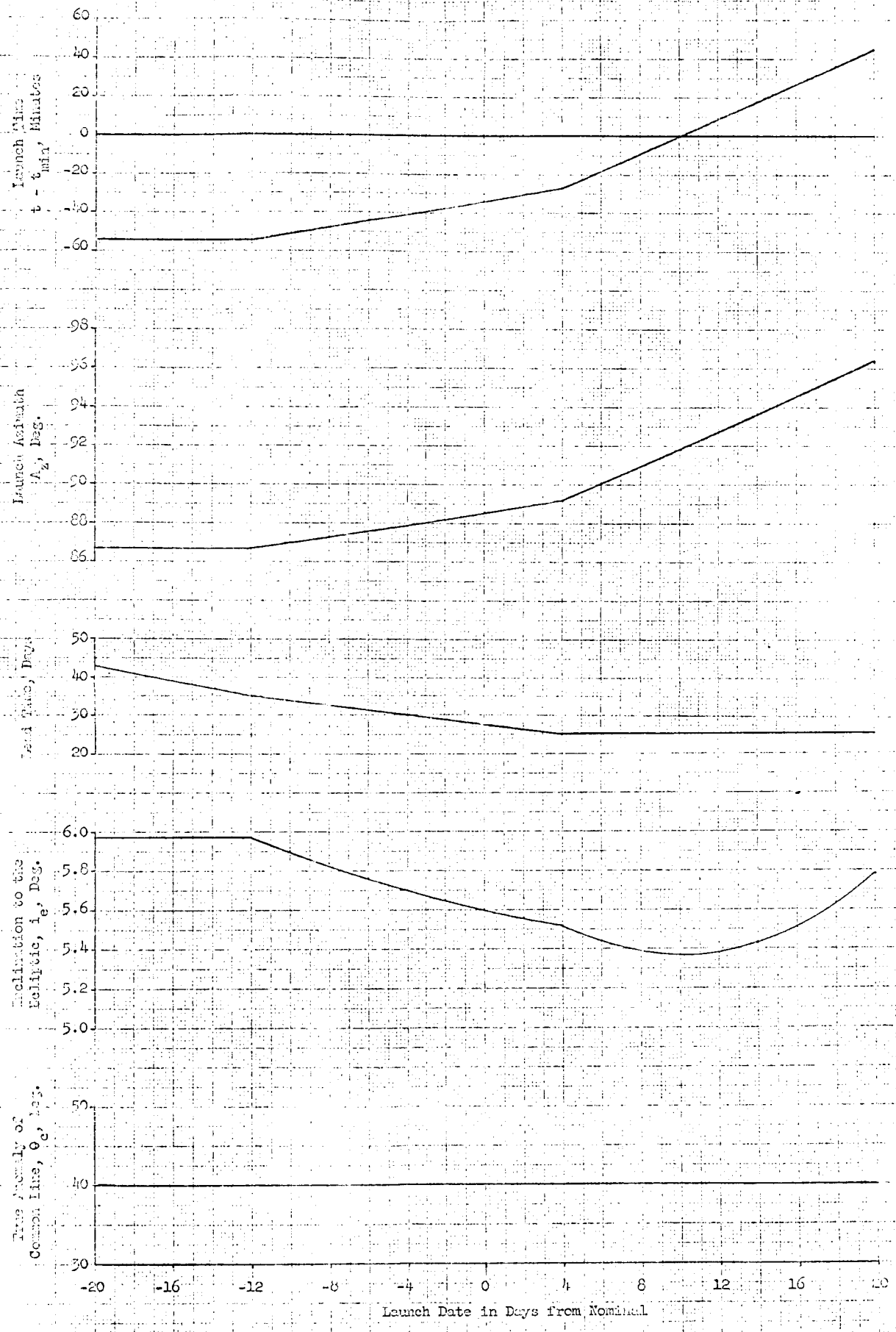

FIGURE J - VARIATION IN LAUNCH CONDITION WITH LAUNCH DATE, ϕ_p = 30 DEG.
t and A_z CHOSEN TO KEEP θ_c = 40 DEG, MINIMUM INCLINATION,
FAVORING SHORT LEAD TIME

3.0 SOLAR AND LUNAR PERTURBATIONS

The final items to be considered here with regard to the launch window are the effects of solar and lunar perturbations. Consideration of these perturbations has been deferred not because these effects are less important but because they are more complicated. However simplified treatment of the solar and lunar perturbations are available in the literature* which permit at least a qualitative evaluation of some of the main effects on the selection of launch window to be obtained. In particular the Multiple Satellite nominal orbit is fairly close to that of the EGO (Eccentric Geophysical Observatory) so that the results given in the literature for the latter orbit can be expected to be generally representative of the effects to be expected for the Multiple Satellite.

In addition to effects on the orientation of the orbital plane which will influence the values of i_e and θ_c (and to a lessor degree s_a), the solar and lunar perturbations have an important influence on perigee altitude. There is no effect on orbital period. Hence, as in the case of an in-plane normal velocity increment, the effect on apogee radius is of equal magnitude but in opposite direction to the effect on perigee altitude.

The effects of solar and lunar perturbations on each of the orbital parameters of interest can be expressed approximately as a sum of a secular and an oscillatory term. In the case of the solar perturbation the oscillatory term has a period of 1/2 year. In the case of the lunar perturbation, the period of the oscillatory term is 1/2 the period of the lunar orbit, i.e., about 15 days.

For the Multiple Satellite orbit, the lunar perturbation of the gravitational acceleration is greater than the solar perturbation. Hence the secular terms of the lunar perturbations generally exceed the secular terms of the solar perturbations. However, because of the shorter period the amplitude of the oscillatory

---

* See NASA SP-33, "Orbital Flight Handbook", Martin Marietta, 1963, Vol. 1, Chapter IV.

terms for the lunar perturbations are much smaller than the amplitudes of the oscillatory terms for the solar perturbation.

The effects of launch date on both the secular terms and the initial phases of the oscillatory terms varies approximately with a period equal to that of the corresponding oscillatory term. That is to say if all launch conditions other than the launch date were kept constant, a complete cycle of lunar perturbation effects would be obtained in launch date interval of about 1/2 month; a complete cycle of solar perturbation effects is obtained in a launch date interval of 1/2 year. Therefore it can be expected that adverse effects produced by the solar or lunar perturbation will not extend over a launch date interval greater than half the interval in which a complete cycle of conditions is obtained, and that strong adverse effects will not extend over a launch date interval greater than 1/4 the complete cycle interval. Hence, for lunar perturbations intervals of strong adverse effects may extend for 3 to 4 days; for the solar perturbation strong adverse effects may extend for about 45 days. Accordingly it appears that adverse lunar perturbation effects, which if necessary can be avoided by blanking out a few days of the launch window, are more readily dealt with than adverse solar perturbation effects.

Since i_e, the inclination of the orbital plane relative to the ecliptic plane will be quite small, the approximations for the solar perturbation effects given by Equations (167) to (171) of the aforementioned reference can be further simplified by neglecting higher order effects of the departure of i_e from zero. Upon (a) making small i_e approximations, (b) converting the per-orbit effects to continuous derivatives and integrating, (c) applying the parameters of the reference orbit, and (d) transcribing to the notation used herein; the following expression for the effect of the solar perturbation on perigee altitude is obtained:

$$h_p = h_{p_o} + 264 \left[\cos 2\delta_h - \cos 2 \left(S - S_o + \delta_h \right) \right] \text{km} \qquad (3)$$

$$+ 4.6 \left(\frac{i_e}{57.3} \right)^2 \left(\sin 2\, \theta_c \right) \left(S - S_o \right) \text{km}$$

where

$$\delta_h = S_o - A_c + \theta_c \tag{4}$$

the subscript $_o$ indicates initial values; and A_c is the value of A for $\varphi = \varphi_c$. The integration has been performed on the assumption that A_c and θ_c and hence δ_h are constant. The value of A_c is given approximately by:

$$A_c = S_o + s_a + \theta_c + 180 \tag{5}$$

Hence

$$\delta_h \doteq -s_a + 180; \; 2\delta \doteq -2\, s_a \tag{6}$$

In Equation (3) only the leading terms in i_e have been retained. The second term in the expression for h_p is the oscillatory term and is of zeroth order in i_e. The third term is the secular term and is of second order in i_e.

During a six-month period the value of $(S-S_o)$ will increase to about 180 deg. With i_e = 15 deg, the maximum change in h_p arising from the secular term will be about 6 km. The secular term for the lunar perturbation will have a factor about twice that for the solar perturbation, and the inclination with respect to the lunar orbital plane will generally be about twice as great. Hence, the contribution of the lunar secular term can be 8 times the solar secular term i.e., in the order of 50 km in a 6-month period.

If undesirable values are avoided, θ_c will be between 0 and 60 deg, so that for the solar perturbation the secular term would contribute a small increasing trend. The true anomaly of line common to the satellite and lunar orbital planes may be large enough to cause the lunar secular contribution to be negative, but a large negative contribution is not expected.

It should be noted that the "secular" term will actually vary in consequence of the variations in θ_c due to perturbation effects. (As previously noted a decrease in θ_c of about 35 deg due to earth's oblateness effects is anticipated.)

Eventually the secular contribution will become dominant over the oscillatory contribution to h_p. The sign of the secular contribution will depend upon the ultimate value of θ_c. (The sign of the secular lunar perturbation term will depend upon the ultimate value of a similar phase parameter.) However, the main concern for the Multiple Satellite mission is not the ultimate effects on the perigee altitude but the effects encountered in the first several months in orbit. During these months the secular contributions will be of less importance than the oscillatory.

From Equations (3) and (6) it is seen that the only parameter having a strong effect on the oscillatory term is the lead time. Since the launch conditions will be selected to fix the lead time within relatively narrow limits, conditions with respect to the effect of the solar perturbation on perigee altitude will be relatively restricted.

With respect to the effect on perigee altitude the most desirable lead time would be zero (or 1/2 year). This corresponds to $s_a = 0$ (or 180 deg) and $\delta_h = 0$. The history of perigee altitude (neglecting the secular contribution) for this case is shown in Figure K. It is seen that in this case perigee altitude always remains above its initial value. A maximum increase in perigee altitude of about 530 km is reached after 3 months in orbit, and after 6 months perigee altitude returns to its initial value.

The history of perigee altitude for any lead time can be obtained in the manner illustrated in Figure K. The point P is found by projecting back, on the curve that applies for zero lead time, through the sunline rotation angle corresponding to the lead time. The curve is then translated to bring the point P to the origin.

Illustrated in Figure J is the generation of the plot for a lead time of 35 days. It is seen that in this case during the first 40 days in orbit perigee altitude dips by about 175 km. Thereafter perigee altitude increases returning to its initial value after about 2 months in orbit. The increase continues adding about 350 km to perigee altitude and then returns to its initial value in 6 months.

The net effect of the variation in perigee altitude would be unfavorable since for the factors of importance to the Multiple Satellite mission, e.g., the

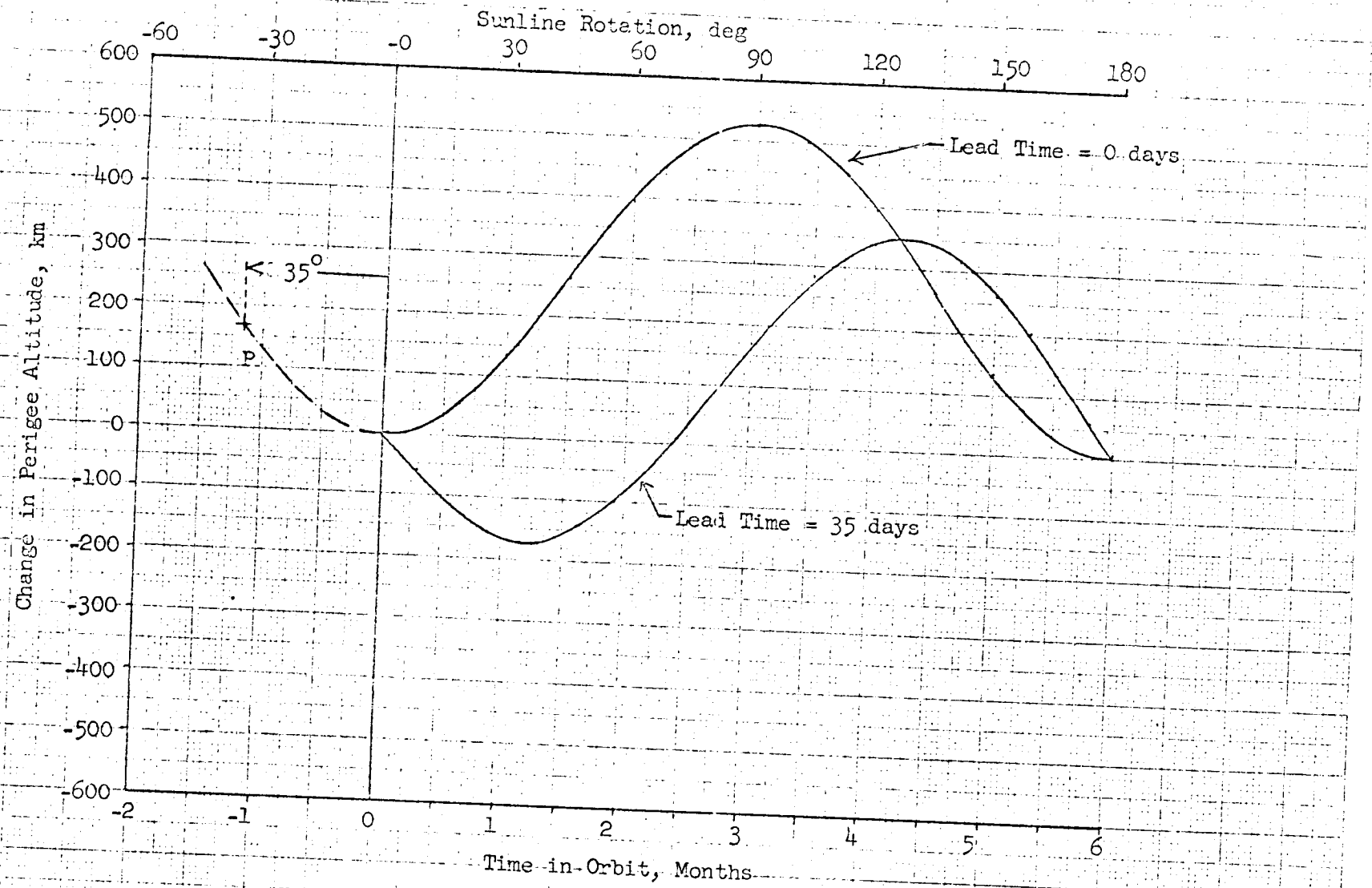

FIGURE K. EFFECT OF SOLAR PERTURBATION ON PERIGEE ALTITUDE

differences in orbital decay between satellites, the effects of the initial drop would outweigh the effects of the subsequent increase.

An increase in lead time will increase the initial drop in perigee altitude. For a lead time of 45 deg the initial drop would be about 264 km. For a decrease in lead time to 25 days, the initial drop would decrease to about 95 km.

The solar (and lunar) perturbation effects on perigee altitude are proportional to the 2.5 power of the major axis of the orbit and hence these effects are quite sensitive to apogee radius. Present estimates indicate that as a result of boost flight guidance errors there could be a 3σ dispersion in apogee radius in the order of 10%. Because the Option 3 deployment will not provide a desirable array of intersatellite separation distances near apogee, a lower than nominal apogee radius will be more objectionable than a higher than nominal apogee radius. Consequently it can be expected that the nominal apogee radius will be raised somewhat so as to increase the 3σ low value. This will increase the 3σ high value, perhaps to about 23 R_e, i.e., 15% above the nominal 20 R_e. With an apogee radius of 23 R_e, the magnitudes of the solar perturbation would be increased by about 40%.

As described in Appendix III, in order to avoid excessive differences in orbit decay, it is necessary to keep the perigee altitude of the lowest satellite above a minimum value. Because of the drop in perigee altitude resulting from the solar perturbation an increase in the initial perigee altitude will be necessary in order to satisfy this requirement.

The amplitude of perigee altitude oscillations due to the lunar perturbation is about 1/5 of the solar perturbation, i.e., in the order of 50 km. Because of its smaller amplitude and shorter period this contribution is of relatively little consequence.

c In the case of the inclination of the orbit to the ecliptic both the secular and oscillatory terms of the solar perturbation are of first order in i_e. Hence upon integration of the per-orbit perturbation effects the expression for i_e takes an exponential form; viz:

$$i_e = i_{eo} e^{\left\{3.3\times10^{-4} \sin 2\theta_c (S-S_o) + A_i \left[\cos 2\delta_i - \cos 2 (S-S_o+\delta_i)\right]\right\}} \quad (7)$$

Since it appears that for the orbital lifetime presently contemplated the exponent will always be small, an approximate linear expression for i_e can be written:

$$i_e = i_{eo} + 3.3\times10^{-4} \sin 2\theta_c (S-S_o)\, i_{eo}$$

$$+ A_i \left[\cos 2\delta_i - \cos 2 (S-S_o + \delta_i)\right] i_{eo} \quad (8)$$

The secular term has maximum effect when $\sin 2\theta_c = \pm 1$. However even in this case its effect is quite small. In the exponential form the factor of secular term then corresponds to a time constant of nearly 8.5 years. With an initial inclination of 5 deg, the maximum change in inclination due to the secular term would be about .3 deg during the first 6 months in orbit.

Since the inclination with respect to the lunar orbit is in the order of twice as great and the factor for the secular term would be larger by a factor of two, the maximum secular effect of the lunar perturbation on the inclination during the first six months in orbit would be in the order of 1.2 deg.

The amplitude and initial phase of the oscillatory term for the solar perturbation effect on inclination can not be reduced to as simple an expression as that obtained in the case of the effect on perigee altitude. However it can be shown that for the Multiple Satellite reference orbit the maximum value of the amplitude of the oscillatory term, i.e., A_i in Equations (7) and (8) is about .046. The maximum excursion of i_e that can arise from the oscillatory term is $2A_i\, i_{eo}$ which is approximately .09 i_{eo}. With $i_{eo} \doteq 5$ deg, the maximum excursion in i_e due to the solar perturbation would be less than 1/2 deg. The effect of the oscillatory term for the lunar perturbation should be much smaller.

Table 3

ESTIMATES OF OUT-OF-PLANE VELOCITY INCREMENT DIRECTIONAL ERRORS

Error Source	Contribution to Directional Error, deg	Contribution to Tangential Velocity, meters/sec	Contribution to Period Difference, % of Period
1. Tilt of pallet's spin axis relative to normal to orbit			
Residual Error in adjusting for off-nominal conditions	.1	.05	.002
Altitude sensor error	1.0	.52	.018
2. Shift in satellite's spin axis relative to pallet's spin axis			
Disturbance on separation from pallet	.01	-	-
Disturbance on separation from partner	.04	.08	.001
Coning motion	.1	.05	.002
3. Deviation in direction of velocity increment relative to satellite's spin axis (due to misalignments)	.1	.05	.002
RSS	1.0	.52	.018

thus allowing a lead time of about 35 days before the sunline passes over the line of apsides. The ± 10 deg variation in the initial direction of the sunline relative to the line of apsides, which would be required to accommodate a ± 40 minute daily launch window, would result in a ± 10 day variation in this lead time. The time of application of the out-of-plane velocity increment would range from about 18 to 21.5 hours after perigee passage. This range of application time could result in some variation in sensitivity to errors in the direction of the velocity increment and in a somewhat less desirable distribution of out-of-plane separation distances. However, these disadvantages are preferable to the acceptance of the error that would otherwise be made.

For the anticipated nominal launch conditions the change in the angle between the normal to the orbital plane and the sunline would be roughly 1/3 of the angle that the earth rotates about its axis from the nominal launch time. For a ± 40 minute daily launch window this change would be about ± 1/3 x 10 = ± 3.3 deg. In addition to the daily launch window, the window with respect to the day of the year would affect the angle between the normal to the orbital plane and the sunline. This effect is roughly estimated to be about 6% of the rotation of the earth-sunline. For a ± 20 day launch window the variation in the angle between the normal and the sunline would be approximately ± 1.2 deg. Adding these effects of the hour of day and the day of year windows leads to a possible ± 4.5 deg variation in the angle between the normal to the orbital plane and the sunline. For the assumed approach to the handling of the out-of-plane deployment, this would result in a possible ± 4.5 deg tilt of the spin axis in the in-plane normal direction which would lead to a possible in-plane normal velocity increment component of approximately ± 1 meter/sec, when the 15 meter/sec axial velocity increment is applied.

In the adjustment of the precession of the pallet's spin axis about the sunline and the selection of time of deployment, correction would also be made for booster flight guidance errors. These are expected to be small in comparison to the launch window variations. Compared to execution errors, the residual errors in effect the correction, such as uncertainties in knowledge of the actual orbital parameters should be quite small. Little difficulty is anticipated in keeping the residual error below .1 deg.

The execution errors will depend primarily upon the accuracy with which the orientation of the spin axis is measured. The angle between the spin axis and the sunline, which will be established by the on-board ACS sun sensor, is not critical since any error made in this angle would result in a tilt in the in-plane normal direction. The critical measurement would be that used to decide when to stop the precession of the pallet's spin axis about the sunline. For this purpose, Pioneer 6 used a fan beam antenna at practically no additional burden to the system since the fan beam antenna was also used to satisfy communications requirements. The system specifications called for a $\pm$ 2 deg accuracy. It is believed that the accuracy actually obtained was somewhat better.

Because of the closer range to the earth a fan beam as narrow as that used by Pioneer 6 (5 deg between 3 db points), would not be very useful for Multiple Satellite communications. Hence it appears that the Pioneer approach to the aspect sensing problem will not be directly applicable and that an equally accurate attitude measurement will not be so simply obtained.

For the interpretation of the scientific data the satellites will be equipped with sensors to determine the orientation of their spin axes. Hopefully these sensors can also be used for the execution of the pallet's reorientation maneuver. For the purpose of aiding the interpretation of the scientific data, attitude measurements with an accuracy of 2 deg are considered to be adequate. Instrument simplicity, reliability, light-weight and low cost will be dominant factors in selecting the attitude sensor. It appears unlikely that the accuracy of attitude sensor selected on this basis would greatly exceed the stated requirements.

For present purposes it is assumed that the sensor used for the pallet reorientation maneuver will have a 1 deg accuracy which is comparable to that achieved by the Pioneer system.

In considering the spin-off velocity increment it was estimated that a lateral impulse of about 1 lb-sec may be applied to the satellite pair at separation from the pallet. If the center of mass of the satellite pairs is line of action of this impulse by .1 inch a moment impulse of about .1 inch-lb-sec could be delivered. Applied to a satellite pair with a pitch/yaw moment of inertia in the

order of 4 slug-ft^2 spinning at a rate of about 140 rpm, this moment impulse would cause a shift in the direction of the angular momentum vector less than .01 deg.

A somewhat larger disturbance might be encountered when the satellites are separated from their partners. Assuming a separation velocity increment of 1 ft/sec imparted to each satellite and an offset of .1 inch of the center of mass from the line of action of the separation impulse and assuming a satellite pitch/yaw moment of inertia of about 2 slug-ft^2 yields a shift in the direction of the angular momentum vector in the order of .04 deg.

A shift in the direction of the angular momentum vector could also arise from the presence of a coning motion at the time of separation if the moment of inertia ratio for the separated parts differs from that of the unseparated assembly. For present purposes it is assumed that a favorable moment of inertia ratio will be maintained for all assemblies and that a precession damper capable of reducing the cone angle to a residual value below .1 deg will be provided. The shift in the direction of the angular momentum vector due to the presence of a coning motion will then be less than .1 deg.

The deployment of booms does not affect the direction of the angular momentum vector. The main possible adverse effect of boom deployment is a shift in the direction of the principal axis. The action of the precession damper will cause the principal axis to become aligned with the angular momentum vector. The shift in the principal axes relative to the body frame would then be eventually reflected in a deviation of the direction of the thrust applied to obtain the out-of-plane velocity increment from the direction of the spin axis.

In consideration of the loading of the satellite booms on deployment it would be preferable that the satellite be despun to the desired rate of about 60 rpm before the booms are deployed. However, it appears likely that the deployment of the booms prior to despin will be required in order to maintain favorable moment of inertia ratios. In this case it is advantageous to apply the out-of-plane velocity increment prior to despin to gain the increased stability of the higher spin rate.

A sizeable deviation in the direction of the velocity increment relative to the direction of spin axes would be incurred if the burning time of the rockets applying the out-of-plane velocity increment were short relative to the satellite's spin cycle period. For present purposes it is assumed that the out-of-plane rockets will have a burning time in the order of several seconds or more. In this case rough computations of the effects of misalignments in applying the out-of-plane thrust indicate that the deviation in the direction of the velocity increment could be kept to about .1 deg.

4.3 GROWTH DUE TO DIFFERENCE IN PERIGEE ALTITUDE

As a consequence of the in-plane separation, a difference in perigee altitude of about 240 km will be obtained between satellites. The results presented in Figure E of Section 2-3 indicate that if a benefit is not obtained from the effects of solar and lunar perturbations in the way of an increasing trend in perigee altitude, a relatively high initial perigee altitude will be required in order to avoid excessive growth due to a difference in perigee altitude of 240 km. In order to reduce the difference in the decay of the orbital period to .02% after 6 months in orbit, an initial perigee altitude of about 470 km would be required.

If the burden of obtaining the higher perigee altitude is placed on the booster a substantial penalty in payload weight would be paid. For example, an increase in perigee altitude from 280 km to 470 km would cost about 45 pounds of payload. The same increase in perigee altitude could be obtained at a cost of one pound of payload if the burden of increasing payload altitude is placed on the pallet.

The pallet would then be equipped with a small solid rocket thrusting in the direction of its spin axis. The rocket would be fired at the first pass of the pallet through apogee. The separation of the satellites from the pallet would of course be deferred until after perigee altitude had been increased in this way.

For present purposes it is assumed that perigee altitude will be raised to the point where the difference in the decay of the orbital period due to the difference in perigee altitude will not exceed .02% after 6 months in orbit.

It should be noted that the same problem is encountered regardless which mission option is selected. However, for Option 4 another approach to handling the problem would be available. Specifically, compensation for the differences in the decay of the orbital period could be made by means of occasional adjustment of period. This could be done because capability for adjustment of orbital period would be provided and the velocity increments required to make the necessary corrections of period when passing near perigee are quite small (in the order of a .2 meter/sec).

5.0 SUMMARY

A summary of the factors that contribute to the growth of the tangential separation distances is presented in Table 4. It is seen that at 10 R_e after 6 months in orbit the growth would be somewhat less than the originally contemplated 15,000 km. At larger distances from the earth the growth would be smaller. It is possible that the system can be feasibly implemented to reduce the growth in the tangential velocity increment below the values shown in Table 4 perhaps by a factor of 2 or 3. The main obstacle to such a reduction in errors is the realization of a reasonably simple attitude sensor that will provide an accuracy better than 1 deg.

Figure G shows the nominal disturbances of the in-plane normal and out-of-plane separation distances attainable with Option 3 implemented as proposed herein. The main drawback is the relatively small in-plane normal separation distances that can be obtained from the spin-off separation, particularly on the ascending leg of the orbit. However, based upon consultation with scientists at Ames Research Center, the in-plane normal separation distances achievable are acceptable.

Table 4

SUMMARY OF ESTIMATES IN GROWTH OF TANGENTIAL SEPARATION DISTANCE

Cause of Tangential Separation Distance Growth	Growth in Tangential Separation Distance, km After 6 months in Orbit				
	Perigee	5 R_e	10 R_e	15 R_e	20 R_e
1. Errors incurred in application of spin-off velocity increment	39,100	16,000	9,400	5,700	2,040
2. Errors incurred in application of out-of-plane velocity increment	28,100	11,500	6,750	4,100	1,500
3. Difference in perigee altitude	15,600	6,390	3,750	2,300	800
RSS	50,000	20,400	12,000	7,200	2,600

NOTES:

1. The spin-off error is due almost entirely to uncertainty in action time of separation mechanism. A simple system having a 1.4 millisecond uncertainty was assumed. With a more complicated system this error could be reduced by an order of magnitude.

2. The out-of-plane velocity increment error is due almost entirely to the attitude sensor error which was assumed to be 1 deg.

3. It is assumed that a perigee altitude of about 470 km will be obtained for the lowest satellite.

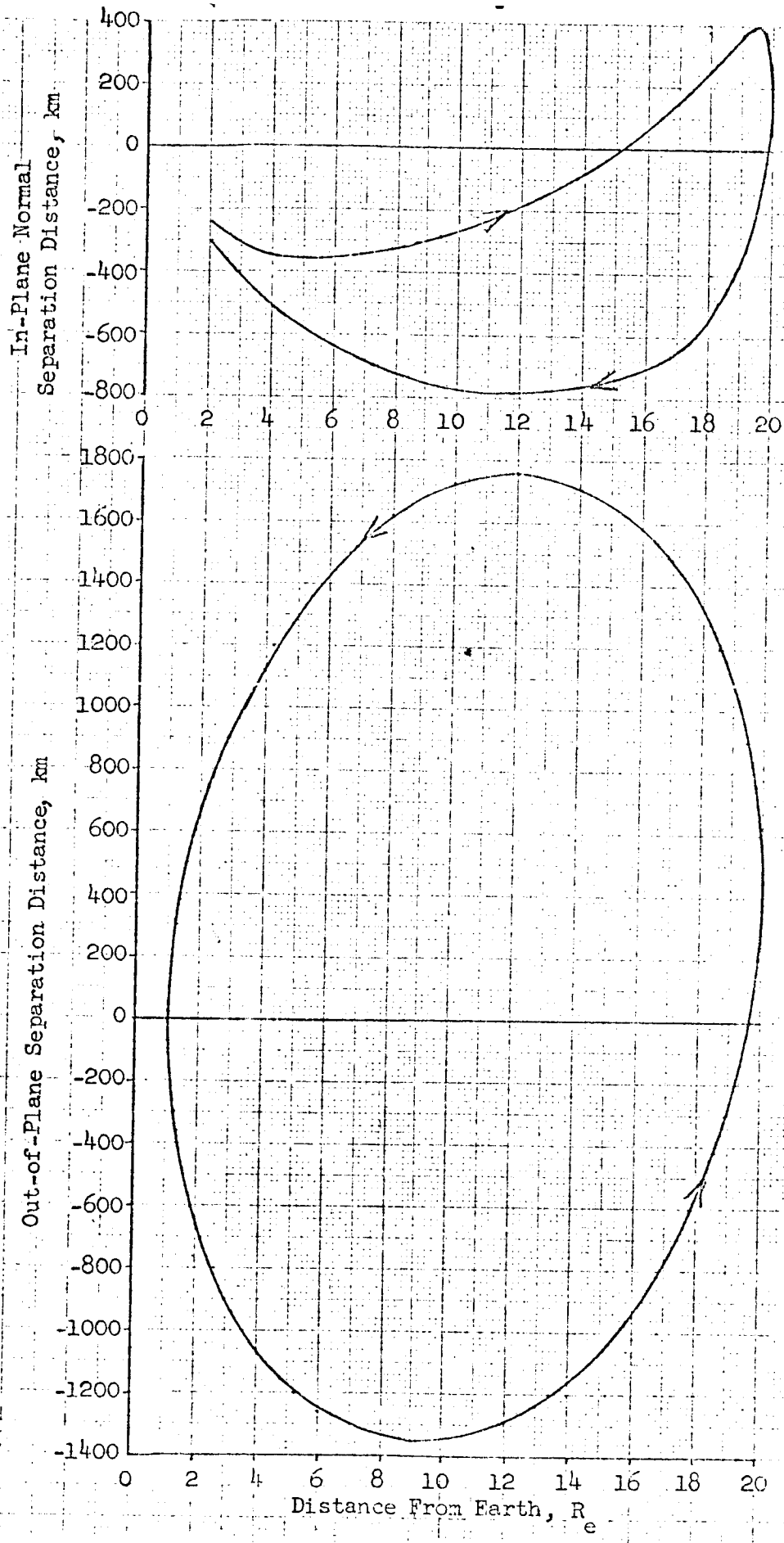

FIGURE G. NOMINAL SEPARATION DISTANCE OBTAINED WITH OPTION 3

Appendix IV

SELECTION OF COMMON ORBIT PARAMETERS

1.0 GENERAL APPROACH

The multiple satellites will be injected into orbit by a single booster and subsequently separated by applying small vehicle increments so as to achieve the desired array of intersatellite separation distances. These separation distances will, of course, be small relative to the orbital dimensions. Hence a logical division can be made between: (a) "common" orbit, and (b) deployment and separation distance considerations.

The initial values of the common orbit parameters are set by the booster flight which is designed to attain the selected values. Subsequent variation from the selected values will be encountered in consequence of (a) errors of the booster guidance system, and (b) a variety of orbital perturbation effects, including the perturbations due to satellite separation.

In the selection of the nominal initial orbital parameters the general approach that will be followed is to: (a) examine in a general way the effects of variations in the parameters on the problems of the system design and meeting scientific objectives, (b) make preliminary assessments of the variations in the parameters that can be expected (for this purpose simple representations such as Keplerian orbit relationships will be used), (c) make a preliminary selection of nominal initial parameters, and (d) confirm the selection by more detailed study of dispersion and perturbation effects. This approach takes account of the absence of simple methods for precise evaluation of long term perturbation effects. The approach taken is intended to narrow the selection of parameters as much as possible by simpler techniques before more expensive and time consuming perturbation computations are undertaken.

2.0 SELECTION OF APOGEE RADIUS

It is desired that scientific data be obtained at radii far enough beyond the maximum extent of the transition region to assure the detection and measurement of approaching disturbances in the solar wind. Along the sub-solar line the transition region may extend out as far as 16 R_e. Hence an apogee radius at least somewhat greater than 16 R_e is called for.

As shown in Figure A, the apogee radius, r_a, has a strong influence on the orbital period. In the region near $r_a = 20\ R_e$, the orbital period increases by about 3 hours for an increase in r_a by 1 earth radius. (In this region the sensitivity of orbital period to perigee altitude is about 3×10^{-4} hrs/km. With this low sensitivity, for the range of perigee altitudes to be considered, the effect of perigee altitude on the period of common orbit can be neglected for most purposes.)

If the apogee radius is larger than necessary the orbital period will be larger than necessary and the maximum number of orbits for which data can be obtained in a given operational lifetime is reduced. Furthermore an increase in apogee radius increases the portion of the orbital period that is spent near apogee, where the orbital velocity is lowest. To the extent that measurements near apogee may be of less interest than measurements closer to earth, e.g., near 10 R_e, an unnecessarily large apogee radius would lead to inefficient utilization of time in orbit. If the recording mode is fixed, an excessive apogee radius may also imply inefficient utilization of recording and communications capacity.

In order to assure the attainment of the minimum acceptable apogee radius it will be necessary to increase the nominal initial apogee radius by the magnitude of the dispersion produced by the booster injection errors. The probability of an apogee radius greater than the minimum acceptable by twice the apogee dispersion is then incurred. In the absence of a cut-off capability for the last stage of the TAID booster an uncertainty of apogee radius in the order of 2 R_e, 3σ is anticipated. Also to be taken into account are the effects of orbital perturbations; particularly the orbital decay due to atmospheric drag which could reduce the apogee radius in by a significant fraction of an R_e over a 6-month period.

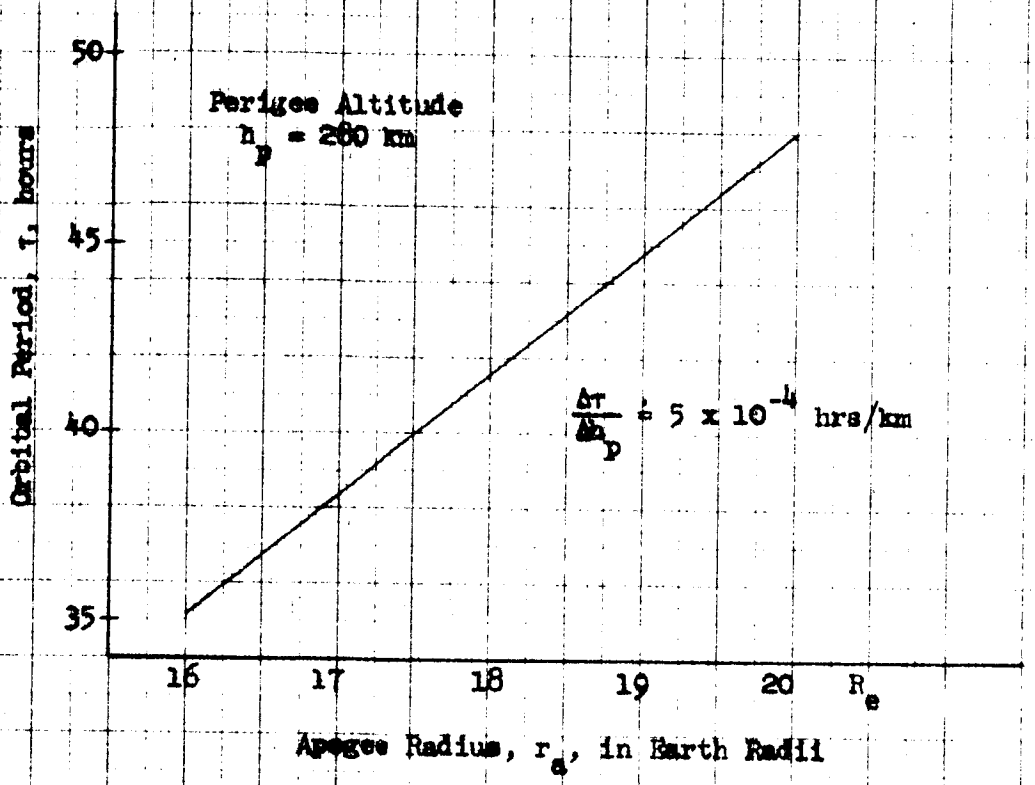

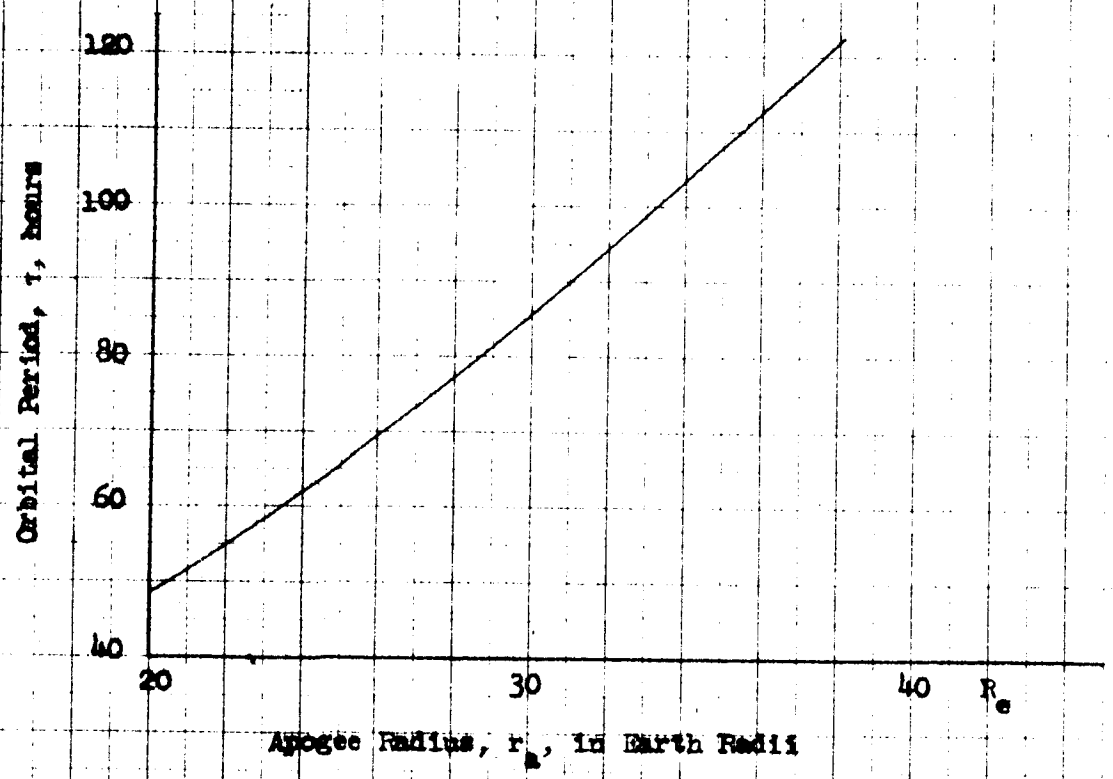

FIGURE 3. RELATIONSHIP BETWEEN ORBITAL PERIOD AND APOGEE RADIUS

PRINTED IN U.S.A. ON CLEARPRINT TECHNICAL PAPER NO. 1015
CLEARPRINT PAPER CO. NO. C38X MILLIMETERS 200 BY 250 DIVISIONS

It is noted that an apogee radius of 20 R_e corresponds closely to an orbital period of 48 hours. Unusual conditions could be encountered if the period were exactly equal to twice the period of the earth's rotation. At any point in the orbital cycle, each orbital transit would find the earth at the same orientation relative to the earth-satellite line. Thus given ground station would always see the satellites during the same portions of the orbit. Since the rotation of the earth affects the direction of the earth's magnetic field, the earth's orientation could have an influence on solar wind phenomena. An orbital period sub-harmonic to the earth's rotation would reduce the range of conditions with respect to the earth's magnetic field that is encountered.

It is not clear at present whether or not these conditions would be desirable. However, it is apparent that if a sub-harmonic synchronous orbit were desired, greater accuracy in orbital injection than can be expected for TAID would be needed. The uncertainty of apogee radius in the order of 2 R_e, 3σ anticipated for TAID, would correspond to a 3σ dispersion in orbital period of about 7 hours. This factor alone would preclude planning for a nearly sub-harmonic synchronous orbit. Even if the required injection accuracy could be obtained, the sub-harmonic orbital period could not be maintained for a long operational lifetime in the absence of compensation for the orbital decay.

On the other hand if the sub-harmonic condition is not desired it would be reasonably safe to plan on a nominal 48-hour orbit. The probability that the initial orbit period would actually be very close to the sub-harmonic period would be quite small. This along with the orbital decay can be counted on to prevent the orbit from remaining in phase with the earth's rotation for a large number of orbits.

Additional considerations relating to apogee radius are:

- The trade-off between apogee radius and payload capability.
- The effect of apogee radius on deployment and separation distance problems.
- The effect of apogee radius on duration of occultation periods, view times from ground stations, and communication problems.

These items will be covered in future work.

3.0 SELECTION OF PERIGEE ALTITUDE

The nominal initial perigee altitude is perhaps the most critical parameter of the common orbit to be selected. This parameter has a strong influence on the booster payload capability. Figure B shows the effect of perigee altitude on maximum payload capability for the TAID (FW4) for direct-ascent east launches from ETR into 20 R_e apogee orbits. In the region of interest the trade-off factor is about .2 lb per km of perigee altitude. A 200 km difference in perigee altitude; viz. h_p = 200 km vs h_p = 400 km, corresponds to a difference of about 40 pounds in payload capability.

Since the Multiple Satellite system is likely to require the maximum practical vehicle payload capability, it is important that the restriction on lowering perigee altitude be carefully examined so that the lowest "safe" altitude can be used, and the maximum payload capability attained.

A lower bound on the useful reduction of perigee altitude is set by the limitations of the launch vehicle with respect to the allowable depression of the booster flight. Generally this limitation is not encountered above a perigee altitude of 200 km and is likely to be superceded by other restrictions against lowering perigee altitude.

Clearly a perigee altitude so low that the apogee radius decays too rapidly would be totally unacceptable; but before this point is reached difficulties may be encountered by one or more of the following adverse effects of a low perigee altitude:

1. Increased requirements for precise matching of the satellites ballistic coefficients and perigee altitudes in order to prevent intersatellite separation distances from growing too rapidly.
2. More rapid precession of the direction of the satellites' spin axes due to increased aerodynamic, gravity-gradient and magnetic torques.
3. Increased difficulties of maintaining precise emphemerides for the satellites over extended time intervals.

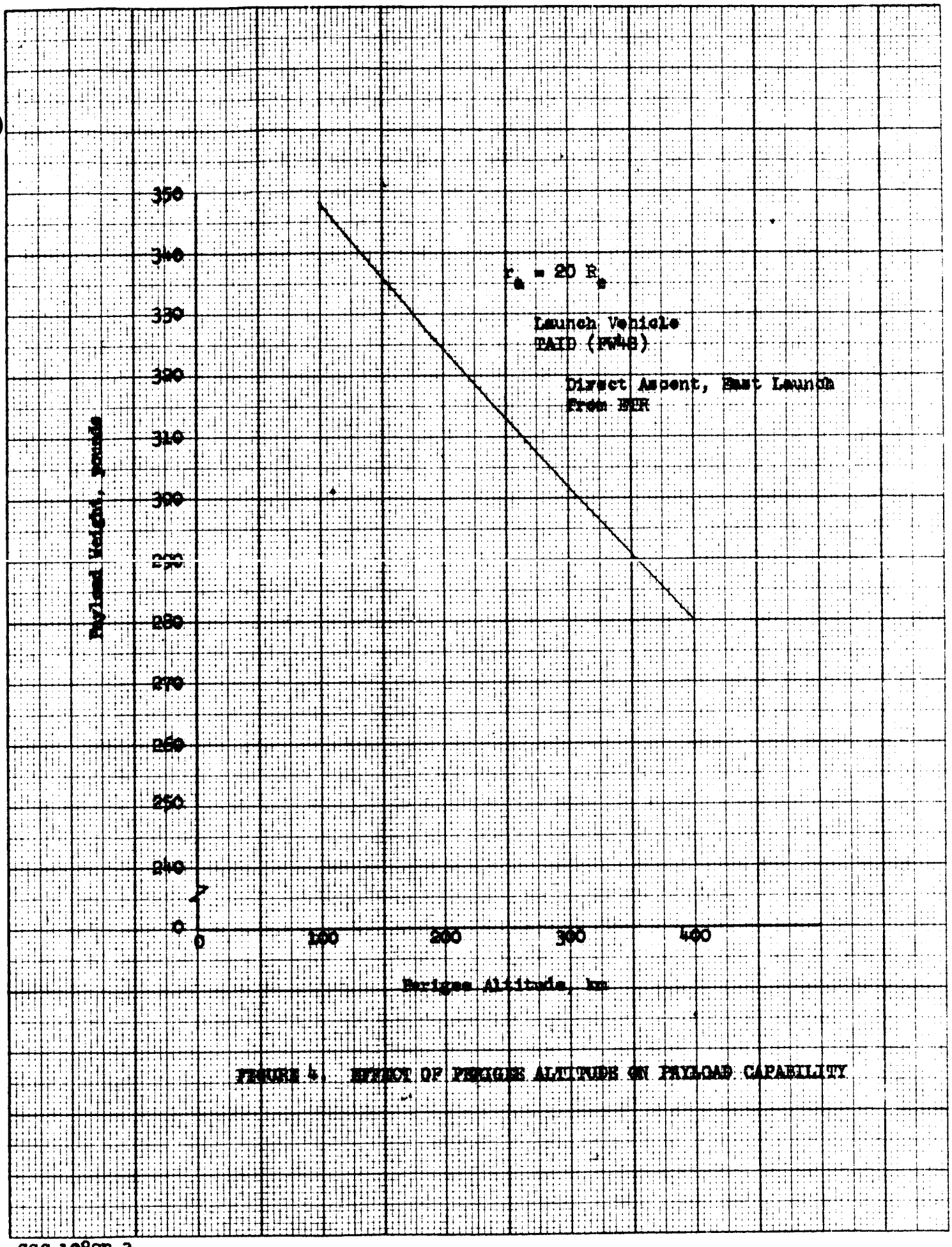

FIGURE 4. EFFECT OF PERIGEE ALTITUDE ON PAYLOAD CAPABILITY

CLEARPRINT PAPER CO. NO. C38X 20 DIVISIONS PER INCH BOTH WAYS 190 BY 200 DIVISIONS PRINTED IN U.S.A. ON CLEARPRINT TECHNICAL PAPER NO. 1015

In determining the lowest safe perigee altitude, account must be taken of (1) the dispersion of the initial perigee altitude due to booster guidance errors, and (2) the changes in perigee altitude arising from orbital perturbations after injection.

The dispersion of the initial perigee altitude will, of course, be far smaller than the dispersion of apogee radius. It is expected that this dispersion will not be much greater than a few km.

Preliminary estimates of the effect of perigee altitude on orbital decay are presented in Figure C. These estimates were obtained by application of the method given in Smithsonian Institute. Astrophysical Obs. Research in Science Special Report Number 135 "Formulae and Tables for the Computation of Lifetime of Artificial Satellites", L. G. Jacchia and J. Slowly, Sept. 16, 1963. Although more refined estimates of orbital decay will be made later, the present estimates serve to provide a reasonable approximation for evaluating the most significant repercusions.

It is expected that for a perigee altitude high enough to keep the decay of apogee radius within reasonable bounds, the decay of perigee altitude due to atmospheric drag will be quite small in comparison to other factors that contribute to the uncertainty or change in perigee altitude. For example, solar and lunar perturbations will undoubtedly have a far greater effect on perigee altitude. Solar and lunar perturbations increase with distance from the earth. Thus in contrast to atmospheric drag these perturbations have more significant effects on perigee altitude than on apogee radius.

If the launch window were inappropriately chosen there may be danger that a large decrease in perigee altitude due to these perturbations would be encountered during the days following injection into orbit. Obviously if such an unfortunate choice of launch time were made, an increase in the initial perigee altitude would be required. However, it is also true that if the launch time is chosen to obtain an increase in perigee altitude at the outset, with perigee altitude remaining well above the minimum acceptable value during the desired operational lifetime, then a lower initial perigee altitude can be used. In this way the benefit of increased payload capability could be obtained without the penalties associated with low perigee altitudes.

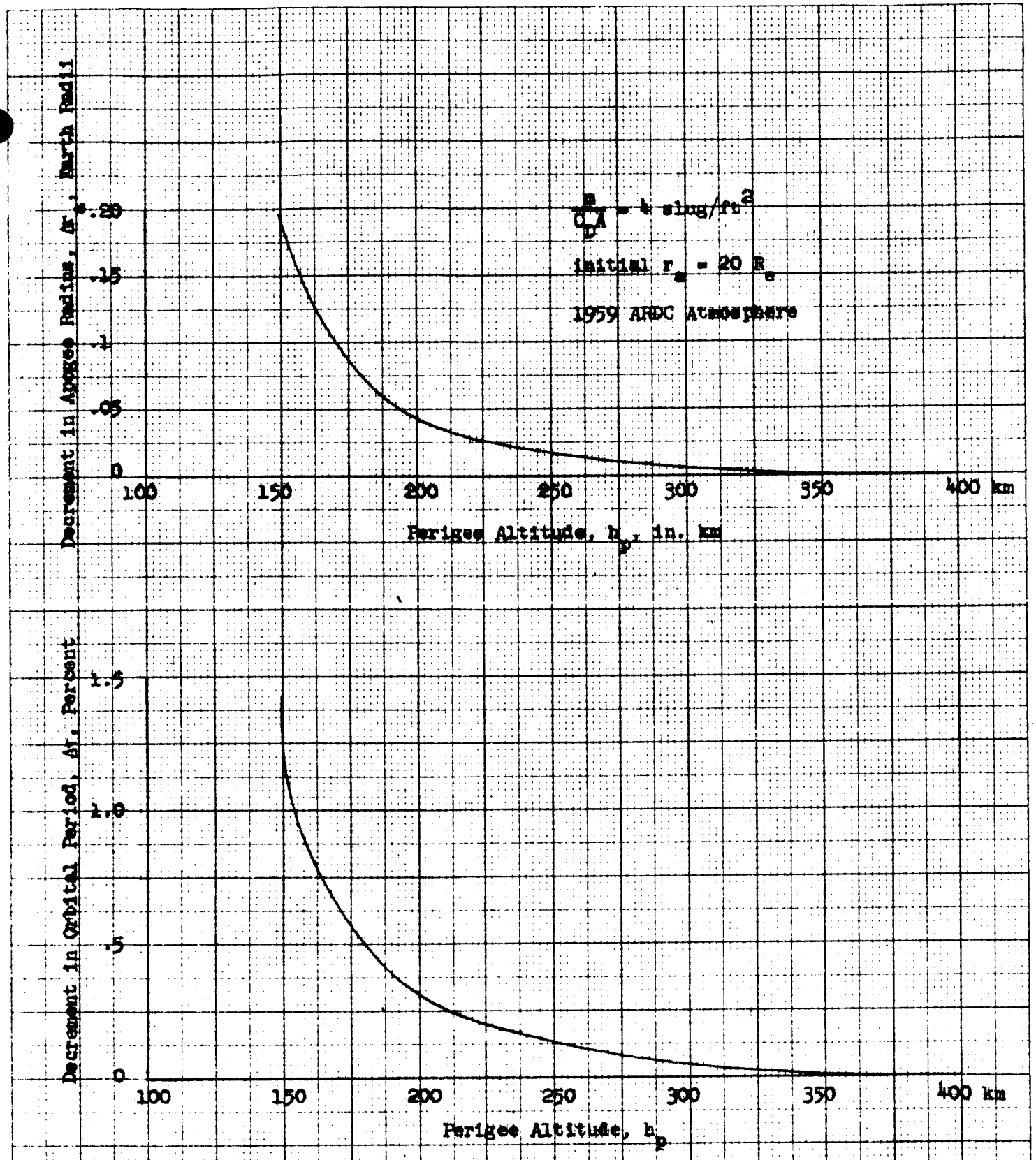

FIGURE 5. PRELIMINARY ESTIMATE OF THE EFFECT OF PERIGEE ALTITUDE ON ORBITAL DECAY AFTER 6 MONTHS IN ORBIT

Preliminary calculations indicate that such fortuitous choice of launch window will be feasible. See for example, Figure B-1 of SGC Proposal P-6873. In this case the perigee altitude remained above the initial value of about 280 km during almost all of the first 6 months in orbit. During this period the average perigee altitude was about 450 km. Other computer runs have also indicated that an initially increasing trend and a high average perigee altitude during the first six months would not be difficult to attain. Hopefully this conclusion will be confirmed by more extensive computations.

Another possibility for gaining the benefits of increased payload capability while avoiding the disadvantages of low perigee altitude is to apply a velocity increment at apogee in the direction of the velocity vector (either through a pallet or individual satellite reaction jet systems). Because of the great sensitivity of perigee altitude to velocity increments applied at apogee, a very small velocity increment at this time can produce a large increase in perigee altitude at a payload penalty that is slight in comparison to that which would be incurred if the booster vehicle were required to provide the higher perigee altitude.

Assuming that the maintenance of the orbital period close to sub-harmonic with the earth's rotation is not desired, the decrement in orbital period due to atmospheric drag is not of concern per se; but since this decrement is dependent upon the ballistic coefficient and perigee altitude, a requirement on the precision of matching ballistic coefficients and perigee altitudes is imposed.

If two of the satellites have a constant difference in period of about .04% of the nominal period (~48 hrs), then the separation distance between the satellites (in the region of 10 R_e) would grow approximately linearly with time to the order of 15,000 km in 6 months. For equal perigee altitudes, the rate of decrease in the orbital period is approximately proportional to the ballistic coefficient. Hence, the difference in period arising from a constant difference in ballistic coefficients will tend to grow approximately linearly with time while the separation distance grows with the second power of time, i.e., like $1/2\ t^2$. Thus a constant difference in ballistic coefficient that produces a difference in period of .08% in 6 months would cause separation distances to grow to the order of 15,000 km in this time.

Taking this increase in separation distance to be the maximum allowable, the decrement of the common period can be related to the maximum difference between ballistic coefficient that can be tolerated. The results of such computations are shown in Figure D.

It appears improbable that the satellites would be deliberately designed to attain specified differences in ballistic coefficient in order to achieve the desired growth of the separation distances. (This might be interpretated as a violation of the requirement that the satellites be identical in design.) If the satellites are designed to have nominally equal ballistic coefficients, the desired separation distance growth presumably would be achieved by means of differential velocity increments imparted at the deployment of the satellites (with a component in the tangential direction). It would then be desired that the additional stochastic growth (or decrease) due to inadvertent differences in ballistic coefficient be small relative to the planned growth of the separation distances. This along with the need to allow for other factors covering differences in period would require much smaller tolerances on the differences in ballistic coefficients than the maximum allowable values computed as described above and shown in Figure D.

A requirement for extremely high precision in matching ballistic coefficients would impose difficult if not unacceptable burdens on the design and fabrication of the satellites. For example in trimming the inertial characteristics of the satellites in spin balance tests it would be necessary to re-adjust balance weights in such a manner that the total weight of all four satellites remains precisely equal. Experience indicates that a practical readily attained tolerance for the ballistic coefficient would be in the order of 1%.

In this connection it is noted that if the satellites are individually equipped with reaction jet systems used either for the generation of deployment thrusts or attitude control moment, when perigee altitude is low care must be taken to avoid differences in propellant utilization which would lead to differences in mass and hence to differences in ballistic coefficient.

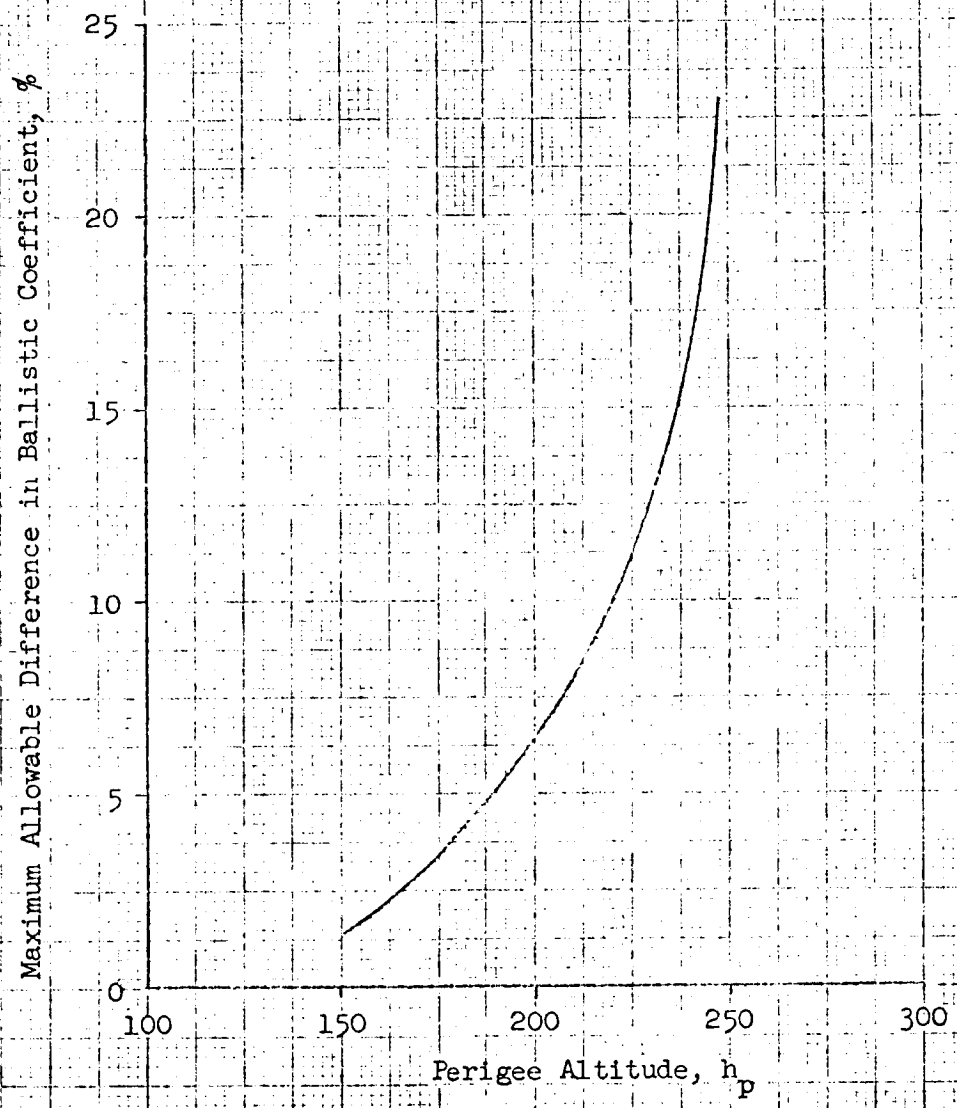

FIGURE D. EFFECT OF PERIGEE ALTITUDE ON ALLOWABLE DIFFERENCES IN BALLISTIC COEFFICIENT

(Based upon maximum allowable separation distance growth due to difference in ballistic coefficient of 15,000 km in 6 months)

-- Differences in perigee altitude, like differences in ballistic coefficient will cause an approximately constant rate of growth in the difference in period and a growth of the separation distances with the second power of time. If the difference in perigee altitudes is such that the differences in orbital period grows to .08% of an orbital period the separation distance between the satellites will grow 15,000 km in the region of 10 R_e in 6 months. Figure E shows the perigee altitude of a second satellite corresponding to various percentage changes in period after 6 months for various (lower) perigee altitude of the first satellite. From these results it is seen that for low perigee altitudes it would be necessary to be very careful in the deployment of the satellites to make sure that the differences in perigee altitude between satellites is extremely small.

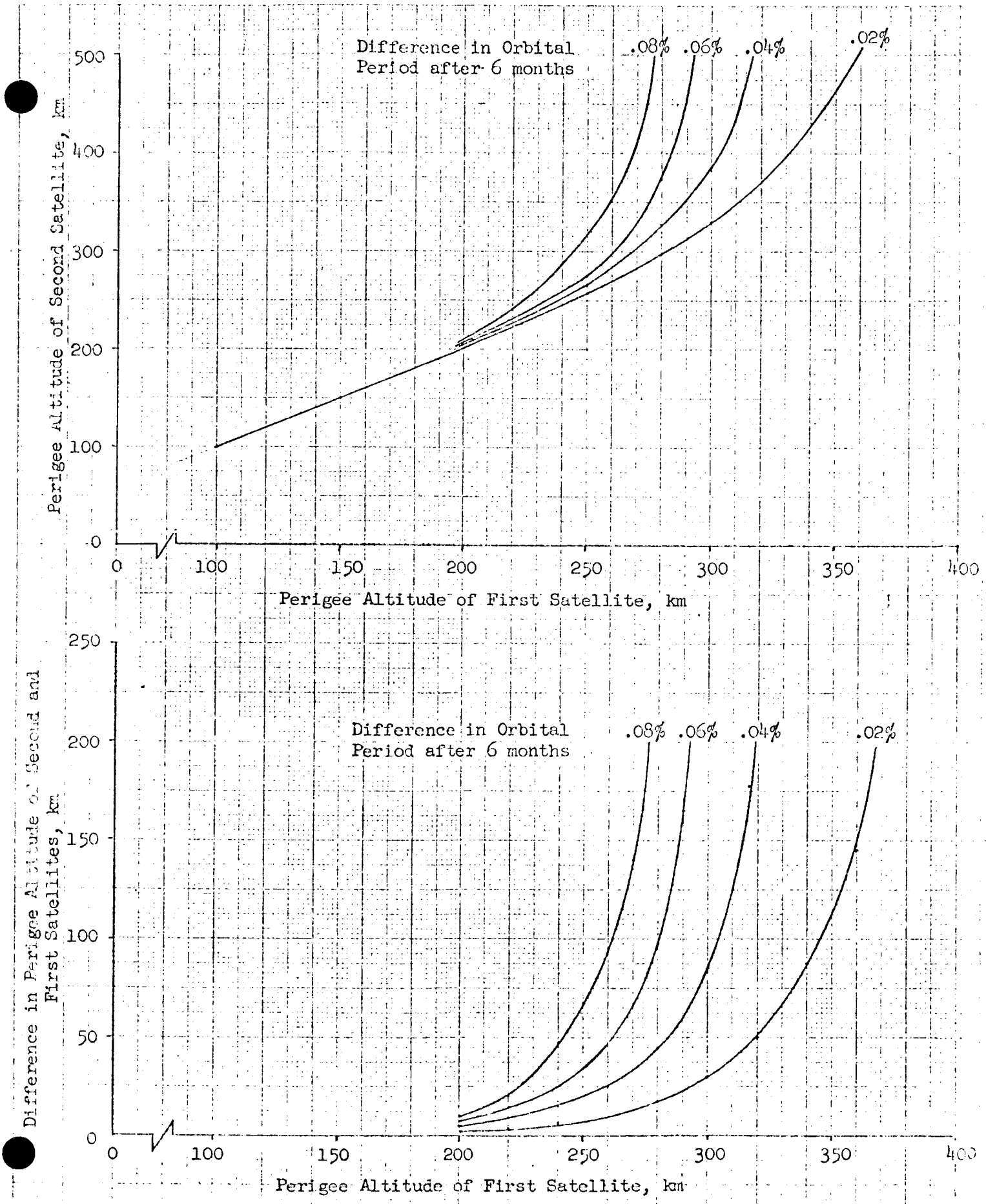

FIGURE E. EFFECT OF PERIGEE ALTITUDE ON GROWTH OF DIFFERENCES IN ORBITAL PERIOD

Appendix V

COVERAGE OF THE SUBSOLAR LINE

COVERAGE OF THE SUBSOLAR LINE

The most important considerations regarding the orbital orientation relate to coverage of the subsolar line. This coverage depends upon the orientation of the orbital plane relative to the ecliptic plane. The relationship between the two planes can be specified in terms of the following parameters: (a) the inclination between the planes, i_e; (b) the position of the line common to the two planes relative to the orbit; this can be conveniently specified by the true anomaly of the common line, θ_c; and (c) the angle between the sunline and the projection of the line of apsides in the ecliptic plane, s_a. Figure A illustrates the significance of these parameters.

In contrast to s_a which is subject to first order changes, the values of i_e and θ_c are subject only to comparatively small changes caused by orbital perturbation effects, particularly those arising from the earth's oblateness. Hence, for first approximations i_e and θ_c are taken to remain constant. Since the orbit stays nearly inertially fixed, the change in s_a is due mainly to the 1 deg/day rotation of the sunline in the ecliptic plane. In a period of a year s_a will take on practically all values in the circle. In a period of six months s_a will traverse a range of about 180 deg.

It is, of course, important that a desirable initial value of s_a be obtained so that the most significant experimental conditions are encountered early in the operational lifetime when the probability of collecting useful data is greatest. The conditions of most interest are obtained when apogee is directed towards the sunline, i.e., when s_a has small values. Thus, it is desirable that the initial value of s_a be such as to provide a suitable lead of the crossing of apogee by the sunline, i.e., the passage of s_a through zero. The attainment of a desirable initial value involves launch window considerations which are discussed more fully in Appendix VII.

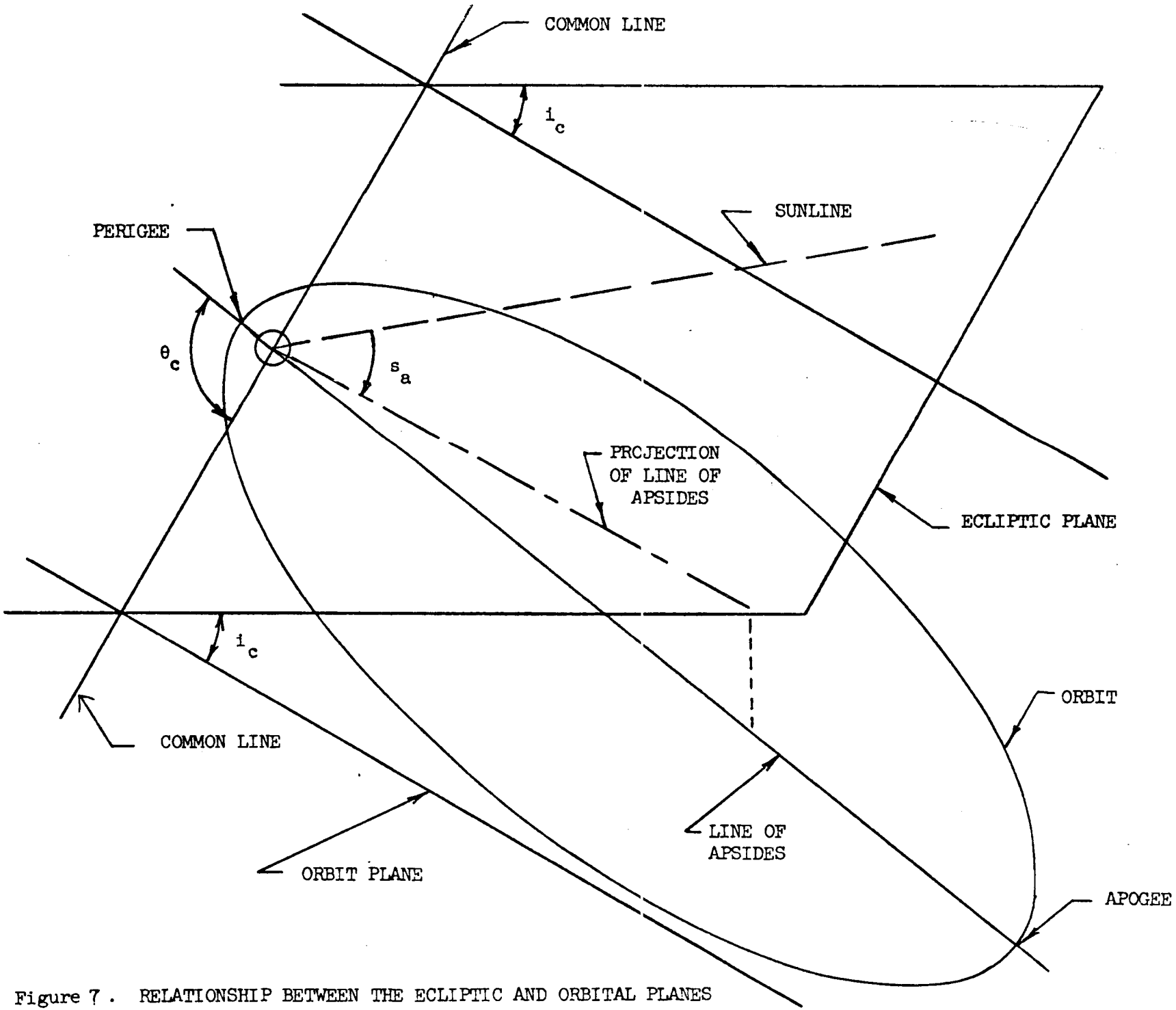

Figure 7 . RELATIONSHIP BETWEEN THE ECLIPTIC AND ORBITAL PLANES

It will be noted that, in the absence of orbital perturbations, the envelope of the subsolar coverage conditions encompassed during a complete circuit of the sunline is not affected by the initial value of s_a but is strongly affected by the other parameters and particularly by the value of i_e.

If $i_e = 0$, the orbit lies entirely in the ecliptic plane. In this case the satellites pass through the sunline at two points in every orbit. During a six-month period the subsolar line would be covered at every distance from the earth between the perigee and apogee radii.

If $i_e \neq 0$ then the only points on the orbit that lie in the ecliptic plane are the two points that lie on the line common to the orbit and ecliptic planes. All other points on the orbit lie either above or below the ecliptic plane, the distance from the ecliptic plane depending upon the magnitude of i_e and the distance from the common line.

When the true anomaly of the common line is 90 deg, i.e., $\theta_c = 90$ deg, the common line passes through the latus rectum of the orbit. In this case apogee is most distant from the ecliptic plane. The distance from the ecliptic plane is symmetrical about the line of apsides, the ascending half of the orbit matching the descending half of the orbit.

When the true anomaly of the common line is zero, the common line passes through the line of apsides. In this case perigee and apogee lie in the ecliptic plane. The points on the semi-minor axis are furthest from the ecliptic plane and the distance from the ecliptic plane is antisymmetric about the line of apsides; the ascending half of the orbit matching the descending half but in opposite direction.

For other values of θ_c, one side of the orbit lies closer to the ecliptic plane than the other side, Figure B illustrates the effect of the value of θ_c on distance from the ecliptic plane as a function of distance from the earth.

Since the region of greatest scientific interest is close to the earth-sunline at a range of about 10 earth radii, it appears that if i_e cannot be made equal to zero, then a value of θ_c near 30 deg would be desirable.

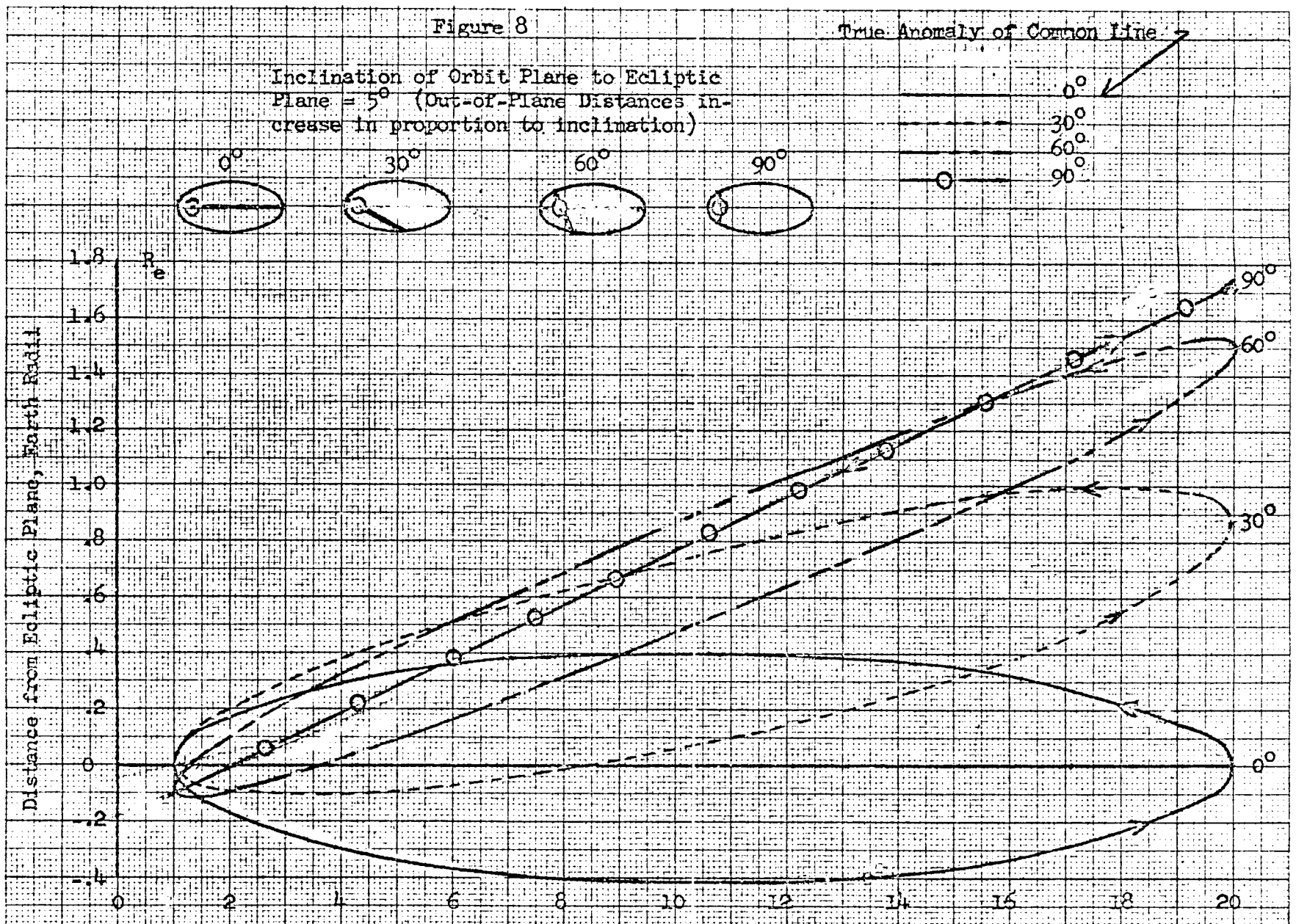

FIGURE 8. EFFECT OF TRUE ANOMALY OF COMMON LINE ON OUT-OF-PLANE DISTANCES

The inclination between the orbital plane and the ecliptic plane, i_e, is equal to the angle between the normal to the orbit and the ecliptic pole. On the assumption that the boost trajectory will not be dog-legged the direction of the normal to the orbit is fixed by (a) the latitude of the launch site, (b) the azimuth of the pitch-over of the boost trajectory, and (c) the time of launch. For a launch out of ETR the launch site latitude will be close to 28.50 deg.

The lowest inclination to the ecliptic, i.e., the smallest value of i_e, is obtained with an east launch, i.e., AZ = 90 deg, at the time of day, $t = t_{min}$, when the launch site is closest to the ecliptic plane. Figure C depicts the relationship of the orbital plane to the ecliptic plane for these launch conditions. It is seen that the minimum inclination between the planes is given by the difference between the launch latitude, 28.5 deg and the obliquity angle, i.e., the angle between the earth's pole and the ecliptic pole which is close to 23.44 deg. Hence the minimum inclination between the orbital and ecliptic planes is about 5.06 deg.

As shown in Figure D, as the launch time departs from t_{min} and/or the launch azimuth departs from 90 deg, the inclination between the planes, i_e, first increases gradually and then more rapidly. An increase in inclination to about 8.5 deg is incurred if the launch time is either an hour early or an hour late and a launch azimuth of ninety degrees is retained. The increased inclination incurred for an hour's delay could be kept to about 6 deg, if the azimuth were increased to about 97 deg. Since the variation in payload capability with azimuth in the vicinity of 90 deg is flat, the payload loss due to a 7 deg shift in azimuth should be small. However, it is unlikely that the launch vehicle could readily provide an on-the-spot adjustment of launch azimuth. Hence, the launch azimuth will probably be fixed by the nominal launch time.

The main perturbation effect that is expected to influence the inclination to the ecliptic is the regression of the line of nodes of the orbit due to earth's oblateness. This corresponds to a rotation of the orbit about the earth's polar axis. Hence, the effect on inclination with respect to the ecliptic is equivalent to that due to a shift in launch time. For the contemplated orbital parameters,

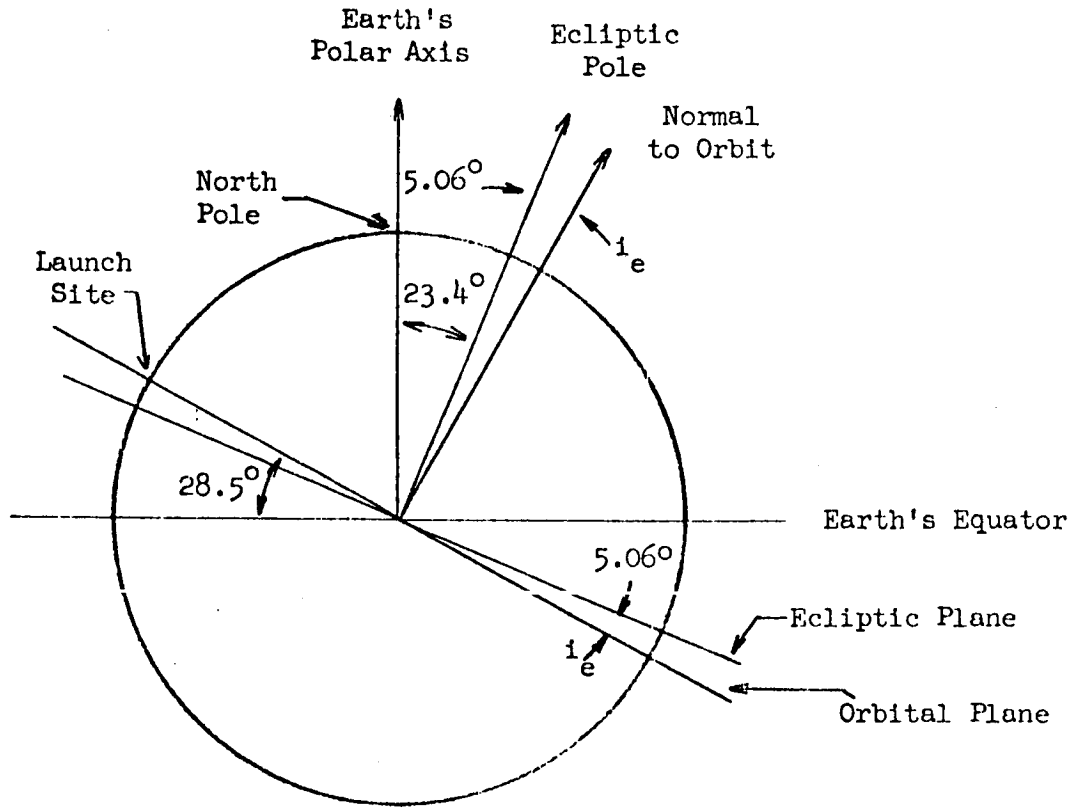

FIGURE 9. RELATIONSHIP OF ECLIPTIC AND ORBITAL PLANES FOR MINIMUM INCLINATION LAUNCH CONDITIONS

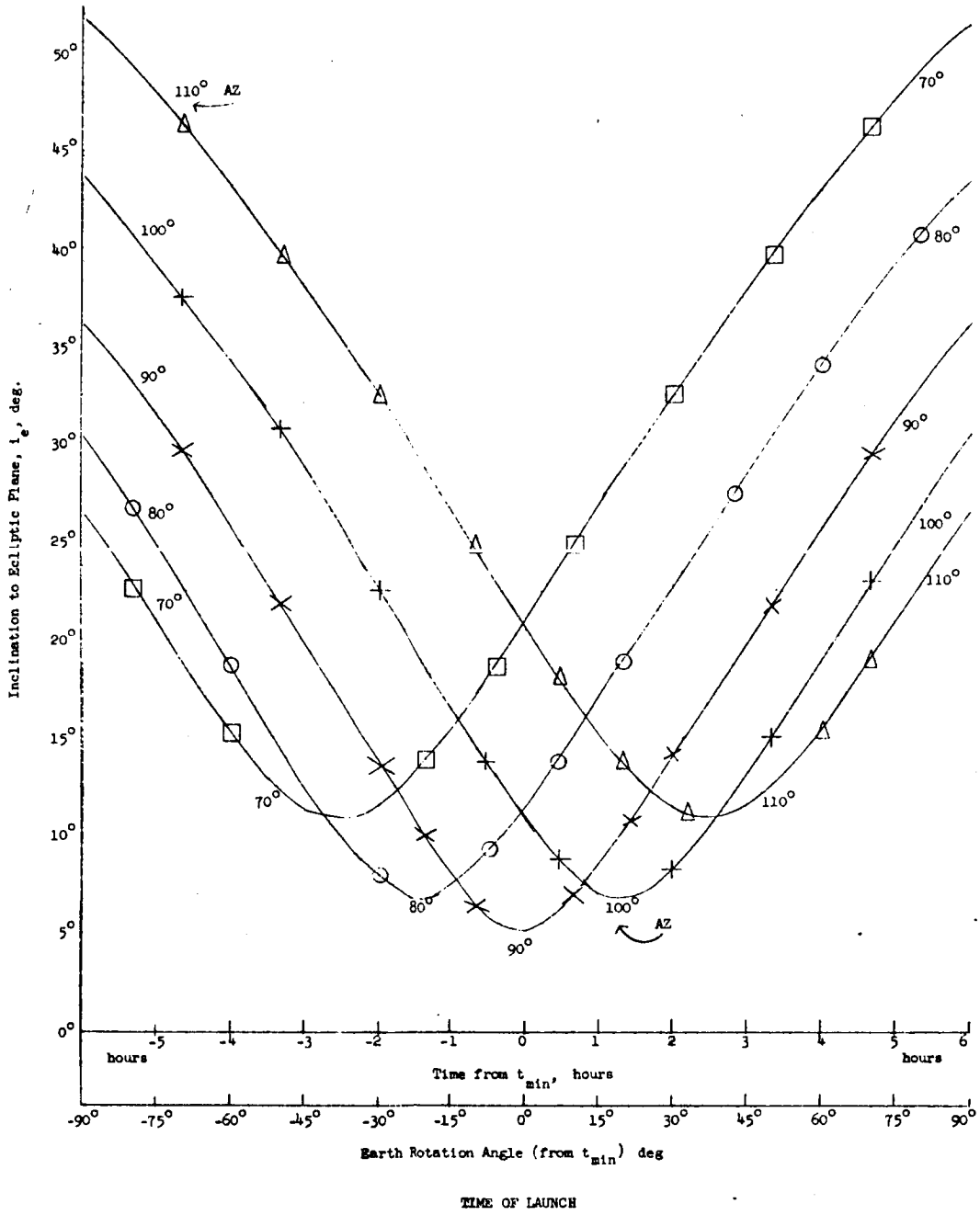

Figure 10. Effect of Launch Time and Azimuth on Inclination to Ecliptic

i.e., prograde inclination with respect to the earth's equatorial plane $\doteq$ 28.5 deg; $r_a \doteq 20\ R_e$; $h_p \doteq 280$ km, the nodal regression in a 6-month period would be about 12.5 deg. This is equivalent to launching early by about 50 minutes. If it were desired that maximum inclination encountered during a 6-month operational lifetime be minimized, a partial compensation for the nodal regression could be obtained by launching about 25 minutes after t_{min}. With a launch azimuth of 90 deg, the initial inclination to the ecliptic would then be about 6 deg; during the first 3 months i_e would decrease to about 6 deg and then increase back to 6 deg in the next 3 months.

The foregoing conditions, i.e.: the launch site latitude; the launch azimuth; and the launch time also fix the angle, φ_c, between the launch site radius and the common line. If the angle between the launch site radius and the perigee radius is designated, φ_p, then the true anomaly of the common line is given by: $\theta_c = \varphi_c - \varphi_p$ (see Figure E). Figure F shows the relationship between φ_c and the launch parameters.

With a due east launch (AZ = 90 deg), at $t = t_{min}$, a value of $\varphi_c = 90$ deg is obtained. It is estimated that if the booster vehicle flies a direct-ascent maximum payload boost trajectory, the value of φ_p will be about 30 deg. The value of $\varphi_c = 90$ deg will then correspond to a value of θ_c of 60 deg. To obtain a value of $\theta_c = 30$ deg requires either a reduction of the value φ_c to 60 deg or an increase in the value of φ_p. Reduction of the value of φ_c calls for a shift in the launch time and/or a shift in the launch azimuth. Either shift would involve some increase in inclination with respect to the ecliptic. However, the increase in i_e required for a decrease in φ_c of from 90 to 60 deg is rather small. This can be seen in the cross plots presented in Figure G and H.

A shift in azimuth would incur a small payload penalty while no payload penalty is incurred by a shift in launch time. However, other factors such as the initial value of s_a and the phase of the long term perturbation of perigee radius may restrict the selection of the launch time.

It is noted that when the inclination is low, φ_c (and hence θ_c) is quite sensitive to the launch time. A launch time shift of 20 minutes (1/3 hour)

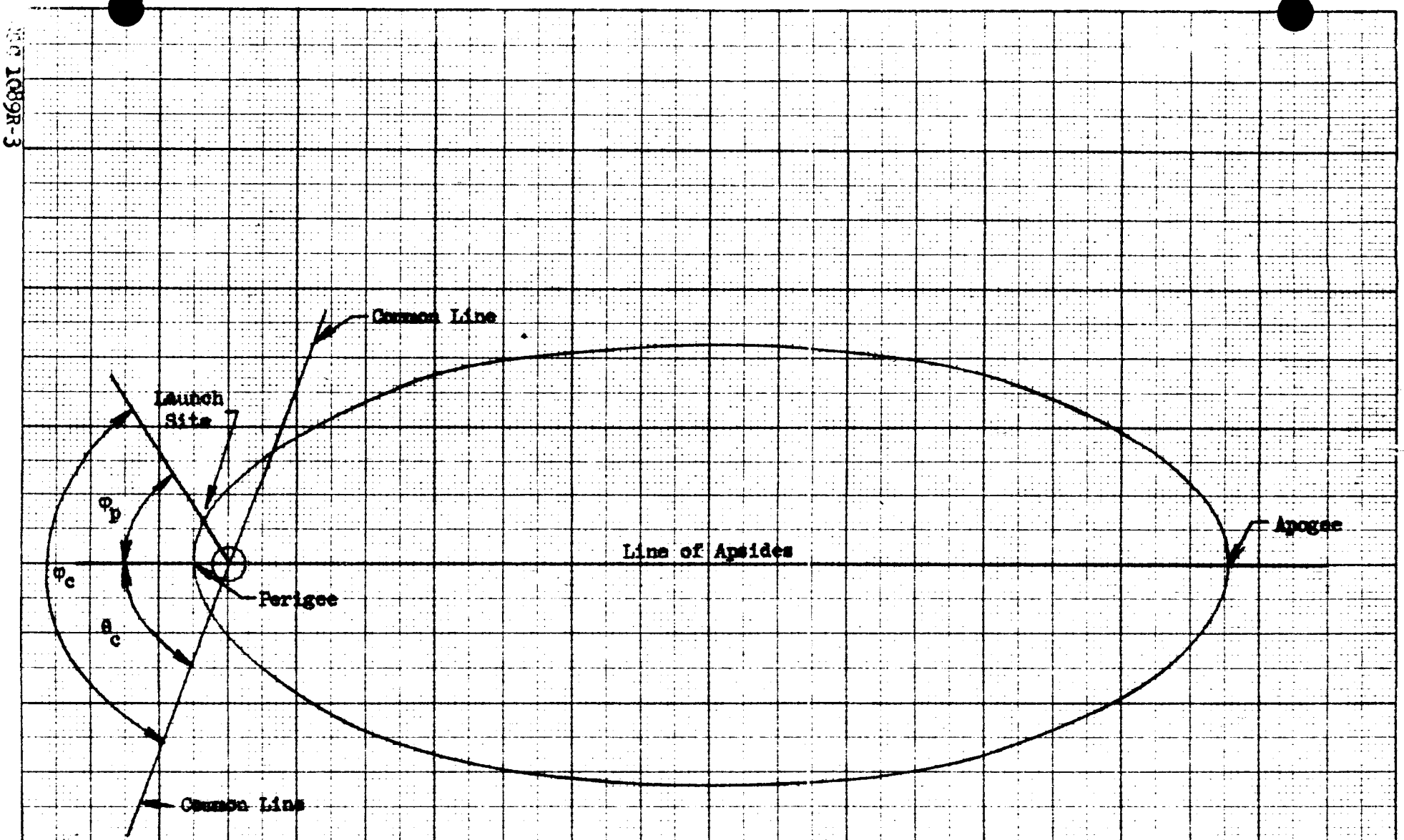

FIGURE 11. RELATIONSHIP BETWEEN LAUNCH RADIUS, PERIGEE RADIUS AND COMMON LINE

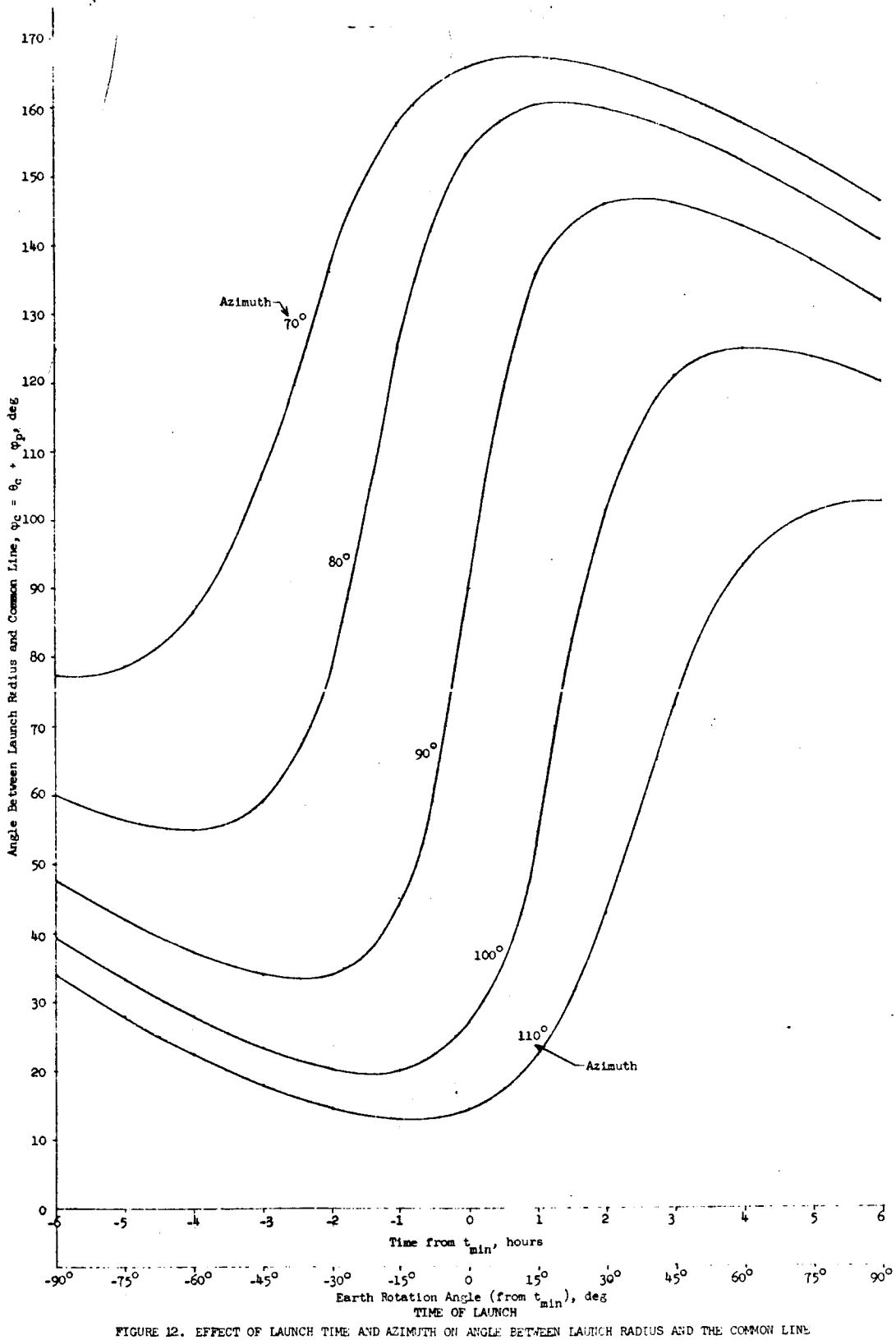

FIGURE 12. EFFECT OF LAUNCH TIME AND AZIMUTH ON ANGLE BETWEEN LAUNCH RADIUS AND THE COMMON LINE

Figure 12. Effect of Launch Time and Azimuth on Angle Between Launch Radius and the Common Line

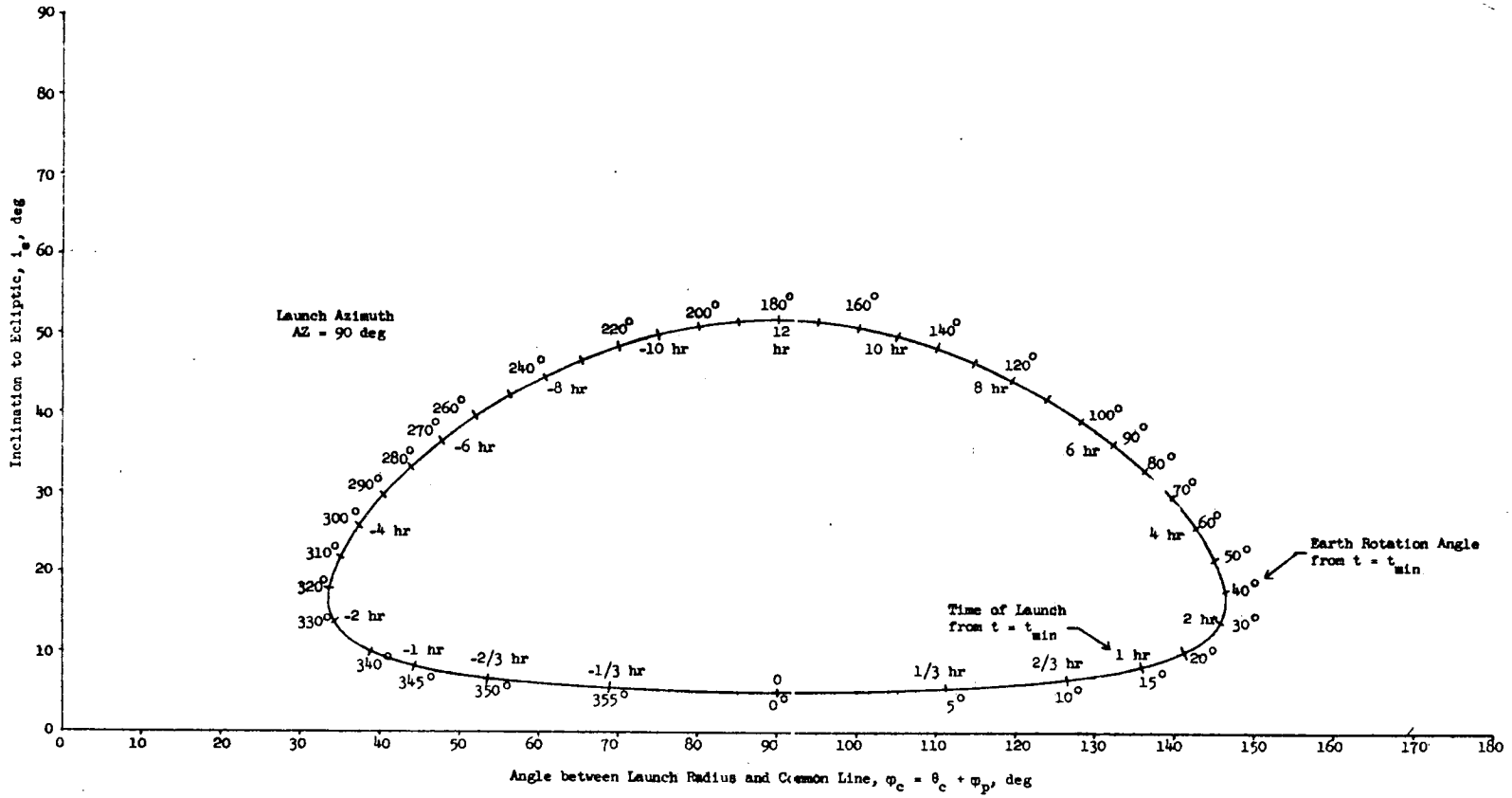

FIGURE 13. CROSS PLOT OF i_e vs φ_c, FOR AZ = 90 DEG

Figure 13. Cross Plot of i_e vs φ_c, for AZ = 90 Degree

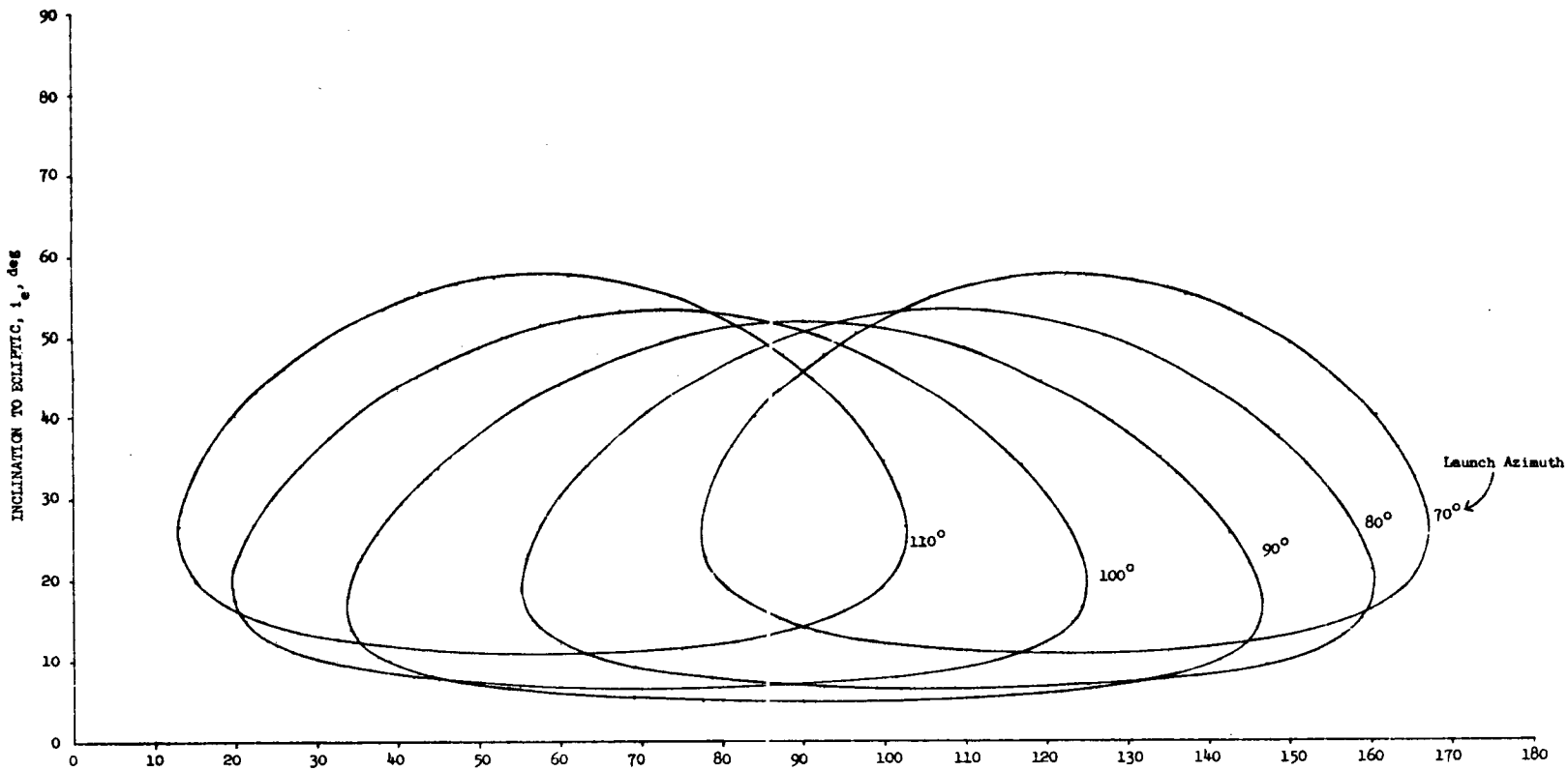

FIGURE 14. CROSS PLOT OF i_e VS φ_c, VARIOUS LAUNCH AZIMUTHS

Figure 14. Cross Plot of i_e vs φ_c, Various Launch Azimuths

corresponds to a change in φ_c of about 20 deg. Hence it is clear that in order to obtain a specified value of θ_c within reasonably small tolerances, stringent limitations on the width of the launch window would be necessary, unless an on-the-spot shift in azimuth, appropriate to the launch time delay were made. Such on-the-spot variations of the nominal boost trajectory would complicate booster guidance and mission planning problems.

Increasing the value of φ_p requires an increase in the coast time prior to firing the last booster stage. This would involve a departure from an optimum boost trajectory with a consequent reduction of payload capability or the use of a low parking orbit with restart of the second stage of the booster. Extending the coast period would allow any desired value of φ_p to be obtained within the limitations on the maximum attainable coast angle which is restricted by the present booster design to about 200 deg. However, with the use of a parking orbit, compensation for launch time delays could not be effected unless an on-the-spot adjustment of the time of firing the last stage were made. The present implementation of the TAID booster does not provide such an adjustment capability.

In addition to difficulties in obtaining the desired initial value of θ_c, the value of θ_c during the operational lifetime is subject not only to variations due to the nodal regression, but also the variations due to apsidal precession of the orbit. As previously noted the nodal regression corresponds to an equivalent shift in the launch time which is expected to be approximately 50 minutes over a 6-month operational lifetime. The apsidal precession is equivalent to a rotation of the orbit about the normal to the orbit and thus is directly additive to θ_c. Over a 6-month operational lifetime the apsidal precession is estimated to be about 20 deg. The sense of both the nodal regression and the apsidal precession are in the direction to reduce θ_c.

If, as discussed above, the nominal launch time were delayed by about 25 minutes to compensate for the effect of the nodal regression on inclination, the initial value of φ_c would be increased to about 115 deg. For φ_p = 30 deg the initial value of θ_c would be about 85 deg. However, in the first three months θ_c would decrease to about 50 deg (a decrease of ~ 25 deg due to nodal regression plus a decrease of ~ 10 deg due to apsidal precession), and by the end of 6 months

θ_c would decrease to about 20 deg. In this case the most desirable values of θ_c would occur late in the operational lifetime.

If the nominal launch time is not advanced but is chosen at $t = t_{min}$ to achieve the minimum initial inclination at the outset, with $\varphi_p = 30$ deg, the initial value of θ_c would be about 60 deg. In 3 months the value of θ_c would drop to about 25 deg [illegible] while the inclination would increase from 5.06 to about 6 deg.

The orientation of the sunline line relative to any vector lying in the orbital plane can be expressed in terms of two angles:

a. The angle, D, between the vector and the ecliptic plane, and

b. The angle, (A-S), between the sunline and the projection of the vector in the ecliptic plane.

As indicated in Figure I, the latter angle can be obtained from the difference between:

a. The angle, A, between Aries (i.e., the direction of the sunline at the vernal equinox), and the projection of the vector in the ecliptic plane, and

b. The angle, S, between Aries and the sunline.

In the case where the vector in the orbital plane is taken to be the apogee radius, the angle (A-S) is equal to s_a. S is zero at the vernal equinox and increases by about 1 deg/day as the earth rotates about the sun in its annual orbit.

The angles A and D depend upon: the launch site longitude; the launch azimuth, AZ; the time of launch, t; and the angle, φ, between the launch site and the position vector at an arbitrary point in the orbit. The effects of the launch variables on the angle A, for a launch from ETR are shown in Figures J, K and L.

The manner in which these graphs can be interpreted to derive the details of the relationship between the orbit and the sunline is illustrated in Figure M. The illustration is based upon a launch at $t = t_{min}$ at an azimuth of 90 deg. The dates shown along the A scale correspond to the position of the sunline relative to Aries. For example, on December 21 the angle between the sunline and Aries

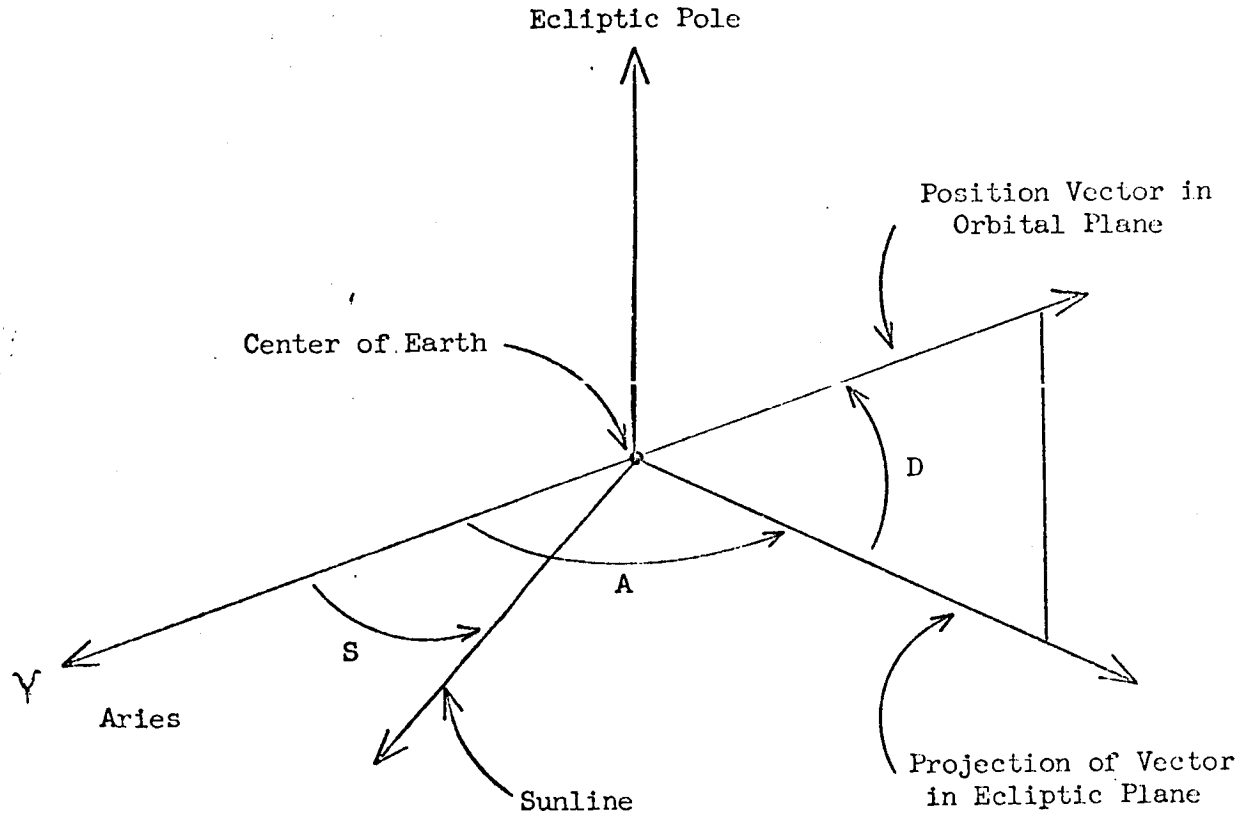

FIGURE I. DEFINITION OF ANGLES RELATING POSITION VECTOR IN ORBITAL PLANE TO THE ECLIPTIC PLANE AND THE SUNLINE

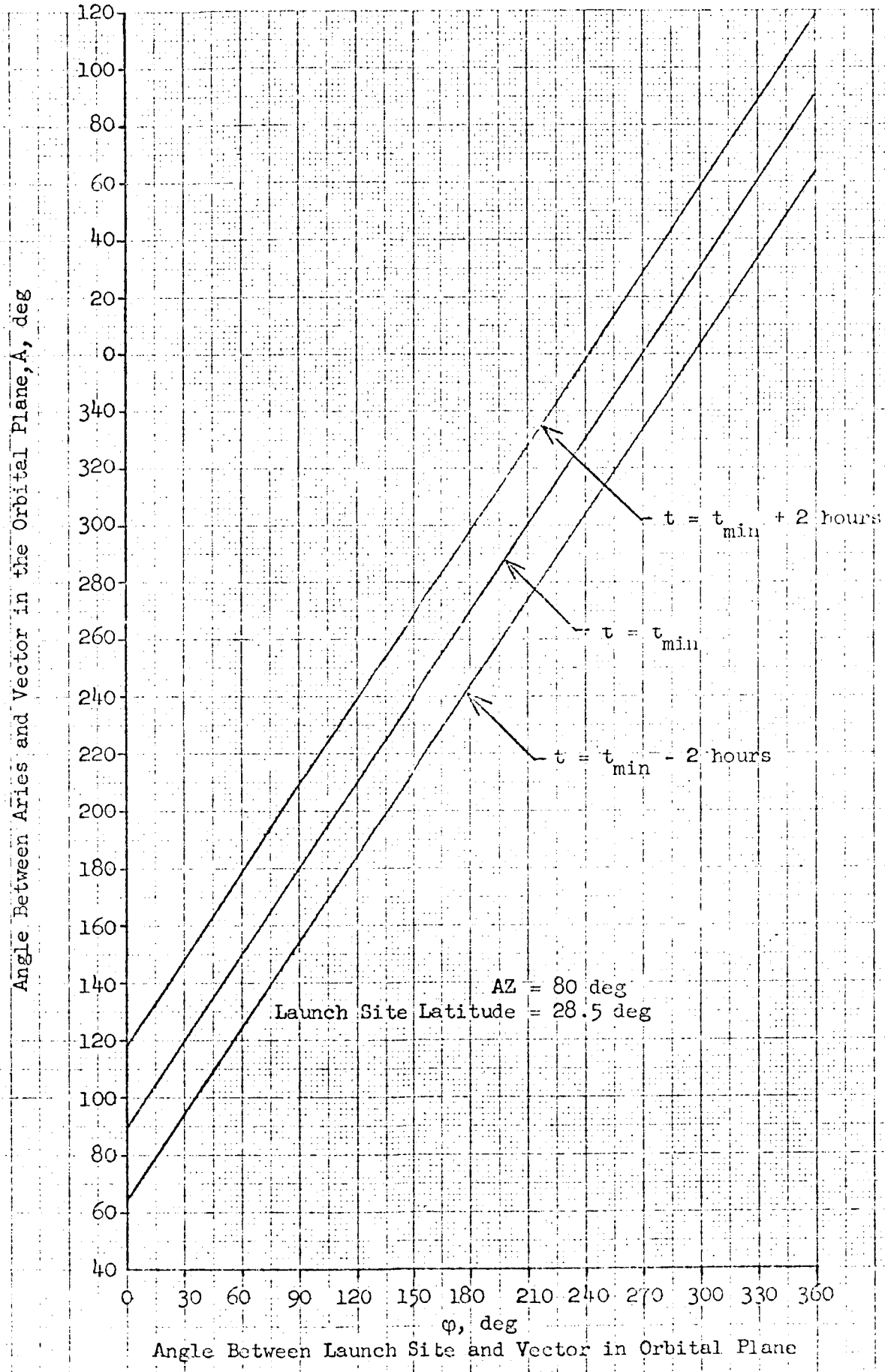

FIGURE J. VARIATION OF A WITH φ AND LAUNCH TIME, AZ = 80 DEG

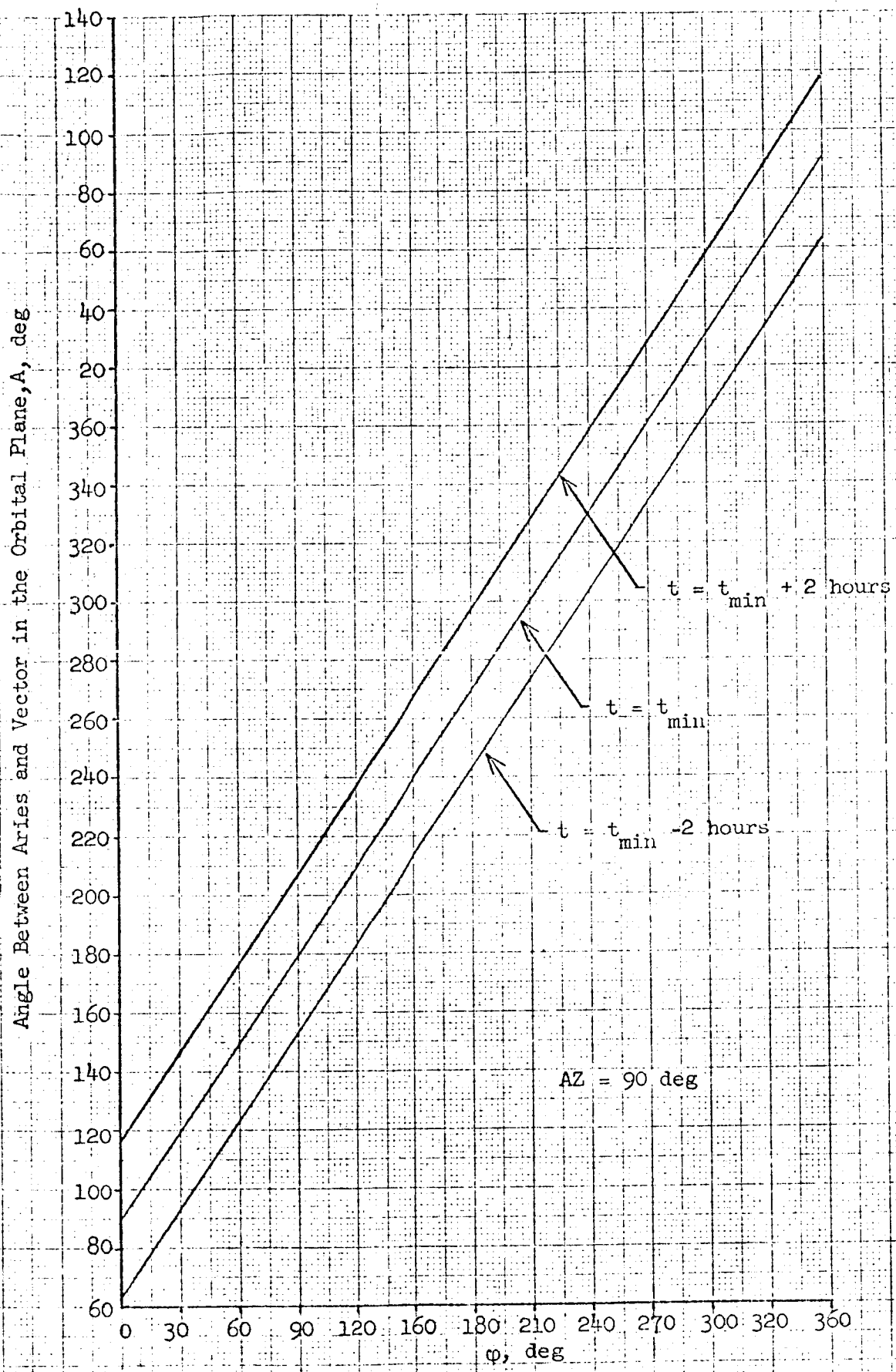

FIGURE K. VARIATION OF A WITH φ AND LAUNCH TIME, AZ = 90 DEG

The effect of the solar and lunar perturbations on θ_c could not be reduced to a form simple enough to warrant hand computation. Machine computations are currently being prepared for the study of these effects. It is noted that the foregoing estimates of the solar and lunar perturbation effects on inclination indicate that these effects will generally be smaller than those previously estimated for the earth oblateness perturbation. However, it is true that there will be interaction between the perturbation effects which have not been taken into account in the present calculations. For example if the inclination increases due to earth oblateness effects, the solar perturbation effect on inclination will increase. Likewise interaction between the perturbation effects may have a significant influence on θ_c and the changes in θ_c can influence both h_p and i_e. In addition to evaluating the solar and lunar perturbation effects on θ_c, a prime objective of the machine computations will be to take account of these interaction effects.

Appendix VIII

REFERENCE ORBIT

1.0 REFERENCE ORBIT

Nominal values of the position and velocity history for the common orbit necessary for separation and deployment studies are presented in this Appendix. Figure A presents a graphical illustration of this reference orbit. Tables 1 to 3 list the details of position and velocity history.

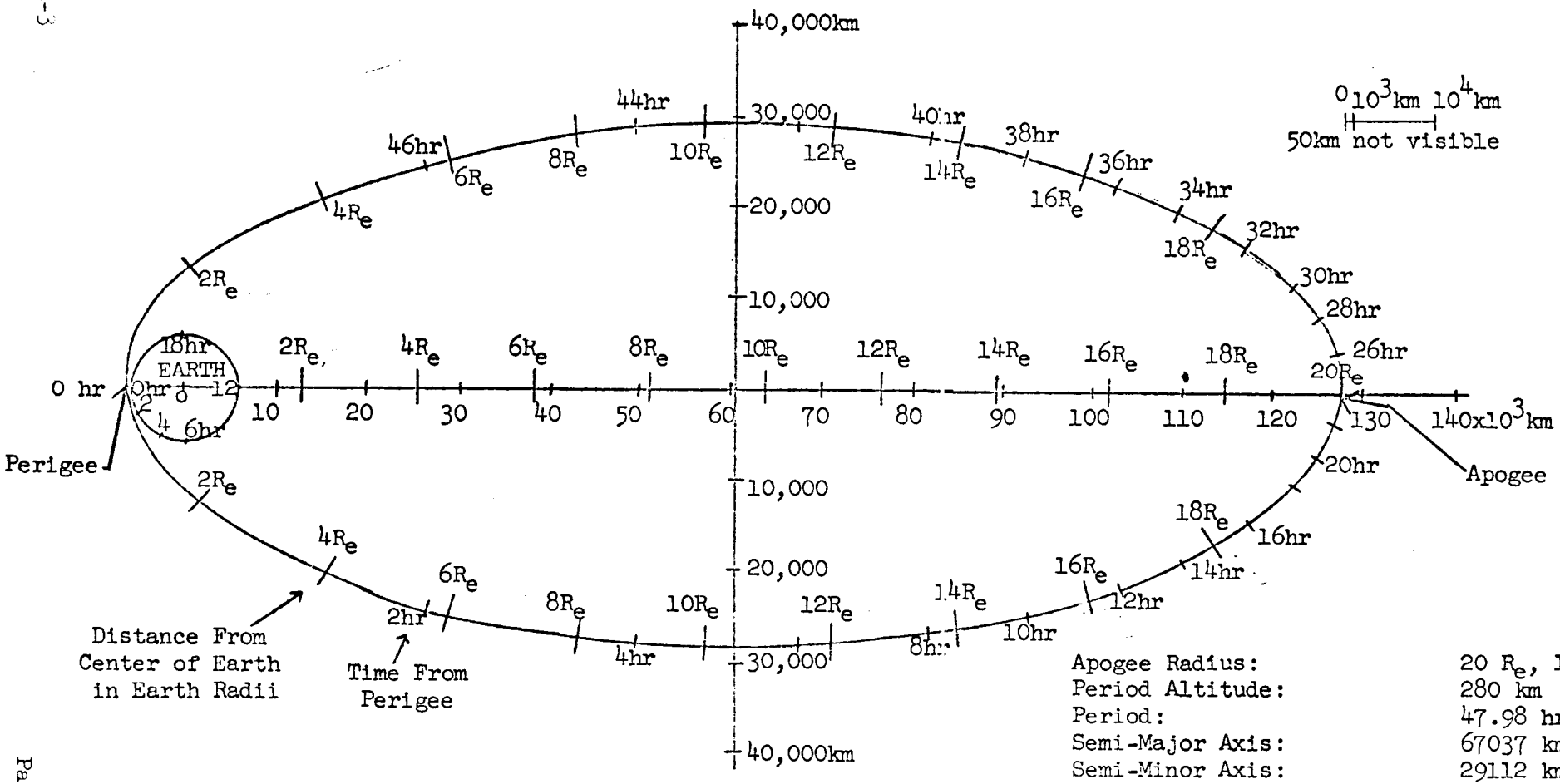

Apogee Radius:	20 R_e, 127,424 km
Period Altitude:	280 km
Period:	47.98 hrs
Semi-Major Axis:	67037 km
Semi-Minor Axis:	29112 km
Semi-Latus Rectum:	12642 km
Velocity at Perigee:	10,673 meters/sec
Velocity at Semi-Minor Axis:	2472.5 meters/sec
Velocity at Apogee:	557.1 meters/sec

FIGURE A. MULTIPLE SATELLITE REFERENCE ORBIT

Table 1

280 km x 20 R_e REFERENCE ORBIT CONDITIONS AS FUNCTIONS OF TIME FROM PERIGEE

Time From Perigee hrs	Distance From Center of Earth		True Anomaly			Position Coordinates		Velocity Coordinates		Velocity Magnitude	Flight Path Angle	Radial Velocity	Angular Velocity
	R_e	km	deg	sin θ	cos θ	x km	y km	$\dot{x}$ km/sec	$\dot{y}$ km/sec	v km/sec	γ deg	$\dot{R}$ km/sec	$\dot{\theta}$ 10^{-3} deg/sec
0	1.044	6651	0.00	0.0000	1.0000	-6651	0.	0.000	-10.673	10.673	0.00	0.000	91.94
.25	1.446	9213	65.59	0.9106	0.4133	-3807	-8389	5.113	-7.378	8.977	30.87	4.606	47.92
.5	2.146	13674	94.81	0.9965	-0.8377	1146	-13626	5.595	-4.588	7.236	44.15	5.040	21.75
1.0	3.491	22241	118.63	0.8778	-0.4791	10656	-19522	4.329	-2.368	5.468	54.29	4.440	8.22
1.5	4.665	29718	129.63	0.7701	-0.6379	18956	-22887	4.324	-1.476	4.569	58.48	3.895	4.61
2.0	5.705	36347	136.39	0.6898	-0.7240	26316	-25072	3.873	-0.993	3.998	60.76	3.489	3.08
3.0	7.504	47809	144.74	0.5772	-0.8166	39041	-27597	3.241	-0.47[illegible]	3.275	63.04	2.920	1.78
4.0	9.037	57574	150.04	0.4994	-0.8664	49881	-28753	2.804	-0.19[illegible]	2.811	63.98	2.523	1.23
5.0	10.376	66109	153.88	0.4403	-0.8978	59355	-29109	2.472	-0.016	2.472	64.26	2.227	0.93
6.0	11.564	73679	156.88	0.3927	-0.9197	67759	-28936	2.205	0.10[illegible]	2.208	64.12	1.986	0.74
7.0	12.628	80457	159.34	0.3527	-0.9357	75284	-28384	1.981	0.19[illegible]	1.991	63.69	1.784	0.62
8.0	13.586	86559	161.44	0.3183	-0.9480	82058	-27548	1.787	0.26[illegible]	1.807	63.00	1.610	0.54
9.0	14.451	92071	163.28	0.2877	-0.9577	88177	-26493	1.616	0.32[illegible]	1.647	62.09	1.455	0.48
10.0	15.234	97056	164.91	0.2603	-0.9655	93712	-25260	1.461	0.364	1.506	60.94	1.316	0.43
11.0	15.941	101564	166.40	0.2352	-0.9720	98715	-23884	1.320	0.40[illegible]	1.380	59.56	1.189	0.39
12.0	16.580	105632	167.76	0.2120	-0.9773	103231	-22390	1.190	0.42[illegible]	1.265	57.92	1.072	0.36
13.0	17.154	109292	169.03	0.1903	-0.9817	107295	-20797	1.069	0.454	1.161	55.99	0.962	0.34
14.0	17.669	112570	170.22	0.1699	-0.9855	110933	-19123	0.954	0.475	1.066	53.72	0.859	0.32
15.0	18.126	115485	171.35	0.1505	-0.9886	114170	-17378	0.845	0.493	0.978	51.07	0.761	0.30
16.0	18.529	118055	172.42	0.1319	-0.9913	117023	-15575	0.741	0.508	0.898	47.98	0.667	0.29
17.0	18.881	120294	173.45	0.1141	-0.9935	119508	-13723	0.641	0.520	0.825	44.36	0.577	0.28
18.0	19.182	122213	174.44	0.0968	-0.9953	121639	-11830	0.543	0.531	0.760	40.13	0.490	0.27
19.0	19.434	123822	175.41	0.0800	-0.9968	123425	-9904	0.449	0.539	0.701	35.21	0.405	0.26
20.0	19.640	125128	176.36	0.0635	-0.9980	124875	-7951	0.357	0.546	0.652	29.53	0.321	0.25
21.0	19.798	126137	177.28	0.0474	-0.9989	125996	-5977	0.266	0.551	0.612	23.07	0.240	0.25
22.0	19.91	126855	178.20	0.0314	-0.9995	126792	-3987	0.176	0.554	0.582	15.86	0.159	0.25
23.0	19.978	127283	179.11	0.0156	-0.9999	127267	-1987	0.088	0.556	0.563	8.06	0.079	0.25
24.0	20.000	127424	180.01	-0.0001	-0.9999	127423	17.54	-0.001	0.557	0.557	-0.07	-0.001	0.25
25.0	19.977	127278	180.91	-0.0159	-0.9999	127261	2022	-0.089	0.556	0.563	-8.20	-0.080	0.25
26.0	19.909	126845	181.82	-0.0317	-0.9995	126781	4021	-0.178	0.554	0.582	-15.99	-0.160	0.25

Table 2

280 km x 20 R_e REFERENCE ORBIT CONDITIONS AS FUNCTION OF TRUE ANOMALY

True Anomaly θ deg	Time From Perigee hrs	Distance From Center of Earth		Position Coordinates		Velocity Coordinates		Velocity Magnitude v km/sec	Flight Path Angle γ deg	Radial Velocity $\dot{R}$ km/sec	Angular Velocity $\dot{\theta}$ 10^{-3} deg/sec
		R_e	km	x km	y km	$\dot{x}$ km/sec	$\dot{y}$ km/sec				
0	0.000	1.044	6651	-6651	0	0.000	-10.673	10.673	0.00	0.000	91.94
5	0.015	1.046	6663	-6637	-580	0.489	-10.652	10.663	2.37	0.441	91.61
10	0.030	1.052	6699	-6598	-1163	0.975	-10.588	10.633	4.74	0.878	90.62
15	0.045	1.061	6760	-6530	-1750	1.453	-10.482	10.582	7.11	1.309	89.00
20	0.062	1.075	6847	-6434	-2342	1.920	-10.334	10.511	9.47	1.730	86.76
25	0.078	1.092	6960	-6308	-2942	2.373	-10.147	10.421	11.84	2.138	83.96
30	0.095	1.115	7102	-6151	-3551	2.808	-9.921	10.310	14.20	2.529	80.64
35	0.112	1.142	7275	-5959	-4173	3.221	-9.658	10.180	16.56	2.901	76.86
40	0.131	1.174	7481	-5731	-4808	3.609	-9.359	10.031	18.91	3.251	72.68
45	0.151	1.212	7723	-5461	-5461	3.970	-9.028	9.863	21.26	3.577	68.19
50	0.172	1.257	8007	-5147	-6133	4.301	-8.667	9.676	23.61	3.875	63.45
55	0.195	1.308	8336	-4781	-6828	4.600	-8.279	9.471	25.94	4.143	58.54
60	0.219	1.368	8717	-4358	-7549	4.863	-7.865	9.247	28.27	4.380	53.53
65	0.247	1.437	9157	-3870	-8299	5.089	-7.431	9.007	30.60	4.584	48.51
70	0.277	1.517	9665	-3306	-9082	5.276	-6.978	8.749	32.91	4.753	43.54
75	0.311	1.609	10252	-2653	-9903	5.424	-6.511	8.474	35.21	4.886	38.70
80	0.349	1.716	10932	-1898	-10766	5.530	-6.033	8.184	37.49	4.981	34.03
85	0.393	1.840	11722	-1022	-11678	5.594	-5.547	7.878	39.76	5.039	29.60
90	0.443	1.984	12642	0.0	-12642	5.615	-5.058	7.557	42.01	5.058	25.45
95	0.502	2.153	13720	1196	-13667	5.594	-4.569	7.222	44.24	5.039	21.61
100	0.573	2.352	14987	2602	-14759	5.530	-4.083	6.874	46.44	4.981	18.11
105	0.657	2.588	16486	4267	-15924	5.424	-3.605	6.512	48.61	4.886	14.97
110	0.760	2.868	18272	6249	-17170	5.276	-3.137	6.139	50.74	4.753	12.18
115	0.887	3.204	20414	8627	-18501	5.089	-2.685	5.754	52.82	4.584	9.76
120	1.048	3.610	23003	11501	-19921	4.863	-2.250	5.358	54.83	4.380	7.69
125	1.254	4.106	26157	15003	-21426	4.600	-1.837	4.953	56.77	4.143	5.94
130	1.522	4.713	30031	19303	-23005	4.301	-1.449	4.539	58.61	3.875	4.51
135	1.880	5.466	34823	24624	-24624	3.970	-1.088	4.117	60.32	3.577	3.35
140	2.366	6.402	40787	31245	-26218	3.609	-0.757	3.688	61.84	3.251	2.44
145	3.040	7.570	48231	39509	-27664	3.221	-0.458	3.253	63.10	2.901	1.75
150	3.991	9.024	57492	49790	-28746	2.808	-0.195	2.814	63.98	2.529	1.23
155	5.349	10.807	68854	62403	-29099	2.373	0.031	2.373	64.25	2.138	0.858
160	7.298	12.924	82340	77374	-28162	1.920	0.218	1.933	63.51	1.730	0.600
165	10.055	15.275	97317	94001	-25188	1.453	0.366	1.498	60.87	1.309	0.429
170	13.811	17.576	111978	110277	-19445	0.975	0.472	1.083	54.18	0.878	0.324
175	18.571	19.332	123168	122700	-10735	0.489	0.536	0.726	37.41	0.441	0.268
180	23.991	20.000	127424	127424	0.	0.000	0.557	0.557	0.00	0.000	0.251

Table 3

280 km x 20 R_e REFERENCE ORBIT CONDITIONS AS FUNCTION OF DISTANCE FROM CENTER OF EARTH

Distance From Center of Earth		Time From Perigee	True Anomaly			Position Coordinates		Velocity Coordinates		Velocity Magnitude	Flight Path Angle	Radial Velocity	Angular Velocity
R_e	km	hrs	deg	sin θ	cos θ	X km	Y km	$\dot{X}$ km/sec	$\dot{Y}$ km/sec	V km/sec	γ deg	$\dot{R}$ km/sec	$\dot{\theta}$ 10^{-3} deg/sec
1.044	6651	0	0.00	0.0000	1.0000	-6651	0.	0.000	-10.673	10.673	0.00	0.000	91.94
1.5	9557	0.270	69.00	0.9336	0.3584	-3426	-8922	5.242	-7.071	8.802	32.44	4.722	44.53
2.0	12742	0.449	90.50	1.0000	-0.0087	111	-12742	5.615	-5.009	7.524	42.24	5.058	25.05
2.5	15928	0.626	103.24	0.9734	-0.2290	3647	-15505	5.466	-3.772	6.641	47.85	4.924	16.03
3.0	19114	0.810	112.08	0.9267	-0.3759	7184	-17712	5.203	-2.948	5.980	51.61	4.687	11.13
4.0	25485	1.209	124.02	0.8289	-0.5594	14257	-21124	4.654	-1.917	5.033	56.40	4.192	6.26
5.0	31856	1.655	132.03	0.7428	-0.6696	21330	-23661	4.171	-1.298	4.368	59.32	3.757	4.01
6.0	38227	2.152	137.99	0.6693	-0.7430	28403	-25585	3.758	-0.861	3.861	61.25	3.385	2.78
7.0	44598	2.702	142.70	0.6060	-0.7954	35476	-27028	3.403	-0.591	3.454	62.56	3.065	2.04
8.0	50969	3.308	146.59	0.5506	-0.8348	42548	-28063	3.092	-0.371	3.114	63.43	2.785	1.57
9.0	57341	3.974	149.92	0.5011	-0.8654	49621	-28734	2.814	-0.199	2.821	63.97	2.535	1.24
10.0	63712	4.706	152.86	0.4562	-0.8899	56694	-29068	2.562	-0.061	2.563	64.23	2.308	1.00
11.0	70083	5.511	155.49	0.4149	-0.9099	63767	-29075	2.330	0.051	2.330	64.23	2.098	0.828
12.0	76454	6.397	157.91	0.3761	-0.9266	70840	-28756	2.112	0.145	2.117	63.98	1.924	0.696
13.0	82825	7.376	160.17	0.3393	-0.9407	77913	-28100	1.905	0.224	1.918	63.46	1.716	0.593
14.0	89197	8.466	162.33	0.3036	-0.9528	84986	-27081	1.705	0.292	1.730	62.60	1.536	0.511
15.0	95568	9.691	164.43	0.2685	-0.9633	92059	-25658	1.508	0.351	1.548	61.32	1.358	0.445
16.0	101939	11.088	166.52	0.2331	-0.9725	99132	-23757	1.309	0.402	1.369	59.43	1.179	0.391
17.0	108310	12.721	168.68	0.1962	-0.9806	106205	-21251	1.102	0.448	1.189	56.56	0.992	0.347
18.0	114681	14.712	171.03	0.1560	-0.9878	113278	-17887	0.876	0.488	1.003	51.88	0.789	0.309
19.0	121052	17.376	173.83	0.1075	-0.9942	120351	-13016	0.603	0.525	0.800	42.84	0.544	0.278
20.0	127424	23.991	180.00	0.0000	-1.0000	127424	0.	0.000	0.557	0.557	0.00	0.000	0.251

Appendix IX

DEPLOYMENT SENSITIVITIES

1.0 GENERAL APPROACH

In order to achieve the scientific objectives of measuring the direction and speed of the propagation of disturbance fronts in the solar wind and measuring the spatial derivatives of physical variables pertinent to solar wind phenomena, a non-coplanar array of 4 satellites is required. The desired array is to be obtained by applying small velocity increments during or subsequent to the separation of the satellites from the pallet. In addition to these deployment velocity increments, differential orbital perturbations may be caused by differences in the forces acting on the satellites while in orbit; this includes differences in accelerations due to atmospheric drag and perhaps solar pressure and gravitational forces.

As long as the separation distances are small, the satellites will experience practically the same gravitational accelerations. Hence gravitational perturbations can have only indirect secondary effects on the intersatellite separation distances.

Different accelerations due to atmospheric drag can be effective even when the separation distances are small; but these accelerations and particularly the differences in these accelerations can be expected to be so small that a large number of orbits is required before there is a significant velocity difference accumulation.

Hence, the initial array of intersatellite separation distances can be attributed almost entirely to the initial deployment velocity increments, and the history of the separation distances at least during the early portion of the operational lifetime can be expected to be very close to that which would be obtained for purely Keplerian orbits.

For the purpose of studying the effects of the deployment velocity increments on the array of intersatellite separation distances, it is convenient to use

is concerned. In addition, the design of the pallet's systems is burdened by the requirement for a longer period of operation in orbit.

On the favorable side the magnetometer is a relatively simple, low cost, low weight and low power consuming instrument. Because of the scanning obtained from the spinning of the vehicle each satellite could be equipped with a single probe. Mounted so that its sensitive axis is at an angle of about 45 deg to the spin axis the measurement of the component of the field in this one body fixed direction is sufficient to permit determination of the direction of the satellites spin axis. The satellites would be mounted on the pallet so that their probe axes are 90 deg apart, thus providing complete instantaneous measurement of all components of the magnetic field with some redundancy. In addition to the inertial orientation of the pallet's spin axis, this would permit any shift in the direction of the pallet's spin axis relative to the body axis to be detected.

Technical data for available magnetometers are listed in Table 1.

4.0 IR HORIZON CROSSING INDICATOR

The angle between the local vertical and the spin axis can be determined with the use of an IR horizon crossing indicator. Since the local vertical, i.e., the line from the center of the earth to the satellite rotates through 360 deg as the satellite traverses its orbit, this sensor can provide sufficient data to completely define the orientation of the satellites' spin axes. Two measurements of the angle between the satellite's spin axis and the local vertical obtained at convenient points for which the local vertical is separated by about 90 deg would be adequate. For use with the pallet's ACS only the angle between the spin axis and the local vertical that is perpendicular to the sunline is required inasmuch as the angle between the spin axis and the sunline will be fixed by the pallet's ACS solar sensors.

The optical and mechanical elements of the horizon crossing indicator are rigidly fixed to the sensor base, i.e., no moving parts are used. Instead advantage is taken of the spinning of the vehicle to provide the scanning of the sensor's view field. Discussions with representatives of Barnes Engineering indicate that their Horizon Crossing Indicator Series 13-205 could be adapted to the Multiple Satellite application. This sensor has a conical view field with a cone angle of about 1.3 deg. It detects the thermal discontinuity between earth and space as its view field is scanned across the horizon by the spinning of the spacecraft. Separate outputs indicating sky-earth and earth-sky crossings are generated.

In principle the angle between the spin axis and the local vertical can be determined from the time spacing of the two output signals. If the sensor view field were perpendicular to the spin axis there would be an ambiguity in the determination of the spin axis orientation as indicated by Figure 1a. This ambiguity can be avoided by mounting the sensor so that its view field is not perpendicular to the spin axis as shown in Figure 1b.

Mounting the sensor so that its view field is perpendicular to the spin axis would also be undesirable in that when the spin axis is close to the desired direction, i.e., normal to the orbital plane, the field would sweep across nearly an earth diameter and minimum sensitivity of the time between horizon crossing to a shift in the direction of the spin axis would be obtained.

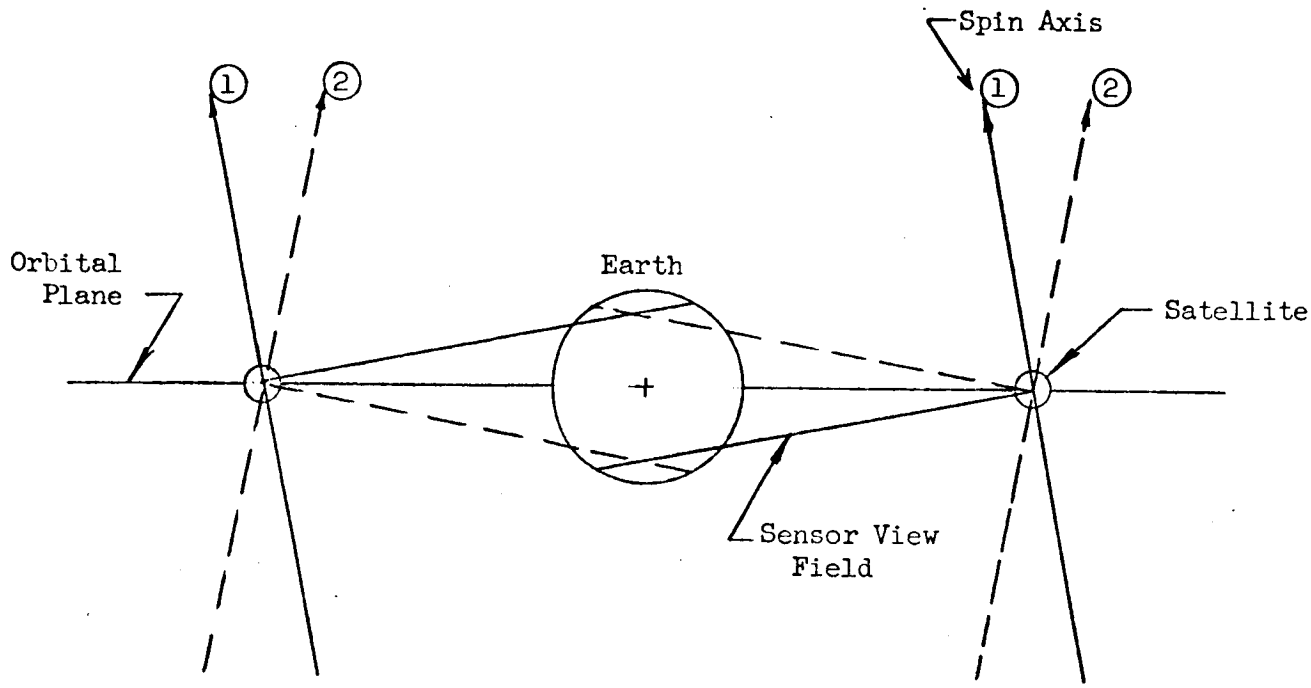

(a) IR sensor view field perpendicular to spin axis orientation of spin axis 1 solid line and 2 dashed line produce same spacing of horizon intercept at all points in orbit.

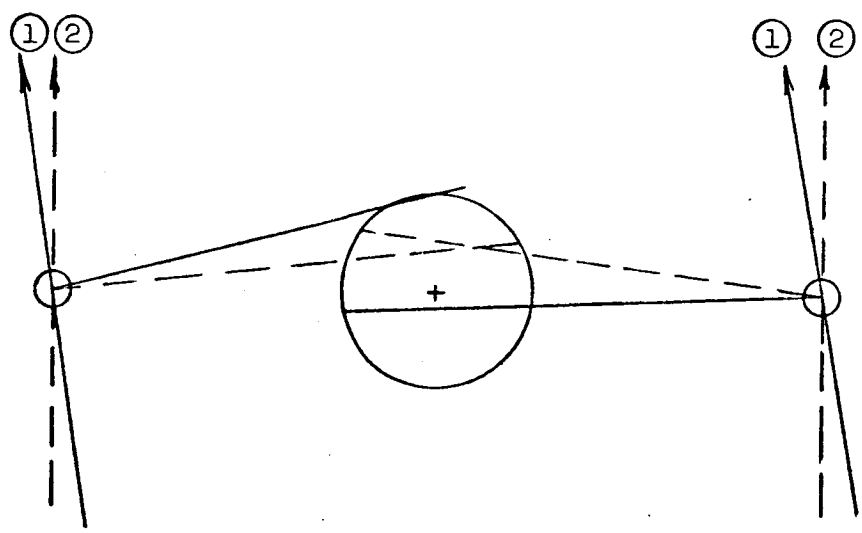

(b) IR sensor view field not perpendicular to spin axis orientation of spin axis 1 and 2 produce same spacing of horizon intercepts on one side of orbit but different spacing on the other side.

FIGURE 1. AVOIDANCE OF AMBIGUITY IN DIRECTION OF SPIN AXIS

A better way of avoiding ambiguity and improving sensitivity is to use two view fields as indicated in Figure 2. The difference between the time between horizon crossings for the two view fields then provides a direct and simple indication of the deviation of the spin axis from perpendicular to the local vertical. Barnes Engineering representatives indicate that a dual field of view sensor can be obtained with a minor modification of the Series 13-205 Horizon Crossing Indicator without a significant increase in size or weight. This is accomplished by mounting a suitable prism at the sensor head and splitting the detector and supporting electronics. In this way two electro-optical systems are provided in a single mechanical housing.

Even if the satellites were confined to single view field sensors, for operation with the pallet four view fields would be available. With two of the view fields inclined toward the pallets spin axis and two away the equivalent of two dual view field sensors would be available.

In contrast to the magnetometer aspect sensor, for operation with the pallet ACS, the IR horizon crossing indicator would provide practically real time attitude data. Even if more or less elaborate corrections are made, the computations required to determine the instantaneous angle between the local vertical and the pallet's spin axis should be quite short; probably less than 1 minute. A few readings made during the portion of the orbit when the angle between the local vertical and the sunline is substantial, say > 45 deg, is all that is required for the completion of the reorientation maneuver.

Furthermore it is possible to get a very quick simple check on any more elaborate computations that may be made; viz. the difference in the timing of the horizon crossings can be quickly and simply determined and would provide an excellent indication that the correction computations had not gone astray. No such check on the reduction of magnetometer data is available.

Although the use of a single view field sensor for the satellites is possible the dual field sensor would be preferable if it can in fact be practicably implemented. In addition to enhancing reliability it would permit any shift in the spin axis relative to body axis to be observed.

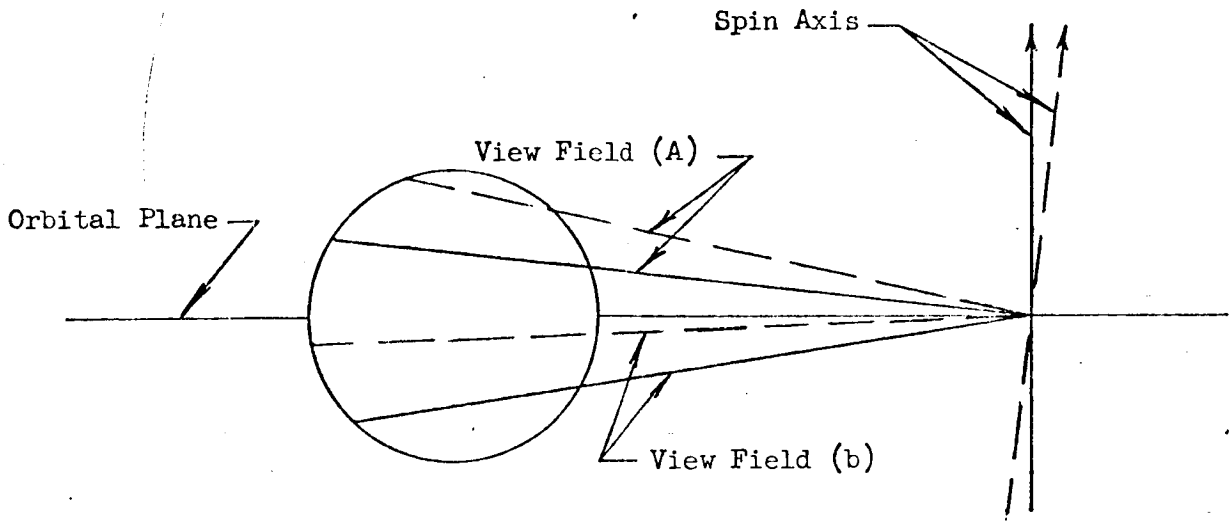

Solid Line indicates spin axis in nominal orientation, i.e., aligned to normal to orbit.

Dashed Line indicates spin axis shifted from nominal orientation.

FIGURE 2. DUAL BEAM HORIZON CROSSING INDICATOR

The optimum choice of the angle between the view field axes and the spin axis will require some study. If the inclinations of the view field axes toward and away from the spin axis are large then at large distances from the earth the view field will completely miss the earth and no data will be obtained. If the inclinations are very small then the field will normally sweep close nearly an earth diameter and sensitivity will be poor. For present purposes view fields inclined about 3 deg towards and away from the spin axis are assumed. With the spin axis in its nominal orientation the field will then skim the horizon at about 20 R_e. Reasonably good sensitivity would then be obtained in the region from about 6 to 20 R_e. It is unlikely that data would be needed as far as or beyond 20 R_e. If data is needed at closer distance the angle could be increased somewhat.

(It should be noted that no matter what orientation the spin axis may have or how the sensor is mounted, provided that the angle between the view field axis and the spin axis is reasonably large, there is no danger that attitude data could be completely lost. While the view field may miss the earth at large distances from earth it is practically impossible for the view field to miss the earth when the satellite is near perigee and for some extended region of the orbit about perigee. From the data obtained when the view field does intercept the earth the direction of the spin axis could always be determined.)

Barnes claims an accuracy of $\pm$ 1 deg in determining spin axis orientation with their Horizon Crossing Indicator. In view of the following considerations it is felt that for the Multiple Satellite application a better accuracy, perhaps as small as .1 to .2 deg, can be obtained:

- The spin rate of the pallet is relatively high providing a stronger thermal gradient signal.
- The altitude at which data is obtained can be optimized.
- Ground based computations can be made to correct for errors that would otherwise be incurred due to earth oblateness and to variation of the curvature of the horizon in the view field and also to some extent variations in earth irradiance.

- While on the pallet the multiplicity of sensors will help to reduce various errors including those arising from the finite signal to noise ratios. Also the smoothing of the many data points obtained with very slowly changing conditions will help to reduce errors due to noise.

Technical data for available IR sensors that might be adapted for the Multiple Satellite mission is listed in Table 2. It appears unlikely that an "on-the-shelf" unit could be applied with no modifications whatsoever. In practice sensors of this type have generally been customized for the particular spacecraft, e.g. adjustments are made for altitude and spin rate. However, although modifications in filters, electronic signal processing, etc. might be made, the same basic optical/mechanical hardware can be used. Any modifications involved would not require state-of-the-art advances or involve departures from proven principles and techniques. Static IR sensors are relatively simple, highly reliable and low power consuming. They can be designed for magnetic cleanliness and are comparitively insensitive to changes in ambient temperature. Unit weights are reasonably small and could probably be reduced if there is sufficient incentive for weight reduction modifications. One of the main drawbacks is the relatively high cost of these sensors which are in the order of 3 or more times more expensive than magnetometers.

However, the costs of the IR sensors would still be a small part of the total cost of the Multiple Satellite system.

The choice of the IR horizon crossing indicator is based upon

- The relative simplicity of using this aspect sensor with the pallet's ACS.
- The assurance that the minimum accuracy requirements can be met and probably exceeded.

5.0 SUN SENSORS

It is noted that since either the magnetometer are IR sensors would be sufficient to completely determine the direction of the satellite's spin axis there is no need for a satellite solar sensor to obtain the angle between the spin axis and the sunline. The IR sensor would be capable of also fixing the roll position of the satellite in its spin cycle. However the use of a sun sensor is preferable for this purpose.

No difficulty is anticipated in obtaining sun sensors to meet the requirements of the Multiple Satellite system. These requirements are not significantly different from those of Pioneer VI. Hence, it appears likely that very similar units will be used.

Table 1

ASPECT SENSORS

MAGNETOMETERS

Description	Schonstedt RAM-3	Schonstedt RAM-5B	Schonstedt RAM-5C	Schonstedt MND-5C	Marshall Labs ML 153-1	Marshall Labs ML 178	Marshall Labs ML 237-1
Sensitivity	.004 Volts DC per millioersted	.004 VDC per millioersted	.004 VDC per millioersted	12.5 mV to 100 mV per millioersted	± 1γ or ± 1% of full scale, whichever is larger	--	± 1% of full scale
Range of Field	0 to ± 600 millioersted	0 to ± 600 millioersteds	0 to ± 600 millioersteds	± 25 to ± 200 millioersteds	± 50γ to ± 5,000 gamma	± 60,000 γ	± 60,000 γ
Linearity	within 3% of full scale reading	± 3% of full scale	± 3% of full scale	± 3% of full scale	2% of full scale	5% of full scale	± 1% of full scale
Stability of Sensitivity	--	± 3% from +165°F to 0°F	± 3% from +165°F to 0°F	±0% from +165°F to 0°F	± 5% of full scale	± 5% of full scale	--
Accuracy	--	--	--	--	--	--	± 1% of full scale
Operating Temp.	--	+185°F to -50°F	+185°F to -50°F	+185°F to -50°F	0°F to +120°F	0°F to +100°F	-15°C to 65°C
Input voltage	6.3 VDC	10.2-14 VDC	24-32 VDC	22-32 VDC	± 12V ± 1%	± 12 V ± 10%	± 12 V ± 5%
Input Current	35 ma	18 ma	11 ma	10 ma	50 ma	40 ma	+12V - 40 ma -12V - 3 ma
Weight	8 oz	6 oz	5 oz	9 oz	0.9 lbs	0.65 lbs	0.57 lbs
Dimensions							
Probe	3.187" x .75" dia	3.0" x .625" dia	3.0" x .62 " dia	3.0" x .62" dia	0.8" dia x 2"	0.8" dia x 2"	0.8" dia x 2"
Electronics	3.0" x 1.75" dia	4.0" x 1.0"x1.59"	2.62"x1.59"x1.0"	2.81"x2.78"x.98"	5.0"x5.5"x0.8"	4"x2"x1"	1"x1.9"x4.1"

Table 2

ASPECT SENSORS

IR HORIZON SENSORS

Description	Barnes 200 C,D,CF,DF	Barnes 200X	Barnes 13-205 DC	Barnes 13-205SC	General Electric Nimbus A	Honeywell - APL OGO
Spectral Bandpass	1.8 to 20 microns	14 to 16 microns	2 to 20 microns	2 to 20 microns	12 to 18 microns	7 microns to germanium cutoff
Operating Temp.	-10°C to +60°C	-30°C to +165°C	14°F to 125°F	14°F to 125°F	0°C to 50°C	-30°F to +120°F
Optical Field of View	1.3° x 1.3°	1.0° x 1.0°	1.3° x 1.3° ± 20%	1.3° x 1.3°	6° x 8°	1° wide - viewing from 2.5° to 19.2
Detector	Germanium immersed thermistor	--	Germanium - immersed thermistor bolometer	--	Germanium - immersed bolometer	Germanium - thermistor bolometer
Input Voltage Input Current	26V DC ± 10% 10 ma	20 milliwatts	70 milliwatts	26V DC 35 milliwatts	22 VDC 3.5 watts	22.7 VDC ± 1% 1.5 watts
Weight	12 oz	16 oz	20 oz	12 oz	3.5 lbs	2.8 lbs
Dimensions	1½"x1½"x4-3/4"	4.0"x2.5"x2.5"	5.3"x2.5"x2.5"	4-3/4"x1½"x1½"	26 in.^{3}	9.2 in.^{3}
Orbital Accuracy		± 0.1°				
Orientation Determ.			± 1°	± 1°		
MTBF	More than 100,000 working hours					7,000 hours
System error	± 0.8°					2°

Appendix XII

SPIN AXIS DRIFT

1.0 INTRODUCTION

The nominal initial orientation of the spin axes of the satellites will be in the direction of the normal to the orbit. Since the initial inclination of orbit relative to the ecliptic plane will be small the initial direction of the spin axes will be nearly aligned with the normal to the ecliptic plane. This orientation assures that the view field of the plasma sensors will sweep through the sunline and generally across the ecliptic plane. Also, except for a relatively small section of the orbit near perigee where the satellites are close to the earth, the entire earth will be encompassed within the width of the downlink fan beam transmission.

In order to retain these conditions, which are required for efficient collection of scientific data and efficient operation of the telecommunications system, excessive drift in the direction of the spin axes due to disturbance moments encountered in orbit must be avoided. No significant degradation of communications coverage is likely to be encountered as long as the total drift in the direction of the spin axis is a small fraction of the half-angle of the fan beam. For the current design, this angle is about 12 deg. Accordingly it is felt that at least during the first 3 months, and hopefully during the first 6 months operation in orbit, the drift in the spin axis orientation should be kept below about 2 deg. A drift of this small magnitude would be quite acceptable with respect to the effect on the fields swept by the plasma sensors.

To determine the restrictions on orbital and design parameters that must be imposed in order to keep the spin axis drift within acceptable bounds, computations based upon the analysis and computer program described in References 1 and 2 were run. This program had been designed primarily for relatively low orbits. It was altered in order to accommodate the Multiple Satellite orbit (which is of very high eccentricity and has a very large apogee radius) without using

excessive machine time. This was accomplished by computing the time averages of the disturbance torques from values at points that are evenly separated in true anomaly instead of points evenly separated in time. This provided a closer spacing of points in the vicinity of perigee, where the most significant torques are generally encountered, and thus reduced the total number of points required to obtain accurate average values.

In addition to the sources of disturbance torques that were included in the existing program; specifically, aerodynamic, gravity gradient and magnetic torques, the program was revised to take account of solar pressure torques. Solar pressure torques are comparatively unimportant for low orbits, but can become significant for an orbit as high as that of the Multiple Satellite. The results obtained did in fact show that in the present case the solar pressure torque would be a significant cause of spin axis drift.

In order that results be automatically given in a coordinate system facilitating interpretation of the effects of the torques, the orbit was generally taken to be equatorial, with the argument of perigee equal to 90 deg. However, the obliquity angle was then adjusted to be equal to the inclination of the orbit to the ecliptic i.e., 5.06 deg. In this way the basic frame used for the computation was made to coincide with the orbital plane, while the true relationship of the sunline to the orbit was preserved. This relationship corresponded closely to that which would be obtained under nominal launch conditions.

Inasmuch as the effects of the disturbance torques tend to increase when the orbit is lowered, for conservatism, a comparatively low value, 17.7 R_e, was used for the apogee radius. Where perigee altitude was an important factor, the computations were made for a range of values. The only orbital perturbation effects that were included were the effects of earth oblateness. Hence the orbital dimensions remained fixed.

Generally the spin axis was taken to be initially in the direction of the normal to the orbit and the computations were run for a 6-month interval. Separate computations were made to determine the effects of each of the disturbance torques acting alone. Computations were also made to determine the combined effects of the disturbance torques. The atmospheric and solar perturbation torques were found to make the most significant contributions to the spin axis drift. At the perigee altitudes of interest the effects of these contributions tend to cancel. The total drift remains within the allowable limit of 2 deg.

2.0 AERODYNAMIC TORQUE COMPUTATIONS

In general the aerodynamic torque could be a rather complicated function of the angle between the spin axis and the velocity vector. However, in the present case, in view of the simple form of the satellite and the fact that the spin axis will remain nearly orthogonal to the velocity vector a simple representation is justified. It is assumed that the satellite will be designed to assure that impeller effects will be negligible. Hence, over a spin cycle, the mean value of the component of aerodynamic torque in any direction that lies in the plane including the spin axis, and the velocity vector can be taken to be zero. The precession of the spin axis will stem from the torque component that in the direction mutually perpendicular to the spin axis and the velocity vector. To the extent that the center of pressure may be displaced axially from the center of mass, this torque component will have a non-vanishing mean value.

The parameters that influence the drift in the orientation of the spin axis due to aerodynamic torques are:

a. Atmospheric density

b. The product, $C_D A x_a$, where C_D is the drag coefficient, A is the laterally projected area and x_a is the effective moment arm of the aerodynamic force, i.e., axial distance between the center of mass and the center of pressure; and

c. The angular momentum of the satellite,, $I_x p$; I_x being the roll moment of inertia and p, the spin rate.

Although some variations in these parameters would occur during the orbital lifetime, for present purposes all of the foregoing parameters were taken to be constant.

The atmospheric density that is encountered at points in the orbit far removed from perigee is insignificant in comparison to the density encountered at perigee. Hence, an atmospheric representation that is accurate at perigee altitude and at points not too far removed perigee is adequate for obtaining a close approximation of the effects of atmospheric torques. The computer program uses a simple exponential representation which permits the density at a reference altitude and the atmospheric scale height at the reference altitude to be inputted so as to match the orbital perigee altitude used in the computation.

Table 1 lists the values that were used for these parameters for the range of perigee altitudes for which computations were made. These values were based upon the ARDC 1959 Model Atmosphere as given in "Orbital Flight Handbook," Vol. 1 NASA, GSFC, Martin-Marietta SSD, 1963. This atmosphere corresponds to a period of high solar activity similar to that applicable to the period expected for the Multiple Satellite launch. During the early part of the operational lifetime perigee will occur in or near the earth's shadow. Hence, a benefit will actually be gained from the lower densities of the night time atmosphere. No attempt was made to take account of this advantage.

For conditions wherein the drift of the spin axis remains reasonably small, which was found to be true for all of the computations, the drift of the spin axis is very nearly proportional to $(C_D A x_a)/I_x p$. The values used for the parameters were:

$$C_D A x_a = .16 \text{ ft}^3$$

and

$$I_x p = 3.14 \text{ slug ft}^2 \text{ rad/sec}$$

These values were based upon rough estimates made at the outset of the study. Using these values,

$$\frac{C_D A x_a}{I_x p} = \frac{.16}{3.14} = .051 \text{ ft/(slug rad/sec)}$$

Re-evaluation of the parameters for the current design indicates that while both of the initial estimates were too small, the value of the ratio is not far off. The value of $C_D A x_a$ increased primarily as a result of the location of the station of center of mass which is below the center of the lateral projected area. In order to obtain the required favorable moment of inertia ratio for the

Table 1

ATMOSPHERIC REPRESENTATION

Perigee Altitude, km	Density at Perigee Altitude slug/ft^3	Scale Height, n. miles
200	$.70 \times 10^{-12}$	26.3
300	$.92 \times 10^{-13}$	32.3
400	$.17 \times 10^{-13}$	38.3
600	$.44 \times 10^{-14}$	50.0

pallet in the simplest manner, the satellites were designed to keep the center of mass as low as possible. This placed the center of mass about 3.5 inches below the center of pressure. The projected area is about 2.6 ft^2. Hence taking $C_D \doteq 2$, for the current design:

$$C_D A x_a \doteq 1.5 \text{ ft}^2$$

The value of I_x increased because the satellite mass was greater than had been anticipated and the satellite had a larger radius of gyration. The roll moment of inertia is now estimated to be about 3.4 slug ft^2. With a spin rate of 60 rpm, $p = 2\pi$ and

$$I_x p \doteq 21.4 \text{ slug ft}^2 \text{ rad/sec}$$

Hence for the current design the ratio of the parameters is approximately:

$$\frac{C_D A x_a}{I_x p} = \frac{1.5}{21.4} = .070 \text{ ft/(slug rad/sec)}$$

This ratio is 1.37 times greater than used in the computations. Hence the drift rates were increased by this factor.

It is noted that if it should prove to be necessary, the value of x_a could be drastically reduced either by going to a design with a more central location of the center of mass and achieving the favorable moment of inertia ratio for the pallet in some other way, or by adding a light weight flexible skirt to the satellite so as to shift the station of the center of pressure as closely as possible to the station of the center of mass. This would result in a large reduction in the drift due to aerodynamic torques.

The results obtained from the computations showed that the aerodynamic torque caused a precession of the spin axes about the direction of the velocity vector at perigee at a virtually constant rate. The effect of perigee altitude on the total drift, i.e., the angle between the initial direction and the direction

of the spin axis after 6 months in orbit, is shown in Figure 1. Because of the need to restrict the difference in orbital decay between satellites it is presently estimated that the lowest perigee altitude will be above 370 km. For the current design the spin axis due to atmospheric torques will then be less than 1.8 deg.

Figure 2 shows the history of the angle between the spin axis and the sunline. For the higher perigee altitude where the drift of the spin axis due to the aerodynamic torque is small, the variation in the angle between the spin axis and the sunline arises mainly from the rotation of the sunline in the ecliptic plane.

CLEARPRINT PAPER CO. NO. C3PX MILLIMETERS 200 BY 250 DIVISIONS. PRINTED IN U.S.A. ON CLEARPRINT TECHNICAL PAPER NO. 1018

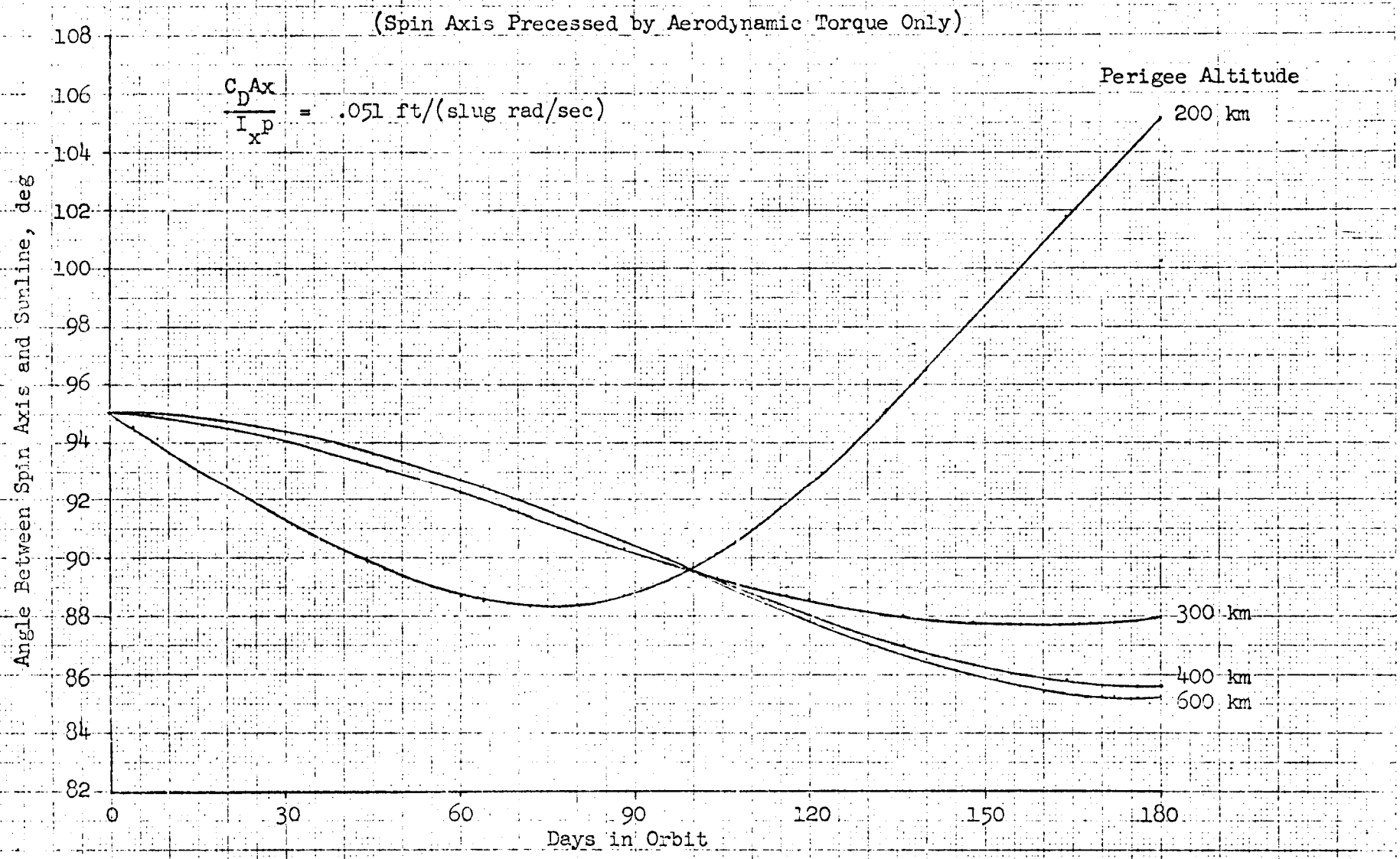

FIGURE 2. HISTORY OF ORIENTATION OF THE SPIN AXIS RELATIVE TO THE SUNLINE

3.0 SOLAR TORQUE COMPUTATIONS

As in the case of the aerodynamic torque, the simple form of the satellite argues against the presence of any significant impeller effect. The component of torque that may cause precession of the spin axis is in the direction mutually perpendicular to the spin axis and the sunline. Using the expressions for the solar pressure forces given in Reference 3, and taking the satellite to be represented by a simple right circular cylinder (see Figure 3), having properties with respect to the absorption and reflection of solar radiation that are uniform on the sides and uniform on the ends, this component of the solar torque can be written:

$$M_S = PAx_S \left[\left(1 + \frac{\rho s}{3}\right) \sin^2 \psi + (1-s) \frac{\rho\pi}{6} \sin \psi\right]$$

$$+ PAx_S \frac{r}{L} \left(1 - \rho_e s_e\right) \frac{\pi}{4} \sin \psi \cos \psi$$

$$+ PA \frac{\pi}{4} \left[r (1 - \rho s) - L \left(1 - \rho_e s_e\right)\right] \sin \psi \cos \psi$$

where

P	=	the solar radiation pressure in the vicinity of earth, approximately .47 dyne/meter^2
A	=	the laterally projected area, i.e., $A = 2rL$
r	=	the radius of the cylinder
L	=	the length of the cylinder
x_s	=	the axial distance between the center of volume and the center of mass
ψ	=	the angle between the spin axis and the sunline
ρ	=	the ratio of reflected to total incident radiation for the sides
s	=	the ratio of specularly reflected to total reflected radiation on the sides
ρ_e, s_e	=	the analogous ratios applicable to the ends

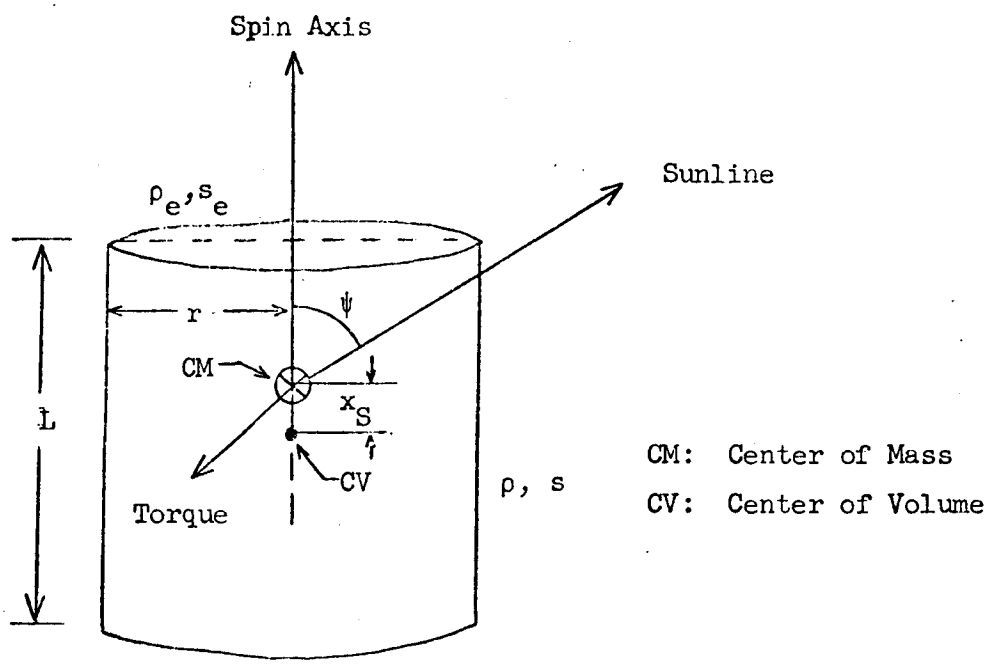

FIGURE 3. GEOMETRY OF FACTORS AFFECTING SOLAR RADIATION TORQUE

Since ψ remains close to 90 deg the solar pressure torque is given to a close approximation by:

$$M_S = PAx_S \left[1 + \frac{\pi}{6}\rho - \left(\frac{\pi}{6} - \frac{1}{3}\right) s\rho\right]$$

The values of ρ and s lie between 0 and 1. Minimum torque is obtained when $\rho = 0$, in which case $M_S = PAx_S$. Maximum torque is obtained when all radiation is diffusely reflected; then $\rho = 1$, $s = 0$, and $M_S = \left(1 + \frac{\pi}{6}\right) PAx_S$. For the current design the value of ρ would be about .2 while the value of s would be close to 1. In this case, $M_S = 1.07\ PAx_S$.

Although the computer program permitted the more complicated expression for M_S to be used, the results obtained indicated that the use of the simplified expressions for M_S would cause little difference in the results. In fact, since the solar torque does not vary with position in orbit (the effect of the vahishing of the solar torque during occultation periods was not included), it is possible to integrate the effects of solar torques without recourse to the use of the computer program. The drift rate is equal to $M_S/I_x p$. Letting $M_S = P2rLx_s$ and using values corresponding to those inputted for the computer, viz

$P = .47$ dyne/meter^2

$r = .5$ ft

$L = 1$ ft

$x_S = .1$ ft

$I_x = .5$ slug ft^2

$p - 2\pi$ rad/sec

yields a drift rate of .0154 deg/day. Taking account of the fact that the axis of precession will rotate through 180 deg with the sunline rotation in 180 days the total drift is given by $\frac{2}{\pi} \times 180 \times .0154$ deg = 1.76 deg. Within a few percent, this agrees with the more exact result of 1.81 deg obtained by the computer.

Using the values applicable to the current design: $M_S = 1.07\ P2rLx_S$

$P = .47$ dyne/meter^2

$r = 11$ inches

$L = 17$ inches

$x_S = 3.5$ inches

$I_x = 3.36$ slug ft^2

$p = 2\pi$ radians

and scaling the results obtained from the computer to take account of the differences between these values and those inputted to the computers, yields a value of 2.18 deg for the total drift of the spin axis during the first 6 months in orbit as a result of the solar torques.

The center of solar pressure can be expected to lie very close to the center of the aerodynamic forces. If necessary the design could be adjusted so that the separation between these centers is very small. Hence, the solar torque could be drastically reduced by the same devices mentioned in the discussion of the aerodynamic torque.

4.0 GRAVITY GRADIENT AND MAGNETIC TORQUES

In the nominal case, i.e., when the spin axis is normal to the orbital plane, the gravity gradient torque will vanish. In order to obtain some assessment of the potential effects of the gravity gradient torque when the spin axis departs from its nominal orientation, computations were made for cases where the spin axis was initially tilted away from the normal to the orbit. The cases considered were those where the initial orientation spin axis was: (a) tilted 10 deg in the direction of the line of apsides, and (b) tilted 10 deg in the direction perpendicular to the line of apsides. The results obtained indicated that the gravity gradient torque causes the spin axis to precess in a cone about the normal to the orbit, maintaining a nearly constant angle to the normal to the orbit, and that the rate of precession is nearly insensitive to the direction of the initial tilt.

The precession rate due to the gravity gradient torque depends on the satellite's moment of inertias and its spin rate. The following values, which are applicable to the current design, were used:

$$I_x = 3.38 \text{ slug ft}^2$$

$$I_y = 2.49 \text{ slug ft}^2$$

$$I_z = 1.02 \text{ slug ft}^2$$

$$p = 2\pi \text{ rad/sec}$$

The computations were made for perigee altitudes of 200 km and 600 km. The results, which are summarized in Table 2, show that the gravity gradient torque will produce a total drift not exceeding 1/3 deg. Since normally the angle between the spin axis and the normal will be very much smaller than 10 deg and, for small angles, the precession rate is proportional to this angle, it is apparent that the drift due to gravity gradient torque will be negligible.

Inasmuch as the earth's magnetic field is not spherically symmetric, the magnetic torque is affected by the rotation of the earth. Hence the formal integration of the effects of magnetic torque must take account of the earth's position

Table 2

EFFECT OF GRAVITY GRADIENT TORQUES ON SPIN AXIS ORIENTATION

Perigee Altitude	Total Drift in Orientation of Spin Axis in 6-months	
	Spin axis initially tilted 10 deg from normal to orbit in direction of line of apsides	Spin axis initially tilted 10 deg from normal to orbit in direction perpendicular to the line of apsides
200 km	.31 deg	.33 deg
600 km	.29 deg	.30 deg

as well as the position of the satellite in orbit, and is therefore far more burdensome than the integration of the effects of the other torques. This is particularly true for the Multiple Satellite orbit where the orbital period is not short relative to the period of the earth's rotation, i.e., one day.

It can be anticipated that the effects of the magnetic torques will be quite small; not only because of the height of the orbit, but also because the satellite must be very clean magnetically. Hence its magnetic dipole moment of necessity must be very small so that the magnetic torque must be small even at points in the orbit where the ambient magnetic field may be strong.

To avoid the trouble of directly integrating the effects of the magnetic torques, computations were made to determine an upper bound for these effects in the following manner: Fictitious orbital elements were not inputted; i.e., the proper value of inclination with respect to the equator, 28.5 deg, and argument of perigee, 120 deg, were used. The direction of the normal to the orbit relative to the earth reference frame was therefore properly established. With the earth position fixed, mean values of the magnitude of the magnetic torque over an orbit were computed. The relative position of the earth was varied (this was actually accomplished by keeping the earth position fixed and rotating the orbit relative to the earth by varying the longitude of the ascending node), and the position at which the maximum mean value of the magnetic torque is obtained was determined. The drift in the spin axis that would be obtained in the event that the maximum mean torque were steadily applied in an inertially fixed direction was then calculated. For this purpose the current estimates; $I_x = 3.38$ slug ft^2; $p = 2\pi$ rad/sec were used.

The magnetic torque is proportional to the component of the satellite's magnetic dipole moment that is parallel to the spin axis. The other components of the dipole moment produce torques that have zero mean value over a spin cycle and/or do not cause a secular drift of the spin axis orientation. For the computations, the component of the satellite's dipole moment parallel to the spin axis was taken to be large enough; viz 100 in cgs units, to contribute a field

of about $3/4\gamma$ at a lateral distance of 8 feet. This field is about three times greater than the magnetic cleanliness requirements would allow for the combined effects of all of the components of the spacecraft dipole moment.

Table 3 summarizes the results obtained for the effects of the magnetic torques. It is seen that for the worst-worst case conditions that have been assumed the maximum drift in spin axis orientation is about .4 deg. It can be expected that actual drift will be a small fraction of this maximum value.

Table 3

EFFECTS OF MAGNETIC TORQUE ON SPIN AXIS ORIENTATION

Satellite Dipole Moment Parallel to Spin Axis	100 (cps)
Roll Moment of Inertia	3.38 slug ft^2
Spin Rate	2π rad/sec

Perigee Altitude km	Maximum Mean Magnetic Torque ft-lbs s	Maximum Precession Rate deg/day	Maximum Drift of Spin Axis in 6 months deg
200	9.4×10^{-9}	.0022	.39
400	9.0×10^{-9}	.0021	.38
600	8.6×10^{-19}	.0020	.37

5.0 COMBINED EFFECTS

The foregoing results indicate that the spin axis drift will stem primarily from aerodynamic and solar torques. Since both of these torques arise mainly from the low station of the center of mass, and during the first 6 months in orbit the mean direction of the solar force will be nearly opposite to the mean direction of the aerodynamic drag, there is a tendency for these torques to cancel each other to some extent. This was demonstrated by the results of computations which took account of the combined effects of all of the disturbance torques. For these computations, values of the parameters applicable to the current design were used. The initial direction of the sunline was taken to correspond to a lead time of 35 days before the sunline passes over apogee.

The results of the computations, shown in Figure 4 and 5, indicate that, as would be expected, at low perigee altitudes the aerodynamic torque will dominate. Thus at a perigee altitude of 200 km the drift of the spin axis caused by the combined torques is practically the same as that due to the aerodynamic torque alone. The most effective cancellation of the two major torques is obtained at perigee altitudes of 350 to 450 km. At higher perigee altitudes the solar torque dominates. (Because of the rotation of the sunline, the solar torque has a cyclical effect on the spin axis drift with a period of about 1 year.) In the region of interest, i.e., perigee altitudes ranging from about 350 to 650 km, the total drift of the spin axis during the 6 month operational lifetime remains below 2 degrees.

CLEARPRINT PAPER CO NO. C39X. MILLIMETERS. 200 BY 250 DIVISIONS. PRINTED IN U.S.A. ON CLEARPRINT TECHNICAL PAPER NO. 1015

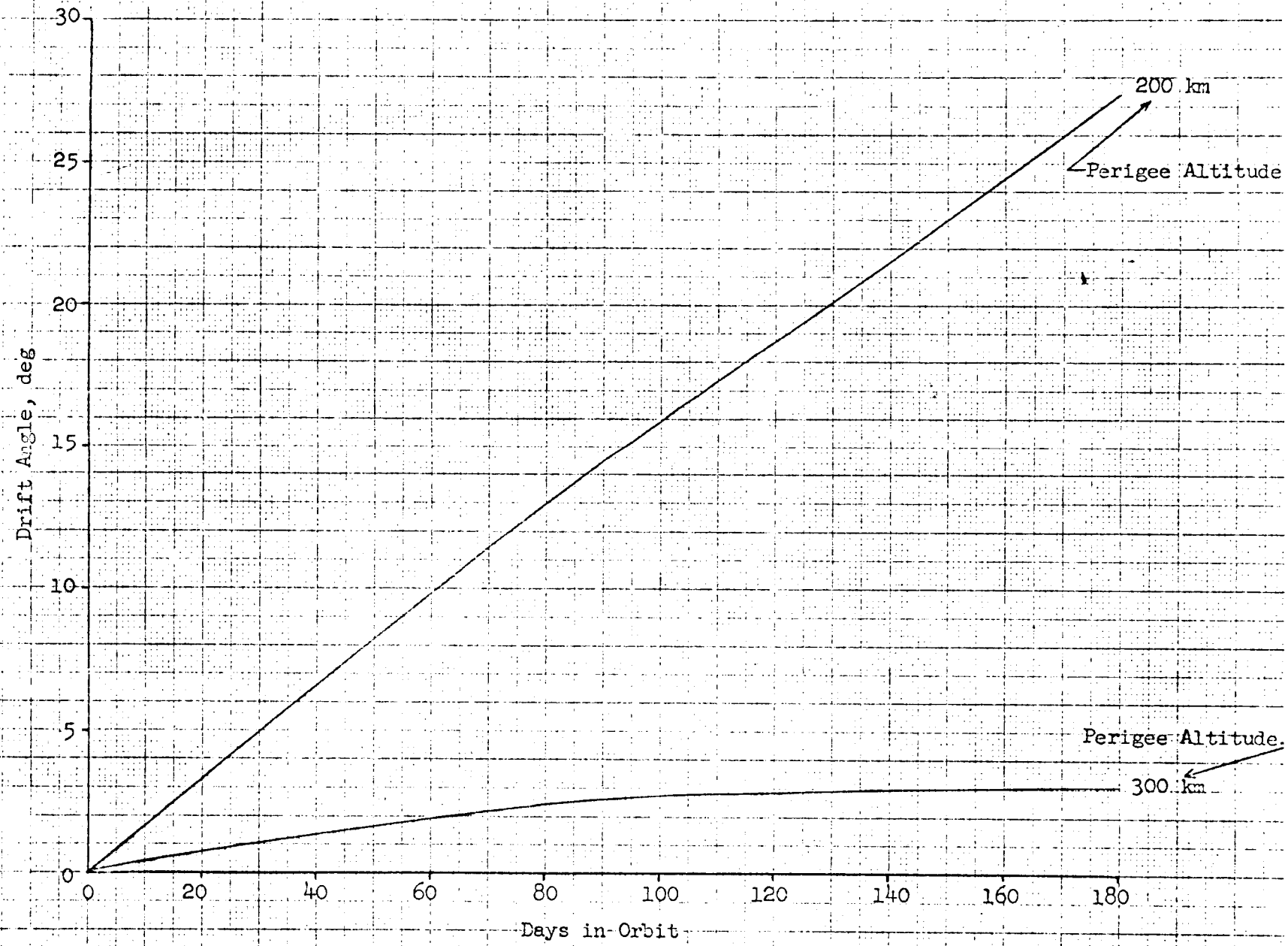

FIGURE 4. COMBINED EFFECT OF TORQUES ON SPIN AXIS DRIFT PERIGEE ALTITUDE = 200 km AND 300 km

CLEARPRINT PAPER CO. NO. C39X MILLIMETERS, 100 BY 250 DIVISIONS. PRINTED IN U.S.A. ON CLEARPRINT TECHNICAL PAPER NO. 1015

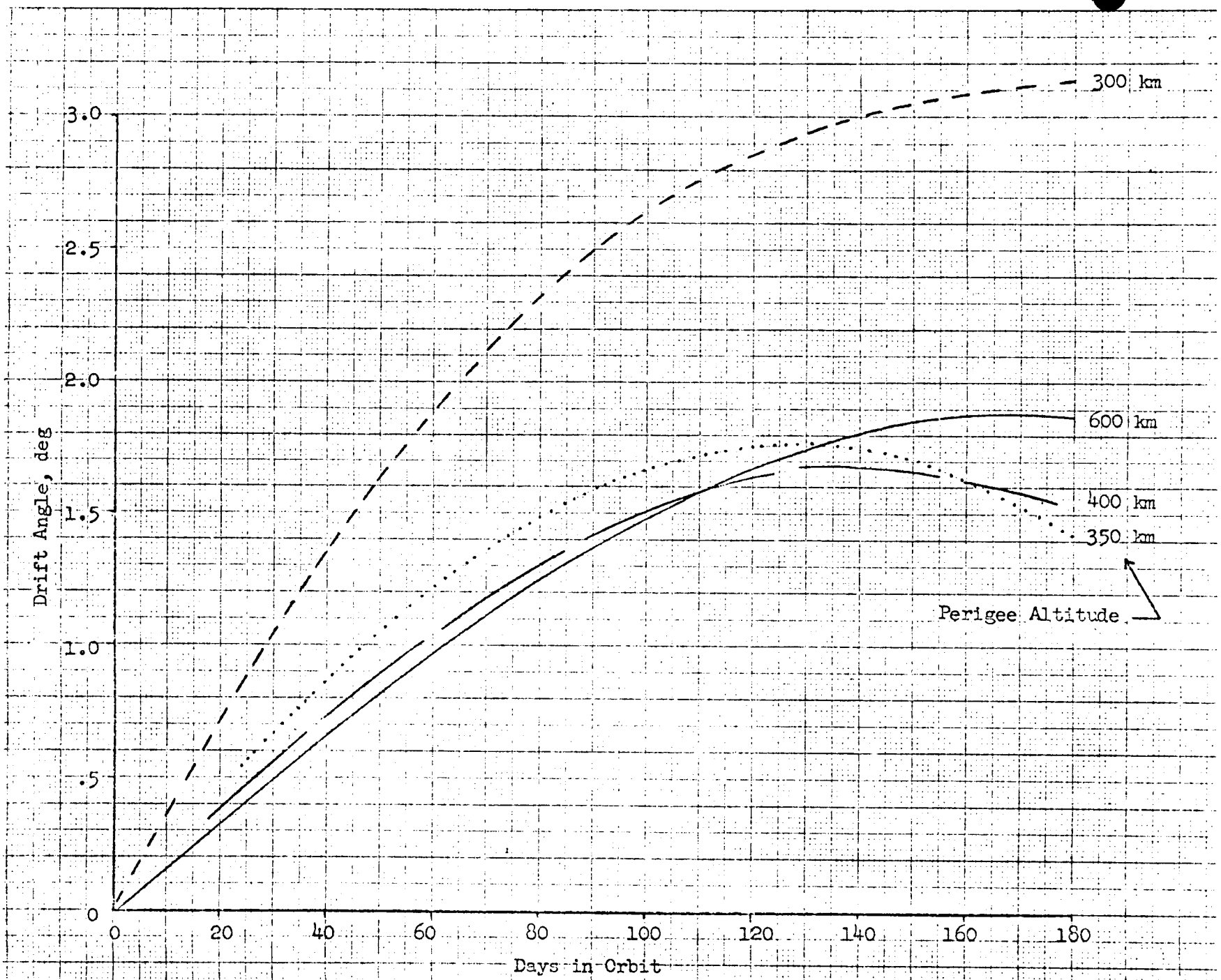

FIGURE 5. COMBINED EFFECT OF TORQUES ON SPIN AXIS DRIFT PERIGEE ALTITUDES - 300 TO 600 km

REFERENCES

1. SGC Report No. 5412-65-25, 16 June 1965, "Prediction of Spin Axis Drift", L. Pode.

2. SGC Report No. 5412-65-33, 23 November 1965, "Computer Program for Prediction of Spin Axis Drift", L. Pode, M. Schaffer, J. E. Freeman.

3. JPL Tech Report No. 32-467, May 15, 1966, "Theoretical and Practical Aspects of Solar Pressure Attitude Control for Interplanetary Spacecraft", Acord and Nicklas.

Appendix XIII

STADAN INTERFACE

1.0 INTRODUCTION

This Appendix defines the projected characteristics of the STADAN network which will support the Multiple Satellite System during its 1970-1975 operational time period.

The following references are pertinent to this interface:

Report X-530-66-33 "Space Tracking and Data Acquisition Network Facilities Report (STADAN)"

Specification S-531-P-17 (May 1966) "Goddard Range and Range Rate System Specifications"

X-560-63-2 (2 May 1966) "Aerospace Data Systems Standards"

The information presented on the following pages was obtained through contact with Dr. Robert Coates at Goddard Space Flight Center.

2.0 EQUIPMENT AVAILABILITY

The following equipment may be assumed as available within the STADAN network for the 1970-1975 multiple satellite mission:

Station Location	Antenna Size	Receivers
Ulaska	85', 40' (new) and 30' dishes	At least four receivers meeting the new Range/Range Rate system specification at either 136 megacycles or S-band.
Rosman	2 - 85' dishes 1 - 30' dish 1 - 40' dish	
Orroral	1 - 85' dish 1 - 30' dish 1 - 40' dish	
Santiago	1 - 30' dish 1 - 40' dish	
Tananarive	1 - 30' dish 1 - 40' dish	
Quito	1 - 40' dish	No $R/\dot{R}$ capability

There will be no additional 85' or 40' dishes added to the STADAN network prior to the multiple satellite operational period.

Each station with 85' or 40' antennas will have at least two PCM data processing systems. Maximum data processing rate at the station will be 200K BPS.

Johannesburg and Tananarive should be considered as one station only.

All receivers can be coupled to either the 30', the 40' or the 85' dishes.

Ground data links with a capacity of at least 2400 BPS from all remote stations to GSFC will be available.

Only one $R/\dot{R}$ system will be available at each station; $R/\dot{R}$ determination cannot be performed for more than one satellite simultaneously.

All 40' dishes now have feed structures for S-band but may not currently have the parametric amplifier or first converter. For the multiple satellite operational period, S-band capability for all 40' dishes may be assumed.

The Gilmore station is actually a Weather Bureau station and not really part of the STADAN network. East Grand Forks and Blossom Point will be phased out.

There will be 136 megacycle SATAN antennas at all active stations by 1970.

The STADAN command systems are based on the following techniques:

Tone Standard

Tone Digital Standard

PCM Standard

All command links are currently 148 megacycles - no S-band command links are now in use; however, they will be utilized in the 1970-1975 time period.

A more capable command system is currently under development per a memo provided by Dr. Coates.

3.0 PERFORMANCE AND OPERATIONAL FACTORS

The following performance characteristics and operational requirements were indicated:

The $R/\dot{R}$ system may be utilized either as a single station measurement or through the use of multiple stations simultaneously for maximum accuracy (the latter approach has never been operationally practiced).

The $R/\dot{R}$ system accuracy at S-band was given as:

$\pm$ 7 meters RMS resolution

$\pm$ 20 meters RMS system accuracy

The range measurements are taken over a period of 5 to 10 minutes tracking in different parts of the orbit.

Main limitations on the use of 136 megacycles for the multiple satellite include the 90 KC RF bandwidth restriction per satellite, and the reduced $R/\dot{R}$ accuracy relative to the S-band system.

The receiving system performance was specified as 220°K system noise, for the uncooled parametric amplifiers at S-band.

No pre-detection recording is utilized or planned for the STADAN network. Demodulated data may be recorded for later analysis.

Doppler can be read out in all receivers, but normally isn't due to spacecraft transmitter stability.

Bandwidth occupancy for an S-band system was given at 1750 - 1850 mc uplink, and 2200 to 2270 mc downlink. A specific downlink and R/Ṙ spectrum utilization example was indicated as follows:

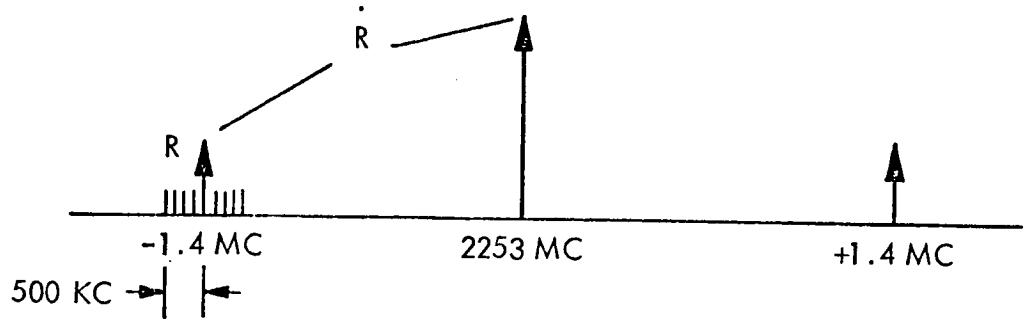

Rosman facilities are capable of indicating the incoming signal polarization for determining satellite orientation. This signal will exist internal to all R/Ṙ system receivers per the new specifications; however, it will be necessary to make minor additions to provide an external indication from the polarization diversity equipment.

The use of a 136 megacycle beacon on all satellites for initial acquisition was highly recommended.

4.0 STATION DUTY CYCLE

Current GSFC projections suggest four competing S-band satellites in orbit in 1970, and 10 to 12 competing satellites in orbit in 1975. On this basis, it was suggested that the multiple satellite system should expect to be limited to a maximum of three to six hours per day coverage from any one STADAN station.

Appendix XIV

COMMUNICATIONS LINK AND TRACKING PERFORMANCE ANALYSIS

1.0 COMMUNICATIONS LINK ANALYSIS

The link analyses were performed by programming the computer to iterate parameters in the design control table. Extensive printout is available for variations in antenna gain and data transmission rates. Certain of these calculations also were plotted by machine and displayed graphically for easy reference and comparison. The procedure used to perform the analysis is based on the suggested AMES design control format, with modifications appropriate to this particular program. A typical result is shown below:

DOWNLINK DESIGN CONTROL TABLE

	Parameter	Value	Tolerance
1.	Transmitter Power	+ 30 dBm	+1.0, -0.5
2.	Transmit Circuit Loss	- 1.0 dBm	±0.1
3.	Transmit Antenna Gain	+ 6.4 dB	+0, -0.4
4.	Transmit Antenna Pointing Loss	0 dB	--
5.	Space Loss at 2250 MHz, R = 80,000 mi.	- 202.1 dB	--
6.	Polarization Loss	- 3 dB	--
7.	Receiving Antenna Gain	+ 44.0 dB	+1.0, -0.5
8.	Receiving Antenna Pointing Loss	0 dB	--
9.	Receiving Circuit Loss	- 0.5 dB	±0.1
10.	Net Circuit Loss	-156.2 dB	
11.	Total Received Power	-126.2 dB	+2.2, -1.6
12.	Receiver Noise Spectral Density, N/B ($T_{system} \cong 200^{\circ}K$)	- 175.7 dBm	±0.8
13.	Carrier Modulation Loss ($\theta = 76^{\circ}$)	- 12.4 dB	±0.5
14.	Received Carrier Power	-138.6 dBm	+3.5, -2.9
15.	Carrier APC Noise BW ($2 B_{LO} = 12$ Hz)	+10.8 dB	+0, -0.5

	Parameter	Value	Tolerance
	Carrier Performance		
16.	Threshold SNR in 2 B_{LO}	+6.0 dB	--
17.	Threshold Carrier Power	-158.9 dBm	+0, -1.0
18.	Carrier Performance Margin	+20.3 dB	+3.5, -4.4
	Data Performance		
19.	ST/N/B Required for 1280 BPS	+7.0 dB	+0, -1.0
20.	ST/N/B Achieved for 1280 BPS	18.4 dB	
21.	Data Performance Margin	11.4 dB	+3.5, -5.4

The analysis indicates that real-time data coverage at the nominal 1280 BPS is achievable with adequate performance margin over all portions of the orbit. However, because of the beamwidth of the antenna, coverage at slant ranges of less than 16,000 miles (4 R_e) is limited.

2.0 NON-REAL TIME DATA PERFORMANCE

The non-real time data will be transmitted at a rate 24 times the input rate, or 30,720 BPS for a nominal real-time rate of 1280 BPS. Under the same conditions as expressed in the above design control table, together with the requirement that a minimum data performance margin of 6.0 dB must be maintained, the maximum communications distance is limited to 30,000 miles (7.5 R_e) for transmission of non-real time data. Trajectory considerations indicate that ample time is available to playback the tape recorder when the satellite range is between 4.0 and 7.5 R_e; indeed, sufficient time exists to playback the recorder of all four satellites, even at maximum intersatellite separations, between these two range figures. The times available for playback are related to the visibility of the satellites from the major STADAN stations; a computer analysis has been ; performed which indicates that aminimum of 4 hours is available under worst-case conditions to playback the tape recorders in the four satellites. Typical view times range from 6 to 8 hours. Thus, it will be possible to playback the data from all four satellites in every orbit and meet the STADAN requirement to use a given ground station less than 6 hours in any 24 hour period.

3.0 TRACKING DOPPLER EFFECTS

Since the satellites will be spinning, both while on the pallet as well as after deployment, doppler effects may arise which could limit the capability of tracking accurately. This situation is considerably worse on the pallet, since the spin rate could be as high as 3 RPS, and the distance from the antenna to the spin axis could be as much as 3 feet. To obtain an estimate of the doppler error and the ability of the GSFC ranging equipment to track out the doppler, the following analysis was performed.

Consider the following diagram,

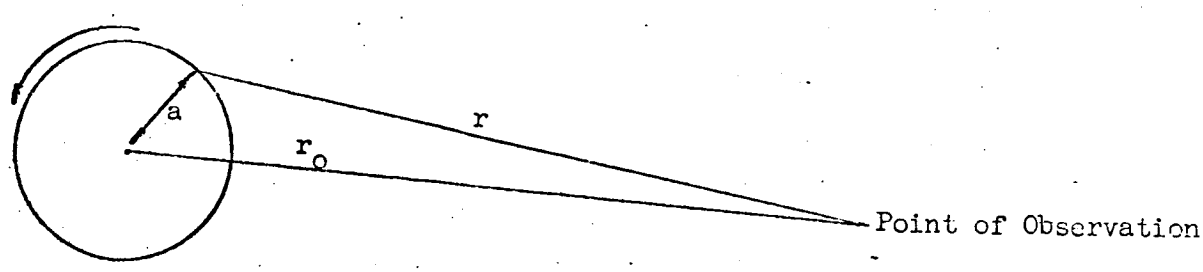

Figure 1. Simplified Spinning System

It is assumed that the time required to make a single ranging measurement is small compared both to the spin rate as well as the rate of change of r_o. The rate of angular rotation is assumed to be Ω. Thus we have

$$\dot{r} \approx \dot{r}_o + a\, r \cos \Omega\, t \tag{1}$$

$$\dot{r} \approx \ddot{r}_o + a\, r^2 \sin \Omega\, t \tag{2}$$

and

$$f_d = f_o \left[\frac{\dot{r}_o + a\, r \cos \Omega\, t}{c} \right] \tag{3}$$

where

c = velocity of propagation (cm/sec)

$\dot{r}_o$ = true range-rate (cm/sec)

a = radius of rotation (cm)

Ω = angular velocity (radians/sec)

d = wavelength (cm)

f_d, f_o = doppler frequency, transmit frequency, in Hz

Combining terms and simplifying, we have

$$\left| f_d - \frac{f_o \dot{r}_o}{c} \right|_{max} = \frac{a \Omega f_o}{c} = \frac{a \Omega}{\lambda} \tag{4}$$

for the maximum difference doppler shift, that is, the change in doppler caused by vehicle spin. For the RMS error, we have

$$\sqrt{\overline{\left(f_d - \frac{f_o \dot{r}_o}{c} \right)^2}} = \frac{a \Omega f_o}{c2} = \frac{a \Omega}{\lambda 2} \tag{5}$$

Given, from the first paragraph above, that

$$\begin{aligned} \Omega &= 2\pi (3) \\ c &= 3 \times 10^{10} \text{ cm/sec} \\ a &\cong 10^2 \text{ cm} \\ f_o &= 1 \text{ mHz, we have, then} \end{aligned} \tag{6}$$

$$\left| f_d - \frac{f_o \dot{r}_o}{c} \right|_{max} = \frac{(2\pi)(3)(10^2)}{(3)(10^{10})} \times 10^6 = \frac{2\pi}{100} \text{ Hz} \tag{7}$$

Now, for several values of f_o, the following maxima of doppler result, by substitution into the left-hand side of Equations (7) above:

f_o	Doppler Shift, max.
10^6 Hz	.0628 Hz
100 mHz	6.28 Hz
1000 mHz	62.8 Hz
2000 mHz	125.6 Hz

This rate of change is well within the tracking rate of the smallest loop bandwidth of the receiver, as described in GSFC S-531-P-17, Section 4.5.4.2.3.

Another doppler change to be considered is the change in the translation doppler caused by vehicle rotation, or phase acceleration. An expression for this is given by the following:

$$\left| \frac{\dot{r} - \dot{r}_o}{c} \times f_o \right|_{max} = \frac{a\,\Omega^2}{c} \times f_o \tag{8}$$

For this case we have

$$\bar{a}\,\frac{\Omega^2}{c} \times f_o = \frac{2\pi}{100} \times 6\pi \cong \frac{120}{100} \text{ Hz/sec} \tag{9}$$

Tabulations, for several values of f_o, are shown below:

f_o	Phase Acceleration
1 mHz	1.2 Hz/sec^2
100 mHz	120 Hz/sec^2
1000 mHz	1200 Hz/sec^2
2000 mHz	2400 Hz/sec^2

The maximum rate above is again within the capability of the receiver, but at a larger loop bandwidth, which results in a drop of 10 dB in acquisition and tracking threshold. However, for the ranges involved, no problem can be anticipated as a consequence of this reduced sensitivity.

It is not self-evident as to whether the tracking specifications mentioned above, from the GSFC document, imply tracking of carrier frequency or modulation frequency. It is, however, most probable that reference is made to the modulating frequency. If so, then the narrowest band loop can be used always, since, with a tracking tone rate of 100 kc, both doppler shifts are negligible. Additional material is anticipated from GSFC which will clarify this matter.

Appendix XV

SATELLITE TRACKING

1.0 TRACKING REQUIREMENTS

Tracking data from which orbital parameters and satellite positions can be derived is required for two purposes:

a. In executing the deployment of the satellites, orbital data is needed to permit correct timing of the velocity increment commands, taking account of off-nominal orbital conditions.

b. After deployment, precise knowledge of the positions of the four satellites is required for the interpretation of scientific data.

The latter requirement is likely to be the more demanding. Errors in the knowledge of the position of the satellites leads to errors in determination of the intersatellite separation distances. Errors in the separation distance will propagate, proportionately to errors in the determination of velocities of propagation and spatial derivatives.

The magnitude of intersatellite separation distances will vary with direction and will also vary as the orbit is traversed. If useful results are to be derived from data obtained at points where the separation distance in the critical direction may be as small as 200 km, knowledge of separation distance to within 4 km will be needed, if the errors arising from the uncertainty in separation distance are to be kept below 2%. Since the separation distances will be determined by subtracting position coordinates, assuming statistical independence of errors, the position coordinates must be known more accurately, i.e., to within about 2.8 km. This order of accuracy is far better than required to support the deployment maneuver alone.

It should be noted, however, that the accuracy requirements on position determination could be relaxed to the extent that (a) consideration is restricted to points where larger separation distances are obtained, and (b) error contributions larger than 2% can be tolerated. For example, with 1,000 km separation distances and a 4% allowable error, errors in the separation distances as large as 40 km could be tolerated.

The requirements on accuracy of orbital determination in support of deployment stem mainly from the need to establish the precise direction of the normal to the orbit and the direction of the tangent to the orbit at the time of application of the in-plane velocity increment. A 15 km error in position corresponds roughly to a 0.1 deg uncertainty in the direction of the tangent. As indicated in the study of deployment errors presented in Appendix III, this order of accuracy would be quite satisfactory.

The accuracy of position determination depends upon:

a. The frequency of collection of tracking data points.

b. The degree of sophistication used in correlating the tracking data points.

c. The accuracy of the measurements obtained at the tracking data points.

d. The accuracy of establishing the time associated with the scientific data points.

2.0 TRACKING SYSTEM DESCRIPTION

The tracking system to be used in this mission is the Goddard Space Flight Center range and range-rate system (GRARR), operating at S-Band. This system, which is capable of a high degree of accuracy, operates with a transponder located in each of the satellites in conjunction with a set of ground equipment comprised (at S-Band) of a 30-foot antenna, multiple receivers, and a tone-code and doppler range and range-rate subsystem. At S-Band, the major system parameters include the following:

GROUND SYSTEM

Parameter	Value
1. Transmit Frequency	1800 MHz nominal
2. Transmit Power	1 kw or 10 kw
3. Receive Frequency	2253 MHz nominal
4. Receive Antenna Gain	42 dB nominal
5. Receive Antenna Type	30' paraboloid
6. Down Converters	Uncooled paramp, 100 MHz BW

GROUND SYSTEM (Continued)

Parameter	Value
7. No. of Receivers	4
8. Receive Frequencies	136 MHz nom, 2250 MHz nom.
9. Receiver Modes	A. Auto Track B. Auto Track and Ranging C. Auto Track and Telemetry (closed loop) D. Auto Track and Telemetry (open loop) E. Auto Track, Ranging and Telemetry F. Ranging G. Telemetry (coherent) H. Telemetry (non-coherent)

10. Tracking Rates

Loop BW	Rate
10 Hz	200 Hz/sec^2
30 Hz	2,000 Hz/sec^2
100 Hz	20,000 Hz/sec^2
300 Hz	200,000 Hz/sec^2
1,000 Hz	2,000,000 Hz/sec^2
3,000 Hz	20,000,000 Hz/sec^2

11. Receiver noise power density	-174 dBm/Hz

SPACECRAFT SYSTEM

Parameter	Value
1. Weight	~ 8 lbs
2. Power Input	~ 7 watts
3. Receive frequency	1800 MHz nom.
4. Transmit Frequency	2253 MHz nom.
5. Transmit Power	~ $\frac{1}{2}$ watt

The basic system accuracies are as tabulated below:

Parameter	Value
Frequency	nom. S-Band
Ranging Tone	100 KHz
Range Measurement	< 15 meters RMS
Range-Rate Measurement	0.1 meter/sec
Direction	0.1 degree
Basic Range Resolution	~ 1.5 meters
Basic Range-Rate Resolution	0.1 λ/sec of $f_{carrier}$

Range-rate measurements are obtained through the use of a two-way Doppler technique utilizing coherent carrier techniques. Range is obtained by measurement of the delay time in a series of sidetones or a combination of code and sidetones.

3.0 TRACKING ACCURACY

The system description above indicates that, for the tracking equipment likely to be used in the Multiple Satellite mission, the accuracy of range data will be about 15 meters, while range rate data will be accurate to about 0.1 meter/sec. With this order of tracking data-point accuracy, there is little doubt that the desired accuracy (i.e., ~ 3 km) in position determination can be obtained if very frequent data points are collected and a reasonably effective computer program is used to correlate the data.

At the outset of the mission, intensive coverage by the STADAN ground stations could be requested. In support of the deployment, and perhaps for several days afterward, it would be operationally acceptable to provide coverage to obtain a tracking data point about every hour. Subsequently such frequency of observation would impose an unacceptable burden on the STADAN stations.

To estimate how infrequently the collection of tracking data points can be made while avoiding excessive errors in position, some approximate calculations simulating the process of position determination were made. These calculations are intended to establish by a relatively straightforward approach that the required accuracies are indeed feasible -- they are not meant to represent the actual operational system calculations. For this simplified analysis, only the data obtained from one assumed Keplerian orbit was considered. In practice, data obtained over many successive orbits could and probably would be included in the correlation process to establish emphemeris, thus reducing position errors below the values obtained in the present computations.

Also, account will be taken of all known orbital perturbation effects such as the solar, lunar, and earth oblateness as well as atmospheric drag. These perturbations can produce differences in satellite positions, in comparison with the unperturbed, i.e., the Keplerian orbit of the order of 20 km, from orbit to orbit. Knowledge of the perturbation effects should be good to at least a few percent, so that the residual error due to uncertainties in the effects of perturbations from one orbit to the next will be far smaller than the order of accuracy required in determining satellite position. Hence, the simplification gained in the present calculations by assuming a Keplerian orbit is justified.

Since, at low altitudes, the coverage of the satellites by the STADAN stations is relatively poor, consideration was restricted to sightings made at relatively large distances from earth. At such distances, the view of an orbit from a ground station is like that obtained if the earth were transparent and the station were at the center of the earth. However, the difference between such a location for the ground stations and the actual locations is important. If only range and range rate data as seen from the center of the earth were available, it would not be possible to determine the direction of the orbital plane or the direction of the line of apsides in the orbital plane, and the position of the satellite relative to any fixed three dimensional coordinate system could not be established. Knowledge of the directions of the orbital plane and the line of apsides derives from the fact that the sightings are obtained from sites displaced from the center of the earth in directions both normal to the orbital plane and in the orbital plane.

The establishment of the pertinent directions is obtained through triangulation, the triangulation base being established by (a) the separation distances between the different STADAN stations, and (b) the variation of the positions of the stations relative to the orbit arising from the rotation of the earth. Although the triangulation base obtained in this way is small relative to the dimensions of the orbit, it can be quite adequate since a considerable amplification of error can be tolerated. An allowable position error of 3 km is some 200 times greater than the range error of 15 meters in the individual tracking data points.

To simplify the computations, the orbit was taken to be equatorial, with apogee at zero longitude. Three stations were used; the first was located at zero deg longitude and 30 deg north latitude; the second was at 50 deg west longitude, and 30 deg south latitude; the third was at 50 deg east longitude, and 30 deg south latitude. These station locations were kept fixed, i.e., they were not rotated with the earth. Data from sightings obtained at 3 different points on the orbit were included in the computation. These were:

1. Sightings by the first and second stations when the satellite is at 10 R_e on the ascending leg.

2. Sightings by the second and third stations when the satellite is at apogee.

3. Sightings by the first and third stations when the satellite is at 10 R_e on the descending leg.

The foregoing representation of the stations and the orbit is, of course, highly fictitious. It does, however, provide reasonably realistic conditions with respect to the separation distances between the stations, the positions of the stations relative to the orbit, and the coverage of the satellite obtained from the stations. Computations of the visibility of the satellite from the STADAN stations show that when the range of the satellite is above 10 R_e, the satellite generally will be visible by two or more stations. Although the sightings were

taken to be simultaneous, in practice there would be no real need for exact simultaneity. While the computations may be more complex, the correlation process can be expected to handle non-simultaneous data with no loss of accuracy (as long as the exact time of the sightings is known).

Three sightings by each of two stations yield 6 range measurements. Keeping the times of the sightings fixed, orbital computations were made to determine the effects of small departures of the 6 orbital elements, from their nominal values, on the 6 range measurements. By inverting the matrix relating the deviations in the orbital elements to the deviations in the range measurements, the matrix relating the errors in the orbital elements to the errors in the range measurements was obtained.

The 3σ values for the errors in the elements listed in Table 1, were then computed, under the assumption that the range measurements are statistically independent and each measurement has a 3σ error of 15 meters. These errors in the orbital elements were then used to compute the position errors at various points in the orbit as listed in Table 2.

From the results listed in Table 2, it is seen that the largest errors in the position components are less than 2.3 km. This accuracy is quite satisfactory, particularly in view of the fact that it was obtained with no redundancy of tracking data. A substantial improvement in accuracy can be expected with the use of additional data points and the inclusion of range-rate data in the determination of the orbital elements. The 6 measurements could be obtained with a few minutes of tracking during each orbit. With an orbital period of about 2 days the operational burden on the ground stations would be quite modest.

There is, of course, no necessity for the actual sightings to conform to the case used here for illustrative purposes. In practice, it would be convenient to have the stations obtain tracking data points when the stations are in communication with the satellites for other purposes, such as collection of real time data or tape recorder playback. Special tracking data points would be called for only when the tracking data obtained routinely with the other data is not

Table 1

ESTIMATE OF ORBITAL ELEMENT ERRORS

Orbital Element	Error, 3σ
Perigee Altitude	.025 km
Apogee Altitude	.015 km
Inclination	.00014 deg
Longitude of Ascending Node	.00070 deg
Argument of Perigee	.00078 deg
Time of Perigee Passage	.011 sec

Table 2

ESTIMATE OF POSITION ERRORS

Nominal Time From Perigee, hours	Nominal Distance From Earth R_e	Components of Position Error			Total Magnitude of Position Error km
		In Tangential Direction km	In In-Plane Normal Direction km	In Out-Of-Plane Direction km	
0	1.04	.16	.03	.02	.17
2	5.7	.27	.58	.15	.66
5	10.4	.42	1.08	.21	1.18
12	16.6	.85	1.64	.27	1.86
24	20.0	2.21	.18	.32	2.24
36	16.6	1.10	1.47	.31	1.86
43	10.4	.59	.99	.25	1.18
46	5.7	.40	.52	.17	.68

adequate for establishing position as closely as desired. The present computations indicate that, in the worst case, the need for such special tracking data would impose no serious burden on the ground stations.

In the region of most interest, the orbital velocity of the satellites will be of the order of a few km/sec. Assuming that the time corresponding to a scientific data point is known to .01 sec, the error in position due to time uncertainty will be of the order of a few hundredths of a kilometer. Knowledge of time to the order of .01 seconds will be required for accurate measurement of propagation velocities. The times of transit of disturbances from one satellite to another will be typically of the order of 1 sec or less. A .01 second error in time will contribute a 1% error in determination of velocity relative to the satellites and about a 5% error in propagation velocity relative to the medium.

Assuming that the satellite clocks are synchronized once each orbit with a master ground clock, a timing accuracy of .01 second will require that the drift rate of the clocks in the satellites be less than 1 part in about 2×10^7. This order of accuracy can be attained with a crystal controlled clock provided that it incorporates adequate temperature compensation.

Appendix XVI

COMMUNICATIONS COVERAGE

1.0 INTRODUCTION

As presently conceived, the Multiple Satellite system will be designed such that real time communications can be supported whenever the satellite is in view of a STADAN station. These communications functions include command, tracking, and real time downlink data transmission. Because NASA OTDA desires to limit the operational burden on the STADAN stations to 4 to 6 hours per station per day, it is necessary to record and subsequently readout data accumulated during substantial portions of the orbit. Since the recorder playback is at a rate of 24 times that of the real-time rate, playback cannot be accomplished at the long ranges from the STADAN stations that are possible for real-time transmission. Thus the questions relating to communications coverage can be divided between recorder playback and real time coverage.

The current design provides a capability for recording data throughout the sections of the orbit of greatest scientific interest; specifically from 8 to 18 R_e on the ascending and on the descending legs of the orbit. Sufficient time for readout must be available during the section of the orbit between the end of recording to the next start of recording, that is from 8 R_e on the descending leg to 8 R_e on the ascending leg.

With regard to real time coverage, the main question relates to the extent that sections of the orbit may be blanked out due to the absence of any STADAN station that can view the satellite. This question is of particular importance with respect to the support of the deployment operation. During deployment operations and perhaps for a few subsequent orbits, it is considered operationally acceptable to exceed the limitations on the utilization of the STADAN stations. The deployment operation requires extensive use of command, tracking, and data transmission functions. In support of this operation, continuous coverage for the real time communications functions would be desirable.

In order to determine the adequacy of communications coverage, three sets of computations were performed. These were:

a. Visibility computations designed primarily to guide the selection of the distance range for tape recorder playback.

b. Computations designed to establish the real time coverage that will be available.

c. Computations designed to verify the recorder readout coverage, based upon the characteristics of the current communications system design.

The purpose of this section is to describe these computations.

2.0 VISIBILITY COMPUTATIONS

One of the critical factors that affects the communications system design is the range over which the tape recorder playback transmission will be made. To minimize the power requirements on the communications system it is desirable that this transmission be made at as short a range as possible. However, when the satellites are close to the earth, visibility from the STADAN stations is degraded.

To assist in resolving this problem, a computer program was written to determine the visibility of the satellites from the STADAN stations. For this purpose, the visibility of a single satellite from each of the STADAN stations was computed, i.e., no account was taken of the possibility that one station may, at times, be able to receive from two or more satellites simultaneously. Since the differences in orbital elements between satellites will be quite small, it is not expected that there will be significant differences in visibility among the individual satellites.

Computations were made for a range of orbital elements as listed in Table 1. Since visibility can be expected to degrade as perigee altitude is reduced, a conservatively low perigee altitude of 280 km was used. Apogee altitude was varied in the range of 17 to 23 R_e. To take account of the potentially wide range of coast angles prior to injection into orbit, a wide range in the argument of perigee was covered. A smaller range in the longitude of the ascending node was covered since this parameter is subject to less variation.

Table 1

ORBITAL ELEMENTS USED FOR COMPUTATIONS

Apogee Alt km	Arg Per deg	Longitude of Ascending Node deg	Orbit Time hrs
146537.23	150.0	-165.0	4333.4
146537.23	120.0	-165.0	4333.4
121052.50	120.0	-165.0	4333.2
121052.50	150.0	-165.0	4331.2
108310.13	180.0	-165.0	4416.8
108310.13	120.0	-180.0	48.3
108310.13	120.0	-150.0	413.4
121052.50	120.0	-180.0	499.3
121052.50	120.0	-150.0	500.8
146547.23	120.0	-180.0	692.0
146537.23	120.0	-150.0	694.1
108310.13	150.0	-165.0	413.3
146537.23	150.0	-165.0	692.9
146537.23	180.0	-165.0	694.1
146537.23	210.0	-165.0	691.3
146537.23	240.0	-165.0	692.4
146537.23	270.0	-165.0	694.1
146537.23	300.0	-165.0	693.6
146537.23	330.0	-165.0	692.2
108310.13	210.0	-165.0	416.3
108310.13	240.0	-165.0	414.3
108310.13	270.0	-165.0	414.2
108310.13	300.0	-165.0	414.5
108310.13	330.0	-165.0	416.5
121052.50	150.0	-165.0	498.2
121052.50	180.0	-165.0	500.8
121052.50	210.0	-165.0	500.8
121052.50	240.0	-165.0	500.8
121052.50	270.0	-165.0	500.8
121052.50	300.0	-165.0	500.8

Perigee Altitude = 280 km

For the most likely orbital parameters, which correspond approximately to a launch near the optimum date and time of day, the computations were run for long periods in orbit. For other orbital parameters, the computations were run for shorter times in orbit. Because of the lack of synchronism between the orbital period and the period of the earth's rotation, it is expected that the long term behavior of the visibility patterns will be much the same regardless of launch date and time. The shorter runs are sufficient to determine whether any unusual difficulties in communication coverage might be encountered at the outset as a result of variations in the launch timing.

The satellite was assumed to be visible from a station whenever the line-of-sight from the station to the satellite is above the horizon, i.e., whenever the elevation angle of the line-of-sight is positive. The computation was designed to determine the point at which the satellite first appears above the horizon and the subsequent point at which the satellite drops below the horizon. Starting at perigee, the satellite position was advanced in its orbit, which was taken to be Keplerian, in steps of 1/4 R_e; the positions of the STADAN station were advanced in accordance with the rotation of the earth. When a change in the sign of the elevation angle of the line-of-sight from any of the 5 STADAN stations was noted, a linear extrapolation method was used to evaluate the point at which the elevation angle went through zero. Data relating to these critical points were printed in half-orbit sections. At each point, data was given for all stations for which the elevation angle had not remained negative. This data included: elevation angle, elevation angle rate; communications range; slewing rate, and time since the last appearance of the satellite at the horizon. Each point was identified by: time, distance from earth, and the true anomaly.

From the horizon crossing points, compilations were made to show the visibility time for each station, in 1 R_e intervals of distance of the satellite from the center of the earth. This was printed out for each half orbit along with the critical point data. At the end of the orbit time a similar computation for the total orbit time was printed out.

Table 2 presents the printout key for reading the computer output. Table 3 is a sample of the computer printout. SGC and ARC have copies of the complete printouts of these computations as well as all the other computations described herein.

The results obtained indicate that, in the range from 7.5 to 4 R_e, including the descending and ascending orbital legs, more than 4 station hours of communication coverage would be available. Since the communication system currently is designed for a recorder playback period of 1 hour, sufficient time would be available for readout of the 4 satellites without recourse to simultaneous transmissions.

It should be noted that in many cases the Ulaska station provides very little coverage. The number of available ground stations is then practically reduced to 4.

3.0 REAL TIME COVERAGE

The data obtained from the computation of the points at which the satellite crosses the horizon at the STADAN stations are useful not only for evaluating the recorder playback coverage but also for evaluating the coverage obtained for real time communications. However, for real time communications coverage, primary interest is in determining sections of the orbit for which little or no coverage is available. To facilitate this evaluation, the computation of the horizon crossing points was repeated but the data was compiled in a different way. In this case, the time required for the distance of the satellite from earth to change 1 R_e was divided into 6 categories, numbered 0 to 5; the time assigned to each category corresponded to the interval wherein the satellite is within view of the respective number of stations simultaneously. As in the previous computations, the horizon crossing points and the compilation of the time distribution was printed out for each half orbit. The compilation was made for each interval of 1 R_e from perigee to apogee. The same range of orbital parameters was covered, and at the end of the orbit time, a compilation of the total orbit time was printed.

Table 2

PRINTOUT KEY
FOR COMMUNICATIONS VISIBILITY COMPUTATION

INITIAL CONDITIONS

SATELLITE	APOGEE ALT ECC	PERIGEE ALT SMA	ARG PER PERIOD	NODE TP	T ANOMALY VA	INCL VP

SATELLITE - Initial orbital conditions for Nth satellite conic where N may be up to 5.

APOGEE ALT - Apogee altitude - km

PERIGEE ALT - Perigee altitude - km

ARG PER - Argument of perigee - deg

NODE - Longitude of the ascending node - deg (measured with respect to Aries)

T ANOMALY - True anomaly of the satellite at the initial time point - deg

INCL - Equatorial orbital inclination - deg

ECC - Eccentricity

SMA - Semi-major axis - km

PERIOD - Orbital period - seconds

TP - Time from perigee passage - seconds

VA - Apogee velocity - km/sec

VP - Perigee velocity - km/sec

RECEIVING STATION LOCATION

NUMBER	LATITUDE	LONGITUDE	RADIUS

NUMBER - Nth number of the receiving station, where N goes from 1 - 5.

LATITUDE - Geodetic latitude of the Nth receiving station + north latitude, - south latitude - deg

LONGITUDE - Longitude of the Nth receiving station - + east of Greenwich, - west of Greenwich - deg

RADIUS - Radius of the Nth receiving station - km

Table 2 (Continued)

			STATION N				
T	R	TA	E	ED	CR	SL	DTM

T - time from the initial time point - hours

R - Radial distance to the satellite - Earth radii (1 Earth radius = 6371.184 km)

TA - True anomaly of the satellite - deg

The following data are given for each of the five receiving stations. One line of printout occurs whenever any one of the five stations go "on" or "off". (An "on" status results from an acquisition, "off" from a loss condition.)

E - Elevation angle - The angle measured from the local horizontal of the receiving station to the satellite - deg

ED - Rate of change in elevation (deg/sec) x 10^{-3}

CR - Communication range - km x 10^{2}

SL - Slewing rate - angular velocity of the communication range vector $\frac{\text{deg}}{\text{sec}} \times 10^{-3}$

DTM - Time accumulation of the "on" status hours

Immediately following the lines of on-off data is a summation matrix of the time each station is "on" during an increment of one earth radius. This matrix is computed and printed at apogee and at perigee for each orbit. The succeeding pages are the same as page two with the exception of the last matrix of the last page. The terminal matrix is a summation of the "on" time status for each station as a function of R for the entire computer run.

Table 3

SAMPLE OF PRINTOUT OF VISIBILITY COMPUTATION

APOGEE RADIUS = 20 RE

INITIAL CONDITIONS

SATELLITE	APOGEE ALT ECC	PERIGEE ALT SMA	ARG PER PERIOD	NODE TP	T ANOMALY VA	INCL VP
1	121052.50 0.90078402	280.00 67037.43	150.0000 172737.061	-165.0000 -0.	0. 0.557104	28.5000 10.673019

RECEIVING STATION LOCATION

NUMBER	LATITUDE	LONGITUDE	RADIUS	NAME
1	-35.63	148.95	6371.95	ORRORAL
2	35.20	-80.00	6371.88	ROSMAN
3	-33.13	-70.68	6371.69	SANTIAGO
4	-17.00	48.00	6371.00	TANANARIVE
5	64.98	-147.50	6371.29	ULASKA

Table 3

SAMPLE OF PRINTOUT OF VISIBILITY COMPUTATION (Continued)

T	R	TA	STATION 1 E	ED	CR	SL	DTM	STATION 2 E	ED	CR	SL	DTM	STATION 3 E	ED	CR	SL	DTM	STATION 4 E	ED	CR	SL	DTM	STATION 5 E	ED	CR	SL	DTM
0.2	1	53	0	0	0	0	0.	0	0	0	0	0.	0	0	0	0	0.	39	123	27124		0.1	0	0	0	0	0.
0.6	2	104	6	19	141	19	0.1	0	0	0	0	0.	0	0	0	0	0.	44	-4	110	4	0.5	0	0	0	0	0.
6.7	12	158	-1	-2	762	3	5.6	0	0	0	0	0.	0	0	0	0	0.	84	-0	719	3	6.2	0	0	0	0	0.
8.2	13	162	0	0	0	0	0.	0	0	0	0	0.	1	2	875	3	0.1	60	-0	819	0	7.7	0	0	0	0	0.
11.2	16	166	0	0	0	0	0.	2	2	1017	3	0.2	33	2	985	2	2.9	29	-2	989	21	0.5	0	0	0	0	0.
13.7	17	170	0	0	0	0	0.	26	1	1088	3	2.8	63	0	1060	2	5.5	-3	-3	1120	3	12.8	0	0	0	0	0.
16.4	19	175	0	2	1226	3	0.0	26	-1	1199	3	7.4	45	-1	1183	21	0.1	0	0	0	0	0.	2	1	1225	3	0.6

1- 2	0.	0.	0.	0.27	0.
2- 3	0.19	0.	0.	0.36	0.
3- 4	0.39	0.	0.	0.39	0.
4- 5	0.44	0.	0.	0.44	0.
5- 6	0.49	0.	0.	0.49	0.
6- 7	0.54	0.	0.	0.54	0.
7- 8	0.59	0.	0.	0.59	0.
8- 9	0.65	0.	0.	0.65	0.
9-10	0.72	0.	0.	0.72	0.
10-11	0.79	0.	0.	0.79	0.
11-12	0.87	0.	0.	0.87	0.
12-13	0.33	0.	0.	0.96	0.
13-14	0.	0.	0.11	1.06	0.
14-15	0.	0.	1.19	1.19	0.
15-16	0.	0.	1.36	1.36	0.
16-17	0.	1.45	1.58	1.58	0.
17-18	0.	1.90	1.90	1.08	0.
18-19	0.	2.48	2.48	0.	0.
19-20	5.62	4.60	5.03	0.	6.17
20-21	-0.00	-0.00	-0.00	-0.00	-0.00
21-22	-0.00	-0.00	-0.00	-0.00	-0.00
22-23	-0.00	-0.00	-0.00	-0.00	-0.00
23-24	-0.00	-0.00	-0.00	-0.00	-0.00
24-25	-0.00	-0.00	-0.00	-0.00	-0.00
25-26	-0.00	-0.00	-0.00	-0.00	-0.00

Table 4 presents the printout key for these computations. Table 5 is a sample of the printout. The results obtained indicate that, except for small periods near perigee, the satellites will be in view of one or more stations at all times. The results also show that the assumption used in considering tracking requirements (see Appendix XV), namely that the satellite will generally be in view of two or more stations when its distance from earth is equal to or greater than 10 R_e, is justified.

Although for almost all of the orbit the satellites will be in view of one or more stations at all times, the use of real time coverage only for data collection does not appear to be feasible. Even if it were always possible for one station to service all four satellites simultaneously, the station duty cycles would be tight at best. In general the separation distances between satellites will be too great to allow simultaneous coverage of all four satellites. It is expected that main reliance will be placed on the 30-foot dishes. These antennas have a beam width of about 1 degree. In order to be assured of remaining within this beam width, the maximum separation between satellites, as a function of distance from the station is as follows:

Distance From Station	Maximum Separation Distance Between Satellites to Assure Remaining Within Beam Width of 1 deg
20 R_e	2200 km
16 R_e	1800 km
12 R_e	1300 km
8 R_e	900 km

Except near apogee, the initial separation distances between satellites will exceed these distances, and the problem will be aggravated by the growth of the tangential separation distance to an order of magnitude larger than the initial separation distances. While it is possible that, as a result of a favorable orientation of the line-of-sight relative to the separation distance array, at times all four satellites will be within the antenna's beam width. This will be the exception rather than the rule. When two or more stations are required to

Table 4

PRINTOUT KEY
FOR REAL TIME COVERAGE COMPUTATIONS

INITIAL CONDITIONS

SATELLITE	APOGEE ALT ECC	PERIGEE ALT SMA	ARG PER PERIOD	NODE TP	T ANOMALY VA	INCL VP

SATELLITE - Initial orbital conditions for Nth satellite conic where N may be up to 5.

APOGEE ALT - Apogee altitude - km

PERIGEE ALT - Perigee altitude - km

ARG PER - Argument of perigee - deg

NODE - Longitude of the ascending node - deg (measured with respect to Aries)

T ANOMALY - True anomaly of the satellite at the initial time point - deg

INCL - Equatorial orbital inclination - deg

ECC - Eccentricity

SMA - Semi-major axis - km

PERIOD - Orbital period - seconds

TP - Time from perigee passage - seconds

VA - Apogee velocity - km/sec

VP - Perigee velocity - km/sec

RECEIVING STATION LOCATION

NUMBER	LATITUDE	LONGITUDE	RADIUS

NUMBER - Nth number of the receiving station, where N goes from 1 - 5.

LATITUDE - Geodetic latitude of the Nth receiving station + north latitude, - south latitude - deg

LONGITUDE - Longitude of the Nth receiving station - + east of Greenwich, - west of Greenwich - deg

RADIUS - Radius of the Nth receiving station - km

Table 4 (Continued)

ORBIT NUMBER

TIME	TA	R	TI	N = 0	N = 1	N = 2	N = 3	N = 4	N = 5

TIME - Orbital time from Time = 0 - hours

TA - True Anomaly - deg

R - Radial distance to the satellite - Earth radii (1 Earth radius = 6371.184 km)

TI - Value of elapsed time between preceding R and present R - hours

N=0 - Portion of TI for which none of the five communication stations receive.

N=1 - Portion of TI for which one of the five communication stations receive.

N=2 - Portion of TI for which two of the five communication stations receive.

N=3 - Portion of TI for which three of the five communication stations receive.

N=4 - Portion of TI for which four of the five communication stations receive.

N=5 - Portion of TI for which all of the five communication stations receive.

These data are computed over each half orbit and printed at the corresponding apogee or perigee point. Subsequent pages follow the format of Page 2 with the orbit number being incremented by .5. The last page of the computer run is entitled "Summation Matrix of all Preceding Orbits". This matrix gives a summation of viewing time as a function of R for the total time in orbit.

Table 5

SAMPLE OF PRINTOUT OF REAL TIME COVERAGE

APOGEE RADIUS = 18

INITIAL CONDITIONS

SATELLITE	APOGEE ALT ECC	PERIGEE ALT SMA	ARG PER PERIOD	NODE TP	T ANOMALY VA	INCL VP
1	108310.13 0.89036434	280.00 60666.25	120.0000 148706.578	-180.0000 -0.	0. 0.617305	28.5000 10.643726

RECEIVING STATION LOCATION

NUMBER	LATITUDE	LONGITUDE	RADIUS	NAME
1	-35.63	148.95	6371.95	ORRORAL
2	35.20	-80.00	6371.88	ROSMAN
3	-33.13	-70.68	6371.69	SANTIAGO
4	-17.00	48.00	6371.00	TANANARIVE
5	64.98	-147.50	6371.29	ULASKA

Table 5

SAMPLE OF PRINTOUT OF REAL TIME COVERAGE (Continued)

COVERAGE

ORBIT NUMBER 0.

COMMUNICATION TIME IN HOURS FOR WHICH N STATIONS RECEIVE OVER AN INCREMENT OF ONE EARTH RADIUS

TIME (HR)	TA (DEG)	R (RE)	TI (HR)	N = 0	N = 1	N = 2	N = 3	N = 4	N = 5
0.47	92	1	0.47	0.26	0.21	0.	0.	0.	0.
0.83	113	2	0.37	0.	0.37	0.	0.	0.	0.
1.24	125	3	0.41	0.	0.41	0.	0.	0.	0.
1.70	133	4	0.46	0.	0.46	0.	0.	0.	0.
2.21	139	5	0.51	0.	0.51	0.	0.	0.	0.
2.78	144	6	0.57	0.	0.57	0.	0.	0.	0.
3.41	148	7	0.63	0.	0.63	0.	0.	0.	0.
4.11	151	8	0.70	0.	0.58	0.12	0.	0.	0.
4.89	154	9	0.78	0.	0.	0.78	0.	0.	0.
5.76	157	10	0.87	0.	0.	0.87	0.	0.	0.
6.72	160	11	0.97	0.	0.	0.97	0.	0.	0.
7.82	162	12	1.09	0.	0.	1.09	0.	0.	0.
9.07	165	13	1.26	0.	0.	0.37	0.89	0.	0.
10.55	167	14	1.47	0.	0.	0.20	1.28	0.	0.
12.36	170	15	1.81	0.	0.	1.81	0.	0.	0.
14.80	173	16	2.44	0.	0.	2.36	0.08	0.	0.
20.65	180	17	5.85	0.	1.05	1.94	2.86	0.	0.

obtain coverage of the satellites for extended intervals, the station duty cycle requirements would become prohibitive if all data had to be obtained from real time transmission.

The separation distance problem is, of course, not a factor when the satellites are still mounted on the pallet. Also near apogee the separation distances are not only small initially but will remain fairly small. While it may not always be possible for one station to service all four satellites simultaneously, it can be expected that one station will generally be able to service two and often three satellites particularly when the satellites are above 16 R_e. In addition above 16 R_e the satellites are generally in view of two or more stations. Hence, simultaneous real time data transmission from all four satellites will generally be possible for the section of the orbit above that covered by tape recording.

4.0 VERIFICATION OF RECORDER PLAYBACK COVERAGE

To verify the recorder playback coverage, computations were made of the intervals wherein the satellite would not only be in view of a ground station, but that conditions permitting transmission at the playback bit rate would also be satisfied. With the use of a collinear array antenna for downlink communication, the required conditions depend upon the angle between the spin axis and the line-of-sight from the satellite to the ground station, as well as the range.

Based upon the current system design, the envelope of conditions acceptable for recorder playback is approximately as shown in Figure 1. Computations were made in a manner similar to that followed previously, but using the crossing of boundary of acceptable conditions in place of the change in sign of the elevation angle, as the criterion for the critical points. The range of orbital conditions previously used and listed in Table 1 was again covered. The printout listed the points at which the boundary of acceptable conditions was crossed for each station during half orbit periods. Also shown in the printout is the time interval during which acceptable recorder playback conditions exist at each station in the half orbit periods.

CLEARPRINT PAPER CO. NO. C39X MILLIMETERS, 200 BY 250 DIVISIONS PRINTED IN U.S.A. ON CLEARPRINT TECHNICAL PAPER NO. 1015

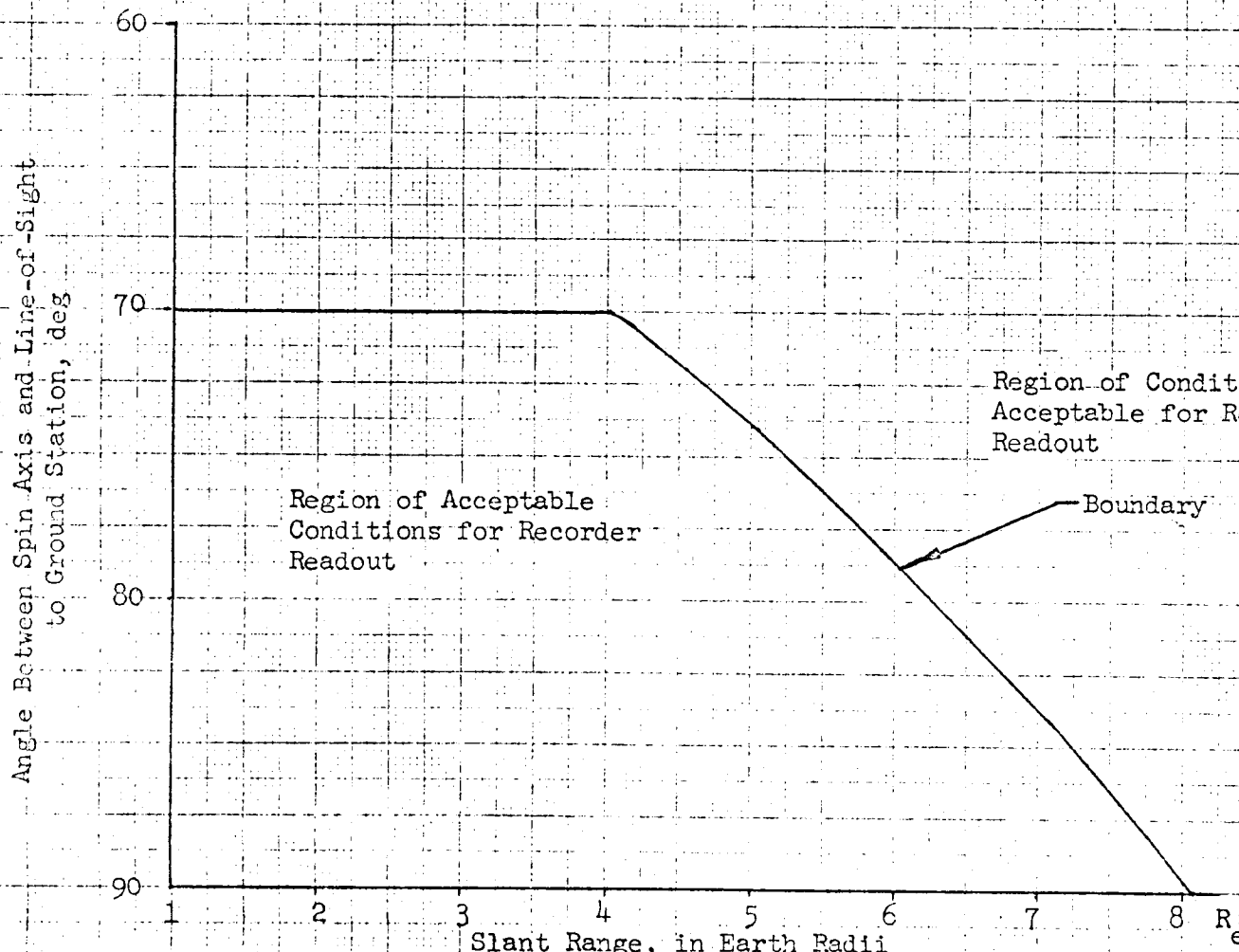

FIGURE 1. ENVELOPE OF CONDITIONS ACCEPTABLE FOR RECORDER READOUT

Table 6 presents the printout key for these computations. Table 7 is a sample of the printout. Review of the complete printout indicates that the requirement of 4 station hours for recorder playback, for the 4 satellites, will be fulfilled readily.

Table 6

PRINTOUT KEY
FOR RECORDER READOUT COVERAGE VERIFICATION COMPUTATIONS

INITIAL CONDITIONS

SATELLITE	APOGEE ALT ECC	PERIGEE ALT SMA	ARG PER PERIOD	NODE TP	T ANOMALY VA	INCL VP

SATELLITE - Initial orbital conditions for Nth satellite conic where N may be up to 5.

APOGEE ALT - Apogee altitude - km

PERIGEE ALT - Perigee altitude - km

ARG PER - Argument of perigee - deg

NODE - Longitude of the ascending node - deg (measured with respect to Aries)

T ANOMALY - True Anomaly of the satellite at the initial time point - deg

INCL - Equatorial orbital inclination - deg

ECC - Eccentricity

SMA - Semi-major axis - km

PERIOD - Orbital period - seconds

TP - Time from perigee passage - seconds

VA - Apogee velocity - km/sec

VP - Perigee velocity - km/sec

RECEIVING STATION LOCATION

NUMBER	LATITUDE	LONGITUDE	RADIUS

NUMBER - Nth number of the receiving station, where N goes from 1 - 5.

LATITUDE - Geodetic latitude of the Nth receiving station + north latitude, - south latitude - deg

LONGITUDE - Longitude of the Nth receiving station - + east of Greenwich, - west of Greenwich - deg

RADIUS - Radius of the Nth receiving station - km

Table 6 (Continued)

The data given on page 2 of Table 7 (Section 3.11) and all subsequent pages within a given computer run pertain to the high data rate recorder playback coverage. The communication range for the high data rate is restricted to the approximate interval of 1.3 R_e (8280 km) to 7.8 R_e (49700 km) on both the ascending and descending orbit legs.

STATION	TIME ON	RADIUS ON	TIME OFF	RADIUS OFF	DT

STATION - Communication station number

TIME ON - Time from injection at which recorder playback begins - hrs

RADIUS ON - Distance from center of Earth to satellite at time on - R_e (1 R_e = 6371.184 km)

TIME OFF - Time from injection at which recorder playback terminates - hrs

RADIUS OFF - Distance from center of Earth to satellite at time off - R_e

DT - Recorder playback time from time on to time off - hrs

Table 7

SAMPLE PRINTOUT OF VERIFICATION OF RECORDER PLAYBACK COVERAGE

APOGEE RADIUS = 20 RE

KEY

INITIAL CONDITIONS

SATELLITE	APOGEE ALT ECC	PERIGEE ALT SMA	ARG PER PERIOD	NODE TP	T ANOMALY VA	INCL VP
1	121052.50 0.90078402	280.00 67037.43	150.0000 172737.061	-165.0000 -0.	0. 0.557104	28.5000 10.673019

RECEIVING STATION LOCATION

NUMBER	LATITUDE	LONGITUDE	RADIUS	NAME
1	-35.63	148.95	6371.95	ORRORAL
2	35.20	-80.00	6371.88	ROSMAN
3	-33.13	-70.68	6371.69	SANTIAGO
4	-17.00	48.00	6371.00	TANANARIVE
5	64.98	-147.50	6371.29	ULASKA

Table 7

SAMPLE PRINTOUT OF VERIFICATION OF RECORDER PLAYBACK COVERAGE (Continued)

COVERAGE

STATION	TIME ON	RADIUS ON	TIME OFF	RADIUS OFF	DT
ORBIT NO. 1					
1.	0.64	2.54	2.87	7.29	2.23
2.	0.	0.	0.	0.	0.
3.	0.	0.	0.	0.	0.
4.	0.19	1.29	2.87	7.29	2.69
5.	0.	0.	0.	0.	0.
ORBIT NO. 2					
1.	48.62	2.54	50.86	7.29	2.23
2.	45.42	6.75	47.53	2.00	2.11
3.	44.83	7.75	47.36	2.50	2.53
4.	48.17	1.29	50.86	7.29	2.69
5.	45.56	6.50	47.27	2.75	1.70
ORBIT NO. 3					
1.	96.61	2.54	98.84	7.29	2.23
2.	93.41	6.75	95.60	1.75	2.20
3.	92.97	7.50	95.25	2.75	2.28
4.	96.15	1.29	98.84	7.29	2.69
5.	93.55	6.50	95.25	2.75	1.70
ORBIT NO. 4					
1.	144.59	2.54	146.82	7.29	2.23
2.	141.39	6.75	143.59	1.75	2.20
3.	140.95	7.50	143.14	3.00	2.19
4.	144.14	1.29	146.82	7.[illegible]	2.69
5.	141.53	6.50	143.23	2.75	1.70

Appendix XVII

MAGNETIC TAPE RECORDERS

1.0 INTRODUCTION

Tape recorders have been used in spacecraft and satellites for many years. In the early days of satellites, most recorders were of the endless loop type, which used a lubricated tape. The tape was pulled, by means of a capstan arrangement, from the inside of the tape pack and was rewound onto the outside of the reel. In this way the reel maintained an essentially constant diameter throughout all modes of operation. A successful example of such a tape recorder is the machine flown on the Mariner Mars mission. This recorder had a tape loop of approximately 150 ft and recorded data and sync information on two tracks. The data was recorded at a relatively high speed and played back with a record-to-playback ratio of 1:1280, resulting in a playback speed of .01 ips. Much of the development cost associated with this machine went into two principal areas: (1) the mechanical drive system to insure smooth operation at the low playback speed, and (2) the electronics and the playback head, to insure adequate reproduced signal to noise ratio.

Many recorders of the endless loop type have been built by vendors, principally for the Goddard Space Flight Center. These recorders have been flown on many satellites with varying degrees of success. In general, the recorders have been subject to premature failures in flight, or else, extensive rework was necessary after delivery to GSFC before the recorders could be made operational. There are several vendors who have been manufacturing such machines, among them Raymond Engineering Laboratories of Middletown, Conn., the Lockheed Electronics Company of Metuchen, New Jersey, Borg-Warner Controls Division of Santa Ana, California and the Data Sciences Corporation of San Diego, California.

2.0 ENDLESS LOOP RECORDER LIMITATIONS

For the Multiple Satellite mission, the principal objection to the use of endless loop recorders, aside from an undistinguished history, is the limitation on the tape capacity. The most recent of such machines cannot be expected to hold more than 300 ft of tape. Experiments which have been tried in the past using tape loops up to and including 1200 ft have been markedly unsuccessful. The reasons are many: (1) the support required for the tape loop as it rotates, (2) the frictional problems encountered because of the rubbing of many layers of tape against each other, and (3) the inability to maintain proper guidance have all contributed to prevent the use of longer tape loops. Such a recorder for the Multiple Satellite mission would be restricted to recording data only over sections of the region of maximum scientific interest, and would result in an increased load on the STADAN stations. For example, if the nominal data acquisition rate is 1280 bits per second and a typical recorder with 300 ft of tape, 4 tracks, and capable of recording 2,000 bits per inch per track is utilized, the recorder would become filled in approximately 6 hours. Therefore, since the region of interest extends over a portion of the orbit during which the spacecraft system takes 12 hours to traverse, or a total of 24 hours on the ascending and descending legs combined, approximately 4 complete record/reproduce cycles must be employed. To prevent loss of data during playback, real time data transmission would be required at the same time to prevent significant loss of data. Clearly, such a situation is highly undesirable from an operational standpoint and appears to be incompatible with the requirements of NASA OTDA to limit the use of any one STADAN station to not more than 6 hours per day. Hence, to summarize, (1) because of the previous poor history of operational reliability of endless loop tape recorders, coupled with (2) the limited data storage that can be achieved on even the best of these recorders, which results in a (3) high duty cycle for the STADAN stations, the use of endless loop tape recorders is not recommended for the Multiple Satellite mission.

3.0 REEL-TO-REEL RECORDERS

There is another basic type of recorder which appears much more suitable for use for the Multiple Satellite mission which is the reel-to-reel recorder. This type of recorder has not been used as extensively in scientific satellites as the endless loop recorder because of the apparent simplicity and ease of operation of the endless loop recorder. However, certain classified programs have used many of the reel-to-reel recorders since the programs required storage of considerably more data than the typical scientific satellite. Hence, a not as well publicized but equally as long development history exists for the reel-to-reel recorder.

Several vendors which manufacture tape recorders of the reel-to-reel type which are suitable for the Multiple Satellite Mission include (1) the Kinelogic Corporation of Pasadena, Calif., (2) the Raymond Engineering Laboratory of Middletown, Conn., (3) the Leach Corporation of Azusa, Calif. Recently, the Space-General Corporation, as part of the OV3 program, utilized a Leach reel-to-reel recorder. Four of the OV3 satellites were launched and have been orbiting for periods of four to twelve months as of this writing. During this period, all the recorders have functioned perfectly. Indications with respect to the classified programs are that, after an initial period in which failures were experienced, solutions have been derived which have solved these problems. A recent and spectacular use of a reel-to-reel tape recorder has been in the Gemini program. This tape recorder, built by Raymond Engineering Laboratory under subcontract to IBM, provided storage for computer programs for use by the on-board computer for precise terminal guidance. The use of an auxiliary tape memory of this type has prompted Raytheon Corporation to use such a recorder in conjunction with the Apollo Guidance Computer. In general, the use of the endless loop machine is diminishing while the use of the reel-to-reel recorder is increasing, since the operational problems are minimized and the storage capacity of reel-to-reel recorders is considerably greater than that of the endless loop recorder.

For the Multiple Satellite mission, reel-to-reel tape recorders having a data capacity somewhat in excess of 10^8 bits are available as off-the-shelf items which can record the scientific data on both 12 hour legs of the orbit for a total of 24 hours without having to playback the recorder at any point during the data acquisition mode. Thus,

1. The STADAN duty cycle is minimized,
2. Communications system complexity is minimized, since subcarrier operation of two data links is not required,
3. All the desired scientific data is obtained without interruption.

4.0 MECHANICAL CONSIDERATIONS

In spite of the fact that many manufacturers currently can provide reel-to-reel recorders much care must be taken in the construction of such recorders to achieve the reliability required to meet the long-life time for the Multiple Satellite program. The mechanical performance of a tape recorder probably is dependant critically on the bearing assemblies. It is extremely important that high class (class 6+) bearings be used throughout a recorder in order to insure maximum possible lifetime. The bearings must be properly lubricated to prevent binding, clogging, and chemical reactions which may result in poor speed control. The masses suspended from the bearings must be as light as possible, to prevent vibration damage from occurring to the bearing assemblies during the boost phase. It is extremely important that all tolerances in the mechanical structure be held closely, otherwise cumulative errors build up which result in poor tape guidance and consequent loss of signal to noise ratio.

There are two basic approaches to the packaging of the mechanical transport: (1) isolation of the transport by means of vibration isolators and snubbers, or (2) direct coupling of the transport to the spacecraft structure. Each technique has relative advantages and disadvantages, and the use of one method over another is predicated upon several things:

1. The actual boost environment.

2. The physical size of the shaft/bearing/pulley assemblies which must be protected.

3. The class of bearing used and whether it is simplex or a duplex pair.

4. If a duplex pair, the preload used.

5. The flutter deterioration allowed after a certain amount of brinelling of the bearings.

6. The possibility of catastrophic failure because of damage to bearing or shaft assemblies.

The choice of packaging to be used depends on a detailed analysis of the vibration loads and spectrum to be anticipated and must be done at a later stage in the program.

5.0 MOTORS

While the use of DC motors for driving spacecraft recorders has been attempted in the past, practically all recorders currently built use AC hysteresis-synchronous motors. The DC motors have several major disadvantages, including (1) arcing, causing radio frequency interference, and (2) rapid wear of the motor brushes (less than 500 hrs). The development of brushless DC motors has, for many reasons, been relatively unsuccessful. Invariably, the techniques used to eliminate brushes result in a complex device utilizing electronic control whose reliability is low compared to that of the AC hysteresis motor.

The AC hysteresis-synchronous motor is used in most spacecraft tape recorders. The development of a high efficiency, small motor, of this type has been pursued by several manufacturers over the past several years. Current designs are available which demonstrate reasonable efficiency at the low power levels at which such motors run. However, it is difficult to reduce the input power of these motors to below 1 watt, since the materials require a minimum amount of excitation power, regardless of the output power. Therefore, there are

many motors available which consume slightly in excess of 1 watt and produce sufficient torque to operate a tape recorder at the speeds which are required. In addition, the hysteresis-synchronous motor has the advantage of precise speed control capability. The speed of this type of motor is rather independent of power supply voltage fluctuations, once synchronous operation has been achieved. Of course, it is susceptible to speed variations if the frequency control of the power supply is not adequate; indeed, multiple speed operation, at a sacrifice in efficiency, is achieved by changing the frequency of the supply voltage. Therefore, the type of motor that would be used in the Multiple Satellite recorder would be of the AC hysteresis-synchronous type.

6.0 MAGNETIC TAPE

There are many instrumentation quality magnetic tapes manufactured by Minnesota Mining and Manufacturing, St. Paul, Minn. or Memorex Corporation, Santa Clara, California which are suitable for use in a spacecraft recorder. These tapes have been developed primarily for use with large scale, high frequency instrumentation ground recorders. The tapes available that would be used on the Multiple Satellite recorder generally have a Mylar base.

Such tape, however, does have limitations if stretched because high torque loads are applied. Generally, such torque loads can not be applied in a spacecraft recorder because of the limited torque characteristics of the drive motors.

A more important problem is the thermal stability problem. The Mylar base tapes tend to exhibit either sticking or decomposition if stored at temperatures in excess of 200°F. Therefore, care must be taken in all testing, storage and handling not to exceed a temperature well below this. In addition, the thermal control of the spacecraft should limit the maximum temperature to approximately 125°F to permit a suitable margin of safety during operation.

There are several experimental tapes which use polyester bases of a different type. These are the so-called H film, or similar to H film materials.

Since the requirement for high temperature tape is not usually required by any customer, the development of such tapes has been quite limited. However, experimental quantities of such tapes are available if one is willing to pay a high price from several manufacturers. The H film base material has the advantage that it can withstand considerably higher temperatures, approximately 300°F to 400°F. If thermal problems were to become paramount, i.e., the possibility arose that the tape recorder would be subject to temperatures as high as 150°F, consideration must be given to utilizing H film type base tapes. However, it would be more desirable to lower the temperature than to develop a new tape for the Multiple Satellite program because of cost considerations.

7.0 METALLIC AND PLATED-METAL TAPES

There are several experimental tapes utilizing plating of magnetic material on H film or which are made entirely of metal. Such tapes have been manufactured principally by small independent laboratories, such as Thin Films, Inc.,Los Angeles, or Lash Laboratories, San Diego. A major manufacturer (3M Co.) also experimented with such tapes. The Dupont Company, Wilmington, Delaware is said to have a coating material which is suitable for use on such tapes; however, these are experimental at this stage and, unless significant production in test quantities will become available in the next few years, cannot be considered as likely candidates for the Multiple Satellite program.

8.0 MAGNETIC RECORDING AND PLAYBACK HEADS

A most important element in any tape recorder are the recording and playback heads. This section will include a lengthy discussion of basic head requirements. It is here that the transformation of signal energy from an electrical current to a magnetic field and vice versa is made. The performance characteristics of magnetic heads has shown considerable improvement over the past several years. There are several independent manufacturers of heads, including Applied Magnetics Corporation, Goleta, California and the Ferroxcube Corporation, Saugerties, New York. The heads, which are generally available,

are of conventional design, built of laminated sections of magnetic material. The head is built up of these laminations maintaining a precise separation between the two pole pieces (the gap). To impress a signal on the tape, the gap lengths must be controlled precisely, since the frequency response (in playback) is dependent, critically, on the gap length.

The following is an excerpt from a NASA document, by Dr. S. W. Athey, No. SP-5038, concerning magnetic heads. It is quoted here because of the lucidity and completeness of the presentation.

Two main types of reproduce heads and one type of record head are in current use. Essentially all heads use the fringing effect that occurs at a well-defined gap in a soft magnetic structure as the primary mechanism of inducing magnetomotive force into the tape or for extracting flux from the tape.

The form of record head in most common use is effectively a ring of soft magnetic material, interrupted by a narrow gap of nonmagnetic material, with windings placed somewhere around the circumference of the ring. When current is passed through the windings, most of the magnetomotive force produced in the magnetic circuit by the windings appears across the nonmagnetic gap and the fringing fields at this gap are relatively strong. These fringing fields are the means for producing a magnetomotive force in the tape. Although the foregoing states the principle on which such heads work, the current use of shorter gaps and the trend to recording higher and higher frequencies, for which the effective permeability of the magnetic material of the head may be low, invalidate the statement that most of the magnetomotive force appears across the gap. It is more accurate to say that a controlled amount of the total magnetomotive force appears across the gap.

The two basic kinds of reproduce heads are the so-called "$d\phi/dt$" and flux-sensitive heads. The $d\phi/dt$ head is almost identical in construction to the record head just described and "obtains its information" about the flux in the magnetic tape by determining the voltage induced in the reproduce head winding as the flux intercepted by the gap and passed through the head changes with time.

The output of such a head is effectively the time derivative of the flux intercepted. The remanent flux induced in the tape by the record head is almost linearly proportional to the record current. The overall transfer characteristic of a record/reproduce system using the $d\phi/dt$ head is therefore differentiated. In a particular record/reproduce system, such differentiation may be a disadvantage or an advantage.

When the rate of movement of tape is extremely slow, the $d\phi/dt$ output is correspondingly low. For such applications, heads of a different basic operating mode are often used. These are so-called flux-sensitive heads, of which there are two basic types. In one type, the flux intercepted by the head from the tape is introduced in the same magnetic circuit as the flux induced by an auxiliary signal applied to some auxiliary windings. A pickup winding detects changes induced in the auxiliary signal as the tape flux modifies the magnetic characteristics of the nonlinear magnetic circuit used. This is the so-called "modulator head". A variation of this type is one in which the tape flux is caused to vary the reluctance of a magnetic path where the reluctance is externally measured by some method other than the carrier technique described.

The second type of flux-sensitive head employs the so-called "Hall effect." The Hall effect occurs when a steady current and a magnetic flux are applied orthogonally to a material exhibiting the Hall phenomenon. The Hall effect occurs in most of the common semiconductors, and is especially strong in gallium arsenide. The "Hall voltage" appears across electrodes orthogonal to the current and flux directions and is proportional to the product of the flux intensity and the steady current intensity. Although very simple and quite effective in many applications, Hall effect heads suffer from thermal sensitivity and many other complicating properties which have been discussed in the literature (Stein [1961a]).

Conventional recording heads and $d\phi/dt$ reproduce heads are almost identical in construction. Reproduce heads usually have much smaller gaps than record heads and there are differences in the windings on the core structure for the two types. For each head application there is an optimum number of turns and size of wire for the winding. For a record head the wire is usually heavier and the

winding is designed to induce as many ampere-turns in the head as possible with the recording amplifier available. In the corresponding reproduce heads, the wire may be finer and more turns may be desirable to obtain as much induced voltage as possible, but the winding is also optimized for the reproduce amplifier chosen. For multitrack record heads the winding size required may lead to serious space problems.

Cross-talk between the tracks of a multitrack head poses a continual problem. In recording, there is, of course, simple transformer action between the adjacent magnetic structures with their windings. The bodies of the heads themselves may be shielded from each other but the fringing flux at the gap may result in a transfer between adjacent cores which resembles transformer action. This may be influenced by the presence of the magnetic material of the tape as it moves past the head. For the reproduce head, there is, of course, also transformer pickup, but because of sensitivity of the head, it is also possible for one track to pick up the signal directly from the adjacent track. The flux source in this case is in the track rather than in the core structure. In pulse recording there is relatively little flux available in an adjacent track from the record current in a given track, but in carrier or FM recording, where there is always a large signal present in every track, a small cross-talk flux can produce a detectable recording (Davies [1961]). On reproduction, the transformer action cross-talk is usually limited to relatively high frequencies since these are the hardest to shield. Adjacent-track flux pickup in the reproducing process is usually limited to long-wavelength and hence low-frequency signals. An array of pole tips and gaps in a multi-track head is a fairly sophisticated magnetic structure and quite unusual means are sometimes needed to provide adequate shielding between tracks at the pole tips, both for record and reproduce.

Because flux-sensitive heads are used in specialized applications, their construction is likewise specialized. Modulator and variable-reluctance heads may resemble conventional $d\phi/dt$ heads quite closely except for extra windings and additional applied magnetic circuits.

The front surface of any magnetic head must be extremely smooth. This is essential for good head-tape contact, and for low head and tape wear. Since the typical recording head material is mechanically soft, it is difficult to produce a very high finish on such a surface. Since this soft material carries a very small gap which must be clearly defined, the process of polishing the head metal must avoid "smearing" the gap. The head lapping process is thus often a magnetic head manufacturer's most closely guarded secret. Most manufacturers have, by now, managed to work out individual processes which produce reasonably uniform results.

There have been many attempts to increase the number of tracks per inch across the tape with a view to using the tape surface more efficiently for storage. There are theoretical limits to how narrow a track can be used but these limits are seldom approached in any practical head. There is therefore considerable justification for attempting to increase the lateral track density.

A specific investigation of what can be done by straightforward methods to increase the track density was undertaken in 1964 by Jet Propulsion Laboratory (Clement [1964]). The investigation so far has concerned itself with determining the performance obtainable using commercial techniques to provide a large number of tracks per inch. Twelve tracks are fitted in this head onto quarter-inch tape which, when interleaved, would produce 24 tracks per quarter inch or 96 tracks per inch. Each track is 0.006 inch wide and the track-to-track pitch is 0.020 inch. When head elements are spaced this closely, interaction between heads becomes a severe problem as does the physical task of fitting the large number of coils and windings into the small space available. The results so far of the investigation show that at this track density reasonable cross-talk values (down 34 db) can be obtained for pulse recording, presumably at about 1,500 bits per lineal inch. The results show promise that the final goal of the program, which is to record at 100 tracks per inch at a density of 10,000 bits per lineal inch, may well be achieved.

9.0 RECENT DEVELOPMENTS - HIGH DENSITY RECORDING

Most tape recorders for spacecraft use record digital signals at a bit packing density of 1000 - 2000 bits per inch. If bi-phase recording is used, the number of flux reversals per inch is, respectively, 2000 and 4000 FRI. These densities are used because of several reasons:

1. Limitations on the tape surface
2. Limitations of record/playback head
3. Non-optimum playback circuit design
4. Conservatism in design

The writer, and Mr. Warren G. Clement, while at JPL, demonstrated in 1963 the capability of recording and reproducing a digital signal at 10,000 BPI, utilizing a standard Ampex FR 1400 and Memorex 62L recording tape. The raw signal amplified from the playback head and unreconstructed, exhibited considerable pulse crowding with loss of resolution, and broad regions of dropout (to 40% of peak signal level), extending over 50-100 bit periods. However, it was obvious that recording at this density was practical, provided that hard limiting was employed in the data reconstruction circuitry, and if the head/tape interface were to be improved.

Within the past month, the writer witnessed a demonstration at the Leach Corporation, Azusa, California of a standard Leach spacecraft recorder operating at a bi-phase bit packing density of 10,000 BPI (20,000 FRI). The tape used was 3M 991, and a 50 μ inch gap record and playback head manufactured by Applied Magnetics Corporation, Goleta, California was employed. The signal was recorded with a high-frequency bias (~ 5 MHz) for an input data rate of 1 MHz, with a bias/signal ratio of about 10:1. Hard limiting and clipping at about 40% of peak reproduced level was used in the reconstruction circuitry. At the high data rate, very few dropouts could be observed; Leach Corporation engineers claim to be able to meet the standard dropout rate of 10^{-5}. No special techniques are used to achieve this level of performance, other than careful attention to the head/tape area and selection of the proper playback operating levels.

It is apparent that pending some further development of this approach by the Leach Corporation, this high-density recording technique may be desirable for the Multiple Satellite program. To illustrate this point the following is a comparative listing of significant parameters of two recorders, one utilizing a recording density of 2000 BPI, "A", the other 10,000 BPI, "B".

Parameter	Recorder "A"	Recorder "B"
1. Recording density, BPI	2000	10,000
2. Total Storage, data bits	1.1×10^8	1.1×10^8
3. Tape length/1 track	4600 ft*	920 ft (B)
4. Tape length/4 tracks	1150 ft (A)	230 ft
5. Tape reversals/record cycle		
(A)	3	----
(B)	----	1
6. Recording	Serial	Serial
7. Electronic Switching	required in Rec. & PB	None
8. Electronics, sets of	4 ea, rec. & PB	1 ea, rec. & PB
9. Power, input	8 watts	5 watts
10. Weight	8.5 lbs	6.5 lbs

Obviously, several trade-offs between tape length, number of tracks, and sets of electronics are possible with recorder "B". The above comparison, however, was taken to illustrate that the entire data collection period can be recorded in one pass of recorder "B", with concomitant improvements in reliability because of the absence of switching functions. Reductions in required electronics also can be achieved by using recorder "B", thus producing net reductions in required power and in recorder weight.

---

* Unachievable for reasonable weight (8 - 10 lbs)

Appendix XVIII

MULTIPLE SATELLITE MAGNETIC DESIGN

1.0 INTRODUCTION

One of the primary objectives of the Multiple Satellites is the systematic and continuous measurement of the magnetic field in interplanetary space, the transition region and within the magnetosphere. This magnetic field can be as small as 5 gamma in the interplanetary region, and the spacecraft must be able to detect this magnetic field with reasonable accuracy. If the magnetic field contributed by the spacecraft design exceeds the field to be measured, but is predictable and steady, then measurement of the small interplanetary field would be possible. Detection of the interplanetary magnetic field, when the spacecraft field exceeds it, is generally not possible, since the spacecraft field is not predictable and steady within the accuracy required for the measurements. Therefore, it is necessary to maintain the spacecraft field, at a level sufficiently lower than the field to be measured. This level has been specified as 0.5 gamma which includes all causes (permanent and stray fields).

In the following paragraphs, terms are defined, design guidelines to achieve this high degree of magnetic cleanliness are presented, and preliminary individual component design requirements are established. Preliminary qualification and test procedures are also indicated. More detailed specification of the components and spacecraft requirements and the qualification procedures will be developed as the design becomes definitized. Much of the following information has been abstracted from "Magnetic Guidelines for Project Pioneer Experiments", Ames Research Center, January 25, 1965.

2.0 DEFINITION OF TERMS

1. Magnetic Material. Materials which have magnetic properties similar to iron, such as nickel, cobalt and many alloys of these three elements, are classed as magnetic materials. These materials are ferromagnetic, exhibit hysteresis, and have permeabilities which are dependent on field strength and temperature.

2. Non-Magnetic Material. Diamagnetic and paramagetic materials having permeabilities less than 1.02 are classed as non-magnetic. Paramagnetic materials usually do not show hysteresis, and have permeabilities essentially independent of

temperature and field strength.

3. Induced Fields. The external portion of the field associated with a part or assembly being magnetized by an external source is called the induced field. In general, the magnitude of the induced field may be considered directly proportional to the magnetizing field for ratios of body length to diameter up to 10 to 1 and magnetizing field intensities up to 0.5 oersted.

4. Stray Fields. The external magnetic fields of parts or assemblies which result from internal current elements are termed stray fields and may be considered as being approximately proportional to the current producing them. Excessive stray fields may occur in circuits of milliamperes or more where appreciable area is enclosed between forward and return path and in parts such as relays, solenoids, and inductors where discontinuities in the magnetic circuit exist.

5. Remanence or Perm. That portion of the external magnetic field that remains after removal of either an internal or external magnetizing field is considered Perm. The word Perm is a common-use contraction of permanent magnetization.

6. Magnetic History. The magnitude and configuration of the permanent magnetizations of a body at any point in time is the result of many factors such as:

(1) Previous magnetic exposure
(2) Configuration of the magnetic circuit
(3) Alloy composition and homogeneity
(4) Heat treatment
(5) Mechanical treatment
(6) Temperature.

The combined effect of these antecedents is commonly called the magnetic history of the body.

7. Component Magnetometer. A component magnetometer measures the magnitude and polarity of magnetic field strength along a given axis. The sensor is uniaxial, having a polar sensitivity following the cosine law.

8. Scalar Magnetometer. A scalar magnetometer measures only the magnitude of the magnetic field intensity. The scalar magnetometer is typified by devices using nuclear magnetic resonance principles.

9. Magnetic Noise. The sum of all unwanted magnetic signals originating aboard the spacecraft which are detectable by the magnetometer experiment and

specifically includes steady state or DC fields. For Multiple Satellites, only magnetic noise in the band of 0-25 cps will be considered to be of importance.

3.0 DESIGN GUIDELINES

3.1 GENERAL SPACECRAFT REQUIREMENTS

The goal of the magnetic control program is to reduce the level of the "magnetic noise" originating in the spacecraft to a value substantially less than the ambient intensities found in interplanetary space, that is less than 0.5 gamma over a 0-25 cps spectrum at the magnetometer sensor. The magnetic field from a static dipole source falls off as $1/r^3$. The desired field at the magnetometer sensor could be achieved, no matter what the spacecraft field is, by locating the sensor far enough from the spacecraft to reduce the field at the sensor. Practical limitations due to achievable boom lengths, etc., soon limit the separation distance between the sensor and spacecraft, however. Assuming a 0.5 gamma requirement at the magnetometer sensor, the spacecraft magnetic cleanliness requirement at a distance three feet from the centroid (a standard distance for establishing the magnetic specifications) is given as a function boom length in Figure 1. Based upon preliminary estimates of the achievable magnetic cleanliness of the spacecraft and discussions with E. J. Iufer (A.R.C. Systems Division, responsible for the Pioneer magnetic cleanliness program), boom lengths on the order of 6 to 8 feet will be required. The allowable minimum field at three feet is thus 4 to 10 gamma. This requirement will be distributed among the basic subsystem in Section 4.3.

Magnetic design consideration should start with the component, subsystem and system layouts and material selection to prevent design decisions which neglect magnetic considerations and thereby create future magnetics problems. The following section on non-magnetic materials, shielding, component location and orientation have been developed to provide general design guidelines for magnetically clean spacecraft. It is recommended that reference 1, which contains additional information on this subject, be referred to for necessary details.

3.2 NON-MAGNETIC MATERIALS

The first step in minimizing the magnetic field produced by an experimental package is the use, whenever possible, of non-magnetic materials in place of materials with high magnetic susceptances. In general, no magnetic materials or parts shall be used when a reliable non-magnetic substitute can be found. Each part and material used in construction shall be magnetically inspected.

Maximum Allowable Spacecraft Magnetic Field
As a Function of Sensor Boom Length

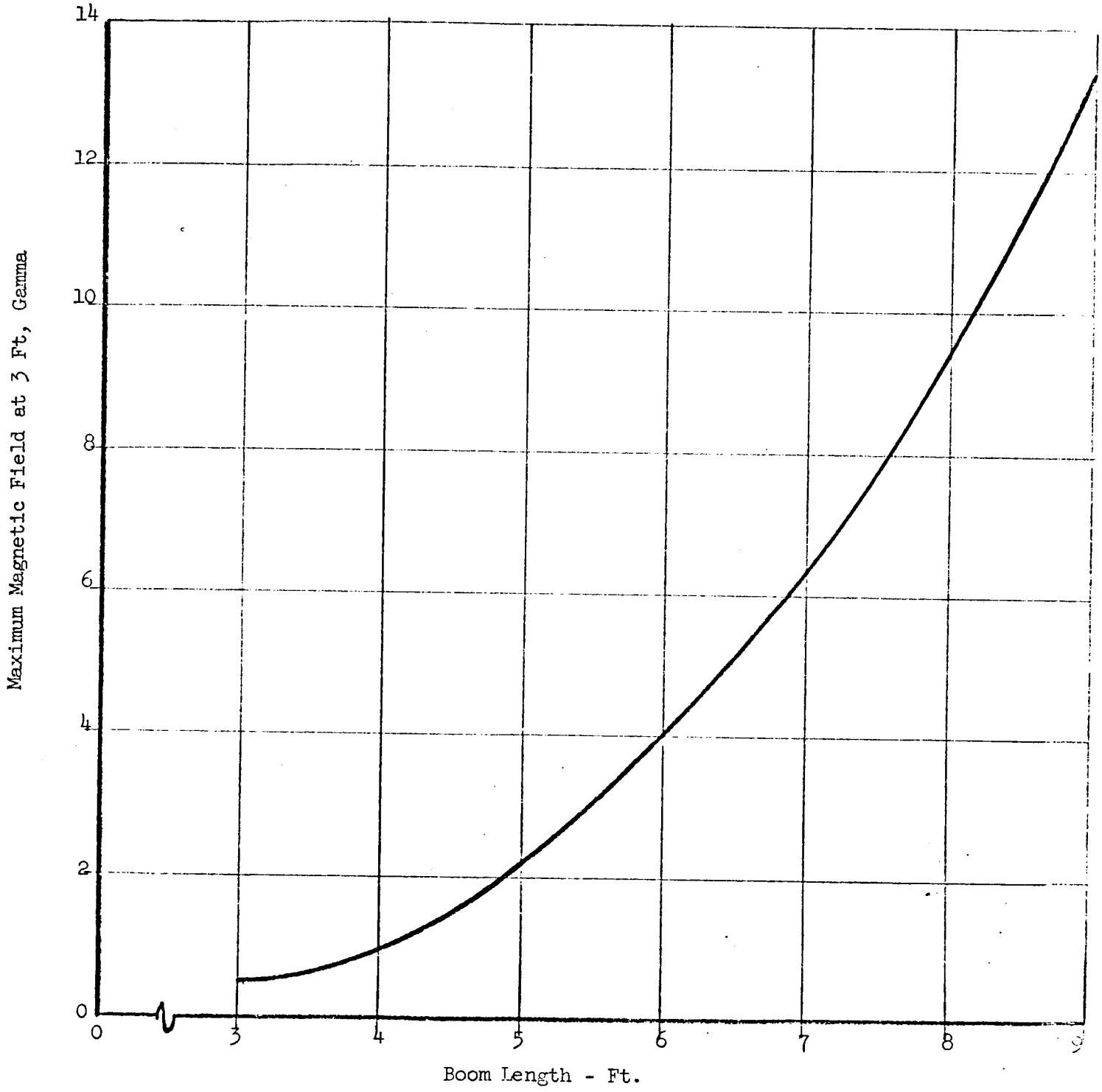

Figure 1

Non-magnetic stock hardware is available from several sources. The non-magnetic property should be clearly indicated on all purchase orders for these materials. Communicating this requirement to the vendor will not guarantee magnetic cleanliness. It will be necessary to magnetically inspect parts and materials on a 100% basis.

Only non-magnetic materials shall be used for fabricating parts. Fabricated parts may not be considered non-magnetic unless magnetically inspected. Chips, fillers, and machine shop lubricants have been found to cause magnetic contamination.

Lists of high reliability electrical or electronic parts which are preferred have been prepared. A preferred parts list from the Pioneer program including vendor lists of transistors, resistors, diodes, cable and wire, connectors, capacitors, transformers and conductors, crystals, switches, relays, fuses, etc. is available. In the event that a circuit function cannot be achieved by a non-magnetic part, reduction in the degree of magnetic contamination can be achieved by special selection. Parts from certain vendors may be less magnetic than parts from others. Certain parts within a given lot may be appreciably less magnetic than the rest. Powder iron cores should not be used. Stray fields from inductors and electromechanical devices can be reduced by increasing the efficiency of the magnetic circuit. Substantial variations exist among commercially available parts of a single type.

Tables 1, 2 and 3 list materials which have been magnetically checked by JPL after exposure to high intensity fields in a solenoid. Samples of each material 3/8 inch diameter by 2 inch long were placed in 1000 and 100 oersted fields. After exposure, the magnetic field was measured at a distance of one foot from the sample. The tables list the magnetic field density measured in gammas. Table 1 is a list of preferred metals. Table 2 is a list of borderline materials which should be avoided, if possible, and metals in Table 3 should be avoided entirely. Included in Table 1 are materials from a Pioneer non-magnetic materials list. These are assumed to be non-magnetic, but some may be borderline materials. They have permeabilities less than 1.02 and are valid for temperatures of -40°C to +50°C and H = 0.5 oersted. Other acceptable materials are all ceramics except those containing iron oxides and generally all polymeric materials. For additional data on materials see Pages 322, 324 and 325 of Reference 1.

The most highly magnetically susceptible material listed in Table 3 is nickel. Unfortunately, nickel is the most preferred material for interconnects in welded electronic modules because of its excellent thermal, mechanical and electrical

NON-MAGNETIC ALLOYS

Metal	Field (γ) After Exposure to Field Intensity of	
Stainless Steel (18-8*)		
CPT 193*		
CPT 195*		
Non-Magnetic Steel		
CPT 790*		
CPT 320*		
CPT 350*		
CK-20 (572-BB)	0	0
CDC 720	0	0
Crobalt Tool Steel	0	0
RA-600	0	0
Incoloy 800	0	0
Hardsteel HD-32M	0	0
Chromel D	0	0
Copel	0	0
Alloy 843	0	0
Chromel A	0	0
Firth Brown NMCW	0	0
Firth Brown FNMC	1	.8
OFHC Copper	0	0
Alloy 53 (Coast Metals)	0	0
Hadfield 14% MN A-128-33	.8	0
Kennametal K-601	0	0
Chromel AA	0	0
17-14 CuMo	0	0
Hella 8302 MN Steel	0	0
22-4-9 SS	0	0
Monel k-500	0	0
Resista PH Hi MN Steel	0	0
Incone X-750	0	0
Alloy 64 (Coast Metals)	0	0
Inconel Alloy 718	0	0
Zinc	0	0
Inconel Alloy 700	0	0
VX-9338	0	0
Inconel Alloy 722	0	0
Nochrome 5	0	0
Haynes Star J Alloy	0	0
Inconel Alloy 901	0	0
Haynes Alloy No. 31	0	0
Inconel 600	.5	.5
Inconel X750	0	0
Haynes R-41	0	0
Hastelloy Alloy B	0	0
Haynes Alloy No. 25	0	0
Haynes Alloy No. 12	0	0
403 Monel	0	0

NON-MAGNETIC ALLOYS

Metal		Field (γ) After Exposure to Field Intensity of	
Hastelloy Alloy C		0	0
Alloy No. 90		0	0
Haynes 98M2		0 0	0
Alloy No. 800		0	0
Alloy No. 30		0	0
Calo 74117		1	1
Pyro 74302		0	0
Alloy No. 45		0	0
Alloy No. 60		0	0
Alloy No. 180		0	0
Haynes Stellite Alloy No. 21		0	0
Haynes Stellite Alloy No. 19		0	0
Haynes Stellite Alloy No. 3		0	0
Jessop No. 9	CPT 265*		
Jessop No. 200	CPT 270*		
Jessop No. 200	CPT 275*		
Dualoy	CPT 310		
	CPT 315		
Eligiloy			
Thermaloys 30	CPT 815		

NOTE: (1) Readings taken at distance of 1 foot
(2) * Non-magnetic materials from Ames Research Center Pioneer Program

Table 2

BORDERLINE ALLOYS

Metal	Field (γ) After Exposure to Field Intensity of 10^3 Oe	10^2 Oe
Stainless Steel 303	8	0
304	23	1.5
321	9	3
RA 330	2	2
S-28 (Coast Metals)	6	4
Ni-Resist D-2	4.5	3
Ni-Resist D-2B	2	2
Haynes Alloy No. 3	2	1.5
Haynes Alloy No. 6B	3	3
Haynes Alloy No. 6	6	4
Haynes Alloy No. 10	3.5	4

NOTE: Readings taken at distance of 1 foot from sample 3/8 inch diameter x 2 inches long

Table 3

MAGNETIC ALLOYS

Metal	Field (γ) After Exposure to Field Intensity of 10^3 Oe	10^2 Oe
Stainless Steel 410	525	195
416	525	193
440	990	169
Monel	125	138
Nickel	1250	710
Iron Oilite	575	295
Steel 4130HT	610	282
4140	725	177
4340N	490	170
Cold Rolled	285	113
Drill Rod	540	238
Graph-Mo	525	161
Nitralloy	400	151
Screw Rod	150	56
Starrett	545	358
Armco Iron	77	33
Invar	-	67.5
Alloy 56 (Coast Metals)	21	20
Kennametal 3411	540	78
Kennametal 3109	645	45
Kennametal 3047	570	57
Kennametal K-151A	100	12
Kennametal K-162B	170	35
Kennametal K-6	380	8.5
Kentanium K-165	90	6
Kentanium K-138A	16	25
Kovar	225	14

NOTE: Readings taken at distance of 1 foot from sample 3/8 inch diameter x 2 inches long

properties. It is a matter of record that the greatest magnetic contribution in any scientific space probe to date has been the welded cordwood modules which comprise the electronics systems. Goddard Space Flight Center and other agencies have advocated the use of Alloy 180 as a fairly non-magnetic replacement for the nickel ribbon. Some welding experts, however, feel that Alloy 180 is an unreliable material because of problems with weld joint embrittlement. This is a problem that is difficult to ascertain with the usual optical inspection techniques used on the assembly line. Careful quality control during manufacture is required. All Alloy 180 material used shall be procured to ARL Specification 301 or its equivalent. Soldered cordwood could be used, but does not allow the component packaging density concordant with the high degree of reliability attained with the welded module. It is recommended that other non-magnetic interconnect materials be investigated and that they should be required for use on all welded assemblies in the Multiple Satellite. Until more suitable materials are discovered, however, Alloy 180 or copper are recommended.

When using cordwood modular construction leads should be clipped to 1/32 to 1/16 inch in length. Parts having leads of Kovar (Ni 29%, Fe 53%, Co 17%) Dumet (Ni 42%, Fe 58%) or nickel generally exhibit dipole moments parallel to these leads even after clipping. To achieve the lowest overall moment for the scientific instrument, attention should be given to distributing these parts equally along three axes. The rules of linear superposition generally apply.

Another significant offender on Table 3 and an extremely common material is Kovar. Virtually all glass to metal seals use Kovar because its temperature coefficient of expansion is almost identical to that of glass. There appears to be no satisfactory replacement for Kovar as a glass to metal seal material; therefore, care should be taken to minimize its use. All transistor header and diodes use Kovar leads. If care if exercised and the leads are cut off as close to the components as possible, consistent with good reliability practice, problem should be significantly reduced. For headers sometimes required in hermetic seal applications, the Harrison Seal Corporation is now advertising a non-magnetic, hermetic, header for spaceborn applications.

The second greatest offender after welded cordwood modules found on today's space probes are miniature relays. In the interests of conserving power, many designers will use a magnetic latching relay. These devices change state on a pulse basis, magnetically latch, and do not require constant excitation power. Because of this unique feature, they are generally used in large numbers on space-

Reduce the effective area of current loops to zero. This may be accomplished by using coaxial or twisted pairs of conductors to handle both forward and return current in any circuit handling more than 5.0 milliamperes at 0-25 cps. (Experience indicates that 3 twists/inch is optimum). This will require close attention to conductor placement in wiring harness and in connectors. The separation between the forward and the return path imposed by the thickness of a printed circuit board has been found to be unacceptable in certain instances.

Reduce the stray field by compensation. This technique applies the principle of superposition. In a region that is free of iron, the total stray field at a point is equal to the vector sum of the component stray fields. Consequently, stray fields can be reduced by deliberately producing a magnetic field that is equal and opposite to the undesired field. To obtain the smallest resultant, the following conditions must also be met:

(1) The magnetic moment of each current loop must be as small as possible.

(2) The distance between the current loop and the compensating loop should be as small as possible.

(3) The magnetic moments of the two loops must be equal and opposite.

In practice, the compensating loop cannot be superimposed upon the current loop. In those cases where high levels of compensation are needed, it is useful to split the current between two compensating loops, one on each side of the current loop.

Mathematically, the fields around an opposed pair of current loops may be found by a spherical harmonic analysis (or expansion). If the current pairs perfectly cancel, they will produce no net field. In practice, such current pairs will not perfectly match and some net field will result. If a large number of these closely matched loop pairs are combined in random orientations, the total net field will approach zero. (As more loop pairs are added, the net field will approach more closely to null.) In practice, the degree of compensation using a single loop will range from 50 to 90%.

Leads carrying currents greater than 5 milliamperes should be routed so that any magnetic material present will not form a core for the current loop. A notable exception to this rule is the employment of required toroidal inductors. Separate signals and unrelated types of power should have separate two-wire transmission systems.

If it is necessary to pass a circuit through a magnetic enclosure, the two legs of the circuit must be as close together as possible and pass through the same hole.

Part groups such as electromechanical devices which carry common currents can frequently be oriented to obtain at least partial cancellation of stray fields.

The number of ground loops should be minimized. Chassis grounds will be combined with circuit grounds at the common system ground point inside the spacecraft. The chassis ground connection brought out from the experiment package should carry no current and be isolated from all power and signal circuits.

3.4 MAGNETIC SHIELDING CONSIDERATIONS

It is most desirable to produce a magnetically-clean spacecraft through: first, elimination of magnetic fields; second, compensation of the fields; and third, magnetic shielding. Only elimination and compensation were used in the design of Pioneer. There was no need to resort to shielding for this spacecraft. Because of the current state-of-the-art of shielding, it should not be considered except for applications for reducing the external field of permanent magnets. Shielding is useful if the magnet is small and is likely to be less stable than the magnetic properties of the shield. Shielding is not a cure-all. Improper application as well as improper design can be detrimental. Discontinuities in the magnetic circuit such as air gaps or stress and the degree of departure from a spheroidal shape seriously degrade the effectiveness of a shield. The attenuation factor of a shield is influenced by conditions such as external field intensities, mechanical and thermal shock, temperature and stress.

Once it is determined that shielding is the only solution, several additional factors must be considered. Because shielding material is magnetic and will have remanence, the shield can introduce instabilities. By only shielding the offending device rather than the complete subassembly, instability can be reduced since the amount of magnetic material is less.

The shielding factor, s, or effectiveness, is a function of the shield dimensions and the effective permeability of the shielding material:

$$s \propto \frac{\mu \quad T}{L},$$

where μ is the effective permeability, T is the thickness, and L the outside dimension of the shield.

Although shielding effectiveness increases with the thickness of the shield, it has been found in practice that the structural rigidity of the shield to prevent distortion and stresses is a more important consideration in small shield design. The materials most frequently used for shielding are the mumetals or molypermalloys. These high nickel alloys are mechanically sensitive in their magnetic characteristics and must be handled with some care after their fabrication and subsequent annealing. Materials of 0.025 and 0.050 inch thicknesses have been used for shielding spacecraft components. The 0.050 inch material is favored in most applications for mechanical stability.

The construction of shields from these materials requires high temperature annealing in a hydrogen atmosphere after all fabrication work such as welding, bending, drilling, grinding, etc. Bends should have as large a radius as possible, and welding should be done with the shield material as the filler.

Although theoretical shielding factors of several thousand should be possible, in practice, shielding factors of less than a hundred are generally attained. The reason for these low efficiencies is not completely known, but in part is due to the large openings necessary in the shield for the passage of leads or to facilitate installation of the shield and the fact that the shield material probably becomes magnetically saturated due to the proximity of the source of field to the shield.

In tests of a five-sided rectangular shield of mumetal to shield a miniature latching relay, shielding factors of 12 to 20 were obtained. In this case, the shields were made so small as to inhibit the operation of the relay by short circuiting the relay magnetic circuit. Where a magnetic circuit is being shielded, it is important that adequate space be left between the device being shielded and the inside surface of the shield.

Partial shields have also been used where weight is critical. These shields which have been used with relays and circulator switches have shielding factors from two or three to about ten, depending on the extent of the partial shield. Mumetal and moly permalloy in a 0.050 inch sheet weigh about 2.4 lbs/sq. ft. In the case of the mumetal shield used to replace the crystal type case on the miniature latching relay, the weight was increased by 0.35 ounce.

Because of the uncertainties of shielding effectiveness, every effort should be made to improve the designof magnetic devices and eliminate unnecessary magnetic material so that the necessity for shielding is reduced. It is virtually

impossible to define curves of shield weight versus field attenuation as it varies widely with shield volume and configuration.

3.5 COMPONENT LOCATION AND ORIENTATION CONSIDERATIONS

Subsystem and component location and orientation within the spacecraft from a magnetic standpoint should be considered beginning with the preliminary layouts. In general, dirty parts, or those with large currents (tenths of amps to amps) which will produce large stray fields should be located as far from the sensor as possible, on the side of the spacecraft opposite the sensor boom. Those components drawing milliamps may be located in the spacecraft region close to the sensor boom. As the program progresses into design layout and the magnetic performance of the various components becomes available, more definitive location specifications can be provided.

Because of the measurement of the X and Y field components by alternate sensors on a spinning vehicle (the Z axis is the spin axis), it is possible to establish the radial component of the spacecraft produced field. Therefore, it is desirable to orient components so that their largest field components are in the X and Y directions while keeping the Z-axis component to a minimum. The X-Y components may be allowed to be five times the Z axis component for equivalent sensor accuracies. Because parts usually have magnetic field components three to five times one axis over another, judicial orientation of the parts should be undertaken to achieve the X-Y-Z axis relationships prescribed above.

4.0 PRELIMINARY SUBSYSTEM SPECIFICATIONS

It is not possible to specify in detail the magnetic requirements for each subsystem at this time, but design goals are specified in Table 4 based upon the overall spacecraft requirement and potentially achievable subsystem capabilities. These goals are not firm and are not meant to either severely restrict component design or provide an unreasonably easy design goal. During the design phase as more data on subsystem capability becomes available, these preliminary goals will be revised.

The preliminary specs are based on using the boom length and allowable field at the sensor to establish the magnetic moment at the spacecraft centroid. Then, based on the number of major experiments and components, and the potential magnetic contribution of each, the magnetic allowance is distributed among the components. Linear superposition of the component effects is assumed.

Table 4

MAGNETIC DESIGN GOALS

SUBSYSTEM	DESIGN GOAL (γ at 3 ft) After 25 Gauss Exposure	Stray Field DC thru 25 CPS	Depermed Condition
1. Pallet			
a. Structure	0	0	0
b. Attitude Control (includes electronics and valve relays)	2	0.2	0.5
c. Command receiver	2	0.2	0.5
2. Satellite			
a. Structure	0	0	0
b. Separation jets (extended solid rockets)	2	0	0.5
c. Transmitter	2	0.2	0.5
d. Receiver and command decoder	2	0.2	0.5
e. Data processor, including tape recoder	2	0.2	0.5
f. Thermal control system (passive)	0	0	0
g. Power distribution and conditioning system	2	0.2	0.5
h. Plasma instruments	2	0.2	0.5
i. Magnetometer (electronics)	2	0.2	0.5

(Typically the magnetic specification for electroinics is 7 CGS units--dyne-cm/gauss).

The magnetic acceptance criteria for each component of the satellite is based upon the total magnetic noise permitted at the magnetometer without mission degradation. However, in view of the strict magnetic specification imposed by the mission and the research nature of the experiments, it will be the responsibility of each experimenter and component designer to achieve the absolute minimum practical magnetic noise level for units under his control.

It will be noticed that no special privileges have been provided the pallet when specifying the magnetic requirements even though the only effect of the pallet will be to induce a magnetic field into the separate satellites. This has been done to maintain the entire spacecraft design at a high level of magnetic cleanliness and keep the induced field to a minimum. But should the pallet requirements be very difficult to meet (e.g., dueto the requirement for ACS relays), they may be reduced.

5.0 PRELIMINARY QUALIFICATION PROCEDURES

Preliminary qualification procedures are presented here primarily for information purposes, although they may be useful in making the initial parts selections. The watchword in the acceptance of parts and subsystems is measure everything as often as possible to avoid inadvertant acceptance of magnetic parts. Each part should be re-measured every time something is done to it. All parts, even "non-magnetic" parts should be subjected to 100% receiving inspection.

It will be necessary to magnetically test each and every part placed aboard spacecraft. The magnetic characteristics listed in order of importance are:

(1) Perm fields
(2) Stray fields
(3) Induced fields

In view of the strict limitation placed on Perm and the low level of ambient field during the mission, the induced magnetization characteristics may be generally disregarded.

5.1 INSTRUMENTATION

The magnetometry set-up used for surveying parts must be able to measure a change of 5 micro oersted (1/2 gamma) and have a stable Earth's field compensator of zero suppression. Instruments meeting this requirement are commercially available. Measurements at this level will require control of the ambient noise in the sensor area. A practical solution to this problem is to very rigidly orient the magnetometer sensor in the vertical direction. The sensor is then enclosed in a square or circular tube mounted horizontally normal to the ambient magnetic meridian. This tubing will shield the sensor from ambient noise. This shield can be fabricated from Mu metal sheet approximately 0.030 inch thick, rolled or brake formed and joined by continuous weld. It is important that the alloy of the weld be the same as the sheet to prevent dicontinuity in the flux path. The dimensions of the shield may be nominally 8" in diameter and 24" long. After fabrication the shield must be thoroughly cleansed, and annealed in an oxygen-free dry hydrogen atmosphere (dew point below -40°F) for two hours at 2050°F and slowly cooled per vendors recommendations. All stressing after anneal should be avoided.

Mu metal is available from the Alleghany Ludlum Co. and is a 79% nickel-iron non-oriented alloy. Hi Mu 80, available from Carpenter Steel Company is equally suitable.

5.2 PROCEDURE

After the axis of the shield is oriented east and west the output of the magnetometer is biased to zero and the most sensitive range is selected. The part or parts to be inspected are held over or slowly passed over the sensor and the magnetometer reading noted. The measurement distance should be standardized. A distance of 3 inches is preferred for single parts.

In the event that the ambient magnetic field changes rapidly enough as to present a nuisance, it is suggested that a filter be added to the output circuitry of the magnetometer having a pass band of .01 to 1 cps. The parts may then be moved over the sensor at a velocity that will produce a signal in this pass band. This technique has been tested and found to be effective after little experimentation.

The residual induction field in the shield will be fairly small. It is therefore possible that a magnetic specimen would not be discovered if it had been fully depermed. To avoid this hazard, all parts should be exposed to a steady state magnetic field of approximately 25 gauss parallel to the long axis of the specimen prior to the magnetic screening test. This pre-treatment will greatly increase the effectiveness of the magnetometer to find low levels of contamination.

Those parts which indicate a Perm but pass the screening test will be in a state of unstable remanence which is not typical. To correct this situation, the parts may be exposed to an AC magnetic field of 25-50 gauss and slowly removed so as to cycle the parts over a hysteresis loop of slowly decreasing area. The presence of Earth's field during this treatment will result in a Perm due to the offset in the induction field. The value of the Perm produced by this method should be approximately 1/5 of that produced by the 25 gauss DC field exposure. A Perm of this value is tentatively though to be fairly typical of the post launch Perm of the Spacecraft.

Stray fields may be measured by noting the change of magnetic field intensity due to an operating or failure mode. These tests may be conducted in Earth's field where the ambient noise level is low. The test set-up should be

REFERENCES

1. J. G. Bastow, "Proceedings of the Magnetics Workshop", JPL TM No33-216, March 30, April 1, 1965.

2. "Magnetic Guidelines on Project Pioneer Experiments", Ames Research Center, January 25, 1965.

Appendix XIX

RELIABILITY CRITERIA AND ANALYSES

1.0 INTRODUCTION

The mission of the Multiple Satellite program dictates that the initial design be characterized by a high level of inherent reliability. This objective shall be considered in performing reliability tradeoff studies and making hardware and configuration selections. The reliability requirement shall be met through the utilization of proven state-of-the-art components with known flight qualification status and failure free test histories, wherever possible. This basic feature shall be complemented by maintaining design simplicity, prudent usage of derating and safety factors, selective application of parallel redundancy in critical components, and the imposition of mandatory reliability design practices.

The following sections present reliability goals, preliminary budget, and reliability related design considerations.

2.0 RELIABILITY GOAL AND PRELIMINARY BUDGET

2.1 RELIABILITY GOAL

Reliability shall be a primary design consideration and maximized consistent with performance and cost. For the purpose of this study, the effective life of the array of four satellites should have a high probability of exceeding three months. As a design goal, the reliability figure for the system of four satellites to function over a period of three months shall be 0.70.

2.2 MISSION SUCCESS

Mission success, for the Multiple Satellite Mission in terms of hardware operation is defined as follows:

<u>Pallet</u>

Structure	Normal operation until after satellite deployment
Thermal Control	Not to exceed design limits until after satellite deployment
Electrical Power	Normal power until after satellite deployment

Command Receiver	Normal operation until after satellite deployment
Deployment	Provide at least 500 km separation between satellites and not more than 15,000 km after 6 months
Attitude Control	Align all satellite spin axes within $\pm 10^{\circ}$ of the normal of the ecliptic plane

Satellites

Structure	Normal operation for 6 months
Thermal Control	Not to exceed design limits for 6 months
Data Control	Normal down link data stream after 6 months
Electrical Power	Normal operation after 6 months
Power Distribution	Sufficient power available at all necessary instruments and subsystems for 6 months
Attitude Control	Coning shall be less than $\pm 1^{\circ}$; aspect sensing with $\pm 1^{\circ}$; spin rate between 50 and 70 rpm

Instruments

Plasma Detectors	
(a) Peak velocity and ion flux detectors	Successful operation for at least three months
(b) Plasma spectrum detector	All channels operate for at least 3 months; 3/4 channels operate for 6 months
Magnetometer(s)	Successful operation for at least 3 months

2.3 PRELIMINARY RELIABILITY BUDGET

A preliminary reliability budget has been prepared to meet the reliability goal. Table 1 summarizes the budget.

Table 1

APPORTIONMENT FOR MULTIPLE SATELLITE

Subsystem or Event	Quantity/ System	Reliability Goal	Reliability Objective
*Thorad	1	.9705	.9705

Subsystem or Event	Quantity/ System	Reliability Goal	Reliability Objective
Multiple Satellite System During Boost	1	.9967	.9960
Pallet			
Structure	1	.9958	.9954
Thermal Control	1	.9975	.9963
Command Receiver	1	.9802	.9802
Antenna Omni	1	.9958	.9952
Battery 100 Watt	1	.9900	.9900
PCDU	1	.9794	.9754
Cabling	1	.9950	.9945
ACS	1	.9713	.9713
Deployment			
Spin-Off Release	2	.9925	.9925
Solid Motors	4	.9950	.9950
Satellites			
Structure	4	.9971	.9971
Thermal	4	.9967	.9967
Data System			
Data Processor	4	.9934	.9868
Tape Recorder	4	.9673	.9051
Command Rec-Decoder	4	.9876	.9730
Transponder	4	.9967	.9894
Transmitter	4	.9934	.9848
Antenna, Fan	4	.9917	.9917
Power System			
Solar Cells	4	.9900	.9802
Battery	4	.9803	.9764
PCDU	4	.9774	.9730
Cabling	4	.9950	.9945
Precession Dumper	4	.9876	.9514
Instruments			
*Plasma Ion Flux Detector	8	.9835	.9835
*Magnetometer	4	.9786	.9786
*Peak Velocity	8	.9876	.9876
*Plasma Spectrum	4	.9835	.9835
*GFE			
	Overall	.70	

This preliminary reliability budget is based on a reliability goal of .70 for the mission, including: (a) the pallet being injected into the proper orbit, operating for up to five days, being injected into the and providing proper orientation and deployment of the satellites into their respective orbits; and, (b) the satellites, their communications and the scientific instruments performing for the ensuing 3 months. However, the satellites will be designed for one year's operation. Potential difficulties in meeting the individual goals may arise for some of the subsystems. The reported design goal for the Thorad by its manufacturer (0.85) is less than that assigned in Table 1. Also, there may be difficulty in meeting the tape recorder and separation system goals. On the other hand, the allocated pallet ACS goal may be less than its true reliability potential.

The reliability apportionment is based on a model which includes the complexity and growth potential of each subsystem. Factors are allocated to the relative complexity and growth potential of the subsystems. Low factors indicate simple design and relatively little room for reliability improvement; (hence, higher reliability goals). Higher factors indicate necessarily more complex design and relatively greater opportunity for reliability improvement (hence, lower reliability goals). The calculation of reliability goals assumed that all subsystems operated in series and any failure would abort the mission. A secondary reliability allocation is presented in Table 1 entitled Reliability Objectives which includes the relative importance of the subsystems for mission success, in addition to complexity and growth potential. The Reliability Objective deflates the Reliability goal by taking into account that some component failure modes are not critical to mission success. The importance factor associated with a subsystem is given a value of one when virtually any failure mode would result in a mission abort. Higher values are assigned to those subsystems whose modes of failure would degrade the mission but not abort it. The less likely a failure would abort the mission, the higher the importance factor assigned. When the importance factor is inserted, the resulting reliability budget is reduced. This budget may be interpreted as indicating a mission success rate of 70% can be obtained if the probability that all subsystems operate properly is the same as that listed in the table. The reliability effort will concentrate on meeting the reliability objectives.

As the design of each subsystem becomes more definite, updated apportionments will be made and potential reliability problems assessed.

3.0 RELIABILITY ANALYSES

Reliability monitoring and analysis will be performed continually during the design phase in order to meet the design goal established. These analyses will be presented in later reports. Particular emphasis during these analyses will be placed upon avoiding the use of design concepts or operational sequences whereby the failure of a single component can result in complete loss of the mission. Each potential failure mode will be critically examined and the effects of these failure modes on mission objectives assessed. Adherence to the apportioned reliabilities given in Table 1 will be carefully policed.

4.0 DESIGN RELIABILITY PRACTICES

4.1 INTRODUCTION

This section states the policy to be followed for the creation and application of standard, reliability-related, Multiple Satellite design practices. In addition, it describes the scope of practices and procedures to be followed when taking necessary exception to these standard practices. The design practices are intended to include design guidelines, rules and techniques which, in general, should pervade all Multiple Satellite designs so that high design reliability is maintained. These practices will reflect experience gained in other space flight programs, announced ARC design philosophies, program management judgments, and system engineering analysis; and will generally be an indication of the stringent environmental, reliability, and long-life requirements of the Multiple Satellite program.

4.2 INITIATION OF DESIGN RELIABILITY PRACTICES AND EXCEPTIONS

A design practice should be initiated each time a design principle is applied which has general applicability and is consistent with the Multiple Satellite mission objectives. All practices shall be submitted to the Systems Analysis Task Manager for approval. The submittal shall include a concise statement of the practice to be followed, motivation for creating the practice, and evidence substantiating its validity.

Once established, a design practice becomes a mandatory characteristic of all designs. However, due to certain constraints, it may be clearly desirable to violate an established practice. This eventuality is anticipated and the procedure for taking exception to an accepted practice is as follows. The exception shall be submitted to the System Analysis Task Manager in writing with

substantiating evidence for the advisability of the action. Approval or disapproval will determine the ultimate design course of action.

4.3 PARTS AND MATERIALS

Proven, state-of-the-art parts and materials will be used in the Multiple Satellite design wherever possible. Component parts and materials lists have been compiled for parts and materials having high reliability and low magnetic field characteristics. Vendor data on candidate major components and subsystems are currently being compiled and evaluated; these data will be presented in a later section. The following derating plan will be employed to contribute to the fulfillment of the one year mission requirement:

Component	Derating Factor
Capacitor	50%
Diodes (Silicon)	60%
Inductors	50%
Resistors	40%
Transformers	50%
Transistors (Silicon)	40%
Integrated Circuits	75%

Integrated circuits and solid state electronics should be utilized whenever possible.

Materials which are classified as corrosive, toxic, flammable, or explosive, shall be avoided.

4.4 EQUIPMENT DESIGN CONSIDERATIONS

1. Generally, the use of electrical connectors should be avoided; however, where design dictates their use, connectors such as the Apollo-approved, MC 414-0365, connectors will be used.

2. Moving parts which, as a part of their function, operate on a duty cycle, or some recurring activity, should be kept to a minimum. Those movable parts which are required to operate for only one cycle are to be hermetically sealed, if possible, free of moisture prior to sealing, dust free, and well lubricated.

3. For all moving mating surfaces, direct contact between the same or similar metal should be avoided where possible. Where direct contact is necessary, approved dissimilar metal surfaces should be used.

4. If loading permits, the use of metal to non-metallic mating surfaces is indicated, such as steel-Teflon. Where the loading does not permit this type of mating surface, phosphate, oxide, or chromate passivating coating should be used, when these are thermodynamically and/or vacuum stable.

5. Solid lubricants such as molybdenium disulfide, turgsten disulfide, or niobium diselinide should be used. The latter material possesses the best combination of electrical conductivity and high-vacuum/high-temperature stability. Graphite lubricants shall not be used.

6. For duty cycled moving parts, additional precautions are indicated

   (a) Filled, porous metal surfaces (e.g., Teflon, Kel-F, or niobium disilenide in porous steel or brass metal bearing surfaces) should be used to minimize metal surface contact areas.

   (b) Sufficient protection to eliminate collection of dust should be provided where long interval transient duty cycle is involved.

7. A minimum use of tight tolerances for all moving parts should be maintained.

8. Redundancies in design should be incorporated when feasibility and the overall design requirements permit.

9. All attachment devices of the design shall be shakeproof.

10. Large flat plates which can diaphragm and generate acoustical noise should be avoided.

11. Only Class 1 and 2 packaging, with no unsupported parts, should be employed.

12. A minimum of 1.3 should be imposed as a design safety factor, and an overall margin of safety shall be adequately maintained.

13. Components selected should have end-of-life expectancy well beyond the one-year service requirement and two-year shelf life.

Appendix XX

ELECTROMAGNETIC INTERFERENCE CONTROL

Beginning early in the design phase and continuing throughout the Multiple Satellite Program, considerable attention must be given to electromagnetic interference control. Electromagnetic interference produced by the spacecraft will be controlled to eliminate undesired malfunctioning of all electronic and electrical subsystems in or associated with the spacecraft. This requirement applies to the entire frequency range of the installed subsystems, including when operating with their installed antennas and when performing their intended radiation or reception pattern. Specific attention will be given to:

1. equipment problems where EMI can adversely affect individual equipments during manufacture, checkout, or operation;
2. vehicle and stage problems when EMI affects boost vehicle operation causing undesirable response or degradation of performance; and
3. facility and environment problems where EMI affects manufacturing, assembly, checkout, operation and testing.

EMI control has been the subject of considerable previous work, e.g. MIL-E-60516, MIL-STD-826; Apollo Program, NHB 5320.3, Electromagnetic Compatibility Principles and Practices, etc. These and related documents will be used to guide EMI control in the Multiple Satellite Program.

Basic EMI control features, such as grounding, bonding, shielding packaging, filtering, and cable design, will be considered during the design; alternate approaches will be evaluated as they arise. A consistent grounding approach must be used as the most effective means of controlling EMI. The basic premise on this approach maintains all portions of the system, (electrical, mechanical, or structural) at the same potential by providing separate, non-redundant low-impedance paths to a single grounding reference, so that the ground potential is equalized throughout the system. Therefore, in the course of satellite preliminary design, a consistent grounding concept will be established for

component interaction. Bonding will be accomplished in accordance with the requirements of MIL B-5087 and will be provided for current return paths, antenna installation, and to provide equal potential between all equipment and the basic structure of the spacecraft. Interference control filters shall be in accordance with MIL-F-15733.

From the packaging and equipment interfacing considerations, it is recommended that individual interference source suppression and shielding be on an elemental chassis or black box basis. Using this approach includes three actions:

1. Prevent the generation of signals that are undesirable at the source. In many cases, it will be found easier to prevent the generation of interference than to prevent transmittal to susceptible circuits. It is important to recognize the factors which contribute to the generation of EMI so that prevention can be made at the outset on a scientific basis. These factors include:
   a. waveform
   b. voltage, current, and impedance levels, and
   c. rise time and duration of voltage changes.
2. Prevent any residual interference remaining after the above steps from being either conducted or radiated from the generating circuit to any of the susceptible circuits or the environment.
3. Prevent any remaining interference which reaches the susceptible circuit from adversely affecting performance.

The unique requirements of this program, i.e., multiple satellites operating in close proximity, will be considered when selecting frequencies and bandwidths as well as when performing the EMI control functions.

A complete design guide or specification of EMI control criteria is not possible, or warranted, within the scope of the current study. However, the designers must be aware of its requirements and the purpose of this section is to call it to attention. The referenced documents are more than adequate design guides for preliminary work, and should be referred to during the design process. Additional EMI control considerations and criteria will be developed as required in subsequent implementation phases of the program.

Appendix XXI

ENVIRONMENTAL CRITERIA

1.0 INTRODUCTION

The following is intended to provide a summary of minimum basic test requirements and recommended test levels for environmental testing of prototype and flight models of the Multiple Satellite. It covers not only the mechanical environment of the satellites during flight ascent and spacecraft separation, but also the orbital environmental considerations. These basic requirements are considered to be a minimum for the demonstration of the structural, mechanical and electronic requirements of the satellite.

2.0 LAUNCH VEHICLE CONSIDERATIONS

This section, extracted from the Delta Payload Planner's Guide, provides a summary of minimum basic test requirements and recommended test levels for the environmental testing of prototype and flight models to be launched by Delta vehicles.

VIBRATION ENVIRONMENT

The Improved Delta Launch Vehicle will be subjected to maximum random vibrations during liftoff and transonic flight, with low frequency sinusoids superimposed on random vibrations at liftoff. Sinusoidal oscillation, varying between 17 and 25 cps, will occur during last 25 seconds of first stage operation.

It is recommended that spacecraft structure stiffness be selected to produce fundamental frequencies above 35 cps in the thrust axis and 20 cps in the lateral axis to avoid dynamic coupling between low frequency sinusoids and spacecraft structural modes.

Sinusoidal and ramdom qualification and acceptance test criteria for the Improved Delta configuration are shown in the four vibration schedule charts.

These criteria are NASA Goddard Space Flight Center criteria and are based on flight data from Delta launches. In general, the acceptance test criteria represents flight equivalent vibration levels; the qualification test levels represent flight equivalent levels combined with a 1.5 test factor.

3 STAGE IMPROVED DELTA (DSV-3E & 3F) - SPACECRAFT DESIGN QUALIFICATION - RANDOM VIBRATION

Axis	Frequency cps	PSD Level g^2/cps	Acceleration g - RMS	Duration Min.
Thrust (Z-Z)	20-150	0.023	9.23	4 minutes each axis
Lateral (X-X)	150-300	Increasing from 150 cps at constant rate of 3 dB octave	9.23	
Lateral (Y-Y)	300-2000	0.045	9.23	

Grand Total: 12 Minutes

3 STAGE IMPROVED DELTA (DSV-3E & 3F) - SPACECRAFT FLIGHT ACCEPTANCE - RANDOM VIBRATION

Axis	Frequency cps	PSD Level g^2/cps	Acceleration g - RMS	Duration Min.
Thrust (Z-Z)	20-150	0.01	6.15	2 minutes each axis
Lateral (X-X)	150-300	Increasing from 150 cps at constant rate of 3 dB octave	6.15	
Lateral (Y-Y)	300-2000	0.02	6.15	

Grand Total: 6 Minutes

3 STAGE IMPROVED DELTA (DSV-3E & 3F) - SPACECRAFT DESIGN QUALIFICATION - SINUSOIDAL VIBRATION

Axis	Frequency cps	Duration Min.	Level g. 0-Peak	Sweep Rate
Thrust	10-19	.46	3.0	2 Octaves per Minute
	19-25	.20	4.5	
	25-250	1.66	3.0	
	250-400	.34	4.5	
	400-2000	1.17	7.5	
		Total: 3.83		
Lateral	5-250	2.83	2.3	2 Octaves per Minute
	250-400	.35	3.0	
	400-2000	1.16	7.5	
		Total: 4.34 (Each Axis)		

GRAND TOTAL: 12.51 Minutes

3 STAGE IMPROVED DELTA (DSV-3E & 3F) - SPACECRAFT FLIGHT ACCEPTANCE - SINUSOIDAL VIBRATION

Axis	Frequency cps	Duration Min.	Level g. 0-Peak	Sweep Rate
Thrust	10-19	.23	2.0	4 Octaves per Minute
	19-25	.10	3.0	
	25-250	.83	2.0	
	250-400	.17	3.0	
	400-2000	.58	5.0	
		Total: 1.91		
Lateral	5-250	1.42	1.5	4 Octaves per Minute
	250-400	.17	2.0	
	400-2000	.58	5.0	
		Total: 2.17 (Each Axis)		

GRAND TOTAL: 6.25 Minutes

THIRD STAGE SPINUP

The third stage system uses four to eight spin rockets on a spin table providing the impulse for spin stabilization prior to third stage motor ignition.

All items installed, including their mountings, must be designed for maximum angular acceleration at spin-up and the maximum anticipated angular velocity during spin.

Minimum Allowable Spin Rate - 90 rpm
Maximum Allowable Spin Rate - 200 rpm
Maximum Angular Acceleration - 45 rad/sec^2 (200 rpm spin rate)
Minimum Angular Acceleration - 10 rad/sec^2 (100 rpm spin rate)
Maximum Transient Angular Acceleration - 55 rad/sec^2 (200 rpm spin rate)
Minimum Transient Angular Acceleration - 15 rad/sec^2 (100 rpm spin rate)

PAYLOAD BALANCE

Since the Delta third stage is spin stabilized during flight, it must be statically and dynamically balanced.

To be statically balanced the spacecraft center of gravity must be within .015 inches of the spacecraft centerline -- defined as a line which is perpendicular to the spacecraft/vehicle interface and passing through the center of its diameter.

To be dynamically balanced the spacecraft principal axis of inertia in roll and the spacecraft axes of inertia in pitch and yaw must be respectively parallel and perpendicular to the spacecraft centerline within .002 radians.

The Spacecraft's rigidity must be such as to make all frequencies of the entire structure and/or subassemblies greater than 2.0 times the spacecraft spin rate at spinup but not less than 5 cps.

On or near the top of the spacecraft, physical means must be provided to measure runout (total indicator reading) of the rotating fully assembled third stage and spacecraft.

THERMAL ENVIRONMENT

Thermal environment will vary for each spacecraft since the exit trajectory depends on the specific mission. However. . . The fairing surface can be held below a specific temperature -- 450 degrees F. is adequate in preventing contamination of quartz, potassium bromide glass, and vapor deposited aluminum. External as well as internal insulation can be used to protect a particularly heat sensitive spacecraft.

DESIGN LOAD FACTORS (Including 1.5 Safety Factor)

Maximum axial acceleration - 1st stage ~ 13.5

Maximum axial acceleration - 2nd stage ~ 3.0

Maximum axial acceleration - 3rd stage ~ 3.0

Side load factors < 1.5g

3.0 ORBITAL CONSIDERATIONS

This section was extracted from the Space Environmental Criteria, Aerojet Report 3147, January 1966, performed under NASA contract NAS-8-11285.

Radiation Flux Rate Densities (trapped)

Shielding (Al)	Electrons	Protons
3 mg/cm^2	pk $1 \cdot 10^8$/cm^2 sec (>40 kev)	pk $5 \cdot 10^6$/cm^2 sec (> 1 Mev)
	avg $1 \cdot 10^7$/cm^2 sec (>40 kev)	avg $1 \cdot 10^5$/cm^{2}sec (> 1 Mev)
700 mg/cm^2	pk $4 \cdot 10^6$/cm^2 sec (>1,5 Mev)	pk $2 \cdot 10^4$/cm^2 sec (>22 Mev)
	avg $1 \cdot 5 \cdot 10^5$/cm^{2}sec(>1.5 Mev)	avg $4 \cdot 10^2$/cm^{2}sec (>22 Mev)

Radiation Flux Rate Densities (transient solar)

Protons peak $3 \cdot 10^5$/cm^2 sec (> 10 Mev)

Protons peak $5 \cdot 10^3$/cm^2 sec (> 100 Mev)

Appendix XXII

SYSTEM EVALUATION FOR DESIGN

1.0 INTRODUCTION

The primary objective of the Multiple Satellite program is the collection and return to earth of specific plasma and magnetic field data. The value of the data returned will vary with the reliability of the system, the number and type of instruments, the data transmission rate and the length of time that the multiple satellites function. Data value, together with cost, becomes the criteria for system evaluation. Cost effectiveness is, therefore, defined on a per launch basis as

$$C.E. = \frac{\text{total data value}}{\text{total costs}} = \frac{V_T}{C_T} \qquad (1)$$

Since subsystem and system data are generally unavailable at this point in the program, detailed evaluations are not currently possible. However, the approach to the evaluation is described and a preliminary example of component evaluation provided. The evaluation approach presented could be particularly useful in the preliminary and detail design phases of the program. During these program phases, alternate component and subsystem data is available. The following technique provides a relatively simple means for comparing alternate approaches and providing decision input based upon the effect that each alternative has on the entire program. Thus the total program effects can be considered in each decision without the burden of complete program re-evaluation for each case.

Data value and cost are now defined in quantitative terms which will allow for subsequent evaluation of systems and subsystems.

2.0 PRELIMINARY EVALUATION APPROACH

2.1 VALUE

The expected incremental value of scientific data from an individual experiment accumulated over a period of time, Δt, is $(V_i)(R_{sc})\ \Delta t$, where V_i is the instantaneous data value, and R_{sc} is the satellite reliability at a given time. The total expected value of the experiment can be determined by summing the value increments over the total period of data accumulation; i.e.,

$$V = \left[\sum_{o}^{T} \{(V_i)(R_{sc})\ \Delta t\}\right] R_V \qquad (2)$$

where T is the total operating time

R_V is the launch vehicle and pallet reliability

The individual experiment total expected values can be summed to represent total mission value.

For purposes of establishing preliminary satellite evaluation criteria, the total satellite system including experiments will be used as if it were a single component with one reliability and a single data source. Partial mission success effects on value will not be discussed on the basis of losing operational capability of individual experiments, but the influence of the number of satellites simultaneously returning data will be described. If possible, the consideration of individual experiment failures on the mission value will be considered during later phases of the program.

The following two assumptions were made to establish a physical interpretation of the value associated with data being accumulated by four satellites.

1. Individual satellite data value is shown as a function of time in Figure 1. The maximum value occurs initially when measurements are made in the transition region near the sub-solar point. The value is then assumed to decrease linearly to zero when apogee is in the magnetosphere tail.

Figure 1

Individual Satellite

Value vs Time

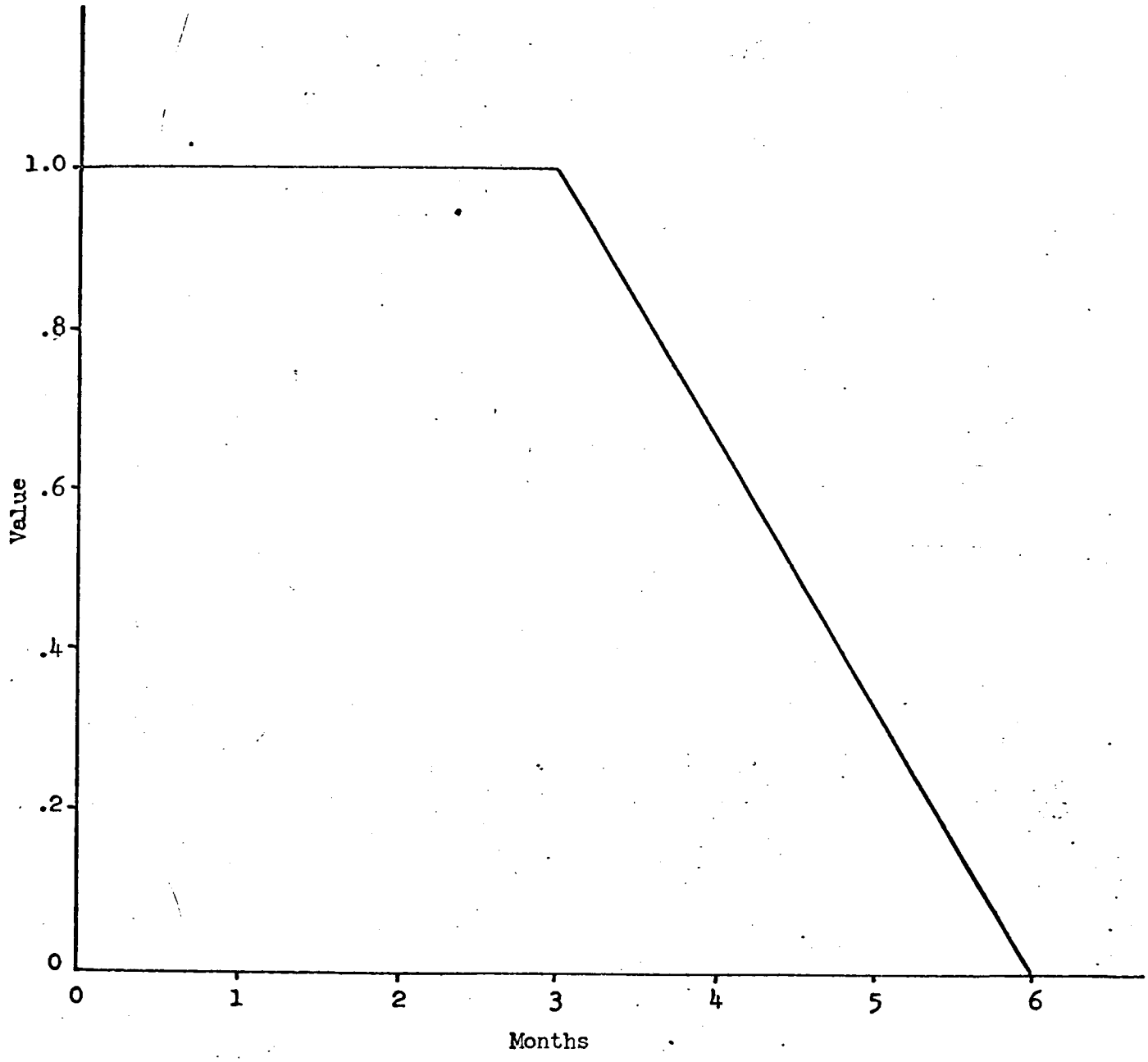

2. The influence of decreased value due to a reduced number of operational satellites is represented in Figures 2 and 3. The value is assumed to be decreased by one-half with each successive spacecraft loss.

The number of operational satellites, N_s, decreases as a function of time by the following relationship:

$$N_s = n\, e^{-t/\theta} \tag{3}$$

where n = initial number of satellites = 4

t = time after launch.

θ = mean time between failure for an individual satellite $\cong$ 54.5 months

For the multiple satellite case in which the individual satellites have estimated reliabilities of 0.9465 after three months, and the total system (including boost vehicle and pallet) has a reliability of 0.70 after three months, the expected number of survivors is shown in Figure 4 as a function of time.

Based upon the above assumptions, the total value for the Multiple Satellite program can be stated as: the integral over time of the value corresponding to the expected number of survivors times the vehicle and pallet reliability. The pallet and vehicle reliability, R_V, has been estimated in Appendix XIX to be 0.8705. The integral over time of the value corresponding to the expected number of survivors was determined as follows. After one month, the average value for N_s is established from Figure 4. (3.96 for this case). Using this number, the average total instantaneous value after one month is read from Figure 2, interpolating between the curves as required. This value is then $V\,\Delta T = 3.92(1)$. Similar values are established for the second through sixth month and summed giving a total value of $V_T = 16.6\ (R_V)$. The total value if all four spacecraft worked for six months is 18.0. The degradation due to spacecraft unreliability is then illustrated. Inserting the vehicle and pallet reliability, the total value becomes $V_T = 16.6\ (.8705) = 14.45$.

Figure 2

Total Value

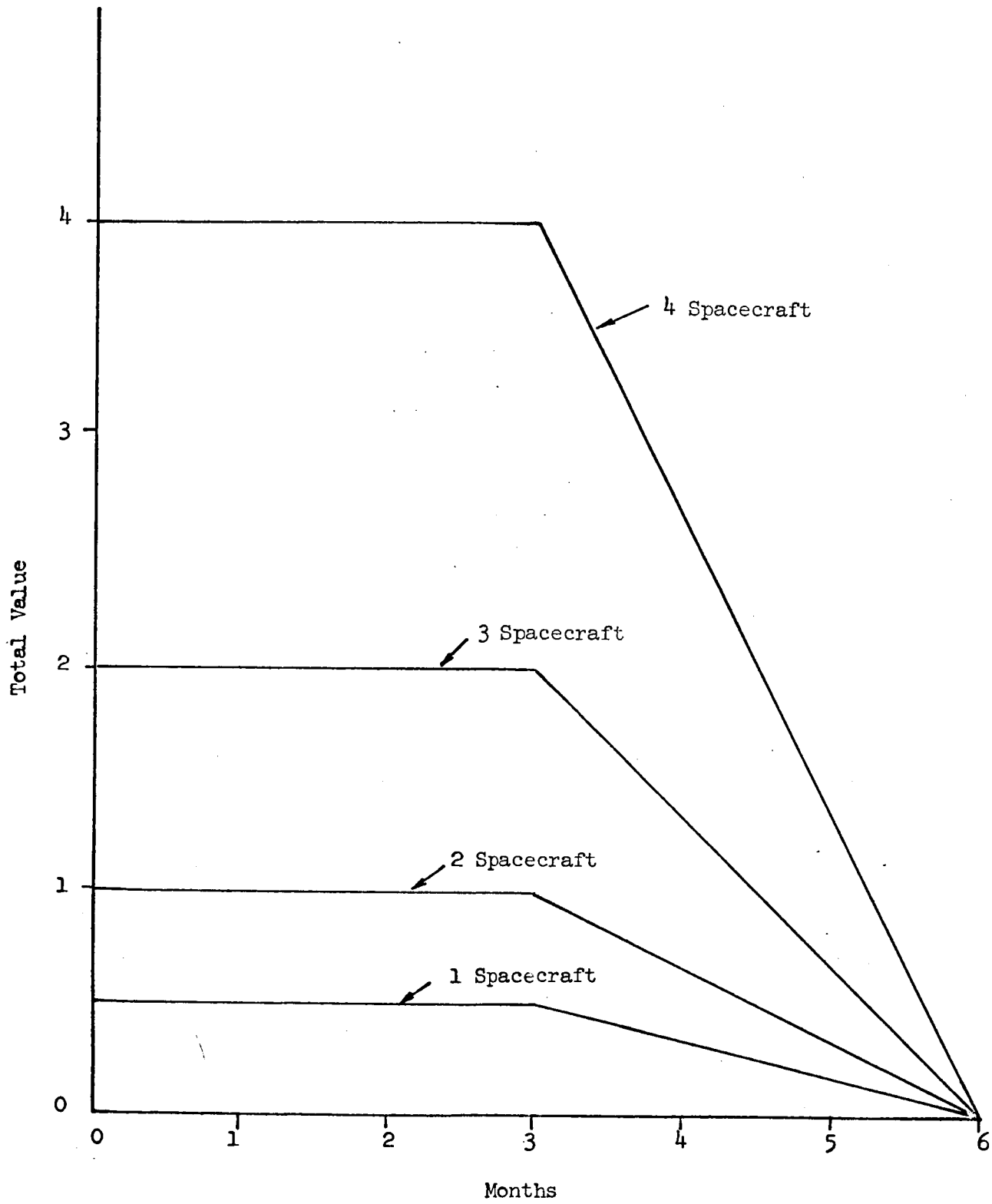

Figure 3

Total Cumulative Value

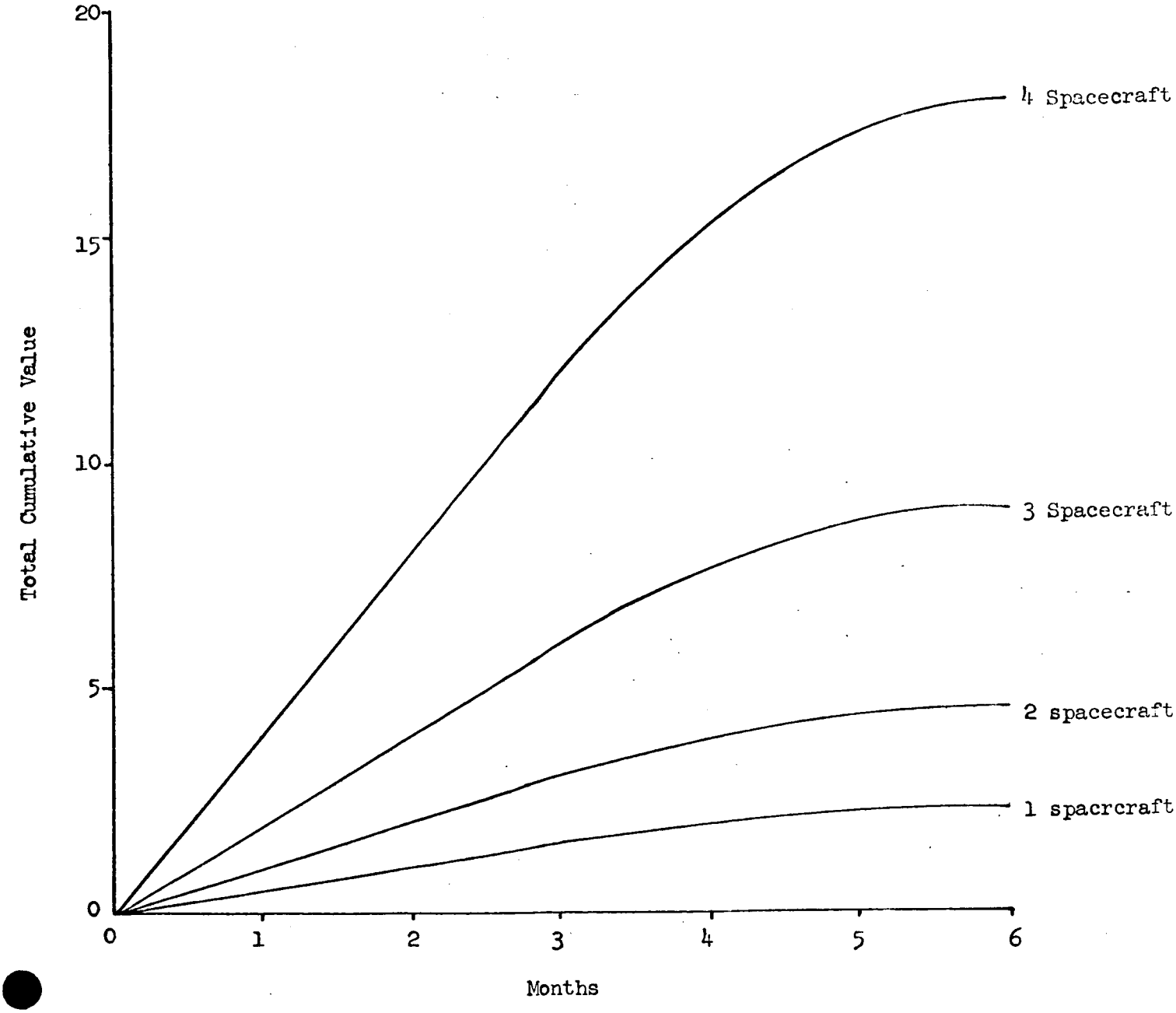

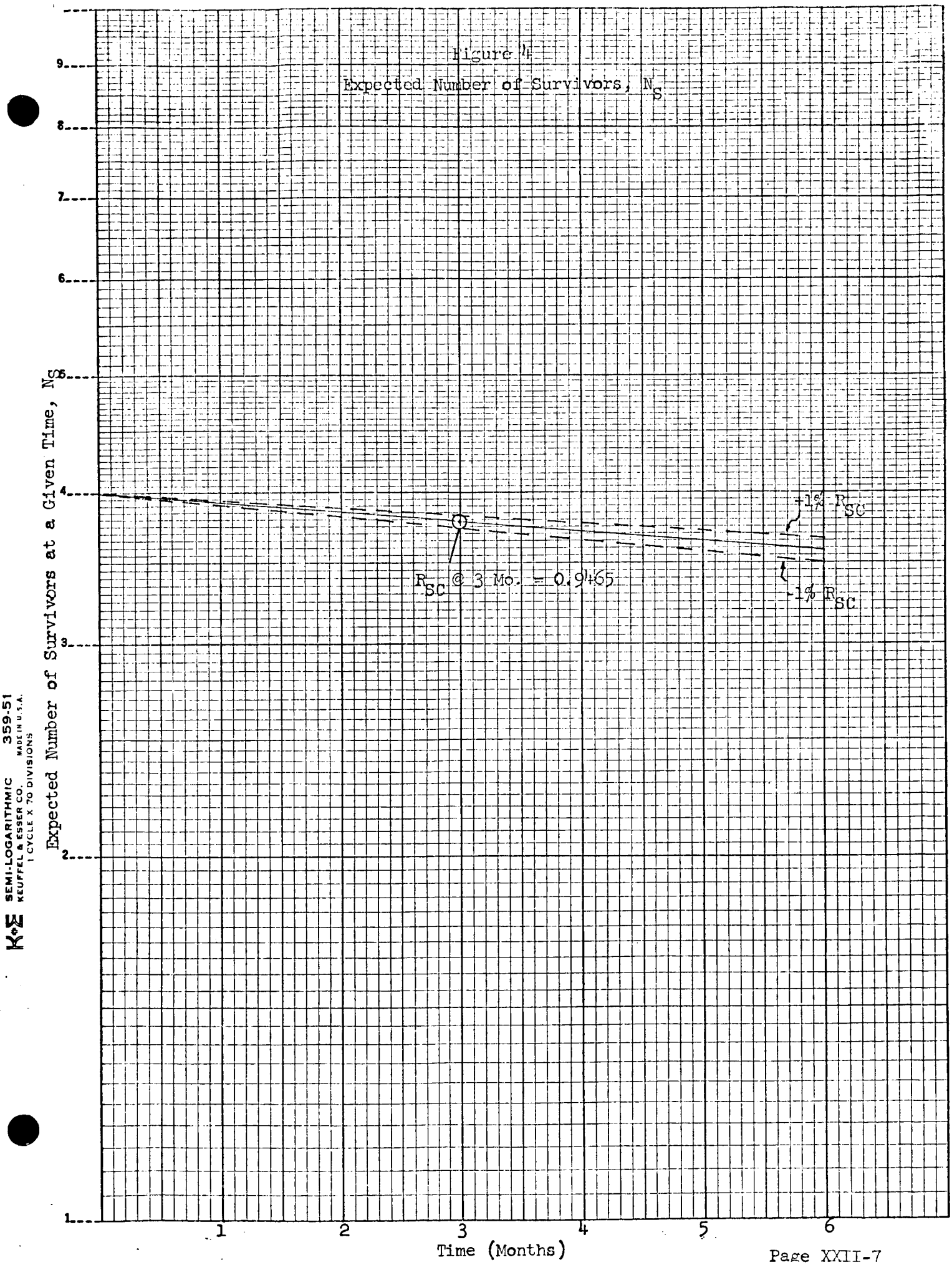
Figure 4
Expected Number of Survivors, N_S
Expected Number of Survivors at a Given Time, N_S
Time (Months)
R_{SC} @ 3 Mo. = 0.9465
+1% R_{SC}
-1% R_{SC}
1
2
3
4
5
6
7
8
9
SEMI-LOGARITHMIC 359-51
KEUFFEL & ESSER CO. MADE IN U.S.A.
1 CYCLE X 70 DIVISIONS

2.2 COST EFFECTIVENESS RELATIONSHIPS

System costs have not yet been worked out in detail and, therefore, in order to continue this analysis, a total cost including boost vehicle and amortized spacecraft development of $10 million/launch is assumed. This estimate will be altered when improved data is made available. Using the estimated cost, the cost effectiveness for the nominal system becomes

$$CE = \frac{V_T}{C_T} = \frac{14.45}{10 \times 10^6} = 1.445 \text{ units of value/million dollars}$$

2.3 INFLUENCE COEFFICIENTS

The overall cost/effectiveness estimate can now be used to determine the influence of component and alternate system costs, reliability, values and usage of excess weight on the total system cost effectiveness. For example, the influence of cost on the system cost effectiveness is $\frac{\partial CE}{\partial C_T}$ which, for the preliminary cost effectiveness estimate, is

$\frac{\partial CE}{\partial C_T}$ = a 10% change in CE (value units/$) for a $1 million change in cost at a nominal cost of 10 million dollars.

From this, alternate system and subsystem costs on the overall cost effectiveness can be established.

Less obvious is the influence of reliability. A change in individual spacecraft reliability affects the slope of the N_s curve of Figure 4 (Equation 3) which in turn affects the value, V_T and hence the C.E. This influence coefficient is

$\frac{\partial CE}{\partial R_{sc}}$ = a 2.2% change in CE for a 1.0% change in R_{sc}, at a nominal R_{sc} of 0.9465.

The booster and pallet reliability affects V_T and hence CE directly, therefore

$$\frac{\partial CE}{\partial R_v} = \text{a 1.0\% change in CE for a 1.0\% change in } R_v \text{ at a nominal } R_v \text{ of .8705.}$$

For the value shown in Figures 2 and 3

$$\frac{\partial CE}{\partial V_T} = \text{a 1\% change in CE for a 1\% change in total cumulative value.}$$

2.3 EFFECT OF VARIATIONS IN THE DEFINED VALUE

The above relationships are based upon a specific definition of the relative value for various numbers of spacecraft functioning versus time (Figure 2). The effect of varying the relative value is as follows.

Since the expected reliability for the individual satellites results in the expected number of survivors shown in Figure 4, the total value is only affected by the relative value assigned to four spacecraft working and three spacecraft working. The expected reliabilities are high enough that never less than three spacecraft can be expected to function for the six month lifetime of the mission. In the previous calculations, it was assumed that three spacecraft were always half as valuable as four spacecraft, and that for expected number of survivors between 3 and 4 satellites a linear interpolation of the value was made. If V_r is the relative value between V_4 and V_3, then

$$V_R = \frac{V_3'}{V_4} \tag{4}$$

$$V_R = 1/2 = \text{nominal}$$

The difference between perfect V_T (all satellites working) and the actual V_T is what is affected, i.e., where $V_R = 3/4$, the difference ($V_{T\ perfect}$ - $V_{T\ actual}$) is reduced by 1/2. (again assuming linear interpolation between the

value for 3 and 4 satellites). That is, the value of three satellites working is increased, reducing the difference between the value for perfect functioning and the value for actual functioning. The relationship between V_R and $V_{T\ act}$ is shown in Figure 5, and is represented by the expression

$$V_{T\ act} = (V_{T\ perf}) - 2(1 - V_R)\ (V_{T\ perf} - V_{T\ act})_{nom.} \qquad (5)$$

The influence coefficient of CE with respect to V_R is

$$\frac{\partial CE}{\partial V_R} = \frac{\partial (V_{T\ act}/C)}{\partial V_R}$$

With changes in V_R from the nominal, changes in the other influence coefficients will result giving corresponding changes in the influence of value, reliability and cost on the total cost effectiveness.

2.4 PAYLOAD WEIGHT VARIATIONS

Weight effects have not been considered in the above development. But in the final analysis payload weight utilization should be optimized on a cost/effectiveness basis. For example, excess weight can be used for additional instruments, to increase reliability through redundancy, or the use of alternate but more reliable or less costly subsystems, or combinations of these alternatives. Each alternate approach will affect the cost effectiveness; the approach producing the greatest positive change in CE at any time should be selected for implementation. Because of lack of data, it is not possible to illustrate this except by a qualitative example. Take the following effects on weight (there will be others in an actual case).

1) Reliability (Increase due to redundancy or use of simpler components)

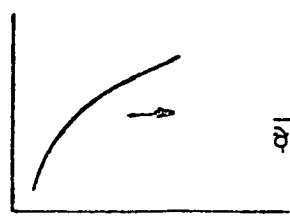

$$\frac{\partial \text{ Reliability}}{\partial \text{ (weight increase)}}$$

Figure 5

Effect of V_R on the Total Value

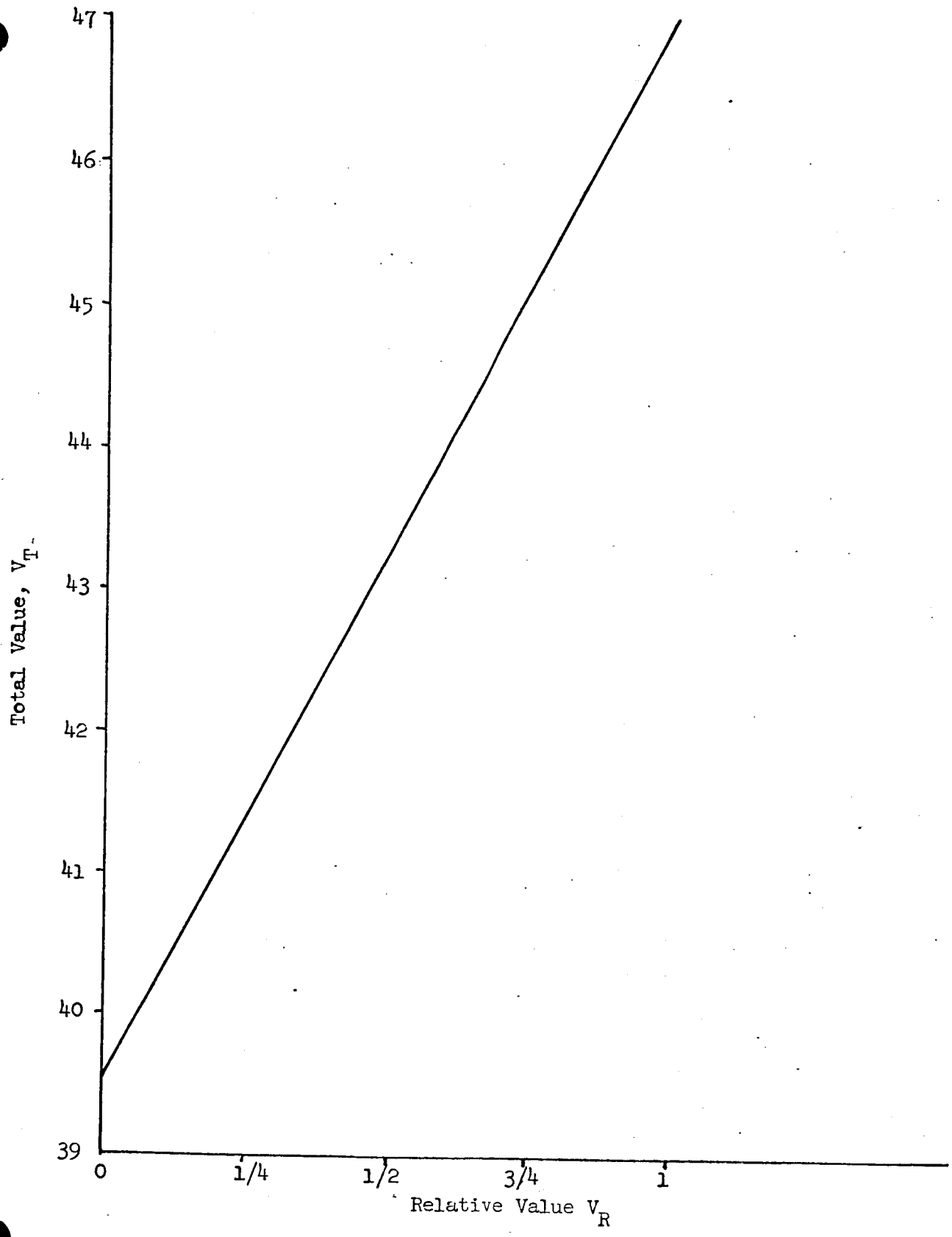

2) Cost (Decrease)

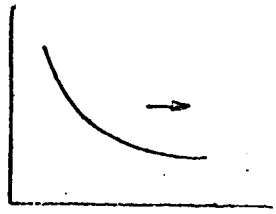

$$\frac{\partial \text{ Cost}}{\partial \text{ (weight increase)}}$$

3) Value (Increase due to higher bit rate or additional instruments

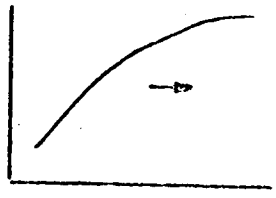

$$\frac{\partial \text{ Value}}{\partial \text{ (weight increase)}}$$

The influence coefficients will vary depending upon the point where they are determined and therefore a realistic nominal case must be selected when establishing them. The effect on system cost effectiveness due to the above influence is then determined. Reliability is used as example

$$\Delta CE_{Rel} = \left(\frac{\partial CE}{\partial Rel}\right)\left(\frac{\partial \text{ Rel}}{\partial \text{ weight increase}}\right)\left(\Delta \text{ weight increase}\right)$$

This is repeated for all potential uses for excess weights or alternate weight uses. The optimum allocation of the weight can then be made by comparing the CE expressions. The best use for any excess weight can be established by selecting the alternative yielding the greatest positive change in C.E. at a specific excess payload value. This optimum allocation of excess weight can be represented as a combined influence of payload weight on CE and plotted schematically as represented by the hypothetical example below.

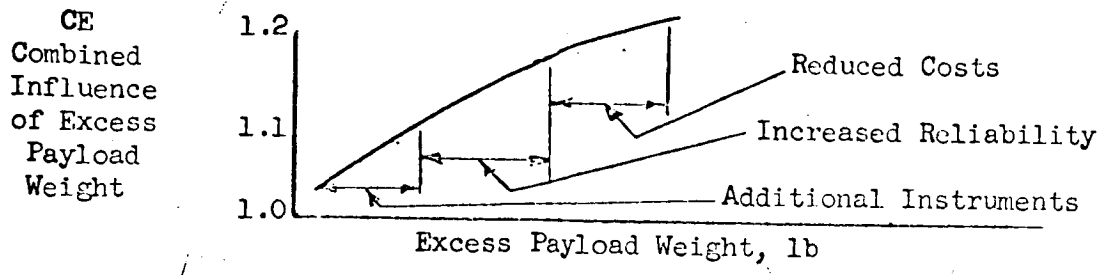

In addition to the above approach to defining the optimum usage of excess payload, the technique can be used to evaluate alternative approaches for other payload weight related questions. .For example, the required perigee altitude can be achieved in at least two ways: (1) boost directly to achieve the perigee altitude; (2) boost to a low perigee altitude and then kick at apogee to raise perigee. The latter alternative will allow provision for between 50 and 70 lb of additional weight over alternative (1), but requires an additional subsystem -- the apogee kick motor. The effects of these two alternatives on the program C.E. can be readily established when component data is made available, and would allow selection of the most effective alternative. For example, the use of a solid apogee kick motor will reduce the reliability by about -0.5% (motor reliability = .995). Using the $\frac{\partial CE}{\partial R_v}$ relationship given previously, gives a -0.5% change in C.E. If the additional 50 to 70 pound can be distributed among the satellites (or the pallet) to increase C.E. more than 0.5%, then it would be more effective to raise perigee with the apogee motor than the booster. Subjects such as these may be explored more thoroughly in the follow-on program when more component data will be available.

3.0 SPECIFIC EVALUATION EXAMPLE

The above analysis has defined evaluation expressions and influence coefficients. The use of these expressions to evaluate alternative designs and aid in the design of the optimum system requires further illustration. A specific example is now provided to illustrate the use of the technique in the selection of

components. The three alternatives for aspect sensing, i.e., magnetometer, IR horizon sensor, and fan beam antenna, are compared on the basis of their effect on the total system cost effectiveness. The change in CE with respect to a nominal system can be written

$$\Delta CE = \frac{\partial CE}{\partial V_T} \Delta V_T + \frac{\partial CE}{\partial C} \Delta C$$

V_T is a complex term including instantaneous value times time, the spacecraft reliability, and the booster and pallet reliability. Since the instantaneous value for the mission will be the same despite which sensor is used, ΔCE can be written

$$\Delta CE = \frac{\partial CE}{\partial R_{sc}} \Delta R_{sc} + \frac{\partial CE}{\partial R_v} \Delta R_v + \frac{\partial CE}{\partial C} \Delta C$$

The use of the magnetometer will delay the taking of data, but this will not change V; it will, however, increase operational costs and decrease the spacecraft reliability when data taking is initiated. The estimated reliabilities, costs, and weights for the three sensors are as follows.

Sensor	Reliability After Completion of Attitude Maneuver (1)	Reliability After 3 Months (1)	Cost (1000$)	Weight (lb)
Magnetometer	.9935 (2)	.955	0.6 (3)	0.56
IR Horizon Sensor	.995	.96	17.0	1.25
Fan Beam Antenna	.98	.975	5.5 (4)	5.0

NOTES:

(1) These reliability data are based on actual flight records. Based on the overall reliability requirements, improvement in these values would be necessary. This improvement and the related reliability and cost changes have not been considered.

(2) This value allows for reliability degradation due to the requirement for additional orbits to make the required measurements.

NOTES (Continued):

(3) Operational costs due to the longer duration required to establish attitude must be added, i.e., about \$200/hr/station for 24 hours ~ \$4800, plus 100 hours of other engineering time gives a total additional operational cost of \$6800.

(4) Includes \$25,000 development amortized over ten units.

Two cases will be considered: (1) that the primary job of the sensor is completed after the attitude maneuver, and (2) that the sensor must function for at least three months. Assuming that the change in cost effectiveness is referenced to a nominal case having a perfect sensor, i.e., zero cost and 1.0 reliability, the following results are achieved. The influence coefficients as given before are repeated.

$$\frac{\partial CE}{\partial R_{sc}} = \text{a 2.2\% change in CE for a 1.0\% change in } R_{sc}$$

$$\frac{\partial CE}{\partial R_{v}} = \text{a 1.0\% change in CE for a 1.0\% change in } R_{v}$$

$$\frac{\partial CE}{\partial C} = \text{a 1.0\% change in CE for a \$}10^5 \text{ change in cost}$$

In Case (1), the spacecraft reliability is not affected, but the pallet reliability is; in Case (2), both $R_{s/c}$ and R_v are affected. The delta cost and reliability coefficients for each case are listed and the change in cost effectiveness established below for both cases.

	Case 1			Case 2			
Sensor	$\frac{\partial CE}{\partial R_v} \Delta R_v$ (%)	$\frac{\partial CE}{\partial C} \Delta C$ (%)	ΔCE (%)	$\frac{\partial CE}{\partial R_v} \Delta R_v$ (%)	$\frac{\partial CE}{\partial R_{sc}} \Delta R_{sc}$ (%)	$\frac{\partial CE}{\partial C} \Delta C$(%)	ΔCE (%)
Magnetometer	-.65	-.074	-.724	-.65	-3.75	-.074	-4.474
IR Sensor	-.5	-.17	-.67	-.5	-3.5	-.17	-4.17
Fan Beam Antenna	-2.0	-.055	-2.055	-2.0	-.5	-.055	-2.555

Based on the basic data used, the following conclusions can be reached. If the importance of the sensor is to be used only during the pallet operation, Case (1), then the IR sensor should be selected as providing the least negative change in cost effectiveness when referenced to the perfect sensor. If, more realistically, the sensors are required to function on each satellite for some time after deployment, Case (2), then the above table indicates that the antenna may be preferred. The antenna's apparent superiority is due primarily to the small reliability degradation after the antenna is deployed. However, the antenna weighs considerably more than the other two instruments. If additional redundant magnetometer or IR sensors were assumed, to provide a weight equal to the antenna (redundancy in systems other than these sensors might be employed to better use the excess weight), then the reliability effects on the cost effectiveness for these two sensors would become very small and they would be preferable to the fan beam antenna. It is not clear from this analysis and the preliminary data available that the IR sensor is superior to the magnetometer, since weight effects cannot be analyzed in detail, however. When performance and ease of use is considered, however, (see Appendix XI), the IR sensor appears to be the best current selection.

The above analysis shows how the evaluation process can be implemented. When detailed component data is made available, more sophisticated evaluations of subsystems and systems may be conducted; the influence coefficients can be refined and the sensitivity of the total system cost effectiveness to changes in subsystem alternatives can be investigated.

Appendix XXIII

BALANCE REQUIREMENTS

1.0 INTRODUCTION

The Multiple Satellite system has unusual and restricting balance requirements. It must be balanced and/or stable in the required spin mode for the following cases:

1. Total payload on the booster
2. Pallet (with satellites attached) separated and deployed
3. Satellite pairs separated and deployed
4. Individual satellites separated and deployed

The balance requirements for each of the four different modes of operation are as follows.

2.0 TOTAL PAYLOAD ON BOOSTER*

Since the Delta third stage is spin stabilized during flight, it must be statically and dynamically balanced.

To be statically balanced the spacecraft center of gravity must be within 0.015 inches of the spacecraft center line - defined as a line which is perpendicular to the spacecraft/vehicle interface and passing through the center of its diameter (Longitudinal Reference Axis - LRA).

To be dynamically balanced the spacecraft principal axis of inertia in roll and the spacecraft axis of inertia in pitch and yaw must be respectively parallel and perpendicular to the spacecraft centerline within 0.002 radians.

---

* From the Delta Payload Planner's Guide

The spacecraft's rigidity must be such as to make all frequencies of the entire structure and/or subassemblies greater than 2.0 times the spacecraft spin rate at spin up, but not less than 5 cps.

On or near the top of the spacecraft, physical means must be provided to measure runout (total indicator reading) of the rotating fully assembled third stage and spacecraft.

3.0 PALLET SEPARATED AND DEPLOYED

The spacecraft must be statically balanced so that the center of mass of the total system is within 0.1 inch of the LRA. For dynamic balance, the principal axis of the total system must be within 0.1 degree of the LRA and the moment of inertia ratio (roll/pitch or yaw) of the total system must be greater than 1.1.

The centers of mass of the satellite pairs as nominally mounted on the pallet must be of equal distance from the LRA and diametrically opposite. For static balance, the pairs must be within 0.1 inch of this nominal location. For dynamic balance, the principal axes of the satellite pairs as mounted on the pallet must be aligned within 0.1 degree of the LRA.

4.0 SATELLITE PAIRS SEPARATED AND DEPLOYED

For static balance, the satellite pairs must have their centers of mass within 0.1 inch of the system LRA, and the individual satellites must be mounted so that their center of mass is within 0.1 inch of the LRA.

For dynamic balance, the principal axis of the pairs must be within 0.1 degree of the LRA, and the principal axis of each satellite as mounted must be within 0.1 degree of the LRA. The total satellite pairs system must have a moment of inertia ratio greater than 1.1.*

---

* If the satellite pairs are separated immediately upon spin-off, the moment of inertia ratio need not be met.

5.0 SATELLITES SEPARATED AND DEPLOYED

For static balance, the center of mass of the individual satellites with booms deployed must be aligned to the LRA within 0.1 inch. For dynamic balance, the principal axis must be aligned within 0.1 degree of the LRA and the moment of inertia ratio must be greater than 1.1.

The tracking antenna must be aligned with the satellite LRA to within 0.1 degree and within 0.1 inch of the LRA.

The deployment of booms, together with the maximum booster spin rate (Figure 1), shall not result in a final satellite spin rate of less than 50 rpm.

DELTA VEHICLE MAXIMUM SPIN RATE

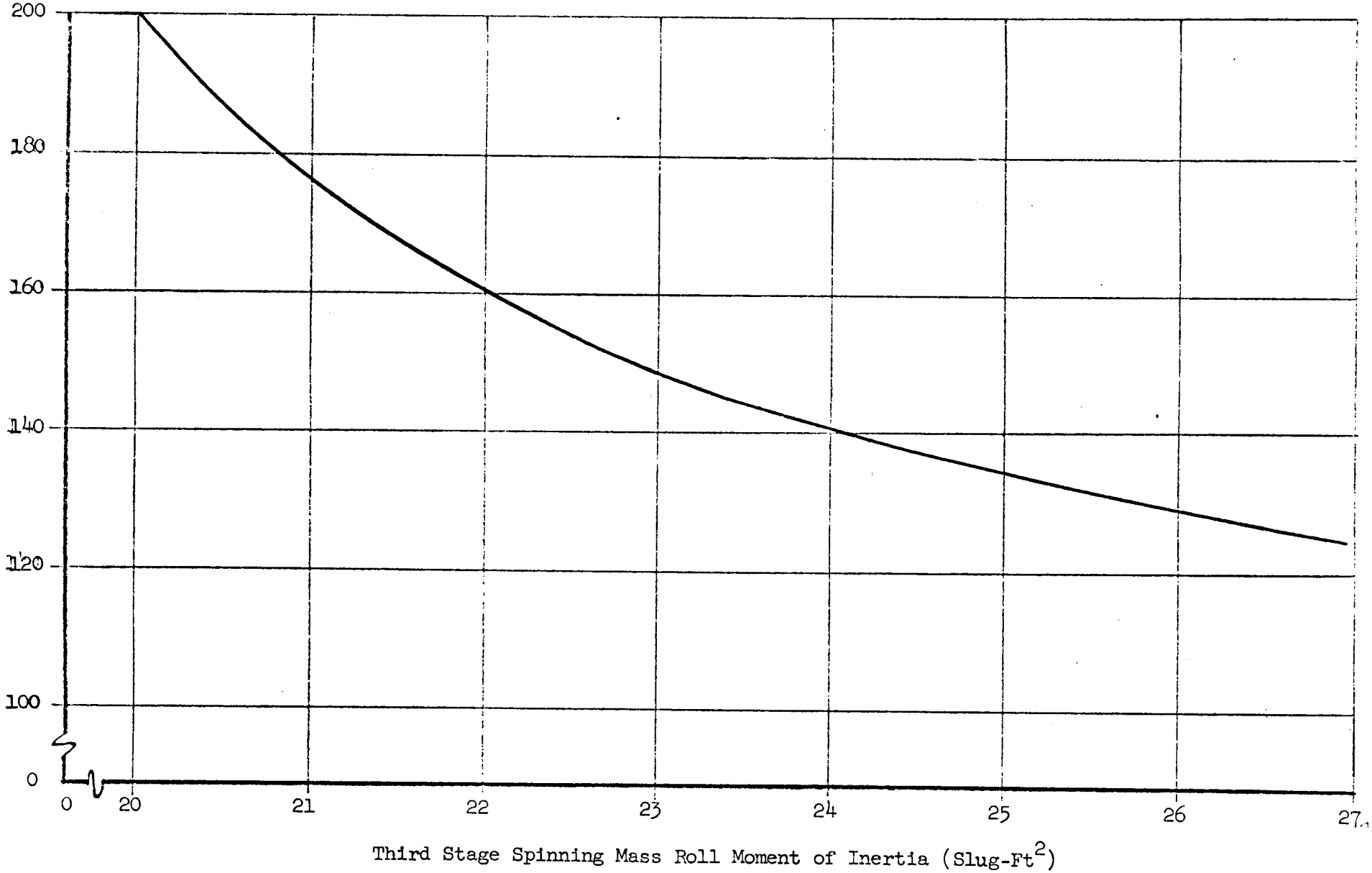

Appendix XXIV

THERMODYNAMIC DESIGN

1.0 INTRODUCTION

A major problem in satellite thermal control is the selection of thermal control finishes that will maintain the satellite temperatures within tolerable limits while the satellite receives the maximum solar and planetary thermal inputs and also while the satellite passes through the earth shadow.

One method of estimating satellite orbit temperatures is to allow the satellite to remain at various points in the orbit for an infinite length of time so that a steady state equilibrium heat balance is obtained. Since this type of analysis is based on a steady state situation, temperature gradients within the satellite are eliminated. The temperatures obtained from such a heat balance represent the temperature extremes a satellite could reach throughout an orbit, but do not necessarily predict the actual temperatures of the various satellite components.

This analysis shows the satellite equilibrium temperature variation throughout an orbit that can be expected for various surface finish combinations when all or part of the satellite surface is covered by solar cells.

The analysis was conducted for a cylindrically shaped satellite in an elliptic orbit with a perigee altitude of 200 km and an apogee altitude of 20 earth radii. The orbit plane was in the plane of the ecliptic and the satellite was spinning at 60 rpm about the satellite longitudinal axis. The satellite was two feet in diameter and 17 inches long. Two orbit orientations were considered as shown in Figure 1; one with apogee at the earth-sunline, the other with apogee in the earth shadow. The orbit period was 48 hours in each case. Equilibrium temperatures were

calculated for the angle θ of 90°, 180° and 270° for each orbit. At θ equal 0° (in the earth shadow) the satellite temperatures were determined by means of a transient temperature equation for a cooling body. The thermal model and the associated equations are discussed in Section 2.0. The equilibrium temperatures were determined from Equation (2) and the shadow temperatures were determined from Equation (4). For the orbit shown in Figure 1A an analysis was also made for the orbit plane inclined about 5° out of the ecliptic such that the satellite does not pass through the shadow.

The solar constant, albedo and planetary emission used for this analysis were based on a planet heat balance. The corresponding values were: solar constant of 443 BTU/hr-ft^2, albedo of 0.40 or 177 BTU/hr-ft^2, and earth emissive power of 67 BTU/hr-ft^2.

2.0 . METHOD OF ANALYSIS

Thermal Model. The average equilibrium temperature for a satellite is given by the heat balance:

$$\dot{q}_{rad1} + \dot{q}_{rad2} = \dot{q}_{s1} + \dot{q}_{r1} + \dot{q}_{p1} + \dot{q}_{s2} + \dot{q}_{r2} + \dot{q}_{p2t} + P_{gen}$$

or

$$\sigma\, \epsilon_1 A_1 T_{eq}^4 + \sigma\, \epsilon_2 A_2 T_{eq}^4 = A_{S1}\, S\, \alpha_1 F_{1S} + A_{r1} Sr\, \alpha_1 F_{1r} + A_{p1}\, \epsilon_1 F_{1p} E$$

$$+ A_{S2} S \alpha_2 F_{2S} + A_{r2}\, \alpha_2\, Sr\, F_{2r} + A_{p2}\, \epsilon_2\, F_{2p}\, E + P_{gen}. \qquad (1)$$

Reference to Figure 1 and the nomenclature list explains the above symbols. For a spinning satellite with a high spin rate relative to the orbit period the temperature gradients around the satellite are eliminated and Equation (1) represents the equilibrium temperature throughout the entire satellite. If the satellite is represented by a right circular cylinder the heat balance sets the heat emitted by

the side and ends of the cylinder equal to the solar, albedo and planet emission inputs to the side and both ends plus the internal power generation. If the cylinder radius to length ratio is $\frac{L}{R}$ and the view factors for the ends; F_{2S}, F_{2r}, and F_{2p} are based on the area of both ends, (as opposed to the area of one end), and the view factors for the side, F_{1S}, F_{1r} and F_{1p} are based on total circumferential area (as opposed to projected area), the following equalities can be made:

$$A_1 = 2\pi RL = A_{S1} = A_{r1} = A_{p1}$$

$$A_2 = 2\pi R^2 = A_{S2} = A_{r2} = A_{p2}$$

and

$$\frac{A_1}{A_2} = \frac{2\pi RL}{2\pi R^2} = \frac{L}{R} \text{ or } A_2 = \left(\frac{R}{L}\right) A_1$$

Also, if the cylinder axis is perpendicular to the ecliptic plane at all times (i.e., ends parallel to solar rays), the fourth term on the right hand side of Equation (1) vanishes since F_{2S} is zero. Then Equation (1) can be rewritten:

$$\sigma \left[1 + \left(\frac{R}{L}\right)\left(\frac{\epsilon_2}{\epsilon_1}\right)\right] T^4 = \left(\frac{\alpha_1}{\epsilon_1}\right) S \left(F_{1S} + rF_{1r}\right) + F_{1p}E + \left(\frac{R}{L}\right)\left(\frac{\alpha_2}{\epsilon_1}\right) SrF_{2r}$$

$$+ \left(\frac{R}{L}\right)\left(\frac{\epsilon_2}{\epsilon_1}\right) F_{2p}E + \frac{P_{gen}}{\epsilon_1 A_1} \qquad (2)$$

The view factors, F_{1S}, F_{1r}, F_{1p}, F_{2r} and F_{2p} were determined by means of the curves shown in Reference (1) for various points in the orbit. The view factors for the cylindrical side were determined for a differential segment of area and integrated over the entire circumferential area. The view factors for the ends were integrated over the area of both ends.

The maximum equilibrium temperature corresponds to the temperature a satellite would reach if allowed to receive the maximum thermal input for an infinitely long period of time, and the minimum equilibrium temperature corresponds to the temperature a satellite would reach if allowed to remain in the planet shadow for an infinitely long period. For high altitude or highly elliptic orbits the orbit period is long compared to the time spent in the earth shadow. Therefore, the maximum satellite temperature could approach the maximum equilibrium temperature due to the relatively long period spent in the sunlight, and since the shadow time is relatively short the change of reaching the minimum equilibrium temperature is unlikely. It is therefore necessary to compute the temperature to which the satellite will drop to as it passes through the planet shadow. This temperature can be represented by the equation,

$$C_p \, w \frac{dT}{dt} = \sigma \, \epsilon \, A \left(T_o^{\,4} - T^4 \right) \tag{3}$$

When Equation (3) is integrated within the limits T_{in} and T_s the solution is,

$$\frac{4 \, \epsilon \, \sigma \, A \, T_o^{\,3} t}{C_p W} = -\mathrm{Ln} \, \frac{T_o - T_s}{T_o + T_s} + 2 \tan^{-1} \left(\frac{T_s}{T_o} \right) + \mathrm{Ln} \, \frac{T_o - T_{in}}{T_o + T_{in}}$$

$$+ 2 \tan^{-1} \left(\frac{T_{in}}{T_o} \right) \tag{4}$$

where T_s is the temperature the satellite will reach after spending t hours in the shadow. In this equation ϵ is the average emissivity of the entire satellite surface. The temperature T_{in} is the temperature of the satellite as it enters the shadow. For circular orbits this temperature is usually the maximum sunlight temperature T_∞, for elliptic orbits a time averaged equilibrium temperature is generally used.

For a surface covered by a combination of two different finishes the average $\frac{\alpha}{\epsilon}$ ratio is given by,

$$\left(\frac{\alpha}{\epsilon}\right)_{ave} = \frac{\alpha' x' + \alpha'' x''}{\epsilon' x' + \epsilon'' x''}$$

where x' is the fraction of the surface area covered by a finish having absorptivity and emissivity α' and ϵ' respectively and x'' is the fraction of the surface area covered by a finish having absorptivity and emissivity α'' and ϵ'' respectively.

3.0 DISCUSSION OF RESULTS

This analysis was conducted for the surface finish combinations shown in Table 1. The sides of the satellite were covered with various proportions of the solar cells and white paint and solar cells and polished aluminum. Two end finishes were included, one was white paint and the other polished aluminum. The $\frac{\alpha}{\epsilon}$ ratio for solar cells as given in Reference (2) was 0.80/0.80, or unity. The $\frac{\alpha}{\epsilon}$ for polished aluminum as obtained from Reference(3)was 0.40/0.05 or 8.0. For white Kemacryl paint the $\frac{\alpha}{\epsilon}$ was 0.26/0.75 or 0.35 also from Reference (3). The average $\frac{\alpha}{\epsilon}$ ratios for the various combinations of finishes are also given in Table 1 for both sides and the ends of the satellite.

The view factors between the satellite and earth and between the satellite and the solar rays are given in Table 2. These view factors were determined for each of the orbits by the method discussed in the Method of Analysis Section.

Using these view factors and the equations previously described, satellite equilibrium temperatures were calculated for the three points in each orbit for the various surface finish combinations. The transient cooling temperatures were determined for the time the satellite spent passing through the shadow.

These satellite temperatures are shown in Figures 3 and 4 versus orbit angle. In the sunlit portion of the orbits only steady state equilibrium temperatures were calculated and therefore the orbit temperatures were symmetrical about

the major axis of the ellipse. The temperature curves shown in Figure 3 with the sun located at apogee and a shadow time of approximately 0.44 hours vary drastically compared to the temperatures of Figure 4 with the sun at perigee and a shadow time of 6.34 hours. This is due to the shorter time spent in the shadow and the fact that the satellite passes closer to the earth just before entering the shadow and hence the earth shine and albedo inputs to the satellite tend to increase the temperature just previous to entering the shadow. Also, for the majority of the orbit the earth inputs to the satellite are small compared to the solar inputs, and the solar input remains constant throughout most of the orbit causing the satellite to remain at a relatively constant temperature. However, in Figure 4 with the sun at perigee, the shadow time is relatively long (6.34 hours) and due to the distance from the earth the satellite receives no thermal input from earth just before entering the shadow. Near apogee the satellite receives albedo, earth-shine, and solar inputs at a maximum, hence the temperature for this portion of the orbit increases greatly. Therefore in this orbit the temperature variation is severe compared to the orbit of Figure 3. However, if the major axis of the orbit is inclined out of the ecliptic plane such that the satellite will not pass through the shadow at all (about 5° inclination), the satellite temperature drop at apogee will be much less. This is shown in Figure 4 by the dashed lines.

From Figure 3 it can be seen that the temperature of case 1 and case 2 fall within reasonable limits. The temperature of cases 4 and 5 are obviously too high and case 3 is somewhat low for most satellite components. Reference to Figure 4 shows that the maximum temperature of case 1 exceeds $100^{\circ}F$, but cases 2 and 3 lie within a more acceptable range provided the orbit is inclined such that the satellite does not pass through the shadow. This reasoning leads to the selection of case 2 as the most satisfactory combination of surface finishes to maintain acceptable satellite temperatures for the complete rotation of the sun.

It can be noted that the cases with the polished aluminum ends exhibit higher temperatures than those with white painted ends for the same side finish. This is due to the low emissivity of the aluminum since no solar input reaches

the ends and the earth inputs to the ends are small. When aluminum ends are used with 50% aluminum on the sides (case 5) the temperature is even greater. This again is caused by the low emissivity of polished aluminum preventing the satellite from cooling itself by radiation to space.

The data presented in Figure 3 and 4 are shown again in Figure 5 and 6 versus the time for one orbit. Figure 5 shows the equilibrium temperature variation with time with the sun at apogee and Figure 6 shows the variation with the sun at perigee. Also shown in Figure 6 is the temperature variation for the inclined orbit where the satellite does not pass through the earth shadow.

REFERENCES

1. F. G. Cunningham, "Power Input to a Small Flat Plate from a Diffusely Radiating Sphere, with Application to Earth Satellites", NASA TND-710, August 1961.

2. F. Krieth, "Radiation Heat Transfer for Spacecraft and Solar Power Plant Design", International Text Book Co., 1962.

3. R. E. Gaumer, L. A. McKellar, "Thermal Radiative Control Surfaces for Spacecraft", Lockheed Missiles and Space Company, LMSD-704014, March 1961.

NOMENCLATURE

A	=	surface area of satellite
C_p	=	average specific heat of satellite
E	=	planet emissive power (177 BTU/hr-ft^2 for earth)
F	=	view factor
H	=	distance from planet center to satellite
L	=	length of cylindrical satellite
P_{gen}	=	internal power generation
$\dot{q}$	=	heat transfer rate
R	=	radius of cylindrical satellite
r	=	planet albedo (.40 for earth)
S	=	solar constant (443 BTU/hr-ft^2 for earth)
T_{eq}	=	equilibrium temperature
T_o	=	minimum equilibrium temperature
T_∞	=	maximum equilibrium temperature
T_{in}	=	equilibrium temperature at entry to shadow
T_s	=	shadow temperature
w	=	satellite weight
α	=	solar absorptivity
ϵ	=	infrared emissivity
σ	=	Stephen-Boltzmann constant ($.174 \times 10^{-8}$ BTU/hr-ft^2 $^oR^4$)

Subscripts

p	=	refers to planet emission input
r	=	refers to albedo input
s	=	refers to solar input
1	=	refers to cylindrical surface area
2	=	refers to area of cylinder ends
rad.	=	refers to satellite radiation to space

Table 1

TABLE OF SURFACE FINISH COMBINATIONS

Material and Percent Area Covered

Case No.	Sides	Ends	(α/ϵ) average Sides	(α/ϵ) average Ends
1	100% solar cells	100% white paint	1.0	0.35
2	80% solar cells - 20% white paint	100% white paint	0.876	0.35
3	50% solar cells - 50% white paint	100% white paint	0.685	0.35
4	100% solar cells	100% polished aluminum	1.41	8.00
5	50% solar cells - 50% polished aluminum	100% polished aluminum	1.00	8.00

White Paint $\alpha/\epsilon = \frac{.26}{.75} = 0.35$ Reference 1

Solar Cells $\alpha/\epsilon = \frac{.80}{.80} = 1.0$ Reference 2

Polished Aluminum $\alpha/\epsilon = \frac{.40}{.05} = 8.0$ Reference 1

Table 2

TABLE OF VIEW FACTORS

Sun at Perigee View Factor	Position 0°	90°	180°
F_{1s}	0	0.319	0.319
F_{1r}	0	0.0411	0.30
F_{1e}	0	0.0822	0.30
F_{2s}	0	0	0
F_{2r}	0	0.05	0.35
F_{2e}	0	0.10	0.35

Sun at Apogee View Factor	Position 0°	90°	180°
F_{1s}	0	0.319	0.319
F_{1r}	0	0.0411	0
F_{1e}	0.30	0.0822	0
F_{2s}	0	0	0
F_{2r}	0	0.05	0
F_{2e}	0.35	0.10	0

ORBIT DIAGRAMS

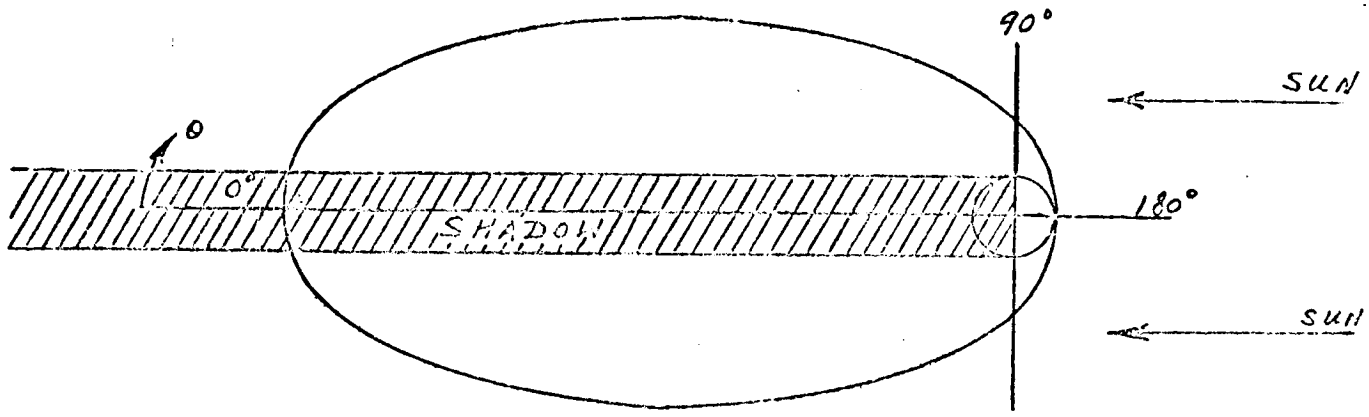

1A ~ SUN AT PERIGEE

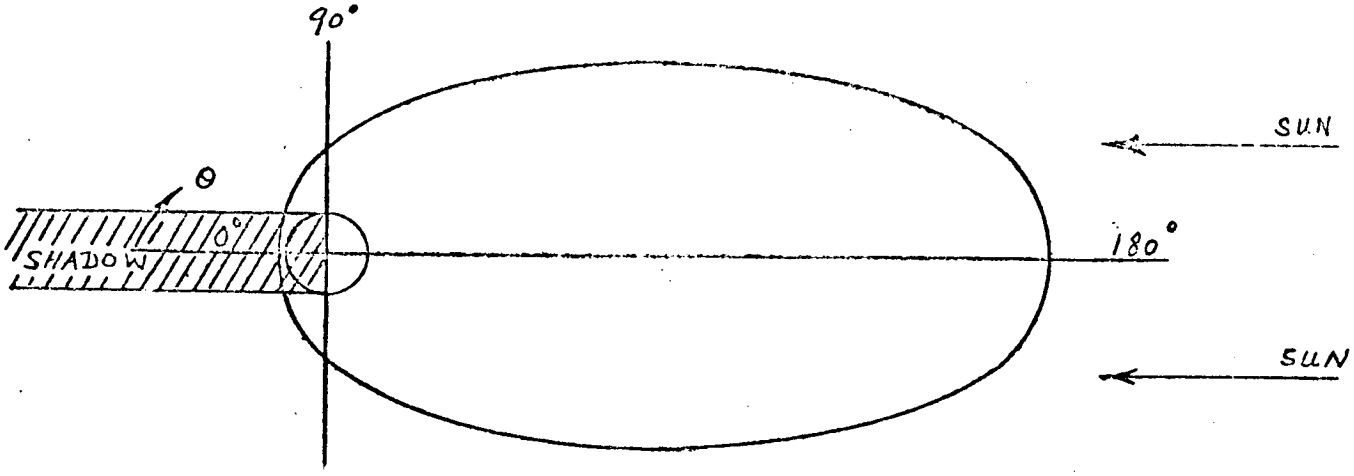

1B ~ SUN AT APOGEE

FIGURE 1

DIAGRAM OF THERMAL MODEL

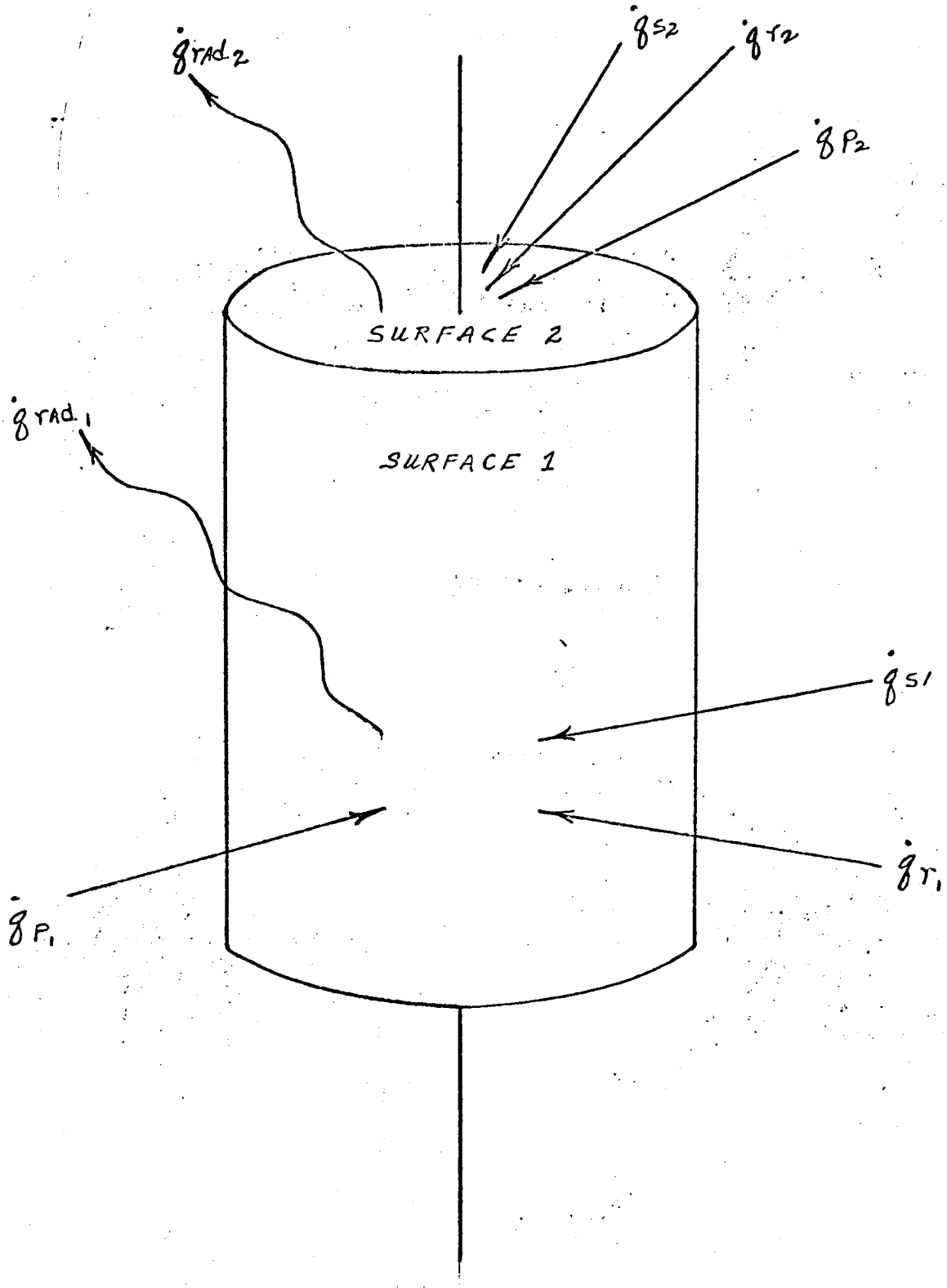

FIGURE 2

Appendix XXV

POWER PROFILE

1.0 INTRODUCTION

Preliminary power profiles have been generated for the pallet and satellite. The profiles are based upon the operational sequence presented in The Summary Volume and the subsystem power requirements presented below. From the power profiles, the power requirements are established and the battery and solar cell characteristics defined.

2.0 SUBSYSTEM POWER REQUIREMENTS

Pallet Subsystems	Average Power	Peak Power (Watts)
1. Command Receiver	1.5 watts	1.5
2. Beacon	10 mw	---
3. Solid Rocket Ignition	Negligible watt-hours	8
4. Attitude Control System	2 watt-hours	50
5. Spin-Off Release (Pyrotechnic)	Negligible watt-hours	80

Satellite Subsystems

1. Instruments*

Magnetometer:		
Pioneer C and D	3.0	6.9
A-Imp (Alternate)	(.71 watts)	(2.7 watts)
Ames Plasma Probe	3.0	3.5
Peak Ion Velocity Detector (2 Instruments)	3.6	4.2
Ion Flux Detector (2 Instruments)	1.0	1.0
Estimated Total - Integrated Instruments	8.0	

*The total average power required by the specified instrument complement is 10.6 watts. However, if an integrated instrument package is considered, it is reasonable to assume that a reduction of about 3 watts in the instrument power required could be achieved. Therefore, for the purposes of establishing the satellite power system, the instrument package power requirement will be assumed to be 8 watts.

2. Support System

Data Handling System	3
Tape Recorder	6
Transmitter	6.5
Command Receiver	1.5
Transponder	7
Aspect Sensor (2 IR Sensors)	.5
Solar Sensors	.5

3.0 PALLET POWER DEMAND

The pallet power demand is shown in Figure 1. The total power demand for the battery is about 95 watt-hours. Assuming a silver-zinc battery at 40 watt-hours/lb., 2.25 pounds of batteries are required.

4.0 SATELLITE POWER DEMAND (PRIOR TO OPERATIONAL DATA MODE)

The satellite(s) power requirement is shown in Figure 2. The average requirement is about 9 watts, which is sufficiently below the 18 watts required during the data mode that the solar cells can provide the required power, even though they are partially shadowed by the other satellites while on the pallet.

The average power required by each satellite after separation, but prior to the data mode, is 9 watts or less which is also less than the data mode requirements. Therefore, the solar array is sized by the real time data mode requirements.

5.0 SATELLITE POWER DEMAND (REAL TIME DATA MODE)

The operational sequence was developed assuming that the satellites would operate in a real time transmission mode for about the first 10 orbits. For the purposes of establishing the power requirements, it will be assumed that the satellites begin transmitting data four hours after perigee passage and continue to transmit until four hours before the subsequent perigee passage with the exception of about 6 hours near apogee. This operational mode allows coverage of the transition and interplanetary region. Twice during the eight hours near perigee when there is no transmission and once near apogee, the transponder will be commanded on and the satellite tracked to up-date the ephemeris.

Figure 1

Pallet Power Demand

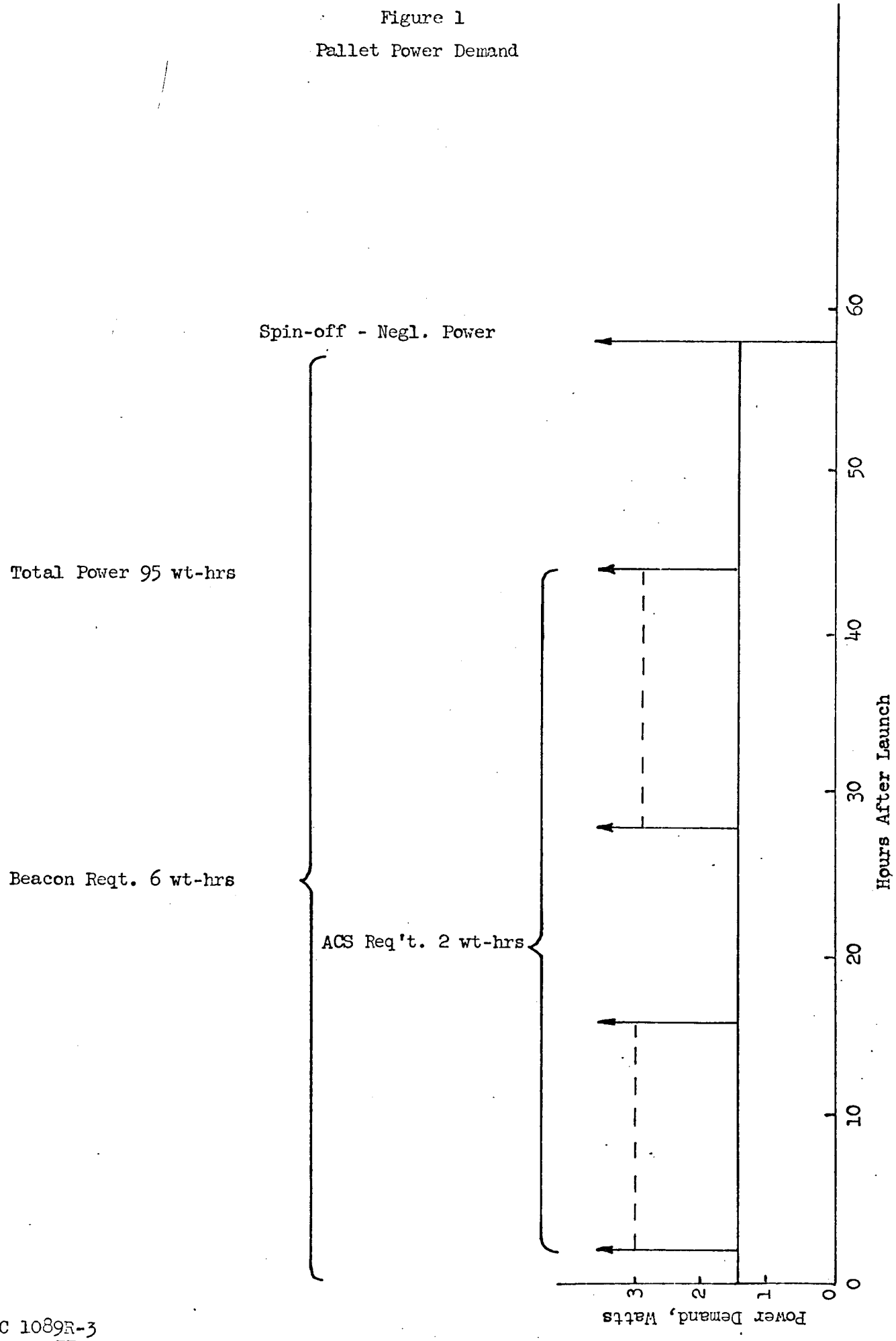

Figure 2

Satellite Power Demand Prior to Data Mode

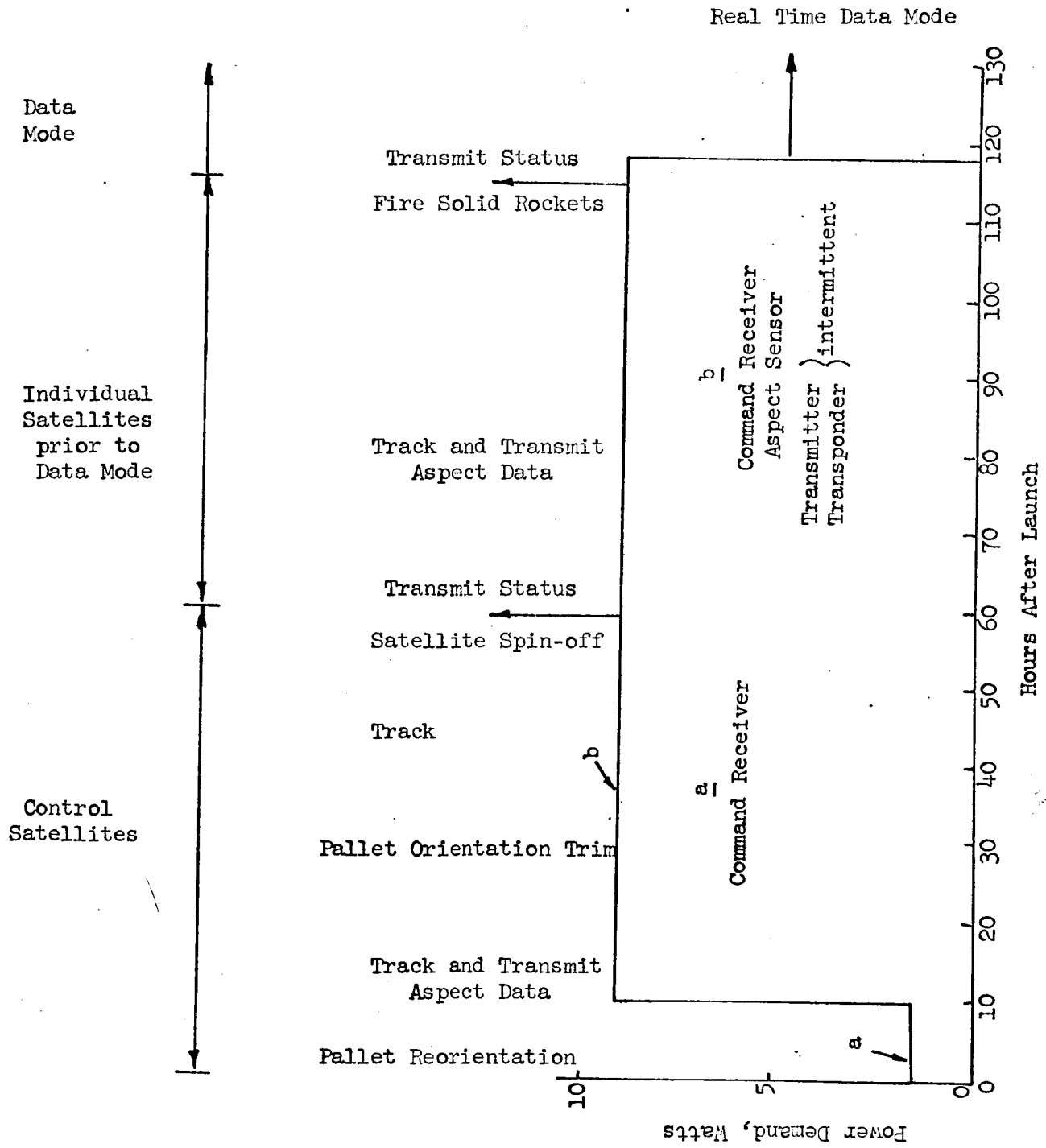

Figure 3

Power Profile - Real Time Data Mode

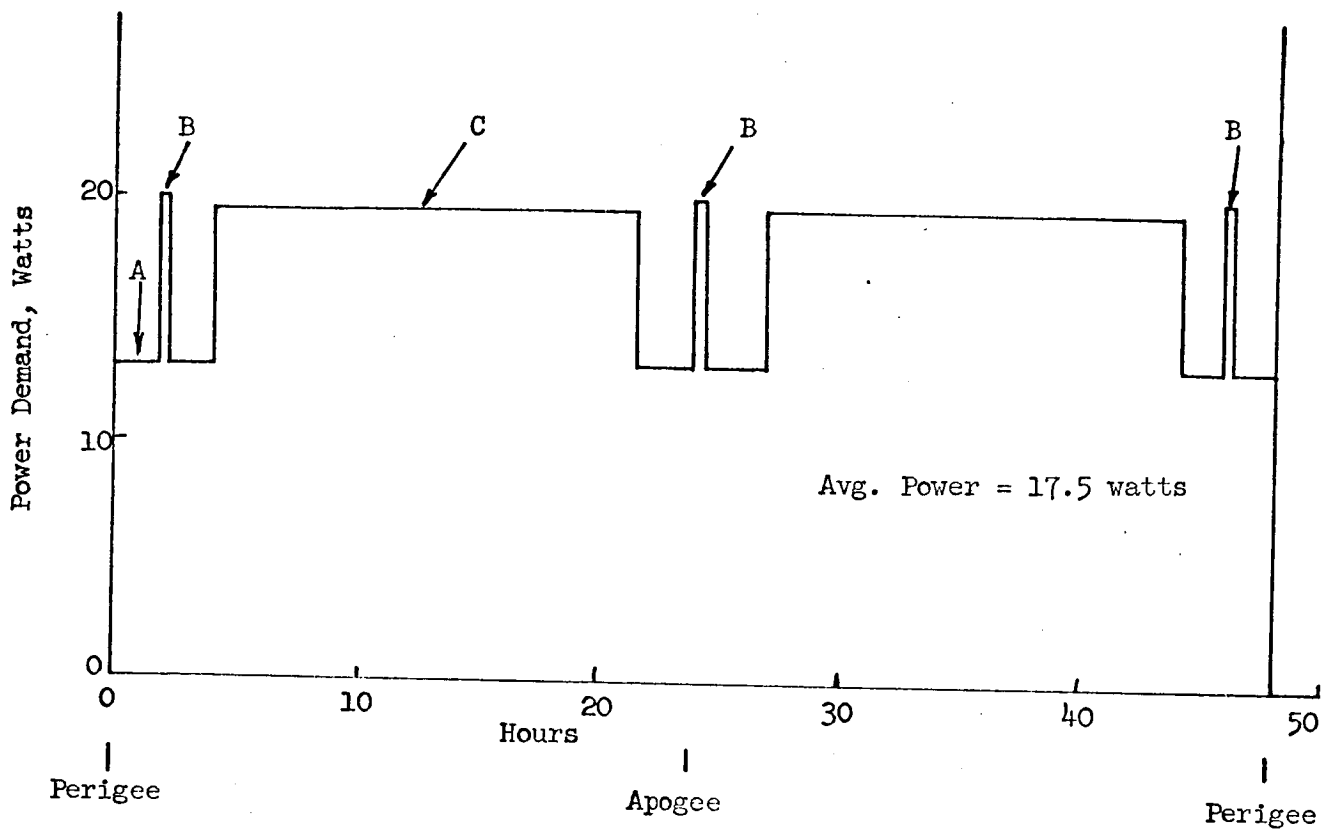

Subsystems On

A	B	C
Instrument	Same as A	Same as A
Command Receiver	+ Transponder	+ Transmitter
Data Handling Syst.		
Aspect Sensor		

The power requirements shown in Figure 3 are based on the assumption that all instruments, the command receiver, data handling system and solar and aspect sensor operate continually and the transmitter and transponder operate intermittently as shown. The time that the transponder will be on will vary from that shown in Figure 3, depending upon the STADAN stations' availability. When computing the instrument power required, the Pioneer C and D magnetometer in an Integrated Instrument package was assumed.

The average power required for the real time data mode is 17.5 watts for the nominal orbit duration and sequence. The battery recharge will require 0.5 watts of continuous power, assuming a battery with depth of charge capability of 20 watt-hours. This allows for in excess of one hour of earth shadow time. To specify the solar cell power output, allowances of 8% loss due to boom shadowing and 10% due to power conditioning losses (see Appendix D-XXVI) must be included. The solar array must therefore be sized for about 22 watts.

For orbits having greater periods than the nominal 48-hour orbit, the 22 watt, requirement remains valid for the real time data mode.

6.0 SATELLITE POWER DEMAND (RECORD DATA MODE)

The satellite power demand for the record mode of operation is shown in Figure 4. No real time transmission is assumed for this mode. The average power required is less than that for the real-time data mode; therefore, some real time transmission or additional record time could be added if desirable and if compatible with other subsystem capabilities. This mode of operation assumes 24 hours of total record time with no recording of data near apogee where the satellite array is bunched. Data will be recorded throughout the transition region and in the interplanetary region somewhat beyond the shock front. The recorded data will be transmitted at a high data rate for about one hour between 4 and 7-1/2 R_e from the earth. Therefore, the time shown for this function will vary as a function of STADAN network availability. The transponder is activated as in the real time data mode.

7.0 SATELLITE SOLAR CELL AND BATTERY REQUIREMENTS

The satellite solar cells and batteries have been sized as follows, based on the real time data mode power profile.

7.1 SOLAR CELL POWER

Solar Cell Degradation Factors:

Effective Surface Area	$F_A = 0.90$
Temperature Rise (10°)	$F_T = 0.95$
Solar Filter	$F_S = 0.95$
Radiation	$F_R = 0.80$

Total $= F_A F_T F_S F_R = 0.65$

Solar Energy = 130 watt/ft^2

Cell Output (10% Efficiency) = 8.45 watt/ft^2

Power Requirement = 22.0 watts continuous

Normal illuminated area required $= \frac{22}{8.45} = 2.6$ ft^2

Assuming solar cells are only on the satellite surfaces normal to the sun line, the surface effectiveness $\cong \frac{1}{\pi}$ (total surface).

The total surface required is then π (2.6) = 8.15 ft^2

The solar cell weight at 1.38 lb/ft^2 = (1.38)(8.15) = 11.2 lb

7.2 BATTERY POWER

Assuming silver-cadmium batteries at 15 watt-hours/lb (50% depth of charge), about 1.5 lb of batteries will provide the necessary power during shadow time.

Figure 4

Power Profile - Data Record Mode

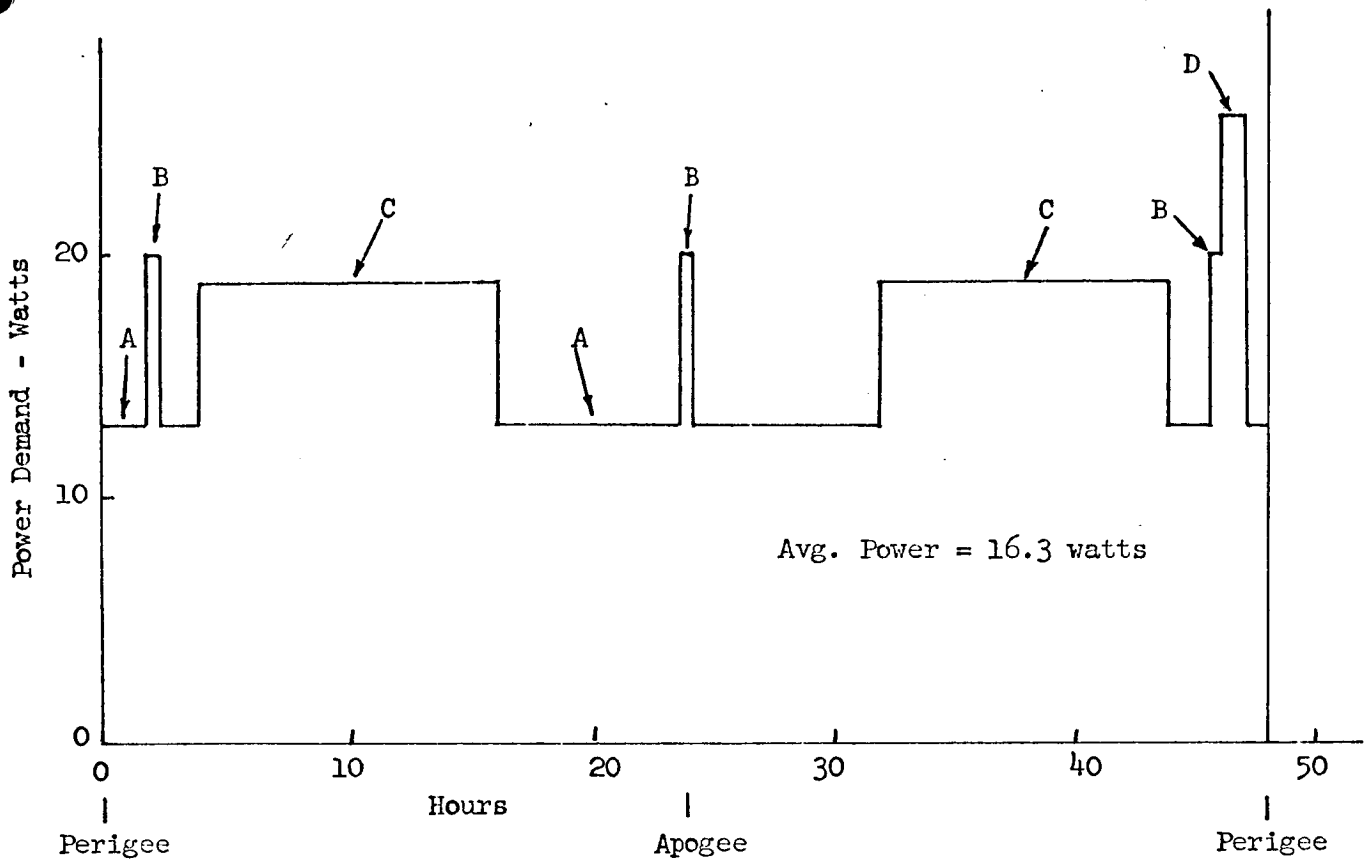

Subsystems On

A	B	C	D
Instruments	Same as A	Same as A	Same as A
Command Receiver	+ Transponder	+ Recorder	+ Transmitter and Recorder
Data Handling Syst.			
Aspect Sensor			

Appendix XXVI

BOOM SHADOW CONSIDERATIONS AND THE EFFECT ON POWER SYSTEM DESIGN

1.0 INTRODUCTION

The spinning satellite's magnetometer boom and sensor will cast a shadow on the satellite surface, blacking out some of the solar cells. This shadow produces a reduction in power output from the solar panels -- the extent of this reduction required investigation. Analyses have been conducted to establish the nature of the shadowing, the effect of varying solar cell layouts on the power output reduction, and the effect of the expected power reduction on the solar array size. The analyses have shown that a power reduction of about 8% can be expected from the boom shadow and that this reduction is relatively sensitive to solar panel design. The average power resulting after consideration of the shadowing is 20.5 watts which is less than the previous design goal of 22 watts. The power reduction due to boom shadowing, together with solar cell area reduction due to instrument view fields (not considered in this analysis), and power conversion inefficiency will probably result in approximately 18 watts of useable power available to the subsystems. Trade-off analyses will be necessary between the power required and the power available, within satellite weight limitations, to establish the final power system design. The supporting analyses are given in the following sections.

2.0 EXPECTED SHADOWING

The angle between the sunline and the orbit plane (orbit shadow angle) will vary as shown in Figure 1. The solid line depicts the case for a no delay, due east launch; while the dotted line is an assumed value to account for launch delays, the spin axis not being exactly perpendicular to the plane, and spin axis drift. The angle between the sunline and the spin axis is thus $90 + \alpha$ (see Figure 2a which shows the extrememes of the sunline).

The shadow cast on the satellite at any time will be radial from the boom/satellite attach point as shown in Figure 2b. The shadow sweeps across the

satellite as a function of the spin rate. When the boom attach point first sees the sun, a shadow is formed on the satellite surface behind the boom (shadow (A)). The shadow then moves through position (b), (c), (d) and (e).

The length of the shadow cast on the satellite as a function of the angle between the sunline and the boom. This shadow angle, γ, is a function of the orbit shadow angle, α, and the spin shadow angle, β, as shown in Figure 2c. The relationship between α, β and γ is

$$\cos \gamma = \cos \alpha \cos \beta$$

The length of the shadow, L_s, is therefore

$$L_s = L_B \tan \gamma$$

where L_B is the boom length.

In most cases, the length of the shadow will be greater than the projected area of the satellite. Thus, the shadow will sweep across the satellite either above or below the boom attach point, depending upon the orbital position (see Figure 1), as a function of the spin rate. When the shadow is first cast in any spin cycle, (shadow (a) of Figure 2b), it will not immediately fall on the solar panel adjacent to the panel where the boom is attached. This is due to the angle of intersection between the adjacent panels for the reference satellite design. A shadow will not impinge on the adjacent panels until the satellite has rotated through an angle of $\beta = 45^\circ$. Due to the shorter distance between the boom attach point and the bottom of the satellite, when the shadow sweeps across the lower portion of the satellite, the adjacent panels are never shadowed. This effect can be seen in the shadow limits presented in Figure 3. As the shadow becomes more nearly parallel with the spin axis, it shortens so that it does not sweep all of the available surface. The length of the shadow at this time is due only to the orbital shadow angle, α, which varies with the precession of the spin axis with respect to the sunline (Figure 1). Figure 3 shows that very little of the satellite surface, either above or below the

boom, is entirely free from shadowing. Only at about 160 days after launch will the area swept out be small. At that time, the shadows would be radially around the girth of the satellite at the boom attach point. It is obvious from Figure 3 that the use of a belly band to eliminate shadow effects is not feasible for the multiple satellites.

3.0 POWER REDUCTION DUE TO BOOM SHADOWING

Power output reduction of the solar panels due to boom shadowing has been established. The geometry of the panels with respect to the sunline is shown in Figure 4. The angle between the sunline and the boom in the orbit plane, β, is assumed to be zero when the boom is aligned with the sunline. When β is zero, panel (1) is shadowed. When the upper part of the satellite is shadowed, panel (3) begins to be shadowed when β is about 25°. When β exceeds 90°, there is no more shadowing until β exceeds 270°. Figure 5 shows how the shadow falls on the adjacent panel illustrating, first, the nature of the shadow on the projected area of the satellite, and second, the nature of the shadow on the panel as rotated 45° (or as seen when directly facing the adjacent panel). The "bend" in the shadow at the interface of the two panels was considered in determining the shadowed solar cells.

Two solar cell array designs were considered to establish the power reduction due to boom shadowing. In both cases, 1 x 2 cm cells were combined in series strings to produce 30 to 32 volts/series. Figure 6 shows the series strings of cells for panels (1) and (2), arranged in a radial or "pie" shape so that the shadow will fall primarily on one series at any time. (Panel (3) is the reverse of Panel (2)) Each square represents two 1 x 2 cm cells. In the alternate arrangement of Figure 7, no attempt is made to orient the series of cells with the shadow, but the arrangement attempts to maximize the length of cell strings in order to reduce the spacing between cells and interconnect complexity. Boom shadow overlays as a function of β were made and the number of cells in each series which were shadowed were established. The power reduction due to solar cell shadowing was extrapolated from data given in Reference 1, and is shown in Figure 8.

The array power loss due to shadowing of any part of one to three strings of cells out of the six used in each upper panel is shown. The power loss falls below the open circuit power due to current drain by the shadowed cells. Blocking diodes between series strings could be used to prevent this. Note the greater power loss when parallel cells are shadowed compared to series cells. Shadowing of 10% of three parallel strings will result in the loss of all strings, while shadowing one entire string will result in only the loss of that string even though a greater number of cells were shadowed. It therefore appears best to attempt to design the solar array so that the shadow falls on only one string at a time.

The power output was computed assuming the deviation of the solar cell output from the cosine curve as shown in Figure 9. The unshadowed and shadowed power outputs are shown in Figure 10. The cyclic variation is due to the octagonal shape of the satellite which has a varying projected area. The "squared off" peak values are due to the deviation of the cell output from the cosine law. The dotted curves show the power output when shadowed. It is obvious that attempting to design the array so that the strings of cells lie radially from the attach point has advantages. Case 1, which has radially aligned cells, has less power reduction than Case 2, where there is no attempt in the design to align the cells radially. The design of Case 1 attempts to reduce the number of parallel cells which are shadowed to minimize the power loss, and, when compared to Case 2, where these attempts were not made, it can be seen to be a successful design approach. It is possible that more sophisticated analysis and design can reduce the power loss due to shadowing more than that shown for Case 1. For example, more attention to the cell layout could possibly further minimize power loss. Blocking diodes between groups of cells will prevent power drain between shadowed and unshadowed cells. Diode shunting of each string of cells reduces loss considerably when parallel cells are shadowed and should be investigated further. All of the above possible design approaches require that the already delicate solar cell mounting procedure be complicated and thus must be considered carefully before implementation.

Based upon the above analysis, if one or more booms is used, a preliminary estimate of the power loss is about 8% per boom.

4.0 POWER CONDITIONING CONSIDERATIONS

Various power conditioning alternatives are available for consideration with the solar array/battery combination. Some of these alternatives are:

1. Battery charge limiting for the battery only
2. Battery charge limiting and voltage transformation
3. Battery charge limiting and voltage regulation

Considering voltage transformations, it is not clear that there are advantages to producing voltages from the solar array sufficiently different from the required voltages to warrant voltage transformation. It is desirable for the voltage to be high to minimize the current and hence magnetic effects. Also, numerous small series strings in parallel to produce low voltages could reduce the power due to shadowing even further than described above. The optimum series string size may be different than that specified above to produce 30-32 volts, however, preliminary considerations indicate that there is no need for voltage transformation.

Voltage regulation must also be considered. The voltage from the solar array/battery system will vary approximately $\pm$ 15% about the design value. Regulation of this can be accomplished in several ways. Pulse width control using oscillatory transistors can be employed, but this method produces stray magnetic fields which are unacceptable to a magnetically clean spacecraft. An alternate scheme is to employ a linear regulator, but this method, due to inefficiencies, can produce a 30% loss in power. Another possible method is to switch battery taps during the charge/discharge cycle. This method requires 15 to 20% more batteries and a resultant weight penalty. Also a 5% switching loss can be expected.

Based upon preliminary consideration, no voltage regulation is recommended. If specific instruments or subsystems are required to operate with voltage regulation better than $\pm$ 15%, then specific regulation will be provided for that subsystem. Therefore, only battery charge limiting is recommended at this time, subject to change due to further analysis.

A final consideration with regard to power conditioning is impedance matching between the solar array and the spacecraft load. Assuming that no complicated impedance matching equipment is used, impedance mismatch can produce a 5 to 15% loss in power.

5.0 POWER REQUIREMENT/CAPABILITY COMPARISONS

The average power requirement for the satellite subsystem, based upon the analysis of Appendix XXV, is 18 watts. This requirement originated from the real time data mode; and it includes allowances on real time data transmission as specified in the referenced section, and provision for battery recharge. The useable power available considering boom shadowing losses, allowance for instrument view fields, power conditioning inefficiency, etc. will be about 18 watts. Thus the current power requirement matches the estimated power available.

It is not inconceivable that the power required will change during future analysis due to changes in the instrument compliment or operational mode. Also, available power may change during future studies due to changes in available weight (solar cell area). During the future phases, continuing system integration analyses will be conducted to assure that the power system design can always meet the power requirements.

REFERENCES

1. Ralph M. Sullivan, Shadow Effects on a Series-Parallel Array of Solar Cells, X-636-65-207, Goddard Space Flight Center.

2. H. Montgomery and F. B. Shaffer, Power Study of Spin Stabilized EGO (S-49), X-643-65-14, Goddard Space Flight Center, March 1965.

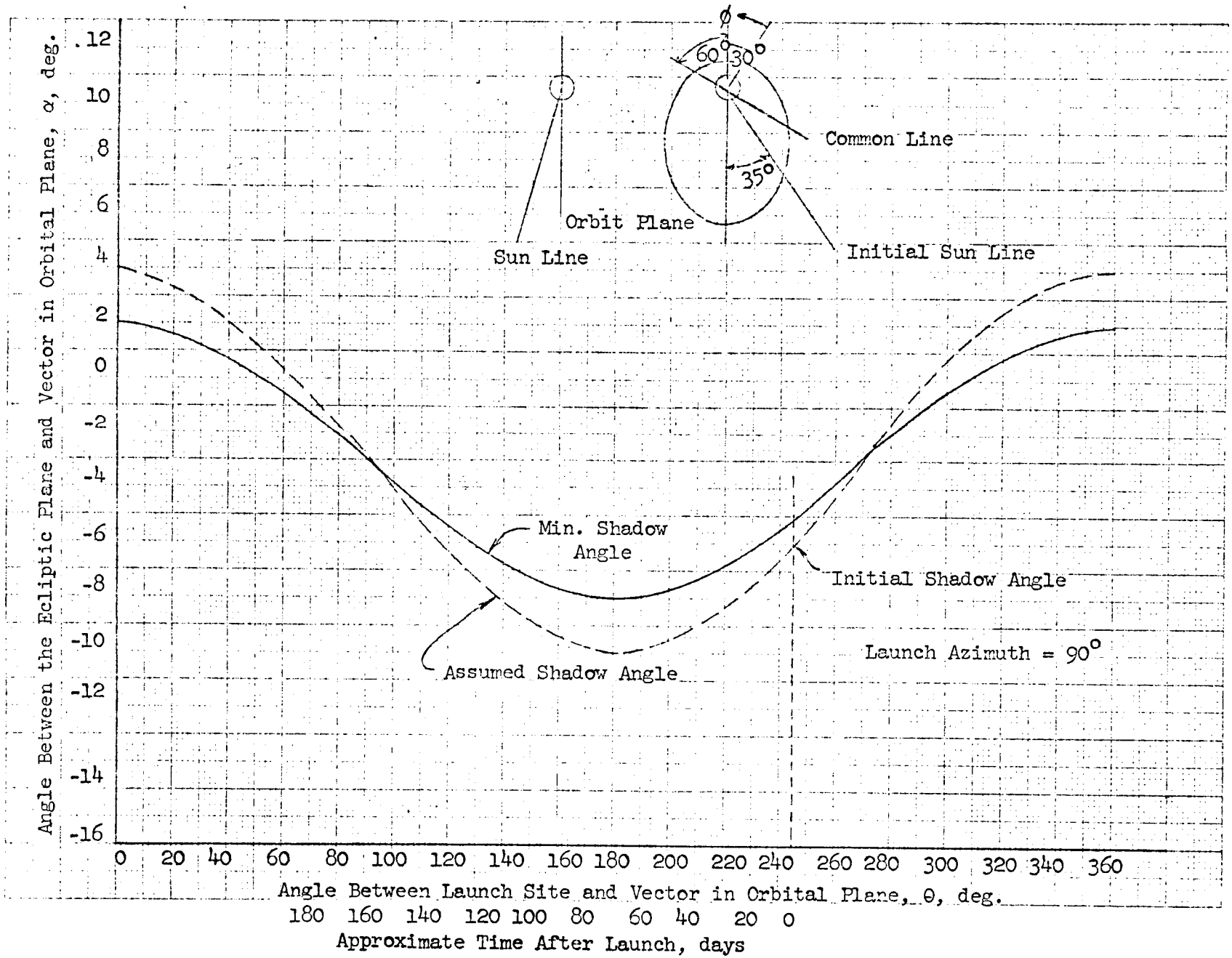

Figure 1 Orbit Shadow Angle

FIGURE 2

SPACECRAFT SHADOW CONSIDERATIONS

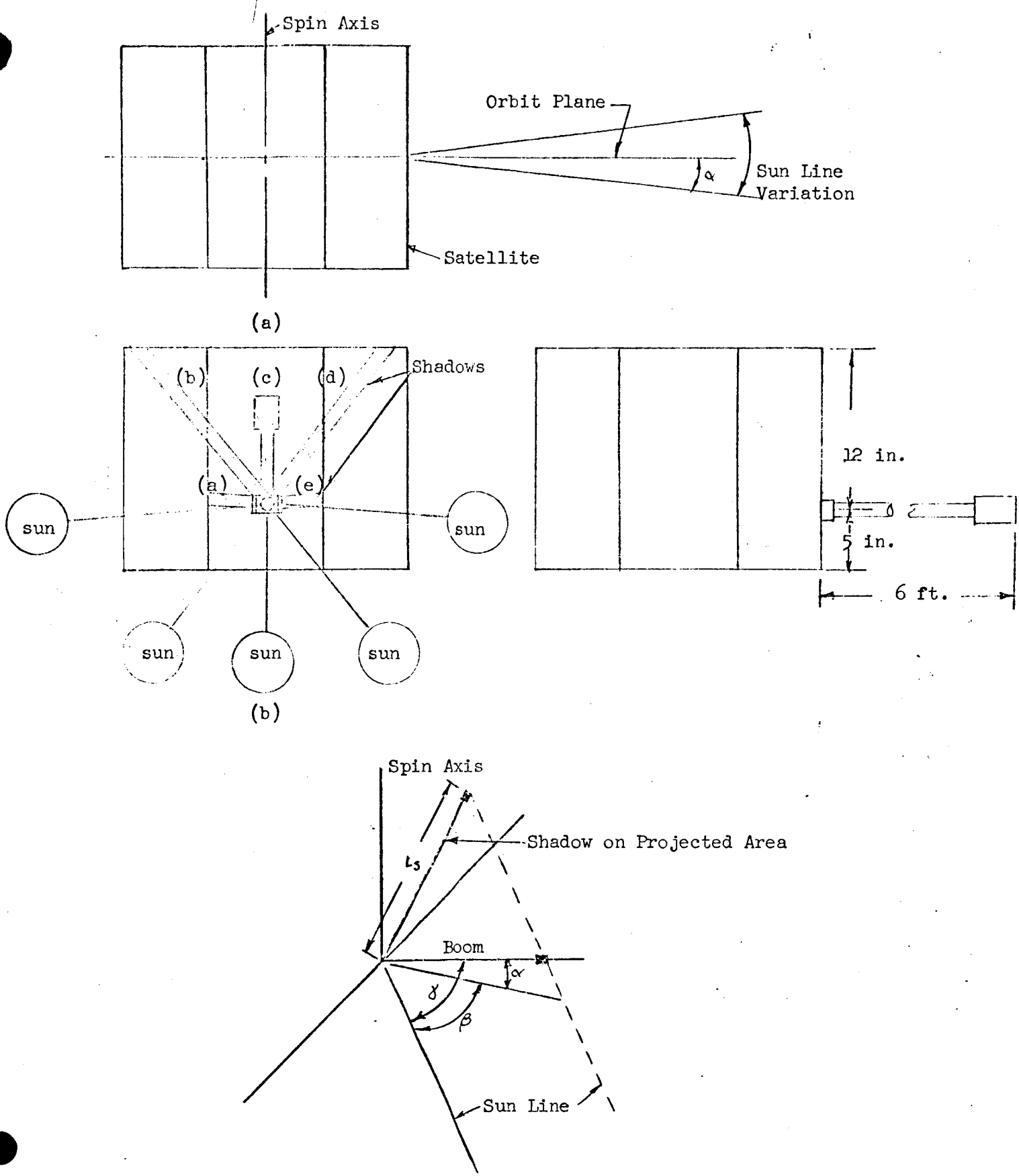

FIGURE 3

SHADOW LIMITS

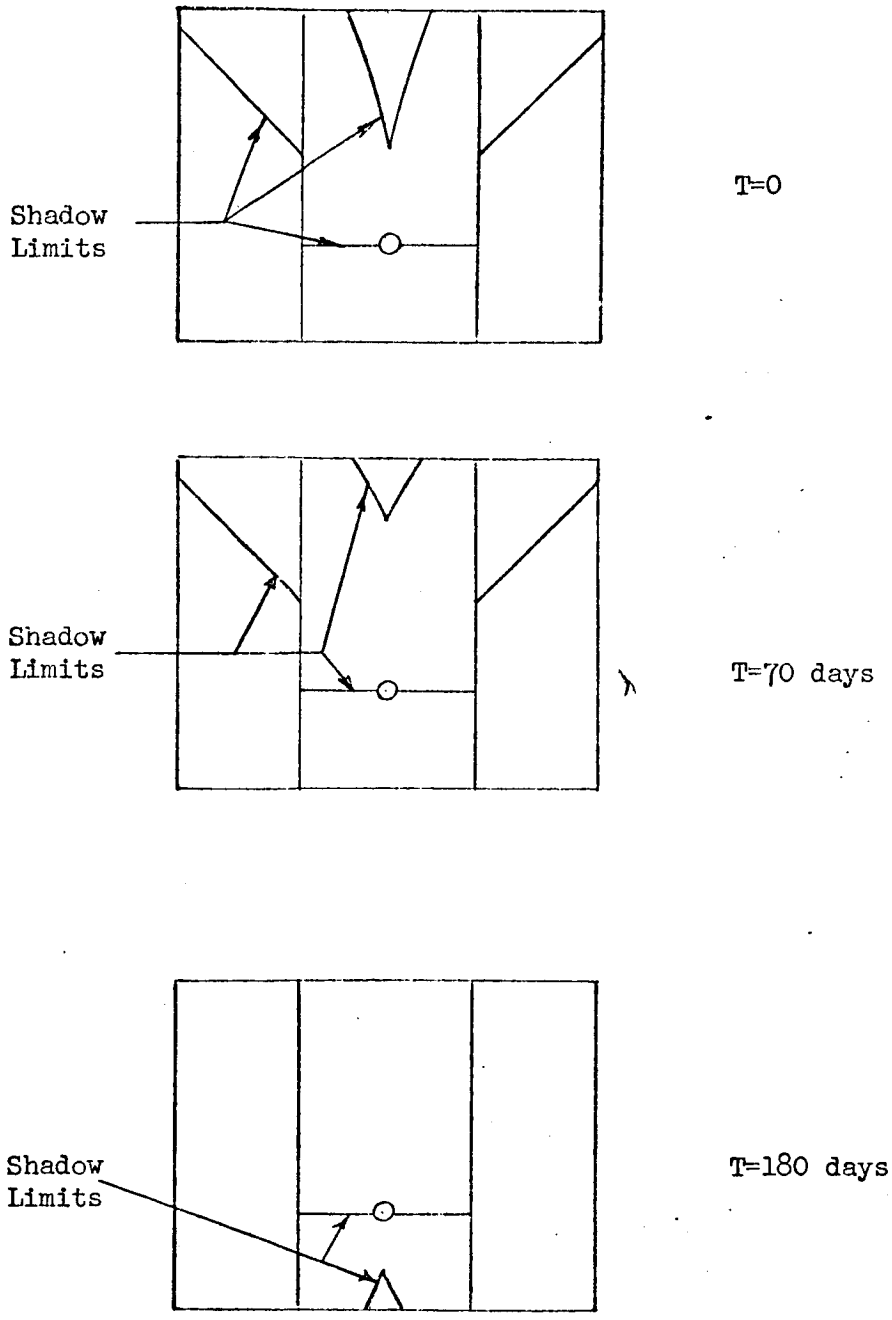

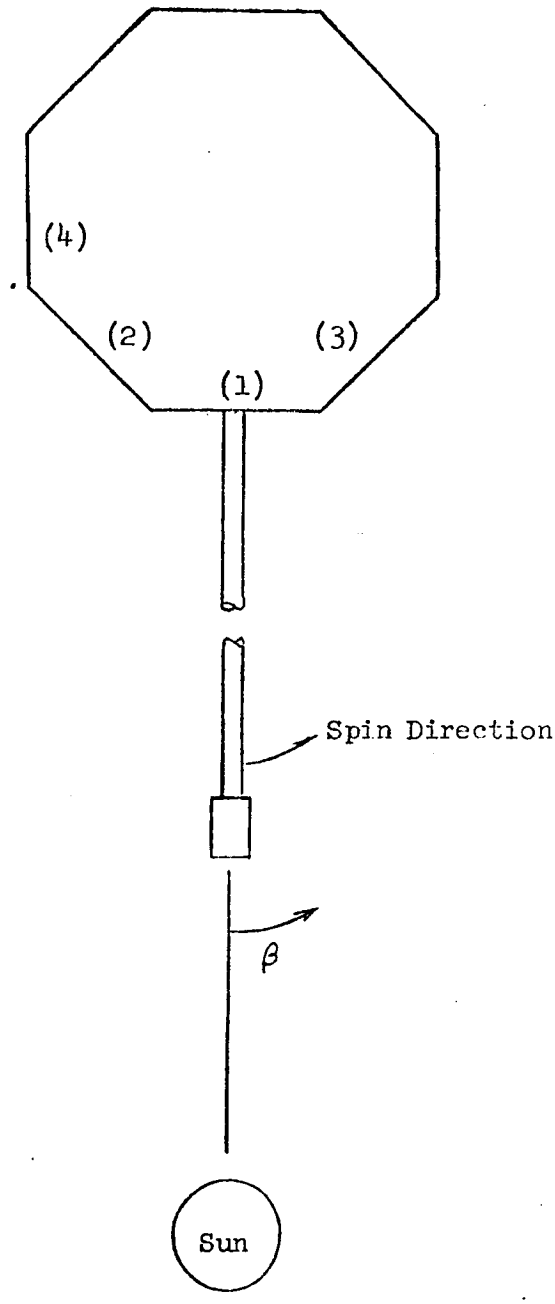

FIGURE 4

PANEL DESIGNATION
AND
INITIAL SPIN SHADOW ANGLE

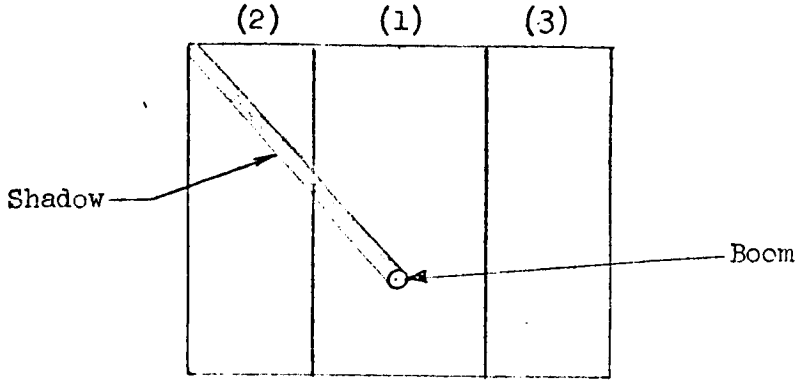

Projected Area

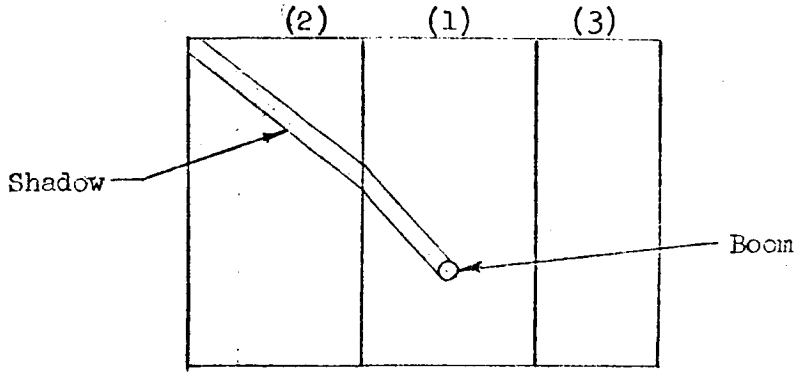

Panel (2) Rotated

FIGURE 5

SHADOW CHARACTERISTICS

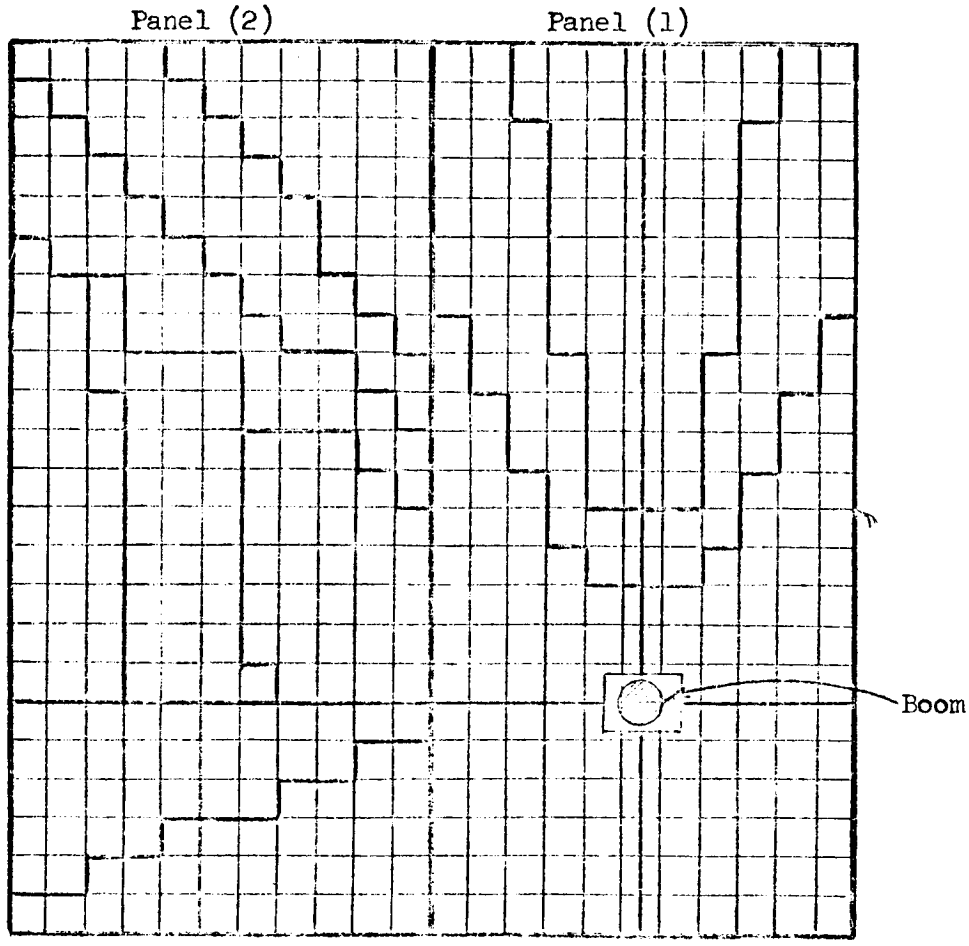

Figure 6

RADIAL SOLAR CELL ARRANGEMENT

(Case 1)

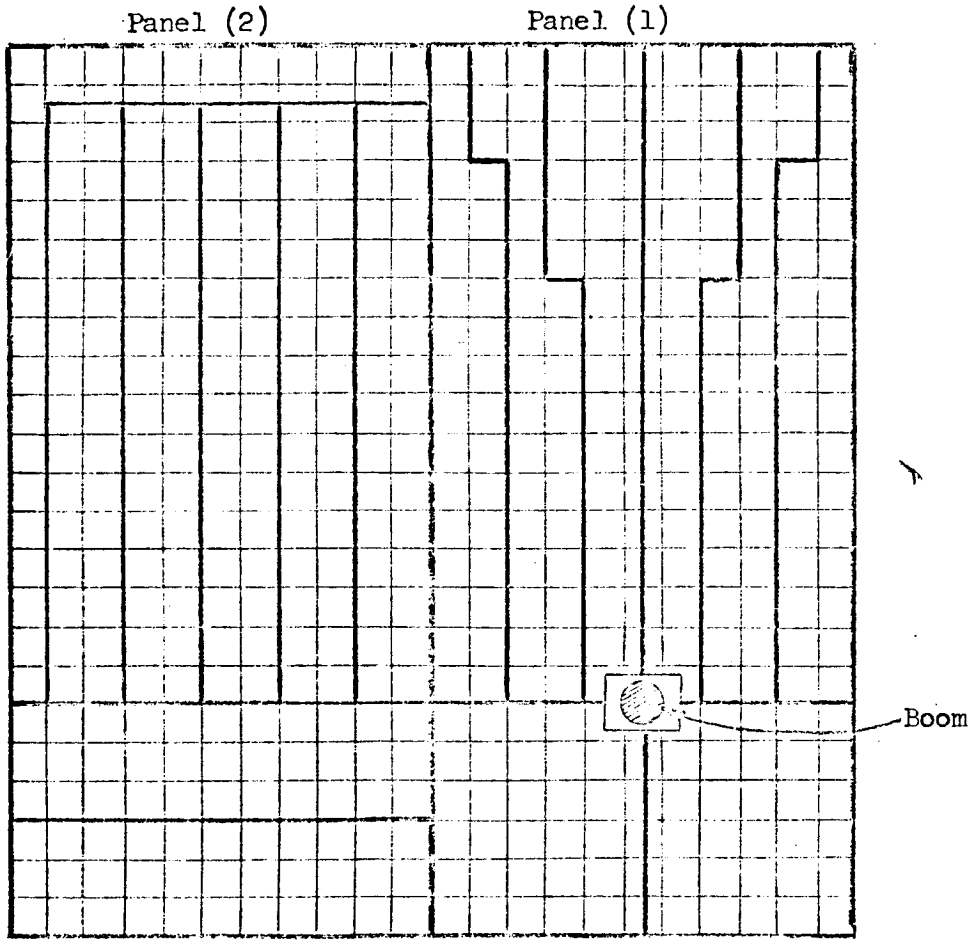

Figure 7

ALTERNATE SOLAR CELL ARRANGEMENT

(Case 2)

Figure 8

Percent Solar Cell Array Power Output with Shadowing

Note: Array has Six Series Strings

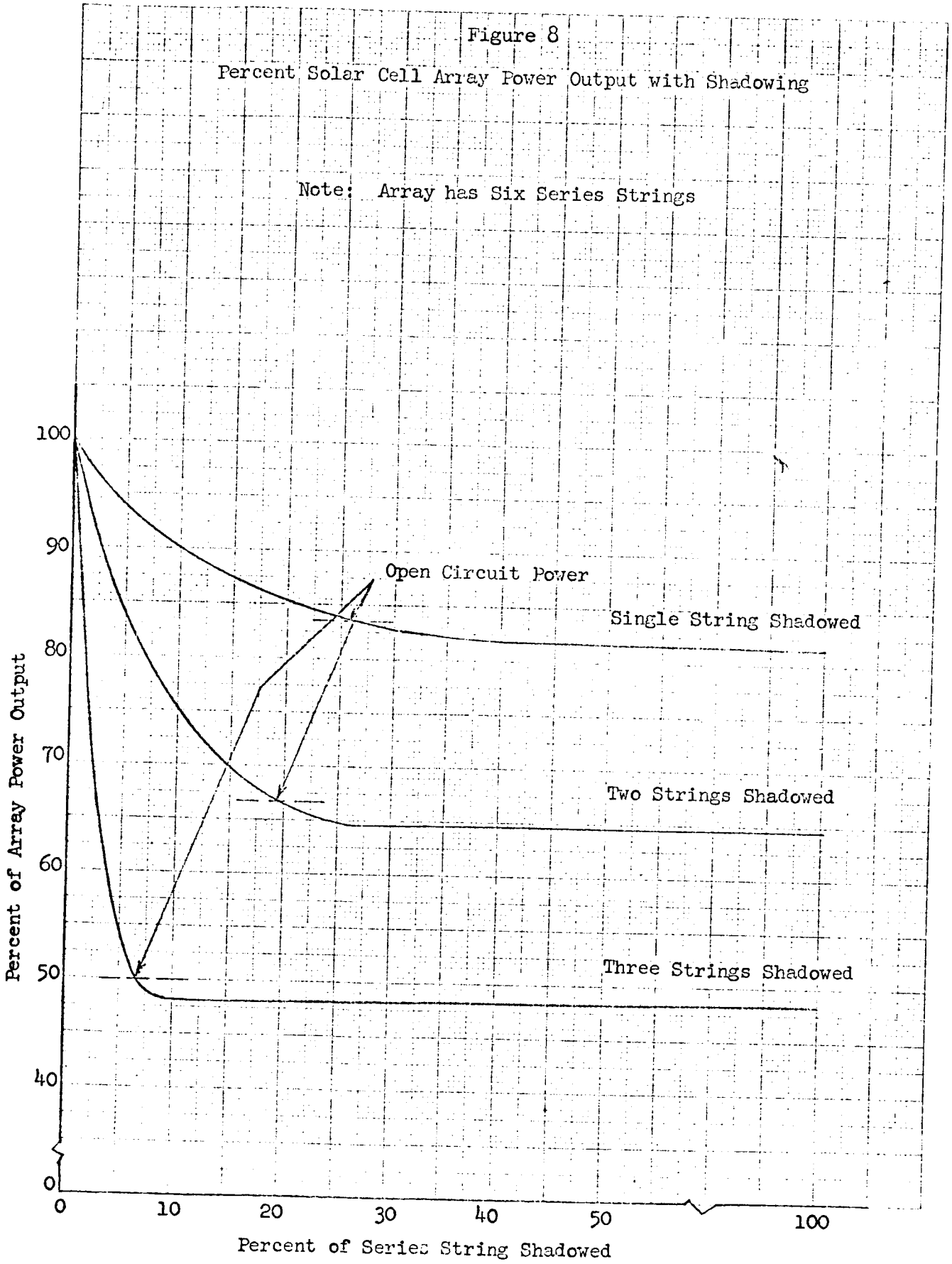

CLEARPRINT PAPER CO. NO. C39 MILLIMETERS BOTH WAYS 150 X 220 DIVISIONS. PRINTED IN U.S.A. ON CLEARPRINT TECHNICAL PAPER 1015

Figure 9

Deviation of Solar Cell Short Circuit Current
From a Cosine Curve

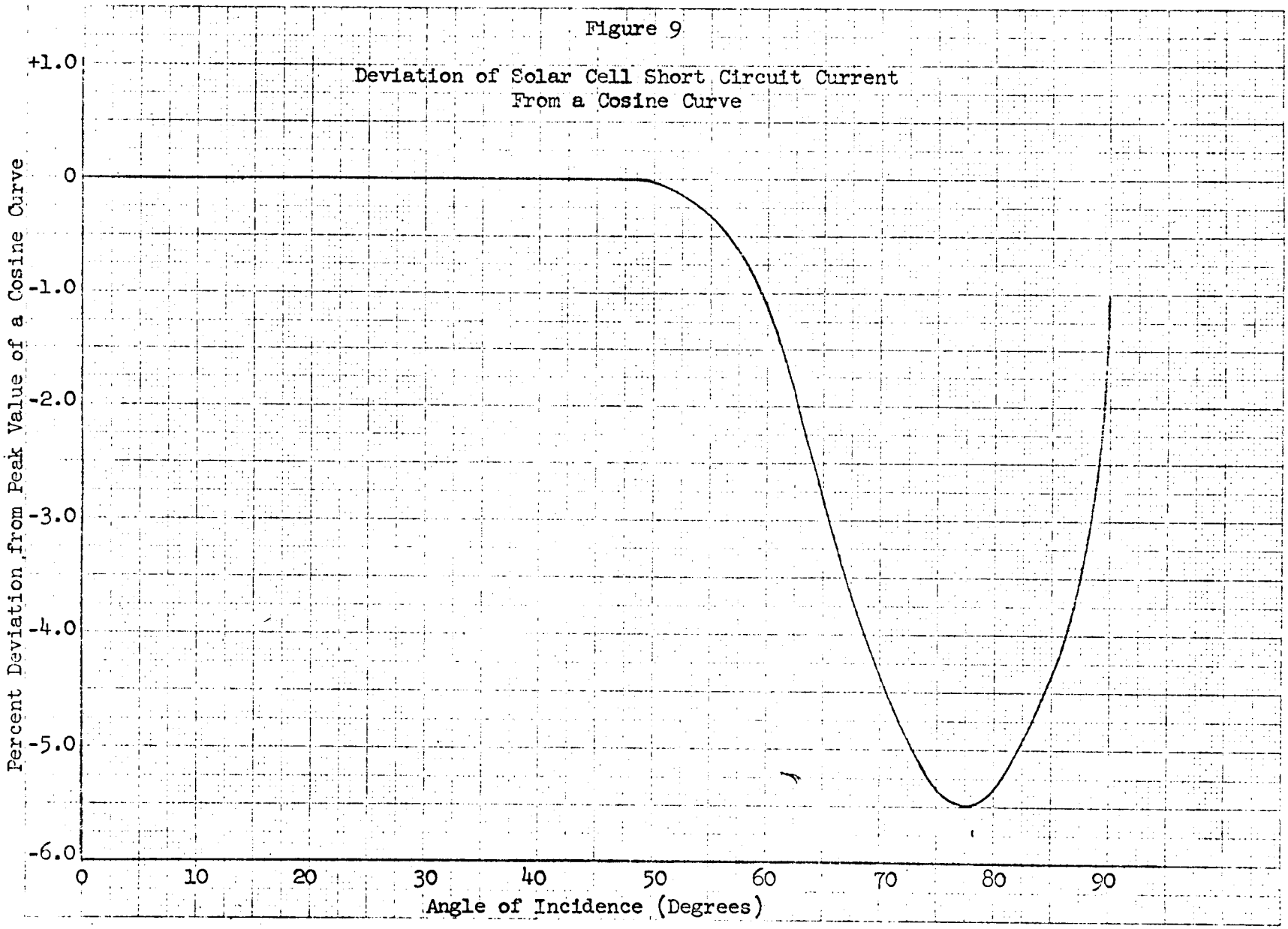

Figure 10
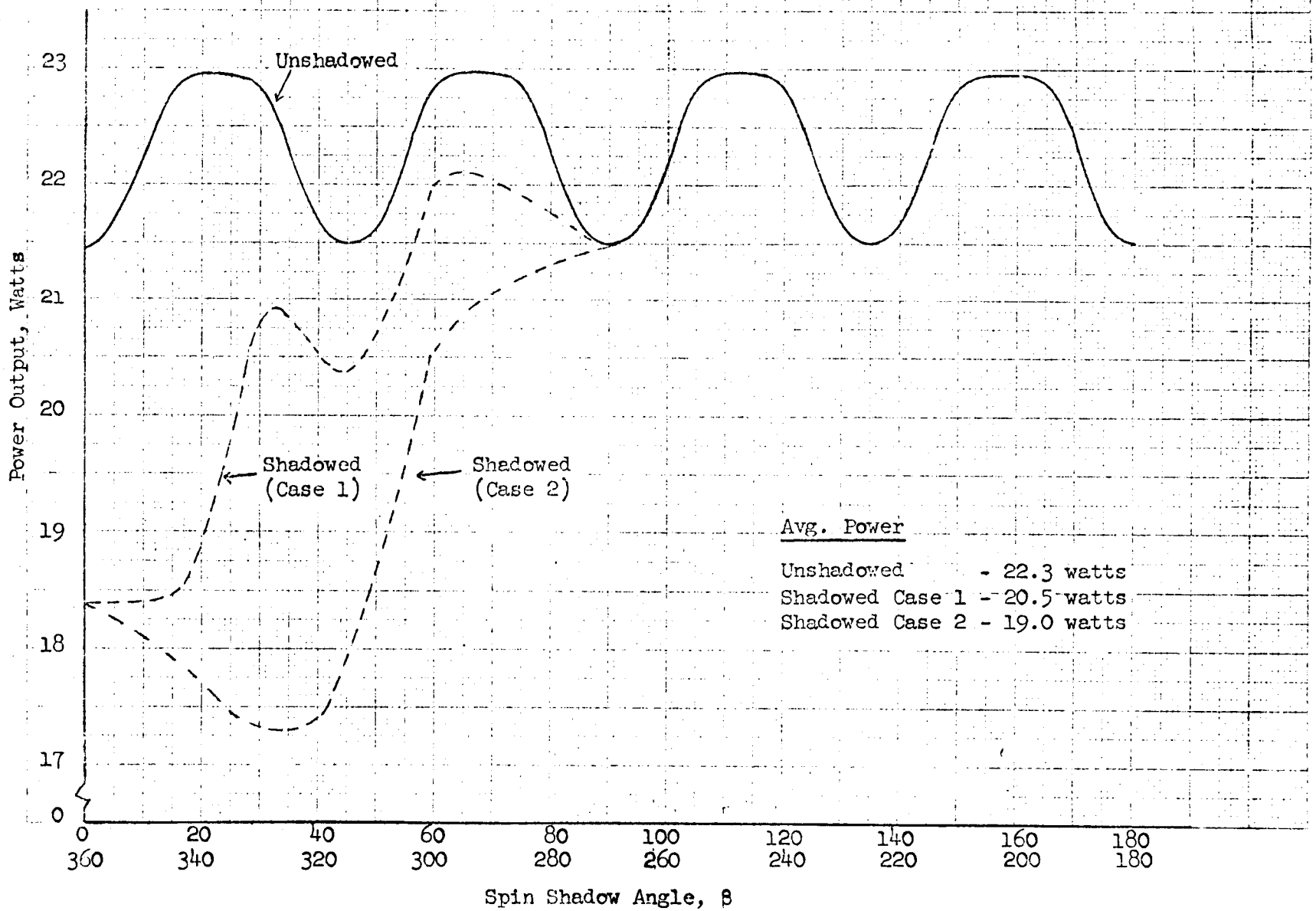
Maximum Power Loss Due to Boom Shadowing